March 2009

Effective Radial Thermal Conductivity in Fixed-Bed Reactor Tubes

Adam Raymond Lirette
Worcester Polytechnic Institute

Amanda K. Gurnon
Worcester Polytechnic Institute

Curtis Joseph Schaaf
Worcester Polytechnic Institute

Nicholas D. Vitello
Worcester Polytechnic Institute

Effective Radial Thermal Conductivity in Fixed-Bed Reactor Tubes

by

Amanda Gurnon
Adam Lirette
Curtis Schaaf
Nicholas Vitello

A Major Qualifying Project
Submitted to the Faculty
of the
WORCESTER POLYTECHNIC INSTITUTE
in partial fulfillment of the requirements for the
Degree of Bachelor of Science
in
Chemical Engineering

by

_____	_____
Amanda Gurnon	Adam Lirette
_____	_____
Curtis Schaaf	Nicholas Vitello

March 2009

APPROVED:

_____
Dr. Anthony G. Dixon, Advisor

Abstract

The purpose of our research is to more accurately model the temperature gradient across a fixed bed reactor used in steam-methane reforming. Heat transfer in the near-wall region was modeled using computational fluid dynamics. Heat transfer in the bed center region was determined through analysis of measured temperature profiles in a packed bed. Using this two-region approach, the effective radial thermal conductivity was used in a 2D pseudo-homogeneous heat-transfer model solved by finite element method and compared to experimental temperatures.

Executive Summary

Methane steam reforming is a major part of the natural gas industry, particularly in the production of syngas and hydrogen. In fact, the syngas generation section at such processing plants make up for over 50% of the capital cost. These fixed-bed reactors used in the process tend to have large temperature gradients, especially near the tube-wall, making analysis of heat transfer in fixed-beds difficult to predict. This becomes a critical problem because a difference of 20K at the tube wall (usually run around 1000K) will shorten the life of the reactor from 10 to less than 5 years. The cost burden also greatly increases as a typical re-tubing runs at around $5-8 million dollars. Thus, knowledge of the heat transfer throughout these fixed-beds is essential to the syngas and hydrogen industries.

Complexities in modeling fixed beds have arisen from the wide variety of catalysts, large temperature ranges, varying flowrates, and varying phases within the reactor. These changing properties make modeling the temperature gradient difficult. A major point of error occurs in the near-wall region where temperature readings are difficult to obtain. These regions have only recently become more attainable through the use of computational fluid dynamics (CFD) software. The use of CFD does not come without its own difficulties. Complexities arise when trying to model the infinitesimally small contact points between particles and the tube-wall.

Our project used the approach of a two-region model, where two descriptions of the behavior of the effective radial thermal conductivity are used, one for the center of the

tube and one for the near-wall region. The thermal conductivity at the center of the fixed bed was investigated using an experimental set-up in the lab. The near-wall region, however, was modeled using CFD software. After sufficient information was supplied by both approaches, radial temperature profiles were obtained using a 2D pseudo-homogeneous heat-transfer model solved by the finite element method, incorporating the two region model for radial thermal conductivity.

Effective radial thermal conductivity values for the near-wall region were found by observing temperature gradients in CFD models run at multiple fluid velocities. It was also observed that the thermal conductivities, as well as the temperature gradient, smoothed out after approximately .27 of a particle length, d_p, which was later used as our wall effect boundary condition. These thermal conductivities in the near-wall area all behaved quadratically until hitting a maximum and flattening out in the bed center region. The bed center thermal conductivity was found to be constant by removing radial positions (IP) and analyzing the collected data with a 2-parameter Inlet Profile Plug Flow model. A linear trend line was plotted onto the IP graph to determine a value for k_r at the center of the bed. By inputting CFD and experimentally calculated effective radial thermal conductivity function into COMSOL, a 2D axial symmetry pseudo-homogeneous heat-transfer model, temperature gradients were computed. These temperature gradients were then compared to those found experimentally and by CFD. The relationships between the experimentally calculated data and those found in COMSOL showed a close relationship. These findings showed a promising start towards the prediction of heat transfer across fixed-bed reactor tubes.

Contents

1 Introduction

Fixed bed reactors are used in steam-methane reforming, a process that accounts for about 95% of the hydrogen produced in the United States (Hartstein, 2003). Currently about 50% of this hydrogen is used to produce ammonia, which is utilized in fertilizers, refrigeration units, and in the production of industrial chemicals. The other half of this hydrogen is primarily used in oil refineries and methanol production, but can also be used to produce other metals, pharmaceuticals, and even foods and beverages. Steam-methane reforming has proved to be an efficient and economical option in industry and has thus led it to be the most common process for hydrogen production (Padro et al.,1999).

Steam-methane reforming converts methane into hydrogen and carbon monoxide. This process is most efficient at very high temperatures, ranging between 700 and 1100 degrees Celsius. The methane is reacted in the presence of a metal catalyst, commonly nickel. In order to improve the efficiency of this reaction, the process uses fixed bed reactors. These reactors are filled with catalyst-coated packing in order to increase the reactive surface area between the two phases.

While fixed bed reactors are an efficient process they do not come without disadvantages. Within fixed bed reactors there are undesired thermal gradients which adversely affect temperature control throughout the reactor. Each year thousands of dollars in damages to steam-methane reforming fixed beds is a direct effect of poor temperature control. The

overall purpose of our research is to more accurately model the temperature gradient across a fixed bed reactor used in steam-methane reforming.

Industry, academia, and government agencies have invested resources into the research and development for improving models of fixed bed reactors. The present research being completed revolves around modeling the temperature gradient across the fixed bed. Complexities in modeling fixed beds have arisen from the wide variety of catalysts, large temperature ranges, varying flowrates, and varying phases within the reactor. These changing properties make modeling the temperature gradient difficult. A major point of error occurs in the near-wall region where temperature readings are difficult to obtain.

Measuring the wall heat transfer coefficient has proven to be a problem in past research. When h_w is plotted versus the thermal conductivity, the plots are scattered, which has caused researchers difficulty in predicting values for the wall heat transfer coefficient (Tsotsas and Schlünder, 1990; Freiwald and Paterson, 1992). Other research has shown that the value of h_w depends on the thermocouples and their location (von Scala, 1999). All prove that a mode of predicting the wall heat transfer coefficient has not been found and that it continues to be a struggle in this type of work.

Past research has worked toward simplifying the description of these complex heat transfer phenomena. The major simplification is the use of a pseudo-homogenous model which allows the temperature of the phases within the bed to be constant throughout. Early models use a constant radial thermal conductivity throughout the bed and a wall

heat transfer coefficient with a step change in temperature idealized at the wall to compensate for a steep temperature change near the wall. As of late, this model has been adapted to what is called the "two-region model" where there are separate thermal conductivities for the main bed and for the region near the wall (Logtenberg et al., 1999). Experimentally, many labs use a fixed bed column set-up with a thermocouple cross that indicates the temperature at certain radial positions across the bed (Smirnov, 2003a). From this information a parabolic temperature profile is developed. However, thermocouples cannot access the near-wall region of the bed without interference, where the majority of the temperature changes take place. This drove researchers to employ the use of computational fluid dynamics (CFD) modeling. Although useful, CFD has had difficulties simulating the contact points that occur between particles or the particle and the wall (Dixon et al., 2006). This past research suggests that a model of the entire temperature gradient across a fixed bed reactor can be achieved by combining the experimentally determined thermal conductivity coefficient in the center of the bed with the thermal conductivity coefficient found using the CFD model for the near-wall region.

In order to model the temperature gradient across a fixed bed reactor our team will meet five specific sub goals; 1) Establish, experimentally, temperature profiles across two-inch and four-inch diameter fixed beds, 2) Determine a constant thermal conductivity coefficient for the center of the fixed bed, 3) Create a CFD model of the near-wall region of the experimental system, 4) Determine a function for the thermal conductivity coefficient in the near-wall region of the fixed bed, 5) Combine these two regional thermal conductivity coefficients to accurately predict the temperature profile across a

fixed bed and compare to data. The thermal conductivity coefficient for the center of the packed bed will be determined experimentally from measured temperature profiles, by fitting plug flow heat transfer models. The thermal conductivity coefficient for the near-wall region will be found by building a near-wall geometry (Gambit) and solving fluid flow and energy balance equations (Fluent) using the finite volume method. These two regional thermal conductivity coefficients will then be used in a 2D pseudo-homogeneous heat-transfer model solved by finite element method in order to model the temperature profile across a fixed bed reactor.

2 Background on Fixed Bed Heat Transfer

For years packed beds have been modeled and analyzed using a variety of methods and experimental set-ups. There are three modes of heat transfer through a fixed bed; conduction, convection and radiation. For the experimental conditions and temperatures, only convection and conduction apply. Conduction is the transfer of energy from particle to particle, while convection is the exchange of energy due to the movement of fluid. The heat transfer within the packed bed is affected by the bed packing size and shape, as well as the fluid flow rate. Of the many variables that have affected the analysis of packed beds, two primary arguments are always discussed; 1) the inlet temperature profile of the air entering the bed and 2) the effect of bed height on the temperature profile and, ultimately, the heat transfer parameters.

Experimental modeling of temperature profiles in fixed beds typically consists of multiple, radial readings spanning the diameter of the column. These readings, however, are unable to span the entire width of a column because the thermocouples cannot come in contact with the heated or cooled wall. Thus, wall effects are not properly measured, which leaves some margin of error in the data set. It is commonly assumed that wall effects take place up to 1-1.5 particle diameters away from the wall. The experimental portion of this project will focus on the thermal conductivity throughout the center of the bed, i.e. outside of the 1-1.5 particle diameters that see wall effects. Concurrently, computational fluid dynamics will be utilized to model the temperature profile near the wall, which will allow a complete profile across the column diameter.

2.1 Pseudo-homogeneous Plug-Flow Model

Multiple models have been written to analyze temperature profile data files, including a Plug Flow (PF) model (Equations 1-7) and an Inlet Profile Plug Flow (IPPF) model (Equations 9-24) (Personal Communication Dixon, 2008).

In order to design the base, pseudo-homogeneous plug-flow model, the following assumptions from Borkink et al. (1993) were used:

- Steady state system
- System is pseudo-homogeneous
- No reaction takes place
- No axial dispersion of heat
- No free convection of heat
- No radiation
- Constant superficial gas velocity
- Constant pressure through the packed bed
- Constant wall temperature
- Physical properties of the gas and solid are independent of temperature

The dimensional energy balance, which the PF model derives from, is written as:

$$\rho v C_p \frac{\partial T}{\partial z} = k_r \left(\frac{\partial^2 T}{\partial r^2} + \frac{1}{r} \frac{\partial T}{\partial r} \right) \qquad 1$$

Given the following boundary conditions:

$$T|_{z=0} = T_{in} \tag{2a}$$

$$\left.\frac{\partial T}{\partial r}\right|_{r=0} = 0 \tag{2b}$$

$$-k_r \left.\frac{\partial T}{\partial r}\right|_{r=R} = h_w (T - T_w) \tag{2c}$$

These equations can be made dimensionless by defining:

$$\theta = \frac{T - T_w}{T_o - T_w} \tag{3a}$$

$$x = \frac{z}{R} \tag{3b}$$

$$y = \frac{r}{R} \tag{3c}$$

$$Pe_R = \left(\frac{G C_p R}{k_r}\right) \tag{3d}$$

$$Bi = \frac{h_w R}{k_r} \tag{3e}$$

Therefore, the dimensionless PF model equation is:

$$\frac{\partial \theta}{\partial x} = \frac{1}{Pe_R}\left[\frac{\partial^2 \theta}{\partial y^2} + \frac{1}{y}\frac{\partial \theta}{\partial y}\right] \tag{4}$$

With boundary conditions of:

$$At\ y = 0: \qquad \frac{\partial \theta}{\partial y} = 0 \tag{5a}$$

$$\text{At y } = 1: \qquad \frac{\partial \theta}{\partial y} + Bi\theta = Bi \tag{5b}$$

$$At\ x = 0: \qquad \theta = f(y) \tag{5c}$$

Assuming a uniform inlet temperature, where f(y) = 1, these equations may be solved to give:

$$\theta = 1 - 2\sum_{n=1}^{\infty} \frac{BiJ_o(\lambda_n y)}{(Bi^2 + \lambda_n^2)J_o(\lambda_n)} exp\left\{\frac{-\lambda_n^2 x}{Pe_R}\right\} \quad 6$$

Where λ_n is the root of:

$$\lambda_n J_1(\lambda_n) - BiJ_o(\lambda_n) = 0 \quad 7$$

The Plug Flow model gives the dimensionless temperature, θ, as a function of both radius and height.

2.2 Length Effects and Heat Transfer Parameters

Research done by De Wasch and Froment (1972); Li and Finlayson (1977); Borkink et. al. (1993) and Dixon (1985) address the systematic length effects on the effective heat transfer parameters k_r and h_w. Borkink et. al. concludes that there are four major reasons for the length dependence of thermal conductivity and heat transfer coefficient parameters as observed in De Wasch and Froment as well as Li and Finlayson; 1) the temperature and velocity profiles have to develop, 2) axial dispersion of heat is neglected, 3) flattening of the measured radial temperature profile due to the thermocouple holding device and 4) preheating or precooling due to conduction of heat through the wall of the tube to the calming section of the bed. According to Dixon (1985), the experimental inadequacies in insulating the calming section are the explanation for the systematic length effects on the effective heat transfer parameters k_r and h_w.

The effective radial thermal conductivity, k_r, and wall heat transfer coefficient, h_w have been estimated by running experimental data through modeling programs. The total heat

flux is therefore dependent on both k_r and h_w so that the same amount of heat can be transferred with a low k_r and high h_w or high k_r and low h_w as described in Equation 8, for the overall heat transfer coefficient, and shown in Figure 1.

$$\frac{1}{\mathrm{U}} = \frac{1}{h_w} + \frac{R/4}{k_r} \qquad 8$$

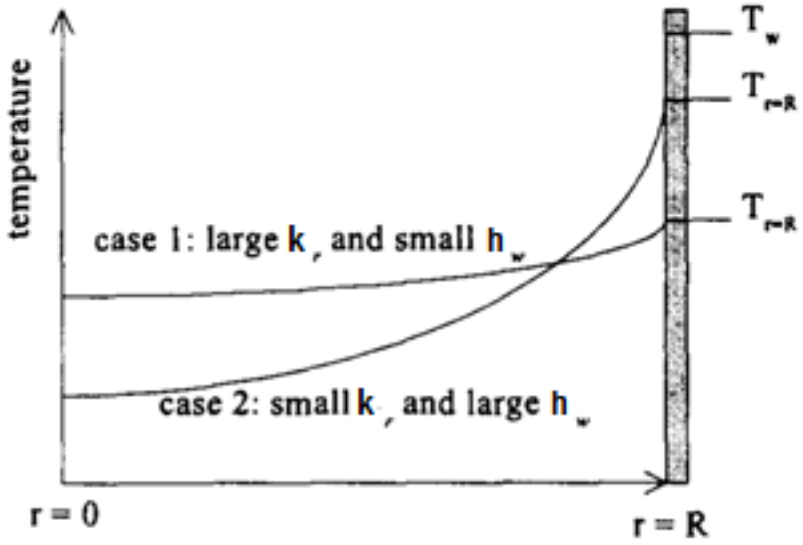

Figure 1: Thermal Conductivity Dependence on Temperature (von Scala et. al, 1999)

Von Scala et al. (1999) performed further experimentation with additional temperature readings closer to the wall in an attempt to improve the accuracy of the calculated heat transfer parameters. Von Scala concluded that additional temperature readings in the near-wall region of the bed did not improve the heat transfer parameters and thus was unnecessary.

2.3 Inlet Temperature Profile

The packed bed utilized in this study uses hot gas, cooled down in a wall-cooled bed, packed with $0.25''$ porous, ceramic spheres. In practical uses, the inlet temperature profile in a packed bed is flat. Conversely in a small-scale laboratory experiment the inlet temperature profile is not usually flat and, in fact, cannot be assumed to be constant. There are two possible ways to account for this discrepancy. The first is to design the experimental apparatus such that the inlet temperature profile is flat by using a heating or cooling section prior to the actual experimental bed. The second possible solution is to adapt the inlet boundary conditions to the experimental situation. The heat loss in the present experimental equipment was so high that only the second approach was feasible.

The PF model was adapted by Borkink et. al (1993) to use the first measured temperature profile as the boundary condition at the tube inlet, which is known as the Inlet Profile Plug Flow (IPPF) model. The dimensional energy balance, from which the IPPF is derived from, is written as:

$$GC_p \frac{\partial T}{\partial z} = k_r \left(\frac{\partial^2 T}{\partial r^2} + \frac{1}{r} \frac{\partial T}{\partial r} \right) \tag{9}$$

Given the following boundary conditions:

$$T|_{z=z_0} = f(r) \tag{10a}$$

$$\left. \frac{\partial T}{\partial r} \right|_{r=0} = 0 \tag{10b}$$

$$-k_r \left. \frac{\partial T}{\partial r} \right|_{r=R} = h_w (T - T_w) \tag{10c}$$

Using Equations 3a-3e, the following derivations can be carried out to make a dimensionless, 2D model:

$$\frac{\partial T}{\partial z} = \frac{\partial T}{\partial \omega}\frac{\partial \omega}{\partial z} = \frac{1}{L}\frac{1}{1 - {z_0}/{L}}\frac{\partial T}{\partial \omega} \tag{11}$$

By substitution and separation of variables:

$$G_{C_p}\frac{1}{L}\frac{1}{1 - {z_0}/{L}}\frac{\partial \theta}{\partial \omega} = k_r\frac{1}{r^2}\left(\frac{\partial^2 \theta}{\partial y^2} + \frac{1}{y}\frac{\partial \theta}{\partial y}\right) \tag{12a}$$

$$\frac{\partial \theta}{\partial \omega} = \frac{L}{Pe_R R}\left(1 - {z_0}/{L}\right)\left(\frac{\partial^2 \theta}{\partial y^2} + \frac{1}{y}\frac{\partial \theta}{\partial y}\right) \tag{12b}$$

Define the following as:

$$\Theta = \frac{\theta}{\theta_0} \quad where \quad \theta_0 = \frac{T_{r=0} - T_w}{T_0 - T_w} \tag{13}$$

Gives:

$$\frac{\partial \Theta}{\partial \omega} = \frac{1}{Pe_R\left({R}/{L}\right)}\left(1 - {z_0}/{L}\right)\left[\frac{\partial^2 \Theta}{\partial y^2} + \frac{1}{y}\frac{\partial \Theta}{\partial y}\right] \tag{14}$$

The boundary conditions for Equation 14 are as follows:

$$-k_r\frac{\partial T}{\partial y} = h_w(T - T_w) \tag{15}$$

Making Equation 15 dimensionless gives:

$$-k_r\frac{1}{R}\frac{\partial \theta}{\partial y} = h_w\theta \quad \rightarrow \quad \frac{\partial \theta}{\partial y} + Bi\theta = 0 \tag{16a}$$

$$\rightarrow \quad \frac{\partial \Theta}{\partial y} + Bi\Theta = 0 \tag{16b}$$

Thus giving the following equation to describe the dimensionless, pseudo-homogeneous system with an inlet temperature profile:

$$\frac{\partial\theta}{\partial\omega} = \frac{1}{Pe_R\left({}^{R}/_{L}\right)}\frac{1}{y}\frac{\partial}{\partial y}\left[y\frac{\partial\theta}{\partial y}\right] \qquad 17$$

With boundary conditions of:

$$\omega = 0,\ \ all\ y,\ \ \ \theta = f(y) \qquad 18a$$

$$at\ all\ \omega, \qquad \frac{\partial\theta}{\partial y} = 0 \qquad 18b$$

$$y = 1,\ \ all\ \omega, \qquad \frac{\partial\theta}{\partial y} = -Bi\theta \qquad 18c$$

Another option to adapt the inlet boundary conditions is to use the first measured radial temperature profile in the packed bed as the inlet temperature profile. By doing this we assume the inlet temperature profile to be parabolic at z = z_0 and the following equations are used (Borkink et al., 1993):

$$T = T_{r=0} + A'r^2 \qquad 19$$

Where $A' < 0\ for\ cooling$

$$\frac{T-T_w}{T_0-T_w} = \frac{T_{r=0}-T_w}{T_0-T_w} + \frac{A'}{T_0-T_w}R^2y^2 \qquad 20$$

$$\theta = \theta_0 + \frac{A'R^2}{(T_0-T_w)}y^2 = \mathrm{f(y)} \qquad 21$$

$$\Theta = \frac{\theta}{\theta_0} = 1 + \frac{\mathrm{A'R^2}}{(\mathrm{T_0 - T_w})\theta_0}\mathrm{y^2} = 1 - \mathrm{Ay^2} \qquad 22$$

And $A = \frac{A'R^2}{(T_w - T_0)\theta_0}$ is always greater than 0

The solution is (Borkink et al., 1993):

$$\Theta(y,\omega) = 2\sum_{i=1}^{\infty}\left\{\frac{\left[\left(Bi{\lambda_i}^2 + 4ABi - 2A\lambda_i^2 - ABi\lambda_i^2\right)J_0\lambda_i y\right]}{\lambda_i^3[\lambda_i J_0(\lambda_i) + BiJ_1(\lambda_i)]} exp\left[\frac{-\lambda_i^2\omega}{Pe_R\left({}^{R}/_{L}\right)}\right]\right\} \quad 23$$

Where λ_i is found from:

$$\lambda_i J_1(\lambda_i) - BiJ_0(\lambda_i) = 0 \quad 24$$

Where J_0 and J_1 are Bessel functions

The position of this first measurement is very important as to ensure proper readings and fitting for the rest of the bed. As suggested by Borkink et al. (1993), the minimum bed length of about 1.5 times the tube diameter is best to use. At this point, length effects of the bed are neutralized and an accurate inlet temperature profile is used.

3 Background on Near Wall Heat Transfer and CFD Modeling

As mentioned previously, obtaining near wall temperature profiles to completely model the heat transfer across a fixed bed has proven difficult in past studies. In recent years there has been much advancement in modeling technology, namely computational fluid dynamics (CFD). CFD has been used to model many applications in the engineering world, including aerodynamics, biological fluid flow, and electrical component heat transfer among others. In our study, CFD's advantage is that it can surpass the limitations of current measurement technology in sensitive areas, as are seen when attempting to measure near wall temperatures in a lab experiments. By applying sophisticated modeling software, such as Fluent, it may be possible to accurately compute the temperature gradients in the small near-wall regions of fixed bed reactors.

3.1 Near-Wall Heat Transfer Behavior

Heat transfer resistance increases near the wall of a packed bed reactor. The increase in resistance occurs because of a viscous boundary layer at the wall, changes in bed conductivity, and a damping of mixing due to lateral displacement of fluid (Tobis and Ziolkowski, 1988; Tsotsas and Schlünder, 1990). The latter two can be attributed to a major increase in void fraction near the walls of a packed tube which in turn leads to a major increase in velocity in those areas. Ambiguity in modeling this phenomenon has produced much discussion. Two major modeling approaches are noteworthy, the classical approach and the two-region approach. The classical approach uses additional heat transfer resistance at the wall only, while the two-region approach uses a region near the wall with additional heat transfer resistance.

The standard model, a two-dimensional pseudo-homogeneous model, is most commonly used by engineers today (Vortmeyer and Haidegger, 1991; Logtenberg et al., 1999). This model uses simplifications of an effective radial thermal conductivity and a lumping together of all heat transfer mechanisms. In order to account for wall effects, a wall heat transfer coefficient, h_w, is used to explain a large change in temperature near the wall, by idealizing it to occur at the wall.

$$q_r = h_w (T|_{r=R} - T_w) \qquad 25$$

Using the wall heat transfer coefficient, h_w, undoubtedly creates errors in predicting temperature profiles near the wall, among other problems. Difficulties in predicting reactor performance and the ability to determine effective heat transfer coefficients have made this model seem over-simplified (Tsotsas and Schlünder, 1990; Logtenberg et al., 1999).

The two-region approach accounts for wall effects in the bed throughout a measurable thickness away from the wall. This is typically seen with two separate thermal conductivities, one for the majority of the bed and one for near the wall. Existing literature on the near-wall region includes four conjectures on the behavior of heat transfer in that area and are discussed below.

Gunn et al. (1987) examined the difference between the two-region model and the standard model at varying physical properties. They discovered that both models were nearly identical in the majority of the experiments, but nonetheless some experiments

showed a significant disagreement between the two models. Using the experiments in which the models disagreed, they noted that the two region model correlated more precisely to experimental data. The quadratic representation of the near-wall temperature profile in Gunn's two-region model is:

$$\frac{T - T_0}{T_1 - T_0} = (2 - \alpha)\left(\frac{R - R_0}{R_1 - R_0}\right) + (\alpha - 1)\left(\frac{R - R_0}{R_1 - R_0}\right)^2 \quad 26$$

Where:

$\alpha = \frac{h(R_0 - R_1)}{K_R}$

T = Temperature at any radial point in the near-wall region

T_0 = Temperature at the wall

T_1 = Temperature at the bulk region/near-wall region interface

R = Radius at any radial point in the near-wall region

R_0 = Radius of the wall

R_1 = Radius of the bulk region/near-wall region interface

h = Wall heat transfer coefficient

K_R = Radial coefficient of thermal dispersion referred to superficial area

Using this equation it was determined that the temperature profile in the wall region was quadratic (Gunn et al., 1987).

Borkink and Westerterp (1996) tested their own two-region model which varied from most. They determined that each region, the bulk region and the near-wall region

(referred to be them as core region and wall region respectively), had constant but different effective radial heat conductivities. This finding was based on the concept that the change in temperature is a direct effect of changes only in porosity (ε) and superficial velocity (u). Thus, the pseudo-homogeneous, two dimensional model (Equation 1) holds in both regions but the u and ε have step changes at the interface of the two regions (Borkink & Westerterp, 1994).

Winterberg et al. (2000) studied the change of porosity and local superficial velocity as a function of radius in a packed-bed reactor. They used the pseudo-homogeneous model accounting for heat and mass transfer in the lateral space coordinate that contains models for velocity and porosity as a function radial positon, both containing adjustable parameters. The mathematical theory used is long and complex and is left out but can be seen in their work (Winterberg et al., 2000). However, an equation representing effective radial thermal conductivity was found and is seen below:

$$\mathrm{k_r}(r) = k_{bed} + K_{1,h} Pe_0 \frac{u_c}{\bar{u}_0} f(R-r) k_f \qquad 27$$

Where:

$\mathrm{k_r}(r)$ = Effective radial thermal conductivity at point r

k_{bed} = Effective thermal conductivity without fluid flow

$K_{1,h}$ = Constant for effective radial mass dispersion coefficient

$\mathrm{Pe_0}$ = Molecular Péclet number

u_c = Superficial velocity in the core of the bed

$\bar{u}_0$ = Average superficial velocity

k_f = Thermal conductivity of fluid

And,

$$f(R-r)=\begin{cases}\left(\frac{R-r}{K_{2,h}d_p}\right)^{n_h} & for:\ 0<R-r\leq K_{2,h}d_p\\ 1 & for: K_{2,h}d_p<R-r\leq R\end{cases} \quad (28)$$

Where:

n_h = Exponential constant of heat transport

$K_{1,h}$ = Constant for effective radial mass dispersion coefficient

Equation 27 plotted against the radial distance from the center of the bed shows a steep decrease in the effective thermal conductivity near the wall. When Winterberg et al. (2000) compared experimental data to modeled data using an n_h value of 2 proved accurate. Thus, the two concluded a quadratic change in effective radial thermal conductivity near the wall.

Smirnov et al. (2000b) created a simple model for the effective radial thermal conductivity near the wall in the two region model. The model, in order to eliminate the steep change in thermal conductivity near the wall, as in the standard model, created a linear change in effective thermal conductivity with change in radius near the wall. It is important to note that this model isn't based on the diameter of the particle, but on the equivalent hydraulic diameter of the packing (d_{eqv}), which allows the model to to be utilized far beyond just spherical packings. Smirnov's simple model (Equations 29 a&b) correlated well with experimental data (Smirnov et al., 2003b).

$$k_{er}(r) = \begin{cases} k_{er,core} & for:\ 0 \leq r \leq R - \delta \\ k_{er,\delta}(r) & for:\ R - \delta < r < R \end{cases} \quad 29a$$

$$k_{er,\delta}(r) = k_f + \frac{k_{er,core} - k_f}{\delta}(R - r) \quad 29b$$

For: $R - \delta \leq r < R$

Where

k_{er} = Effective thermal conductivity

$k_{er,core}$ = Effective thermal conductivity in bulk region

$k_{er,\delta}(r)$ = Effective thermal conductivity in near-wall region

$\delta = d_{eqv} = \frac{4\varepsilon_{bed}}{a_0(1-\varepsilon_{bed})}$

Through CFD modeling, our results will test the validity of the existing two-phase model theories mentioned above and determine which theory, if any, is an accurate description of heat transfer in the region.

3.2 CFD Modeling Near Reactor Wall

Describing heat transfer in fixed-bed reactors has proved difficult throughout history (Borkink & Westerterp, 1994). Currently numerical models for fixed-beds use a single plug-flow velocity profile and also neglect temperature differences between fluid and solid phases (pseudo-homogeneous model in Vortmeyer and Haidegger, 1991). Fixed-bed heat transfer is described by a lumping together of heat transfer mechanisms

throughout the bed, combined with an independent wall heat transfer coefficient to describe the sharp changes in temperature near the wall of the reactor (Figure 1). Based on these simplified models of heat transfer it has been shown that actual flow can vary drastically and cause severe problems (Dixon et al., 2006). The focus of the present section is on the relation between the wall-particle transfer at the wall and the rest of the bed. CFD models of the fluid flow throughout fixed-bed reactors may promise a more accurate definition of the heat transfer through the fixed-bed as well as the influence of the temperature change at the wall.

Describing fluid flow and heat transfer near the wall of a fixed-bed reactor has proven extremely difficult. The use of CFD to explain the effects near the wall of a fixed bed has proven powerful and is becoming increasingly prevalent (Dixon et al., 2006). CFD, while a useful tool for heat transfer modeling, does not come without difficulties, many of which come from the complexity of the model needed to accurately describe a fixed-bed reactor. Contact points between spheres and other spheres and between spheres and the adjacent wall require infinitesimally small mesh particles wherein the computer quickly loses resources to perform the necessary meshing. This problem with the complexity of the meshes at contact points has been the most notable.

Different methods have been used to deal with the contact point problem in CFD simulations. To reduce the fine and skewed computational cells around the contact points the spheres' diameter can be altered after original placement, smaller (Nijemeisland & Dixon, 2001) or larger (Guardo et al., 2006), or bridged with a small particle (Logtenberg

al., 1999). Nijemeisland and Dixon (2001) created the "near-miss" model and determined that altering the size of the particles to 99% of the original diameter kept results in good agreement, but later work at higher Reynolds numbers forced them to change to 99.5%. Likewise, Guardo (2006) altered the particles diameters but, to 100.5% and also got viable results. However, altering the diameter of the particles after original placement has proved to slightly ease the modeling process, but provides a less realistic model and still requires fine computational cells (Kuroki et al., 2007). Bridging the particles can offer a more realistic temperature and velocity profile, but still has its problems (Logtenberg et al., 1999; Ookawara et al., 2007). It is necessary to make the bridges large enough to reduce fine and skewed meshing while also not affecting the fluid flow in the modeled fixed-bed reactor. It should be noted that these particle sizes must be within the dimensions of fluid's stagnant regions around contact points in order to minimize the effects on actual heat transfer and fluid flow. In the past decade, models have been constructed that were successful in using the 3D Navier-Stokes equations in such CFD programs as Fluent (von Scala et al., 1999; Ookawara et al., 2007). It is possible to have a more in-depth analysis of temperature profiles across the bed, more importantly their differences at the wall, than could previously be numerically modeled. The focus of the present paper is on the relation between the wall-particle transfer at the wall and the rest of the bed. CFD models of the fluid flow throughout fixed-bed reactors may promise a more accurate definition of the heat transfer through the fixed-bed as well as the influence of the temperature change at the wall.

4 Experimental Procedure

4.1 Description of Equipment

A schematic diagram of the experimental setup can be found in Figure 2. Temperature profiles and heat transfer measurements were taken in two different columns; one with a 2″ inner diameter (I.D.) and the other with a 4″ I.D.

Inlet air passed a pressure gauge and then entered a ½-27-G-10 rotameter tube with a ½-GSVT-48A float. The rotameter was set to a percentage given in Table 1 corresponding to a particular Reynolds number and column. The air passed through a second pressure gauge and finally entered into the heaters. The four heaters by Wattlo, each of which was a cylinder 5″ long and had a 0.375″ outer diameter, produced 500 Watts of heat used to heat the inlet air. The heaters were mounted within a box of firebrick and then wrapped in thermal insulation to prevent burning and to insulate the system. The column was mounted next to the heaters upon a 6.5″ nylon calming section that sat on aluminum supports through which the air passed prior to entering the column. The calming section was packed with 0.25″ metal spheres. Tests were performed with different packing types in the calming sections to determine the effect on conduction and the inlet temperature profile; once with 0.25″ ceramic spheres and once with 0.25″ metal spheres. The differences were found to be minimal, so both calming sections were packed with the 0.25″ metal spheres during experimentation since a continuous packing of the same material was not necessary.

Table 1 – Reynolds Numbers and Percent Flows

Reynolds Number	Column	Percent Flow
97	4″	20
119	2″	25
171	4″	30
199	2″	40
227	2″	45
259	4″	45
319	2″	60
376	4″	60
424	2″	75
530	4″	75
553	2″	90
735	4″	90

Once the air passed through the calming section it was released into the column packed with 0.25″ porous, ceramic spheres at the experimental heights discussed previously. The column was surrounded by an approximately 18″ copper cooling-jacket with brass end caps. The cooling jacket received cold water from the lab passing through a rotameter and float set at 80% of the maximum. Generally this water kept the cooling jacket at about 10 degrees Celsius.

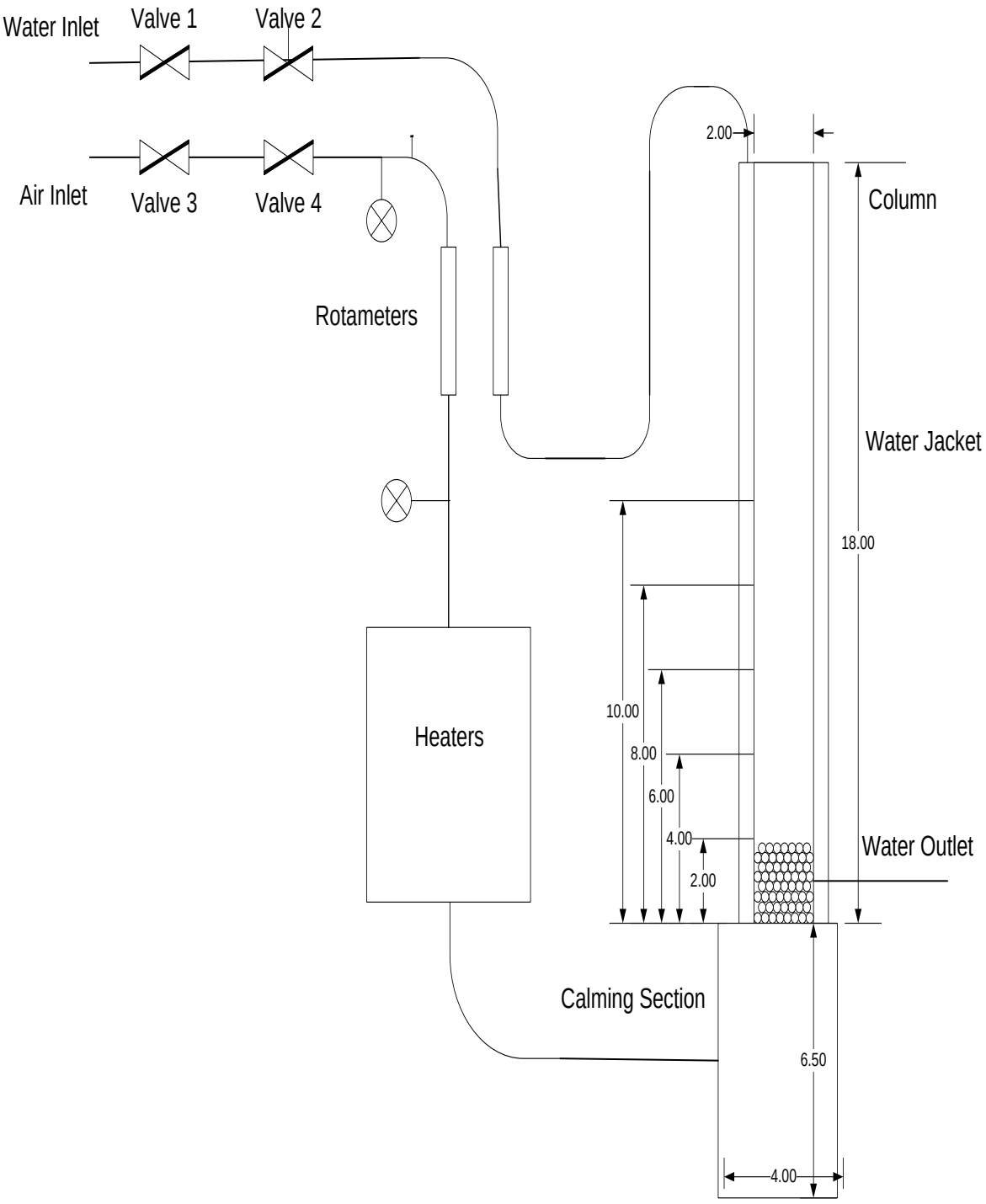

Figure 2- Experimental Setup

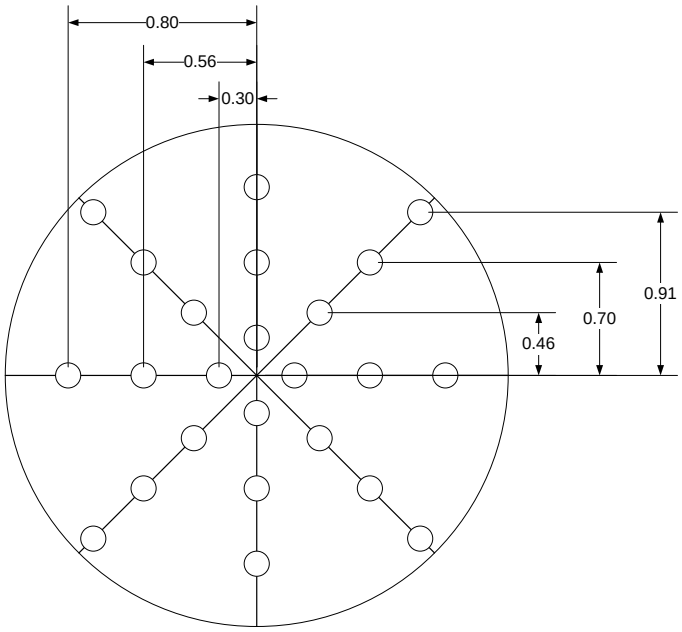

Figure 3- 2" Thermocouple Cross

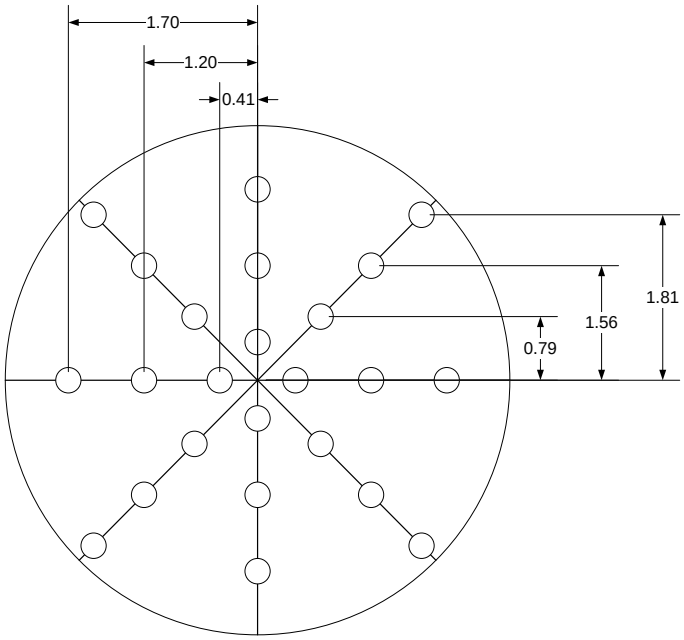

Figure 4- 4" Thermocouple Cross

The 2″ and 4″ thermocouple crosses were placed (in their respective columns) 0.125″ above the packing. Each cross contained 25 thermocouples arranged with three thermocouples on each of eight arms, plus the center location. The thermocouples were set at six different radial positions. This was done by arranging four arms, all having identical thermocouple positioning, 90 degrees apart from one another. Similarly another set of four arms were arranged with thermocouples at different radial positions set 45 degrees apart from the first set. A schematic of each cross for the 2″ and 4″ columns can be seen in Figures 3 and 4, respectively. The cross was made of plastic and was built with the ability to slide up and down the support, therefore the thermocouple cross was placed so that the thermocouples sat approximately 0.125″ above the top of the packing for each run. An additional nine thermocouples were placed within the columns to read the wall temperatures throughout the column and calming section. The column thermocouples were measured from the base of the column at 3″, 9″ and 15″. The calming section thermocouples were 0.25″, 0.625″, 1″, 3″ and 5″ below the column base, with a final thermocouple measuring the inlet air temperature.

The thermocouples on the cross and throughout the wall were connected to a board and wired to the Keithley 2700 Multimeter/Data Acquisition System, which was utilized for thermocouple temperature data recording. The Integra Series Keithley instrument is attached to the computer and runs through Microsoft Excel through the ExceLINX-1A program. Once the Keithley program is installed via CD, the ExceLINX add on is available when opening the program.

4.2 Procedure

1. The column was packed to the desired bed height.
2. The cross was checked to make sure that the thermocouples were properly aligned to ensure that accurate data was being taken. The cross was then placed approximately 0.125″ above the packing in the column. Measurements were taken at different packing heights in each column; 2″,4″,6″,8″ and 10″ for the 2″ I.D. column and 2″, 4″,6″ and 8″ for the 4″ I.D. column. At each bed height and Reynolds number, experimental data was taken at two different angles (0°and 45°) in order to get eight different temperature readings for any given radial position.
3. Valve 1 was fully opened and the flow of the water was adjusted with valve 2 until the float was reading a steady state at 80% of full on the rotameter.
4. Valve 3 was fully opened and the flow of air was adjusted with valve 4 until the float was reading the desired inlet air flow percentage as described in Table 1.
5. The heaters were preset to bring the inlet air from room temperature to 100°C, before the air reached the calming section. The coolant water was brought into the system between 5-15°C, this makes the theoretical temperature differential approximately 90°C.
6. Once the system was running the Keithley Instrument and computer were turned on. The Keithley Instrument uses ExceLinx. Steps a-c describe, in detail, how to set up the ExceLinx file in order to accurately log temperature readings taken from the thermocouples.

a. The program was started under the "DMM Scan" tab
b. The total number of readings and the time between each reading was adjusted to take readings every 3 minutes for a period of 200 readings (600 minutes total).
c. Once the "Worksheet," "Starting Col" and "Starting Row" cells were filled in (see Appendix H), the "Status/Cmds" cell should be set to "Start" to begin data readings.

7. The 34 thermocouple readings taken by the ExceLinx program were recorded onto a data sheet (Appendix I) and then typed into a Notepad file in a specific format (Appendix J) so that the models could read the data using the Fortran program.

Two major models were used to analyze the data, the IPPF and PF model; both were implemented in a nonlinear least squares fitting program. The PF model was utilized solely to determine if the dimensionless thermal conductivity value (k_r/k_f) was dependent on the height of the packing. Analyses for finding a value for the bed thermal conductivity value were done for each Reynolds number at each packing height.

It was determined that the Plug Flow model could not accurately account for the heat losses occurring before and throughout the calming section, therefore the IPPF model was utilized. The IPPF model neglected the thermocouple readings throughout the calming section, as well as the inlet temperature, and took the data results from the first packing height as the inlet profile. Thus, when analyzing data from 2″, 4″, 6″, 8″ and 10″

packings (i.e. the 2″ column) the temperature profiles from the 2″ packing height were read as the inlet temperature profile. This program allows the heat loss upstream to be neglected, resulting in more accurate analysis and specific fitting to the experimental data of each run. The data was analyzed with the IPPF model for each column using all Reynolds numbers at all packing heights. Thus the 2″ I.D. column data input included 2″,4″,6″,8″ and 10″ packings for each Reynolds number as described in Table 1.

Finally the data could be analyzed to find the final value of k_r/k_f for the middle of the bed. To do this, the Data files were run through the IPPF model for each Reynolds number and all packing heights. The Data files were adjusted so that the IPPF model would only read five radial positions, then four, then three, etc. The removal of radial positions gave a new k_r/k_f value each time, which took away the wall effects experienced throughout the bed. In order to determine when the wall effects were diminished or gone, the radial positions were continually removed until the value of k_r/k_f was flat. Once a constant value of k_r/k_f was observed on the graph, it could be assumed that wall effects were negligible and a k_r/k_f value for the center of the bed was found.

Once this was determined, the overall k_r/k_f for each respective column and Reynolds number was determined and thus matched with the k_r/k_f function produced by the wall effects modeling using Fluent and Gambit.

4.3 Preliminary Testing

The thermocouple readings do not input into Excel columns sequentially as one would expect, more specifically, the Excel columns are not necessarily in numerical order. Therefore, to determine the order of the readings, the program should be run while touching a finger to the end of one thermocouple and repeated for all 25 thermocouples on the cross. The touched thermocouple will give a higher reading in the Excel sheet and thus identify that thermocouple's respective Excel column.

Another necessary portion of preliminary testing was the calibration of the thermocouple crosses. To do this, each cross was placed in boiling water and an ice bath, in respective runs, to ensure the thermocouples were reading accurately.

In investigating the actual temperature difference throughout the system, it was discovered that serious heat loss occurred throughout the calming section. It was found that large amounts of heat (commonly a temperature difference of more than 10°C) were being lost before and throughout the calming section, thus entering air was typically in the range of 60-90°C (making the actual temperature differential across the bed between 50-80°C).

4.4 Fitting Parameters

In finding the final values of bed thermal conductivity, k_r and h_w parameters were evaluated and estimated through both the Plug Flow (PF) and Inlet Profile Plug Flow

(IPPF) models. The values of k_r and h_w were fitted by estimating the dimensionless forms of the Peclet number and Biot number. Knowing the different Reynolds numbers and velocities that the experimental data was collected at allowed accurate enough guesses to enable the program to analyze the thermocouple data.

4.4.1 Biot Number

The Biot number is an important parameter in estimating the resistance of heat transfer inside and at the surface of the experimental system. The heated air passing through the columns experiences resistance at the walls of the surface (both the nylon calming section and copper water jacket), as well as resistance by all of the packing throughout the system (both the 0.25″ metal packing in the calming section and 0.25″ ceramic packing in the column). These resistances can be expressed in the following equation to estimate the Biot number:

$$Bi = \frac{h_w R}{k_r} \tag{31}$$

h_w = wall heat transfer coefficient

R = radius of the tube

k_r = thermal conductivity of the body (packing)

When doing analysis with the 2-parameter model a guess for the Biot number was to be provided in order for the iterations to be completed. The Biot number was typically guessed to be 1.0, which was sufficiently close to the actual Biot number in most cases. The Biot number usually ranged between 0.5 and 4.0 when the iterations were completed accurately. Since the Biot number relies heavily on the wall heat transfer coefficient,

which was typically dominated by the value of k_r, we were able to do some one parameter analysis where only Pe_R was guessed.

4.4.2 Peclet Number

In thermal diffusion, the Peclet number relates the advection of flow in a system to its rate of diffusion. An equation can be seen here:

$$Pe_R = \frac{Re * Pr}{k_r / k_f} \qquad 33$$

Re = Reynolds number

Pr = Prandtl number

k_r = thermal conductivity of the body (packing)

k_f = thermal conductivity of the fluid

This number was quite important in the analysis of the thermocouple data through both the PF and IPPF models and was guessed in the 2-parameter IPPF model. From past research with the particular columns used in this experimentation, it was advised that a guess for the Peclet number should be between 5.0 and 12.0. Typically a lower Peclet number was guessed with the lowest Reynolds numbers first and vice versa with the larger Reynolds numbers. Also, a common value of the Prandtl number for air is 0.7, which was used as an estimate by the 2-parameter IPPF model. Knowing the Reynolds numbers for each run and having an estimated Prandtl number of 0.7 allowed the programs to iterate a value of k_r/k_f and Pe_R together.

4.4.3 Sum of Least Squares

The objective of a Sum of Least Squares analysis is to adjust the parameters of a model function, so as to best fit a data set. In the present study, the sum of least squares minimizes the thermal conductivity and the wall heat transfer coefficient by the following:

$$\min_{k_r, h_w} \sum (T_{i,obs} - T_{i,calc})^2$$

$$= \sum (T_{i,obs} - \bar{T}_{obs})^2 + \sum (\bar{T}_{obs} - T_{i,calc})^2$$

5 CFD Modeling Procedure

As previously mentioned, CFD comes with its problems. Contact points are difficult to model because of the need of infinitesimally small meshes. This forces a simplification of the actual contact points and smaller than desirable models are necessary so that the computer does not run out of memory while meshing. Likewise, in our model, some assumptions had to be made in order to ease the computational demand. These assumptions are allowable because the model is designed to represent flow and heat transfer near the wall over a small portion of a fixed bed.

5.1 Geometry and Meshing

Commercially available Gambit was used to produce the geometry and the mesh. Considering the geometry first, determination of the placement of particles in the model was done through a visualization study in a clear tube. Spheres were dropped into a tube multiple times and hexagonal close packing with a few minor exceptions was continually observed. The two exceptions, or irregularities, have been set back from the wall by 0.002 inches so that they don't touch the wall and any spheres that would be overlapping it in the following X-Y plane of spheres has been deleted to account for the experimentally seen natural voids and to ease computational results (Figures 5 and 6). To coincide with the fixed-bed laboratory portion of this study, particle sizes were set to 0.25 in. diameter spheres.

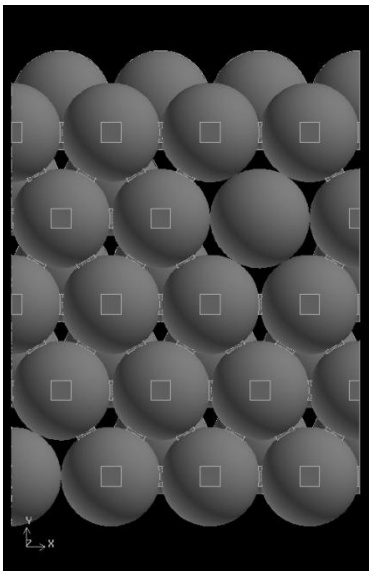

Figure 5: CFD Model Geometry (Wall side view)

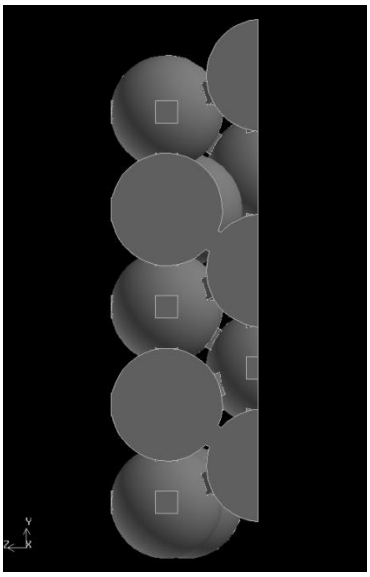

Figure 6: CFD Model Geometry (Cross-section view)

The model created is 1.5 particle diameters in depth (three particle diameters with a plane of symmetry) because the radial position of interest is near the wall only. The curvature of the wall was neglected due to the small area being modeled. The area of the model is five particle diameters in the direction of flow and 3.5 particle lengths wide (10.5 particle diameters with two planes of symmetry). Figures 5 and 6 display the geometry of the

model where the mentioned characteristics can be seen. More information on the geometry of the model and the heat and fluid flow simulations can be seen herein.

The wall, not shown in Figures 5 and 6, is tangent to the spheres on the farthest positive-Z direction (Directly in front in Figure 5 and far left in Figure 6). The back and sides of the geometry seen in Figure 5 are all planes of symmetry which eases computational usage while still extending the wall. The bottom was set as the fluid inlet while the top was set as the fluid outlet.

As mentioned before, the contact points were covered with bridges and can be easily seen in Figures 5 and 6. Shown here are bridges, originally geometric cubes, with sizes of 0.05 in. ($d_p/5$). The spheres and the bridges were all merged as one volume in order for the computational results to exclude the infinitesimally small contact points.

Meshing of the geometry was completed using a uniform mesh 0.0075 in. (approximately $d_p/33$) Due to having contact points so frequently throughout the small model, boundary layers and size functions were rendered nearly useless in reducing volume counts. Pictures of the mesh on a particle and a bridge mesh can be seen in Figures 7 and 8 respectively. The Journal file used to create the geometry and mesh can be seen in Appendix A.

Table 2: Meshed Cell Counts at Various Bridge Sizes

Bridge Size (in.)	Meshed Cell Count
0.05	4924310
0.04	5261630
0.03	5270510

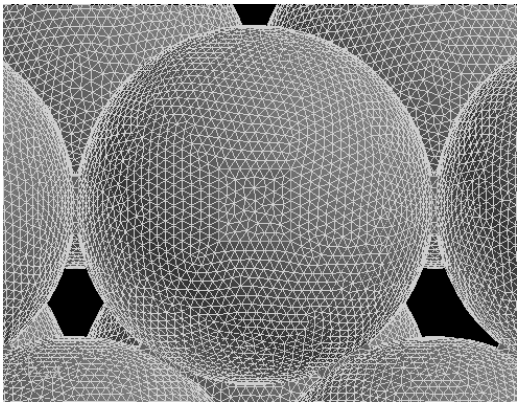

Figure 7: CFD particle's mesh

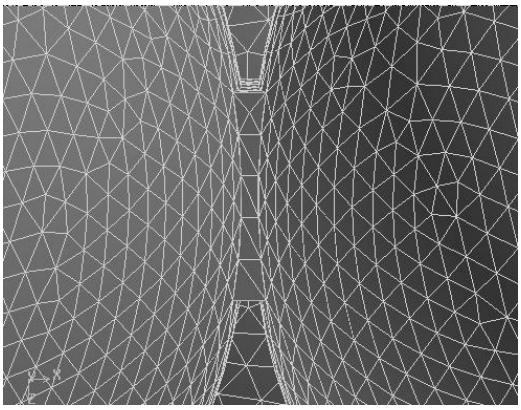

Figure 8: CFD particle bridge's mesh

5.2 CFD Modeling

Fluent was used as the computation fluid dynamics software for the analysis of the created Gambit models. Once the mesh was imported into Fluent it was our responsibility to create parameters that would limit assumptions and error in the analysis of the wall-particle model. It was important to use values and temperatures that were comparable to the experimental part of the project in order to easily combine and analyze the data after running the CFD software. It is also important to note that since the Gambit files were modeled in inches, Fluent's grid scale option was used to give end values in

meters. The parameters our team decided on are listed below. All parameters not specifically mentioned below can be assumed to be the default options in Fluent 3D.

Solver Parameters. Calculations were completed using Fluent 3D's pressure based solver. The solver parameters used at these settings were absolute velocity, steady time, superficial velocity porous formulation, and a Green-Gauss node based gradient option. The model used the energy equation as well as a laminar viscosity model as laminar viscosity can be used for Reynolds numbers of laminar flow and in the transition to turbulent flow range (Dixon et al., 2006).

Materials. To mimic an experimental fixed bed we decided upon using alumina (Al_2O_3) as our solid material and air as our fluid. The input alumina values were a density of 1947 g/cm^3, a C_p value of 1000 J/kg*K, and a thermal conductivity of 0.3 W/m*K. Air was assumed to act as an ideal incompressible gas with Cp of 1006.43 J/kg*K, thermal conductivity of 0.0242 W/m*K, viscosity of 1.7894e-05 kg/m*s and a molecular weight of 28.996 kg/kg*mol.

Fixed Bed. In the particular model used in this project our fixed bed is heated by an inlet flow of air at 353 K. A range of inlet velocity values were used, these were: 0.0799, 0.1877, 0.2229, 0.2765, and 0.5 m/s. The walls of the model were set at a constant temperature of 283 K and modeled as a stationary wall with a no slip condition. The pressure outlet of the model was set at 0 gauge pressure (atmospheric) and a backflow

temperature of 335 K was set in case flow happened to come back into the model from the fluid outlet.

Solving & Analysis. Fluent solves the Navier-Stokes Equations alongside energy balances in small volumes in order to determine properties of flow. First Fluent is initialized with the specified velocity entering at the inlet. Fluent was then set to run 250 iterations solving only for the flow equations using First Order Upwind discretization for momentum and energy. This was done to catch any early problems that may affect a longer set of more in-depth iterations. Once finished, Fluent was set to solve for both flow and energy equations using a Second Order Upwind discretization for momentum and energy. Under-relaxation factors were lowered by 0.1 in order to make the calculations run a little smoother since the model was upwards of eight million cells. It was found that solving our model for the specified parameters took around 20000 iterations and thus that was the number of iterations used to converge each model during our project. The simulations took anywhere from two to five days to run depending on available processing power of the computers. This conclusion was also checked each time by checking that the reported fluxes of mass flow and heat transfer rates had differences less than values of 10^{-3} along with a surface monitor that tracked heat flux through the particles and a volume monitor that tracked the average fluid temperature.

Following the initial iterations, refinement of the mesh was needed to ensure that the simulation was independent of mesh size. In order to determine what cells to refine, mesh adaption registers were created based on gradients of pressure, velocity, and

temperature. Any cells the reported 10% of the maximum value of the adaption function are selected to be refined. This helps in processing power so that the entire mesh isn't refined. Each model then needed to be continued for around 250 more iterations.

The analysis of our model included creating series of y-x plane iso-surfaces at small intervals away from the wall until hitting the center of the first row of spheres. These iso-surfaces were then clipped in the y-direction to only cover the area between the top and bottom row of the bridges against the wall (0.017653 m and 0.00604 m clipped off of the top and bottom of the model, respectively). This was done to cut off the discrepancies in the temperature profiles that would be caused by including the area just after the velocity inlet and before the pressure outlet where no spheres were present since we were only interested in the developed flow through the packed particles. Using these iso-clipped surfaces we were able to find average temperatures of each surface at different radial positions away from the wall in order to create a near-wall temperature profile with the given values.

The above steps were repeated for multiple experimental Reynolds numbers, which were accounted for by changing the inlet velocity. The model was also run at these parameters and velocities for three different bridge sizes using the same mesh size of 0.0075 in. These bridges between the particles added in Fluent were changed to see if they had adverse effects on the computation. The model was set at 0 gauge pressure (atmospheric) and a backflow temperature of 335 K was set in order to prevent negative velocity vectors being modeled back into the system.

6 Experimental Results and Discussion

Our project focused on determining the temperature profiles in packed bed reactor tubes using an experimental system where hot air was run through a cooled water jacket at six different Reynolds numbers.

6.1 Temperature Profiles

Appendices E and F contain the outlet temperature profiles for all runs done on the 2-inch and 4-inch columns, respectively. There are three major trends that were expected and now can be concluded based on this initial data; 1) as the Reynolds number increases, the outlet temperatures of the air also increase, 2) as we approach the center of the bed, the outlet temperature of the air also increases, and 3) as the bed height increases the outlet temperature of the air decreases.

Figures 9 and 10 plot the outlet temperature profiles at different Reynolds numbers. Here the increase in Reynolds number increases the velocity of the air through the column, ultimately decreasing the residence time of the air. This allows less time for the air to lose heat in the column and therefore produces a higher temperature profile. Thus, the temperatures in the profiles increase as the Reynolds numbers increase, which we would expect.

Figures 9 and 10 also demonstrate that as we approach the center of the bed, the bed temperature increases. Since the column is being run with hot air and a cold water jacket,

the thermocouples toward the walls of the bed will read a lower temperature than those toward the center of the bed. This same trend has been demonstrated in past research (Smirnov et al., 2003). In both cases the temperature profiles have a steep temperature increase and then level off as the plot moves from the wall to the center of the bed.

Under the same principles as those that proved that the outlet temperatures should increase with increasing Reynolds numbers, the outlet temperatures should decrease with increasing bed heights. Figures 11 and 12 demonstrate that as the height of the packing increases inside of the reactor, the outlet temperatures decrease at constant Reynolds number. The residence time of the air through the packing is increased as the bed height is increased, which allows more time for the air to lose heat to the column walls. It is expected (Smirnov et al., 2003) that the outlet temperatures of the bed would be lower at higher packing heights, which is demonstrated in our data.

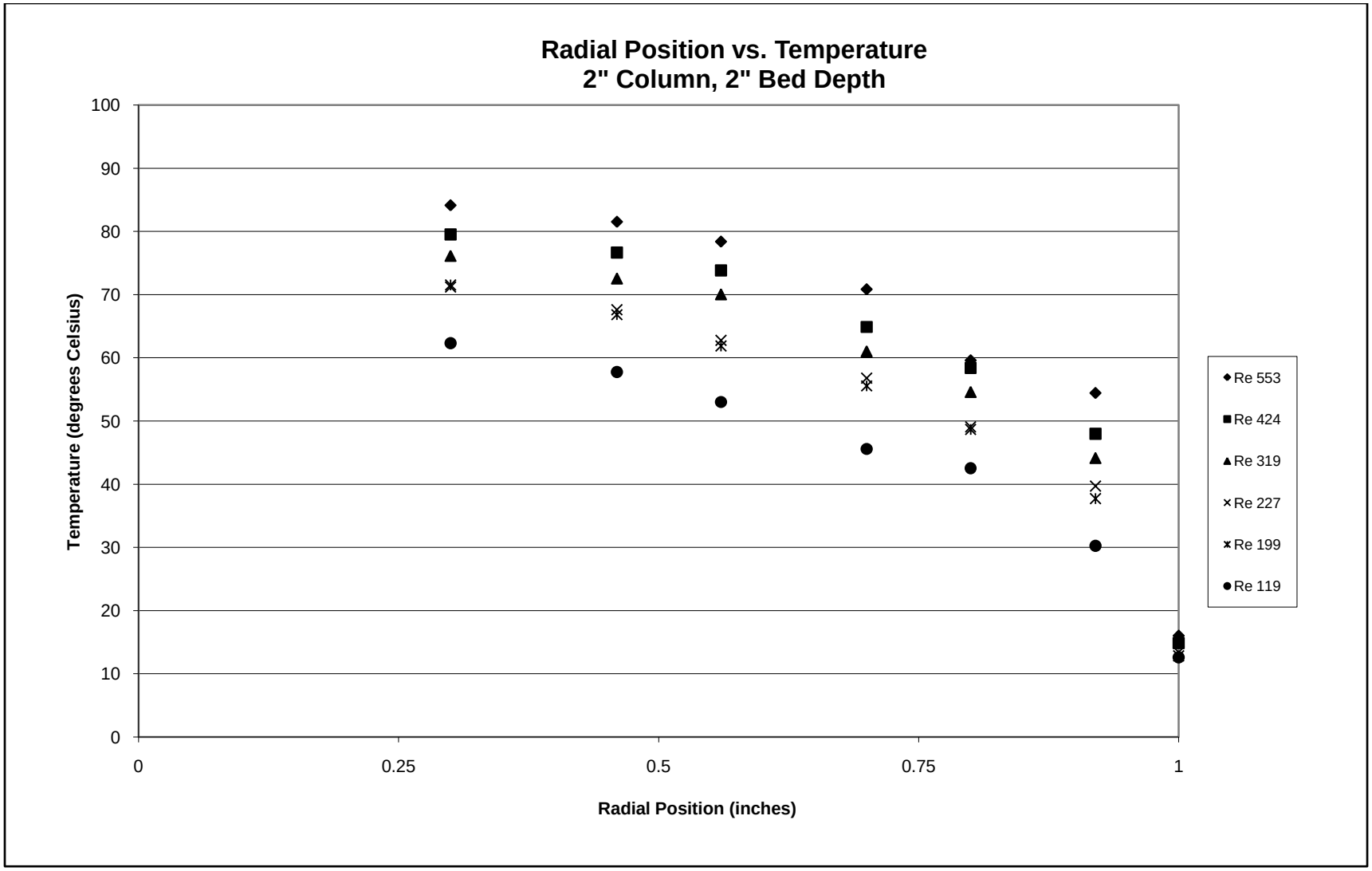

Figure 9- r vs T for 2" Column and 2" Packing

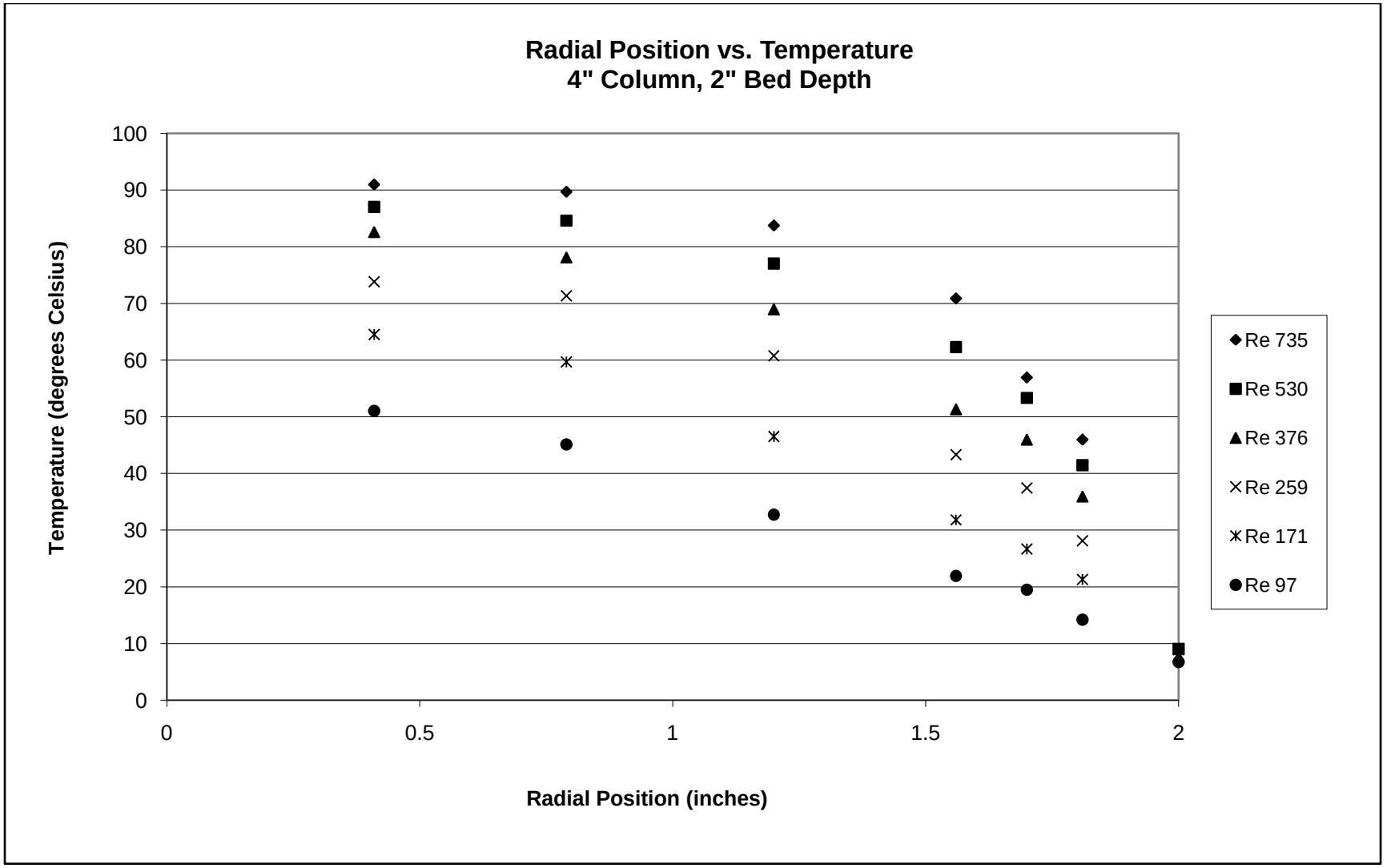

Figure 10- r vs. T for 4" Column with 2" Packing

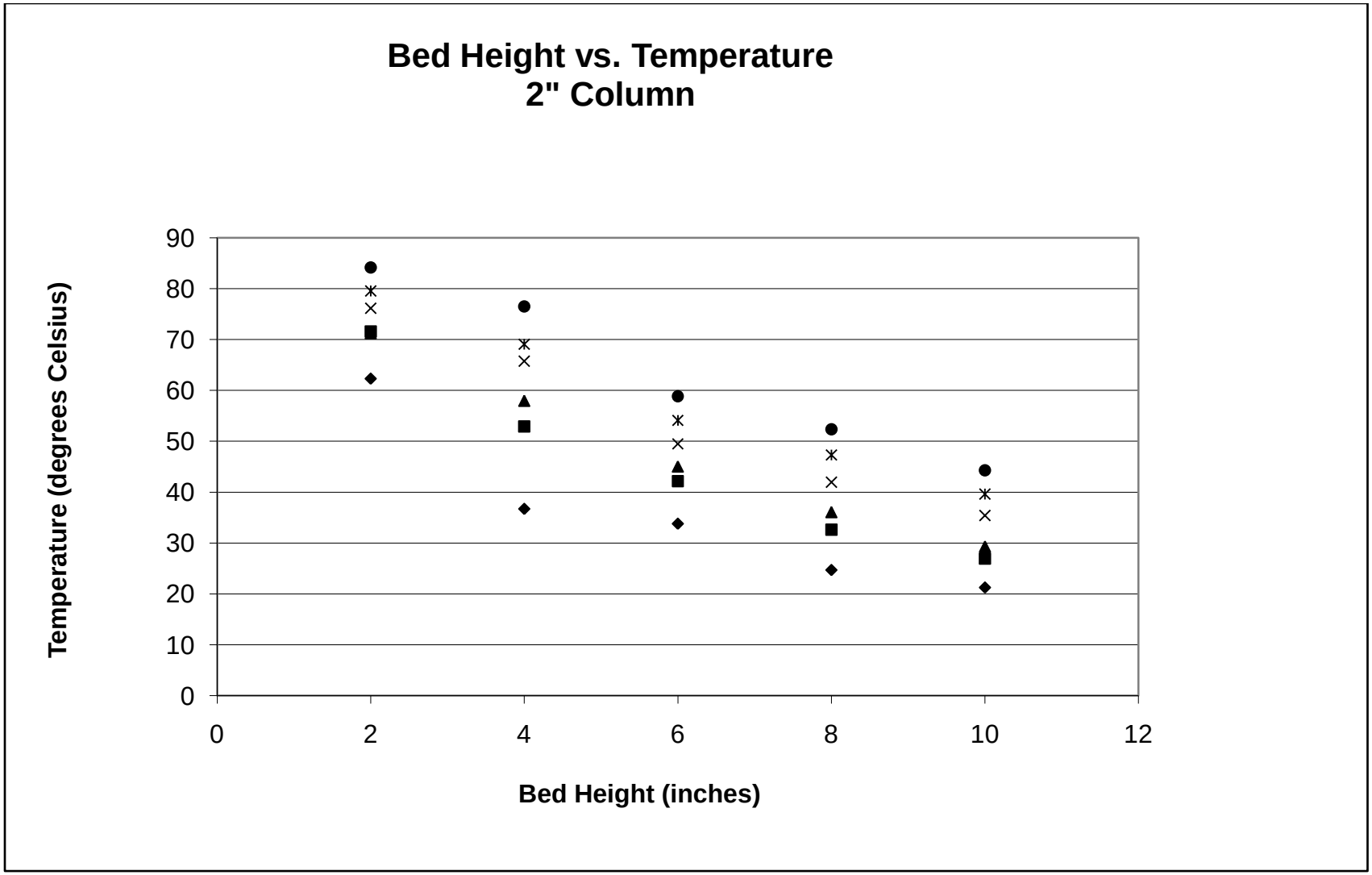

Figure 11- Bed Height vs T in 2" Column

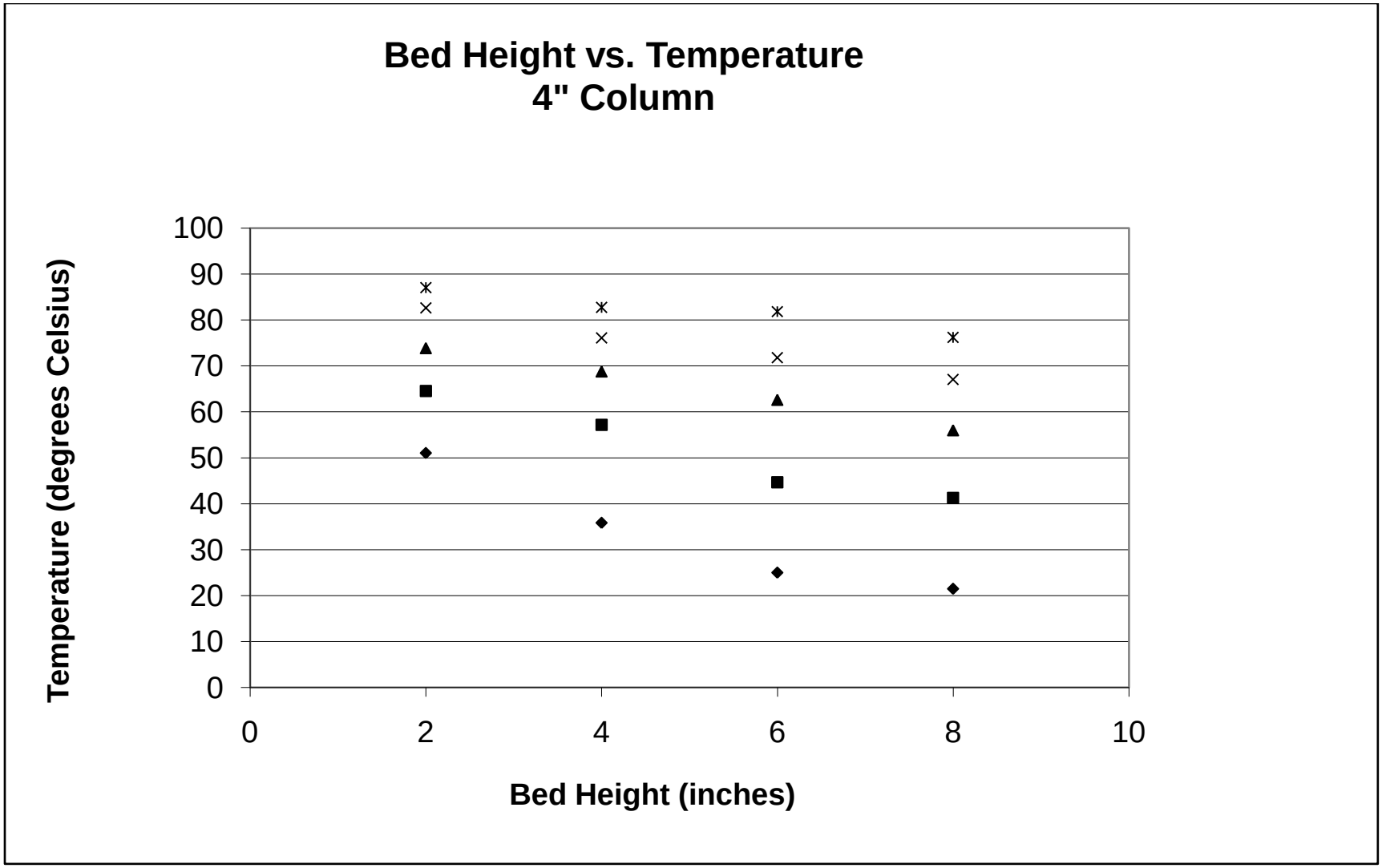

Figure 12- Bed Height vs. T in 4" Column

6.2 PF Model

The Plug Flow (PF) Model is considered the simplest model for analyzing the thermal conductivity of a particular, experimental run. This model is the first means for analysis and uses the thermocouple readings in the calming section as the inlet temperature. We started our analysis by using the 2-parameter Plug Flow (PF) Model, estimated the radial thermal conductivity, k_r, and the wall heat transfer coefficient, h_w. The k_r/k_f values obtained from this model and program are plotted versus bed height in Figures 13 and 14 to show the depth dependence in the system. This plot illustrates that the thermal conductivity values are dependent on the height of the bed and, therefore, that length effects are an issue in our experimental setup. As the bed height increases, the thermal conductivity value decreases, as expected and seen in previous work (Smirnov et al., 2003). This result shows that the analysis performed using the Plug Flow model does, in fact, portray depth dependence in both the 2″ and 4″ column. The PF model cannot fit temperature profiles at several bed depths simultaneously using constant k_r and h_w. The PF model can fit the profiles depth-by-depth, but with the values of k_r and h_w varying for each depth. This depth dependence is unacceptable for accurate analysis of the thermal conductivity.

Another issue with analyzing using the PF model is the presence of heat leaks in the system, which is neglected in the analysis. Since both experimental columns experienced significant heat leaks in the calming section, the inlet temperature was much higher (usually around 30°C) than the temperatures being read at the different packing heights

and got progressively worse as the bed heights increased. This resulted in very poor fitting of both the thermal conductivity and wall heat transfer coefficient because both depend on bed depth.

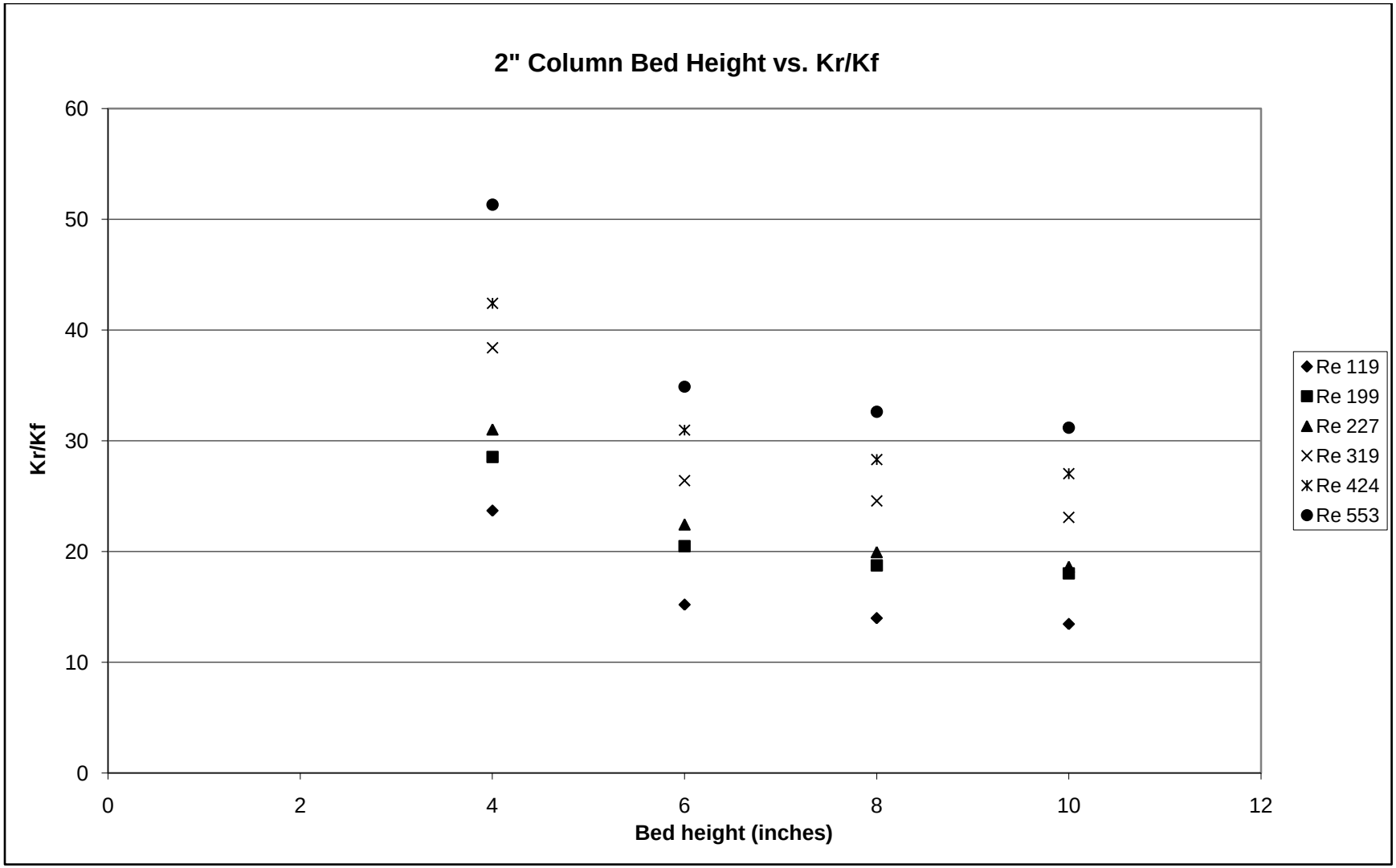

Figure 13- Bed Height vs. Kr/Kf in 2" Column

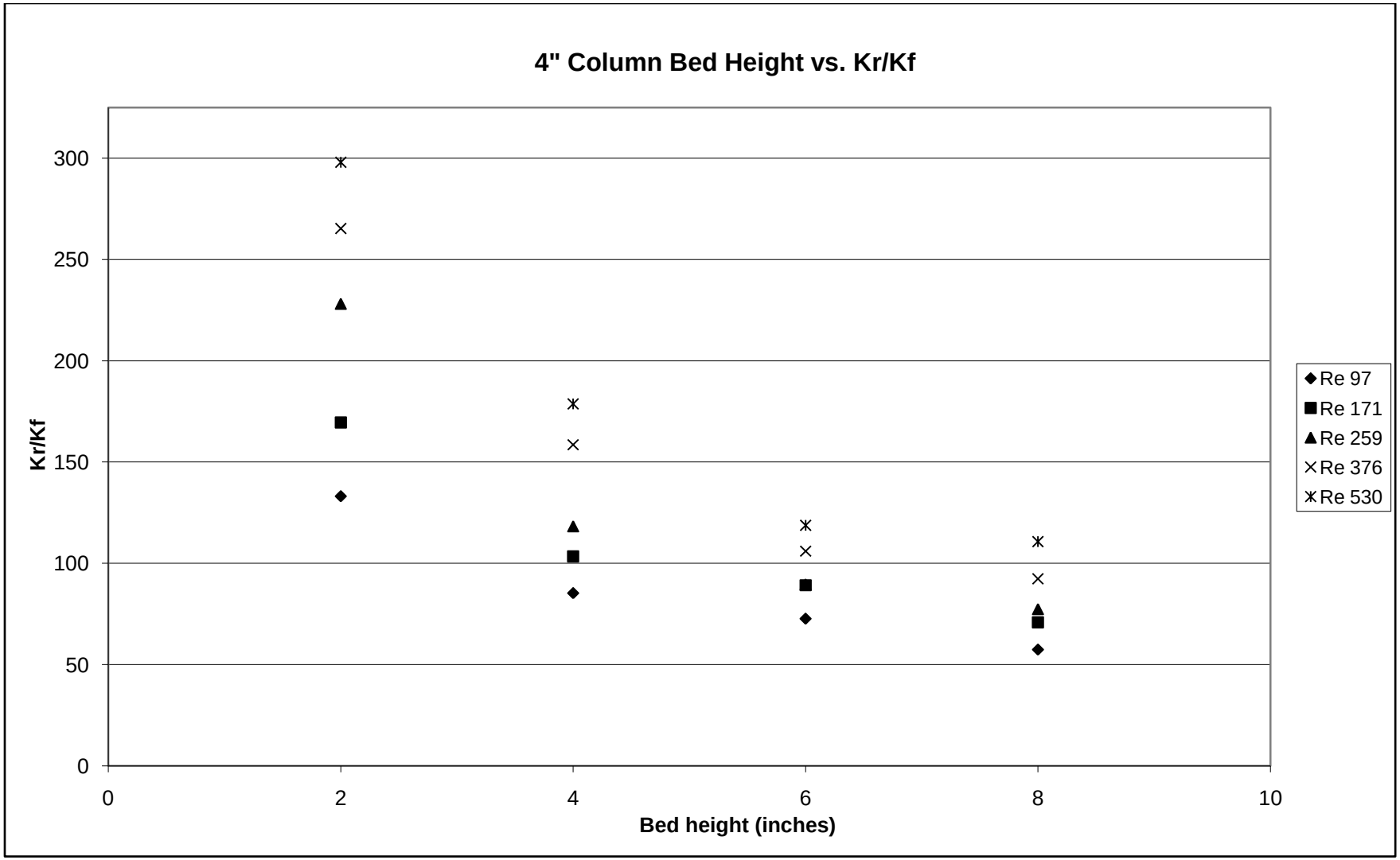

Figure 14- Bed Height vs. Kr/Kf in 4" Column

6.3 IPPF Model

After numerous experimental runs were taken, it became apparent that the temperature readings in the calming section were not constant. A large amount of heat loss (leading to decreases in inlet temperature between 20 and 40°C) was occurring in the calming section, which caused the test bed inlet to be significantly cooler than the temperature at the inlet of the calming section. This caused inaccurate analysis when utilizing the Plug Flow model and therefore the Inlet Profile Plug Flow model was used.

The IPPF model was designed to neglect the thermocouple readings in the calming section and uses the temperature readings gathered for the lowest height (in our case the 2″ data) as the inlet temperature profile. Analysis with the IPPF model, using the 4” thermocouple data as the inlet profile, shows depth dependence, as seen in Figure 15.

6.4 Thermal Conductivity versus Reynolds Number

The first was to see if our data could be compared to data taken in the early 1990s using the same column, but with a steam jacket and cold air. In other words, past heating experiments were in contrast with the present cooling study. Figures 16 and 17 show the comparison between the thermal conductivity values of our data and those from the data taken in the 1990s, all being analyzed using the 2-parameter IPPF model.

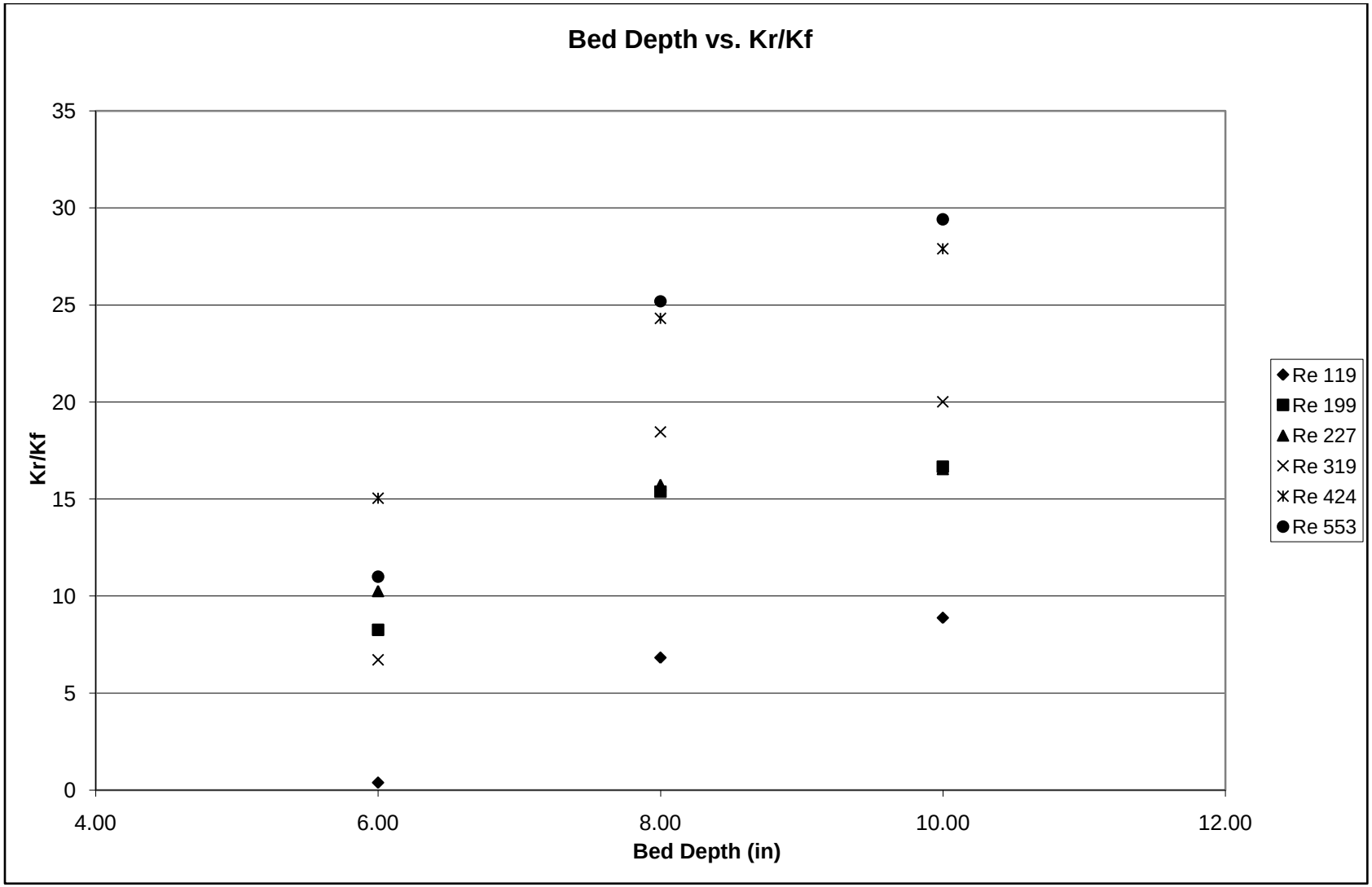

Figure 15- Bed Depth vs. Kr/Kf using IPPF Model

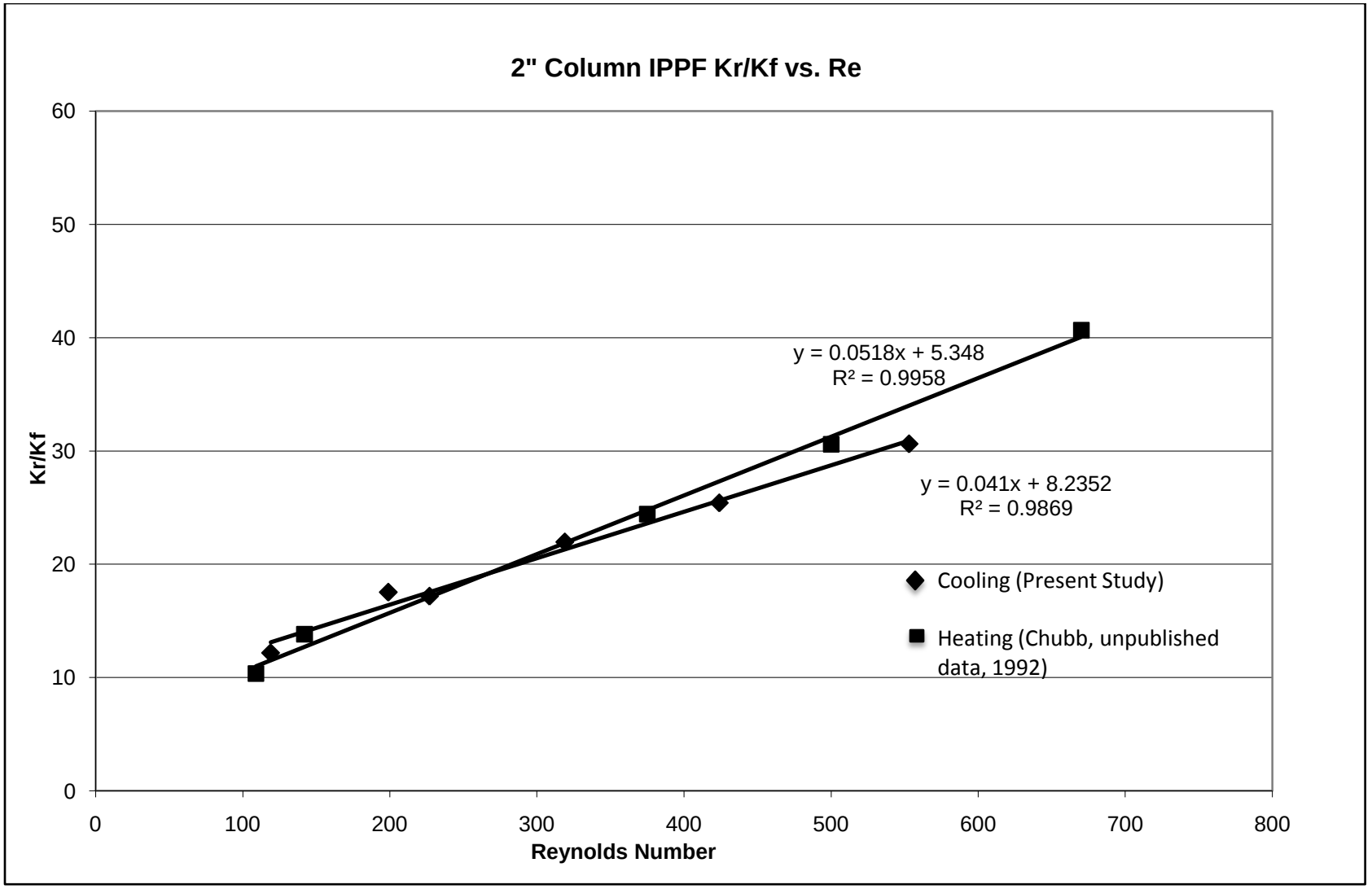

Figure 16- Kr/Kf vs. Re in 2" Column

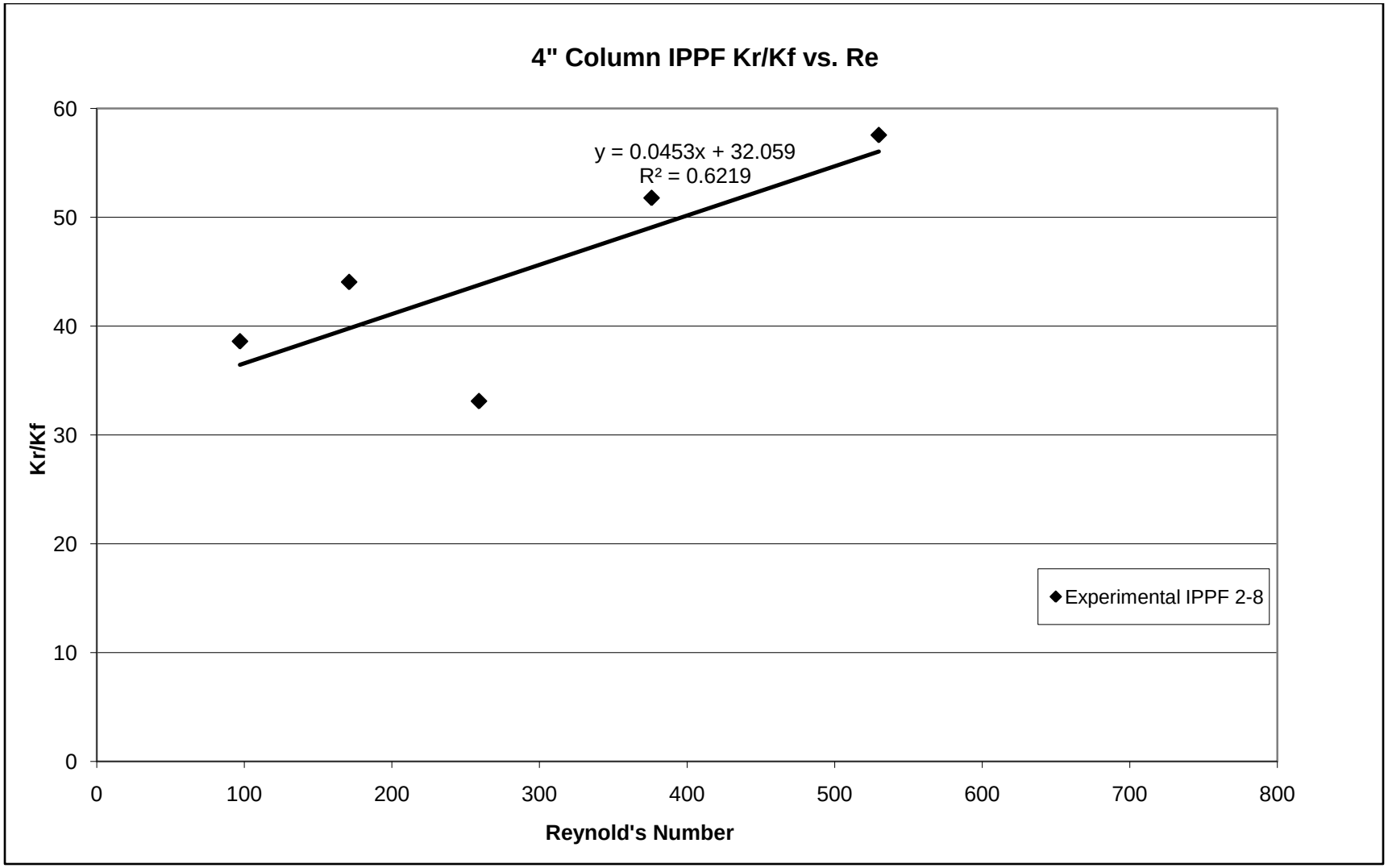

Figure 17- Kr/Kf vs Re in 4" Column

Even though the heating-cooling processes were reversed, the thermal conductivity value still increased along with the Reynolds number, as in past research (Chubb unpublished data, 1992). In addition to the data falling within the same range as previous data, the slopes in both cases were very similar. This assured us that our k_r data was well within the range of what is considered acceptable for thermal conductivity values and validated that the IPPF Model was indeed the correct model to use to analyze our data, since such a large amount of heat loss was occurring.

6.5 Removing Radial Positions

Since our project addressed the column in two parts, the near-wall region and center of the bed, an important piece of the experimental analysis was to observe different thermal conductivities when near-wall, radial positions on the thermocouple cross were not included in the fit to the data. By removing radial positions, we were able to analyze the data better in the center of the bed, thus moving away from the wall effects. As shown in Figures 18, 19 and 20 we removed radial positions first closest to the wall, working inward towards the center thermocouples. Since there were six different radial positions, we were able to produce plots showing all radial positions all the way down to one. The term IP refers to the number of radial positions that were included in the analysis. It should also be noted that the thermal conductivity values found analyzing only one and two radial positions are the least accurate. This is the case because the temperature readings taken in the center of the bed are higher than the IPPF model predicts them to be. Thus the program drives the k_r/k_f value up to account for the unexpected increased temperature in the center of the bed.

Analysis for the 2″ column was completed with the IPPF model for both the 2-10″ packing heights and 4-10″ heights. Thus, for the 2-10″ analysis the 2″ packing height is taken as the inlet condition and the program fits the 4-10″ packings. The IPPF model was written assuming the inlet profile, or first packing, to be at least 1.5 times the tube diameter (3″ in this case). For this reason, it is safe to assume that the data shown and analyzed for the 4-10″ packings (i.e. 4″ is inlet condition fitted to 6-10″ packing heights) are the most accurate.

Figures 18, 19 and 20 also demonstrate that the 4″ column shows severe exponential growth in k_r/k_f when approaching the center of the bed. It was expected that the value of k_r/k_f would level off as the plot moved closer to the bed center, which was not the case in our results. The theory behind removing data near the wall is to analyze data that is influenced less and less by wall effects. In analyzing the data this way, it was expected that the value of k_r would increase to a constant value representative of the bed core, ideally unaffected by the wall. Since the particle size was the same in both columns (0.25″ ceramic spheres), the number of particles across the diameter, N, is 8 in the 2″ column and 16 in the 4″ column. Studies have shown (Borkink and Westerterp, 1993) that wall effects persist over five particle diameters for spheres, which means approximately a 6 particle center core should be present in the 4″ column (uninfluenced by wall effects). It can be assumed that the 2″ column will most likely see wall effects throughout the entire bed at the experimental particle size. Unexpectedly, the data in the 2″ column was found to be more accurate than that collected in the 4″ column. The

specific reasons behind this are unknown and have many possibilities, but the main thought is possible problems with the efficiency and build of the 4″ column versus the 2″ column.

Another demonstration of this effect can be seen in Figures 21 and 22, where temperature profiles of similar Reynolds numbers from both the 2″ and 4″ column are plotted together versus a relative radius. This shows the general trend and increase for both columns as one moves from the wall (1) to the bed center (0) on the graph. As shown clearly in both figures, the 2″ column plot shows a much steeper initial increase in temperature close to the wall and a definite constant temperature being reached. The 4″ column data rises slower and increases much more, never quite leveling off. This shows that the temperatures taken from the 4″ column may have still been increasing and, therefore, too high in the bed center for the IPPF model to predict accurate thermal conductivity values in that region.

Once the IPPF model was established as giving an adequate fit to the data using 2 parameters, as well as good comparison to Chubb's data, it should be used to find a bed-center k_r.

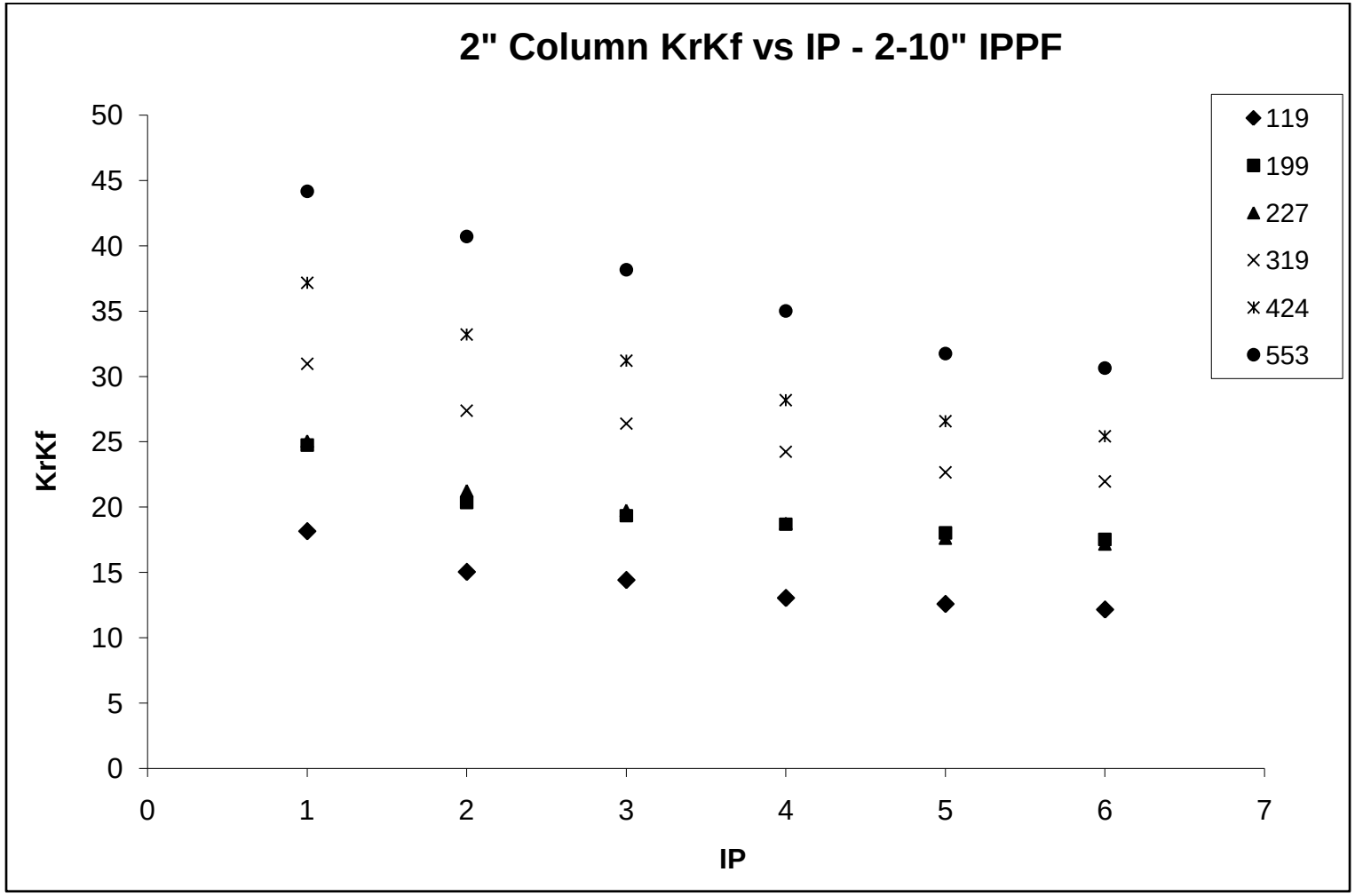

Figure 18- Removal of Radial Positions in 2" Column (2-10" Bed Heights)

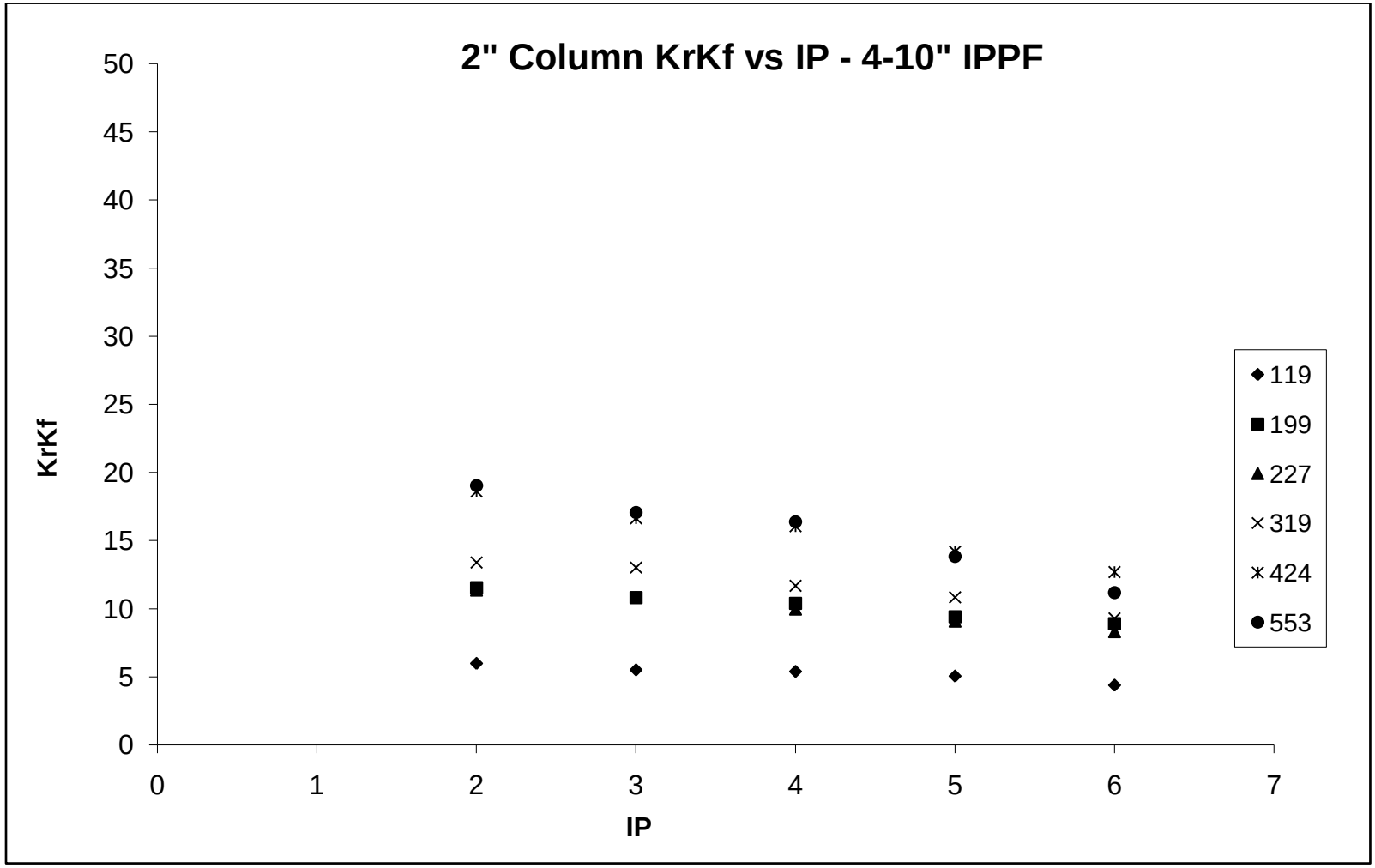

Figure 19- Removal of Radial Positions in 2" Column (4-10" Bed Heights)

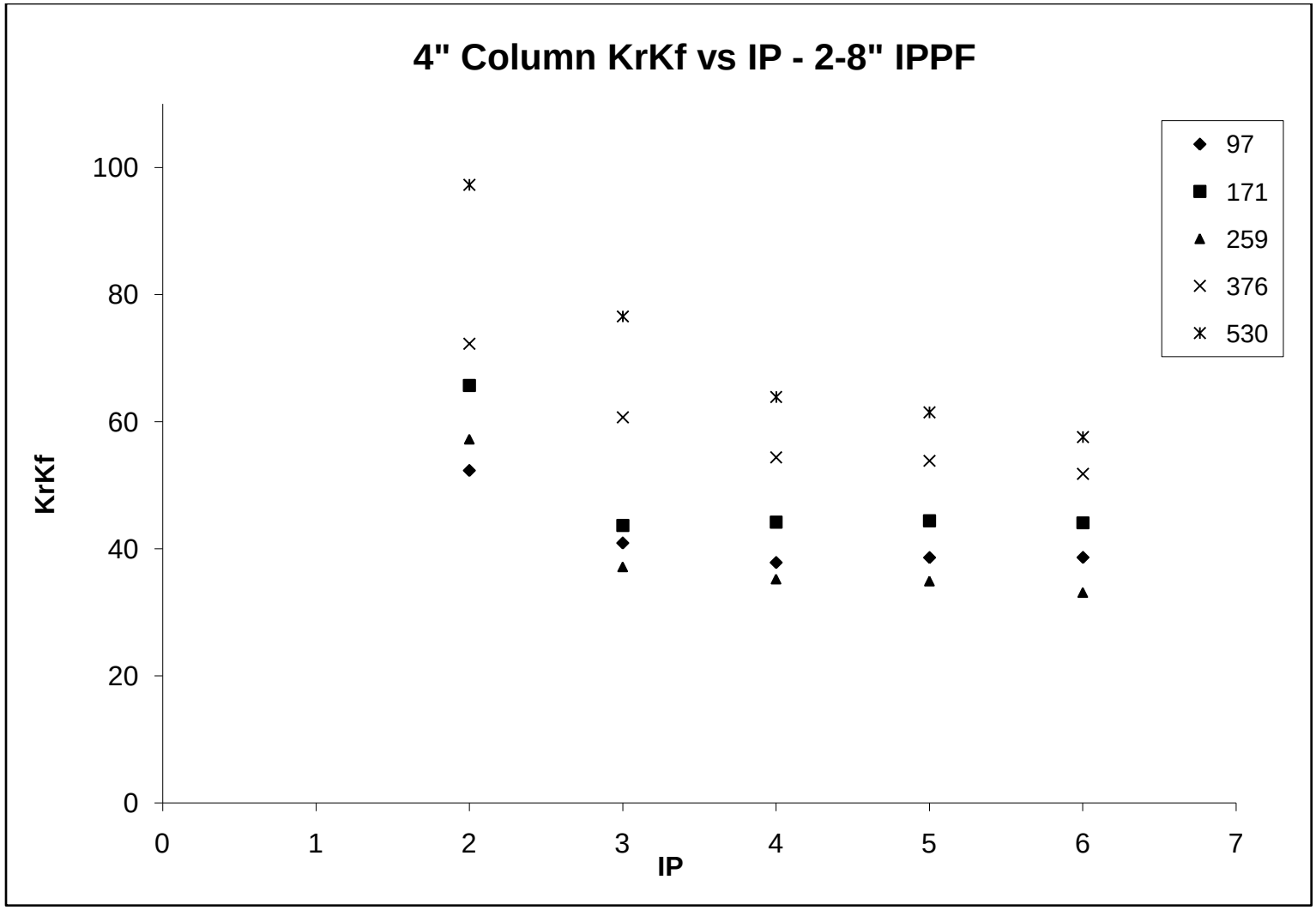

Figure 20- Removal of Radial Positions in 4" Column (2-8" Bed Heights)

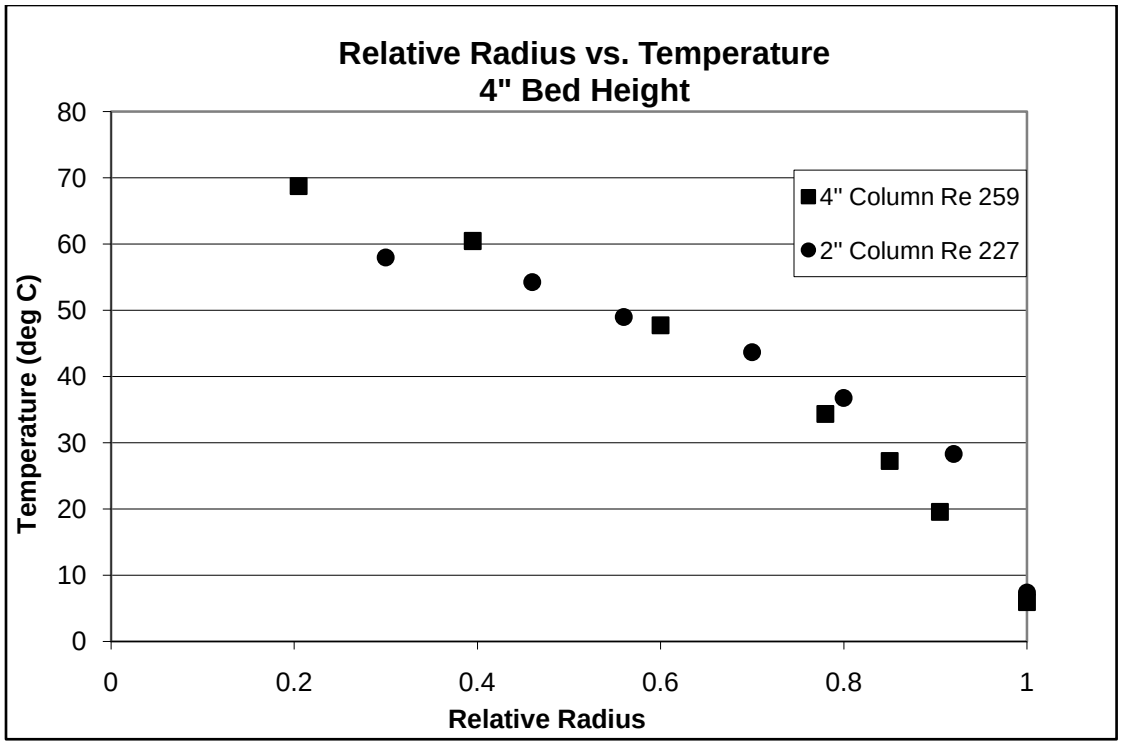

Figure 21- Relative Radius vs. T at 4" Bed Height

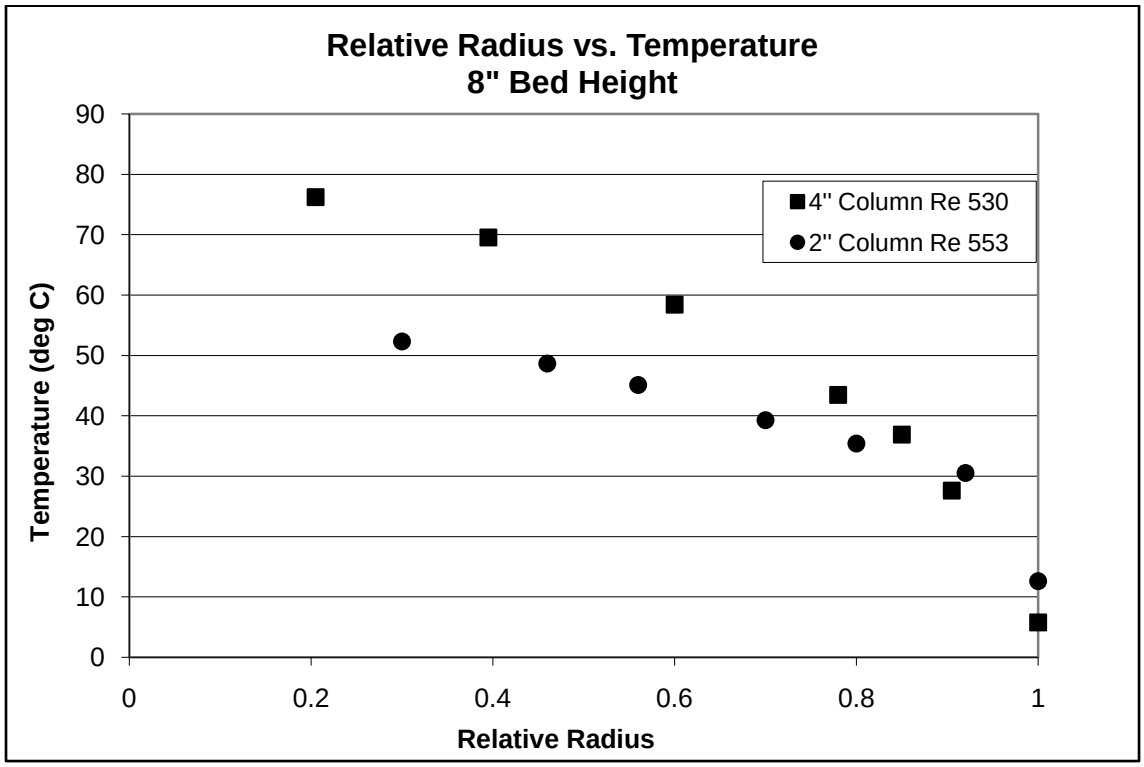

Figure 22- Relative Radius vs. T at 8" Bed Height

6.6 Determining k_r/k_f Values

Once plots showing removed radial positions were produced, a constant value of k_r/k_f could be estimated for each Reynolds number in both columns. As explained in the previous section, the least accurate data points in these plots were found to be when only one or two radial positions were evaluated. This in turn did not show the leveling off of k_r/k_f values that we had hoped for, thus a method for estimating k_r/k_f was developed.

It can be seen above in Figures 18, 19 and 20, especially in the lower Reynold Numbers, that the k_r/k_f values are coming to a steady value as radial positions are removed. Since the data found at one and two radial positions is the least accurate, a means for determining a k_r/k_f value at the very center of the bed had to be found. We began by excluding the one radial position data in the 2″ column and both the one and two radial position data in the 4″ column. Next, a linear trendline was plotted across each data set, which projected a point on the y-intercept, or the bed center. Though the plot is not expected to follow exactly a linear trend, each data set leveled off enough to predict a reasonable k_r/k_f value. A plot of these predictions can be seen in Figures 23 and 24. Thus the k_r/k_f values could be found and can be seen here in Table 3:

Table 3- Final Kr/Kf Values

	Reynolds Number	**k_r/k_f**
2″	119	7.3671
	199	13.378
	227	13.804
	319	16.201
	424	23.04
	553	25.217
4″	97	53.52
	171	65.393
	259	59.708
	376	77.683
	530	109.19

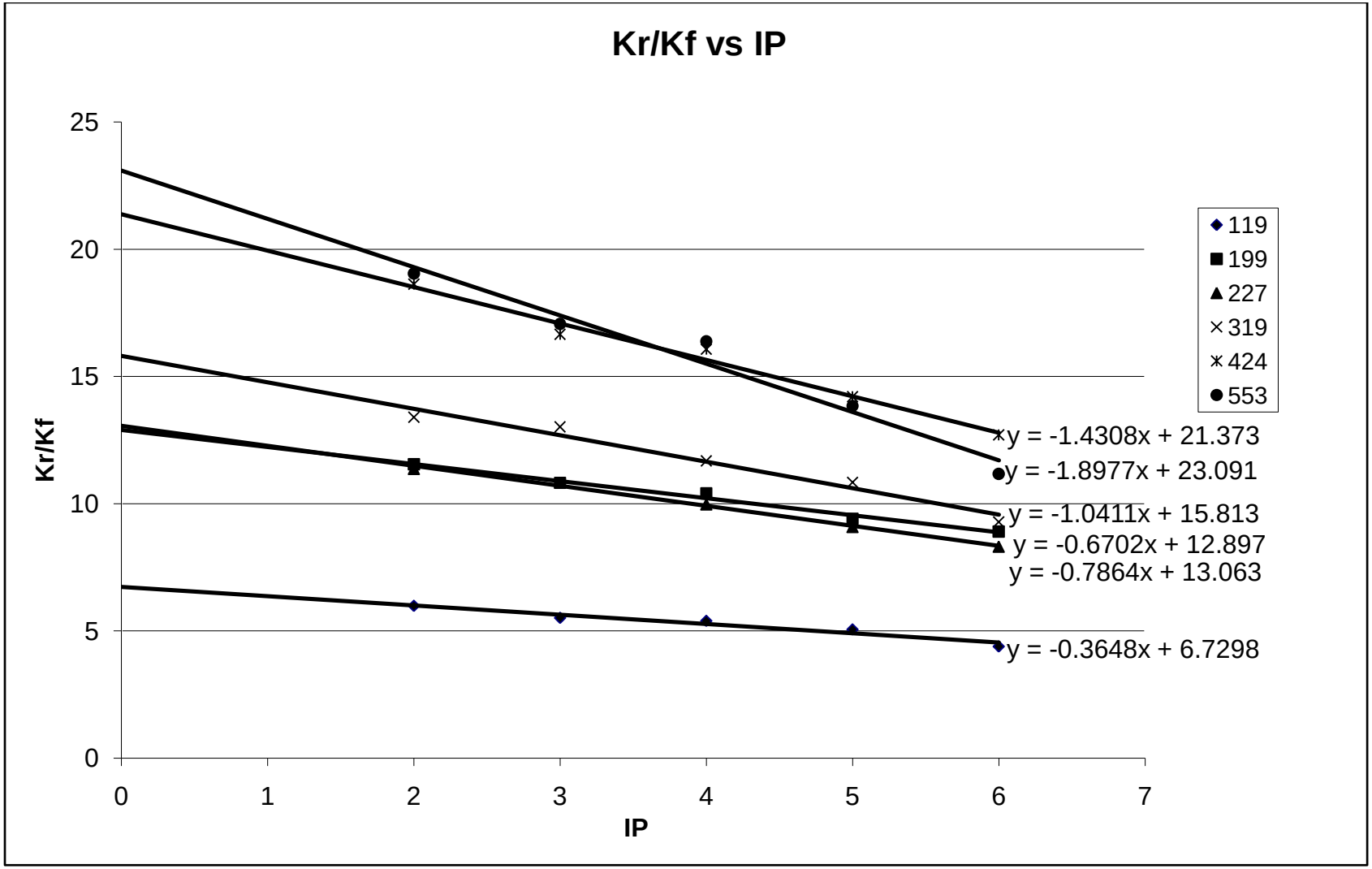

Figure 23- Linear Trendline finding Bed Center Kr/Kf in 2" Column

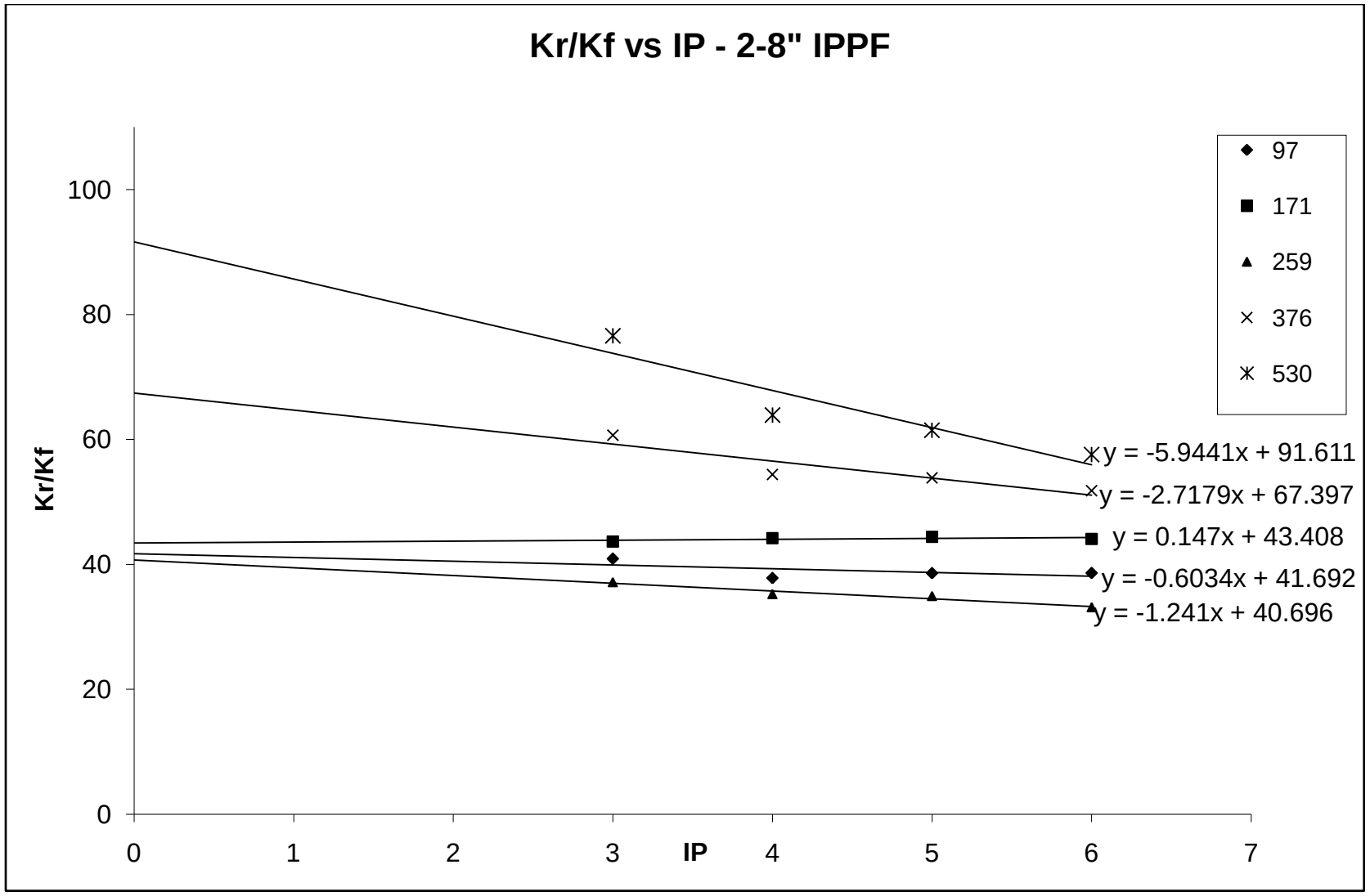

Figure 24-Linear Trendline finding Bed Center Kr/Kf in 4" Column

7 CFD Heat Transfer Results

This section will cover the results provided by the computational fluid dynamics models. Our goals for this section of the project were to create a CFD model of the near-wall region of the experimental system and to then determine a function for the thermal conductivity coefficient in the near-wall region of the fixed bed. By using Fluent to calculate the temperature gradient over particles near the wall we were then able to use point values of temperature to calculate point values of effective radial thermal conductivities . Using this method we were able to graph temperature gradients and thermal conductivities, *k*, within the near wall region. Using these relationships between *k* and the radial position, *r*, our team was able to produce a general equation for the behavior of thermal conductivity near the wall.

7.1 Fluent post-processing

The first step in obtaining usable results was to complete the Fluent models. As mentioned previously the models created were run at various velocities derived from experimental Reynolds number ranges. Three different models were also made and run with different bridge sizes at a constant velocity to determine how much effect the bridge sizes had on the returned values. Each model took an average of 20,000 iterations to converge. These 20,000 iterations took from 60 to 120 hours to complete, depending on computer resources available over the convergence time. Convergence was checked by graphing the residuals and two user-created monitors in Excel. The monitors used were a total surface heat flux over the particles and a volume averaged temperature of the fluid zone. Surfaces were then created as described in the experimental

section. The plotted temperature gradient for a velocity of 0.2675 m/s, a bridge size of 0.05 in., and a particle diameter of 0.25 in. is shown in Figure 25. More temperature vs. radial position graphs can be seen in Appendix C.

Figure 25 covers the distance from the wall to the center of the first particle. As shown in the graph there is a drastic incline in temperature up to about a quarter of a particle length and then the change in temperature begins to steady. Our interest lies in describing the behavior of this temperature jump near the wall. More will be said about the relationships between bridge sizes and fluid velocities and the temperature gradient in the following sections.

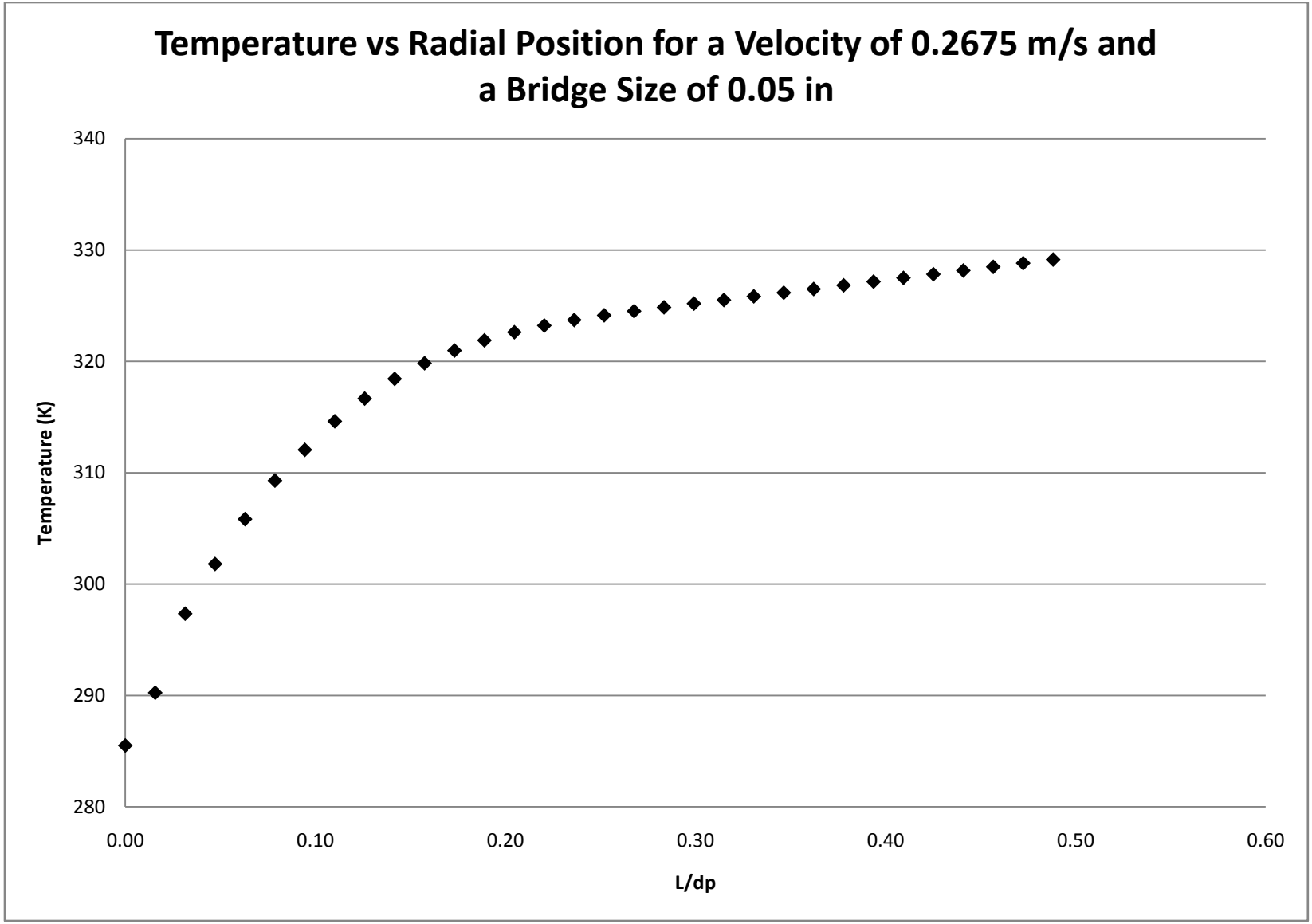

Figure 25: Temperature gradient for a velocity of 0.2675 m/s, a bridge size of 0.05 in.

7.2 Theory

The average temperature of the iso-clips at specific distances away from the wall from Fluent allowed the use of Schuler, Stallings and Smith's (1952) differential equation for temperature change dependent upon radial position with varying effective thermal conductivities. This equation is obtained upon rearrangement of the PF model equations with a varying k_r:

$$\frac{\partial k_r}{\partial r} = f_1(r)k_r + f_2(r) \tag{32}$$

Where

$$f_1(r) = \frac{-\left[\frac{\partial^2 T}{\partial r^2} + \frac{1}{r}\frac{\partial T}{\partial r}\right]}{\frac{\partial T}{\partial r}} \tag{33}$$

$$f_2(r) = \frac{c_p G}{\frac{\partial T}{\partial r}}\left(\frac{\partial T}{\partial z}\right) \tag{34}$$

The equation was numerically solved, using Euler's Method, for all point values of temperature in Microsoft Excel and the spreadsheets can be seen in Appendix B. It is important to note that the second term in Equation 32, $f_2(r)$, becomes insignificant near the wall because of large changes in temperature in the radial position and much smaller changes in temperature in the z-direction ($f_2(r)$ is anywhere from 10^4 - 10^6 times smaller). Because of this insignificance, the second term was dropped from our calculations. Point values of effective radial thermal conductivity were then able to be calculated and plotted. Shown below is the plot of effective radial thermal conductivity against radial position for a velocity of 0.2675 m/s and a bridge size of 0.05 in. All Effective Radial Thermal Conductivities can be seen in Appendix D.

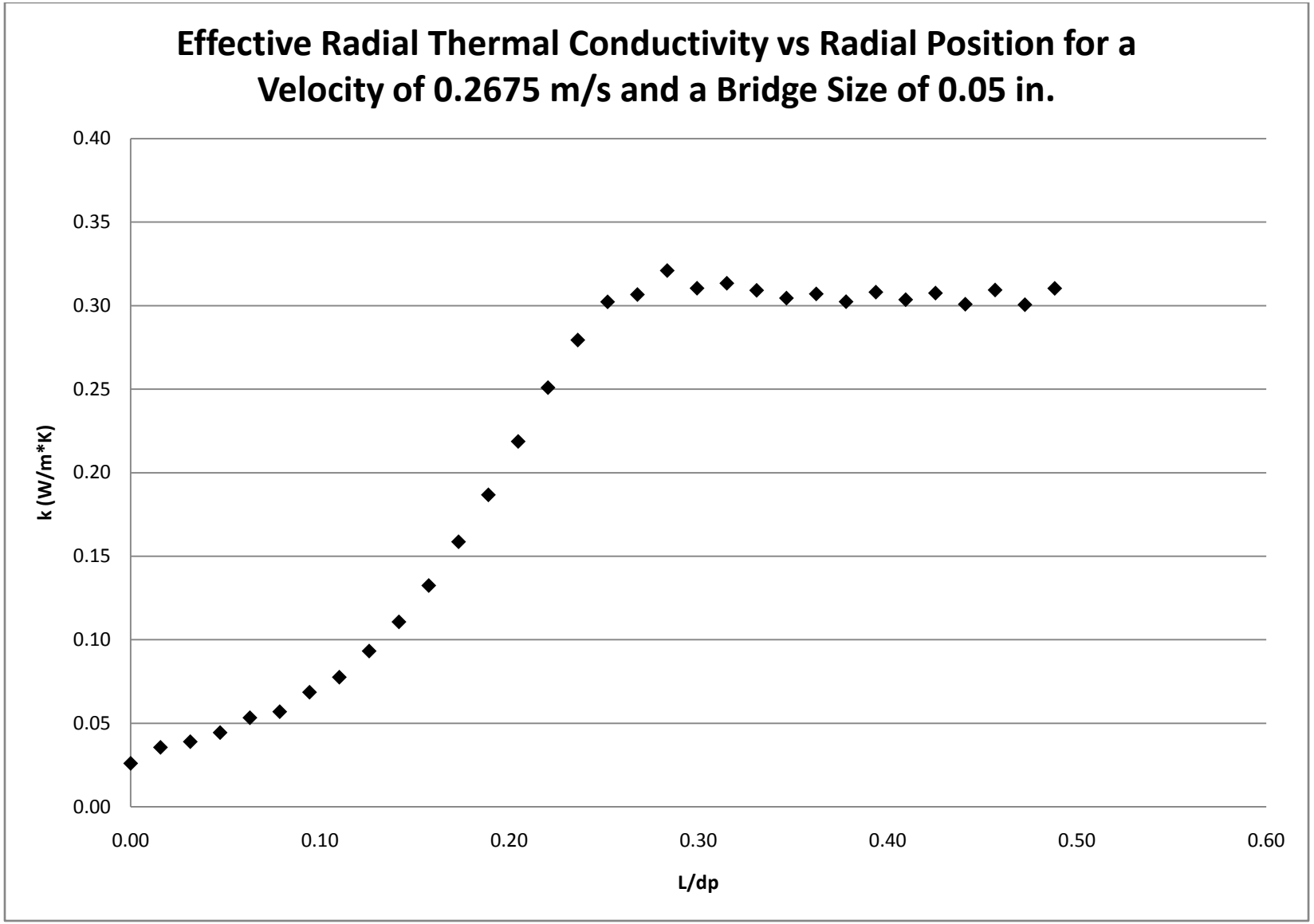

Figure 26: Effective radial thermal conductivity gradient for a velocity of 0.2675 m/s, a bridge size of 0.05 in

7.3 Velocity Comparisons

Since one of our goals for this project was to describe the behavior of thermal conductivity at the wall, we used multiple velocities to observe any general trends. These velocities corresponded to Reynolds numbers from the experimental part of this project. Using five different velocities (all in m/s), the CFD data was processed as mentioned previously and provided us with the following plot of temperature vs. radial position.

In Figure 25, It is noticed that after a dynamic temperature gradient within the first half of a particle diameter the temperature begins to steady. Seeing this, our team used this first half of a particle diameter as our focus for determining heat transfer behavior in the near-wall region. Figure 27 is a plot of temperature vs. radial position at varying velocities. It is also seen that the average temperature values increase with fluid velocity parameters; this makes sense since the incoming air would have less time to cool while flowing past the particles.

As shown in Figure 28, thermal conductivity showed similar trends in all velocity ranges. It should also be noted that thermal conductivity showed a linear increase with the velocity used. From the results above it was concluded that thermal conductivity near the wall increases quadratically with distance from the wall $(R-r)/d_p$. This data agrees with the work of Winterberg et al. (2000). An equation derived to fit this behavior will be discussed in a later section. The next section will show the means by which we showed that the bridge size chosen, .05 in cube, did not have a detrimental effect on the results.

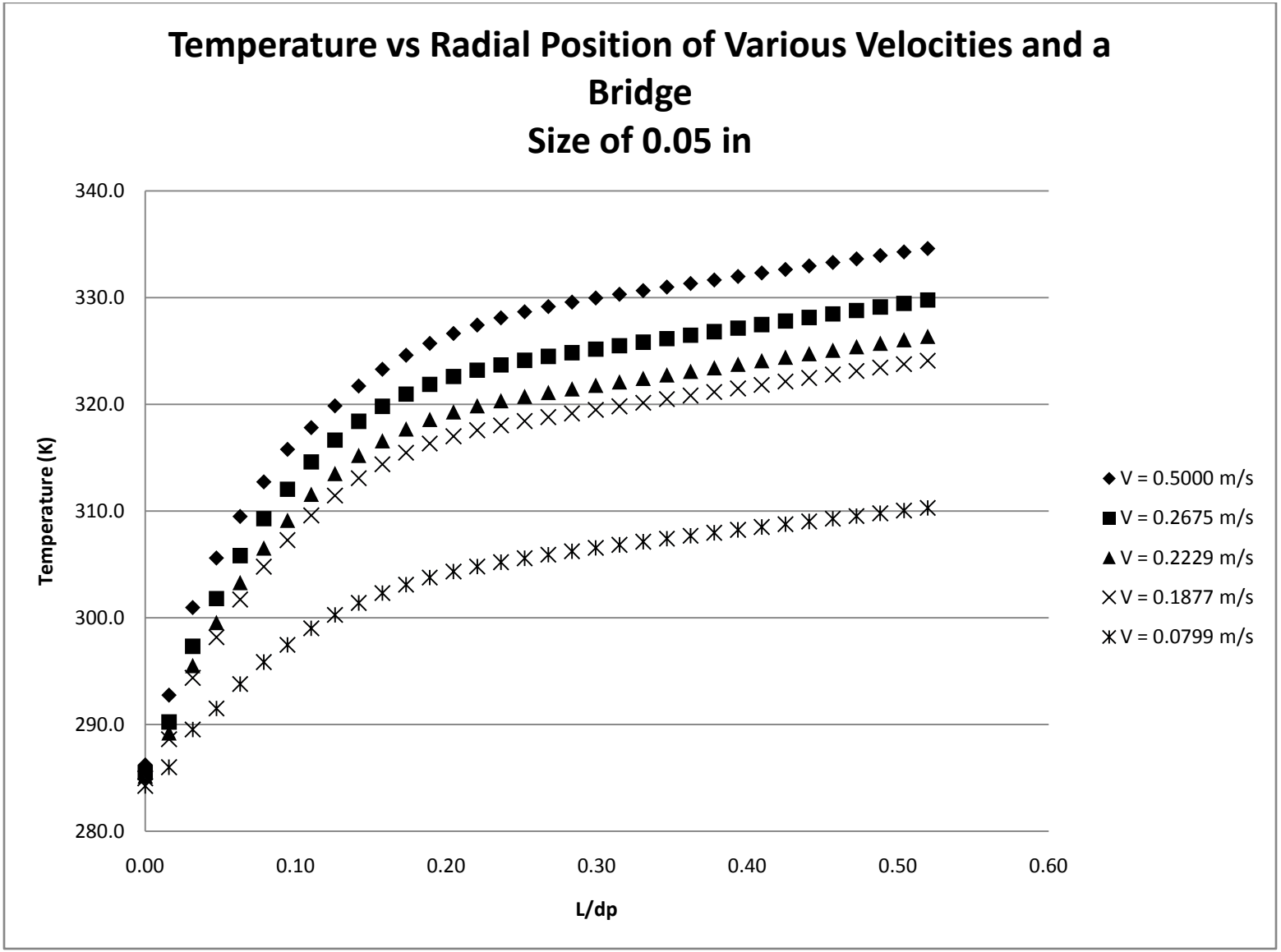

Figure 27: Temperature gradient for various velocities with a bridge size of 0.05 in.

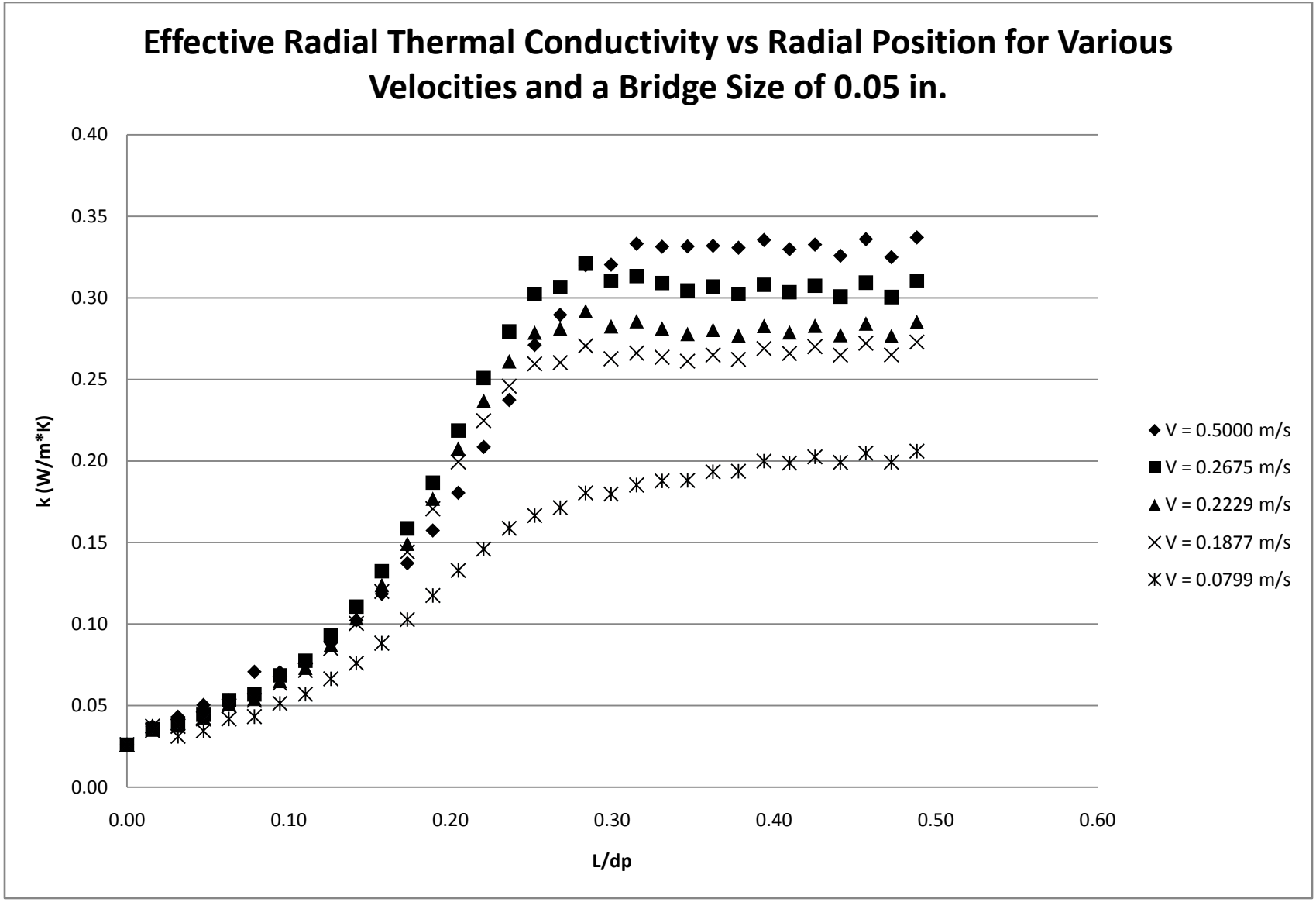

Figure 28: Effective radial thermal conductivity gradient for various velocities with a bridge size of 0.05 in.

7.4 Bridge Size Comparisons

It is important to recall from previous sections that the size of the bridge used between particles can adversely affect mesh volume counts (Table 2). Hence, the largest bridge size possible should be used. In order to determine the size of the bridge used, three bridge sizes were designed and simulated. As shown in Figures 29 and 30 the bridge sizes had minimal effects on temperature and the calculated effective thermal conductivity. Our team then decided that because of the small effect the bridge size has on the effective thermal conductivity, the largest bridge size tested (0.05 in.) would be used in order to save on computer processing power.

7.5 Mesh Refinement

As mentioned before, it was necessary to refine the mesh until it was deemed independent of the solution. Seen in Figure 31 is the plot of effective radial thermal conductivity vs. radial position for a velocity of 0.2675 m/s and a bridge size of 0.05 in. at varying mesh refinements. It is clear that the first refinement created a major difference in effective radial thermal conductivity but the second refinement had nearly no effect. Due to the large amount of processing power these refined meshes took (15,000,000+ cells) this study was done at one velocity and one bridge size and assumed to have minimal effects, if any, on the remainder of the models.

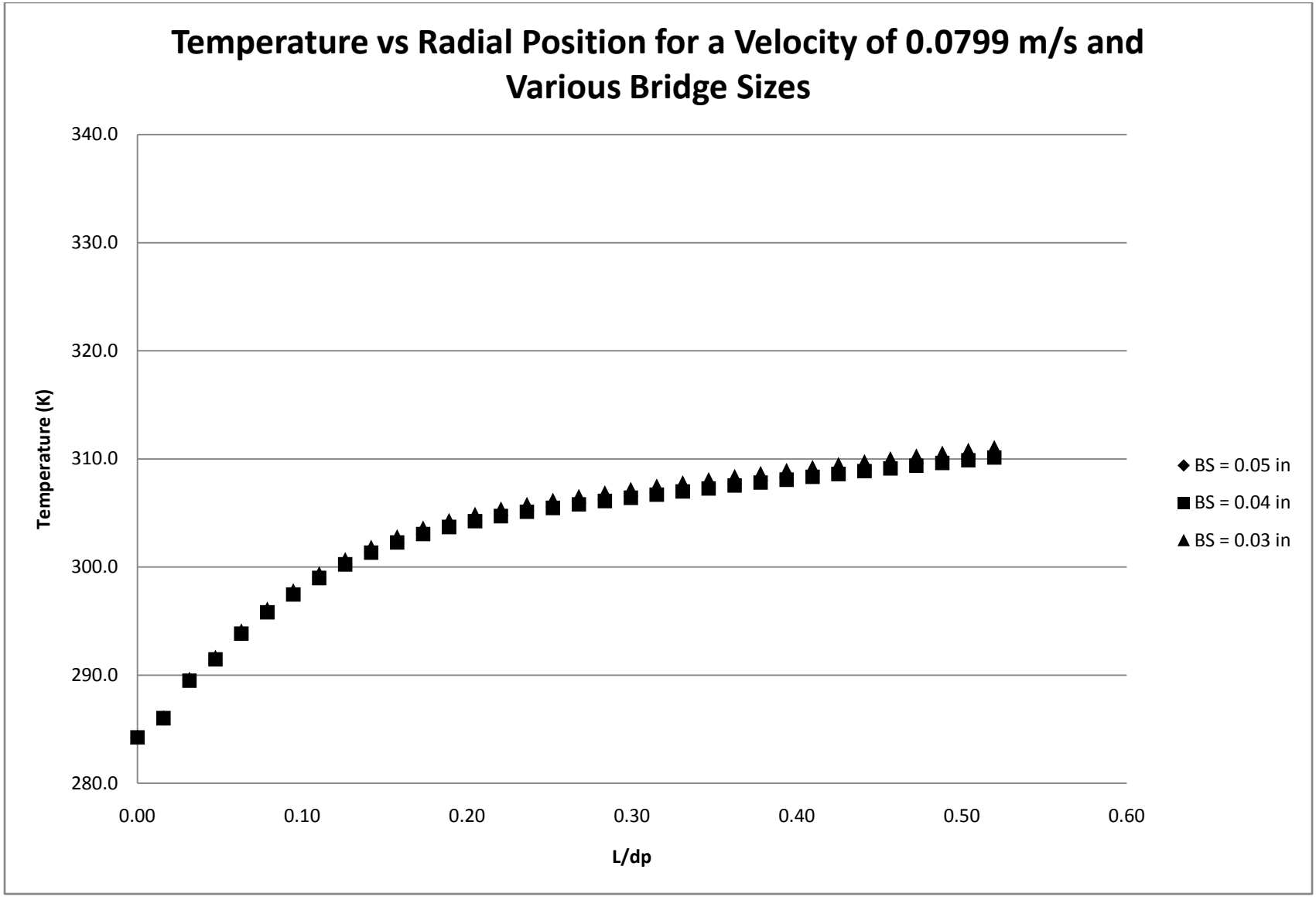

Figure 29: Temperature gradient with a velocity of 0.0799 m/s and varying bridge sizes.

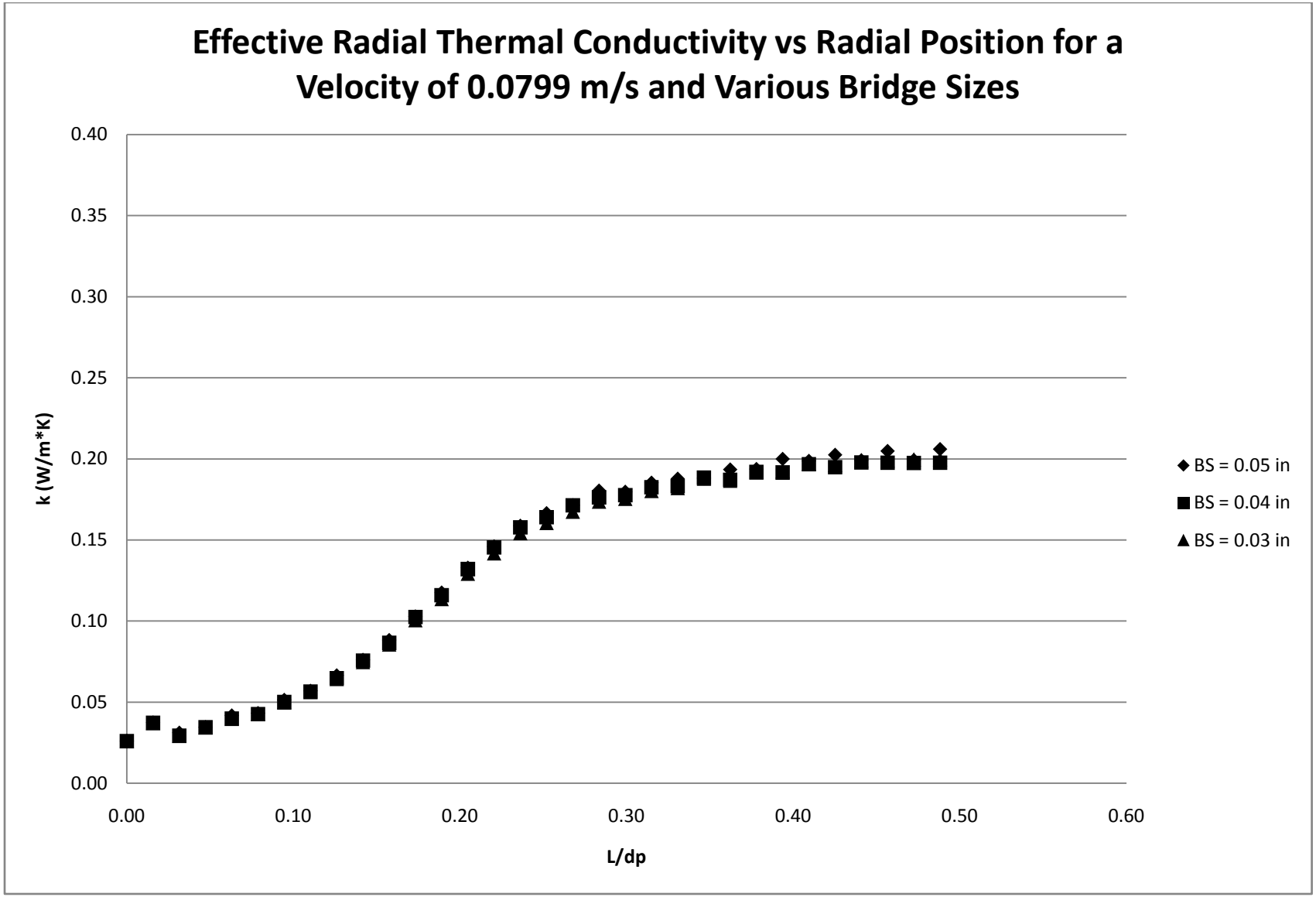

Figure 30- Effective Radial Thermal Conductivity vs Radial Position at Varying Bridge Sizing

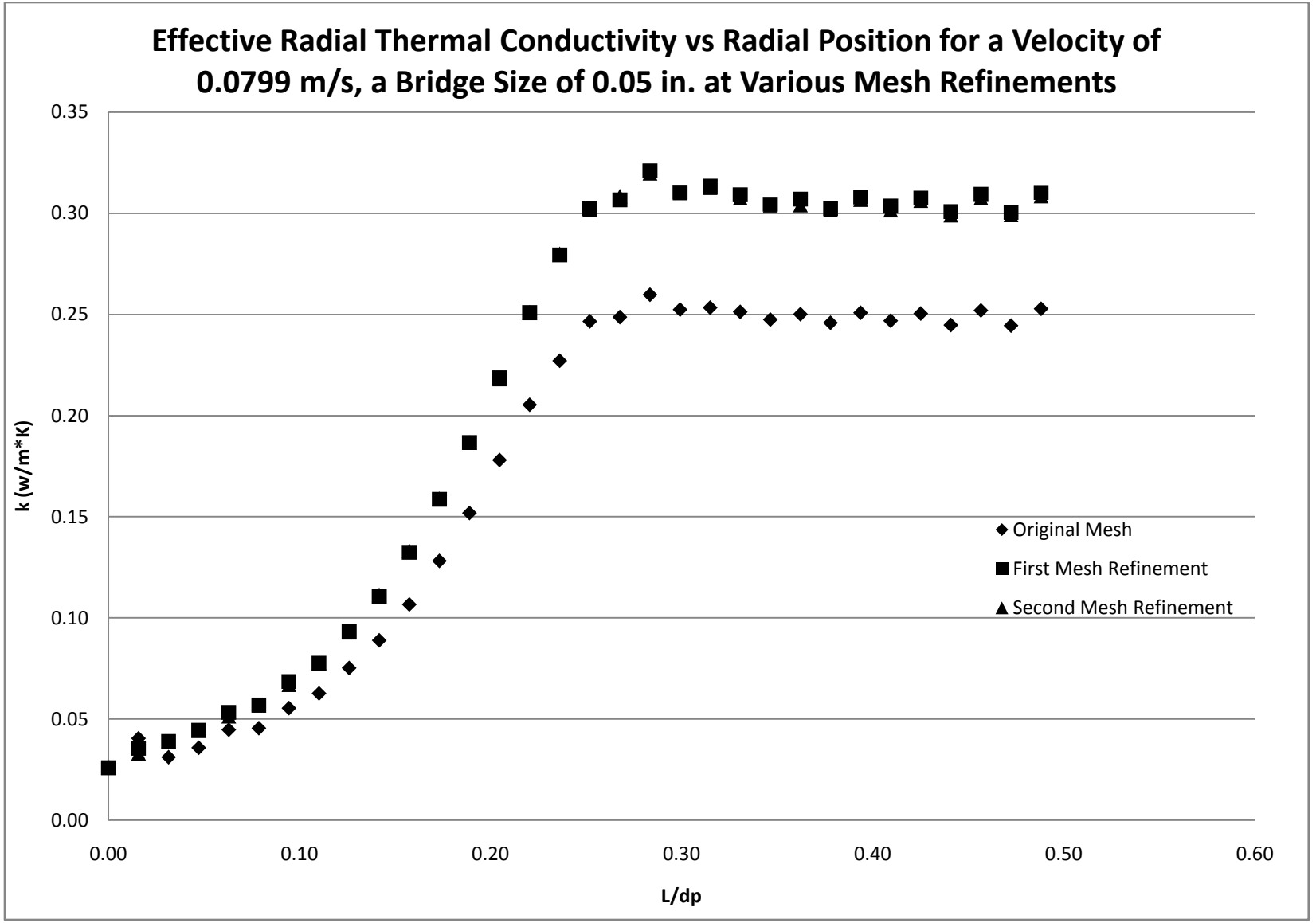

Figure 31- Effective Radial Thermal Conductivity vs Radial Position at Varying Mesh Refinements

7.6 Near Wall Behavior of Thermal Conductivity

Based on the computed results it is viable to assume a quadratic dependence of effective thermal conductivity with respect to radial distance from the wall in a packed bed reactor. This allows the use of the standard quadratic equation:

$$y = A(x + B)^2 + C \quad (35)$$

Which, for our case, can be written as:

$$k_r = A(R_w - r)^2 + C \quad (36)$$

Where:

k_r =Effective radial thermal conductivity near the wall

A = Magnitude constant

R_w =Radius of the wall

r = Radius of interest

C = Constant

Using the following boundary conditions and Equation 36:

i) $r = R_w$; $k_r = k_{wall}$

$$k_{wall} = C \quad (37)$$

ii) $r = R_I$; $k_r = k_{bed}$

$$A = \frac{k_{bed} - k_{wall}}{(R_w - R_I)^2} \quad (38)$$

Gives:

$$k_r = \frac{k_{bed} - k_{wall}}{(R_w - R_I)^2}(R_w - r)^2 + k_{wall} \quad (39)$$

Where:

k_{wall} = Thermal conductivity of the fluid at the wall

k_{bed} = Effective radial thermal conductivity in the center of the bed

Further $(R_w - R_I)$, or the distance that major wall effects are seen, can be simplified to the following because these effects are present through 0.27 particle diameters away from the wall:

$$R_w - R_I = 0.27 * d_p \tag{40}$$

Combining Equations 39 & 40 gives the following model for determining the effective radial thermal conductivity near the wall:

$$k_r = \frac{k_{bed} - k_{wall}}{(.27d_p)^2}(R_w - r)^2 + k_{wall} \tag{41}$$

Equation 41 represents a quadratically increasing effective radial thermal conductivity from k_{wall} to k_{bed} depending on distance from the wall.

8 Two-region Pseudo-homogeneous Model

The current section will test the validity of the effective radial thermal conductivities that were found in the previous sections. Effective radial thermal conductivities were put into COMSOL version 3.4.0.248 and temperature profiles were solved for and compared to our experimentally found temperature gradients.

8.1 Plug Flow Model

The Chemical Engineering Module solving for convection and conduction was used to run calculations in COMSOL Multiphysics. This set-up used our calculated effective thermal conductivity in the 2D axial symmetry pseudo-homogeneous heat-transfer model to compare to our experimental temperature profiles. The thermal conductivity values found from experimental analysis (Chapter 6) and CFD modeling (Chapter 7) were evaluated using Equation 1 as the governing equation taken from Chapter 2.

$$GC_p \frac{\partial T}{\partial z} = k_r \left(\frac{\partial^2 T}{\partial r^2} + \frac{1}{r} \frac{\partial T}{\partial r} \right)$$

8.2 Solving

The following parameters were input into COMSOL to model temperature profiles using the aforementioned plug flow model. Included are the given materials, velocity, boundary conditions, as well as the function used for effective radial thermal conductivity.

Air was used as the fluid with the density set as 1.184 kg/m^3 and the heat capacity set as 1006.43 J/kg*K. The velocity of the fluid in the radial direction is 0 and the axial fluid velocity depends

on the Reynolds number being evaluated, which are provided in Table 4. The equation below was used to find the axial superficial velocity based on a given Reynolds number.

$$v = \frac{Re\mu}{\rho d_p}$$

Where:

μ=0.0000173kg/m*s (the viscosity of air)

d_p=0.00635 m (the diameter of the particle).

Table 4- Corresponding Superficial Velocities

Reynolds Number	Superficial Velocity (m/s)
97	0.223199
119	0.273822
171	0.393475
199	0.457903
227	0.522332
259	0.595965
319	0.734026
376	0.865184
424	0.975633
530	1.219541
553	1.272465

The 2D Axial Symmetric model's dimensions were set at a length of 0.254 m with radius of 0.0254 m, thus having the same dimensions as the physical column described in Chapter 4. The boundary conditions used are shown in Table 5.

Table 5- Boundary Conditions Used in Comsol

r=0	Axial Symmetric
z=0	T_o= 353 K
z=0.254	Convective Flux
r=0.0254	T_o=283K

Based on results in Chapters 6 and 7 the following piecewise function was developed. This two-region approach takes into account the thermal conductivities determined in the bed center area and the near wall area. This equation is a description of the behavior observed experimentally and through CFD during the course of our research.

$$k_r(r) = \begin{cases} k_{bed} \quad for:\ 0 \leq r \leq R - .27d_p \\ \dfrac{k_{bed} - k_{wall}}{(.27d_p)^2}(R_w - r)^2 + k_{wall} \quad for:\ R - .27d_p < r < R_w \end{cases} \qquad 39$$

It was previously determined that the major wall effects end at approximately .27d_p. Thus, the bed center area extends from r = 0m (the center of the bed) to r = 0.02369m. The thermal conductivity from this area (k_{bed}) at varying Reynolds numbers is given in Table 6 .

Table 6- Corresponding Bed Thermal Conductivity Values for Various Reynolds Numbers

2 in Column		**4 in Column**	
Re	**k_{bed}**	**Re**	**k_{bed}**
119	0.191545	97	1.39152
199	0.347828	171	1.700218
227	0.358904	259	1.552408
319	0.421224	376	2.019758
424	0.59904	530	2.83894
553	0.655642	-	-

The second part of the piecewise function describes the near wall area from r = 0.02369m to r = 0.0254m. For the quadratic expression for thermal conductivity discussed in previous sections the thermal conductivity of the wall, k_{wall} is 0.026 and the radius of the column, R_w, is 0.0254m. All of the above parameters were also used to model a 4 in. column in COMSOL, where the dimensions of the COMSOL model were equal to .0508m by .254m, the wall effect region remains .27 particle diameters in length.

8.3 Results and Discussion

The purpose of this project was to more accurately predict the temperature gradient across a packed bed. The thermal conductivity values were evaluated using CFD modeling and experimental analysis and then placed back into the original energy balance using COMSOL. Appendix K contains the complete collection of temperature profiles for each Reynolds number and bed height evaluated using COMSOL and plotted against the actual experimental data. In some cases our model, at a given Reynolds number and bed height, accurately predicted the temperature profile when compared with the results we had received experimentally (Figure 32). The best predictions in the 2" Column were given at the lowest bed heights and highest Reynolds numbers.

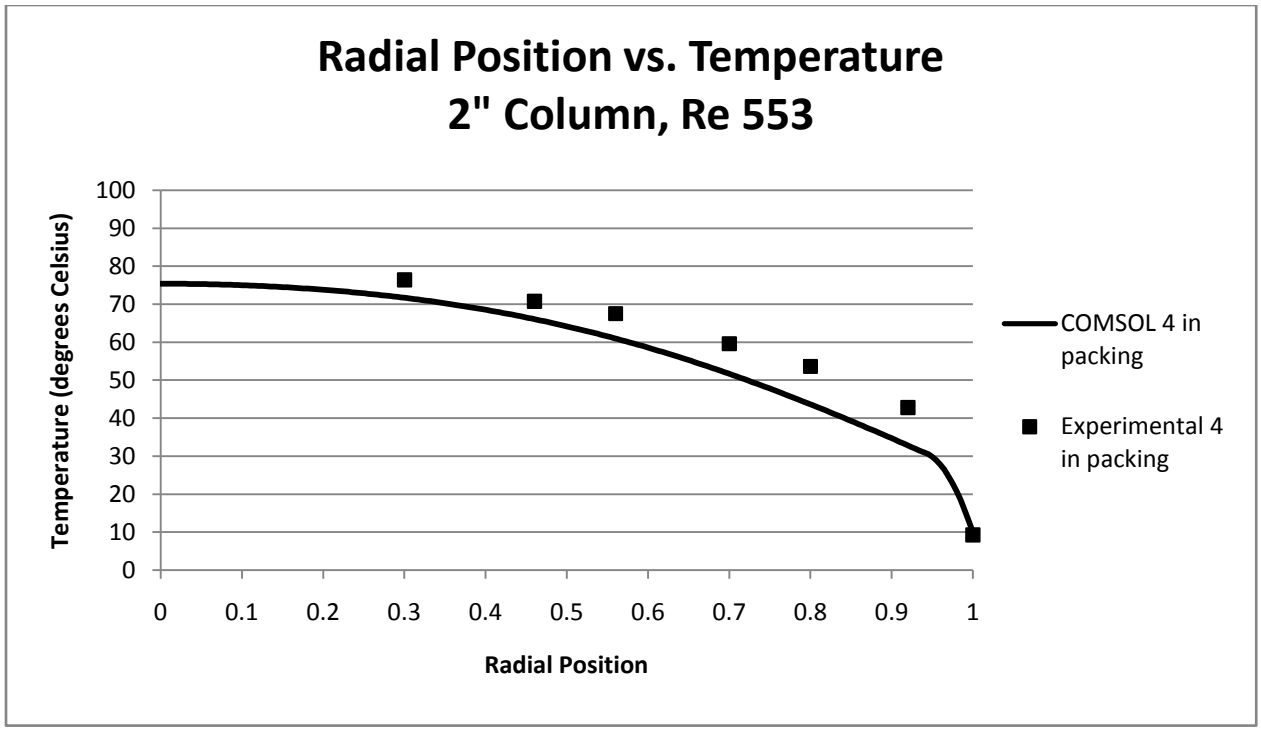

Figure 32-COMSOL vs Experimental Temperature Gradient Comparison#1

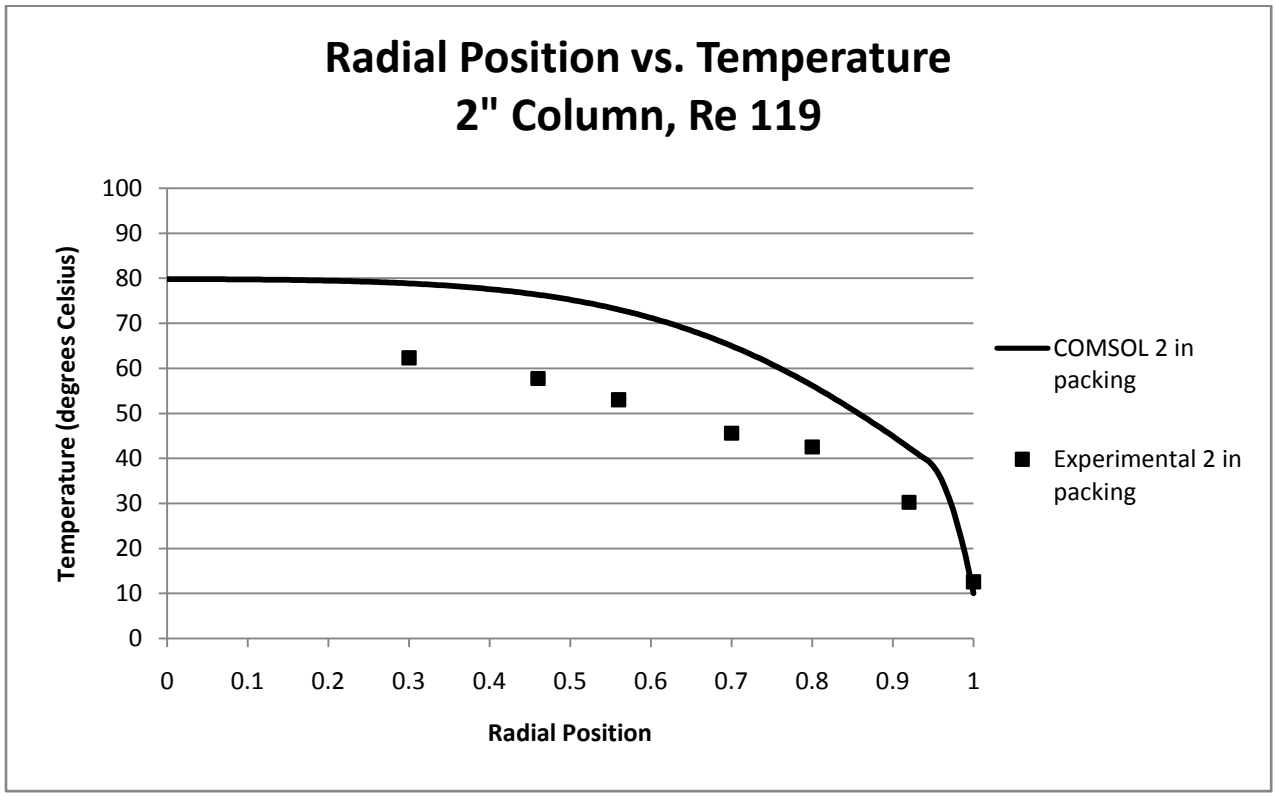

Figure 33- COMSOL vs Experimental Temperature Gradient Comparison#2

At the lower Reynolds numbers (Figure 33) the model usually over predicts the temperature profile. This discrepancy most likely is the result of the inlet temperature being inaccurate. For the COMSOL model the inlet temperature is given as a constant value of 80 degrees Celsius. Experimentally, the measured inlet temperatures ranged from 70 to 90 degrees Celsius. Also there is an enormous amount of heat loss prior to the air entering the column in the calming section. This, in turn, affects the inlet temperature. The inlet temperature is not a constant across the entire bed. In fact, using the IPPF model to determine the bed center thermal conductivity value, the inlet temperature profile is assumed to be parabolic and is represented by the profile of the measured 2" data.

Overall the model predicted better for the 4" Column (Figure 34) compared to the 2" Column (Figure 35). This is most likely because in the 4" Column the wall effects are less throughout the bed.

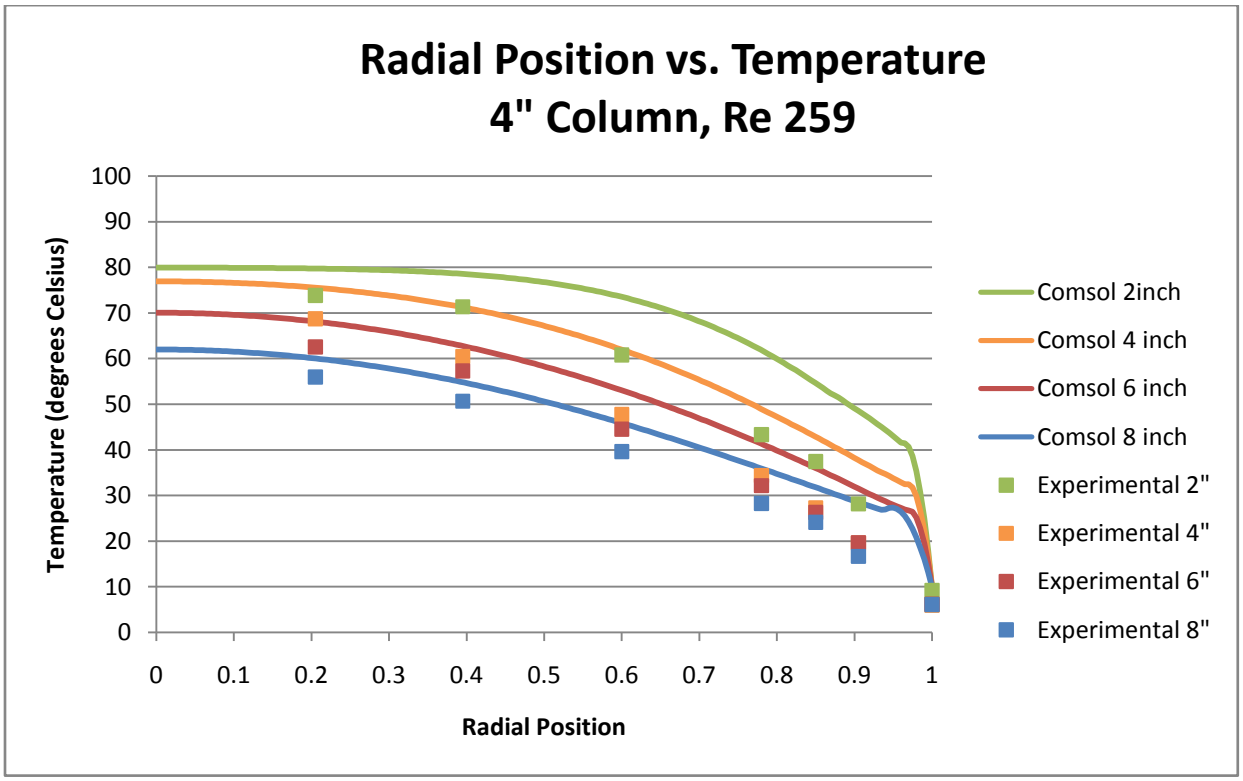

Figure 34- 4 in Column Temperature Gradient Comparisons

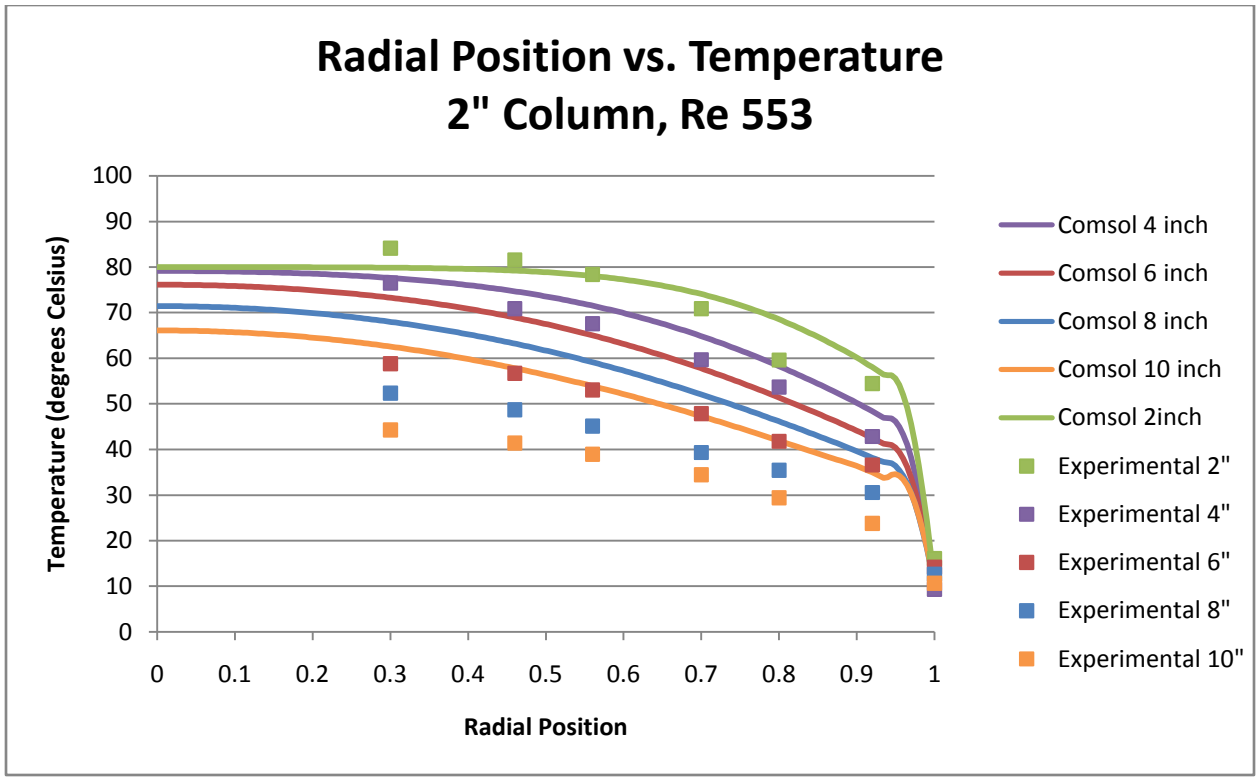

Figure 35- 2 in Column Temperature Gradient Comparisons

Near the wall, the temperature gradient output from COMSOL made an accurate prediction. Figure 36 shows the relationship between the output COMSOL results and the calculated values from CFD.

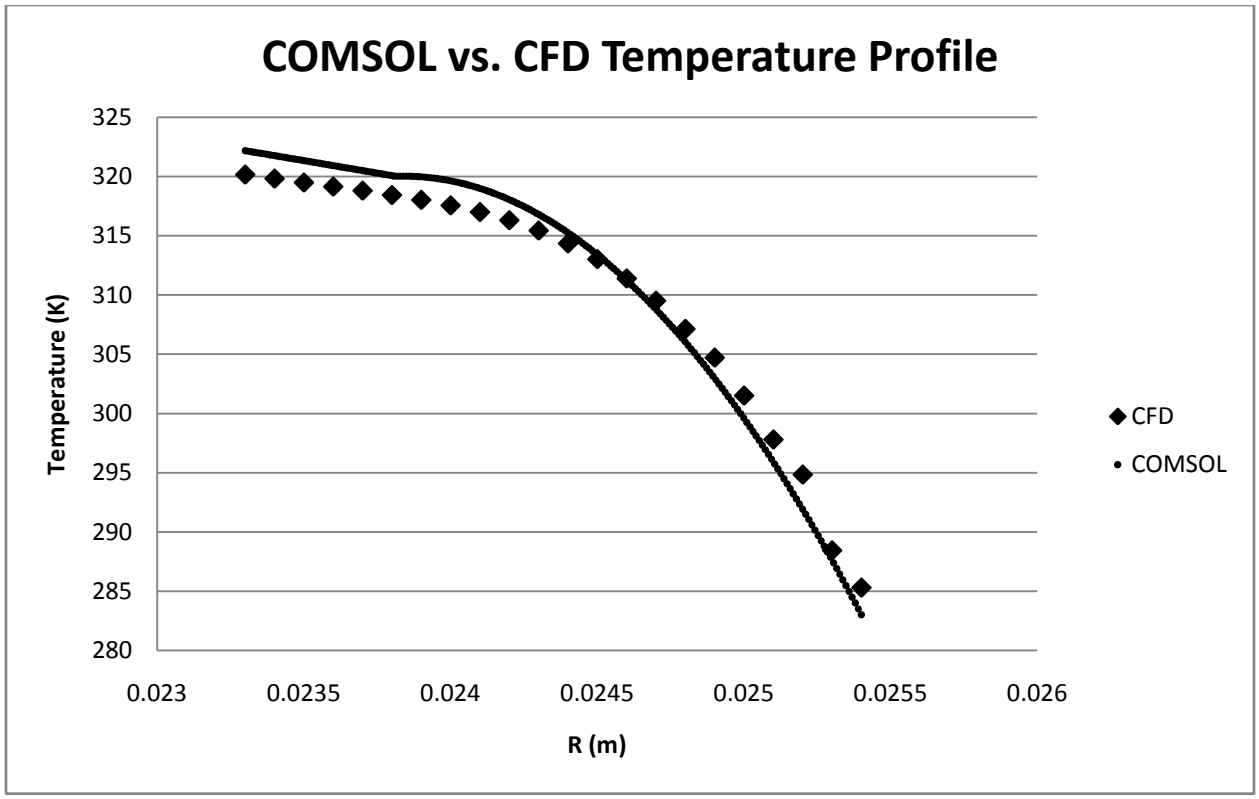

Figure 36- Near-wall COMSOL and CFD Temperature Comparisons

COMSOL was run again after making a 10% increase and 10% decrease to the constant value of .27 of a particle diameter, d_p, used in the piecewise equation for effective radial thermal conductivity, shown again below.

$$k_r(r) = \begin{cases} k_{bed} \quad for:\ 0 \leq r \leq R - .27d_p \\ \dfrac{k_{bed} - k_{wall}}{(.27d_p)^2}(R_w - r)^2 + k_{wall} \quad for:\ R - .27d_p < r < R_w \end{cases}$$

Since this value was determined after observing the temperature gradients from CFD it was necessary to see how much of an effect this value had on the overall equation. Figure 37 shows the difference between values of $.24d_p$, $.27d_p$, $.30d_p$.

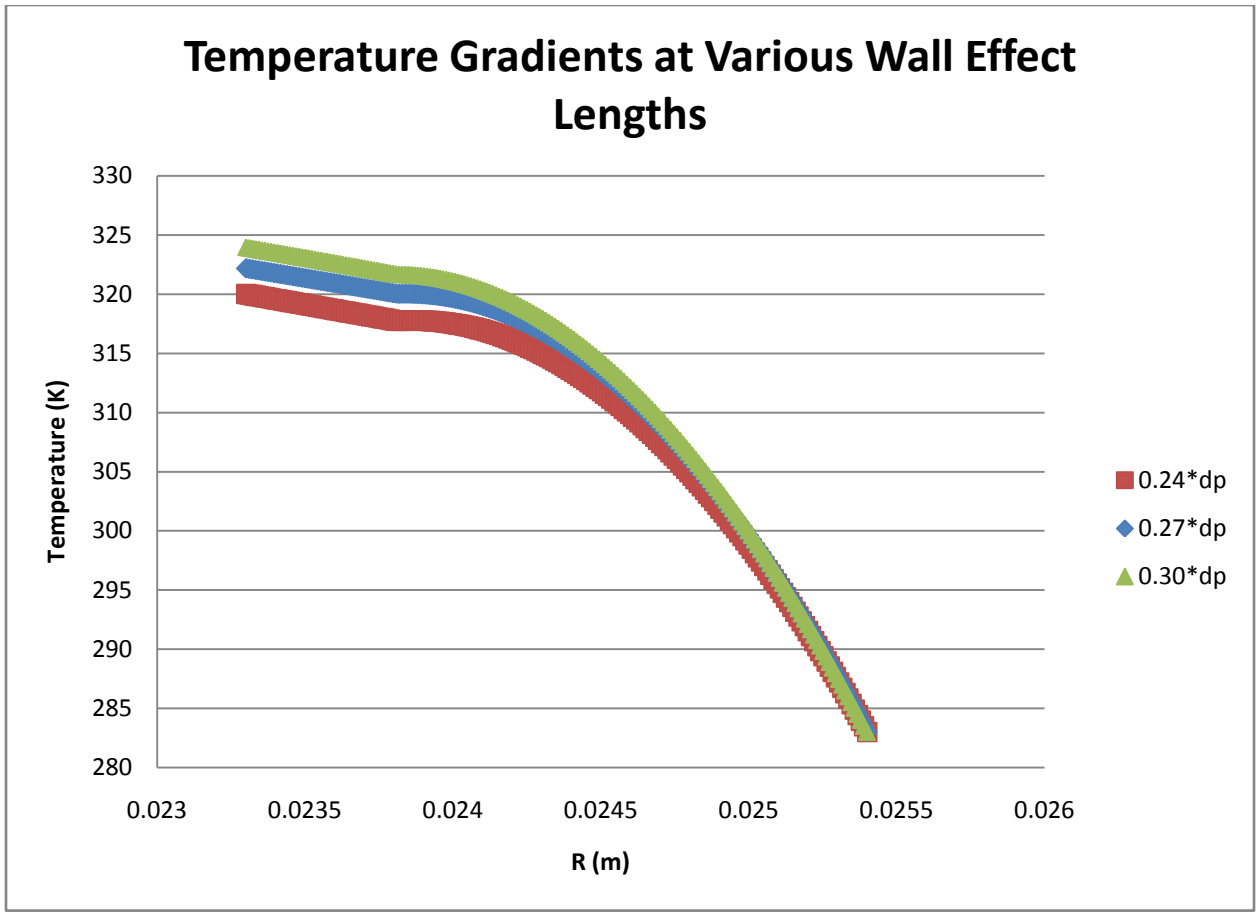

Figure 37- Size of Wall Effects Alteration in COMSOL

As shown above in Figure 37, the discrepancy between a wall effect length differing by 10% was minimal. The points on the graph that were farthest apart from that of $.27d_p$ had less than 1% difference.

9 Conclusions and Recommendations

The main goal of this project was to more accurately predict the temperature gradient across a packed bed. This was completed by creating a function to describe the behavior of effective radial thermal conductivity. By using the two-region approach our team was able to create this expression by using a piecewise function, one to describe thermal conductivity in the bed center region, and one to describe the quadratic behavior of the near-wall region. After inputting calculated thermal conductivities into COMSOL and comparing the resulting temperature gradients with those found experimentally and through CFD it could be seen that while not exact, our results show a promising step towards more accurately describing heat transfer across fixed bed reactor tubes.

In our attempt to accomplish our goal our team used two different methods, each with their own findings and recommendations for the future. The first to be discussed is the CFD modeling of the near-wall region. The model used was only 1.5 particle diameters perpendicular to the wall and 5 particle diameters in the direction of flow due to lack of computer resources and time. In future adaptations of this CFD research a larger model could better show length effects and temperature gradients farther away from the wall. This could alter the effective radial thermal conductivity near the wall. Also, in our model we used bridge sizes of 0.03, 0.04, and 0.05 in. and no significant difference was seen. This does not, however, completely rule out that bridges may affect the temperature gradient calculations in CFD modeling and smaller or larger bridge sizes should be tested. More precise research on either of these issues could lead to more accurately describe fixed bed reactor tube temperature gradients.

The experimental portion of this project focused on determining a thermal conductivity coefficient for the center of the packed bed. The largest experimental error was found in obtaining an accurate inlet temperature profile to the bed; this was due to large amounts of heat loss in the calming section. To adjust for this error we recommend changing one of two things; either a different experimental setup or collecting data at more applicable packing heights. We recommend that future research be completed on either a new column setup or one that minimizes the heat loss in the calming section. Ideally, this would result in a constant inlet air temperature, which would allow analysis using the basic PF model. If this cannot be achieved, we would recommend collecting data at a broader range of packing heights. The IPPF model assumes a minimum packing height of 1.5 times the tube diameter as the inlet temperature profile, which was not the case in this project. This would allow the IPPF model to analyze the data sets much more accurately. In addition we recommend that experimentation be done using different packing materials; the spherical particles used in this project are not necessarily representative of real world steam-methane reform applications. We expect that the difference in shape between particles will make a significant difference in predicting the temperature profiles in a packed bed.

10 References

Borkink, J.G.H, Borman, P.C., Westerterp, K.R. (1993). Modeling of radial heat transport in wall-cooled packed beds. *Chemical Engineering Communications, 121*, 135-155.

Borkink, J. G. H., Westerterp, K. R. (1994). Significance of the radial porosity profile for the description of heat transport in wall-cooled packed beds. *Chemical Engineering Science, 49*, 863-876.

De Wasch, A.P., Froment, G.F. (1972). Heat transfer in packed beds. *Chemical Engineering Science, 27*, 567-576.

Dixon, A. G. (1985). The length effect on packed bed effective heat transfer parameters. *Chemical Engineering Journal, 31*,163-173.

Dixon, Anthony G., Nijemeisland, Michiel, Stitt, E. Hugh (2006). Packed tubular reactor modeling and catalyst design using computational fluid dynamics. *Advance in Chemical Engineering, 31*, 307-389.

Freiwald, M.G., Paterson, W.R. (1992). Accuracy of model predictions and reliability of experimental data for heat transfer in packed beds. *Chemical Engineering Science, 47*,1545–1560.

Guardo, A., Coussirat, M., Recesens, F., Larrayoz, M. A., Excaler, X. (2006). CFD study on particle-to-fluid heat transfer in fixed bed reactors: Convective heat transfer at low and high pressure. *Chemical Engineering Science, 61*, 4341-4353.

Gunn, D. J., Ahmad, M. M., Sabri, M. N. (1987). Radial heat transfer to fixed beds of particles. *Chemical Engineering Science,42*, 2163-2171.

Hartstein, Arthur. *Hydrogen Production from Natural Gas.* June 2, 2003 at the Hydrogen Coordination Meeting.

Kuroki, M., Ookawara, S., Street, D., Ogawa, K. (2007). High-fidelity CFD modeling of particle-to-fluid heat transfer in packed bed reactors. *ECCE-6, Copenhage*n, 16-21 September, 2007.

Li, Chi-Hsiung, Finlayson, B.A. (1977). Heat transfer in packed beds- a reevaluation. *Chemical Engineering Science. 32*, 1055-1066.

Logtenberg, S. A., Nijemeisland, M., Dixon, A. G. (1999). Computational fluid dynamics simulations of fluid flow and heat transfer at the wall-particle contact points in a fixed-bed reactor. *Chemical Engineering Science, 54*, 2433-2439.

Nijemeisland, Michiel, Dixon, Anthony G. (2001). Comparison of CFD simulations to experiment for convective heat transfer in a gas-solid fixed bed. *Chemical Engineering Journal, 82*, 231-246.

Ookawara, S., Kuroki, M., Street, D., Ogawa, K. (2007). High-fidelity DEM-CFD modeling of a packed bed reactors for process intensification. *ECCE-6, Copenhagen,* 16-21 September, 2007.

Padro, C.E.G. and V. Putsche. *Survey of the Economics of Hydrogen Technologies.* National Renewable Energy Laboratory. September 1999.

Schuler, R. W., Stallings, V. P., Smith, J. M. (1952). Heat and mass transfer in fixed bed reactors. *Chem. Engng Prog. Symp. Ser. 4*, 48, 19.

Smirnov, E.I., Muzykantov, A.V., Kuzmin, V.A., Kronberg, A.E., Zolotarskii, I.A. (2003a). Radial Heat Transfer in Packed Beds of Spheres, Cylinders and Rashig Rings Verification of Model with a Linear Variation of λ_{er} in the Vicinity of the Wall. *Chemical Engineering Journal, 91*,243-248.

Smirnov, E. I., Muzykantov, A. V., Kuzmin, V. A., Zolotarskii, I. A., Koning, G. W., Kronberg, A. E. (2003b). Radial heat transfer in packed beds of shaped particles. *Chemistry for Sustainable Development, 11*, 293-296.

Tobis, J, Ziolkowski, D (1988). Modeling of heat transfer at the wall of a packed-bed apparatus. *Chemical Engineering Science, 43*, 3031-3036.

Tsotsas, E., & Schlünder, E. U. (1990). Heat transfer in packed beds with fluid flow: remarks on the meaning and the calculation of a heat transfer coefficient at the wall. *Chemical Engineering Science, 45*, 819-837.

von Scala, C., Wehrli, M., Gaiser, G. (1999). Heat transfer measurements and simulation of KATAPAK-M® catalyst supports. *Chemical Engineering Science, 54*, 1375-1381.

Vortmeyer, D, Haidegger, E.(1991). Discrimination of three approaches to evaluate heat fluxes for wall-cooled fixed bed chemical reactors. *Chemical Engineering Science, 46*, 2651–2660.

Winterberg, M., Tsotsas, E., Krischke, A., Vortmeyer, D. (2000). A simple and coherent set of coefficients for modeling of heat and mass transport with and without chemical reaction in tubes filled with spheres. *Chemical Engineering Science, 55*, 967-979.

11 Appendix

Appendix A: Sample Journal File from Gambit 2.4.6

```
/ Journal File for GAMBIT 2.4.6, Database 2.4.4, lnamd64 SP2007051420
/ Identifier "wall05long"
/ File opened for write Wed Feb 18 10:18:10 2009.
identifier name "wall05long" new nosaveprevious
volume create radius 0.125 sphere
volume cmove "volume.1" multiple 1 offset 0.125 0.125 0.125
volume cmove "volume.1" multiple 1 offset 0.375 0.125 0.125
volume cmove "volume.1" multiple 1 offset 0.625 0.125 0.125
volume cmove "volume.1" multiple 1 offset 0.875 0.125 0.125
volume cmove "volume.1" multiple 1 offset 1.125 0.125 0.125
volume cmove "volume.1" multiple 1 offset 0.25 0.341506 0.125
volume cmove "volume.1" multiple 1 offset 0.5 0.341506 0.125
volume cmove "volume.1" multiple 1 offset 0.75 0.341506 0.125
volume cmove "volume.1" multiple 1 offset 1 0.341506 0.125
volume cmove "volume.1" multiple 1 offset 1.25 0.341506 0.125
volume cmove "volume.1" multiple 1 offset 0.125 0.558013 0.125
volume cmove "volume.1" multiple 1 offset 0.375 0.558013 0.125
volume cmove "volume.1" multiple 1 offset 0.625 0.558013 0.125
volume cmove "volume.1" multiple 1 offset 0.875 0.558013 0.125
volume cmove "volume.1" multiple 1 offset 1.125 0.558013 0.125
volume cmove "volume.1" multiple 1 offset 0.25 0.072169 0.329124
volume cmove "volume.1" multiple 1 offset 0.5 0.072169 0.329124
volume cmove "volume.1" multiple 1 offset 0.75 0.072169 0.329124
volume cmove "volume.1" multiple 1 offset 1 0.072169 0.329124
volume cmove "volume.1" multiple 1 offset 1.25 0.072169 0.329124
volume cmove "volume.1" multiple 1 offset 0.125 0.288675 0.329124
volume cmove "volume.1" multiple 1 offset 0.375 0.288675 0.329124
volume cmove "volume.1" multiple 1 offset 0.625 0.288675 0.329124
volume cmove "volume.1" multiple 1 offset 0.875 0.288675 0.329124
volume cmove "volume.1" multiple 1 offset 1.125 0.288675 0.329124
volume cmove "volume.1" multiple 1 offset 0.25 0.505181 0.329124
volume cmove "volume.1" multiple 1 offset 0.5 0.505181 0.329124
volume cmove "volume.1" multiple 1 offset 0.75 0.505181 0.329124
volume cmove "volume.1" multiple 1 offset 1 0.505181 0.329124
volume cmove "volume.1" multiple 1 offset 1.25 0.505181 0.329124
volume delete "volume.1" lowertopology
volume cmove "volume.27" "volume.28" "volume.29" "volume.30" "volume.31" \
  "volume.26" "volume.25" "volume.24" "volume.23" "volume.22" multiple 1 \
  offset 0 0.433013 0
volume move "volume.38" offset 0 0 -0.045
volume delete "volume.16" "volume.15" lowertopology
window modify shade
volume move "volume.17" offset 0 0 -0.045
volume delete "volume.3" "volume.2" lowertopology
window modify noshade
volume create width 1.5 depth 2 height 0.433013 brick
volume move "volume.42" offset 0 0 0.25
volume move "volume.42" dangle 90 vector 0 0 1 origin 0 0 0
volume move "volume.42" offset 0.375 0 0
volume delete "volume.42" lowertopology
volume create width 0.125 depth 0.125 height 0.125 brick
volume delete "volume.42" lowertopology
volume create width 0.04 depth 0.04 height 0.04 brick
volume move "volume.42" offset 0 0 0.33
volume move "volume.42" offset 0 0 0.125
volume move "volume.42" offset 0.125 0 0
volume move "volume.42" offset 0.5 0 0
volume move "volume.42" offset 0.125 0 0
volume delete "volume.42" lowertopology
volume create width 0.04 depth 0.04 height 0.04 brick
volume move "volume.42" offset 0.25 0.125 0.125
volume cmove "volume.42" multiple 1 offset 0.25 0 0
volume cmove "volume.43" multiple 1 offset 0.25 0 0
volume cmove "volume.44" multiple 1 offset 0.25 0 0
volume delete "volume.43" "volume.42" lowertopology
volume create width 0.04 depth 0.04 height 0.04 brick
```

```
volume cmove "volume.46" multiple 1 offset 0.375 0.341506 0.125
volume cmove "volume.47" multiple 1 offset 0.25 0 0
volume cmove "volume.48" multiple 1 offset 0.25 0 0
volume cmove "volume.49" multiple 1 offset 0.25 0 0
volume cmove "volume.46" multiple 1 offset 0.25 0.558012 0.125
volume cmove "volume.51" multiple 1 offset 0.25 0 0
volume cmove "volume.46" multiple 1 offset 0.375 0.072169 0.329124
volume cmove "volume.53" multiple 1 offset 0.25 0 0
volume cmove "volume.54" multiple 1 offset 0.25 0 0
volume cmove "volume.55" multiple 1 offset 0.25 0 0
volume cmove "volume.46" multiple 1 offset 0.25 0.288675 0.329124
volume cmove "volume.57" multiple 1 offset 0.25 0 0
volume cmove "volume.58" multiple 1 offset 0.25 0 0
volume cmove "volume.59" multiple 1 offset 0.25 0 0
volume cmove "volume.46" multiple 1 offset 0.375 0.505181 0.329124
volume cmove "volume.61" multiple 1 offset 0.25 0 0
volume cmove "volume.62" multiple 1 offset 0.25 0 0
volume cmove "volume.63" multiple 1 offset 0.25 0 0
volume cmove "volume.46" multiple 1 offset 0.25 0.721687 0.329124
volume cmove "volume.65" multiple 1 offset 0.25 0 0
volume cmove "volume.66" multiple 1 offset 0.25 0 0
volume cmove "volume.67" multiple 1 offset 0.25 0 0
volume cmove "volume.65" multiple 1 offset 0.125 0.216506 0
volume cmove "volume.69" multiple 1 offset 0.25 0 0
volume cmove "volume.70" multiple 1 offset 0.25 0 0
volume cmove "volume.71" multiple 1 offset 0.25 0 0
volume delete "volume.45" "volume.53" lowertopology
volume delete "volume.67" "volume.68" lowertopology
volume cmove "volume.46" multiple 1 offset 0.3125 0.233253 0.125
volume cmove "volume.73" multiple 1 offset 0.125 0 0
volume cmove "volume.74" multiple 1 offset 0.125 0 0
volume delete "volume.73" "volume.74" lowertopology
coordinate create "angle" cartesian oldsystem "c_sys.1" offset 0 0 0 axis1 \
  "x" angle1 0 axis2 "y" angle2 109.5 axis3 "z" angle3 0 rotation
coordinate activate "c_sys.1"
coordinate activate "angle"
coordinate activate "c_sys.1"
volume create width 0.04 depth 0.04 height 0.04 brick
coordinate activate "angle"
volume delete "volume.46" lowertopology
volume delete "volume.76" lowertopology
coordinate activate "c_sys.1"
volume create width 0.04 depth 0.04 height 0.04 brick
coordinate activate "angle"
volume delete "volume.76" lowertopology
volume create width 0.04 depth 0.04 height 0.04 brick
coordinate delete "angle"
coordinate create "Angle" cartesian oldsystem "c_sys.1" offset 0 0 0 axis1 \
  "x" angle1 0 axis2 "y" angle2 0 axis3 "z" angle3 109.5 rotation
volume delete "volume.76" lowertopology
volume create width 0.04 depth 0.04 height 0.04 brick
volume move "volume.76" offset 0.1141564934735 -0.2393340656861 0.125
volume move "volume.76" offset -0.08345171480844 -0.235660372773 0
volume cmove "volume.76" multiple 1 offset -0.08345171480844 -0.235660372773 \
  0
volume cmove "volume.77" multiple 1 offset -0.08345171480844 -0.235660372773 \
  0
volume cmove "volume.78" multiple 1 offset -0.08345171480844 -0.235660372773 \
  0
coordinate activate "c_sys.1"
volume cmove "volume.76" "volume.77" "volume.78" "volume.79" multiple 1 \
  offset -0.125 0.216506 0
volume cmove "volume.80" "volume.81" "volume.82" "volume.83" multiple 1 \
  offset -0.125 0.216506 0
volume delete "volume.87" lowertopology
volume delete "volume.86" lowertopology
volume delete "volume.76" lowertopology
coordinate create "Angle2" cartesian oldsystem "c_sys.1" offset 0 0 0 axis1 \
  "x" angle1 0 axis2 "y" angle2 0 axis3 "z" angle3 -109.5 rotation
coordinate activate "Angle2"
volume create width 0.04 depth 0.04 height 0.04 brick
```

```
coordinate activate "c_sys.1"
volume delete "volume.80" "volume.85" "volume.84" "volume.81" "volume.82" \
  "volume.83" "volume.77" "volume.78" "volume.79" lowertopology
volume delete "volume.75" lowertopology
coordinate delete "Angle2" "Angle"
coordinate create "Angle 1" cartesian oldsystem "c_sys.1" offset 0 0 0 axis1 \
  "x" angle1 0 axis2 "y" angle2 0 axis3 "z" angle3 60 rotation
volume delete "volume.86" lowertopology
volume create width 0.04 depth 0.04 height 0.04 brick
coordinate activate "c_sys.1"
volume move "volume.73" offset 0.6875 0.233253 0.125
coordinate activate "Angle 1"
coordinate activate "c_sys.1"
volume cmove "volume.73" multiple 1 offset 0.25 0 0
volume cmove "volume.74" multiple 1 offset 0.25 0 0
volume cmove "volume.73" "volume.74" "volume.75" multiple 1 offset -0.125 \
  0.216506 0
volume move "volume.76" "volume.77" "volume.78" offset -0.25 0 0
volume delete "volume.78" lowertopology
coordinate create "Angle2" cartesian oldsystem "c_sys.1" offset 0 0 0 axis1 \
  "x" angle1 0 axis2 "y" angle2 0 axis3 "z" angle3 -60 rotation
volume create width 0.04 depth 0.04 height 0.04 brick
coordinate activate "c_sys.1"
volume move "volume.78" offset 0.5625 0.233253 0.125
volume cmove "volume.78" multiple 1 offset 0.25 0 0
volume cmove "volume.79" multiple 1 offset 0.25 0 0
volume cmove "volume.78" "volume.79" "volume.80" multiple 1 offset -0.125 \
  0.216506 0
volume delete "volume.83" lowertopology
volume cmove "volume.81" multiple 1 offset -0.25 0 0
coordinate activate "Angle 1"
volume create width 0.04 depth 0.04 height 0.04 brick
coordinate activate "c_sys.1"
volume move "volume.84" offset 0.3125 0.180422 0
volume move "volume.84" offset 0.25 0 0
volume cmove "volume.84" multiple 1 offset 0.25 0 0
volume cmove "volume.85" multiple 1 offset 0.25 0 0
volume cmove "volume.84" "volume.85" "volume.86" multiple 1 offset -0.125 \
  0.216506 0
volume cmove "volume.89" multiple 1 offset 0.25 0 0
volume cmove "volume.87" multiple 1 offset -0.25 0 0
volume cmove "volume.91" "volume.87" "volume.88" "volume.89" "volume.90" \
  multiple 1 offset -0.125 0.216506 0
volume delete "volume.81" "volume.92" lowertopology
volume move "volume.93" "volume.94" "volume.95" "volume.96" "volume.90" \
  "volume.89" "volume.88" "volume.86" offset 0 0 0.329124
volume move "volume.87" "volume.84" offset 0 0 0.329124
volume move "volume.91" "volume.85" offset 0 0 0.329124
volume delete "volume.91" "volume.95" lowertopology
volume cmove "volume.93" "volume.94" "volume.96" multiple 1 offset 0.125 \
  0.216506 0
volume cmove "volume.98" multiple 1 offset 0.25 0 0
volume cmove "volume.97" multiple 1 offset -0.25 0 0
volume delete "volume.100" lowertopology
coordinate activate "Angle2"
volume create width 0.04 depth 0.04 height 0.04 brick
coordinate activate "c_sys.1"
volume move "volume.102" offset 0.1875 0.180422 0.329124
volume move "volume.102" offset 0.25 0 0
volume cmove "volume.102" multiple 1 offset 0.25 0 0
volume cmove "volume.103" multiple 1 offset 0.25 0 0
volume cmove "volume.104" multiple 1 offset 0.25 0 0
volume cmove "volume.105" "volume.104" "volume.103" "volume.102" multiple 1 \
  offset -0.125 0.216506 0
volume cmove "volume.109" "volume.108" "volume.107" "volume.106" multiple 1 \
  offset -0.125 0.216506 0
volume move "volume.113" offset 0.25 0 0
volume cmove "volume.110" "volume.111" "volume.112" multiple 1 offset 0.125 \
  0.216506 0
volume move "volume.116" offset 0.25 0 0
volume cmove "volume.87" multiple 1 offset -0.25 0 0
```

```
volume move "volume.32" "volume.33" "volume.34" "volume.35" "volume.36" \
  "volume.37" "volume.38" "volume.39" "volume.40" "volume.41" "volume.27" \
  "volume.28" "volume.29" "volume.30" "volume.31" "volume.26" "volume.25" \
  "volume.24" "volume.23" "volume.22" "volume.17" "volume.18" "volume.19" \
  "volume.20" "volume.21" "volume.101" "volume.114" "volume.97" "volume.115" \
  "volume.69" "volume.70" "volume.98" "volume.71" "volume.72" "volume.116" \
  "volume.99" "volume.113" "volume.96" "volume.112" "volume.94" "volume.66" \
  "volume.111" "volume.93" "volume.65" "volume.110" "volume.117" "volume.109" \
  "volume.87" "volume.108" "volume.88" "volume.107" "volume.89" "volume.106" \
  "volume.90" "volume.64" "volume.63" "volume.62" "volume.61" "volume.57" \
  "volume.58" "volume.59" "volume.60" "volume.105" "volume.86" "volume.104" \
  "volume.85" "volume.103" "volume.84" "volume.102" "volume.54" "volume.55" \
  "volume.56" offset 0 -0.027965 0
volume cmove "volume.44" multiple 1 offset 0.25 0 0
default set "GRAPHICS.GENERAL.CONNECTIVITY_BASED_COLORING" numeric 1
default set "GRAPHICS.GENERAL.CONNECTIVITY_BASED_COLORING" numeric 0
default set "GRAPHICS.GENERAL.CONNECTIVITY_BASED_COLORING" numeric 1
default set "GRAPHICS.GENERAL.CONNECTIVITY_BASED_COLORING" numeric 0
default set "GRAPHICS.GENERAL.CONNECTIVITY_BASED_COLORING" numeric 1
default set "GRAPHICS.GENERAL.CONNECTIVITY_BASED_COLORING" numeric 0
default set "GRAPHICS.GENERAL.CONNECTIVITY_BASED_COLORING" numeric 1
default set "GRAPHICS.GENERAL.CONNECTIVITY_BASED_COLORING" numeric 0
default set "GRAPHICS.GENERAL.CONNECTIVITY_BASED_COLORING" numeric 1
default set "GRAPHICS.GENERAL.CONNECTIVITY_BASED_COLORING" numeric 0
default set "GRAPHICS.GENERAL.CONNECTIVITY_BASED_COLORING" numeric 1
default set "GRAPHICS.GENERAL.CONNECTIVITY_BASED_COLORING" numeric 0
volume modify "volume.38" "volume.17" color "yellow"
volume modify "volume.4" "volume.5" "volume.6" "volume.7" "volume.8" \
  "volume.9" "volume.10" "volume.11" "volume.12" "volume.13" "volume.14" \
  color "cyan"
volume modify "volume.73" "volume.74" "volume.75" "volume.76" "volume.77" \
  "volume.78" "volume.79" "volume.80" "volume.82" "volume.83" "volume.4" \
  "volume.5" "volume.6" "volume.7" "volume.8" "volume.9" "volume.10" \
  "volume.11" "volume.12" "volume.13" "volume.14" "volume.47" "volume.48" \
  "volume.49" "volume.50" "volume.51" "volume.52" "volume.44" "volume.118" \
  color "cyan"
volume cmove "volume.83" multiple 1 offset 0.25 0 0
volume modify "volume.119" color "cyan"
window modify shade
volume create width 0.05 brick
window modify noshade
volume cmove "volume.120" multiple 1 offset 0.3125 0.070604 0.227074
volume cmove "volume.121" multiple 1 offset 0.25 0 0
volume delete "volume.121" "volume.120" lowertopology
coordinate create cartesian oldsystem "c_sys.1" offset 0.5625 0.070604 \
  0.227074 axis1 "x" angle1 0 axis2 "y" angle2 0 axis3 "z" angle3 0 rotation
volume modify "volume.122" color "orange"
volume move "volume.122" dangle 22.3 vector 1 0 0 origin 0 0 0
volume move "volume.122" dangle 33.6 vector 0 1 0 origin 0 0 0
volume move "volume.122" dangle -33.6 vector 0 1 0 origin 0 0 0
volume move "volume.122" dangle -30 vector 0 1 0 origin 0 0 0
volume move "volume.122" offset 0 0.0075 0
volume move "volume.122" offset 0 0.0075 0
volume cmove "volume.122" multiple 1 offset 0.25 0 0
volume cmove "volume.123" multiple 1 offset 0.25 0 0
volume modify "volume.123" "volume.124" color "orange"
volume cmove "volume.122" "volume.123" "volume.124" multiple 1 offset 0.125 \
  0.216506 0
volume modify "volume.125" "volume.127" "volume.126" color "orange"
volume cmove "volume.125" "volume.126" multiple 1 offset -0.5 0 0
volume modify "volume.125" "volume.129" "volume.128" color "orange"
volume cmove "volume.128" "volume.129" multiple 1 offset 0.125 0.216506 0
volume modify "volume.130" "volume.131" color "orange"
coordinate activate "c_sys.1"
volume create width 0.05 brick
coordinate activate "c_sys.4"
volume move "volume.132" offset 0.6875 0.070604 0.227074
coordinate create cartesian oldsystem "c_sys.1" offset 0.6875 0.070604 \
  0.227074 axis1 "x" angle1 0 axis2 "y" angle2 0 axis3 "z" angle3 0 rotation
volume move "volume.132" dangle 22.3 vector 1 0 0 origin 0 0 0
volume move "volume.132" dangle 30 vector 0 1 0 origin 0 0 0
```

```
volume move "volume.132" offset 0 0.01 0
volume move "volume.132" offset 0 0.005 0
volume modify "volume.132" color "grey"
default set "GRAPHICS.GENERAL.CONNECTIVITY_BASED_COLORING" numeric 1
default set "GRAPHICS.GENERAL.CONNECTIVITY_BASED_COLORING" numeric 0
default set "GRAPHICS.GENERAL.CONNECTIVITY_BASED_COLORING" numeric 1
default set "GRAPHICS.GENERAL.CONNECTIVITY_BASED_COLORING" numeric 0
volume cmove "volume.132" multiple 1 offset 0.25 0 0
volume cmove "volume.133" multiple 1 offset 0.25 0 0
volume modify "volume.132" "volume.133" "volume.134" color "grey"
volume cmove "volume.132" "volume.133" "volume.134" multiple 1 offset -0.125 \
  0.216506 0
volume modify "volume.135" "volume.136" "volume.137" color "grey"
volume cmove "volume.135" multiple 1 offset -0.25 0 0
volume modify "volume.138" color "grey"
volume cmove "volume.138" "volume.135" "volume.136" multiple 1 offset -0.125 \
  0.216506 0
volume modify "volume.139" "volume.140" "volume.141" color "grey"
volume move "volume.4" "volume.5" "volume.6" "volume.7" "volume.8" "volume.9" \
  "volume.10" "volume.11" "volume.12" "volume.13" "volume.14" offset 0 0 \
  -0.01
coordinate activate "c_sys.1"
volume create width 0.05 brick
coordinate activate "c_sys.5"
volume delete "volume.142" lowertopology
coordinate activate "c_sys.1"
volume create width 0.05 brick
coordinate activate "c_sys.5"
coordinate activate "c_sys.1"
volume move "volume.142" offset 0.375 0.328557 0.227074
coordinate activate "c_sys.5"
coordinate activate "c_sys.1"
volume delete "volume.142" lowertopology
volume create width 0.05 brick
volume move "volume.142" offset 0.375 0.328557 0.227074
volume delete "volume.142" lowertopology
volume create width 0.05 brick
volume move "volume.142" offset 0.625 0.192863 0.227074
coordinate create cartesian oldsystem "c_sys.1" offset 0.625 0.192863 \
  0.227074 axis1 "x" angle1 0 axis2 "y" angle2 0 axis3 "z" angle3 0 rotation
volume move "volume.142" dangle -33 vector 1 0 0 origin 0 0 0
coordinate activate "c_sys.1"
volume cmove "volume.142" multiple 1 offset 0.25 0 0
coordinate activate "c_sys.6"
coordinate activate "c_sys.1"
volume delete "volume.143" lowertopology
volume cmove "volume.142" multiple 1 offset 0.25 0 0
volume cmove "volume.143" multiple 1 offset 0.25 0 0
volume modify "volume.142" "volume.143" "volume.144" color "white"
volume cmove "volume.142" "volume.143" "volume.144" multiple 1 offset 0.125 \
  0.216506 0
volume modify "volume.145" "volume.146" "volume.147" color "white"
volume cmove "volume.145" "volume.146" multiple 1 offset -0.5 0 0
volume modify "volume.148" "volume.149" color "white"
volume cmove "volume.149" "volume.148" "volume.145" multiple 1 offset -0.125 \
  0.216506 0
volume modify "volume.150" "volume.151" "volume.152" color "white"
volume cmove "volume.13" "volume.14" "volume.152" "volume.150" "volume.130" \
  "volume.140" "volume.119" "volume.77" "volume.82" "volume.131" "volume.141" \
  "volume.76" "volume.52" multiple 1 offset -0.125 0.216506 0
volume modify "volume.156" "volume.155" color "white"
volume modify "volume.158" "volume.163" color "grey"
volume modify "volume.153" "volume.154" color "cyan"
volume modify "volume.165" color "cyan"
volume modify "volume.157" "volume.162" color "orange"
volume modify "volume.164" "volume.159" color "cyan"
volume modify "volume.160" "volume.161" color "cyan"
volume cmove "volume.153" "volume.154" "volume.156" "volume.155" "volume.157" \
  "volume.162" "volume.158" "volume.163" "volume.165" "volume.159" \
  "volume.164" "volume.160" "volume.161" multiple 1 offset 0.125 0.216506 0
volume cmove "volume.170" "volume.172" "volume.166" "volume.176" "volume.175" \
```

```
  "volume.174" "volume.169" "volume.167" "volume.171" "volume.173" \
  "volume.178" "volume.177" multiple 1 offset 0.5 0 0
volume cmove "volume.174" multiple 1 offset 0.25 0 0
volume cmove "volume.166" "volume.168" "volume.170" "volume.172" "volume.175" \
  "volume.174" multiple 1 offset -0.25 0 0
volume modify "volume.166" "volume.192" "volume.167" "volume.181" \
  "volume.186" color "cyan"
volume cmove "volume.10" "volume.146" "volume.126" "volume.137" "volume.74" \
  "volume.80" multiple 1 offset 0.125 0.216506 0
volume modify "volume.198" color "cyan"
volume cmove "volume.198" "volume.199" "volume.200" "volume.202" multiple 1 \
  offset 0.125 0.216506 0
volume modify "volume.204" color "cyan"
volume delete "volume.194" "volume.193" "volume.168" "volume.169" \
  "volume.185" lowertopology
volume delete "volume.178" "volume.182" "volume.183" "volume.190" \
  lowertopology
volume unite volumes "volume.4" "volume.5" "volume.6" "volume.7" "volume.8" \
  "volume.9" "volume.10" "volume.11" "volume.12" "volume.13" "volume.14" \
  "volume.18" "volume.19" "volume.20" "volume.21" "volume.22" "volume.23" \
  "volume.24" "volume.25" "volume.26" "volume.27" "volume.28" "volume.29" \
  "volume.30" "volume.31" "volume.32" "volume.33" "volume.34" "volume.35" \
  "volume.36" "volume.37" "volume.39" "volume.40" "volume.41" "volume.44" \
  "volume.47" "volume.48" "volume.49" "volume.50" "volume.51" "volume.52" \
  "volume.54" "volume.55" "volume.56" "volume.57" "volume.58" "volume.59" \
  "volume.60" "volume.61" "volume.62" "volume.63" "volume.64" "volume.65" \
  "volume.66" "volume.69" "volume.70" "volume.71" "volume.72" "volume.73" \
  "volume.74" "volume.75" "volume.76" "volume.77" "volume.78" "volume.79" \
  "volume.80" "volume.82" "volume.83" "volume.84" "volume.85" "volume.86" \
  "volume.87" "volume.88" "volume.89" "volume.90" "volume.93" "volume.94" \
  "volume.96" "volume.97" "volume.98" "volume.99" "volume.101" "volume.102" \
  "volume.103" "volume.104" "volume.105" "volume.106" "volume.107" \
  "volume.108" "volume.109" "volume.110" "volume.111" "volume.112" \
  "volume.113" "volume.114" "volume.115" "volume.116" "volume.117" \
  "volume.118" "volume.119" "volume.122" "volume.123" "volume.124" \
  "volume.125" "volume.126" "volume.127" "volume.128" "volume.129" \
  "volume.130" "volume.131" "volume.132" "volume.133" "volume.134" \
  "volume.135" "volume.136" "volume.137" "volume.138" "volume.139" \
  "volume.140" "volume.141" "volume.142" "volume.143" "volume.144" \
  "volume.145" "volume.146" "volume.147" "volume.148" "volume.149" \
  "volume.150" "volume.151" "volume.152" "volume.153" "volume.154" \
  "volume.155" "volume.156" "volume.157" "volume.158" "volume.159" \
  "volume.160" "volume.161" "volume.162" "volume.163" "volume.164" \
  "volume.165" "volume.166" "volume.167" "volume.170" "volume.171" \
  "volume.172" "volume.173" "volume.174" "volume.175" "volume.176" \
  "volume.177" "volume.179" "volume.180" "volume.181" "volume.184" \
  "volume.186" "volume.187" "volume.188" "volume.189" "volume.191" \
  "volume.192" "volume.195" "volume.196" "volume.197" "volume.198" \
  "volume.199" "volume.200" "volume.201" "volume.202" "volume.203" \
  "volume.204" "volume.205" "volume.206" "volume.207"
volume create width 0.875 depth 1.8 height 0.3291 brick
volume move "volume.39" offset 0 0.7 0
volume move "volume.39" offset 0.6875 0 0
volume move "volume.39" offset 0 0 0.004
volume move "volume.39" offset 0 0 0.001
volume move "volume.39" offset 0 0 -0.0005
volume move "volume.39" offset 0 0 -0.0005
volume delete "volume.39" lowertopology
volume create width 0.875 depth 1.8 height 0.3291 brick
volume move "volume.39" offset 0 0 0.125
volume move "volume.39" offset 0 0.7 0
volume move "volume.39" offset 0.6875 0 0
volume move "volume.39" offset 0 0 0.004
window modify noshade
volume move "volume.39" offset 0 0 0.14
volume move "volume.39" offset 0 0 0.02
volume create width 0.05 brick
volume move "volume.40" offset 0.25 0.044204 0.454124
volume move "volume.40" offset 0.25 0 0
volume cmove "volume.40" multiple 1 offset 0.25 0 0
volume cmove "volume.41" multiple 1 offset 0.25 0 0
```

```
volume cmove "volume.42" multiple 1 offset 0.25 0 0
volume cmove "volume.40" "volume.41" "volume.42" "volume.43" multiple 1 \
  offset -0.125 0.216506 0
volume cmove "volume.44" multiple 1 offset -0.25 0 0
volume cmove "volume.48" "volume.44" "volume.45" "volume.46" "volume.47" \
  multiple 1 offset 0.125 0.216506 0
volume cmove "volume.51" "volume.50" "volume.49" multiple 1 offset -0.125 \
  0.216506 0
volume cmove "volume.56" "volume.55" "volume.54" multiple 1 offset 0.125 \
  0.216506 0
volume cmove "volume.58" "volume.59" multiple 1 offset 0.5 0 0
volume cmove "volume.61" multiple 1 offset -0.125 -0.216506 0
volume unite volumes "volume.4" "volume.57" "volume.58" "volume.59" \
  "volume.60" "volume.61" "volume.62" "volume.54" "volume.55" "volume.56" \
  "volume.49" "volume.50" "volume.51" "volume.52" "volume.53" "volume.47" \
  "volume.46" "volume.45" "volume.44" "volume.48" "volume.40" "volume.41" \
  "volume.42" "volume.43"
volume split "volume.4" faces "face.1274" connected
volume split "volume.4" faces "face.1271" connected
volume split "volume.4" faces "face.1273" connected
volume split "volume.4" faces "face.1276" connected
volume delete "volume.4" lowertopology
volume delete "volume.43" "volume.42" "volume.44" "volume.41" "volume.45" \
  "volume.40" lowertopology
volume delete "volume.49" "volume.48" "volume.50" "volume.47" "volume.46" \
  lowertopology
volume delete "volume.54" "volume.52" "volume.51" lowertopology
volume split "volume.17" faces "face.1273" connected
volume delete "volume.54" lowertopology
volume subtract "volume.39" volumes "volume.53" keeptool
volume subtract "volume.39" volumes "volume.38" "volume.17" keeptool
face connect "face.38" "face.1271" "face.1272" "face.1275" "face.4" "face.6" \
  "face.8" "face.10" "face.18" "face.19" "face.20" "face.23" "face.24" \
  "face.25" "face.26" "face.28" "face.29" "face.30" "face.33" "face.34" \
  "face.35" "face.37" "face.39" "face.40" "face.54" "face.72" "face.78" \
  "face.84" "face.92" "face.102" "face.114" "face.116" "face.120" "face.122" \
  "face.128" "face.132" "face.134" "face.138" "face.140" "face.144" \
  "face.146" "face.150" "face.152" "face.156" "face.158" "face.162" \
  "face.164" "face.168" "face.170" "face.176" "face.184" "face.186" \
  "face.190" "face.204" "face.206" "face.210" "face.212" "face.216" \
  "face.218" "face.224" "face.230" "face.233" "face.234" "face.246" \
  "face.248" "face.252" "face.254" "face.263" "face.264" "face.270" \
  "face.274" "face.282" "face.286" "face.296" "face.299" "face.300" \
  "face.302" "face.306" "face.308" "face.312" "face.314" "face.318" \
  "face.320" "face.324" "face.326" "face.348" "face.350" "face.354" \
  "face.356" "face.366" "face.368" "face.372" "face.376" "face.378" \
  "face.382" "face.405" "face.407" "face.408" "face.412" "face.414" \
  "face.418" "face.426" "face.430" "face.432" "face.436" "face.438" \
  "face.442" "face.444" "face.448" "face.456" "face.460" "face.462" \
  "face.466" "face.474" "face.476" "face.480" "face.482" "face.486" \
  "face.488" "face.498" "face.500" "face.504" "face.526" "face.527" \
  "face.531" "face.532" "face.537" "face.538" "face.543" "face.544" \
  "face.549" "face.550" "face.567" "face.568" "face.573" "face.574" \
  "face.579" "face.580" "face.584" "face.586" "face.591" "face.592" \
  "face.603" "face.604" "face.609" "face.610" "face.615" "face.616" \
  "face.621" "face.622" "face.633" "face.634" "face.639" "face.640" \
  "face.644" "face.646" "face.651" "face.652" "face.657" "face.663" \
  "face.664" "face.669" "face.670" "face.687" "face.688" "face.693" \
  "face.694" "face.705" "face.706" "face.709" "face.714" "face.715" \
  "face.721" "face.732" "face.733" "face.734" "face.740" "face.742" \
  "face.746" "face.750" "face.756" "face.757" "face.762" "face.763" \
  "face.770" "face.772" "face.777" "face.794" "face.795" "face.800" \
  "face.801" "face.806" "face.807" "face.812" "face.813" "face.814" \
  "face.820" "face.826" "face.828" "face.832" "face.834" "face.848" \
  "face.854" "face.869" "face.886" "face.887" "face.906" "face.908" \
  "face.941" "face.943" "face.954" "face.955" "face.962" "face.964" \
  "face.1000" "face.1002" "face.1004" "face.1007" "face.1008" "face.1009" \
  "face.1010" "face.1011" "face.1015" "face.1016" "face.1017" "face.1018" \
  "face.1019" "face.1020" "face.1021" "face.1022" "face.1023" "face.1024" \
  "face.1025" "face.1026" "face.1027" "face.1029" "face.1031" "face.1032" \
  "face.1033" "face.1034" "face.1035" "face.1036" "face.1037" "face.1038" \
```

```
"face.1039" "face.1042" "face.1044" "face.1048" "face.1050" "face.1056" \
"face.1061" "face.1062" "face.1063" "face.1064" "face.1065" "face.1066" \
"face.1067" "face.1068" "face.1069" "face.1070" "face.1071" "face.1072" \
"face.1075" "face.1076" "face.1077" "face.1078" "face.1079" "face.1080" \
"face.1081" "face.1082" "face.1083" "face.1084" "face.1089" "face.1090" \
"face.1091" "face.1092" "face.1093" "face.1094" "face.1097" "face.1098" \
"face.1099" "face.1100" "face.1101" "face.1102" "face.1103" "face.1104" \
"face.1107" "face.1108" "face.1109" "face.1110" "face.1113" "face.1114" \
"face.1115" "face.1116" "face.1117" "face.1118" "face.1125" "face.1126" \
"face.1127" "face.1128" "face.1129" "face.1130" "face.1131" "face.1132" \
"face.1133" "face.1134" "face.1139" "face.1140" "face.1141" "face.1142" \
"face.1143" "face.1144" "face.1145" "face.1146" "face.1147" "face.1148" \
"face.1151" "face.1152" "face.1153" "face.1154" "face.1155" "face.1156" \
"face.1157" "face.1158" "face.1161" "face.1162" "face.1163" "face.1164" \
"face.1165" "face.1166" "face.1167" "face.1168" "face.1171" "face.1172" \
"face.1173" "face.1174" "face.1177" "face.1179" "face.1180" "face.1181" \
"face.1182" "face.1185" "face.1186" "face.1187" "face.1188" "face.1193" \
"face.1194" "face.1201" "face.1202" "face.1203" "face.1204" "face.1209" \
"face.1210" "face.1211" "face.1212" "face.1213" "face.1214" "face.1215" \
"face.1216" "face.1218" "face.1224" "face.1226" "face.1227" "face.1229" \
"face.1230" "face.1231" "face.1232" "face.1233" "face.1235" "face.1237" \
"face.1238" "face.1239" "face.1240" "face.1246" "face.1253" "face.1255" \
"face.1256" "face.1260" "face.1280" "face.1281" "face.1287" "face.1288" \
"face.1293" "face.1294" "face.1305" "face.1306" "face.1311" "face.1312" \
"face.1317" "face.1318" "face.1323" "face.1335" "face.1341" "face.1342" \
"face.1347" "face.1348" "face.1353" "face.1354" "face.1365" "face.1366" \
"face.1371" "face.1372" "face.1383" "face.1389" "face.1390" "face.1395" \
"face.1396" "face.1401" "face.1402" "face.1413" "face.1461" "face.1462" \
"face.1463" "face.1464" "face.1465" "face.1466" "face.1467" "face.1470" \
"face.1471" "face.1476" "face.1477" "face.1479" "face.1480" "face.1482" \
"face.1483" "face.1484" "face.1485" "face.1486" "face.1518" "face.1521" \
"face.1522" "face.1523" "face.1524" "face.1525" "face.1526" "face.1527" \
"face.1528" "face.1529" "face.1530" "face.1531" "face.1532" "face.1533" \
"face.1534" "face.1535" "face.1536" "face.1537" "face.1538" "face.1539" \
"face.1540" "face.1541" "face.1542" "face.1543" "face.1544" "face.1545" \
"face.1546" "face.1547" "face.1550" "face.1552" "face.1553" "face.1554" \
"face.1555" "face.1558" "face.1559" "face.1560" "face.1561" "face.1562" \
"face.1563" "face.1564" "face.1565" "face.1566" "face.1567" "face.1568" \
"face.1569" "face.1570" "face.1571" "face.1572" "face.1573" "face.1574" \
"face.1577" "face.1578" "face.1579" "face.1580" "face.1583" "face.1584" \
"face.1585" "face.1586" "face.1587" "face.1588" "face.1589" "face.1590" \
"face.1591" "face.1592" "face.1593" "face.1594" "face.1595" "face.1596" \
"face.1597" "face.1598" "face.1599" "face.1600" "face.1601" "face.1602" \
"face.1603" "face.1604" "face.1605" "face.1606" "face.1607" "face.1608" \
"face.1609" "face.1610" "face.1611" "face.1612" "face.1613" "face.1614" \
"face.1615" "face.1616" "face.1617" "face.1618" "face.1619" "face.1620" \
"face.1621" "face.1622" "face.1623" "face.1624" "face.1625" "face.1626" \
"face.1627" "face.1628" "face.1629" "face.1630" "face.1631" "face.1632" \
"face.1633" "face.1634" "face.1635" "face.1636" "face.1637" "face.1638" \
"face.1639" "face.1641" "face.1642" "face.1643" "face.1644" "face.1645" \
"face.1646" "face.1647" "face.1648" "face.1649" "face.1650" "face.1651" \
"face.1652" "face.1653" "face.1654" "face.1655" "face.1656" "face.1657" \
"face.1658" "face.1659" "face.1660" "face.1661" "face.1662" "face.1663" \
"face.1664" "face.1665" "face.1666" "face.1667" "face.1668" "face.1669" \
"face.1670" "face.1671" "face.1672" "face.1673" "face.1674" "face.1675" \
"face.1676" "face.1677" "face.1678" "face.1679" "face.1680" "face.1681" \
"face.1682" "face.1683" "face.1684" "face.1686" "face.1687" "face.1688" \
"face.1689" "face.1690" "face.1691" "face.1692" "face.1693" "face.1694" \
"face.1695" "face.1696" "face.1697" "face.1698" "face.1699" "face.1700" \
"face.1701" "face.1702" "face.1703" "face.1704" "face.1705" "face.1706" \
"face.1707" "face.1708" "face.1709" "face.1710" "face.1711" "face.1712" \
"face.1713" "face.1714" "face.1715" "face.1716" "face.1717" "face.1718" \
"face.1719" "face.1720" "face.1721" "face.1722" "face.1723" "face.1724" \
"face.1725" "face.1726" "face.1727" "face.1728" "face.1729" "face.1730" \
"face.1731" "face.1732" "face.1733" "face.1734" "face.1735" "face.1736" \
"face.1737" "face.1738" "face.1739" "face.1740" "face.1741" "face.1742" \
"face.1743" "face.1744" "face.1745" "face.1746" "face.1747" "face.1748" \
"face.1749" "face.1750" "face.1751" "face.1752" "face.1753" "face.1754" \
"face.1755" "face.1756" "face.1757" "face.1758" "face.1759" "face.1760" \
"face.1761" "face.1762" "face.1763" "face.1764" "face.1765" "face.1766" \
"face.1767" "face.1768" "face.1769" "face.1770" "face.1771" "face.1772" \
```

```
  "face.1773" "face.1774" "face.1775" "face.1776" "face.1777" "face.1778" \
  "face.1779" "face.1780" "face.1781" "face.1782" "face.1783" "face.1784" \
  "face.1785" "face.1786" "face.1787" "face.1788" "face.1790" "face.1791" \
  "face.1792" "face.1793" "face.1794" "face.1795" "face.1796" "face.1797" \
  "face.1798" "face.1799" "face.1800" "face.1801" "face.1802" "face.1803" \
  "face.1804" "face.1805" "face.1806" "face.1807" "face.1808" "face.1809" \
  "face.1810" "face.1811" "face.1812" "face.1813" "face.1814" "face.1815" \
  "face.1816" "face.1817" "face.1818" "face.1819" "face.1820" "face.1821" \
  "face.1822" "face.1823" "face.1824" "face.1825" "face.1826" "face.1827" \
  "face.1828" "face.1830" "face.1831" "face.1832" "face.1834" "face.1835" \
  "face.1836" "face.1837" "face.1838" "face.1840" "face.1841" "face.1843" \
  "face.1844" "face.1846" "face.1847" "face.1848" "face.1849" "face.1851" \
  "face.1852" "face.1854" "face.1855" "face.1857" "face.1858" "face.1860" \
  "face.1863" "face.1865" "face.1866" "face.1867" "face.1868" "face.1869" \
  "face.1870" "face.1871" "face.1872" "face.1873" "face.1874" "face.1875" \
  "face.1876" "face.1877" "face.1878" "face.1879" "face.1880" "face.1881" \
  "face.1882" "face.1883" "face.1884" "face.1885" "face.1886" "face.1887" \
  "face.1888" "face.1889" "face.1890" "face.1891" "face.1892" "face.1893" \
  "face.1894" "face.1895" "face.1896" "face.1897" "face.1898" "face.1899" \
  "face.1900" "face.1901" "face.1902" "face.1903" "face.1904" "face.1905" \
  "face.1906" "face.1907" "face.1908" "face.1909" "face.1910" "face.1911" \
  "face.1912" "face.1913" "face.1914" "face.1915" "face.1916" "face.1917" \
  "face.1918" "face.1919" "face.1920" "face.1921" "face.1922" "face.1923" \
  "face.1924" "face.1925" "face.1926" "face.1927" "face.1928" "face.1929" \
  "face.1930" "face.1931" "face.1932" "face.1933" "face.1934" "face.1935" \
  "face.1936" "face.1937" "face.1938" "face.1939" "face.1940" "face.1941" \
  "face.1942" "face.1943" "face.1944" "face.1945" "face.1946" "face.1947" \
  "face.1948" "face.1949" "face.1950" "face.1951" "face.1952" "face.1953" \
  "face.1954" "face.1955" "face.1956" "face.1957" "face.1958" "face.1959" \
  "face.1960" "face.1961" "face.1962" "face.1963" "face.1964" "face.1965" \
  "face.1966" "face.1967" "face.1968" "face.1969" "face.1970" "face.1971" \
  "face.1972" "face.1973" "face.1974" "face.1975" "face.1976" "face.1977" \
  "face.1978" "face.1979" "face.1980" "face.1981" "face.1982" "face.1983" \
  "face.1984" "face.1985" "face.1986" "face.1987" "face.1988" "face.1989" \
  "face.1990" "face.1991" "face.1992" "face.1994" "face.1995" "face.1996" \
  "face.1998" "face.2000" "face.2001" "face.2002" "face.2003" "face.2004" \
  "face.2005" "face.2006" "face.2007" "face.2008" "face.2009" "face.2010" \
  "face.2011" "face.2012" "face.2013" "face.2014" "face.2015" "face.2016" \
  "face.2017" "face.2018" "face.2019" "face.2020" "face.2021" "face.2022" \
  "face.2023" "face.2024" "face.2025" "face.2026" "face.2027" "face.2028" \
  "face.2029" "face.2030" "face.2031" "face.2032" "face.2033" "face.2034" \
  "face.2035" "face.2036" "face.2037" "face.2038" "face.2039" "face.2040" \
  "face.2041" "face.2042" "face.2043" "face.2044" "face.2045" "face.2046" \
  "face.2047" "face.2048" "face.2049" "face.2050" "face.2051" "face.2052" \
  "face.2053" "face.2054" "face.2055" "face.2056" "face.2057" "face.2058" \
  "face.2059" "face.2060" "face.2061" "face.2062" "face.2063" "face.2064" \
  "face.2065" "face.2066" "face.2067" "face.2068" "face.2069" "face.2070" \
  "face.2071" "face.2072" "face.2073" "face.2074" "face.2075" "face.2076" \
  "face.2077" "face.2078" "face.2083" "face.2084" "face.2085" "face.2086" \
  "face.2087" "face.2088" "face.2089" "face.2090" "face.2091" "face.2092" \
  "face.2093" "face.2094" "face.2095" "face.2096" "face.2097" "face.2098" \
  "face.2099" "face.2100" "face.2101" "face.2102" "face.2103" "face.2104" \
  "face.2105" "face.2106" "face.2107" "face.2108" "face.2109" "face.2110" \
  "face.2111" "face.2112" "face.2113" "face.2114" "face.2115" "face.2116" \
  "face.2117" "face.2118" "face.2119" "face.2120" "face.2121" "face.2122" \
  "face.2123" "face.2124" "face.2125" "face.2126" "face.2127" "face.2128" \
  "face.2129" "face.2130" "face.2131" "face.2132" "face.2133" "face.2134" \
  "face.2135" "face.2136" "face.2137" "face.2138" "face.2139" "face.2140" \
  "face.2141" "face.2142" "face.2143" "face.2144" "face.2145" "face.2146" \
  "face.2147" "face.2148" "face.2149" "face.2150" "face.2151" "face.2152" \
  "face.2153" "face.2154" "face.2155" "face.2156" "face.2157" "face.2158" \
  "face.2159" "face.2160" "face.2161" "face.2162" "face.2173" "face.2174" \
  "face.2175" "face.2176" "face.2177" "face.2178" "face.2179" "face.2180" \
  "face.2181" "face.2182" "face.2183" "face.2184" "face.2185" "face.2186" \
  "face.2187" "face.2188" "face.2189" "face.2190" "face.2191" "face.2192" \
  "face.2193" "face.2194" "face.2195" "face.2196" "face.2197" "face.2198" \
  "face.2200" real
volume mesh "volume.17" "volume.38" "volume.39" "volume.53" tetrahedral size \
  0.0075
window modify invisible mesh
physics create "Pout" btype "WALL" face "face.1275"
```

```
physics modify "Pout" btype "PRESSURE_OUTLET" face "face.1275"
physics create "Vin" btype "VELOCITY_INLET" face "face.1272"
physics create "Sym1" btype "VELOCITY_INLET" face "face.2194" "face.2195" \
  "face.1470" "face.1471" "face.2192"
physics create "Sym2" btype "SYMMETRY" face "face.2190" "face.1271" \
  "face.1518" "face.2173"
physics modify "Sym1" btype "SYMMETRY" face "face.2194" "face.2195" \
  "face.1470" "face.1471" "face.2192"
physics create "Sym3" btype "SYMMETRY" face "face.2191" "face.2193" \
  "face.2196" "face.1571" "face.1570" "face.134" "face.1577"
physics create "BigWall" btype "WALL" face "face.2197"
physics create "SmallWalls" btype "WALL" face "face.1635" "face.1636" \
  "face.1637" "face.1632" "face.1631" "face.1628" "face.1627" "face.1629" \
  "face.1630" "face.1633" "face.1623" "face.1624" "face.1625" "face.1626" \
  "face.1620" "face.1621" "face.1622"
physics create "Particle1" btype "WALL" face "face.1639"
physics create "Particle2" btype "WALL"
physics modify "Particle2" btype face "face.38"
physics create "Particles" btype "WALL" face "face.4" "face.6" "face.8" \
  "face.10" "face.18" "face.19" "face.20" "face.23" "face.24" "face.25" \
  "face.26" "face.28" "face.29" "face.30" "face.33" "face.34" "face.35" \
  "face.37" "face.39" "face.40" "face.54" "face.72" "face.78" "face.84" \
  "face.92" "face.102" "face.114" "face.116" "face.120" "face.122" "face.128" \
  "face.132" "face.138" "face.140" "face.144" "face.146" "face.150" \
  "face.152" "face.156" "face.158" "face.162" "face.164" "face.168" \
  "face.170" "face.176" "face.184" "face.186" "face.190" "face.204" \
  "face.206" "face.210" "face.212" "face.216" "face.218" "face.224" \
  "face.230" "face.233" "face.234" "face.246" "face.248" "face.252" \
  "face.254" "face.263" "face.264" "face.270" "face.274" "face.282" \
  "face.286" "face.296" "face.299" "face.300" "face.302" "face.306" \
  "face.308" "face.312" "face.314" "face.318" "face.320" "face.324" \
  "face.326" "face.348" "face.350" "face.354" "face.356" "face.366" \
  "face.368" "face.372" "face.376" "face.378" "face.382" "face.405" \
  "face.407" "face.408" "face.412" "face.414" "face.418" "face.426" \
  "face.430" "face.432" "face.436" "face.438" "face.442" "face.444" \
  "face.448" "face.456" "face.460" "face.462" "face.466" "face.474" \
  "face.476" "face.480" "face.482" "face.486" "face.488" "face.498" \
  "face.500" "face.504" "face.526" "face.527" "face.531" "face.532" \
  "face.537" "face.538" "face.543" "face.544" "face.549" "face.550" \
  "face.567" "face.568" "face.573" "face.574" "face.579" "face.580" \
  "face.584" "face.586" "face.591" "face.592" "face.603" "face.604" \
  "face.609" "face.610" "face.615" "face.616" "face.621" "face.622" \
  "face.633" "face.634" "face.639" "face.640" "face.644" "face.646" \
  "face.651" "face.652" "face.657" "face.663" "face.664" "face.669" \
  "face.670" "face.687" "face.688" "face.693" "face.694" "face.705" \
  "face.706" "face.709" "face.714" "face.715" "face.721" "face.732" \
  "face.733" "face.734" "face.740" "face.742" "face.746" "face.750" \
  "face.756" "face.757" "face.762" "face.763" "face.770" "face.772" \
  "face.777" "face.794" "face.795" "face.800" "face.801" "face.806" \
  "face.807" "face.812" "face.813" "face.814" "face.820" "face.826" \
  "face.828" "face.832" "face.834" "face.848" "face.854" "face.869" \
  "face.886" "face.887" "face.906" "face.908" "face.941" "face.943" \
  "face.954" "face.955" "face.962" "face.964" "face.1000" "face.1002" \
  "face.1004" "face.1007" "face.1008" "face.1009" "face.1010" "face.1011" \
  "face.1015" "face.1016" "face.1017" "face.1018" "face.1019" "face.1020" \
  "face.1021" "face.1022" "face.1023" "face.1024" "face.1025" "face.1026" \
  "face.1027" "face.1029" "face.1031" "face.1032" "face.1033" "face.1034" \
  "face.1035" "face.1036" "face.1037" "face.1038" "face.1039" "face.1042" \
  "face.1044" "face.1048" "face.1050" "face.1056" "face.1061" "face.1062" \
  "face.1063" "face.1064" "face.1065" "face.1066" "face.1067" "face.1068" \
  "face.1069" "face.1070" "face.1071" "face.1072" "face.1075" "face.1076" \
  "face.1077" "face.1078" "face.1079" "face.1080" "face.1081" "face.1082" \
  "face.1083" "face.1084" "face.1089" "face.1090" "face.1091" "face.1092" \
  "face.1093" "face.1094" "face.1097" "face.1098" "face.1099" "face.1100" \
  "face.1101" "face.1102" "face.1103" "face.1104" "face.1107" "face.1108" \
  "face.1109" "face.1110" "face.1113" "face.1114" "face.1115" "face.1116" \
  "face.1117" "face.1118" "face.1125" "face.1126" "face.1127" "face.1128" \
  "face.1129" "face.1130" "face.1131" "face.1132" "face.1133" "face.1134" \
  "face.1139" "face.1140" "face.1141" "face.1142" "face.1143" "face.1144" \
  "face.1145" "face.1146" "face.1147" "face.1148" "face.1151" "face.1152" \
  "face.1153" "face.1154" "face.1155" "face.1156" "face.1157" "face.1158" \
```

```
  "face.1161" "face.1162" "face.1163" "face.1164" "face.1165" "face.1166" \
  "face.1167" "face.1168" "face.1171" "face.1172" "face.1173" "face.1174" \
  "face.1177" "face.1179" "face.1180" "face.1181" "face.1182" "face.1185" \
  "face.1186" "face.1187" "face.1188" "face.1193" "face.1194" "face.1201" \
  "face.1202" "face.1203" "face.1204" "face.1209" "face.1210" "face.1211" \
  "face.1212" "face.1213" "face.1214" "face.1215" "face.1216" "face.1218" \
  "face.1224" "face.1226" "face.1227" "face.1229" "face.1230" "face.1231" \
  "face.1232" "face.1233" "face.1235" "face.1237" "face.1238" "face.1239" \
  "face.1240" "face.1246" "face.1253" "face.1255" "face.1256" "face.1260" \
  "face.1280" "face.1281" "face.1287" "face.1288" "face.1293" "face.1294" \
  "face.1305" "face.1306" "face.1311" "face.1312" "face.1317" "face.1318" \
  "face.1323" "face.1335" "face.1341" "face.1342" "face.1347" "face.1348" \
  "face.1353" "face.1354" "face.1365" "face.1366" "face.1371" "face.1372" \
  "face.1383" "face.1389" "face.1390" "face.1395" "face.1396" "face.1401" \
  "face.1402" "face.1413" "face.1461" "face.1462" "face.1463" "face.1464" \
  "face.1465" "face.1466" "face.1467" "face.1476" "face.1477" "face.1479" \
  "face.1480" "face.1482" "face.1483" "face.1484" "face.1485" "face.1486" \
  "face.1518" "face.1521" "face.1522" "face.1523" "face.1524" "face.1525" \
  "face.1526" "face.1527" "face.1528" "face.1529" "face.1530" "face.1531" \
  "face.1532" "face.1533" "face.1534" "face.1535" "face.1536" "face.1537" \
  "face.1538" "face.1539" "face.1540" "face.1541" "face.1542" "face.1543" \
  "face.1544" "face.1545" "face.1546" "face.1547" "face.1550" "face.1552" \
  "face.1553" "face.1554" "face.1555" "face.1558" "face.1559" "face.1560" \
  "face.1561" "face.1562" "face.1563" "face.1564" "face.1565" "face.1566" \
  "face.1567" "face.1568" "face.1569" "face.1572" "face.1573" "face.1574" \
  "face.1578" "face.1579" "face.1580" "face.1583" "face.1584" "face.1585" \
  "face.1586" "face.1587" "face.1588" "face.1589" "face.1590" "face.1591" \
  "face.1592" "face.1593" "face.1594" "face.1595" "face.1596" "face.1597" \
  "face.1598" "face.1599" "face.1600" "face.1601" "face.1602" "face.1603" \
  "face.1604" "face.1605" "face.1606" "face.1607" "face.1608" "face.1609" \
  "face.1610" "face.1611" "face.1612" "face.1613" "face.1614" "face.1615" \
  "face.1616" "face.1617" "face.1618" "face.1619" "face.1636" "face.1637" \
  "face.1638"
physics modify "Sym2" btype face "face.2190" "face.1271" "face.1518" \
  "face.2173" "face.2174" "face.2175" "face.2176" "face.2177" "face.2178" \
  "face.2179" "face.2180" "face.2181" "face.2182" "face.2183" "face.2184" \
  "face.2185" "face.2186" "face.2187" "face.2188" "face.2189"
physics modify "Particles" btype face "face.4" "face.6" "face.8" "face.10" \
  "face.18" "face.19" "face.20" "face.23" "face.24" "face.25" "face.26" \
  "face.28" "face.29" "face.30" "face.33" "face.34" "face.35" "face.37" \
  "face.39" "face.40" "face.54" "face.72" "face.78" "face.84" "face.92" \
  "face.102" "face.114" "face.116" "face.120" "face.122" "face.128" \
  "face.132" "face.138" "face.140" "face.144" "face.146" "face.150" \
  "face.152" "face.156" "face.158" "face.162" "face.164" "face.168" \
  "face.170" "face.176" "face.184" "face.186" "face.190" "face.204" \
  "face.206" "face.210" "face.212" "face.216" "face.218" "face.224" \
  "face.230" "face.233" "face.234" "face.246" "face.248" "face.252" \
  "face.254" "face.263" "face.264" "face.270" "face.274" "face.282" \
  "face.286" "face.296" "face.299" "face.300" "face.302" "face.306" \
  "face.308" "face.312" "face.314" "face.318" "face.320" "face.324" \
  "face.326" "face.348" "face.350" "face.354" "face.356" "face.366" \
  "face.368" "face.372" "face.376" "face.378" "face.382" "face.405" \
  "face.407" "face.408" "face.412" "face.414" "face.418" "face.426" \
  "face.430" "face.432" "face.436" "face.438" "face.442" "face.444" \
  "face.448" "face.456" "face.460" "face.462" "face.466" "face.474" \
  "face.476" "face.480" "face.482" "face.486" "face.488" "face.498" \
  "face.500" "face.504" "face.526" "face.527" "face.531" "face.532" \
  "face.537" "face.538" "face.543" "face.544" "face.549" "face.550" \
  "face.567" "face.568" "face.573" "face.574" "face.579" "face.580" \
  "face.584" "face.586" "face.591" "face.592" "face.603" "face.604" \
  "face.609" "face.610" "face.615" "face.616" "face.621" "face.622" \
  "face.633" "face.634" "face.639" "face.640" "face.644" "face.646" \
  "face.651" "face.652" "face.657" "face.663" "face.664" "face.669" \
  "face.670" "face.687" "face.688" "face.693" "face.694" "face.705" \
  "face.706" "face.709" "face.714" "face.715" "face.721" "face.732" \
  "face.733" "face.734" "face.740" "face.742" "face.746" "face.750" \
  "face.756" "face.757" "face.762" "face.763" "face.770" "face.772" \
  "face.777" "face.794" "face.795" "face.800" "face.801" "face.806" \
  "face.807" "face.812" "face.813" "face.814" "face.820" "face.826" \
  "face.828" "face.832" "face.834" "face.848" "face.854" "face.869" \
  "face.886" "face.887" "face.906" "face.908" "face.941" "face.943" \
```

```
  "face.954" "face.955" "face.962" "face.964" "face.1000" "face.1002" \
  "face.1004" "face.1007" "face.1008" "face.1009" "face.1010" "face.1011" \
  "face.1015" "face.1016" "face.1017" "face.1018" "face.1019" "face.1020" \
  "face.1021" "face.1022" "face.1023" "face.1024" "face.1025" "face.1026" \
  "face.1027" "face.1029" "face.1031" "face.1032" "face.1033" "face.1034" \
  "face.1035" "face.1036" "face.1037" "face.1038" "face.1039" "face.1042" \
  "face.1044" "face.1048" "face.1050" "face.1056" "face.1061" "face.1062" \
  "face.1063" "face.1064" "face.1065" "face.1066" "face.1067" "face.1068" \
  "face.1069" "face.1070" "face.1071" "face.1072" "face.1075" "face.1076" \
  "face.1077" "face.1078" "face.1079" "face.1080" "face.1081" "face.1082" \
  "face.1083" "face.1084" "face.1089" "face.1090" "face.1091" "face.1092" \
  "face.1093" "face.1094" "face.1097" "face.1098" "face.1099" "face.1100" \
  "face.1101" "face.1102" "face.1103" "face.1104" "face.1107" "face.1108" \
  "face.1109" "face.1110" "face.1113" "face.1114" "face.1115" "face.1116" \
  "face.1117" "face.1118" "face.1125" "face.1126" "face.1127" "face.1128" \
  "face.1129" "face.1130" "face.1131" "face.1132" "face.1133" "face.1134" \
  "face.1139" "face.1140" "face.1141" "face.1142" "face.1143" "face.1144" \
  "face.1145" "face.1146" "face.1147" "face.1148" "face.1151" "face.1152" \
  "face.1153" "face.1154" "face.1155" "face.1156" "face.1157" "face.1158" \
  "face.1161" "face.1162" "face.1163" "face.1164" "face.1165" "face.1166" \
  "face.1167" "face.1168" "face.1171" "face.1172" "face.1173" "face.1174" \
  "face.1177" "face.1179" "face.1180" "face.1181" "face.1182" "face.1185" \
  "face.1186" "face.1187" "face.1188" "face.1193" "face.1194" "face.1201" \
  "face.1202" "face.1203" "face.1204" "face.1209" "face.1210" "face.1211" \
  "face.1212" "face.1213" "face.1214" "face.1215" "face.1216" "face.1218" \
  "face.1224" "face.1226" "face.1227" "face.1229" "face.1230" "face.1231" \
  "face.1232" "face.1233" "face.1235" "face.1237" "face.1238" "face.1239" \
  "face.1240" "face.1246" "face.1253" "face.1255" "face.1256" "face.1260" \
  "face.1280" "face.1281" "face.1287" "face.1288" "face.1293" "face.1294" \
  "face.1305" "face.1306" "face.1311" "face.1312" "face.1317" "face.1318" \
  "face.1323" "face.1335" "face.1341" "face.1342" "face.1347" "face.1348" \
  "face.1353" "face.1354" "face.1365" "face.1366" "face.1371" "face.1372" \
  "face.1383" "face.1389" "face.1390" "face.1395" "face.1396" "face.1401" \
  "face.1402" "face.1413" "face.1461" "face.1462" "face.1463" "face.1464" \
  "face.1465" "face.1466" "face.1467" "face.1476" "face.1477" "face.1479" \
  "face.1480" "face.1482" "face.1483" "face.1484" "face.1485" "face.1486" \
  "face.1521" "face.1522" "face.1523" "face.1524" "face.1525" "face.1526" \
  "face.1527" "face.1528" "face.1529" "face.1530" "face.1531" "face.1532" \
  "face.1533" "face.1534" "face.1535" "face.1536" "face.1537" "face.1538" \
  "face.1539" "face.1540" "face.1541" "face.1542" "face.1543" "face.1544" \
  "face.1545" "face.1546" "face.1547" "face.1550" "face.1552" "face.1553" \
  "face.1554" "face.1555" "face.1558" "face.1559" "face.1560" "face.1561" \
  "face.1562" "face.1563" "face.1564" "face.1565" "face.1566" "face.1567" \
  "face.1568" "face.1569" "face.1572" "face.1573" "face.1574" "face.1578" \
  "face.1579" "face.1580" "face.1583" "face.1584" "face.1585" "face.1586" \
  "face.1587" "face.1588" "face.1589" "face.1590" "face.1591" "face.1592" \
  "face.1593" "face.1594" "face.1595" "face.1596" "face.1597" "face.1598" \
  "face.1599" "face.1600" "face.1601" "face.1602" "face.1603" "face.1604" \
  "face.1605" "face.1606" "face.1607" "face.1608" "face.1609" "face.1610" \
  "face.1611" "face.1612" "face.1613" "face.1614" "face.1615" "face.1616" \
  "face.1617" "face.1618" "face.1619" "face.1638" "face.134"
physics modify "Particles" btype face "face.4" "face.6" "face.8" "face.10" \
  "face.18" "face.19" "face.20" "face.23" "face.24" "face.25" "face.26" \
  "face.28" "face.29" "face.30" "face.33" "face.34" "face.35" "face.37" \
  "face.39" "face.40" "face.54" "face.72" "face.78" "face.84" "face.92" \
  "face.102" "face.114" "face.116" "face.120" "face.122" "face.128" \
  "face.132" "face.138" "face.140" "face.144" "face.146" "face.150" \
  "face.152" "face.156" "face.158" "face.162" "face.164" "face.168" \
  "face.170" "face.176" "face.184" "face.186" "face.190" "face.204" \
  "face.206" "face.210" "face.212" "face.216" "face.218" "face.224" \
  "face.230" "face.233" "face.234" "face.246" "face.248" "face.252" \
  "face.254" "face.263" "face.264" "face.270" "face.274" "face.282" \
  "face.286" "face.296" "face.299" "face.300" "face.302" "face.306" \
  "face.308" "face.312" "face.314" "face.318" "face.320" "face.324" \
  "face.326" "face.348" "face.350" "face.354" "face.356" "face.366" \
  "face.368" "face.372" "face.376" "face.378" "face.382" "face.405" \
  "face.407" "face.408" "face.412" "face.414" "face.418" "face.426" \
  "face.430" "face.432" "face.436" "face.438" "face.442" "face.444" \
  "face.448" "face.456" "face.460" "face.462" "face.466" "face.474" \
  "face.476" "face.480" "face.482" "face.486" "face.488" "face.498" \
  "face.500" "face.504" "face.526" "face.527" "face.531" "face.532" \
```

```
  "face.537" "face.538" "face.543" "face.544" "face.549" "face.550" \
  "face.567" "face.568" "face.573" "face.574" "face.579" "face.580" \
  "face.584" "face.586" "face.591" "face.592" "face.603" "face.604" \
  "face.609" "face.610" "face.615" "face.616" "face.621" "face.622" \
  "face.633" "face.634" "face.639" "face.640" "face.644" "face.646" \
  "face.651" "face.652" "face.657" "face.663" "face.664" "face.669" \
  "face.670" "face.687" "face.688" "face.693" "face.694" "face.705" \
  "face.706" "face.709" "face.714" "face.715" "face.721" "face.732" \
  "face.733" "face.734" "face.740" "face.742" "face.746" "face.750" \
  "face.756" "face.757" "face.762" "face.763" "face.770" "face.772" \
  "face.777" "face.794" "face.795" "face.800" "face.801" "face.806" \
  "face.807" "face.812" "face.813" "face.814" "face.820" "face.826" \
  "face.828" "face.832" "face.834" "face.848" "face.854" "face.869" \
  "face.886" "face.887" "face.906" "face.908" "face.941" "face.943" \
  "face.954" "face.955" "face.962" "face.964" "face.1000" "face.1002" \
  "face.1004" "face.1007" "face.1008" "face.1009" "face.1010" "face.1011" \
  "face.1015" "face.1016" "face.1017" "face.1018" "face.1019" "face.1020" \
  "face.1021" "face.1022" "face.1023" "face.1024" "face.1025" "face.1026" \
  "face.1027" "face.1029" "face.1031" "face.1032" "face.1033" "face.1034" \
  "face.1035" "face.1036" "face.1037" "face.1038" "face.1039" "face.1042" \
  "face.1044" "face.1048" "face.1050" "face.1056" "face.1061" "face.1062" \
  "face.1063" "face.1064" "face.1065" "face.1066" "face.1067" "face.1068" \
  "face.1069" "face.1070" "face.1071" "face.1072" "face.1075" "face.1076" \
  "face.1077" "face.1078" "face.1079" "face.1080" "face.1081" "face.1082" \
  "face.1083" "face.1084" "face.1089" "face.1090" "face.1091" "face.1092" \
  "face.1093" "face.1094" "face.1097" "face.1098" "face.1099" "face.1100" \
  "face.1101" "face.1102" "face.1103" "face.1104" "face.1107" "face.1108" \
  "face.1109" "face.1110" "face.1113" "face.1114" "face.1115" "face.1116" \
  "face.1117" "face.1118" "face.1125" "face.1126" "face.1127" "face.1128" \
  "face.1129" "face.1130" "face.1131" "face.1132" "face.1133" "face.1134" \
  "face.1139" "face.1140" "face.1141" "face.1142" "face.1143" "face.1144" \
  "face.1145" "face.1146" "face.1147" "face.1148" "face.1151" "face.1152" \
  "face.1153" "face.1154" "face.1155" "face.1156" "face.1157" "face.1158" \
  "face.1161" "face.1162" "face.1163" "face.1164" "face.1165" "face.1166" \
  "face.1167" "face.1168" "face.1171" "face.1172" "face.1173" "face.1174" \
  "face.1177" "face.1179" "face.1180" "face.1181" "face.1182" "face.1185" \
  "face.1186" "face.1187" "face.1188" "face.1193" "face.1194" "face.1201" \
  "face.1202" "face.1203" "face.1204" "face.1209" "face.1210" "face.1211" \
  "face.1212" "face.1213" "face.1214" "face.1215" "face.1216" "face.1218" \
  "face.1224" "face.1226" "face.1227" "face.1229" "face.1230" "face.1231" \
  "face.1232" "face.1233" "face.1235" "face.1237" "face.1238" "face.1239" \
  "face.1240" "face.1246" "face.1253" "face.1255" "face.1256" "face.1260" \
  "face.1280" "face.1281" "face.1287" "face.1288" "face.1293" "face.1294" \
  "face.1305" "face.1306" "face.1311" "face.1312" "face.1317" "face.1318" \
  "face.1323" "face.1335" "face.1341" "face.1342" "face.1347" "face.1348" \
  "face.1353" "face.1354" "face.1365" "face.1366" "face.1371" "face.1372" \
  "face.1383" "face.1389" "face.1390" "face.1395" "face.1396" "face.1401" \
  "face.1402" "face.1413" "face.1461" "face.1462" "face.1463" "face.1464" \
  "face.1465" "face.1466" "face.1467" "face.1476" "face.1477" "face.1479" \
  "face.1480" "face.1482" "face.1483" "face.1484" "face.1485" "face.1486" \
  "face.1521" "face.1522" "face.1523" "face.1524" "face.1525" "face.1526" \
  "face.1527" "face.1528" "face.1529" "face.1530" "face.1531" "face.1532" \
  "face.1533" "face.1534" "face.1535" "face.1536" "face.1537" "face.1538" \
  "face.1539" "face.1540" "face.1541" "face.1542" "face.1543" "face.1544" \
  "face.1545" "face.1546" "face.1547" "face.1550" "face.1552" "face.1553" \
  "face.1554" "face.1555" "face.1558" "face.1559" "face.1560" "face.1561" \
  "face.1562" "face.1563" "face.1564" "face.1565" "face.1566" "face.1567" \
  "face.1568" "face.1569" "face.1572" "face.1573" "face.1574" "face.1578" \
  "face.1579" "face.1580" "face.1583" "face.1584" "face.1585" "face.1586" \
  "face.1587" "face.1588" "face.1589" "face.1590" "face.1591" "face.1592" \
  "face.1593" "face.1594" "face.1595" "face.1596" "face.1597" "face.1598" \
  "face.1599" "face.1600" "face.1601" "face.1602" "face.1603" "face.1604" \
  "face.1605" "face.1606" "face.1607" "face.1608" "face.1609" "face.1610" \
  "face.1611" "face.1612" "face.1613" "face.1614" "face.1615" "face.1616" \
  "face.1617" "face.1618" "face.1619" "face.1638" "face.134"
physics modify "Sym3" btype face "face.2191" "face.2193" "face.2196" \
  "face.1571" "face.1570" "face.1577"
physics modify "Particles" btype face "face.4" "face.6" "face.8" "face.10" \
  "face.18" "face.19" "face.20" "face.23" "face.24" "face.25" "face.26" \
  "face.28" "face.29" "face.30" "face.33" "face.34" "face.35" "face.37" \
  "face.39" "face.40" "face.54" "face.72" "face.78" "face.84" "face.92" \
```

```
"face.102" "face.114" "face.116" "face.120" "face.122" "face.128" \
"face.132" "face.138" "face.140" "face.144" "face.146" "face.150" \
"face.152" "face.156" "face.158" "face.162" "face.164" "face.168" \
"face.170" "face.176" "face.184" "face.186" "face.190" "face.204" \
"face.206" "face.210" "face.212" "face.216" "face.218" "face.224" \
"face.230" "face.233" "face.234" "face.246" "face.248" "face.252" \
"face.254" "face.263" "face.264" "face.270" "face.274" "face.282" \
"face.286" "face.296" "face.299" "face.300" "face.302" "face.306" \
"face.308" "face.312" "face.314" "face.318" "face.320" "face.324" \
"face.326" "face.348" "face.350" "face.354" "face.356" "face.366" \
"face.368" "face.372" "face.376" "face.378" "face.382" "face.405" \
"face.407" "face.408" "face.412" "face.414" "face.418" "face.426" \
"face.430" "face.432" "face.436" "face.438" "face.442" "face.444" \
"face.448" "face.456" "face.460" "face.462" "face.466" "face.474" \
"face.476" "face.480" "face.482" "face.486" "face.488" "face.498" \
"face.500" "face.504" "face.526" "face.527" "face.531" "face.532" \
"face.537" "face.538" "face.543" "face.544" "face.549" "face.550" \
"face.567" "face.568" "face.573" "face.574" "face.579" "face.580" \
"face.584" "face.586" "face.591" "face.592" "face.603" "face.604" \
"face.609" "face.610" "face.615" "face.616" "face.621" "face.622" \
"face.633" "face.634" "face.639" "face.640" "face.644" "face.646" \
"face.651" "face.652" "face.657" "face.663" "face.664" "face.669" \
"face.670" "face.687" "face.688" "face.693" "face.694" "face.705" \
"face.706" "face.709" "face.714" "face.715" "face.721" "face.732" \
"face.733" "face.734" "face.740" "face.742" "face.746" "face.750" \
"face.756" "face.757" "face.762" "face.763" "face.770" "face.772" \
"face.777" "face.794" "face.795" "face.800" "face.801" "face.806" \
"face.807" "face.812" "face.813" "face.814" "face.820" "face.826" \
"face.828" "face.832" "face.834" "face.848" "face.854" "face.869" \
"face.886" "face.887" "face.906" "face.908" "face.941" "face.943" \
"face.954" "face.955" "face.962" "face.964" "face.1000" "face.1002" \
"face.1004" "face.1007" "face.1008" "face.1009" "face.1010" "face.1011" \
"face.1015" "face.1016" "face.1017" "face.1018" "face.1019" "face.1020" \
"face.1021" "face.1022" "face.1023" "face.1024" "face.1025" "face.1026" \
"face.1027" "face.1029" "face.1031" "face.1032" "face.1033" "face.1034" \
"face.1035" "face.1036" "face.1037" "face.1038" "face.1039" "face.1042" \
"face.1044" "face.1048" "face.1050" "face.1056" "face.1061" "face.1062" \
"face.1063" "face.1064" "face.1065" "face.1066" "face.1067" "face.1068" \
"face.1069" "face.1070" "face.1071" "face.1072" "face.1075" "face.1076" \
"face.1077" "face.1078" "face.1079" "face.1080" "face.1081" "face.1082" \
"face.1083" "face.1084" "face.1089" "face.1090" "face.1091" "face.1092" \
"face.1093" "face.1094" "face.1097" "face.1098" "face.1099" "face.1100" \
"face.1101" "face.1102" "face.1103" "face.1104" "face.1107" "face.1108" \
"face.1109" "face.1110" "face.1113" "face.1114" "face.1115" "face.1116" \
"face.1117" "face.1118" "face.1125" "face.1126" "face.1127" "face.1128" \
"face.1129" "face.1130" "face.1131" "face.1132" "face.1133" "face.1134" \
"face.1139" "face.1140" "face.1141" "face.1142" "face.1143" "face.1144" \
"face.1145" "face.1146" "face.1147" "face.1148" "face.1151" "face.1152" \
"face.1153" "face.1154" "face.1155" "face.1156" "face.1157" "face.1158" \
"face.1161" "face.1162" "face.1163" "face.1164" "face.1165" "face.1166" \
"face.1167" "face.1168" "face.1171" "face.1172" "face.1173" "face.1174" \
"face.1177" "face.1179" "face.1180" "face.1181" "face.1182" "face.1185" \
"face.1186" "face.1187" "face.1188" "face.1193" "face.1194" "face.1201" \
"face.1202" "face.1203" "face.1204" "face.1209" "face.1210" "face.1211" \
"face.1212" "face.1213" "face.1214" "face.1215" "face.1216" "face.1218" \
"face.1224" "face.1226" "face.1227" "face.1229" "face.1230" "face.1231" \
"face.1232" "face.1233" "face.1235" "face.1237" "face.1238" "face.1239" \
"face.1240" "face.1246" "face.1253" "face.1255" "face.1256" "face.1260" \
"face.1280" "face.1281" "face.1287" "face.1288" "face.1293" "face.1294" \
"face.1305" "face.1306" "face.1311" "face.1312" "face.1317" "face.1318" \
"face.1323" "face.1335" "face.1341" "face.1342" "face.1347" "face.1348" \
"face.1353" "face.1354" "face.1365" "face.1366" "face.1371" "face.1372" \
"face.1383" "face.1389" "face.1390" "face.1395" "face.1396" "face.1401" \
"face.1402" "face.1413" "face.1461" "face.1462" "face.1463" "face.1464" \
"face.1465" "face.1466" "face.1467" "face.1476" "face.1477" "face.1479" \
"face.1480" "face.1482" "face.1483" "face.1484" "face.1485" "face.1486" \
"face.1521" "face.1522" "face.1523" "face.1524" "face.1525" "face.1526" \
"face.1527" "face.1528" "face.1529" "face.1530" "face.1531" "face.1532" \
"face.1533" "face.1534" "face.1535" "face.1536" "face.1537" "face.1538" \
"face.1539" "face.1540" "face.1541" "face.1542" "face.1543" "face.1544" \
"face.1545" "face.1546" "face.1547" "face.1550" "face.1552" "face.1553" \
```

```
  "face.1554" "face.1555" "face.1558" "face.1559" "face.1560" "face.1561" \
  "face.1562" "face.1563" "face.1564" "face.1565" "face.1566" "face.1567" \
  "face.1568" "face.1569" "face.1572" "face.1573" "face.1574" "face.1578" \
  "face.1579" "face.1580" "face.1583" "face.1584" "face.1585" "face.1586" \
  "face.1587" "face.1588" "face.1589" "face.1590" "face.1591" "face.1592" \
  "face.1593" "face.1594" "face.1595" "face.1596" "face.1597" "face.1598" \
  "face.1599" "face.1600" "face.1601" "face.1602" "face.1603" "face.1604" \
  "face.1605" "face.1606" "face.1607" "face.1608" "face.1609" "face.1610" \
  "face.1611" "face.1612" "face.1613" "face.1614" "face.1615" "face.1616" \
  "face.1617" "face.1618" "face.1619" "face.1638" "face.134"
physics create ctype "FLUID" volume "volume.39"
physics modify "fluid.11" ctype label "FLUID" volume "volume.39"
physics create "SOLID" ctype "SOLID" volume "volume.53"
physics create "SOILD1" ctype "SOLID" volume "volume.17"
physics create "SOLID2" ctype "SOLID" volume "volume.38"
export fluent5 "finalwall1.msh"
physics modify "SmallWalls" btype face "face.1635" "face.1636" "face.1637" \
  "face.1632" "face.1631" "face.1628" "face.1627" "face.1629" "face.1630" \
  "face.1633" "face.1623" "face.1624" "face.1625" "face.1626" "face.1620" \
  "face.1621" "face.1622" "face.1634"
export fluent5 "finalwall1.msh"
/ File closed at Tue Feb 10 13:53:52 2009, 806.45 cpu second(s), 1795442472 maximum memory.
/ Journal File for GAMBIT 2.4.6, Database 2.4.4, lnamd64 SP2007051420
/ Identifier "finalwall1"
/ File opened for append Tue Feb 10 14:03:36 2009.
physics delete "Sym1" btype
physics delete "Sym2" btype
physics delete "Sym3" btype
physics create "Sym1" btype "SYMMETRY" face "face.2191" "face.1571" \
  "face.1570" "face.2183" "face.2184" "face.2196" "face.2193" "face.1627" \
  "face.1634" "face.1580" "face.1577" "face.1558"
physics delete btype
physics create "Vin" btype "VELOCITY_INLET" face "face.1272"
physics create "Pout" btype "PRESSURE_OUTLET" face "face.1275"
physics create "Particle1" btype "WALL" face "face.1639"
physics create "Particle2" btype "WALL" face "face.38"
physics create "Sym1" btype "SYMMETRY" face "face.2194" "face.1462" \
  "face.1471" "face.1461" "face.2192" "face.1470" "face.2195"
window modify volume "volume.53" invisible
window modify volume visible
window modify invisible mesh
physics create "Sym2" btype "SYMMETRY" face "face.2190" "face.1518" \
  "face.2173" "face.1271" "face.2181" "face.2180" "face.2187" "face.2174" \
  "face.2175" "face.2176" "face.2177" "face.2178" "face.2179" "face.2182" \
  "face.2183" "face.2184" "face.2185" "face.2186" "face.2188" "face.2189"
physics create btype "SYMMETRY" face "face.2191" "face.1571" "face.2193" \
  "face.1570" "face.2196" "face.1580" "face.1558" "face.1559" "face.1577"
physics modify "symmetry.22" btype label "Sym3" face "face.2191" "face.1571" \
  "face.2193" "face.1570" "face.2196" "face.1580" "face.1558" "face.1559" \
  "face.1577"
physics modify "Sym1" btype face "face.2194" "face.1462" "face.1471" \
  "face.1461" "face.2192" "face.1470" "face.2195" "face.1476" "face.1479"
physics modify "Sym1" btype face "face.2194" "face.1462" "face.1471" \
  "face.1461" "face.2192" "face.1470" "face.2195" "face.1476" "face.1479" \
  "face.1482"
physics modify "Sym3" btype face "face.2191" "face.1571" "face.2193" \
  "face.1570" "face.2196" "face.1580" "face.1558" "face.1559"
physics modify "Sym2" btype face "face.2190" "face.1518" "face.2173" \
  "face.1271" "face.2181" "face.2180" "face.2187" "face.2174" "face.2175" \
  "face.2176" "face.2177" "face.2178" "face.2179" "face.2182" "face.2183" \
  "face.2184" "face.2185" "face.2186" "face.2188" "face.2189"
physics create "Particles" btype "WALL" face "face.4" "face.6" "face.8" \
  "face.10" "face.18" "face.19" "face.20" "face.23" "face.24" "face.25" \
  "face.26" "face.28" "face.29" "face.30" "face.33" "face.34" "face.35" \
  "face.37" "face.39" "face.40" "face.54" "face.72" "face.78" "face.84" \
  "face.92" "face.102" "face.114" "face.116" "face.120" "face.122" "face.128" \
  "face.132" "face.134" "face.138" "face.140" "face.144" "face.146" \
  "face.150" "face.152" "face.156" "face.158" "face.162" "face.164" \
  "face.168" "face.170" "face.176" "face.184" "face.186" "face.190" \
  "face.204" "face.206" "face.210" "face.212" "face.216" "face.218" \
  "face.224" "face.230" "face.233" "face.234" "face.246" "face.248" \
```

```
"face.252" "face.254" "face.263" "face.264" "face.270" "face.274" \
"face.282" "face.286" "face.296" "face.299" "face.300" "face.302" \
"face.306" "face.308" "face.312" "face.314" "face.318" "face.320" \
"face.324" "face.326" "face.348" "face.350" "face.354" "face.356" \
"face.366" "face.368" "face.372" "face.376" "face.378" "face.382" \
"face.405" "face.407" "face.408" "face.412" "face.414" "face.418" \
"face.426" "face.430" "face.432" "face.436" "face.438" "face.442" \
"face.444" "face.448" "face.456" "face.460" "face.462" "face.466" \
"face.474" "face.476" "face.480" "face.482" "face.486" "face.488" \
"face.498" "face.500" "face.504" "face.526" "face.527" "face.531" \
"face.532" "face.537" "face.538" "face.543" "face.544" "face.549" \
"face.550" "face.567" "face.568" "face.573" "face.574" "face.579" \
"face.580" "face.584" "face.586" "face.591" "face.592" "face.603" \
"face.604" "face.609" "face.610" "face.615" "face.616" "face.621" \
"face.622" "face.633" "face.634" "face.639" "face.640" "face.644" \
"face.646" "face.651" "face.652" "face.657" "face.663" "face.664" \
"face.669" "face.670" "face.687" "face.688" "face.693" "face.694" \
"face.705" "face.706" "face.709" "face.714" "face.715" "face.721" \
"face.732" "face.733" "face.734" "face.740" "face.742" "face.746" \
"face.750" "face.756" "face.757" "face.762" "face.763" "face.770" \
"face.772" "face.777" "face.794" "face.795" "face.800" "face.801" \
"face.806" "face.807" "face.812" "face.813" "face.814" "face.820" \
"face.826" "face.828" "face.832" "face.834" "face.848" "face.854" \
"face.869" "face.886" "face.887" "face.906" "face.908" "face.941" \
"face.943" "face.954" "face.955" "face.962" "face.964" "face.1000" \
"face.1002" "face.1004" "face.1007" "face.1008" "face.1009" "face.1010" \
"face.1011" "face.1015" "face.1016" "face.1017" "face.1018" "face.1019" \
"face.1020" "face.1021" "face.1022" "face.1023" "face.1024" "face.1025" \
"face.1026" "face.1027" "face.1029" "face.1031" "face.1032" "face.1033" \
"face.1034" "face.1035" "face.1036" "face.1037" "face.1038" "face.1039" \
"face.1042" "face.1044" "face.1048" "face.1050" "face.1056" "face.1061" \
"face.1062" "face.1063" "face.1064" "face.1065" "face.1066" "face.1067" \
"face.1068" "face.1069" "face.1070" "face.1071" "face.1072" "face.1075" \
"face.1076" "face.1077" "face.1078" "face.1079" "face.1080" "face.1081" \
"face.1082" "face.1083" "face.1084" "face.1089" "face.1090" "face.1091" \
"face.1092" "face.1093" "face.1094" "face.1097" "face.1098" "face.1099" \
"face.1100" "face.1101" "face.1102" "face.1103" "face.1104" "face.1107" \
"face.1108" "face.1109" "face.1110" "face.1113" "face.1114" "face.1115" \
"face.1116" "face.1117" "face.1118" "face.1125" "face.1126" "face.1127" \
"face.1128" "face.1129" "face.1130" "face.1131" "face.1132" "face.1133" \
"face.1134" "face.1139" "face.1140" "face.1141" "face.1142" "face.1143" \
"face.1144" "face.1145" "face.1146" "face.1147" "face.1148" "face.1151" \
"face.1152" "face.1153" "face.1154" "face.1155" "face.1156" "face.1157" \
"face.1158" "face.1161" "face.1162" "face.1163" "face.1164" "face.1165" \
"face.1166" "face.1167" "face.1168" "face.1171" "face.1172" "face.1173" \
"face.1174" "face.1177" "face.1179" "face.1180" "face.1181" "face.1182" \
"face.1185" "face.1186" "face.1187" "face.1188" "face.1193" "face.1194" \
"face.1201" "face.1202" "face.1203" "face.1204" "face.1209" "face.1210" \
"face.1211" "face.1212" "face.1213" "face.1214" "face.1215" "face.1216" \
"face.1218" "face.1224" "face.1226" "face.1227" "face.1229" "face.1230" \
"face.1231" "face.1232" "face.1233" "face.1235" "face.1237" "face.1238" \
"face.1239" "face.1240" "face.1246" "face.1253" "face.1255" "face.1256" \
"face.1260" "face.1280" "face.1281" "face.1287" "face.1288" "face.1293" \
"face.1294" "face.1305" "face.1306" "face.1311" "face.1312" "face.1317" \
"face.1318" "face.1323" "face.1335" "face.1341" "face.1342" "face.1347" \
"face.1348" "face.1353" "face.1354" "face.1365" "face.1366" "face.1371" \
"face.1372" "face.1383" "face.1389" "face.1390" "face.1395" "face.1396" \
"face.1401" "face.1402" "face.1413" "face.1463" "face.1464" "face.1465" \
"face.1466" "face.1467" "face.1477" "face.1480" "face.1483" "face.1484" \
"face.1485" "face.1486" "face.1521" "face.1522" "face.1523" "face.1524" \
"face.1525" "face.1526" "face.1527" "face.1528" "face.1529" "face.1530" \
"face.1531" "face.1532" "face.1533" "face.1534" "face.1535" "face.1536" \
"face.1537" "face.1538" "face.1539" "face.1540" "face.1541" "face.1542" \
"face.1543" "face.1544" "face.1545" "face.1546" "face.1547" "face.1550" \
"face.1552" "face.1553" "face.1554" "face.1555" "face.1558" "face.1560" \
"face.1561" "face.1562" "face.1563" "face.1564" "face.1565" "face.1566" \
"face.1567" "face.1568" "face.1569" "face.1572" "face.1573" "face.1574" \
"face.1577" "face.1578" "face.1579" "face.1583" "face.1584" "face.1585" \
"face.1586" "face.1587" "face.1589" "face.1590" "face.1591" "face.1592" \
"face.1593" "face.1594" "face.1595" "face.1596" "face.1597" "face.1598" \
"face.1599" "face.1600" "face.1601" "face.1602" "face.1603" "face.1604" \
```

```
  "face.1605" "face.1606" "face.1607" "face.1608" "face.1609" "face.1610" \
  "face.1611" "face.1612" "face.1613" "face.1614" "face.1615" "face.1616" \
  "face.1617" "face.1618" "face.1619"
physics modify "Sym3" btype face "face.2191" "face.1571" "face.2193" \
  "face.1570" "face.2196" "face.1580" "face.1558" "face.1559" "face.1638"
physics create "BigWall" btype "WALL" face "face.2197"
physics create "SmallWalls" btype "WALL" face "face.1636" "face.1637" \
  "face.1620" "face.1621" "face.1622" "face.1623" "face.1624" "face.1625" \
  "face.1626" "face.1627" "face.1628" "face.1629" "face.1630" "face.1631" \
  "face.1632" "face.1633" "face.1634" "face.1635"
export fluent5 "finalwall1.msh"
```

Appendix B: Spreadsheets for Determining Effective Radial Thermal Conductivity

Simulation 1 Information

Velocity (m/s)	0.500
Bridge (in)	0.050
kw	0.026
Refinement #	0

Iso-clip Name	Avg Temp (K)	L (m)	L/d	dT (K)	dT/dr	d2T/dr2	F1	Eulers K
115.000	287.209	0.0E+00	0.00	N/A	50166.300	4.060E+08	-8112.409	0.026
114.000	292.226	1.0E-04	0.02	5.017	90764.500	-5.475E+08	6012.723	0.042
113.000	301.302	2.0E-04	0.03	9.076	36011.300	5.432E+07	-1528.234	0.035
112.000	304.903	3.0E-04	0.05	3.601	41443.500	-7.259E+07	1731.643	0.041
111.000	309.048	4.0E-04	0.06	4.144	34184.900	-3.692E+07	1060.021	0.046
110.000	312.466	5.0E-04	0.08	3.418	30493.400	-9.580E+07	3121.684	0.060
109.000	315.516	6.0E-04	0.09	3.049	20913.700	-1.489E+06	51.277	0.060
108.000	317.607	7.0E-04	0.11	2.091	20764.800	-1.780E+07	837.308	0.065
107.000	319.683	8.0E-04	0.13	2.076	18984.700	-3.122E+07	1624.324	0.076
106.000	321.582	9.0E-04	0.14	1.898	15863.000	-2.344E+07	1457.801	0.087
105.000	323.168	1.0E-03	0.16	1.586	13518.700	-2.106E+07	1537.836	0.101
104.000	324.520	1.1E-03	0.17	1.352	11412.600	-1.832E+07	1585.298	0.116
103.000	325.661	1.2E-03	0.19	1.141	9580.400	-1.431E+07	1473.096	0.134
102.000	326.619	1.3E-03	0.20	0.958	8149.800	-1.309E+07	1586.340	0.155
101.000	327.434	1.4E-03	0.22	0.815	6840.500	-1.219E+07	1761.206	0.182
100.000	328.118	1.5E-03	0.24	0.684	5621.900	-7.635E+06	1337.798	0.206
99.000	328.681	1.6E-03	0.25	0.562	4858.400	-7.757E+06	1576.291	0.239
98.000	329.166	1.7E-03	0.27	0.486	4082.700	-2.183E+06	514.329	0.251
97.000	329.575	1.8E-03	0.28	0.408	3864.400	-3.860E+06	978.453	0.276
96.000	329.961	1.9E-03	0.30	0.386	3478.400	-2.630E+05	55.160	0.277
95.000	330.309	2.0E-03	0.31	0.348	3452.100	-8.480E+05	225.156	0.284
94.000	330.654	2.1E-03	0.33	0.345	3367.300	-3.050E+05	70.043	0.286
93.000	330.991	2.2E-03	0.35	0.337	3336.800	-2.160E+05	44.157	0.287
92.000	331.325	2.3E-03	0.36	0.334	3315.200	-1.540E+05	25.834	0.288
91.000	331.656	2.4E-03	0.38	0.332	3299.800	1.110E+05	-54.300	0.286
90.000	331.986	2.5E-03	0.39	0.330	3310.900	-5.530E+05	146.320	0.290
89.000	332.317	2.6E-03	0.41	0.331	3255.600	5.370E+05	-185.693	0.285
88.000	332.643	2.7E-03	0.43	0.326	3309.300	-3.600E+05	87.994	0.287
87.000	332.974	2.8E-03	0.44	0.331	3273.300	5.900E+05	-201.080	0.282
86.000	333.301	2.9E-03	0.46	0.327	3332.300	-1.106E+06	311.026	0.290
85.000	333.634	3.0E-03	0.47	0.333	3221.700	1.023E+06	-338.455	0.280
84.000	333.956	3.1E-03	0.49	0.322	3324.000	-1.334E+06	380.359	0.291
83.000	334.289	3.2E-03	0.50	0.332	3190.600	N/A	N/A	N/A
82.000	334.608	3.3E-03	0.52	0.319	N/A	N/A	N/A	N/A

Simulation 1 Information

Velocity (m/s)	0.500
Bridge (in)	0.050
kw	0.026
Refinement #	1

Avg Temp (K)	dT (K)	dT/dr	d2T/dr2	F1	Eulers K
286.200	N/A	65425.1	166647000	-2566.826733	0.026
292.742	6.54251	82089.8	-356817000	4326.942833	0.037
300.951	8.20898	46408.1	-74676000	1589.352804	0.043
305.592	4.64081	38940.5	-65635000	1665.718237	0.050
309.486	3.89405	32377	-18665000	556.6482134	0.053
312.724	3.2377	30510.5	-101556000	3308.678305	0.071
315.775	3.05105	20354.9	535000	-46.20391629	0.070
317.810	2.03549	20408.4	-18196000	871.6335777	0.077
319.851	2.04084	18588.8	-29186000	1550.085213	0.088
321.710	1.85888	15670.2	-24796000	1562.32645	0.102
323.277	1.56702	13190.6	-21200000	1587.12481	0.118
324.596	1.31906	11070.6	-17765000	1584.580015	0.137
325.703	1.10706	9294.1	-13781000	1462.607348	0.157
326.633	0.92941	7916	-11778000	1467.670643	0.180
327.424	0.7916	6738.2	-10634000	1557.923361	0.209
328.098	0.67382	5674.8	-7957000	1381.879977	0.237
328.666	0.56748	4879.1	-7030000	1420.514296	0.271
329.153	0.48791	4176.1	-2931000	681.4844105	0.290
329.571	0.41761	3883	-4159000	1050.670899	0.320
329.959	0.3883	3467.1	-107000	10.41162917	0.320
330.306	0.34671	3456.4	-1455000	400.4664191	0.333
330.652	0.34564	3310.9	112000	-54.36154106	0.331
330.983	0.33109	3322.1	-87999.99999	5.913137147	0.331
331.315	0.33221	3313.3	-104000	10.77008906	0.332
331.646	0.33133	3302.9	49000	-35.49660466	0.331
331.977	0.33029	3307.8	-543000	143.4535123	0.335
332.307	0.33078	3253.5	482000	-168.8950361	0.330
332.633	0.32535	3301.7	-354000	86.42747323	0.333
332.963	0.33017	3266.3	604000	-205.7520487	0.326
333.290	0.32663	3326.7	-1107000	311.88537	0.336
333.622	0.33267	3216	991000	-329.0672683	0.325
333.944	0.3216	3315.1	-1306000	372.9905729	0.337
334.275	0.33151	3184.5	N/A	N/A	N/A
334.594	0.31845	N/A	N/A	N/A	N/A

Simulation 2 Information

Velocity (m/s)	0.268
Bridge (in)	0.050
kw	0.026
Refinement #	0

Iso-clip Name	Avg Temp (K)	L (m)	L/d	dT (K)	dT/dr	d2T/dr2	F1	Eulers K
115.000	286.008	0.0E+00	0.00	N/A	39612.400	3.885E+08	-9828.407	0.026
114.000	289.969	1.0E-04	0.02	3.961	78467.100	-4.386E+08	5569.702	0.040
113.000	297.816	2.0E-04	0.03	7.847	34608.500	7.891E+07	-2299.810	0.031
112.000	301.276	3.0E-04	0.05	3.461	42499.400	-6.451E+07	1498.055	0.036
111.000	305.526	4.0E-04	0.06	4.250	36048.600	-9.011E+07	2479.840	0.045
110.000	309.131	5.0E-04	0.08	3.605	27037.600	-5.242E+06	173.997	0.046
109.000	311.835	6.0E-04	0.09	2.704	26513.400	-5.815E+07	2173.273	0.055
108.000	314.486	7.0E-04	0.11	2.651	20698.500	-2.766E+07	1316.224	0.063
107.000	316.556	8.0E-04	0.13	2.070	17932.800	-3.633E+07	2005.674	0.075
106.000	318.349	9.0E-04	0.14	1.793	14300.200	-2.623E+07	1814.200	0.089
105.000	319.779	1.0E-03	0.16	1.430	11677.200	-2.351E+07	1992.988	0.107
104.000	320.947	1.1E-03	0.17	1.168	9326.500	-1.902E+07	2019.444	0.128
103.000	321.880	1.2E-03	0.19	0.933	7424.300	-1.385E+07	1845.469	0.152
102.000	322.622	1.3E-03	0.20	0.742	6039.200	-1.055E+07	1726.387	0.178
101.000	323.226	1.4E-03	0.22	0.604	4984.400	-7.754E+06	1535.411	0.205
100.000	323.725	1.5E-03	0.24	0.498	4209.000	-4.544E+06	1059.307	0.227
99.000	324.146	1.6E-03	0.25	0.421	3754.600	-3.294E+06	856.999	0.247
98.000	324.521	1.7E-03	0.27	0.375	3425.200	-3.650E+05	86.197	0.249
97.000	324.863	1.8E-03	0.28	0.343	3388.700	-1.572E+06	443.487	0.260
96.000	325.202	1.9E-03	0.30	0.339	3231.500	8.490E+05	-283.176	0.252
95.000	325.526	2.0E-03	0.31	0.323	3316.400	-1.960E+05	38.608	0.253
94.000	325.857	2.1E-03	0.33	0.332	3296.800	2.040E+05	-82.412	0.251
93.000	326.187	2.2E-03	0.35	0.330	3317.200	4.340E+05	-151.409	0.247
92.000	326.519	2.3E-03	0.36	0.332	3360.600	-4.300E+05	107.335	0.250
91.000	326.855	2.4E-03	0.38	0.336	3317.600	4.940E+05	-169.564	0.246
90.000	327.186	2.5E-03	0.39	0.332	3367.000	-7.480E+05	201.452	0.251
89.000	327.523	2.6E-03	0.41	0.337	3292.200	4.490E+05	-157.130	0.247
88.000	327.852	2.7E-03	0.43	0.329	3337.100	-5.520E+05	144.623	0.250
87.000	328.186	2.8E-03	0.44	0.334	3281.900	6.770E+05	-227.116	0.245
86.000	328.514	2.9E-03	0.46	0.328	3349.600	-1.056E+06	294.385	0.252
85.000	328.849	3.0E-03	0.47	0.335	3244.000	8.950E+05	-296.814	0.245
84.000	329.174	3.1E-03	0.49	0.324	3333.500	-1.200E+06	339.018	0.253
83.000	329.507	3.2E-03	0.50	0.333	3213.500	N/A	N/A	N/A
82.000	329.828	3.3E-03	0.52	0.321	N/A	N/A	N/A	N/A

Simulation 2 Information

Velocity (m/s)	0.268
Bridge (in)	0.050
kw	0.026
Refinement #	1

Avg Temp (K)	dT (K)	dT/dr	d2T/dr2	F1	Eulers K
285.49326	N/A	47384.3	235559000	-4990.931	0.026
290.23169	4.73843	70940.2	-262710000	3683.536	0.036
297.32571	7.09402	44669.2	-43567000	955.5624	0.039
301.79263	4.46692	40312.5	-57022000	1394.697	0.044
305.82388	4.03125	34610.3	-70065000	2004.556	0.053
309.28491	3.46103	27603.8	-19266000	678.0667	0.057
312.04529	2.76038	25677.2	-52979000	2043.35	0.069
314.61301	2.56772	20379.3	-27139000	1311.734	0.078
316.65094	2.03793	17665.4	-36014000	2018.674	0.093
318.41748	1.76654	14064	-26623000	1872.949	0.111
319.82388	1.4064	11401.7	-22635000	1965.15	0.132
320.96405	1.14017	9138.2	-18256000	1977.647	0.159
321.87787	0.91382	7312.6	-13092000	1770.173	0.187
322.60913	0.73126	6003.4	-10400000	1712.15	0.219
323.20947	0.60034	4963.4	-7413000	1473.29	0.251
323.70581	0.49634	4222.1	-4877000	1134.828	0.279
324.12802	0.42221	3734.4	-3133000	818.6315	0.302
324.50146	0.37344	3421.1	-563000	144.2004	0.307
324.84357	0.34211	3364.8	-1644000	468.1796	0.321
325.18005	0.33648	3200.4	989000	-329.4738	0.310
325.50009	0.32004	3299.3	-385000	96.19962	0.313
325.83002	0.32993	3260.8	375000	-135.5363	0.309
326.1561	0.32608	3298.3	428000	-150.3399	0.304
326.48593	0.32983	3341.1	-345000	82.64085	0.307
326.82004	0.33411	3306.6	433000	-151.6114	0.302
327.1507	0.33066	3349.9	-702000	188.8546	0.308
327.48569	0.33499	3279.7	412000	-146.3681	0.303
327.81366	0.32797	3320.9	-500000	129.7716	0.307
328.14575	0.33209	3270.9	641000	-216.8039	0.301
328.47284	0.32709	3335	-1014000	283.1711	0.309
328.80634	0.3335	3233.6	852000	-284.4039	0.300
329.1297	0.32336	3318.8	-1148000	324.9438	0.310
329.46158	0.33188	3204	N/A	N/A	N/A
329.78198	0.3204	N/A	N/A	N/A	N/A

Simulation 2 Information

Velocity (m/s)	0.268
Bridge (in)	0.050
kw	0.026
Refinement #	2

Avg Temp (K)	dT (K)	dT/dr	d2T/dr2	F1	Eulers K
285.04788	N/A	5.3E+04	1.3E+08	-2462.137	0.026
290.39648	5.3486	6.7E+04	-1.8E+08	2745.623	0.033
297.05145	6.65497	4.8E+04	-8.5E+07	1748.947	0.039
301.86609	4.81464	4.0E+04	-5.6E+07	1397.912	0.044
305.82916	3.96307	3.4E+04	-5.5E+07	1597.578	0.051
309.23038	3.40122	2.9E+04	-3.0E+07	1040.622	0.057
312.08148	2.8511	2.5E+04	-4.6E+07	1797.684	0.067
314.63022	2.54874	2.1E+04	-3.4E+07	1601.873	0.078
316.7157	2.08548	1.7E+04	-3.4E+07	1953.616	0.093
318.46295	1.74725	1.4E+04	-2.8E+07	1978.52	0.111
319.86536	1.40241	1.1E+04	-2.2E+07	1955.448	0.133
320.98749	1.12213	9.0E+03	-1.8E+07	1931.015	0.159
321.88794	0.90045	7.2E+03	-1.3E+07	1754.219	0.187
322.6127	0.72476	6.0E+03	-1.0E+07	1682.361	0.218
323.20886	0.59616	4.9E+03	-7.6E+06	1507.877	0.251
323.70352	0.49466	4.2E+03	-4.9E+06	1150.165	0.280
324.12259	0.41907	3.7E+03	-3.0E+06	782.6044	0.302
324.49261	0.37002	3.4E+03	-8.2E+05	220.2963	0.308
324.83292	0.34031	3.3E+03	-1.3E+06	368.3068	0.320
325.16504	0.33212	3.2E+03	9.0E+05	-303.649	0.310
325.48425	0.31921	3.3E+03	-3.4E+05	83.69708	0.313
325.8125	0.32825	3.2E+03	4.7E+05	-164.3014	0.308
326.13733	0.32483	3.3E+03	3.1E+05	-114.9616	0.304
326.46683	0.3295	3.3E+03	-7.6E+04	2.231027	0.304
326.79944	0.33261	3.3E+03	1.8E+05	-75.80655	0.302
327.13129	0.33185	3.3E+03	-6.2E+05	166.0019	0.307
327.46497	0.33368	3.3E+03	4.9E+05	-169.1665	0.302
327.79242	0.32745	3.3E+03	-5.9E+05	155.8523	0.306
328.12473	0.33231	3.3E+03	7.0E+05	-234.3488	0.299
328.45117	0.32644	3.3E+03	-1.0E+06	282.3534	0.308
328.78458	0.33341	3.2E+03	8.1E+05	-270.2246	0.299
329.10788	0.3233	3.3E+03	-1.1E+06	310.6991	0.309
329.43924	0.33136	3.2E+03	N/A	N/A	N/A
329.75961	0.32037	N/A	N/A	N/A	N/A

Simulation 3 Information

Velocity (m/s)	0.223
Bridge (in)	0.050
kw	0.026
Refinement #	0

Iso-clip Name	Avg Temp (K)	L (m)	L/d	dT (K)	dT/dr	d2T/dr2	F1	Eulers K
115.000	285.567	0.0E+00	0.00	N/A	34526.000	3.508E+08	-10179.188	0.026
114.000	289.020	1.0E-04	0.02	3.453	69602.700	-3.802E+08	5442.852	0.040
113.000	295.980	2.0E-04	0.03	6.960	31581.700	7.637E+07	-2438.062	0.030
112.000	299.138	3.0E-04	0.05	3.158	39219.100	-5.574E+07	1401.393	0.035
111.000	303.060	4.0E-04	0.06	3.922	33645.300	-8.211E+07	2420.737	0.043
110.000	306.424	5.0E-04	0.08	3.365	25433.900	-3.734E+06	126.931	0.044
109.000	308.968	6.0E-04	0.09	2.543	25060.500	-5.366E+07	2121.418	0.053
108.000	311.474	7.0E-04	0.11	2.506	19694.200	-2.545E+07	1272.400	0.059
107.000	313.443	8.0E-04	0.13	1.969	17149.000	-3.373E+07	1946.879	0.071
106.000	315.158	9.0E-04	0.14	1.715	13776.000	-2.490E+07	1787.669	0.084
105.000	316.536	1.0E-03	0.16	1.378	11285.700	-2.277E+07	1997.429	0.101
104.000	317.664	1.1E-03	0.17	1.129	9008.800	-1.884E+07	2070.724	0.121
103.000	318.565	1.2E-03	0.19	0.901	7125.200	-1.366E+07	1897.259	0.144
102.000	319.278	1.3E-03	0.20	0.713	5759.000	-1.003E+07	1722.288	0.169
101.000	319.854	1.4E-03	0.22	0.576	4755.500	-7.055E+06	1463.302	0.194
100.000	320.329	1.5E-03	0.24	0.476	4050.000	-3.986E+06	963.914	0.213
99.000	320.734	1.6E-03	0.25	0.405	3651.400	-2.636E+06	701.590	0.228
98.000	321.099	1.7E-03	0.27	0.365	3387.800	-2.870E+05	64.349	0.229
97.000	321.438	1.8E-03	0.28	0.339	3359.100	-1.340E+06	378.508	0.238
96.000	321.774	1.9E-03	0.30	0.336	3225.100	9.090E+05	-302.302	0.231
95.000	322.097	2.0E-03	0.31	0.323	3316.000	-3.720E+05	91.692	0.233
94.000	322.428	2.1E-03	0.33	0.332	3278.800	3.240E+05	-119.351	0.230
93.000	322.756	2.2E-03	0.35	0.328	3311.200	3.630E+05	-130.204	0.227
92.000	323.087	2.3E-03	0.36	0.331	3347.500	-4.520E+05	114.408	0.229
91.000	323.422	2.4E-03	0.38	0.335	3302.300	3.930E+05	-139.669	0.226
90.000	323.752	2.5E-03	0.39	0.330	3341.600	-8.020E+05	219.301	0.231
89.000	324.086	2.6E-03	0.41	0.334	3261.400	4.250E+05	-151.059	0.228
88.000	324.412	2.7E-03	0.43	0.326	3303.900	-5.780E+05	154.155	0.231
87.000	324.743	2.8E-03	0.44	0.330	3246.100	6.200E+05	-211.832	0.226
86.000	325.067	2.9E-03	0.46	0.325	3308.100	-9.580E+05	268.715	0.232
85.000	325.398	3.0E-03	0.47	0.331	3212.300	8.510E+05	-285.840	0.226
84.000	325.719	3.1E-03	0.49	0.321	3297.400	-1.147E+06	326.885	0.233
83.000	326.049	3.2E-03	0.50	0.330	3182.700	N/A	N/A	N/A
82.000	326.367	3.3E-03	0.52	0.318	N/A	N/A	N/A	N/A

Simulation 3 Information

Velocity (m/s)	0.223
Bridge (in)	0.050
kw	0.026
Refinement #	1

Avg Temp (K)	dT (K)	dT/dr	d2T/dr2	F1	Eulers K
285.174	N/A	40390.3	226740000	-5633.4091	0.026
289.213	4.03903	63064.3	-227213000	3583.1545	0.035
295.520	6.30643	40343	-29446000	710.12834	0.038
299.554	4.0343	37398.4	-50028000	1317.9023	0.043
303.294	3.73984	32395.6	-64300000	1964.9962	0.051
306.533	3.23956	25965.6	-15836000	590.00313	0.054
309.130	2.59656	24382	-49322000	2002.9654	0.065
311.568	2.4382	19449.8	-24674000	1248.6391	0.073
313.513	1.94498	16982.4	-33056000	1926.4858	0.087
315.211	1.69824	13676.8	-25657000	1855.9104	0.104
316.579	1.36768	11111.1	-22057000	1965.0517	0.124
317.690	1.11111	8905.4	-18379000	2043.6833	0.149
318.581	0.89054	7067.5	-13219000	1850.2314	0.177
319.287	0.70675	5745.6	-10096000	1736.9687	0.208
319.862	0.57456	4736	-6790000	1413.4564	0.237
320.335	0.4736	4057	-4217000	1019.154	0.261
320.741	0.4057	3635.3	-2525000	674.25296	0.279
321.105	0.36353	3382.8	-368000	88.419023	0.281
321.443	0.33828	3346	-1344000	381.26548	0.292
321.778	0.3346	3211.6	959000	-319.05495	0.283
322.099	0.32116	3307.5	-433000	110.42278	0.286
322.429	0.33075	3264.2	439000	-155.02319	0.281
322.756	0.32642	3308.1	330000	-120.33128	0.278
323.087	0.33081	3341.1	-370000	90.123415	0.280
323.421	0.33411	3304.1	333000	-121.44503	0.277
323.751	0.33041	3337.4	-766000	208.81605	0.283
324.085	0.33374	3260.8	382000	-137.89605	0.279
324.411	0.32608	3299	-547000	145.0178	0.283
324.741	0.3299	3244.3	589000	-202.38251	0.277
325.065	0.32443	3303.2	-912000	255.21908	0.284
325.396	0.33032	3212	796000	-268.74117	0.277
325.717	0.3212	3291.6	-1095000	311.7006	0.285
326.046	0.32916	3182.1	N/A	N/A	N/A
326.364	0.31821	N/A	N/A	N/A	N/A

Simulation 4 Information

Velocity (m/s)	0.188
Bridge (in)	0.050
kw	0.026
Refinement #	0

Iso-clip Name	Avg Temp (K)	L (m)	L/d	dT (K)	dT/dr	d2T/dr2	F1	Eulers K
115.000	285.29776	0.0E+00	0.00	N/A	31426.700	3.252E+08	-10368.497	0.026
114.000	288.44043	1.0E-04	0.02	3.143	63949.600	-3.431E+08	5346.064	0.040
113.000	294.83539	2.0E-04	0.03	6.395	29635.600	7.408E+07	-2519.324	0.030
112.000	297.79895	3.0E-04	0.05	2.964	37043.200	-5.035E+07	1339.314	0.034
111.000	301.50327	4.0E-04	0.06	3.704	32008.600	-7.788E+07	2413.161	0.042
110.000	304.70413	5.0E-04	0.08	3.201	24220.900	-4.111E+06	149.849	0.043
109.000	307.12622	6.0E-04	0.09	2.422	23809.800	-5.033E+07	2093.999	0.052
108.000	309.5072	7.0E-04	0.11	2.381	18776.600	-2.420E+07	1268.931	0.058
107.000	311.38486	8.0E-04	0.13	1.878	16356.500	-3.155E+07	1909.019	0.069
106.000	313.02051	9.0E-04	0.14	1.636	13201.300	-2.338E+07	1750.770	0.081
105.000	314.34064	1.0E-03	0.16	1.320	10863.600	-2.149E+07	1958.085	0.097
104.000	315.427	1.1E-03	0.17	1.086	8714.600	-1.805E+07	2051.575	0.117
103.000	316.29846	1.2E-03	0.19	0.871	6909.200	-1.291E+07	1847.783	0.139
102.000	316.98938	1.3E-03	0.20	0.691	5618.600	-9.424E+06	1657.084	0.162
101.000	317.55124	1.4E-03	0.22	0.562	4676.200	-6.149E+06	1294.714	0.183
100.000	318.01886	1.5E-03	0.24	0.468	4061.300	-3.779E+06	910.206	0.199
99.000	318.42499	1.6E-03	0.25	0.406	3683.400	-2.245E+06	589.166	0.211
98.000	318.79333	1.7E-03	0.27	0.368	3458.900	-1.530E+05	23.867	0.212
97.000	319.13922	1.8E-03	0.28	0.346	3443.600	-1.462E+06	404.148	0.220
96.000	319.48358	1.9E-03	0.30	0.344	3297.400	8.520E+05	-278.835	0.214
95.000	319.81332	2.0E-03	0.31	0.330	3382.600	-4.950E+05	125.845	0.217
94.000	320.15158	2.1E-03	0.33	0.338	3333.100	1.560E+05	-67.337	0.215
93.000	320.48489	2.2E-03	0.35	0.333	3348.700	2.720E+05	-101.802	0.213
92.000	320.81976	2.3E-03	0.36	0.335	3375.900	-6.480E+05	171.330	0.217
91.000	321.15735	2.4E-03	0.38	0.338	3311.100	3.400E+05	-123.346	0.214
90.000	321.48846	2.5E-03	0.39	0.331	3345.100	-9.470E+05	262.397	0.220
89.000	321.82297	2.6E-03	0.41	0.335	3250.400	3.020E+05	-113.659	0.217
88.000	322.14801	2.7E-03	0.43	0.325	3280.600	-6.060E+05	163.932	0.221
87.000	322.47607	2.8E-03	0.44	0.328	3220.000	5.850E+05	-202.510	0.216
86.000	322.79807	2.9E-03	0.46	0.322	3278.500	-1.007E+06	286.276	0.223
85.000	323.12592	3.0E-03	0.47	0.328	3177.800	8.080E+05	-275.184	0.216
84.000	323.4437	3.1E-03	0.49	0.318	3258.600	-1.098E+06	315.990	0.223
83.000	323.76956	3.2E-03	0.50	0.326	3148.800	N/A	N/A	N/A
82.000	324.08444	3.3E-03	0.52	0.315	N/A	N/A	N/A	N/A

Simulation 4 Information

Velocity (m/s)	0.188
Bridge (in)	0.050
kw	0.026
Refinement #	1

Avg Temp (K)	dT (K)	dT/dr	d2T/dr2	F1	Eulers K
284.947	N/A	36635.2	208913000	-5722.21	0.026
288.611	3.66352	57526.5	-194158000	3355.382	0.035
294.363	5.75265	38110.7	-28800000	735.9304	0.037
298.174	3.81107	35230.7	-43967000	1228.172	0.042
301.697	3.52307	30834	-59576000	1912.312	0.050
304.781	3.0834	24876.4	-17303000	675.6781	0.053
307.268	2.48764	23146.1	-45810000	1959.247	0.064
309.583	2.31461	18565.1	-23542000	1248.118	0.072
311.440	1.85651	16210.9	-30636000	1869.84	0.085
313.061	1.62109	13147.3	-24076000	1811.21	0.100
314.375	1.31473	10739.7	-21102000	1944.779	0.120
315.449	1.07397	8629.5	-17713000	2032.49	0.144
316.312	0.86295	6858.2	-12680000	1828.72	0.171
316.998	0.68582	5590.2	-9518000	1682.42	0.199
317.557	0.55902	4638.4	-5991000	1271.366	0.225
318.021	0.46384	4039.3	-3879000	940.0309	0.246
318.425	0.40393	3651.4	-2102000	555.3444	0.260
318.790	0.36514	3441.2	-172000	29.61597	0.260
319.134	0.34412	3424	-1421000	394.6035	0.271
319.477	0.3424	3281.9	891000	-291.939	0.263
319.805	0.32819	3371	-513000	131.6886	0.266
320.142	0.3371	3319.7	250000	-95.8419	0.264
320.474	0.33197	3344.7	226000	-88.1457	0.261
320.808	0.33447	3367.3	-546000	141.5292	0.265
321.145	0.33673	3312.7	271000	-102.468	0.262
321.476	0.33127	3339.8	-921000	255.0611	0.269
321.810	0.33398	3247.7	293000	-110.965	0.266
322.135	0.32477	3277	-583000	157.1166	0.270
322.463	0.3277	3218.7	558000	-194.195	0.265
322.785	0.32187	3274.5	-964000	273.5193	0.272
323.112	0.32745	3178.1	760000	-260.057	0.265
323.430	0.31781	3254.1	-1032000	296.174	0.273
323.755	0.32541	3150.9	N/A	N/A	N/A
324.070	0.31509	N/A	N/A	N/A	N/A

Simulation 5 Information

Velocity (m/s)	0.080
Bridge (in)	0.050
kw	0.026
Refinement #	0

Iso-clip Name	Avg Temp (K)	L (m)	L/d	dT (K)	dT/dr	d2T/dr2	F1	Eulers K
115.000	284.23703	0.0E+00	0.00	N/A	17525.600	1.886E+08	-10783.653	0.026
114.000	285.98959	1.0E-04	0.02	1.753	36390.100	-1.825E+08	4994.992	0.039
113.000	289.6286	2.0E-04	0.03	3.639	18141.500	5.171E+07	-2870.078	0.028
112.000	291.44275	3.0E-04	0.05	1.814	23312.400	-2.555E+07	1076.181	0.031
111.000	293.77399	4.0E-04	0.06	2.331	20757.400	-4.758E+07	2272.450	0.038
110.000	295.84973	5.0E-04	0.08	2.076	15999.200	-2.842E+06	157.753	0.038
109.000	297.44965	6.0E-04	0.09	1.600	15715.000	-3.068E+07	1932.673	0.046
108.000	299.02115	7.0E-04	0.11	1.571	12646.500	-1.450E+07	1126.760	0.051
107.000	300.2858	8.0E-04	0.13	1.265	11196.300	-1.890E+07	1668.326	0.059
106.000	301.40543	9.0E-04	0.14	1.120	9306.000	-1.337E+07	1416.238	0.068
105.000	302.33603	1.0E-03	0.16	0.931	7969.400	-1.297E+07	1607.897	0.079
104.000	303.13297	1.1E-03	0.17	0.797	6672.000	-1.117E+07	1653.440	0.092
103.000	303.80017	1.2E-03	0.19	0.667	5555.400	-8.038E+06	1426.719	0.105
102.000	304.35571	1.3E-03	0.20	0.556	4751.600	-6.287E+06	1302.931	0.119
101.000	304.83087	1.4E-03	0.22	0.475	4122.900	-4.122E+06	979.539	0.130
100.000	305.24316	1.5E-03	0.24	0.412	3710.700	-3.355E+06	883.858	0.142
99.000	305.61423	1.6E-03	0.25	0.371	3375.200	-1.678E+06	476.831	0.148
98.000	305.95175	1.7E-03	0.27	0.338	3207.400	-1.028E+06	300.142	0.153
97.000	306.27249	1.8E-03	0.28	0.321	3104.600	-1.719E+06	533.286	0.161
96.000	306.58295	1.9E-03	0.30	0.310	2932.700	6.100E+04	-41.250	0.160
95.000	306.87622	2.0E-03	0.31	0.293	2938.800	-9.820E+05	313.658	0.165
94.000	307.1701	2.1E-03	0.33	0.294	2840.600	-4.520E+05	138.587	0.168
93.000	307.45416	2.2E-03	0.35	0.284	2795.400	-1.000E+05	15.197	0.168
92.000	307.7337	2.3E-03	0.36	0.280	2785.400	-8.710E+05	292.083	0.173
91.000	308.01224	2.4E-03	0.38	0.279	2698.300	-9.100E+04	13.064	0.173
90.000	308.28207	2.5E-03	0.39	0.270	2689.200	-9.270E+05	324.008	0.179
89.000	308.55099	2.6E-03	0.41	0.269	2596.500	9.700E+04	-58.105	0.178
88.000	308.81064	2.7E-03	0.43	0.260	2606.200	-5.460E+05	188.710	0.181
87.000	309.07126	2.8E-03	0.44	0.261	2551.600	3.690E+05	-165.448	0.178
86.000	309.32642	2.9E-03	0.46	0.255	2588.500	-8.030E+05	289.341	0.183
85.000	309.58527	3.0E-03	0.47	0.259	2508.200	6.260E+05	-270.502	0.178
84.000	309.83609	3.1E-03	0.49	0.251	2570.800	-9.280E+05	340.013	0.184
83.000	310.09317	3.2E-03	0.50	0.257	2478.000	N/A	N/A	N/A
82.000	310.34097	3.3E-03	0.52	0.248	N/A	N/A	N/A	N/A

Simulation 5 Information

Velocity (m/s)	0.080
Bridge (in)	0.050
kw	0.026
Refinement #	1

Avg Temp (K)	dT (K)	dT/dr	d2T/dr2	F1	Eulers K
284.22412	N/A	17605	176706000	-10056.947	0.026
285.98462	1.7605	35275.6	-155332000	4383.6598	0.037
289.51218	3.52756	19742.4	32657000	-1673.9184	0.031
291.48642	1.97424	23008.1	-25396000	1083.9832	0.035
293.78723	2.30081	20468.5	-43385000	2099.7571	0.042
295.83408	2.04685	16130	-5901000	345.95933	0.043
297.44708	1.613	15539.9	-29673000	1889.5514	0.051
299.00107	1.55399	12572.6	-13879000	1083.9484	0.057
300.25833	1.25726	11184.7	-18930000	1672.4906	0.066
301.3768	1.11847	9291.7	-13550000	1438.2507	0.076
302.30597	0.92917	7936.7	-12915000	1607.1703	0.088
303.09964	0.79367	6645.2	-11099000	1650.1074	0.103
303.76416	0.66452	5535.3	-8039000	1432.1539	0.118
304.31769	0.55353	4731.4	-6255000	1301.8168	0.133
304.79083	0.47314	4105.9	-4142000	988.54931	0.146
305.20142	0.41059	3691.7	-3302000	874.1549	0.159
305.57059	0.36917	3361.5	-1709000	488.07878	0.166
305.90674	0.33615	3190.6	-1004000	294.30776	0.171
306.2258	0.31906	3090.2	-1687000	525.51119	0.180
306.53482	0.30902	2921.5	54000	-38.933553	0.180
306.82697	0.29215	2926.9	-970000	310.91685	0.185
307.11966	0.29269	2829.9	-434000	132.82843	0.188
307.40265	0.28299	2786.5	-103000	16.387802	0.188
307.6813	0.27865	2776.2	-851000	285.91555	0.193
307.95892	0.27762	2691.1	-95000	14.640393	0.194
308.22803	0.26911	2681.6	-919000	322.00191	0.200
308.49619	0.26816	2589.7	104000	-60.90598	0.199
308.75516	0.25897	2600.1	-544000	188.4327	0.202
309.01517	0.26001	2545.7	374000	-167.74774	0.199
309.26974	0.25457	2583.1	-801000	289.2157	0.205
309.52805	0.25831	2503	632000	-273.41751	0.199
309.77835	0.2503	2566.2	-924000	339.10111	0.206
310.03497	0.25662	2473.8	N/A	N/A	N/A
310.28235	0.24738	N/A	N/A	N/A	N/A

Simulation 6 Information

Velocity (m/s)	0.080
Bridge (in)	0.030
kw	0.026
Refinement #	0

Iso-clip Name	Avg Temp (K)	L (m)	L/d	dT (K)	dT/dr	d2T/dr2	F1	Eulers K
115.000	284.26974	0.0E+00	0.00	N/A	18097.900	1.853E+08	-10259.547	0.026
114.000	286.07953	1.0E-04	0.02	1.810	36629.900	-1.781E+08	4841.933	0.039
113.000	289.74252	2.0E-04	0.03	3.663	18821.700	6.078E+07	-3249.174	0.026
112.000	291.62469	3.0E-04	0.05	1.882	24900.000	-4.637E+07	1842.567	0.031
111.000	294.11469	4.0E-04	0.06	2.490	20262.700	-3.252E+07	1585.177	0.036
110.000	296.14096	5.0E-04	0.08	2.026	17010.500	-1.117E+07	636.537	0.038
109.000	297.84201	6.0E-04	0.09	1.701	15893.900	-2.801E+07	1742.580	0.045
108.000	299.4314	7.0E-04	0.11	1.589	13092.600	-1.701E+07	1279.247	0.050
107.000	300.74066	8.0E-04	0.13	1.309	11391.600	-1.660E+07	1436.775	0.058
106.000	301.87982	9.0E-04	0.14	1.139	9732.100	-1.594E+07	1617.530	0.067
105.000	302.85303	1.0E-03	0.16	0.973	8138.400	-1.191E+07	1442.738	0.077
104.000	303.66687	1.1E-03	0.17	0.814	6947.900	-1.227E+07	1745.881	0.090
103.000	304.36166	1.2E-03	0.19	0.695	5720.900	-7.548E+06	1299.212	0.102
102.000	304.93375	1.3E-03	0.20	0.572	4966.100	-6.857E+06	1360.560	0.115
101.000	305.43036	1.4E-03	0.22	0.497	4280.400	-4.270E+06	977.327	0.127
100.000	305.8584	1.5E-03	0.24	0.428	3853.400	-3.457E+06	876.846	0.138
99.000	306.24374	1.6E-03	0.25	0.385	3507.700	-1.501E+06	407.591	0.143
98.000	306.59451	1.7E-03	0.27	0.351	3357.600	-1.524E+06	433.529	0.150
97.000	306.93027	1.8E-03	0.28	0.336	3205.200	-1.266E+06	374.575	0.155
96.000	307.25079	1.9E-03	0.30	0.321	3078.600	-3.690E+05	99.410	0.157
95.000	307.55865	2.0E-03	0.31	0.308	3041.700	-9.210E+05	282.299	0.161
94.000	307.86282	2.1E-03	0.33	0.304	2949.600	-3.640E+05	102.873	0.163
93.000	308.15778	2.2E-03	0.35	0.295	2913.200	-9.920E+05	319.943	0.168
92.000	308.4491	2.3E-03	0.36	0.291	2814.000	1.310E+05	-67.172	0.167
91.000	308.7305	2.4E-03	0.38	0.281	2827.100	-8.440E+05	277.878	0.172
90.000	309.01321	2.5E-03	0.39	0.283	2742.700	-1.510E+05	34.351	0.172
89.000	309.28748	2.6E-03	0.41	0.274	2727.600	-7.320E+05	247.621	0.176
88.000	309.56024	2.7E-03	0.43	0.273	2654.400	4.900E+04	-39.250	0.176
87.000	309.82568	2.8E-03	0.44	0.265	2659.300	-4.480E+05	147.632	0.178
86.000	310.09161	2.9E-03	0.46	0.266	2614.500	-5.000E+04	-1.753	0.178
85.000	310.35306	3.0E-03	0.47	0.261	2609.500	-1.300E+05	28.897	0.179
84.000	310.61401	3.1E-03	0.49	0.261	2596.500	-8.900E+04	13.313	0.179
83.000	310.87366	3.2E-03	0.50	0.260	2587.600	N/A	N/A	N/A
82.000	311.13242	3.3E-03	0.52	0.259	N/A	N/A	N/A	N/A

Simulation 6 Information

Velocity (m/s)	0.080
Bridge (in)	0.030
kw	0.026
Refinement #	1

Avg Temp (K)	dT (K)	dT/dr	d2T/dr2	F1	Eulers K
284.256	N/A	18196.1	174775000	-9624.77	0.026
286.075	1.81961	35673.6	-154292000	4305.379	0.037
289.643	3.56736	20244.4	42252000	-2106.86	0.029
291.667	2.02444	24469.6	-43371000	1752.642	0.035
294.114	2.44696	20132.5	-30854000	1512.706	0.040
296.127	2.01325	17047.1	-13138000	750.8076	0.043
297.832	1.70471	15733.3	-26705000	1677.435	0.050
299.405	1.57333	13062.8	-16914000	1274.862	0.056
300.711	1.30628	11371.4	-16579000	1437.956	0.064
301.849	1.13714	9713.5	-15962000	1623.24	0.075
302.820	0.97135	8117.3	-11916000	1447.895	0.086
303.632	0.81173	6925.7	-12256000	1749.52	0.101
304.324	0.69257	5700.1	-7508000	1297.009	0.114
304.894	0.57001	4949.3	-6899000	1373.732	0.129
305.389	0.49493	4259.4	-4231000	973.0895	0.142
305.815	0.42594	3836.3	-3445000	877.7167	0.154
306.199	0.38363	3491.8	-1498000	408.6799	0.161
306.548	0.34918	3342	-1508000	430.8602	0.167
306.882	0.3342	3191.2	-1251000	371.6074	0.174
307.201	0.31912	3066.1	-369000	99.89843	0.175
307.508	0.30661	3029.2	-900000	276.6163	0.180
307.811	0.30292	2939.2	-352000	99.2266	0.182
308.105	0.29392	2904	-982000	317.5781	0.188
308.395	0.2904	2805.8	131000	-67.3076	0.187
308.676	0.28058	2818.9	-830000	273.7799	0.192
308.958	0.28189	2735.9	-156000	36.31569	0.192
309.231	0.27359	2720.3	-719000	243.5622	0.197
309.503	0.27203	2648.4	50999.99999	-40.0469	0.196
309.768	0.26484	2653.5	-446000	147.2466	0.199
310.033	0.26535	2608.9	-45000	-3.62818	0.199
310.294	0.26089	2604.4	-129000	28.61106	0.200
310.555	0.26044	2591.5	-85000	11.83518	0.200
310.814	0.25915	2583	N/A	N/A	N/A
311.072	0.2583	N/A	N/A	N/A	N/A

Simulation 7 Information

Velocity (m/s)	0.080
Bridge (in)	0.040
kw	0.026
Refinement #	0

Iso-clip Name	Avg Temp (K)	L (m)	L/d	dT (K)	dT/dr	d2T/dr2	F1	Eulers K
115.000	284.237	0.0E+00	0.00	N/A	17642.200	1.805E+08	-10248.681	0.026
114.000	286.001	1.0E-04	0.02	1.764	35688.400	-1.738E+08	4851.467	0.039
113.000	289.570	2.0E-04	0.03	3.569	18303.900	5.955E+07	-3272.949	0.026
112.000	291.400	3.0E-04	0.05	1.830	24258.500	-4.535E+07	1849.687	0.031
111.000	293.826	4.0E-04	0.06	2.426	19723.400	-3.283E+07	1644.679	0.036
110.000	295.798	5.0E-04	0.08	1.972	16440.400	-9.737E+06	572.380	0.038
109.000	297.442	6.0E-04	0.09	1.644	15466.700	-2.856E+07	1826.627	0.045
108.000	298.989	7.0E-04	0.11	1.547	12610.700	-1.638E+07	1279.016	0.051
107.000	300.250	8.0E-04	0.13	1.261	10972.600	-1.636E+07	1470.987	0.058
106.000	301.347	9.0E-04	0.14	1.097	9336.600	-1.581E+07	1673.189	0.068
105.000	302.281	1.0E-03	0.16	0.934	7755.700	-1.128E+07	1433.818	0.077
104.000	303.057	1.1E-03	0.17	0.776	6628.100	-1.232E+07	1838.632	0.092
103.000	303.719	1.2E-03	0.19	0.663	5396.100	-7.217E+06	1317.286	0.104
102.000	304.259	1.3E-03	0.20	0.540	4674.400	-6.531E+06	1376.983	0.118
101.000	304.727	1.4E-03	0.22	0.467	4021.300	-4.162E+06	1014.746	0.130
100.000	305.129	1.5E-03	0.24	0.402	3605.100	-3.141E+06	850.982	0.141
99.000	305.489	1.6E-03	0.25	0.361	3291.000	-1.367E+06	395.050	0.147
98.000	305.818	1.7E-03	0.27	0.329	3154.300	-1.474E+06	446.932	0.153
97.000	306.134	1.8E-03	0.28	0.315	3006.900	-9.430E+05	293.204	0.158
96.000	306.434	1.9E-03	0.30	0.301	2912.600	-2.750E+05	73.967	0.159
95.000	306.726	2.0E-03	0.31	0.291	2885.100	-8.790E+05	284.177	0.163
94.000	307.014	2.1E-03	0.33	0.289	2797.200	-1.460E+05	31.661	0.164
93.000	307.294	2.2E-03	0.35	0.280	2782.600	-8.660E+05	290.644	0.169
92.000	307.572	2.3E-03	0.36	0.278	2696.000	1.270E+05	-67.725	0.167
91.000	307.842	2.4E-03	0.38	0.270	2708.700	-7.560E+05	258.440	0.172
90.000	308.113	2.5E-03	0.39	0.271	2633.100	-1.600E+04	-14.627	0.171
89.000	308.376	2.6E-03	0.41	0.263	2631.500	-7.600E+05	268.062	0.176
88.000	308.639	2.7E-03	0.43	0.263	2555.500	1.810E+05	-91.618	0.174
87.000	308.895	2.8E-03	0.44	0.256	2573.600	-4.370E+05	148.968	0.177
86.000	309.152	2.9E-03	0.46	0.257	2529.900	-3.700E+04	-6.252	0.177
85.000	309.405	3.0E-03	0.47	0.253	2526.200	-3.000E+04	-9.045	0.177
84.000	309.658	3.1E-03	0.49	0.253	2523.200	-7.900E+04	10.345	0.177
83.000	309.910	3.2E-03	0.50	0.252	2515.300	N/A	N/A	N/A
82.000	310.161	3.3E-03	0.52	0.252	N/A	N/A	N/A	N/A

Simulation 7 Information

Velocity (m/s)	0.080
Bridge (in)	0.040
kw	0.026
Refinement #	1

Avg Temp (K)	dT (K)	dT/dr	d2T/dr2	F1	Eulers K
284.223	N/A	1.8E+04	1.7E+08	-9604.7905	0.026
285.999	1.77515	3.5E+04	-1.5E+08	4312.1473	0.037
289.475	3.47665	2.0E+04	4.2E+07	-2141.0857	0.029
291.446	1.97061	2.4E+04	-4.3E+07	1779.5483	0.034
293.835	2.38864	2.0E+04	-3.1E+07	1560.8902	0.040
295.793	1.95884	1.6E+04	-1.2E+07	695.49644	0.043
297.443	1.6492	1.5E+04	-2.7E+07	1750.3021	0.050
298.974	1.53122	1.3E+04	-1.6E+07	1284.8742	0.056
300.234	1.26016	1.1E+04	-1.6E+07	1473.6161	0.065
301.330	1.09573	9.3E+03	-1.6E+07	1669.7472	0.076
302.262	0.93207	7.7E+03	-1.1E+07	1443.3123	0.087
303.036	0.77457	6.6E+03	-1.2E+07	1838.4135	0.102
303.698	0.66122	5.4E+03	-7.2E+06	1314.8934	0.116
304.236	0.53833	4.7E+03	-6.6E+06	1388.922	0.132
304.702	0.46646	4.0E+03	-4.1E+06	1011.1248	0.145
305.103	0.40073	3.6E+03	-3.1E+06	852.28141	0.158
305.462	0.3594	3.3E+03	-1.4E+06	395.78259	0.164
305.791	0.32804	3.1E+03	-1.5E+06	446.56937	0.171
306.105	0.31439	3.0E+03	-9.3E+05	288.89083	0.176
306.405	0.29971	2.9E+03	-2.8E+05	75.266946	0.178
306.695	0.29044	2.9E+03	-8.6E+05	278.81988	0.183
306.983	0.28766	2.8E+03	-1.4E+05	30.711416	0.183
307.262	0.27905	2.8E+03	-8.6E+05	288.47941	0.188
307.539	0.27762	2.7E+03	1.3E+05	-69.681893	0.187
307.808	0.26904	2.7E+03	-7.5E+05	257.4865	0.192
308.079	0.27036	2.6E+03	-1.4E+04	-15.377499	0.192
308.342	0.26284	2.6E+03	-7.5E+05	265.13054	0.197
308.604	0.2627	2.6E+03	1.7E+05	-88.582646	0.195
308.860	0.25519	2.6E+03	-4.3E+05	144.97704	0.198
309.116	0.25692	2.5E+03	-3.7E+04	-6.2326409	0.198
309.369	0.25266	2.5E+03	-2.8E+04	-9.8221629	0.197
309.621	0.25229	2.5E+03	-7.9E+04	10.383602	0.198
309.873	0.25201	2.5E+03	N/A	N/A	N/A
310.125	0.25122	N/A	N/A	N/A	N/A

Appendix C: Temperature Gradients in the Near-Wall Region at Varying Velocities and Bridge Sizes

C.1: Individual Temperature Gradients

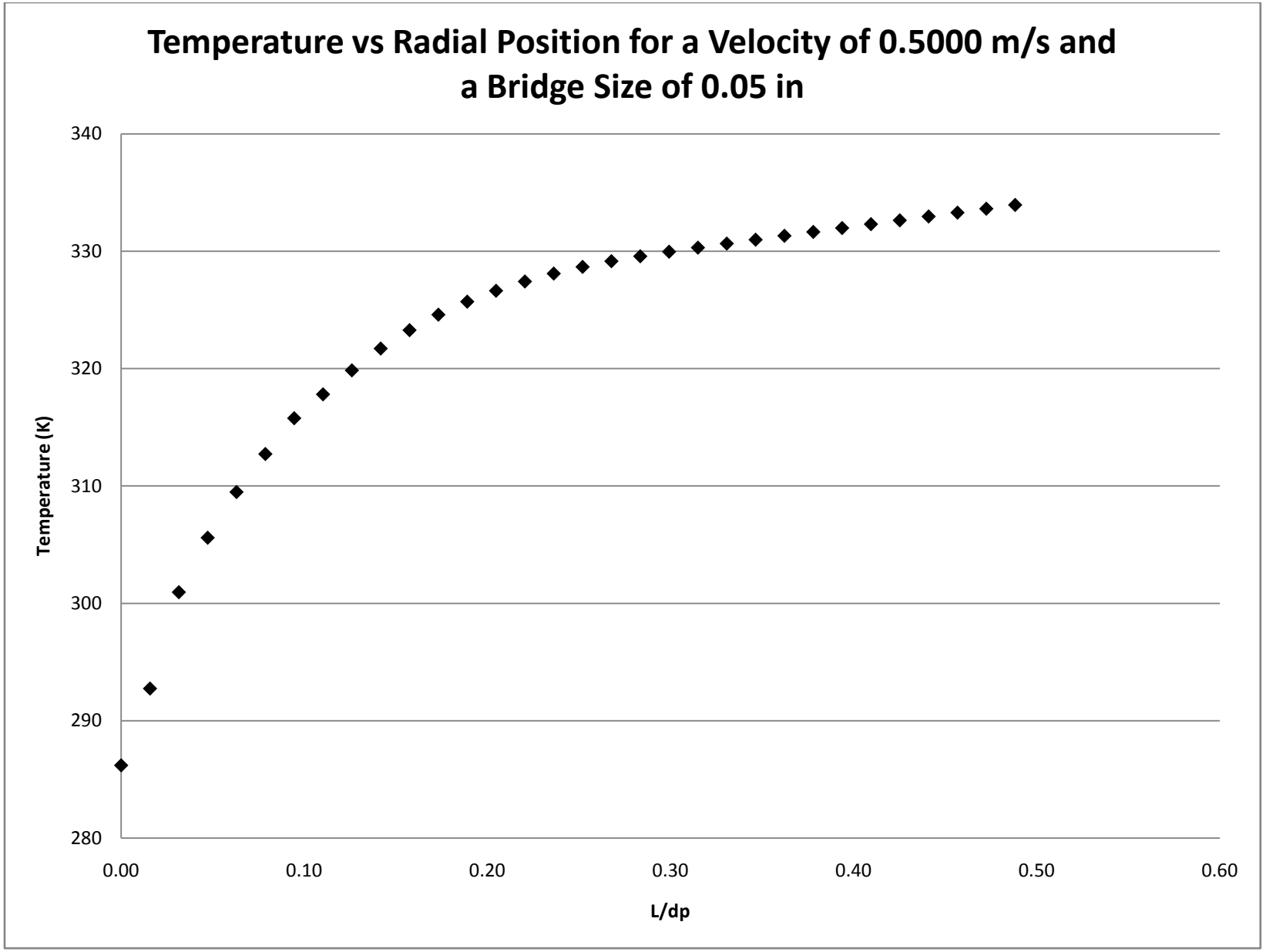
Temperature vs Radial Position for a Velocity of 0.5000 m/s and a Bridge Size of 0.05 in
340
330
320
310
300
290
280
Temperature (K)
0.00
0.10
0.20
0.30
0.40
0.50
0.60
L/dp

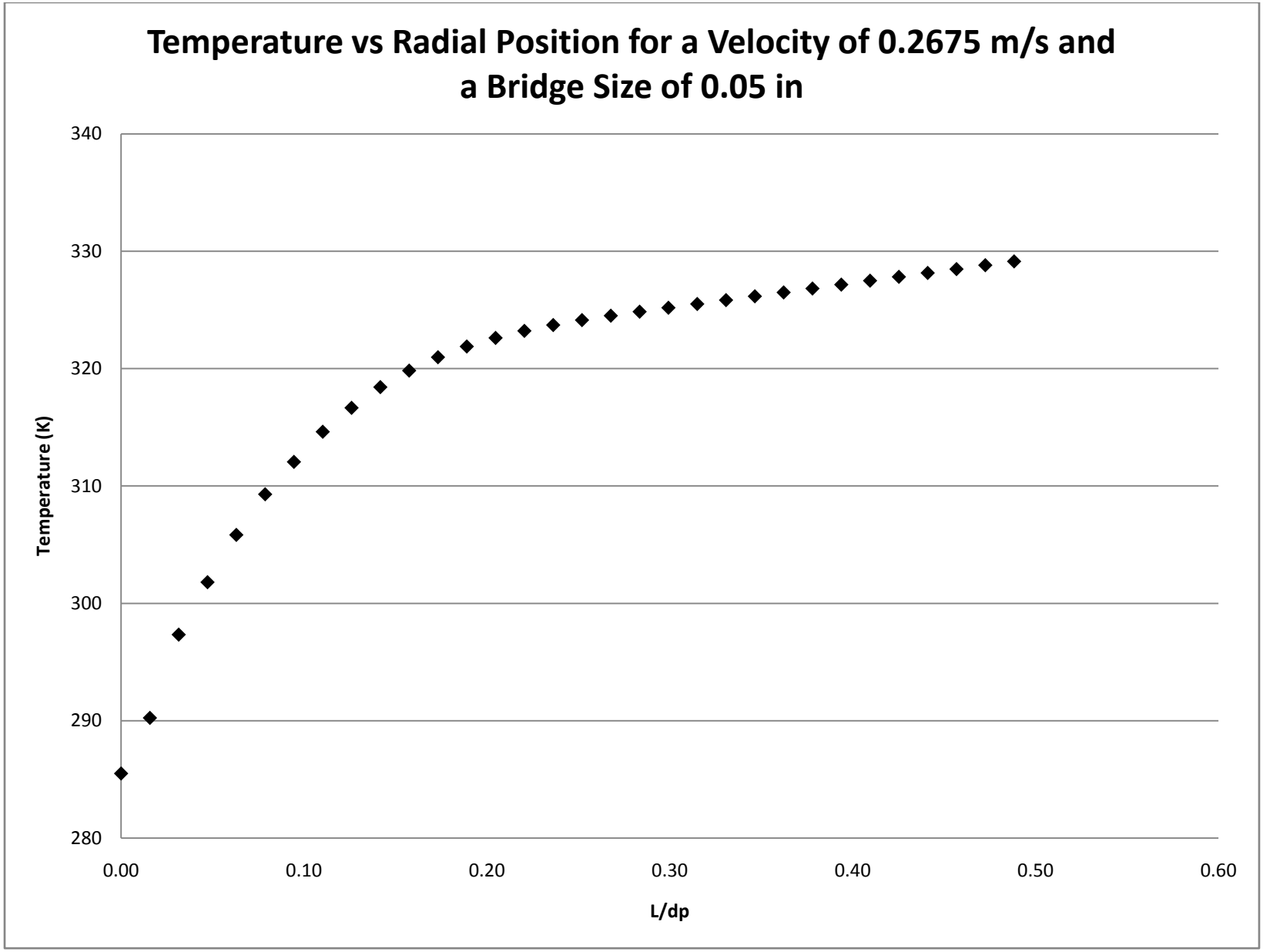
Temperature vs Radial Position for a Velocity of 0.2675 m/s and a Bridge Size of 0.05 in
340
330
320
310
300
290
280
Temperature (K)
0.00
0.10
0.20
0.30
0.40
0.50
0.60
L/dp

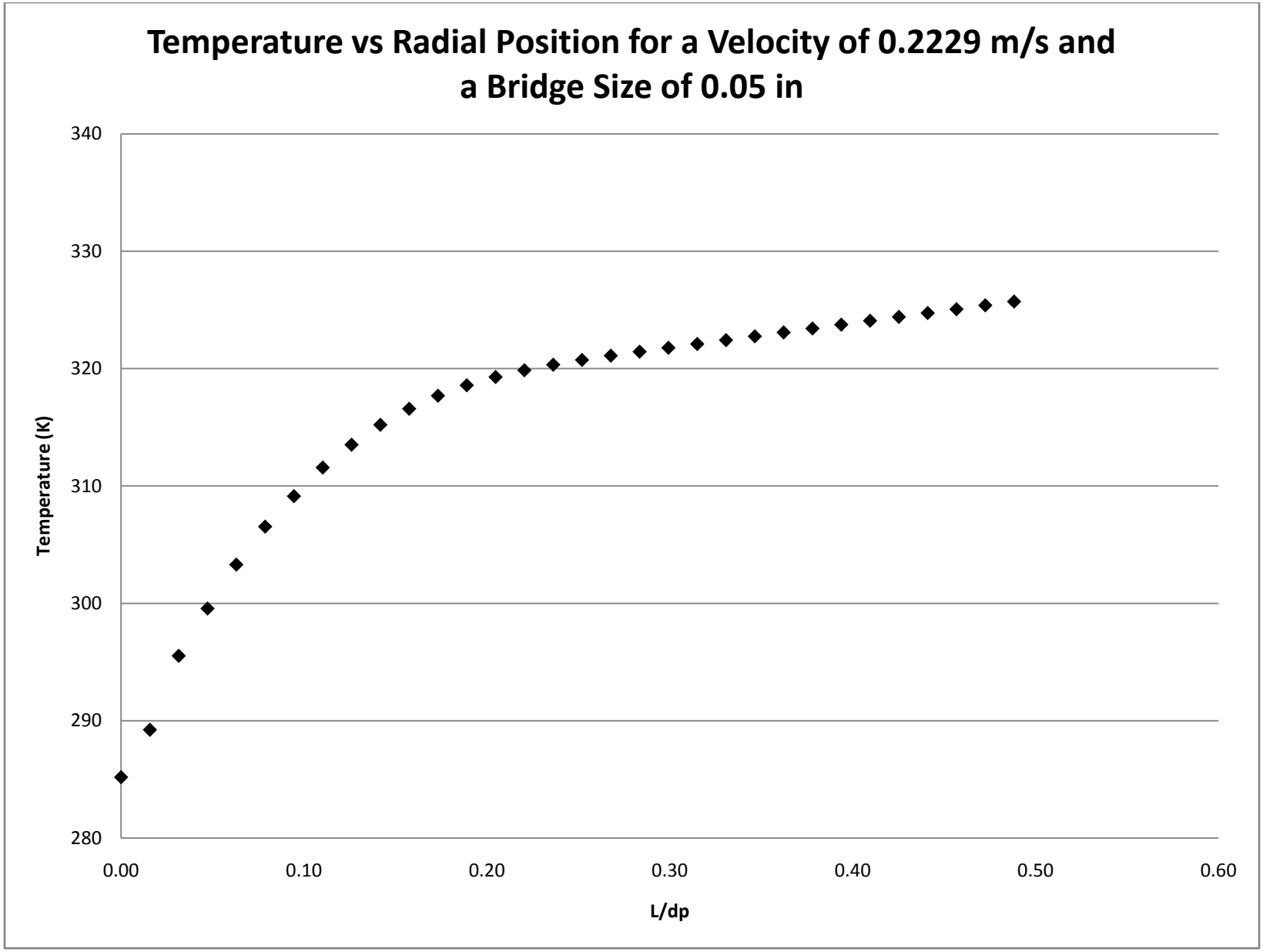
Temperature vs Radial Position for a Velocity of 0.2229 m/s and a Bridge Size of 0.05 in
340
330
320
310
300
290
280
Temperature (K)
0.00
0.10
0.20
0.30
0.40
0.50
0.60
L/dp

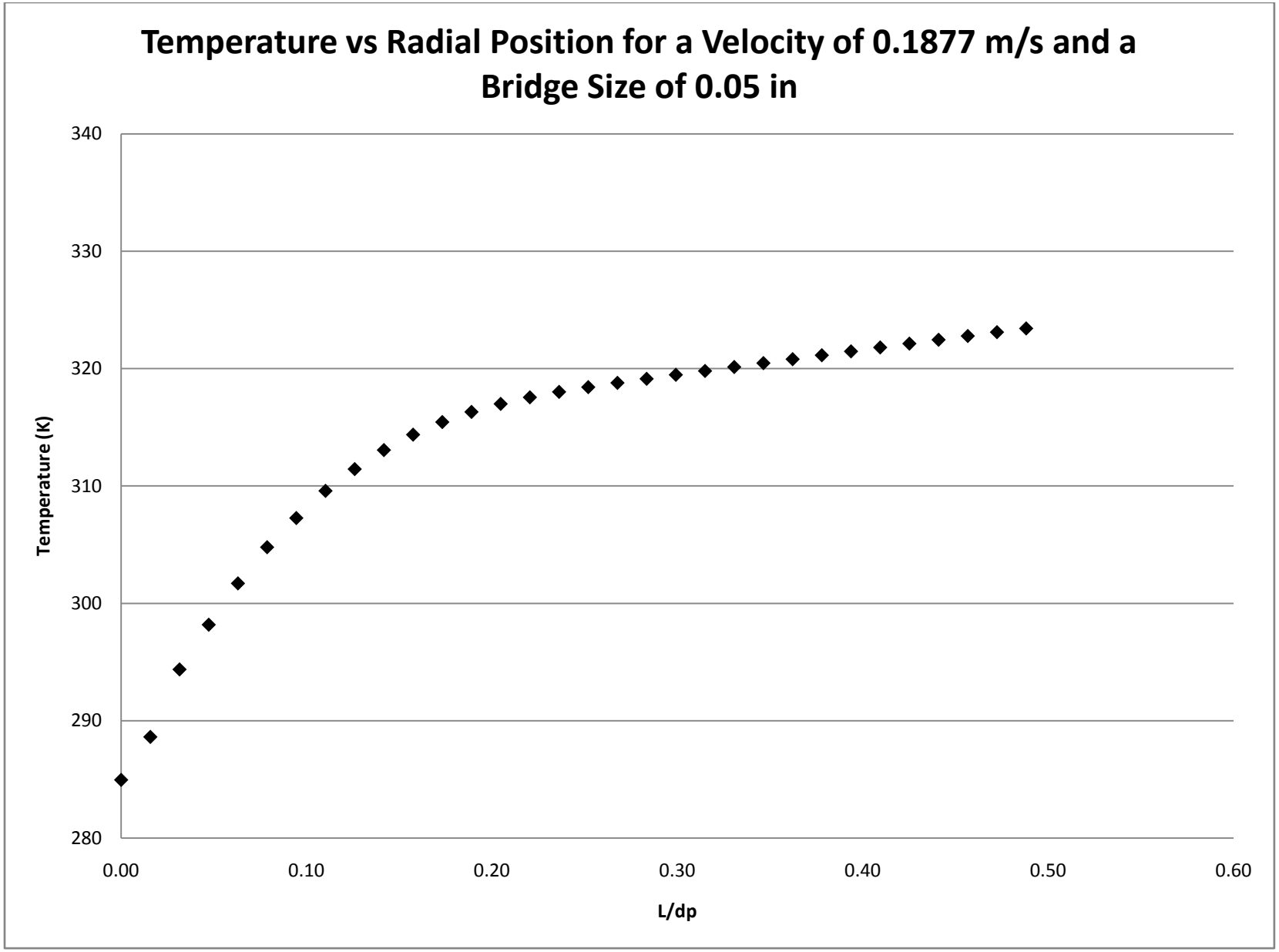
Temperature vs Radial Position for a Velocity of 0.1877 m/s and a Bridge Size of 0.05 in
340
330
320
310
300
290
280
Temperature (K)
0.00
0.10
0.20
0.30
0.40
0.50
0.60
L/dp

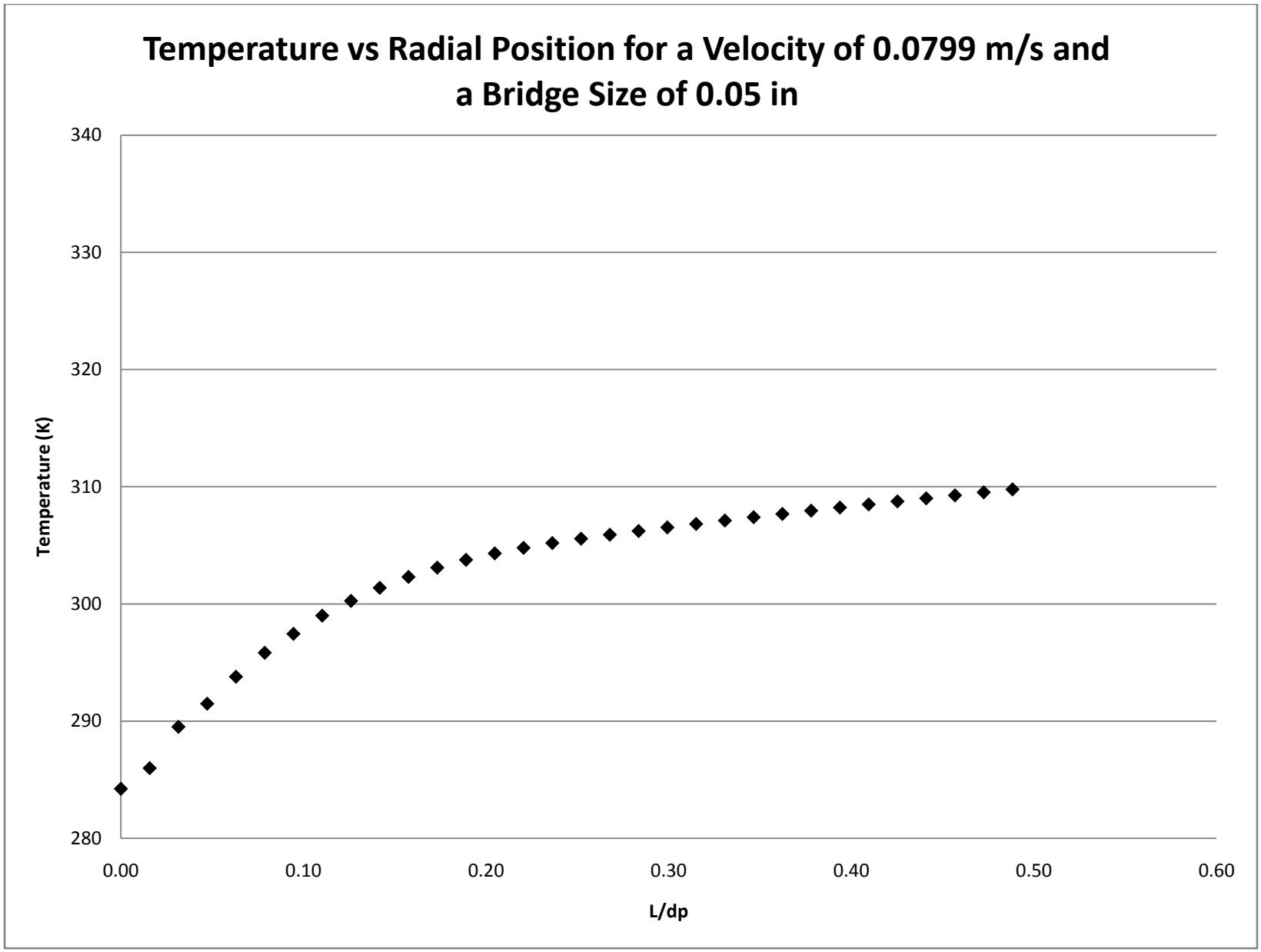
Temperature vs Radial Position for a Velocity of 0.0799 m/s and a Bridge Size of 0.05 in
340
330
320
310
300
290
280
Temperature (K)
0.00
0.10
0.20
0.30
0.40
0.50
0.60
L/dp

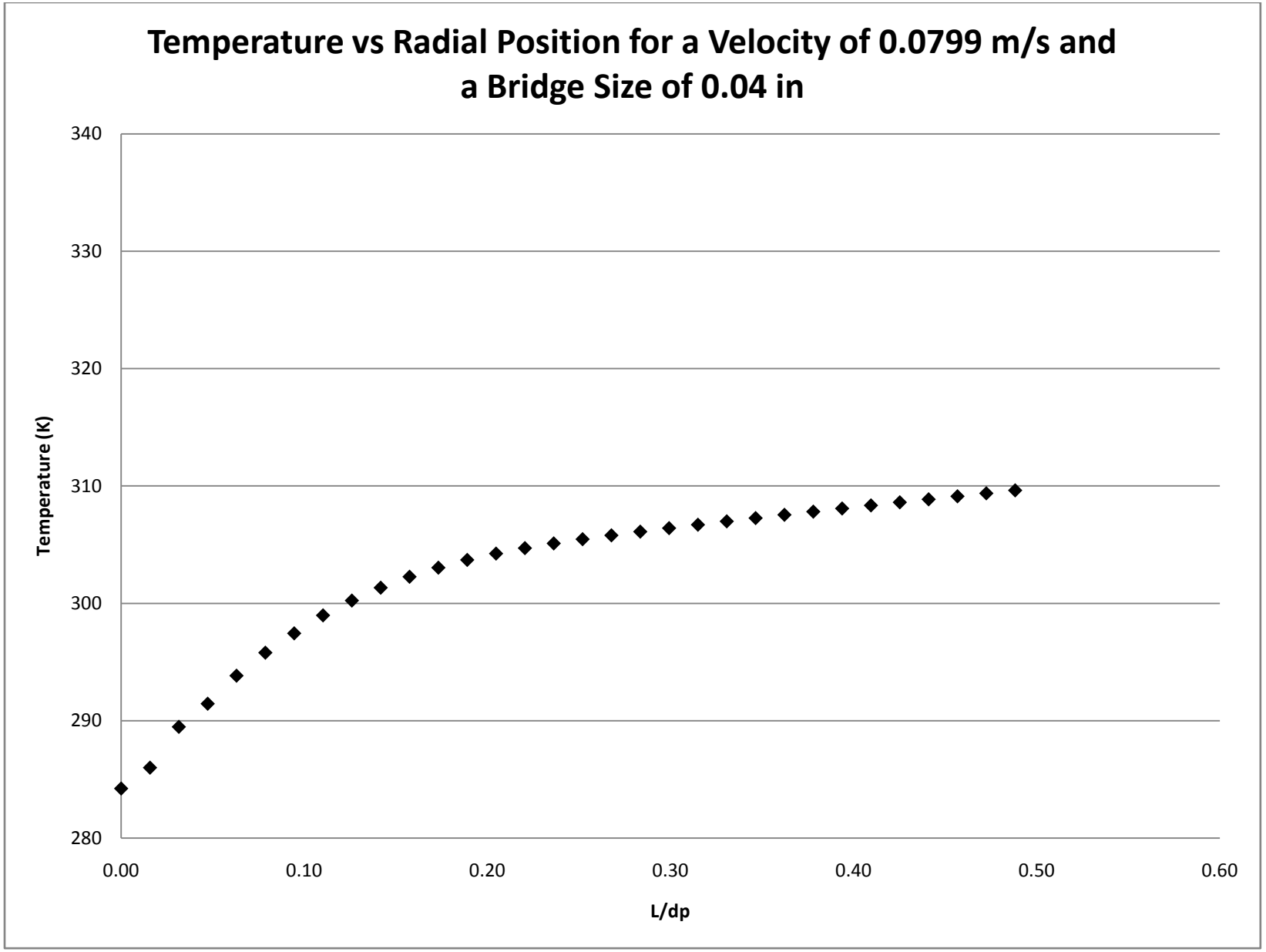
Temperature vs Radial Position for a Velocity of 0.0799 m/s and a Bridge Size of 0.04 in
340
330
320
310
300
290
280
Temperature (K)
0.00
0.10
0.20
0.30
0.40
0.50
0.60
L/dp

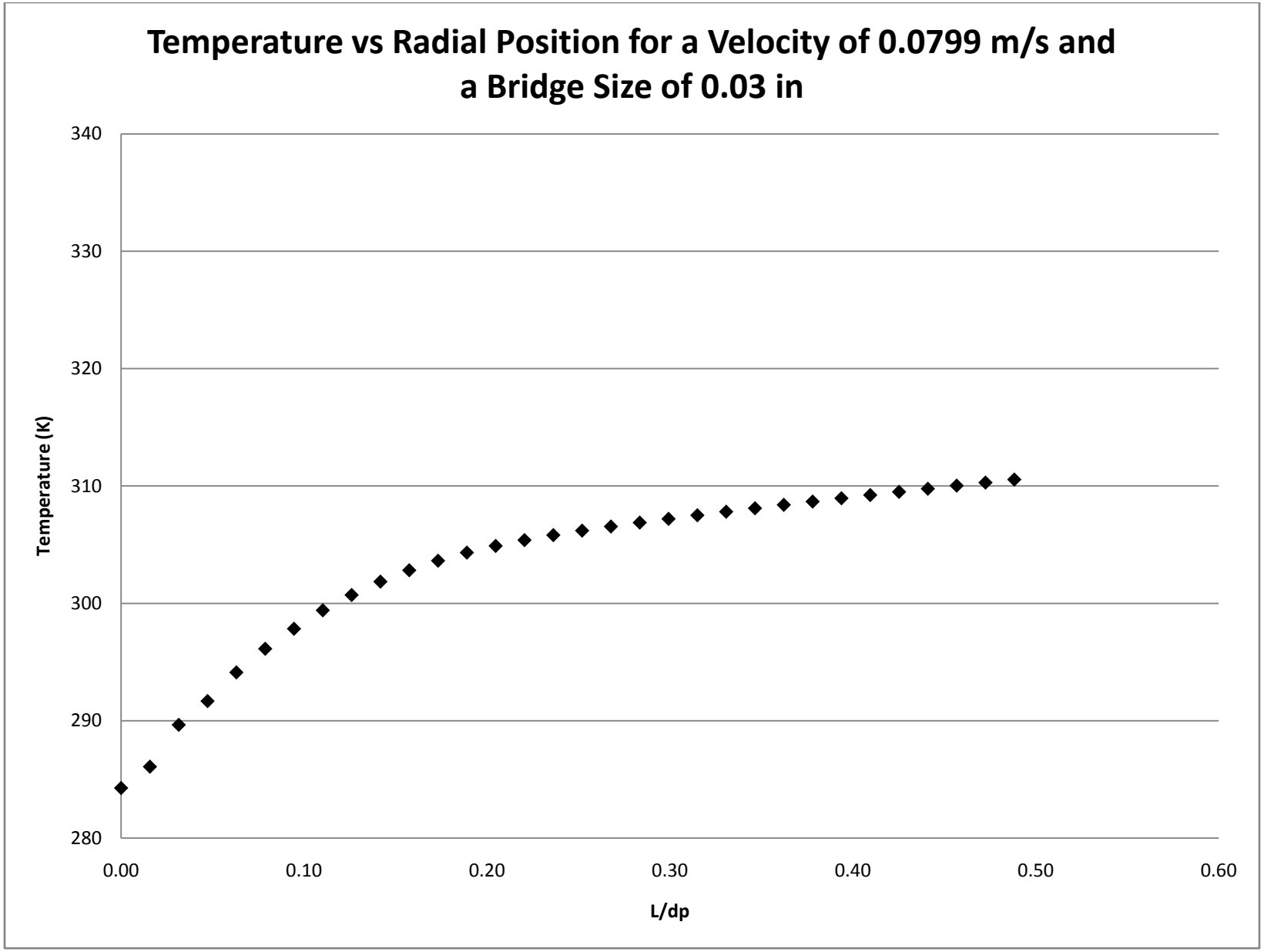
Temperature vs Radial Position for a Velocity of 0.0799 m/s and a Bridge Size of 0.03 in
340
330
320
310
300
290
280
Temperature (K)
0.00
0.10
0.20
0.30
0.40
0.50
0.60
L/dp

C.2: Combined Temperature Gradients

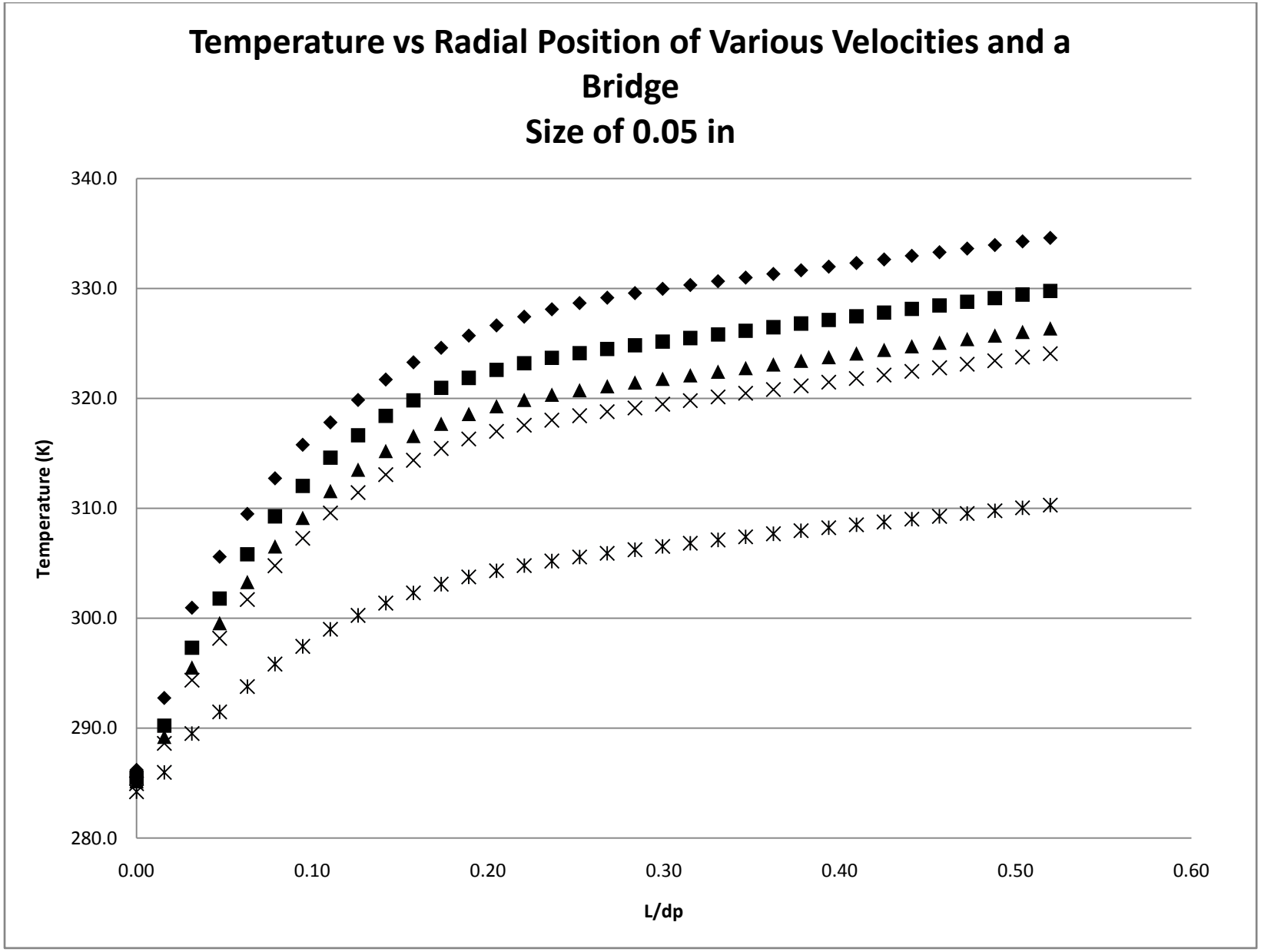
Temperature vs Radial Position of Various Velocities and a Bridge
Size of 0.05 in
340.0
330.0
320.0
310.0
300.0
290.0
280.0
Temperature (K)
0.00
0.10
0.20
0.30
0.40
0.50
0.60
L/dp

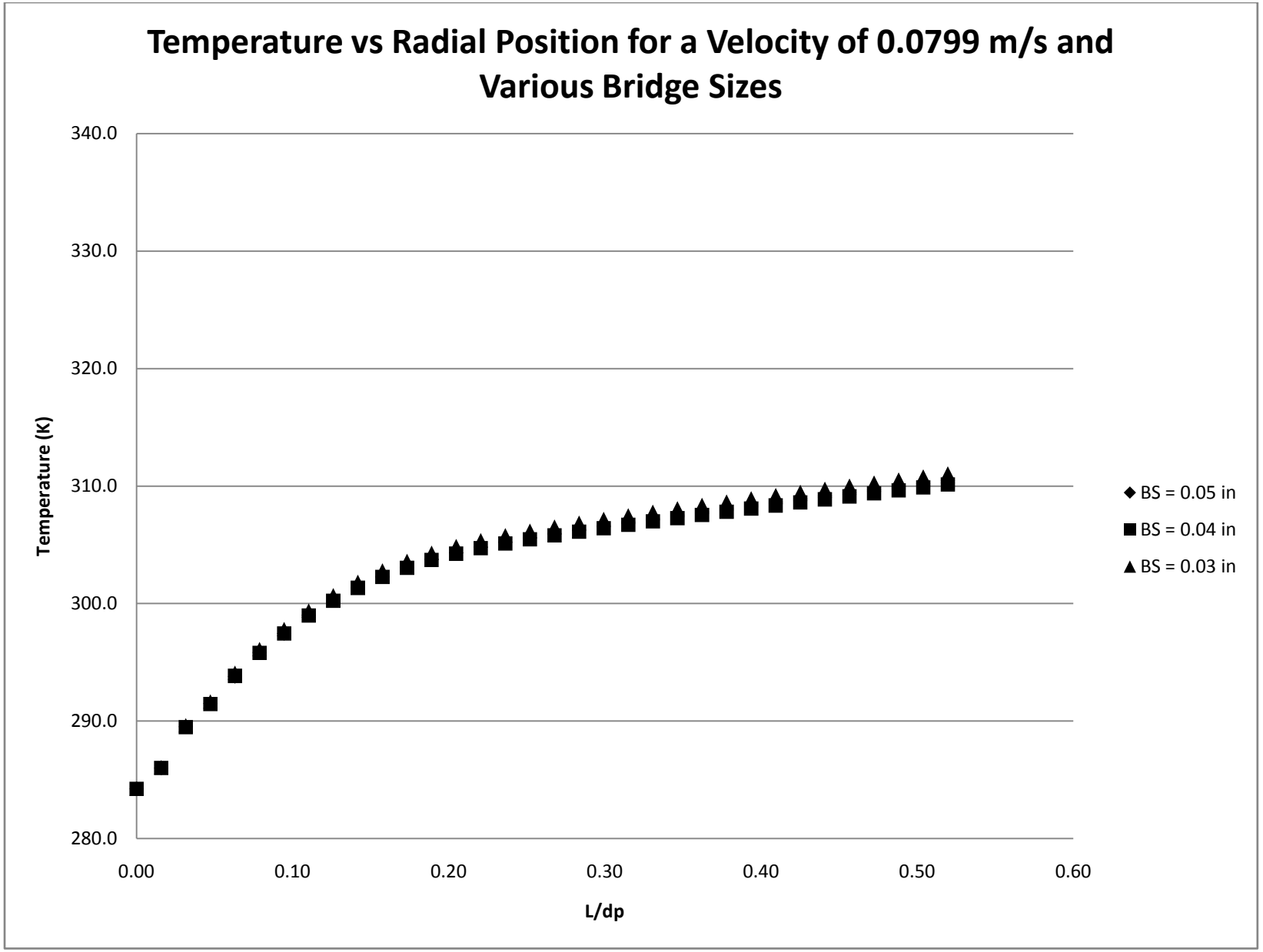
Temperature vs Radial Position for a Velocity of 0.0799 m/s and Various Bridge Sizes
340.0
330.0
320.0
310.0
300.0
290.0
280.0
Temperature (K)
0.00
0.10
0.20
0.30
0.40
0.50
0.60
L/dp
BS = 0.05 in
BS = 0.04 in
BS = 0.03 in

Appendix D: Effective Radial Thermal Conductivity Gradients in the Near-Wall Region at Varying Velocities, Bridge Sizes, and Mesh Refinements

D.1: Individual Effective Radial Thermal Conductivity Gradients

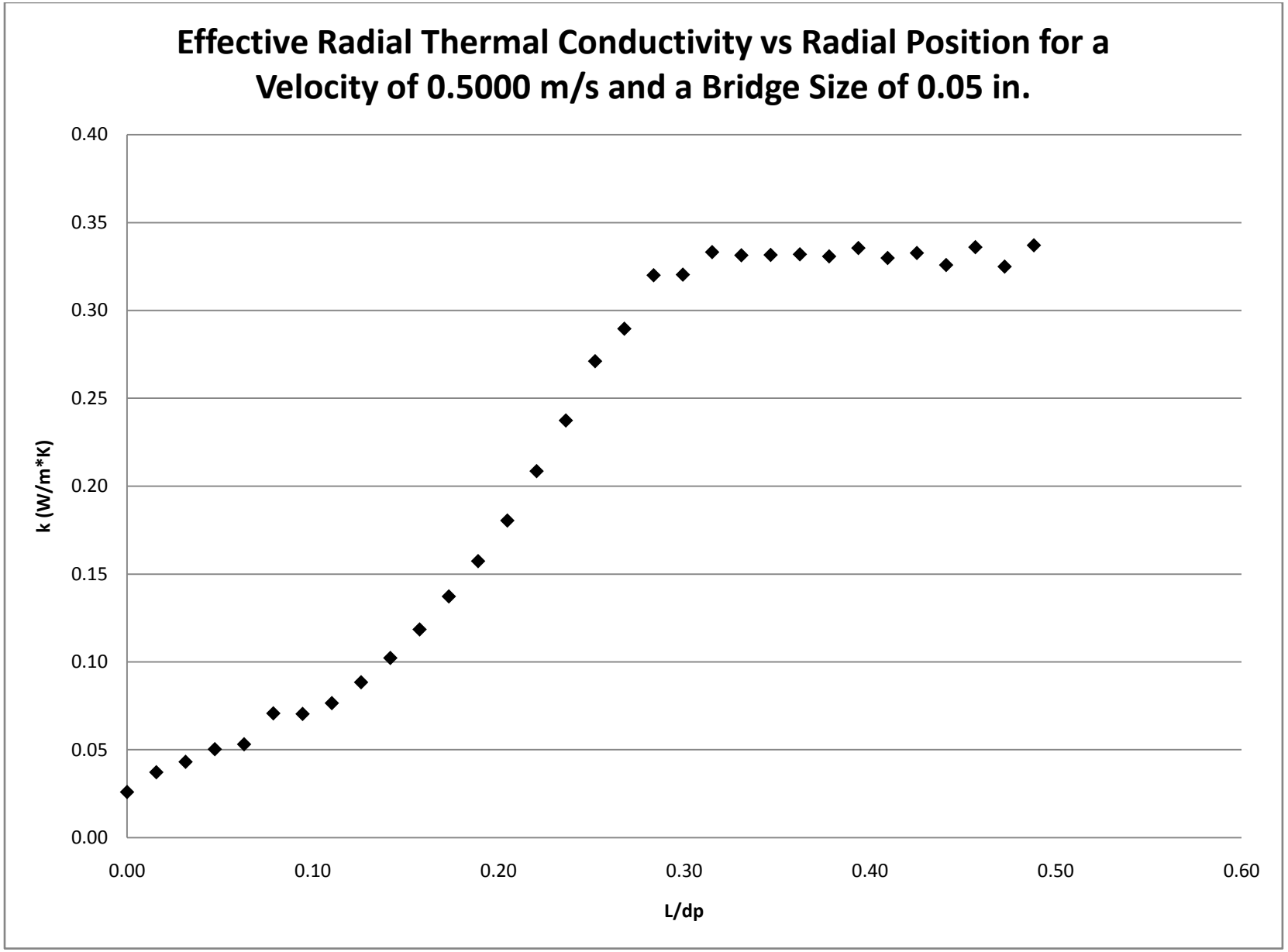
Effective Radial Thermal Conductivity vs Radial Position for a Velocity of 0.5000 m/s and a Bridge Size of 0.05 in.
k (W/m*K)
0.40
0.35
0.30
0.25
0.20
0.15
0.10
0.05
0.00
0.00
0.10
0.20
0.30
0.40
0.50
0.60
L/dp

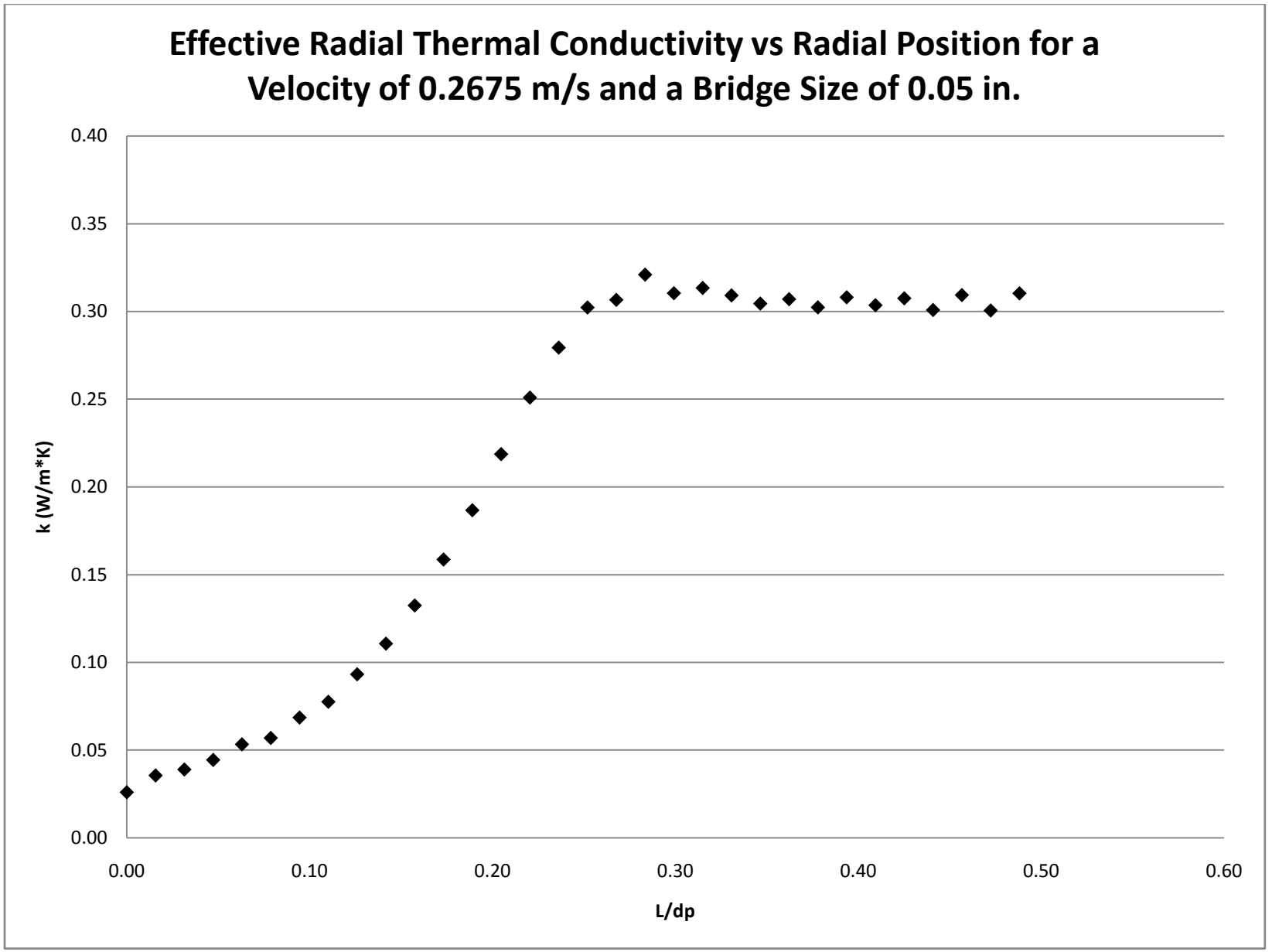
Effective Radial Thermal Conductivity vs Radial Position for a Velocity of 0.2675 m/s and a Bridge Size of 0.05 in.
k (W/m*K)
0.40
0.35
0.30
0.25
0.20
0.15
0.10
0.05
0.00
0.00
0.10
0.20
0.30
0.40
0.50
0.60
L/dp

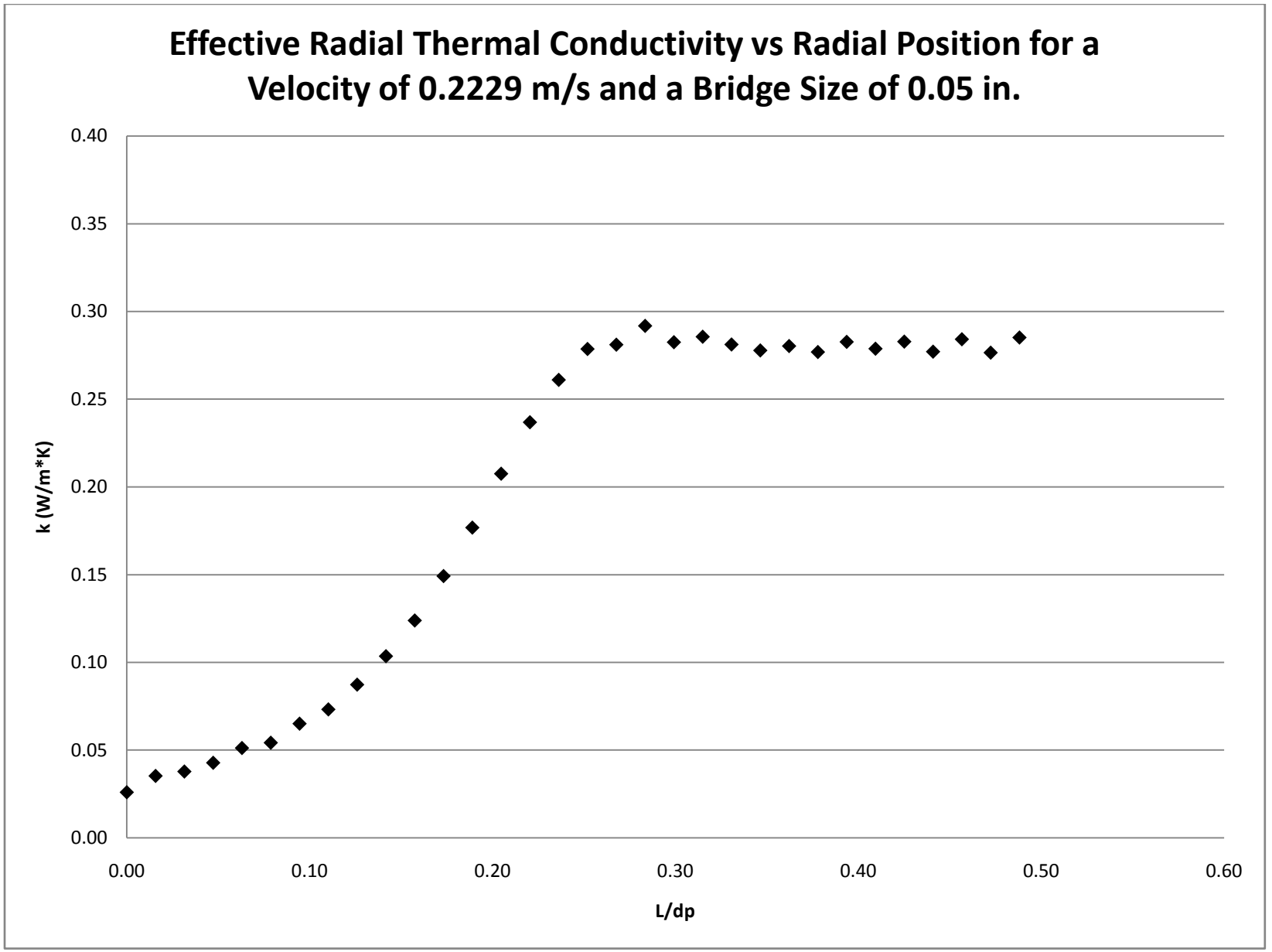
Effective Radial Thermal Conductivity vs Radial Position for a Velocity of 0.2229 m/s and a Bridge Size of 0.05 in.
k (W/m*K)
0.40
0.35
0.30
0.25
0.20
0.15
0.10
0.05
0.00
0.00
0.10
0.20
0.30
0.40
0.50
0.60
L/dp

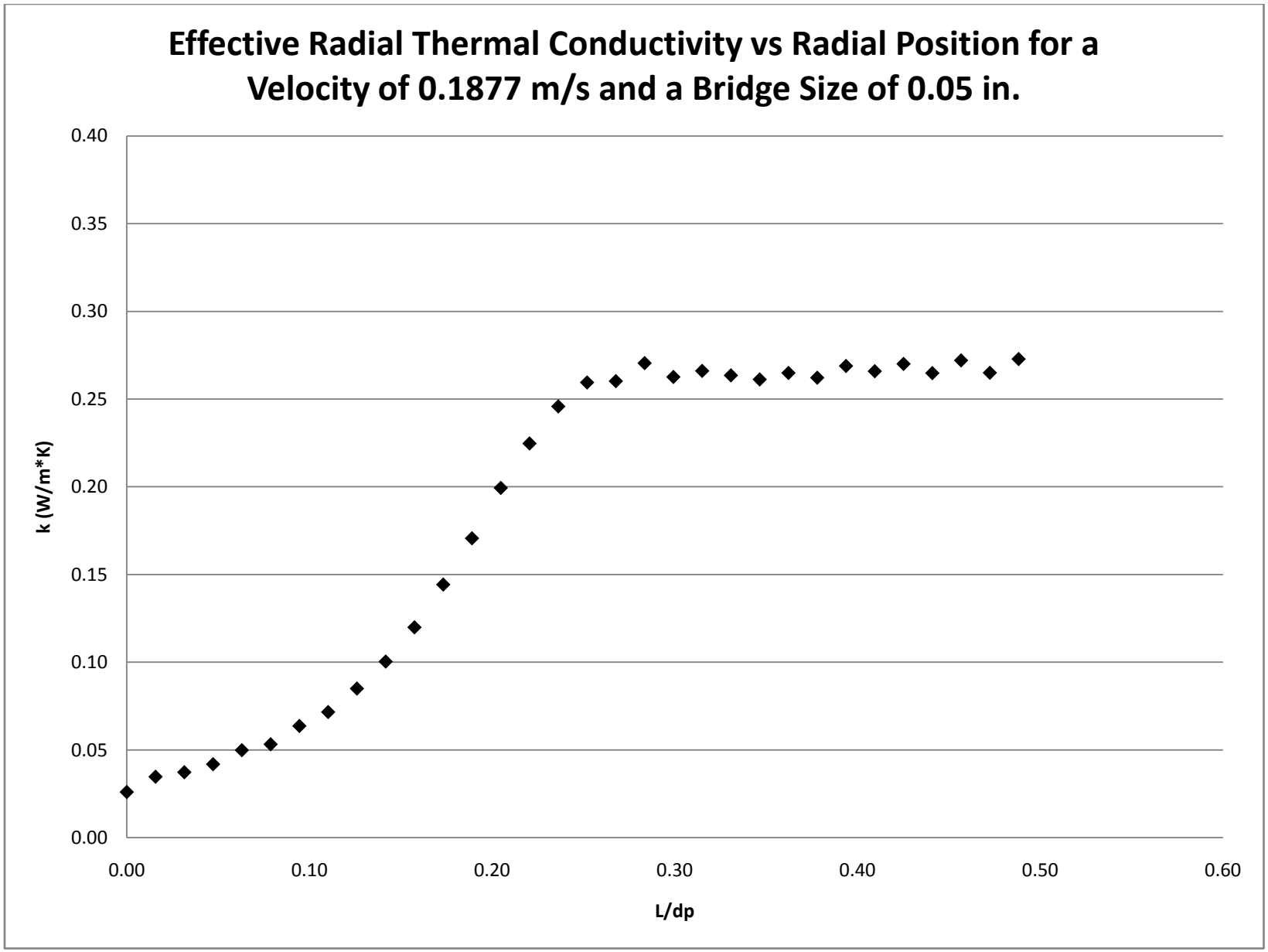
Effective Radial Thermal Conductivity vs Radial Position for a Velocity of 0.1877 m/s and a Bridge Size of 0.05 in.
k (W/m*K)
0.40
0.35
0.30
0.25
0.20
0.15
0.10
0.05
0.00
0.00
0.10
0.20
0.30
0.40
0.50
0.60
L/dp

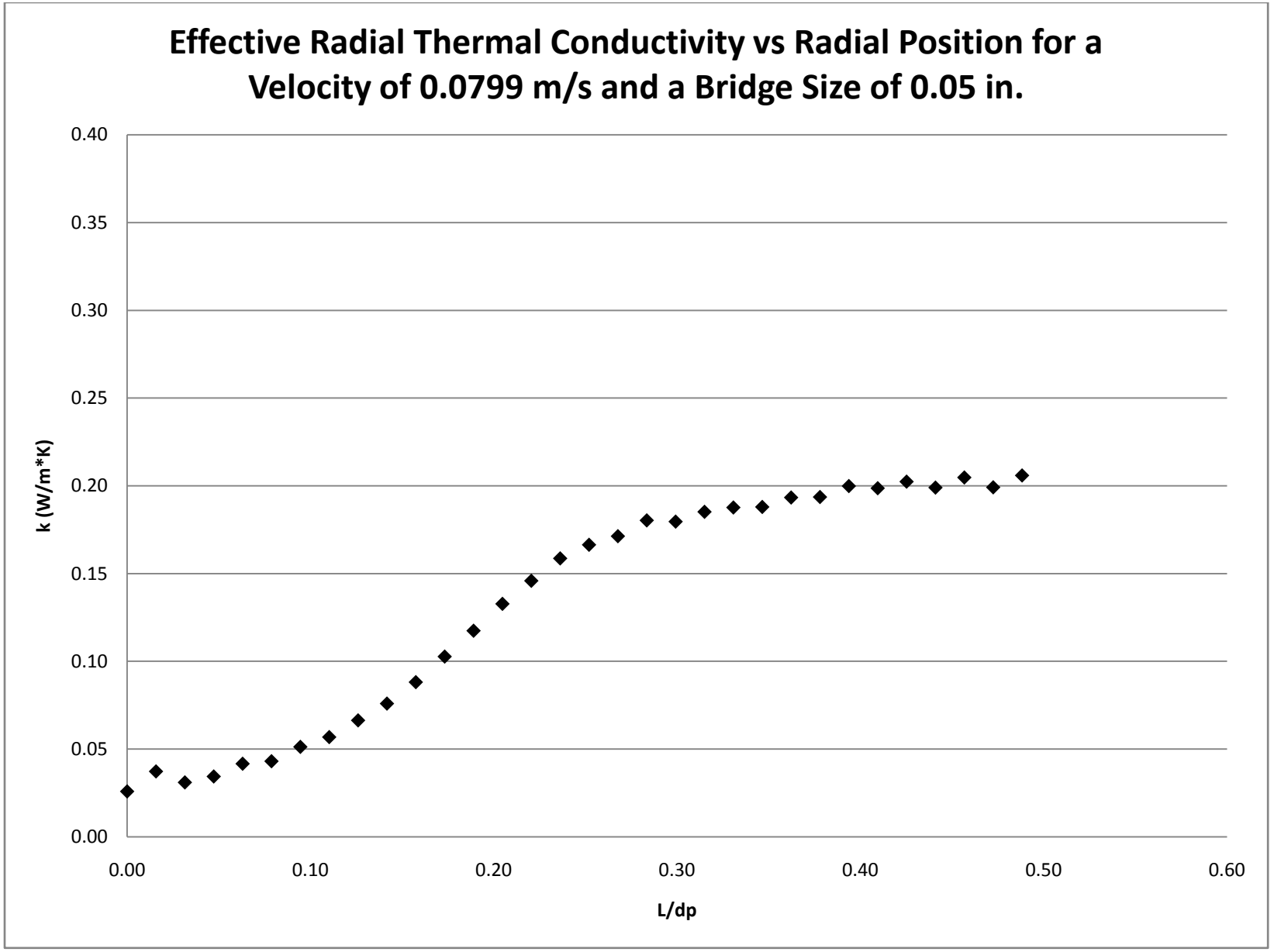
Effective Radial Thermal Conductivity vs Radial Position for a Velocity of 0.0799 m/s and a Bridge Size of 0.05 in.
k (W/m*K)
0.40
0.35
0.30
0.25
0.20
0.15
0.10
0.05
0.00
0.00
0.10
0.20
0.30
0.40
0.50
0.60
L/dp

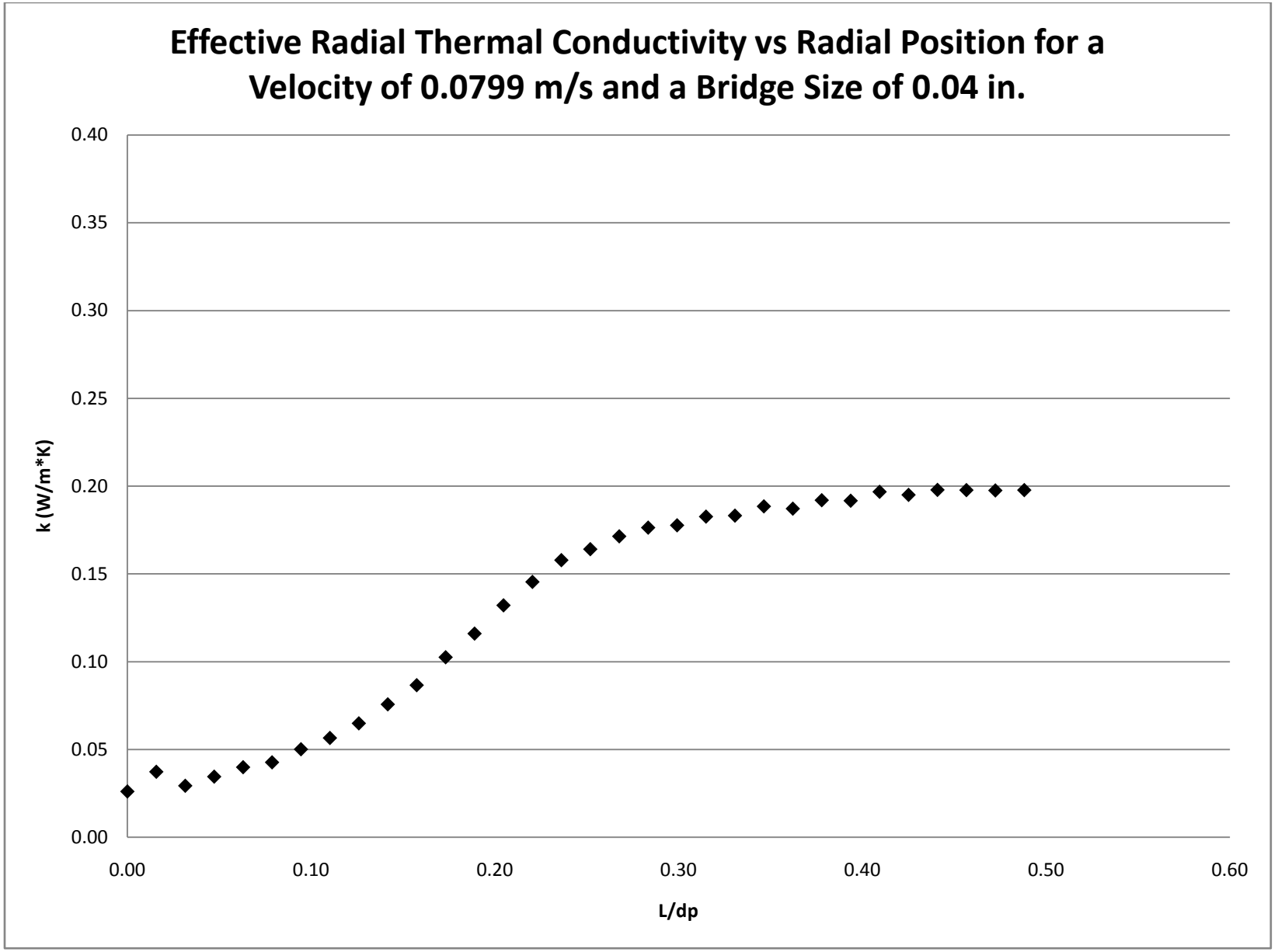
Effective Radial Thermal Conductivity vs Radial Position for a Velocity of 0.0799 m/s and a Bridge Size of 0.04 in.
k (W/m*K)
0.40
0.35
0.30
0.25
0.20
0.15
0.10
0.05
0.00
0.00
0.10
0.20
0.30
0.40
0.50
0.60
L/dp

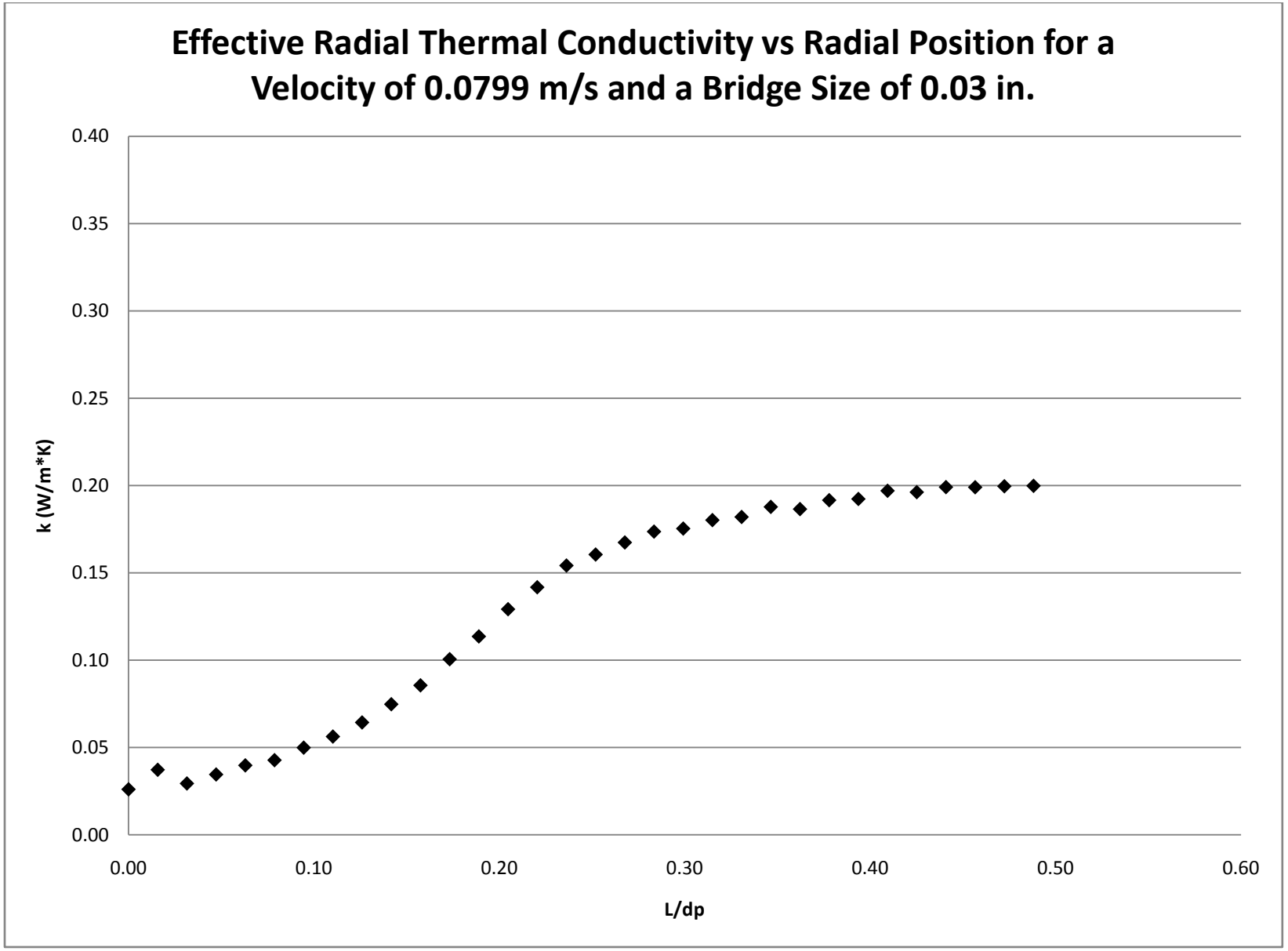
Effective Radial Thermal Conductivity vs Radial Position for a Velocity of 0.0799 m/s and a Bridge Size of 0.03 in.
k (W/m*K)
0.40
0.35
0.30
0.25
0.20
0.15
0.10
0.05
0.00
0.00
0.10
0.20
0.30
0.40
0.50
0.60
L/dp

D.2: Combined Effective Radial Thermal Conductivity Gradients

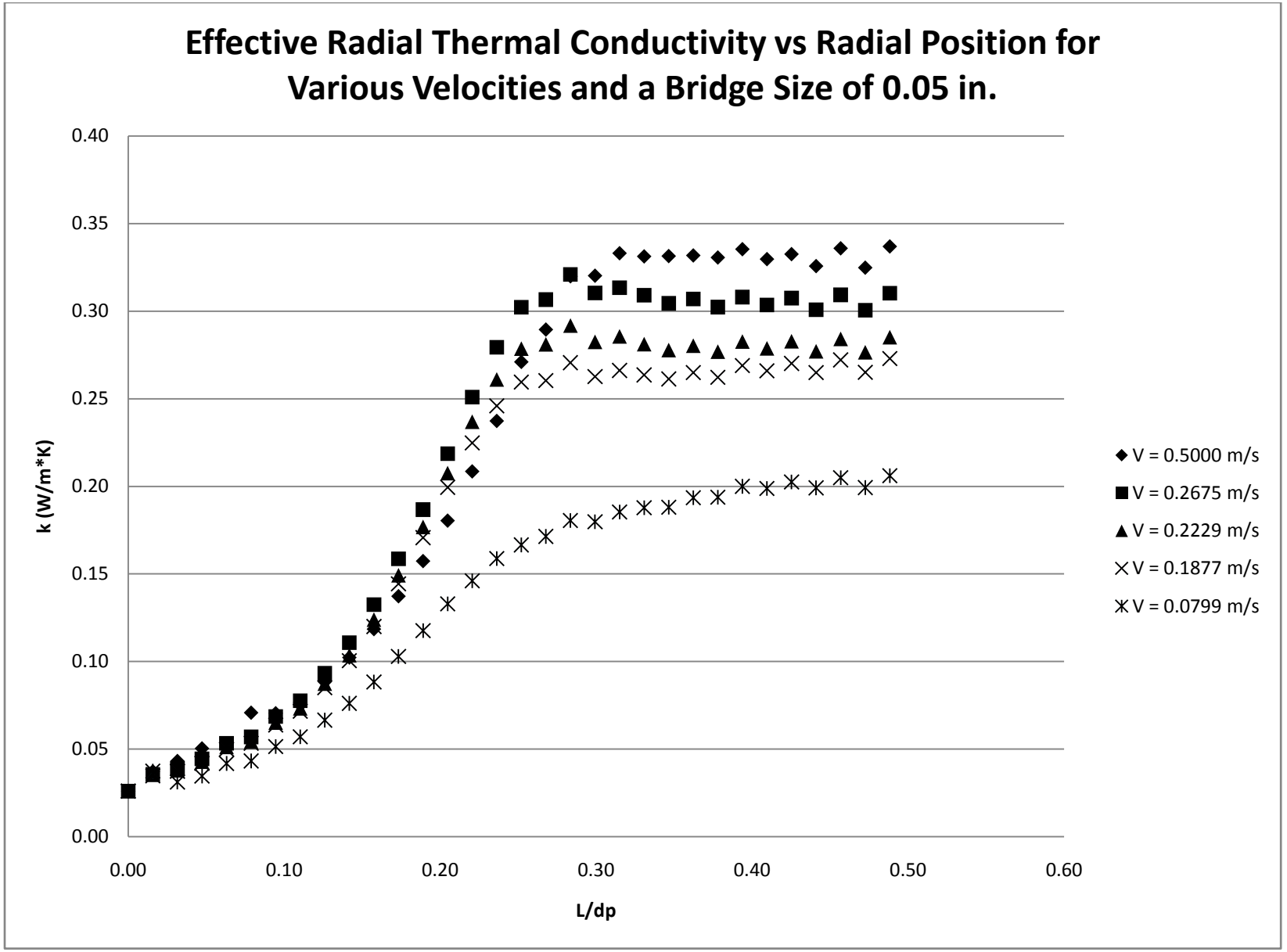
Effective Radial Thermal Conductivity vs Radial Position for Various Velocities and a Bridge Size of 0.05 in.
k (W/m*K)
0.40
0.35
0.30
0.25
0.20
0.15
0.10
0.05
0.00
0.00
0.10
0.20
0.30
0.40
0.50
0.60
L/dp
V = 0.5000 m/s
V = 0.2675 m/s
V = 0.2229 m/s
V = 0.1877 m/s
V = 0.0799 m/s

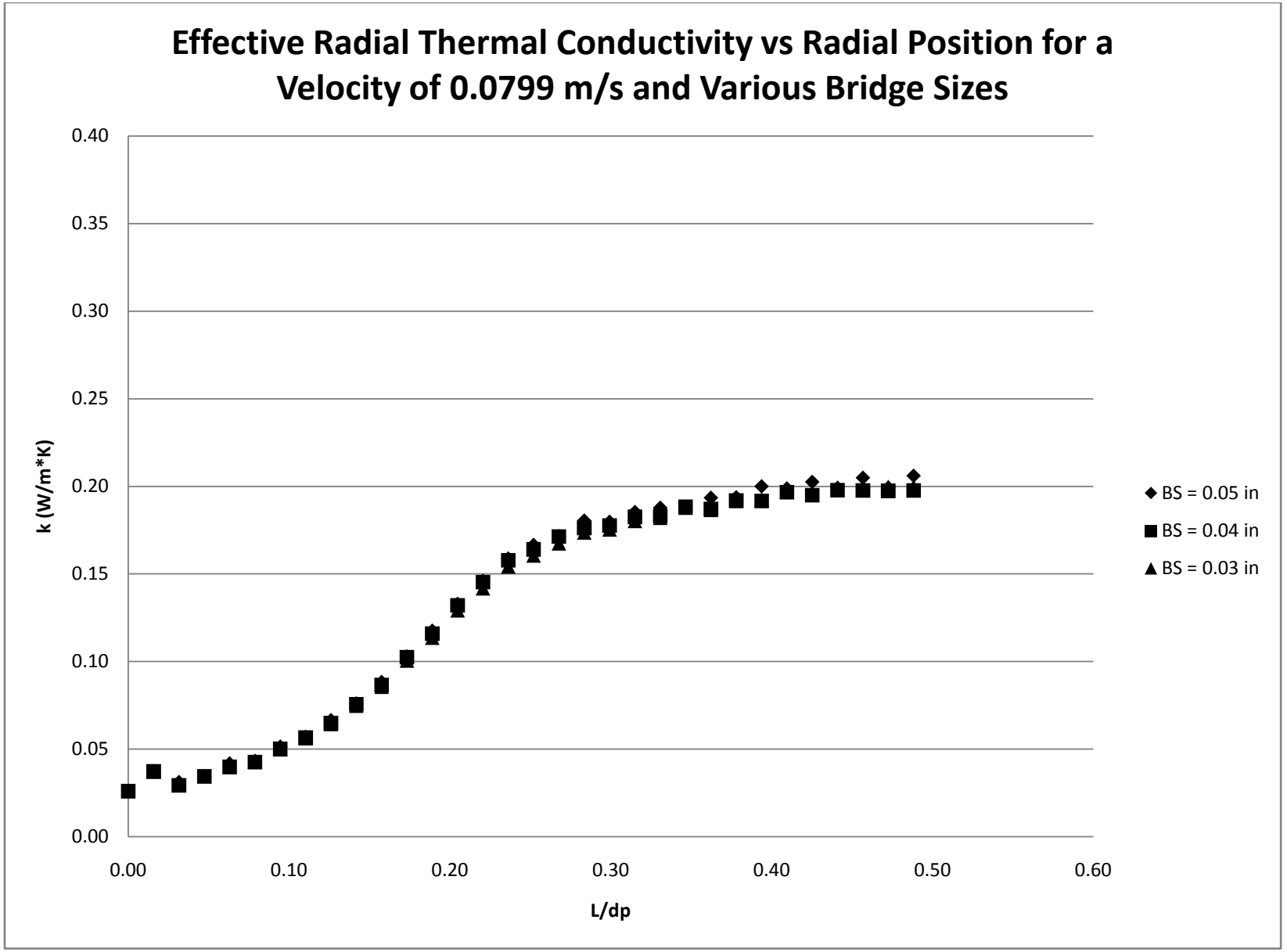
Effective Radial Thermal Conductivity vs Radial Position for a Velocity of 0.0799 m/s and Various Bridge Sizes
k (W/m*K)
0.40
0.35
0.30
0.25
0.20
0.15
0.10
0.05
0.00
0.00
0.10
0.20
0.30
0.40
0.50
0.60
L/dp
BS = 0.05 in
BS = 0.04 in
BS = 0.03 in

D.3: Combined Effective Radial Thermal Conductivity Gradients at Varying Mesh Refinements

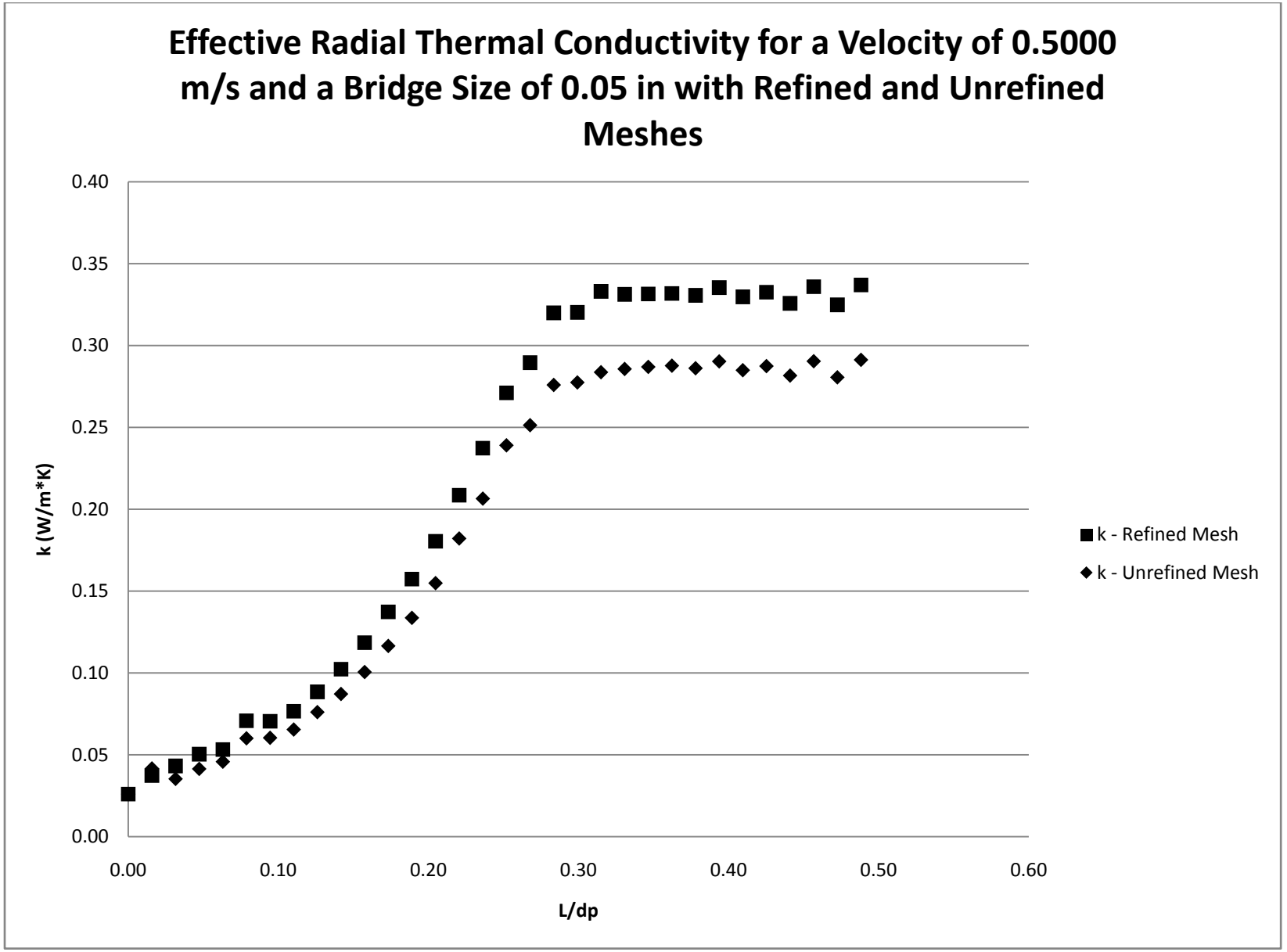
Effective Radial Thermal Conductivity for a Velocity of 0.5000 m/s and a Bridge Size of 0.05 in with Refined and Unrefined Meshes
0.40
0.35
0.30
0.25
0.20
0.15
0.10
0.05
0.00
k (W/m*K)
0.00
0.10
0.20
0.30
0.40
0.50
0.60
L/dp
k - Refined Mesh
k - Unrefined Mesh

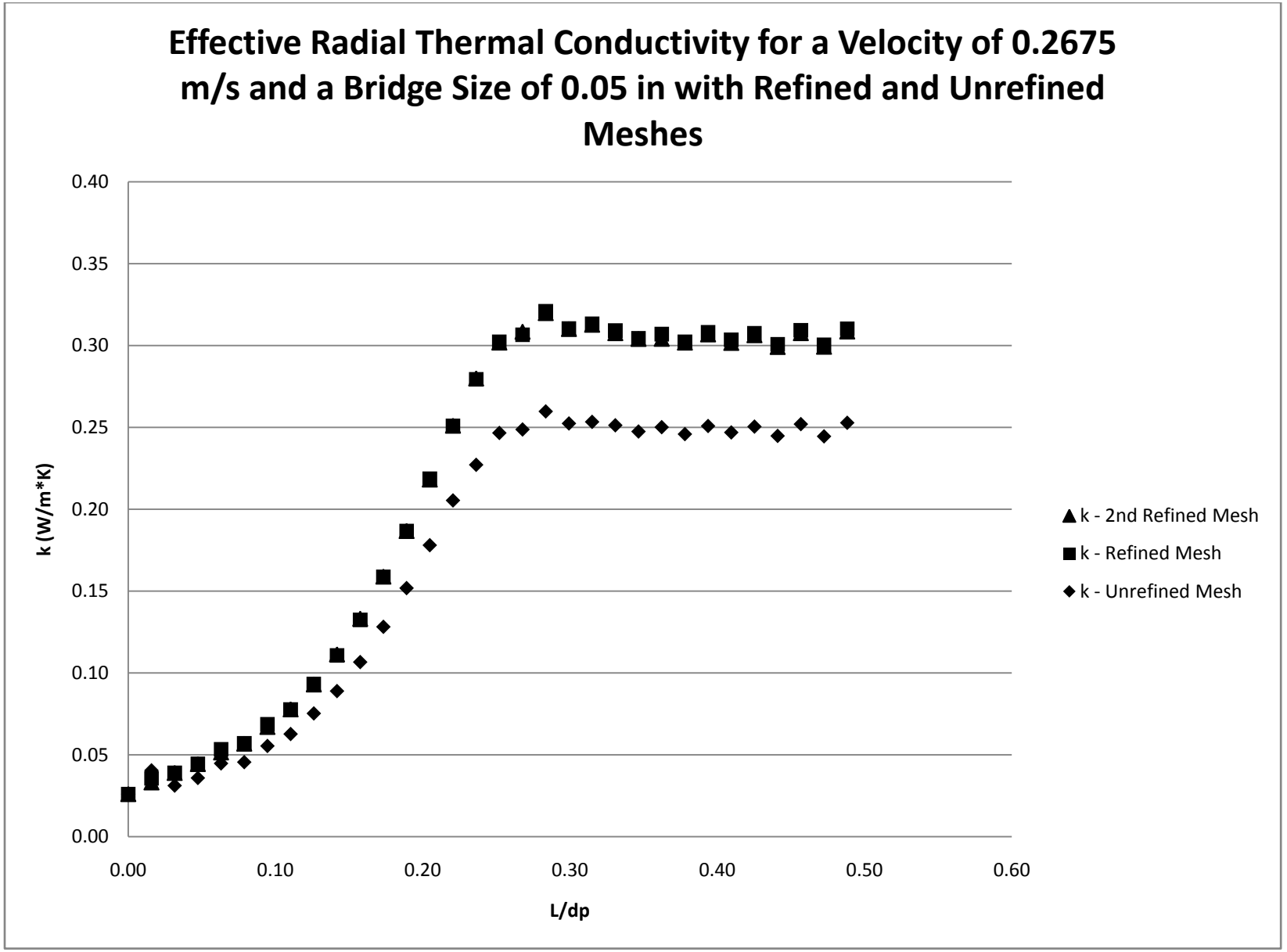
Effective Radial Thermal Conductivity for a Velocity of 0.2675 m/s and a Bridge Size of 0.05 in with Refined and Unrefined Meshes
0.40
0.35
0.30
0.25
0.20
0.15
0.10
0.05
0.00
k (W/m*K)
0.00
0.10
0.20
0.30
0.40
0.50
0.60
L/dp
k - 2nd Refined Mesh
k - Refined Mesh
k - Unrefined Mesh

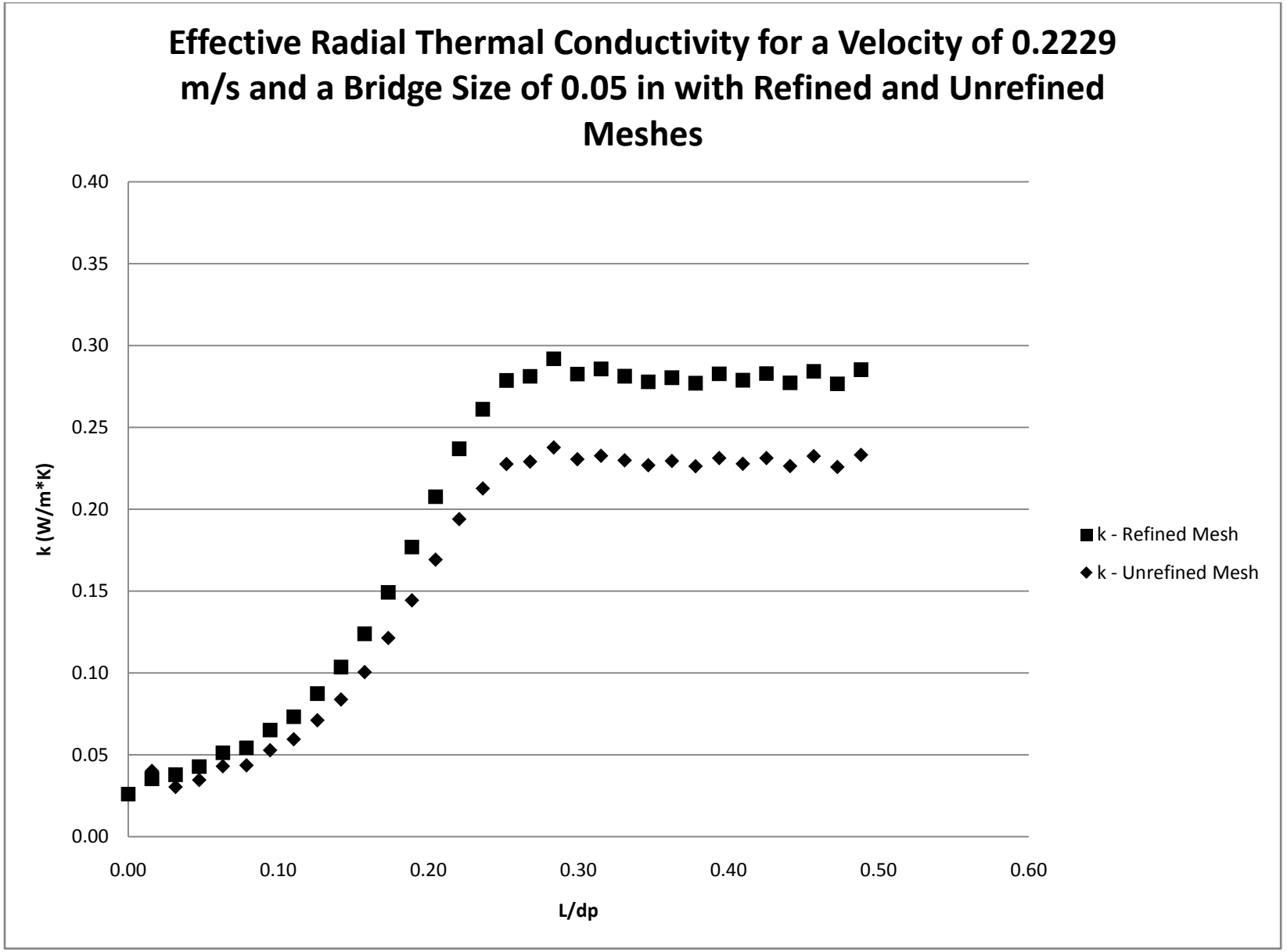
Effective Radial Thermal Conductivity for a Velocity of 0.2229 m/s and a Bridge Size of 0.05 in with Refined and Unrefined Meshes
0.40
0.35
0.30
0.25
0.20
0.15
0.10
0.05
0.00
k (W/m*K)
0.00
0.10
0.20
0.30
0.40
0.50
0.60
L/dp
k - Refined Mesh
k - Unrefined Mesh

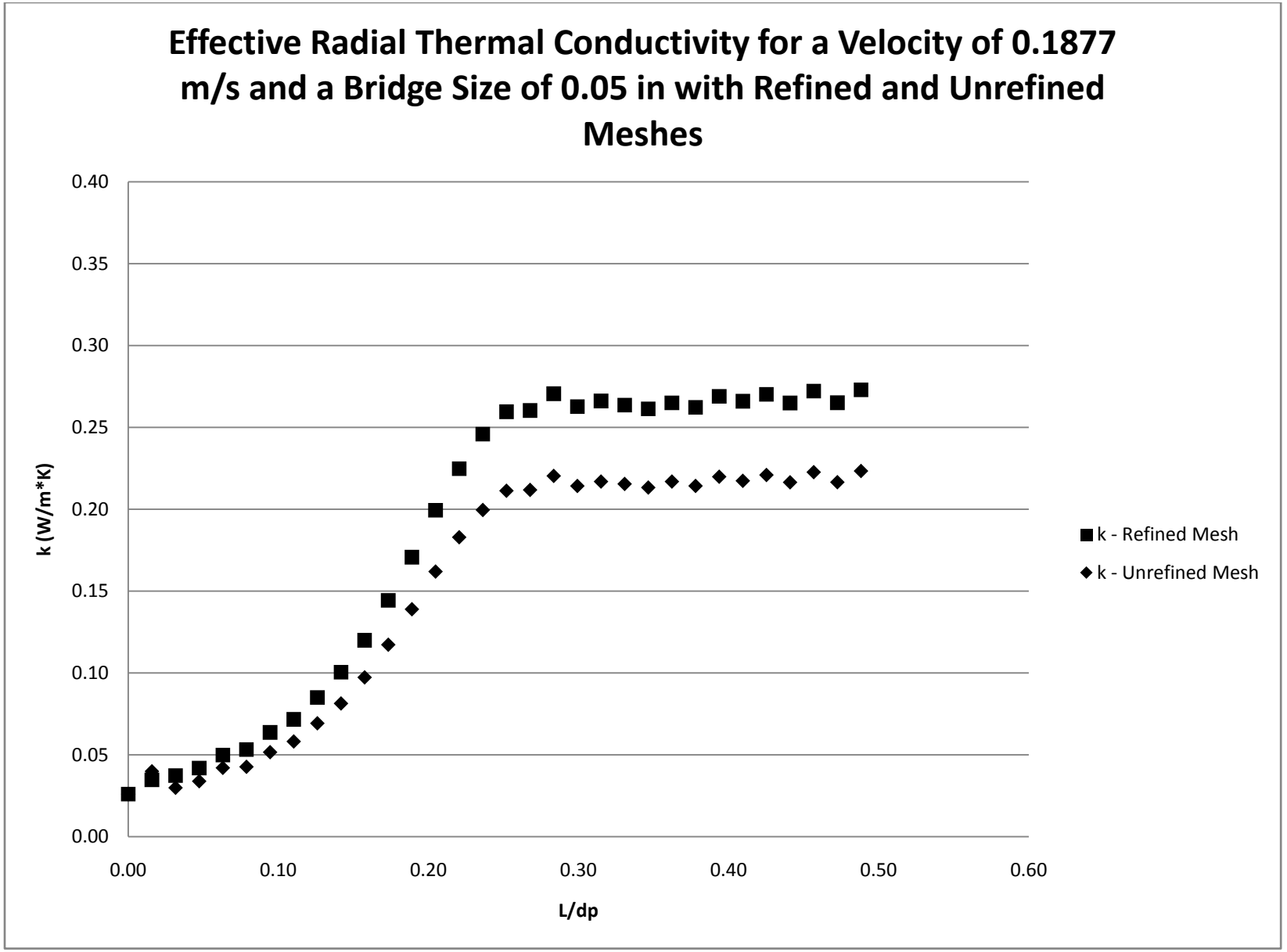
Effective Radial Thermal Conductivity for a Velocity of 0.1877 m/s and a Bridge Size of 0.05 in with Refined and Unrefined Meshes
0.40
0.35
0.30
0.25
0.20
0.15
0.10
0.05
0.00
k (W/m*K)
0.00
0.10
0.20
0.30
0.40
0.50
0.60
L/dp
k - Refined Mesh
k - Unrefined Mesh

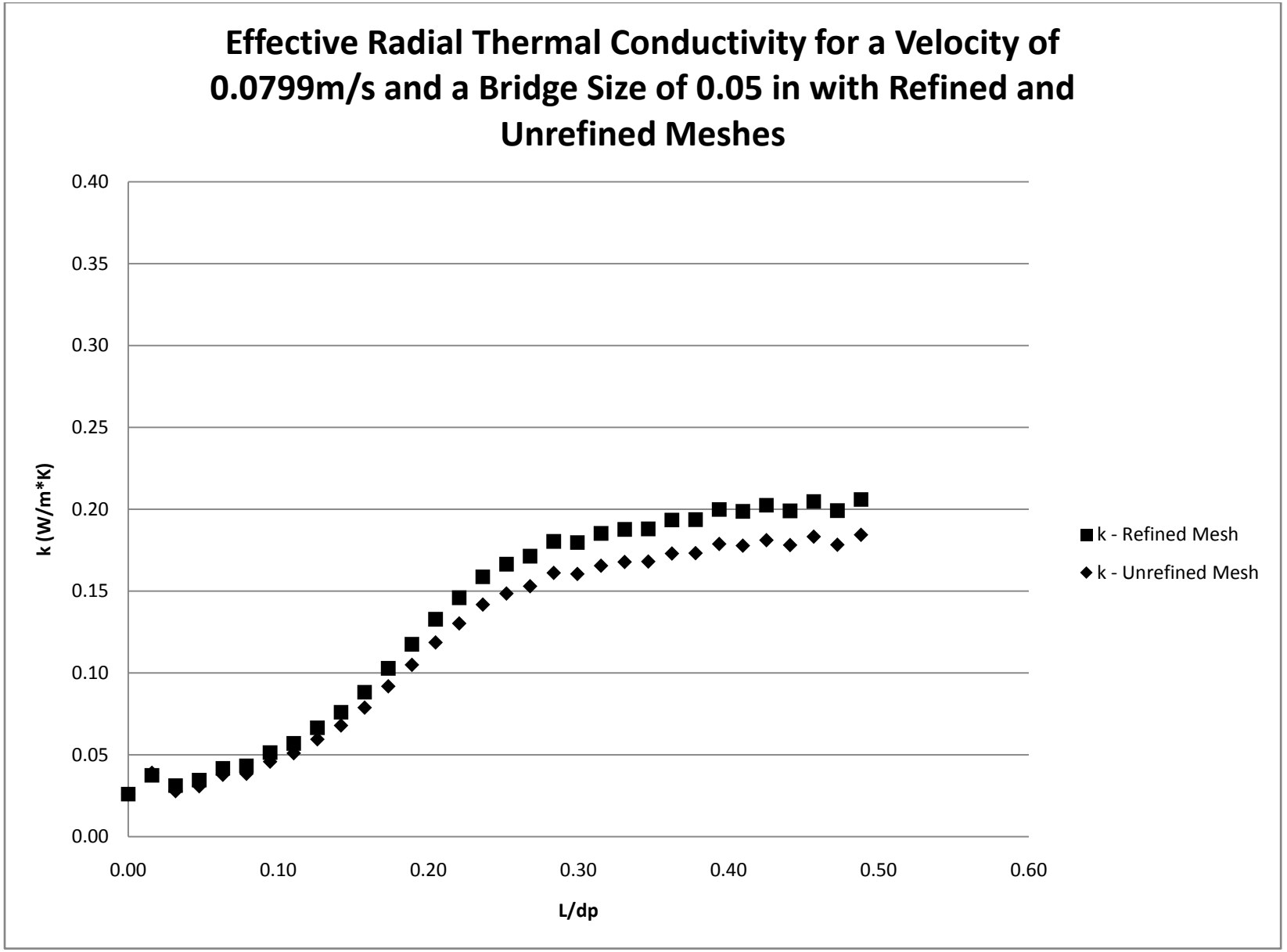
Effective Radial Thermal Conductivity for a Velocity of 0.0799m/s and a Bridge Size of 0.05 in with Refined and Unrefined Meshes
0.40
0.35
0.30
0.25
0.20
0.15
0.10
0.05
0.00
k (W/m*K)
0.00
0.10
0.20
0.30
0.40
0.50
0.60
L/dp
k - Refined Mesh
k - Unrefined Mesh

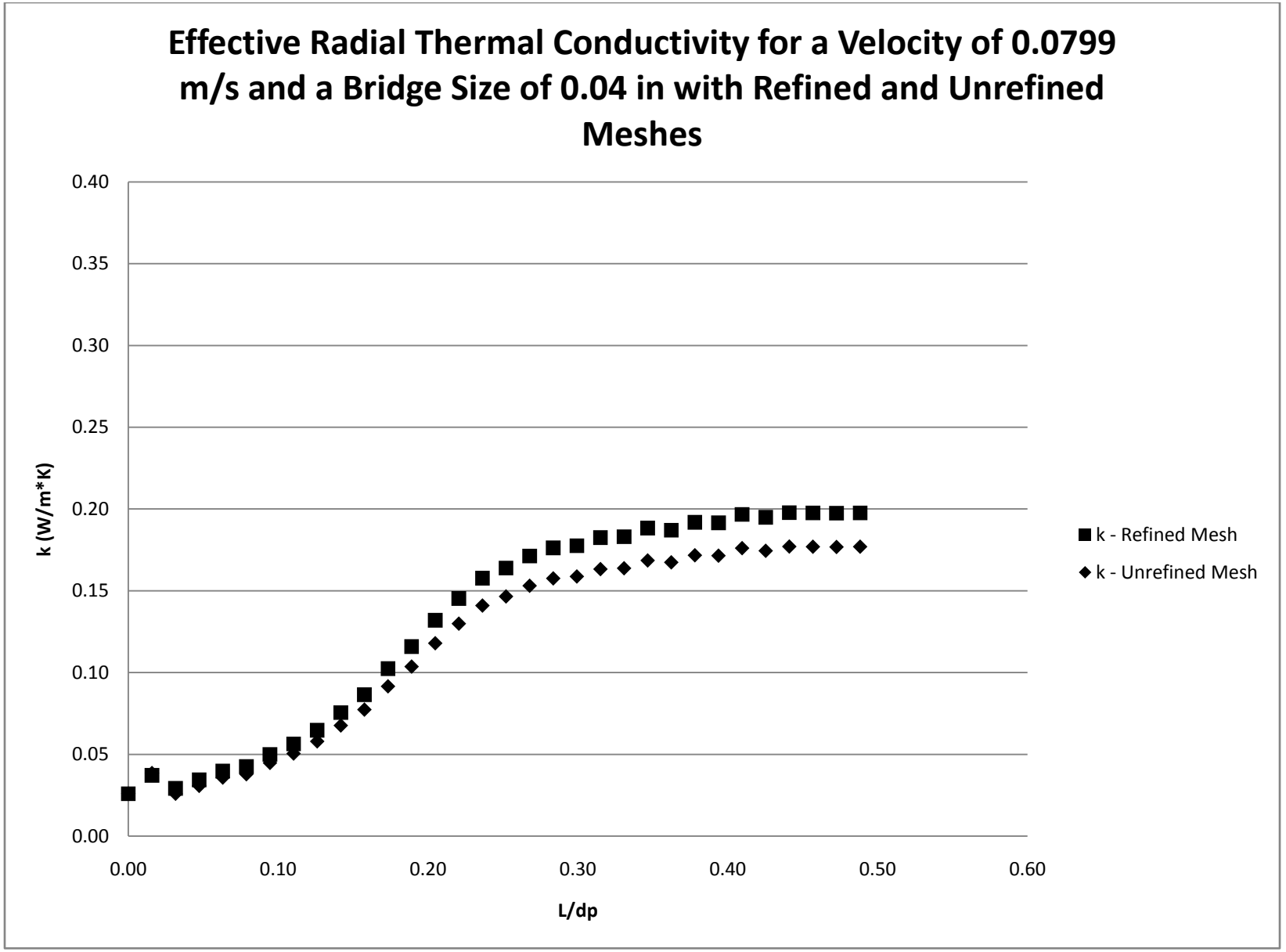
Effective Radial Thermal Conductivity for a Velocity of 0.0799 m/s and a Bridge Size of 0.04 in with Refined and Unrefined Meshes
0.40
0.35
0.30
0.25
0.20
0.15
0.10
0.05
0.00
k (W/m*K)
0.00
0.10
0.20
0.30
0.40
0.50
0.60
L/dp
k - Refined Mesh
k - Unrefined Mesh

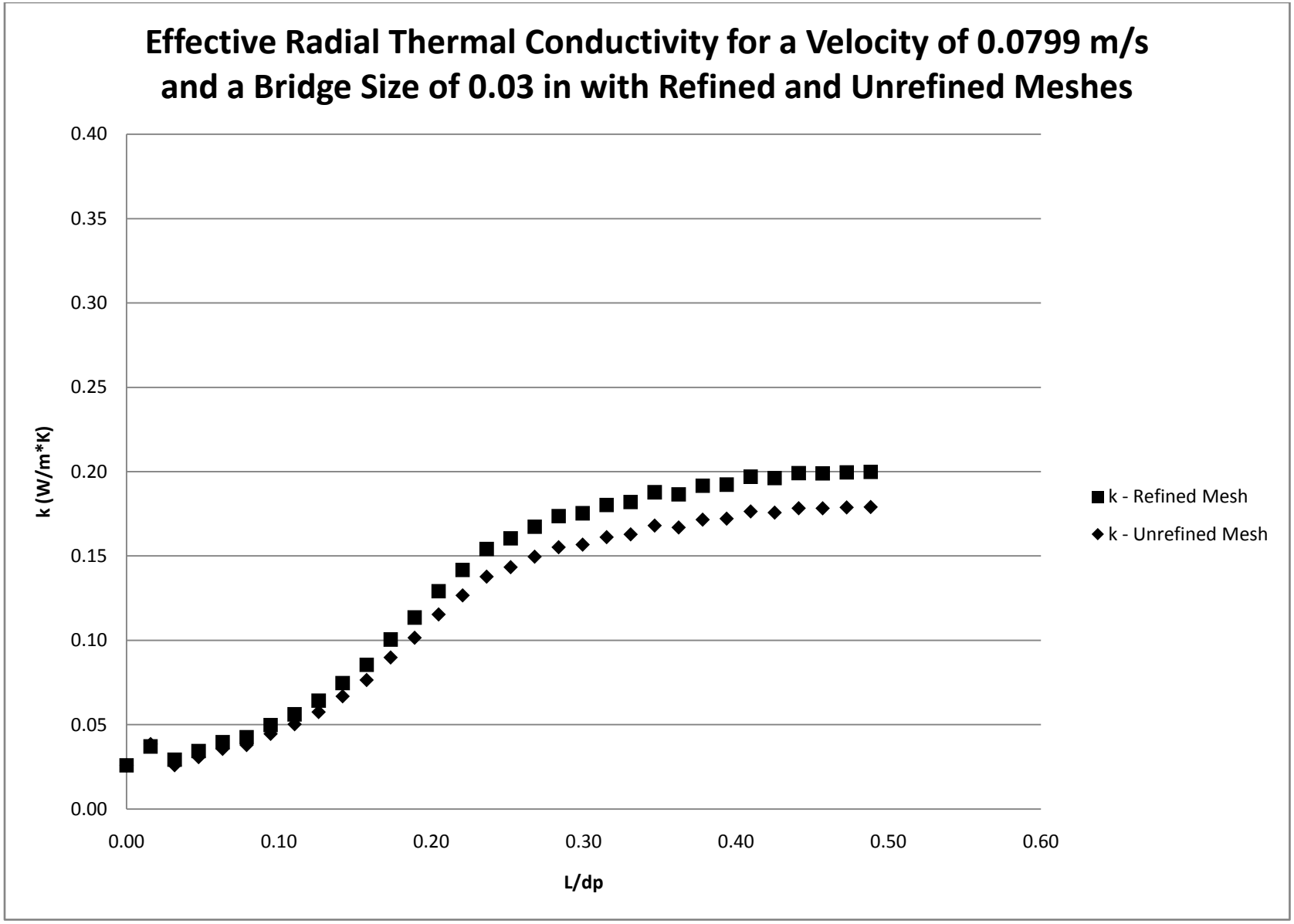
Effective Radial Thermal Conductivity for a Velocity of 0.0799 m/s and a Bridge Size of 0.03 in with Refined and Unrefined Meshes
0.40
0.35
0.30
0.25
0.20
0.15
0.10
0.05
0.00
k (W/m*K)
0.00
0.10
0.20
0.30
0.40
0.50
0.60
L/dp
k - Refined Mesh
k - Unrefined Mesh

Appendix E: 2″ Column Temperature Profiles

E.1: Comparing Reynolds Numbers

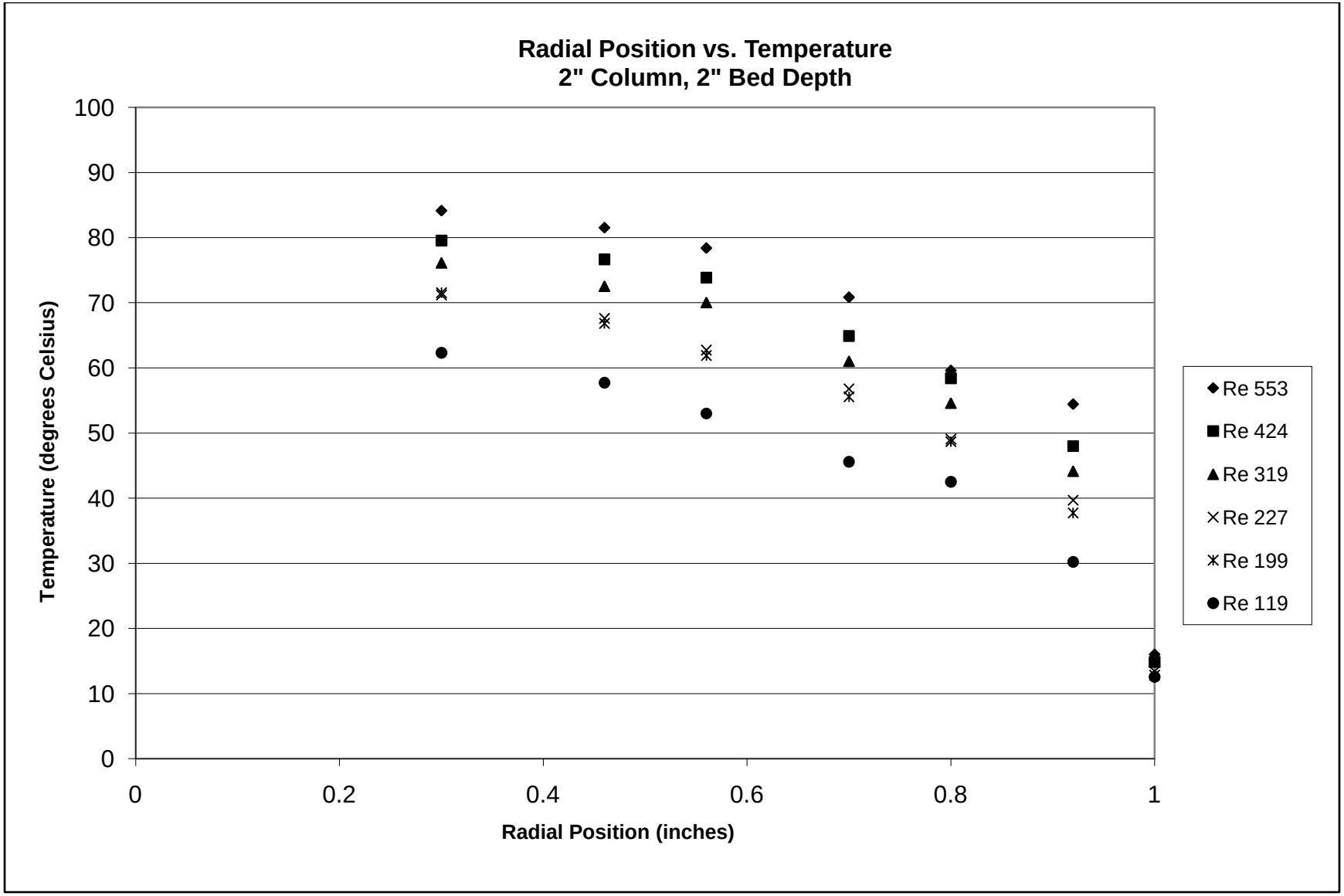
Radial Position vs. Temperature
2" Column, 2" Bed Depth
Temperature (degrees Celsius)
100
90
80
70
60
50
40
30
20
10
0
0
0.2
0.4
0.6
0.8
1
Radial Position (inches)
Re 553
Re 424
Re 319
Re 227
Re 199
Re 119

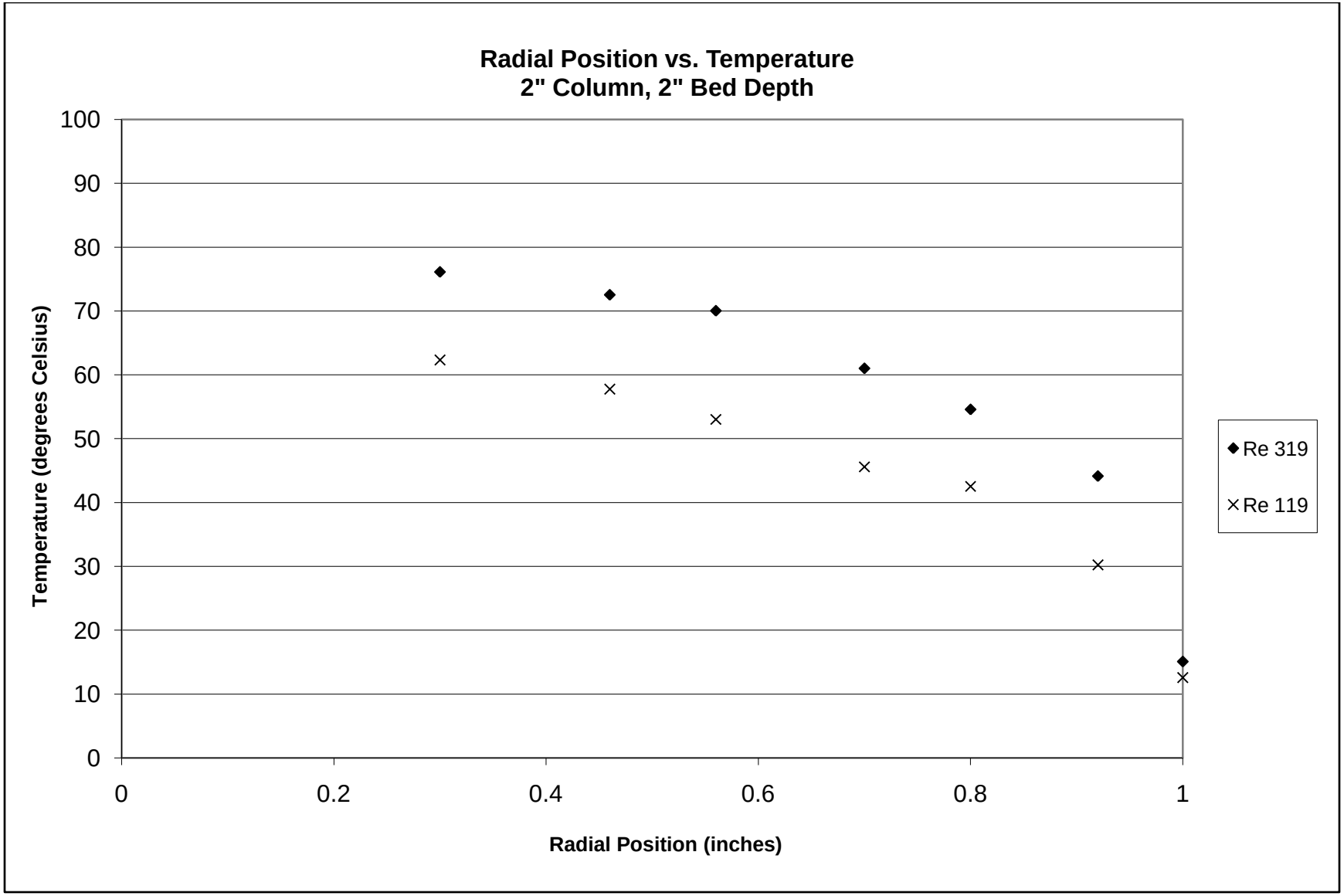
Radial Position vs. Temperature
2" Column, 2" Bed Depth
Temperature (degrees Celsius)
100
90
80
70
60
50
40
30
20
10
0
0
0.2
0.4
0.6
0.8
1
Radial Position (inches)
Re 319
Re 119

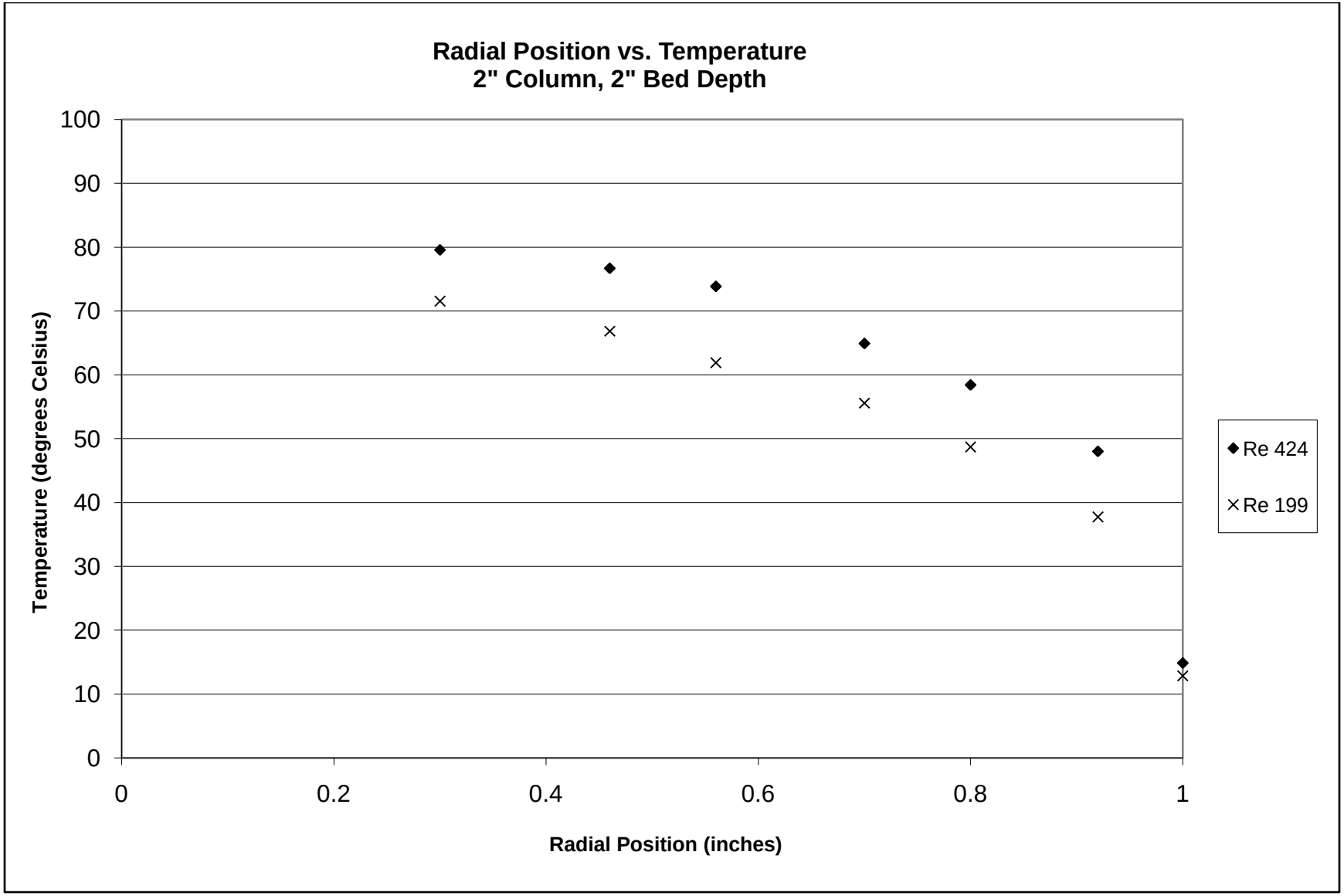
Radial Position vs. Temperature
2" Column, 2" Bed Depth
Temperature (degrees Celsius)
100
90
80
70
60
50
40
30
20
10
0
0
0.2
0.4
0.6
0.8
1
Radial Position (inches)
Re 424
Re 199

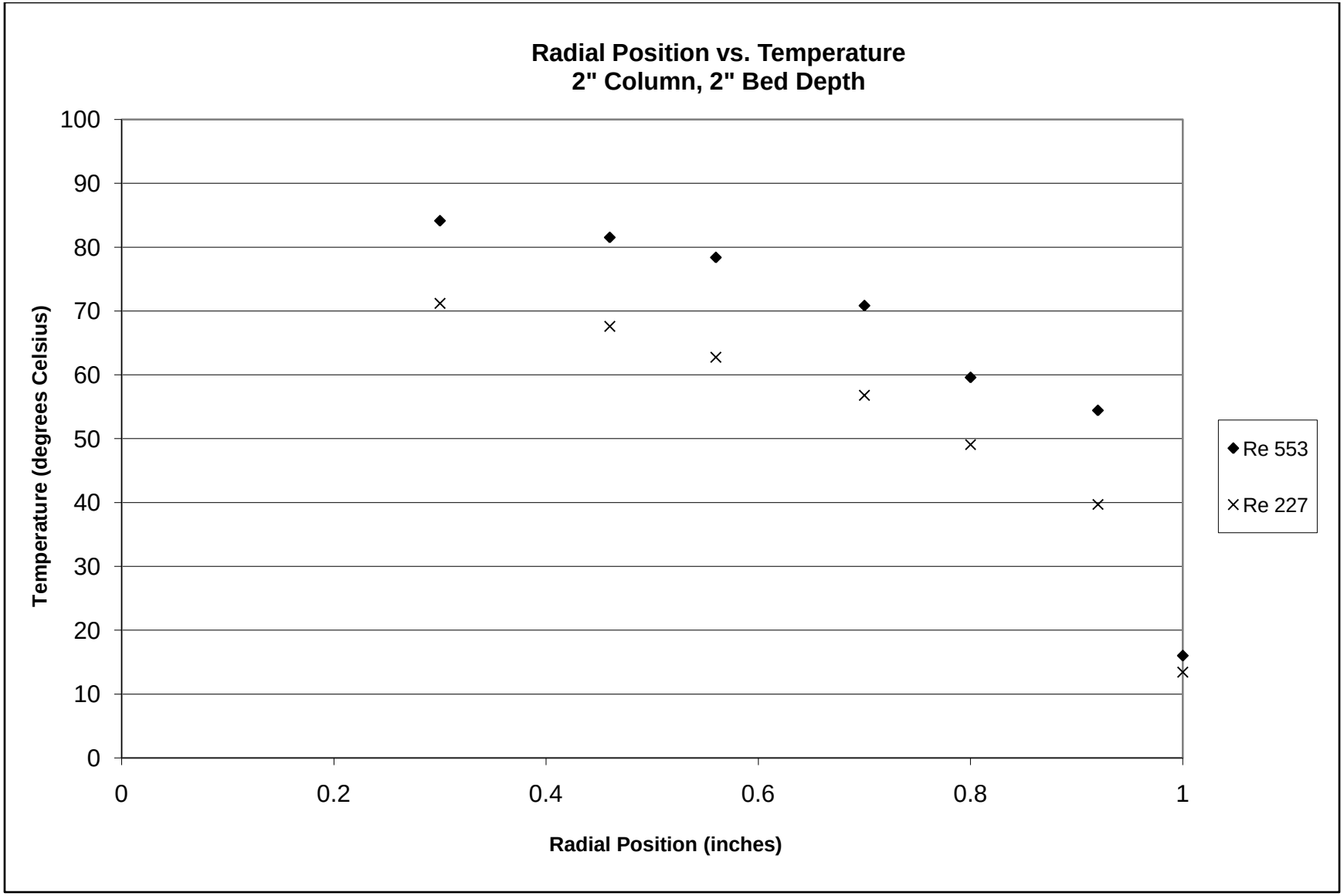
Radial Position vs. Temperature
2" Column, 2" Bed Depth
Temperature (degrees Celsius)
100
90
80
70
60
50
40
30
20
10
0
0
0.2
0.4
0.6
0.8
1
Radial Position (inches)
Re 553
Re 227

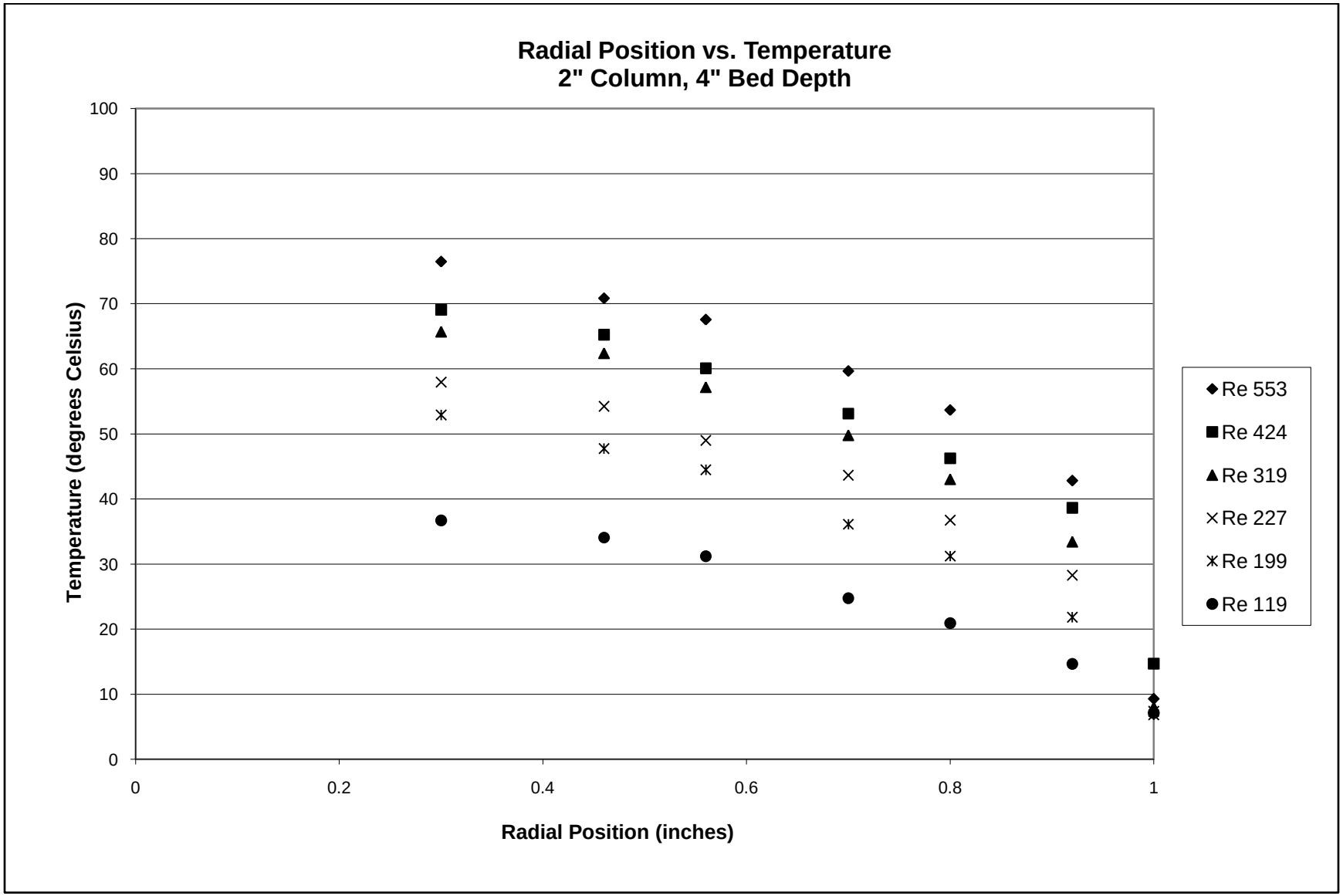
Radial Position vs. Temperature
2" Column, 4" Bed Depth
Temperature (degrees Celsius)
100
90
80
70
60
50
40
30
20
10
0
0
0.2
0.4
0.6
0.8
1
Radial Position (inches)
Re 553
Re 424
Re 319
Re 227
Re 199
Re 119

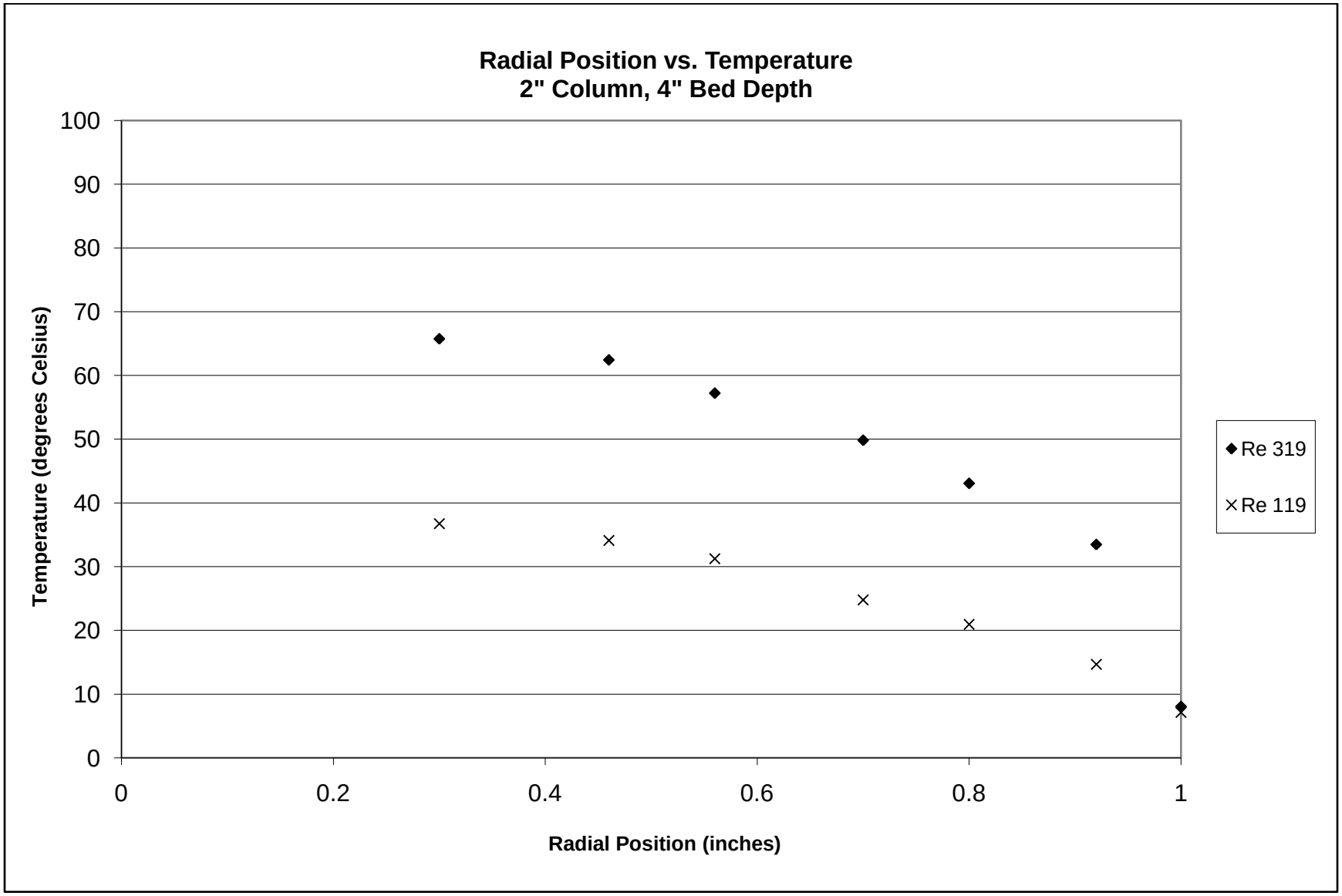
Radial Position vs. Temperature
2" Column, 4" Bed Depth
Temperature (degrees Celsius)
100
90
80
70
60
50
40
30
20
10
0
0
0.2
0.4
0.6
0.8
1
Radial Position (inches)
Re 319
Re 119

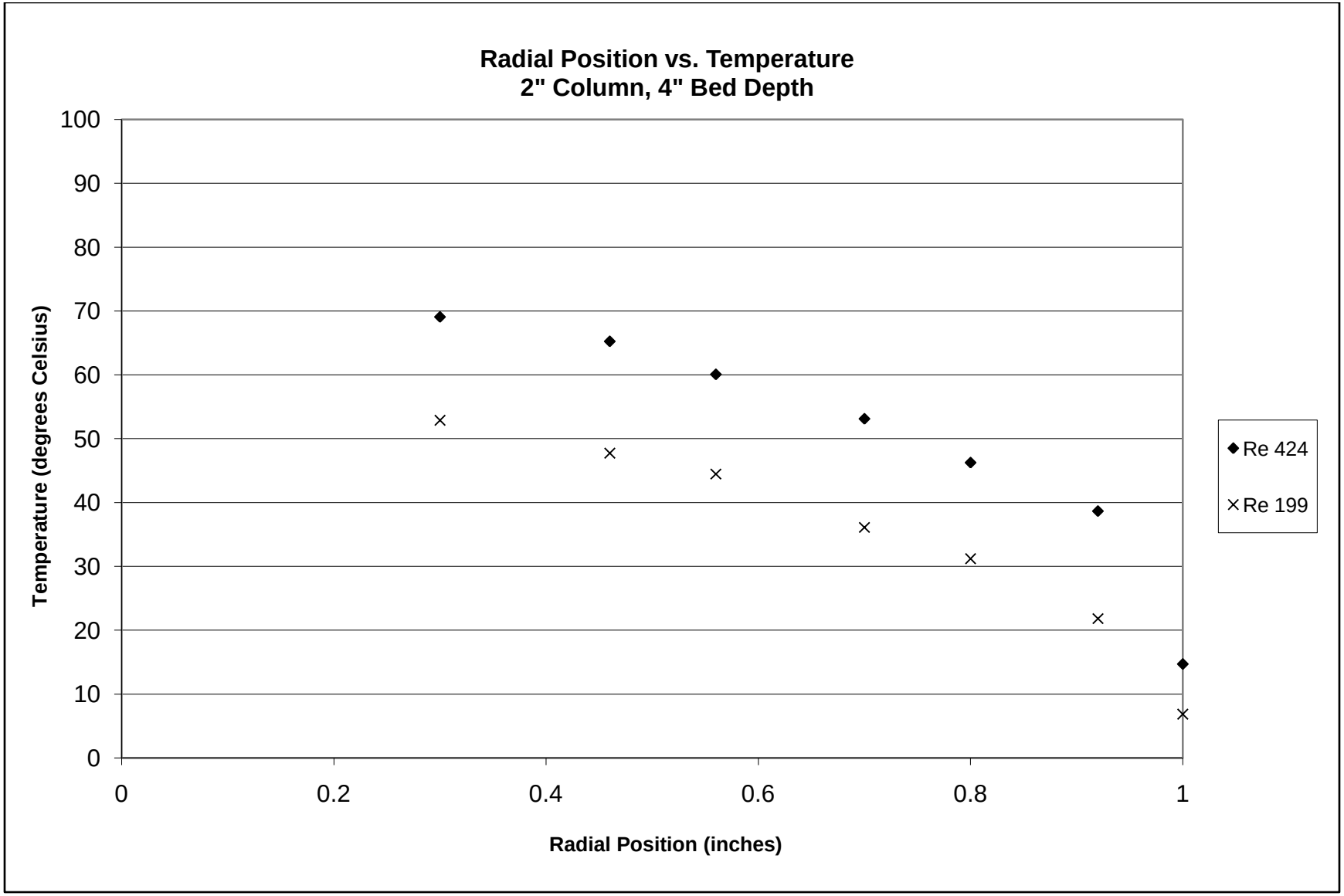
Radial Position vs. Temperature
2" Column, 4" Bed Depth
Temperature (degrees Celsius)
100
90
80
70
60
50
40
30
20
10
0
0
0.2
0.4
0.6
0.8
1
Radial Position (inches)
Re 424
Re 199

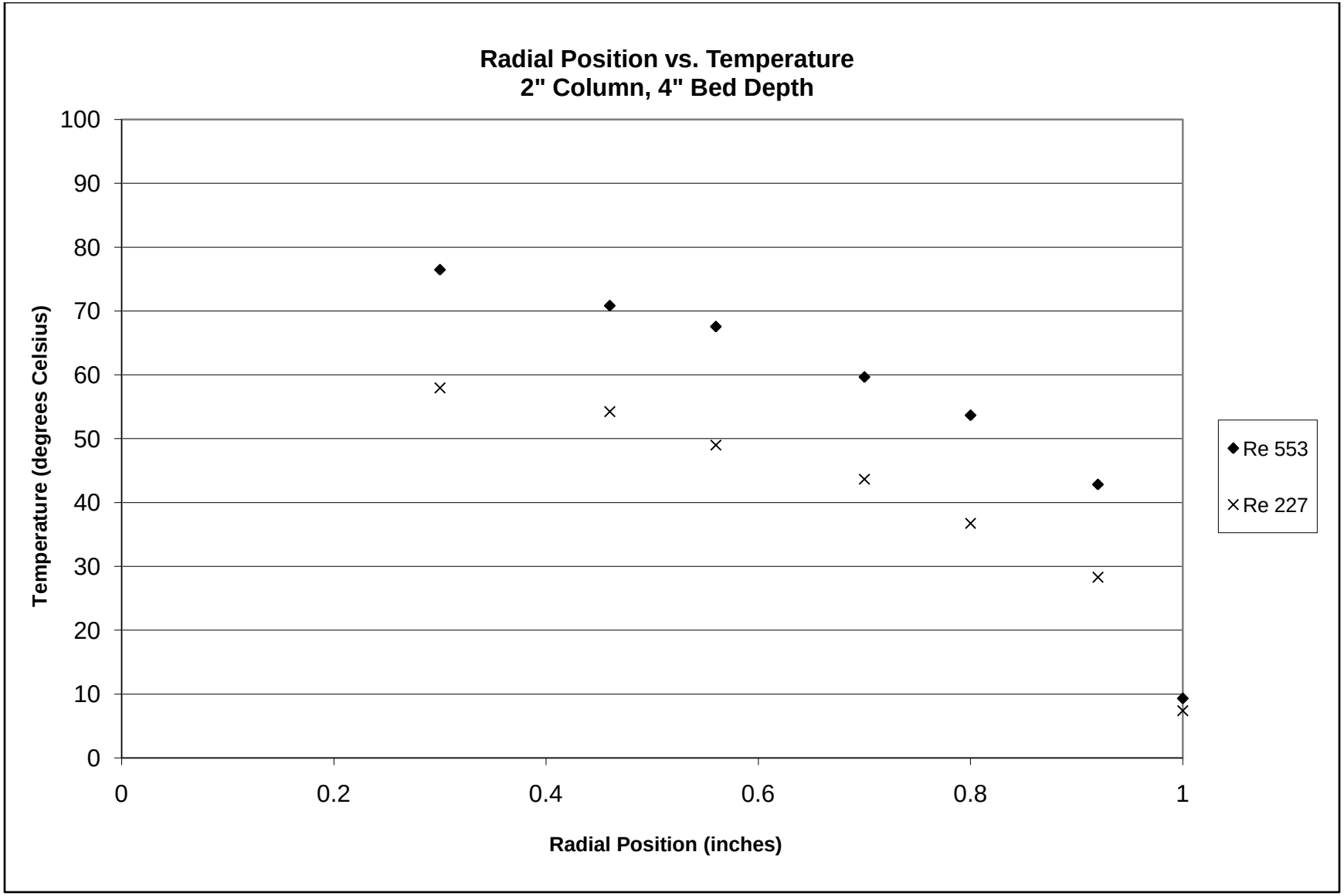
Radial Position vs. Temperature
2" Column, 4" Bed Depth
Temperature (degrees Celsius)
100
90
80
70
60
50
40
30
20
10
0
0
0.2
0.4
0.6
0.8
1
Radial Position (inches)
Re 553
Re 227

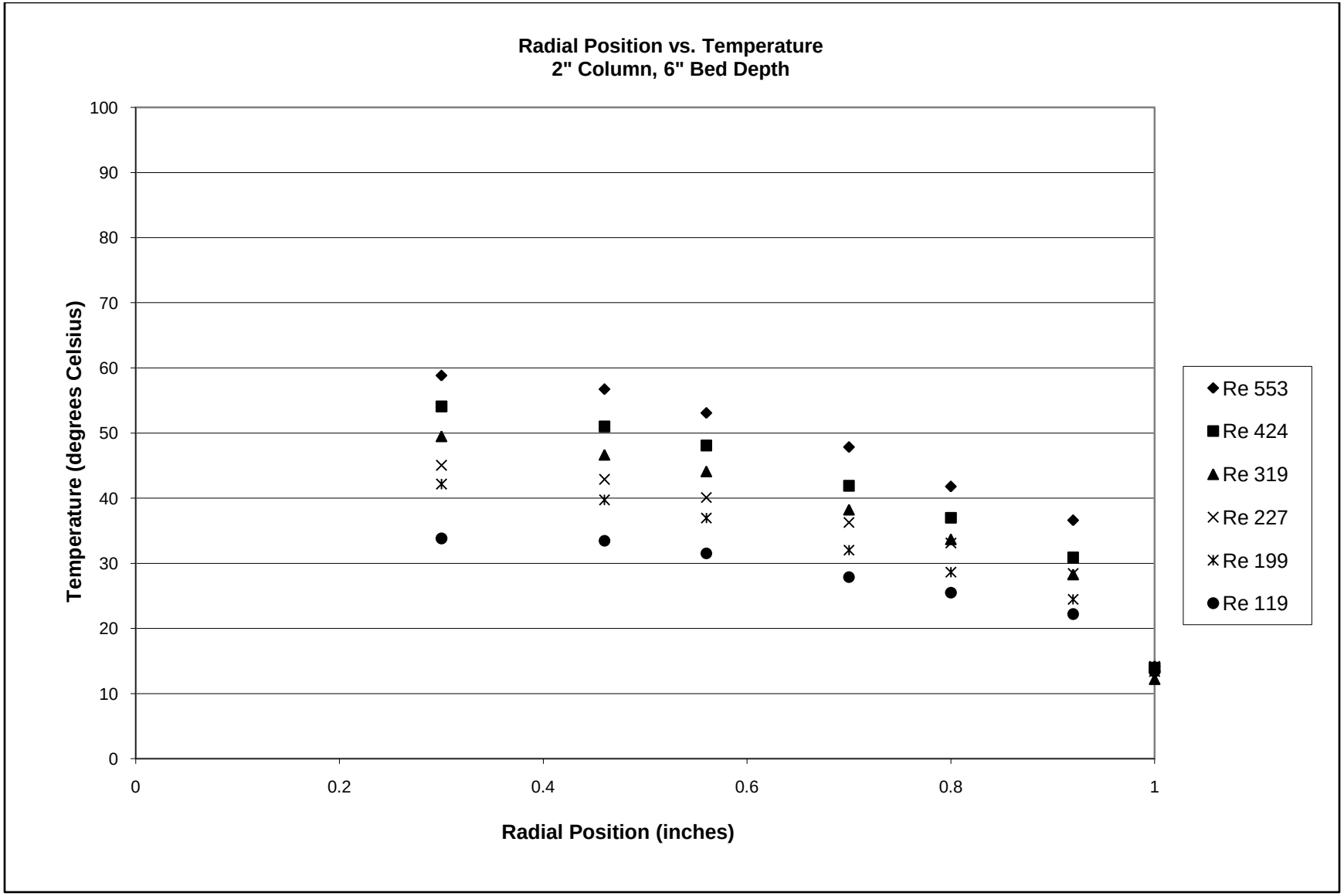
Radial Position vs. Temperature
2" Column, 6" Bed Depth
Temperature (degrees Celsius)
100
90
80
70
60
50
40
30
20
10
0
0
0.2
0.4
0.6
0.8
1
Radial Position (inches)
Re 553
Re 424
Re 319
Re 227
Re 199
Re 119

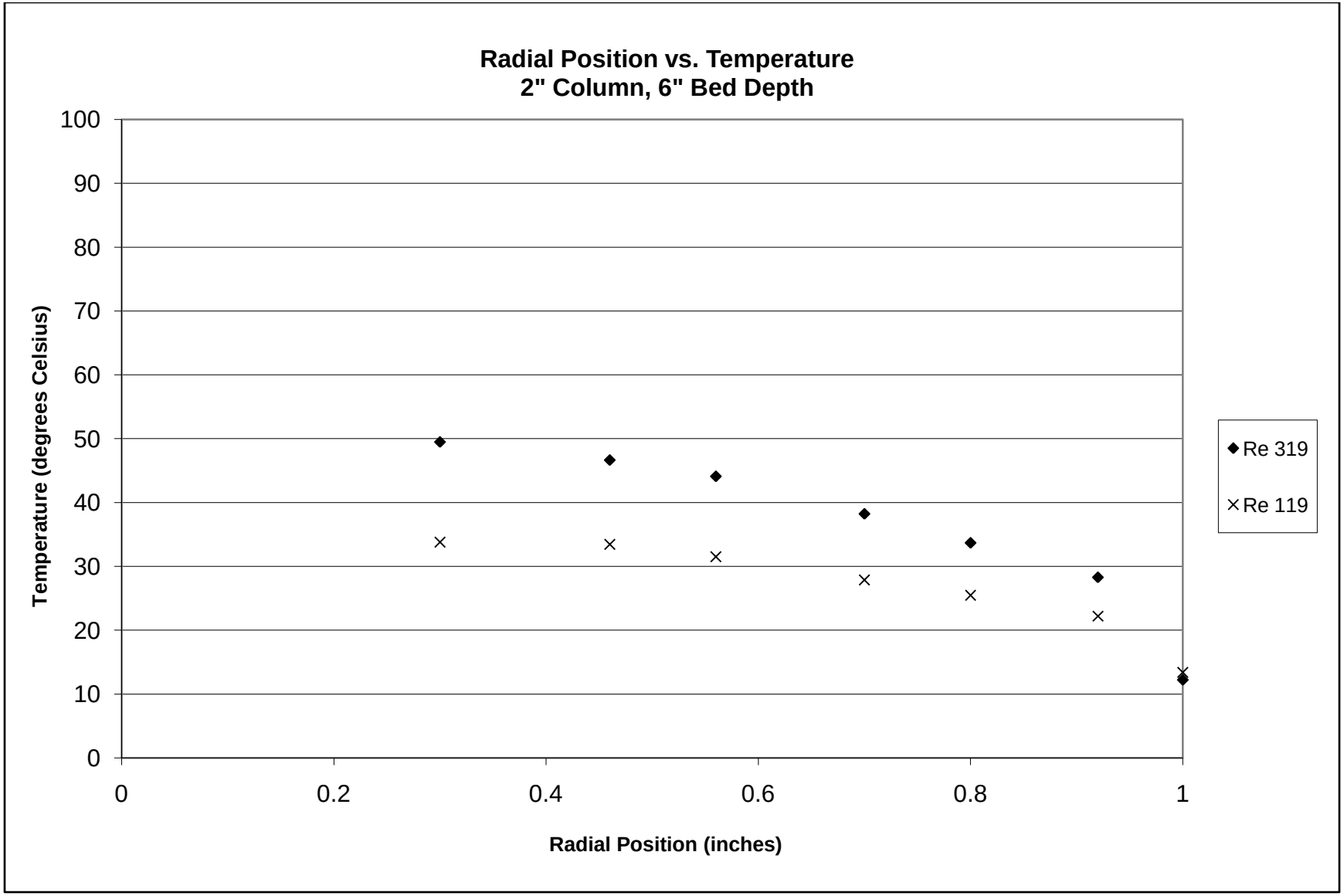
Radial Position vs. Temperature
2" Column, 6" Bed Depth
Temperature (degrees Celsius)
100
90
80
70
60
50
40
30
20
10
0
0
0.2
0.4
0.6
0.8
1
Radial Position (inches)
Re 319
Re 119

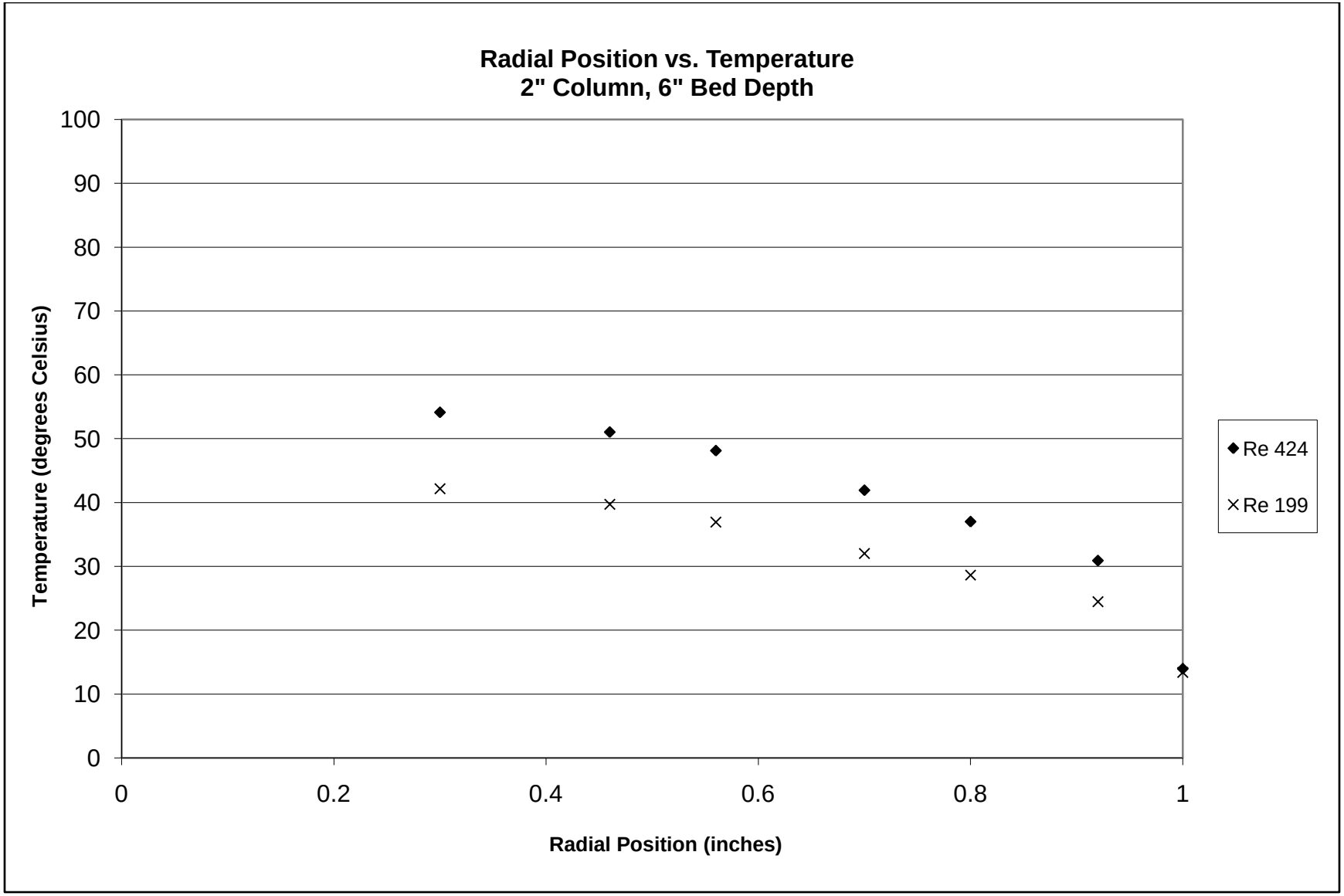
Radial Position vs. Temperature
2" Column, 6" Bed Depth
Temperature (degrees Celsius)
100
90
80
70
60
50
40
30
20
10
0
0
0.2
0.4
0.6
0.8
1
Radial Position (inches)
Re 424
Re 199

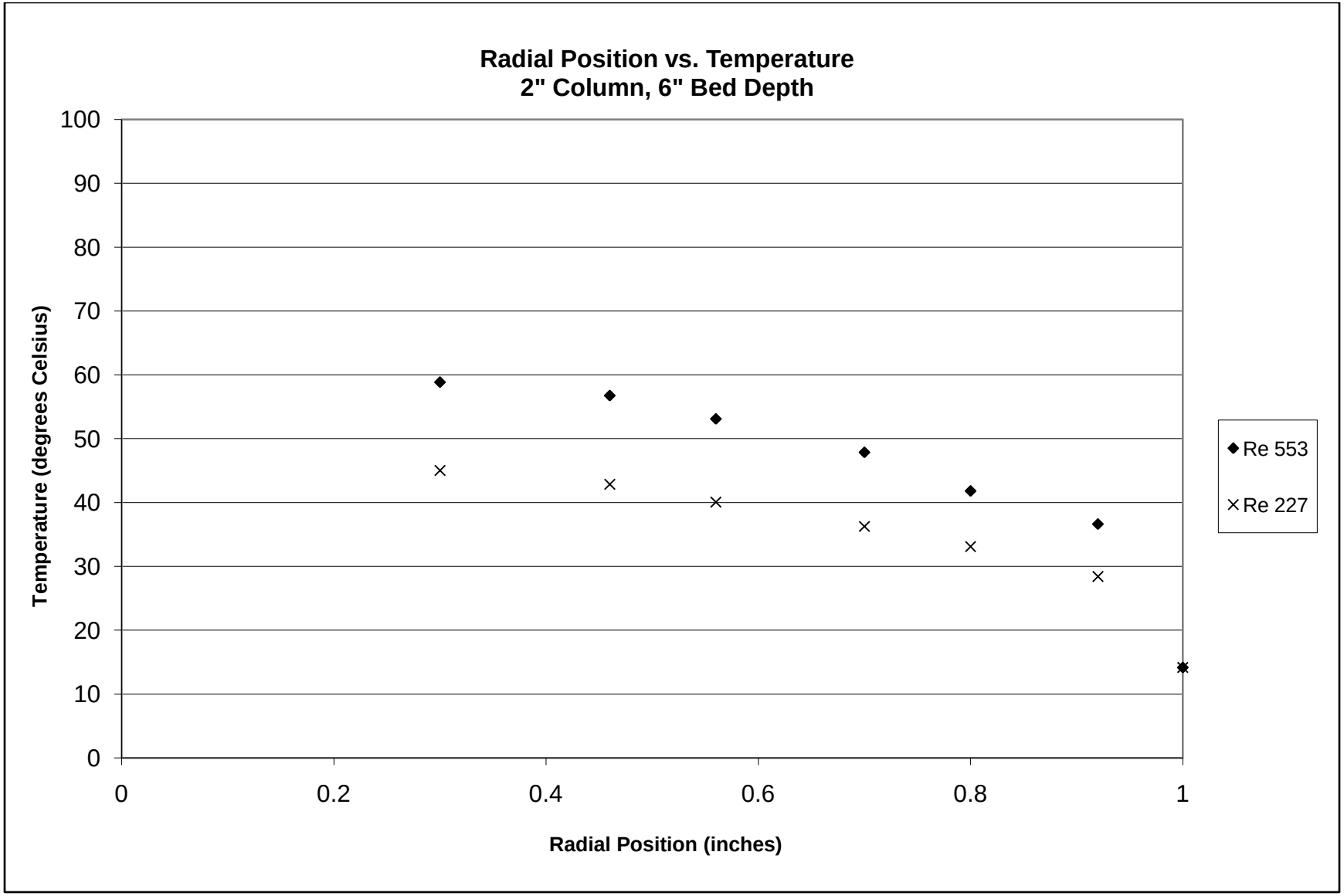
Radial Position vs. Temperature
2" Column, 6" Bed Depth
Temperature (degrees Celsius)
100
90
80
70
60
50
40
30
20
10
0
0
0.2
0.4
0.6
0.8
1
Radial Position (inches)
Re 553
Re 227

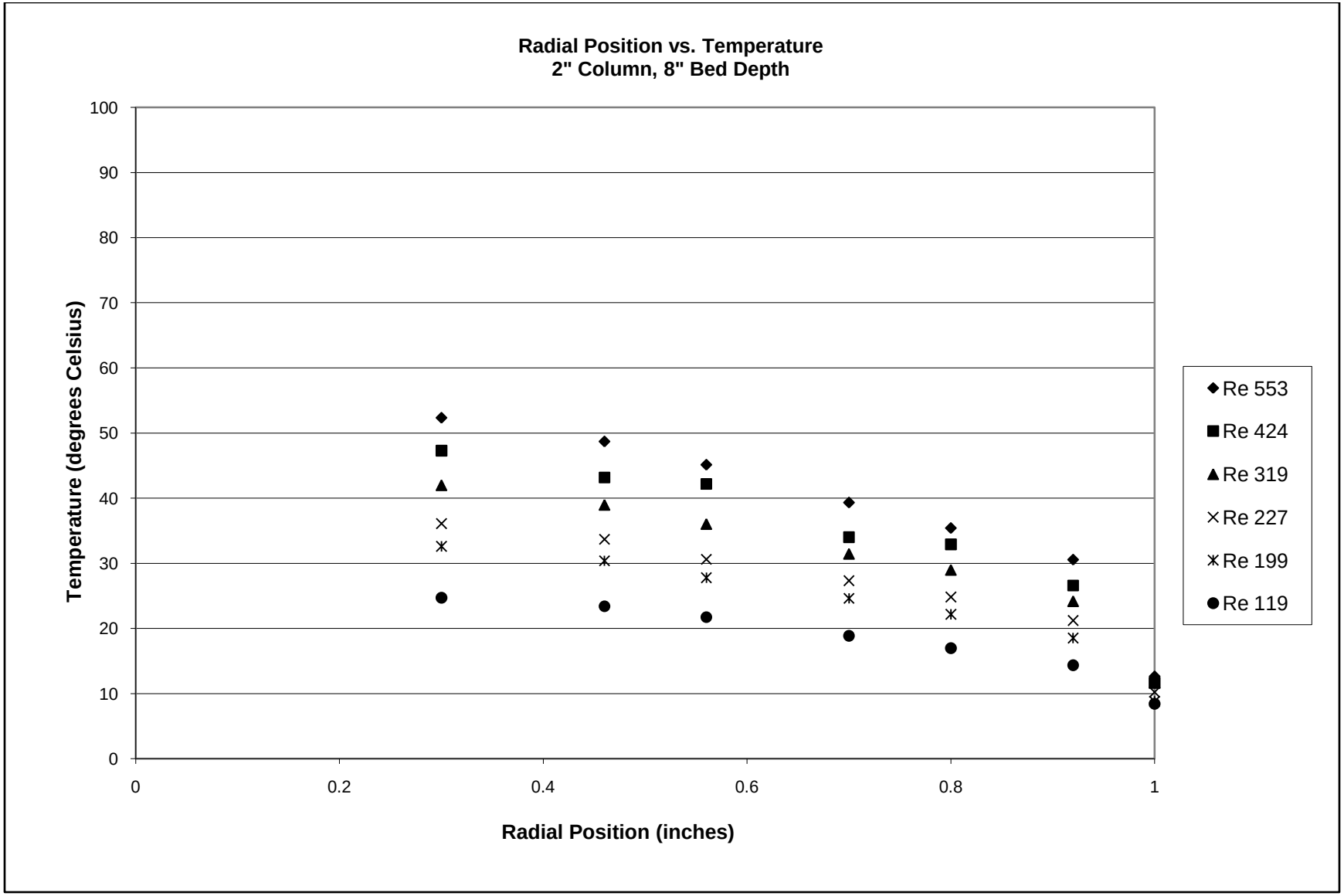
Radial Position vs. Temperature
2" Column, 8" Bed Depth
Temperature (degrees Celsius)
100
90
80
70
60
50
40
30
20
10
0
0
0.2
0.4
0.6
0.8
1
Radial Position (inches)
Re 553
Re 424
Re 319
Re 227
Re 199
Re 119

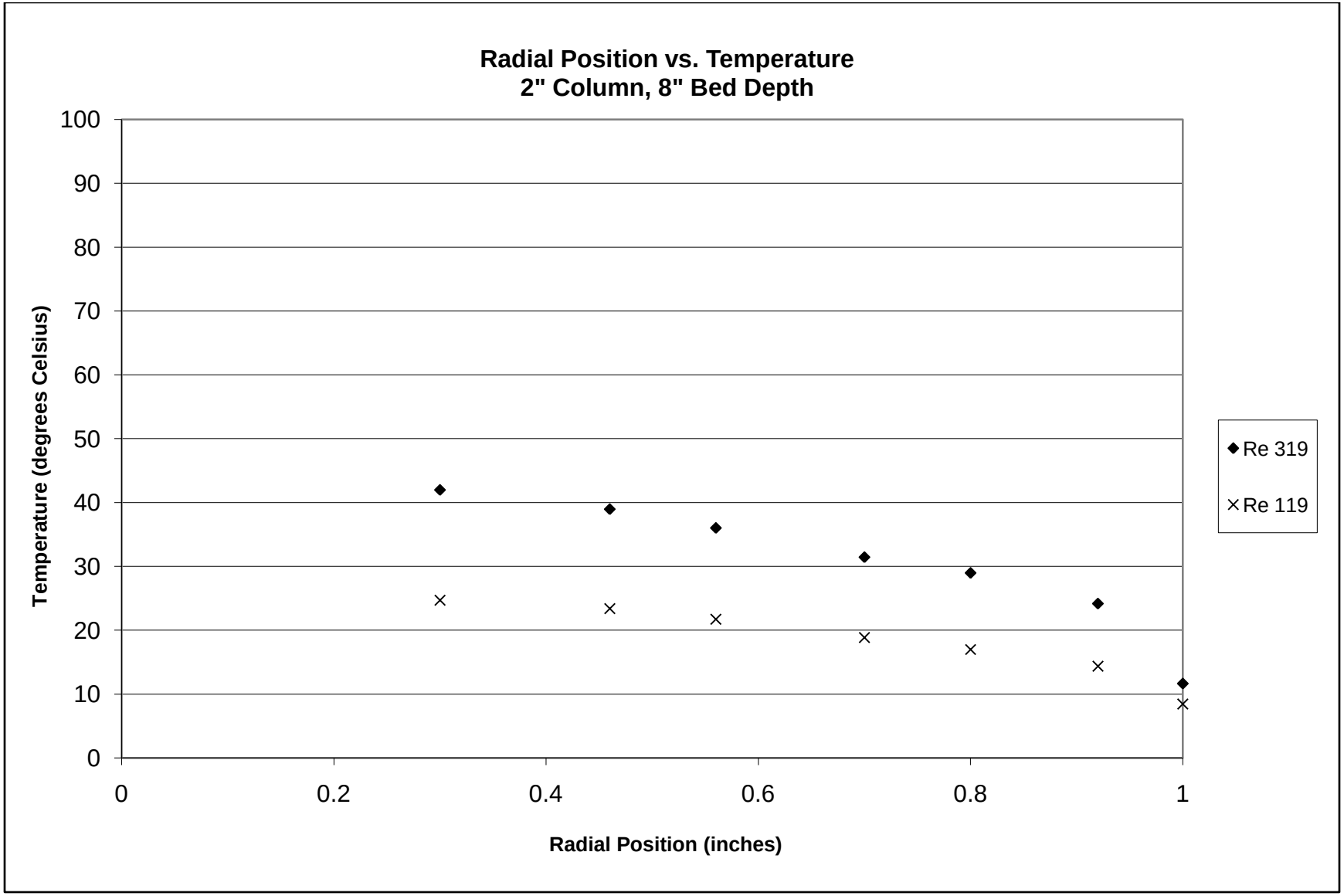
Radial Position vs. Temperature
2" Column, 8" Bed Depth
Temperature (degrees Celsius)
100
90
80
70
60
50
40
30
20
10
0
0
0.2
0.4
0.6
0.8
1
Radial Position (inches)
Re 319
Re 119

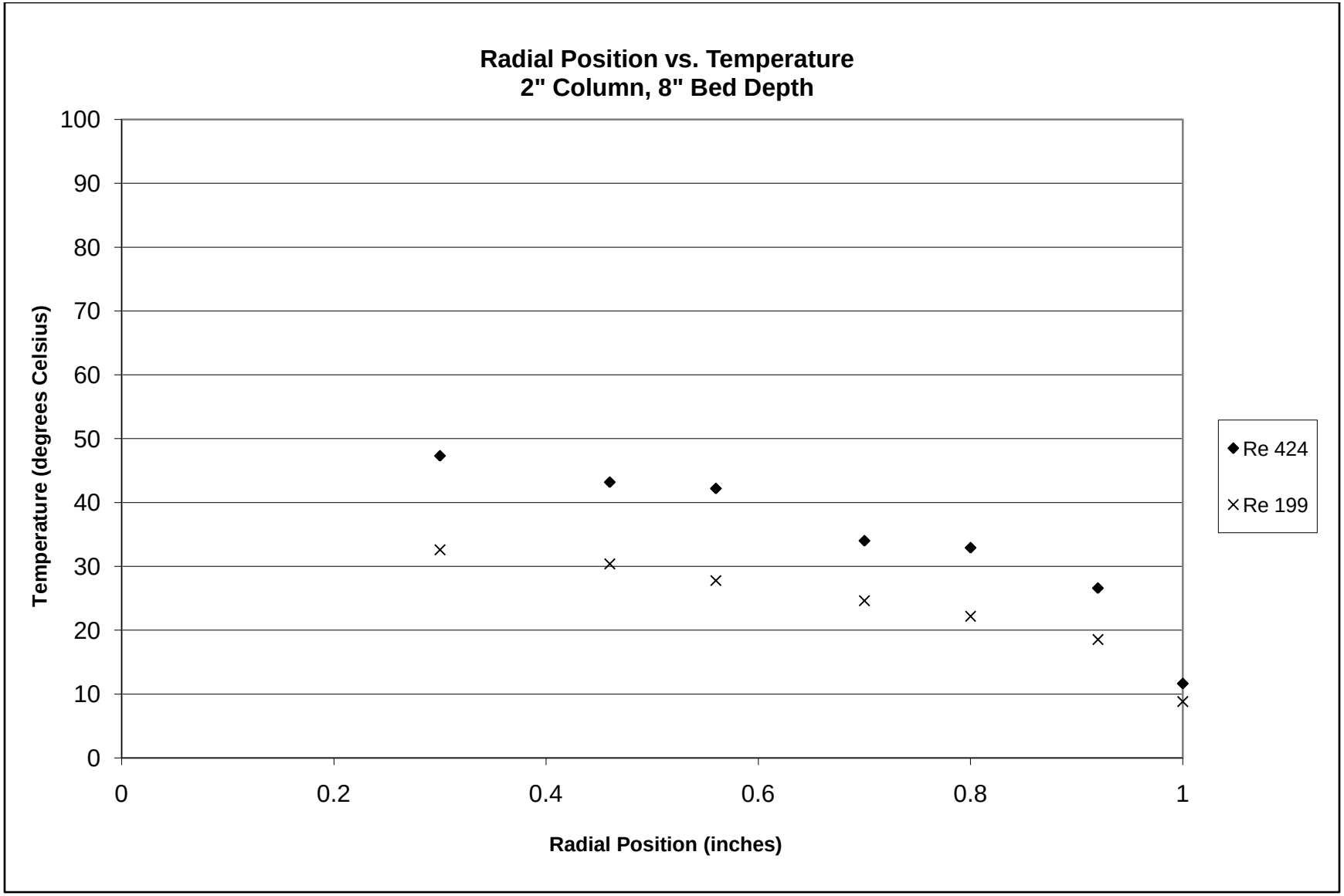
Radial Position vs. Temperature
2" Column, 8" Bed Depth
Temperature (degrees Celsius)
100
90
80
70
60
50
40
30
20
10
0
0
0.2
0.4
0.6
0.8
1
Radial Position (inches)
Re 424
Re 199

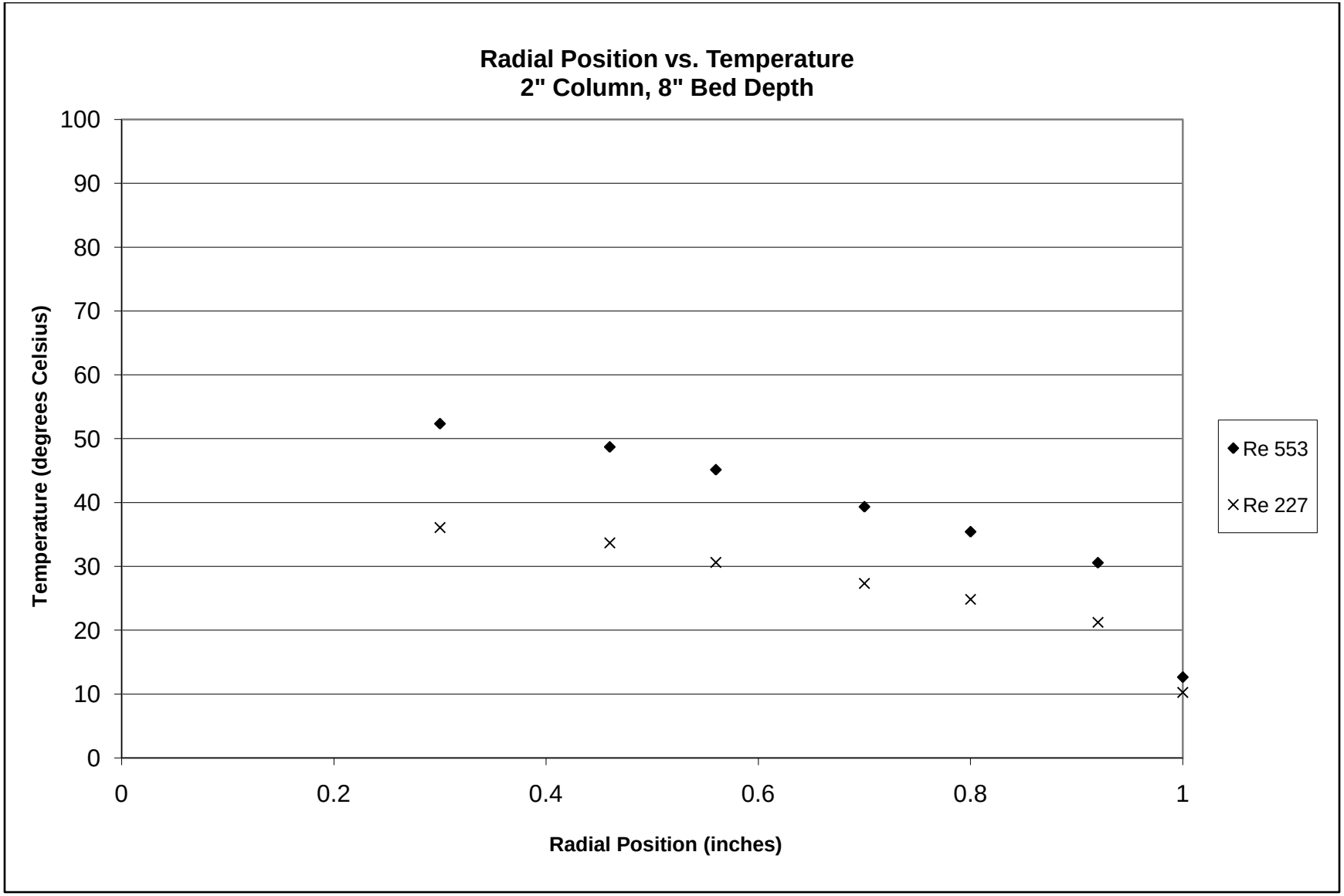
Radial Position vs. Temperature
2" Column, 8" Bed Depth
Temperature (degrees Celsius)
100
90
80
70
60
50
40
30
20
10
0
0
0.2
0.4
0.6
0.8
1
Radial Position (inches)
Re 553
Re 227

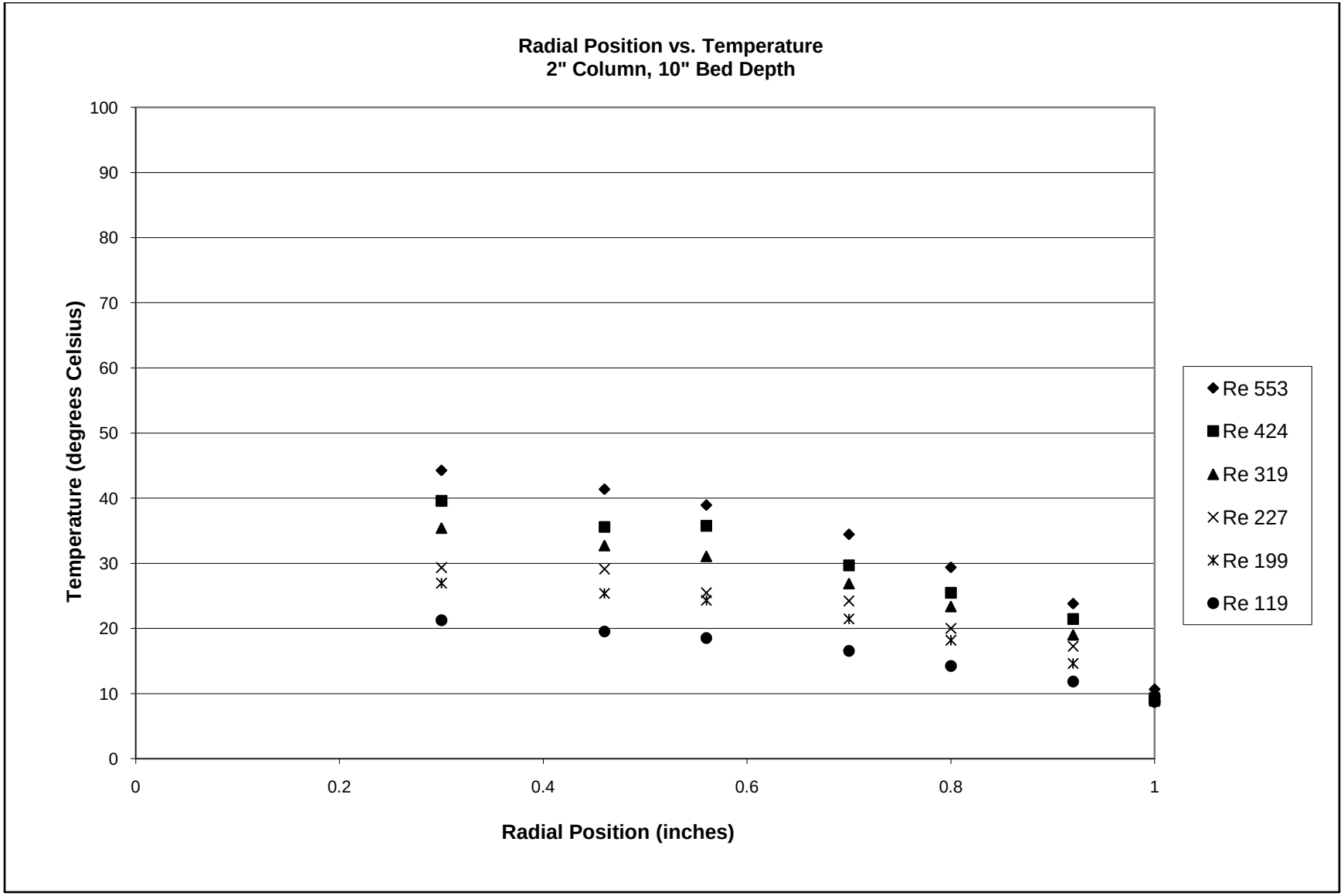
Radial Position vs. Temperature
2" Column, 10" Bed Depth
Temperature (degrees Celsius)
100
90
80
70
60
50
40
30
20
10
0
0
0.2
0.4
0.6
0.8
1
Radial Position (inches)
Re 553
Re 424
Re 319
Re 227
Re 199
Re 119

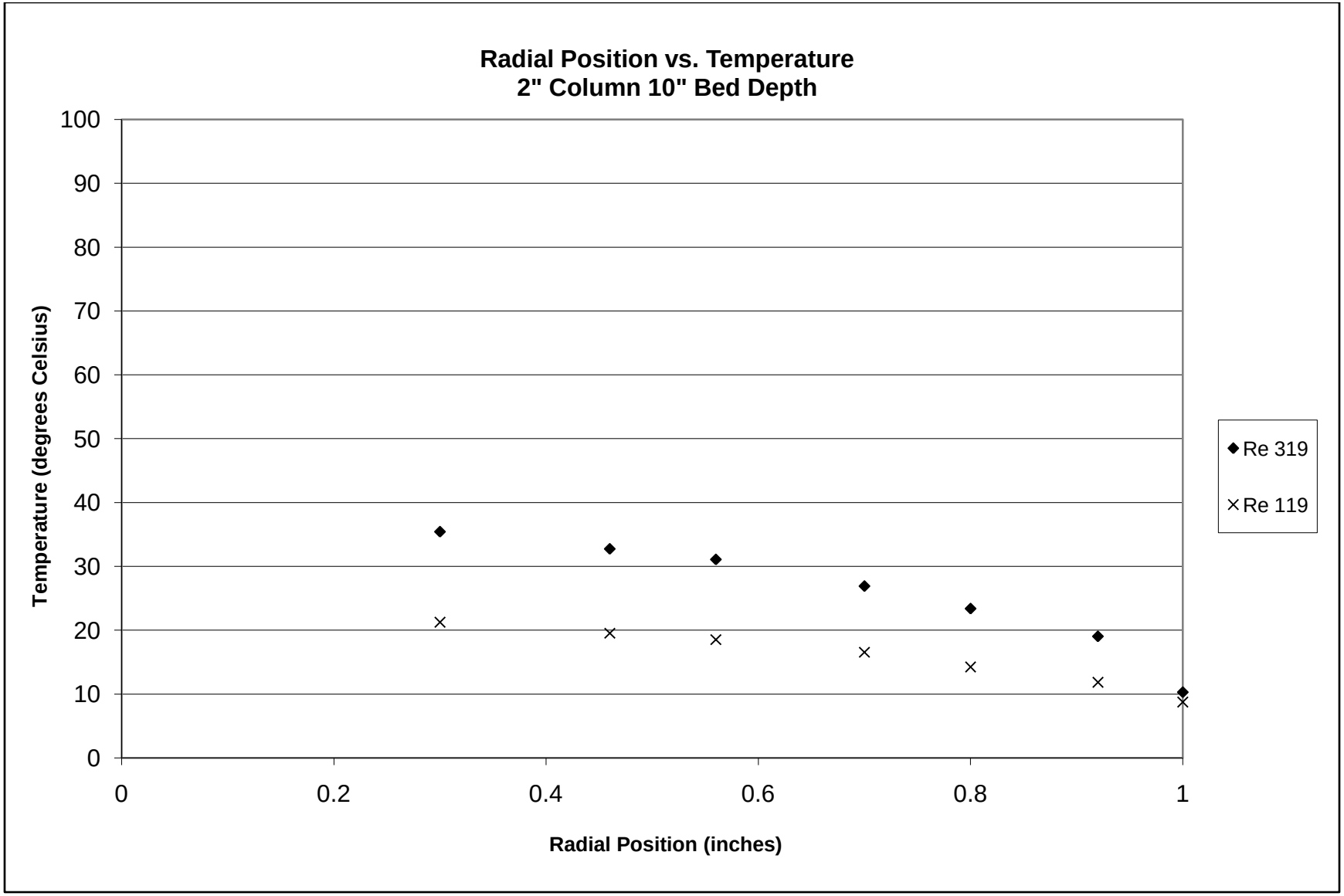
Radial Position vs. Temperature
2" Column 10" Bed Depth
Temperature (degrees Celsius)
100
90
80
70
60
50
40
30
20
10
0
0
0.2
0.4
0.6
0.8
1
Radial Position (inches)
Re 319
Re 119

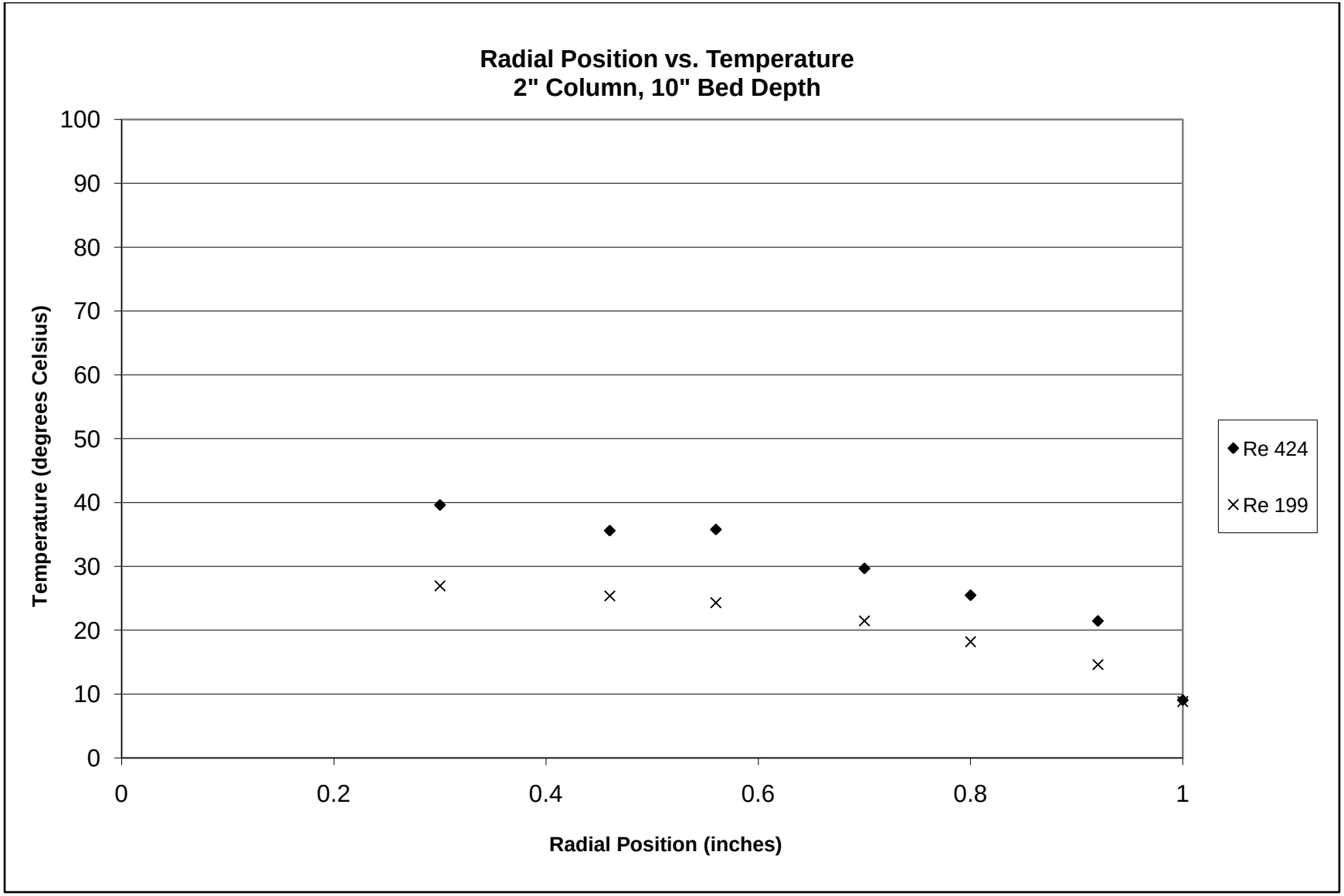
Radial Position vs. Temperature
2" Column, 10" Bed Depth
Temperature (degrees Celsius)
100
90
80
70
60
50
40
30
20
10
0
0
0.2
0.4
0.6
0.8
1
Radial Position (inches)
Re 424
Re 199

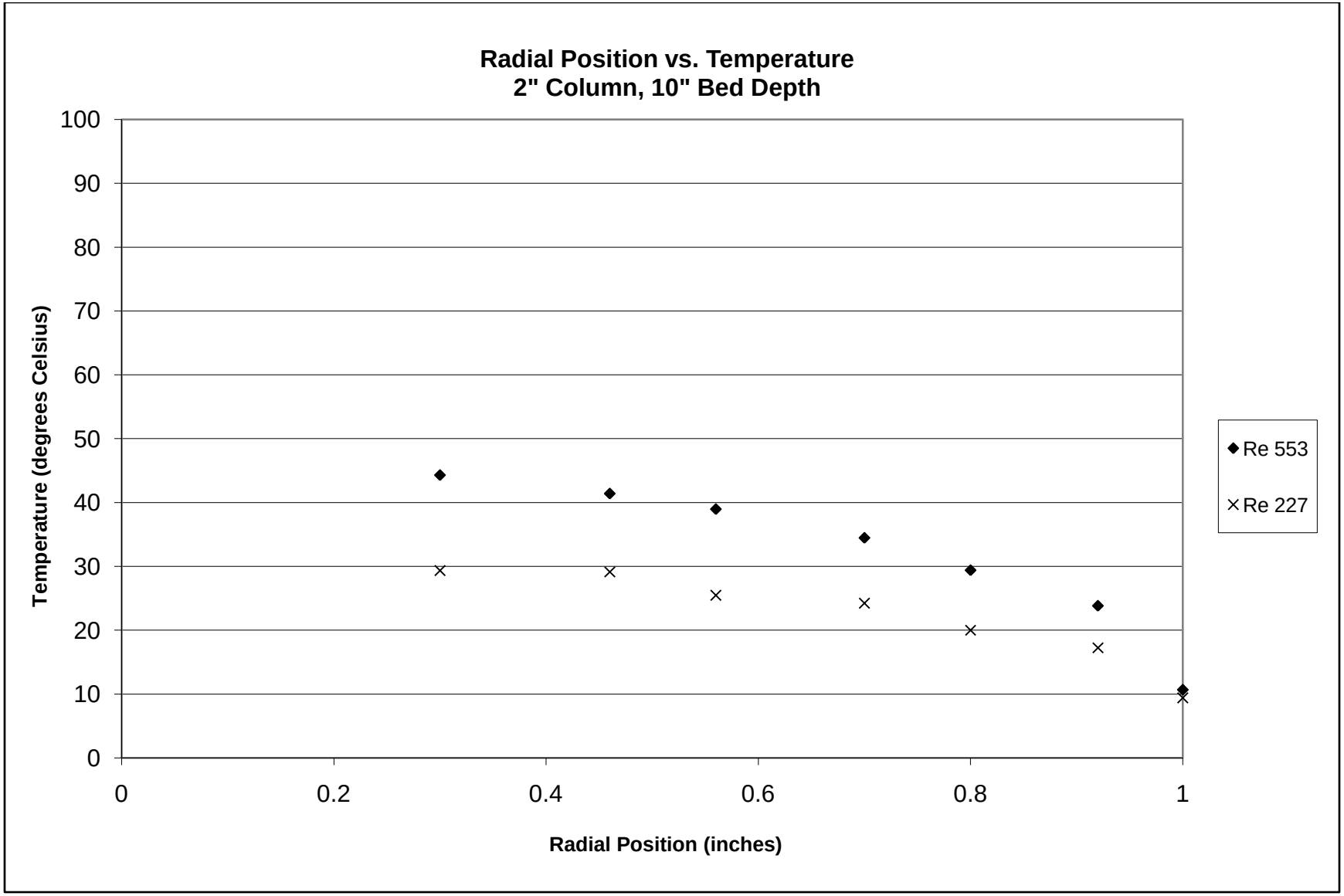
Radial Position vs. Temperature
2" Column, 10" Bed Depth
Temperature (degrees Celsius)
100
90
80
70
60
50
40
30
20
10
0
0
0.2
0.4
0.6
0.8
1
Radial Position (inches)
Re 553
Re 227

E.2: Comparing Bed Heights

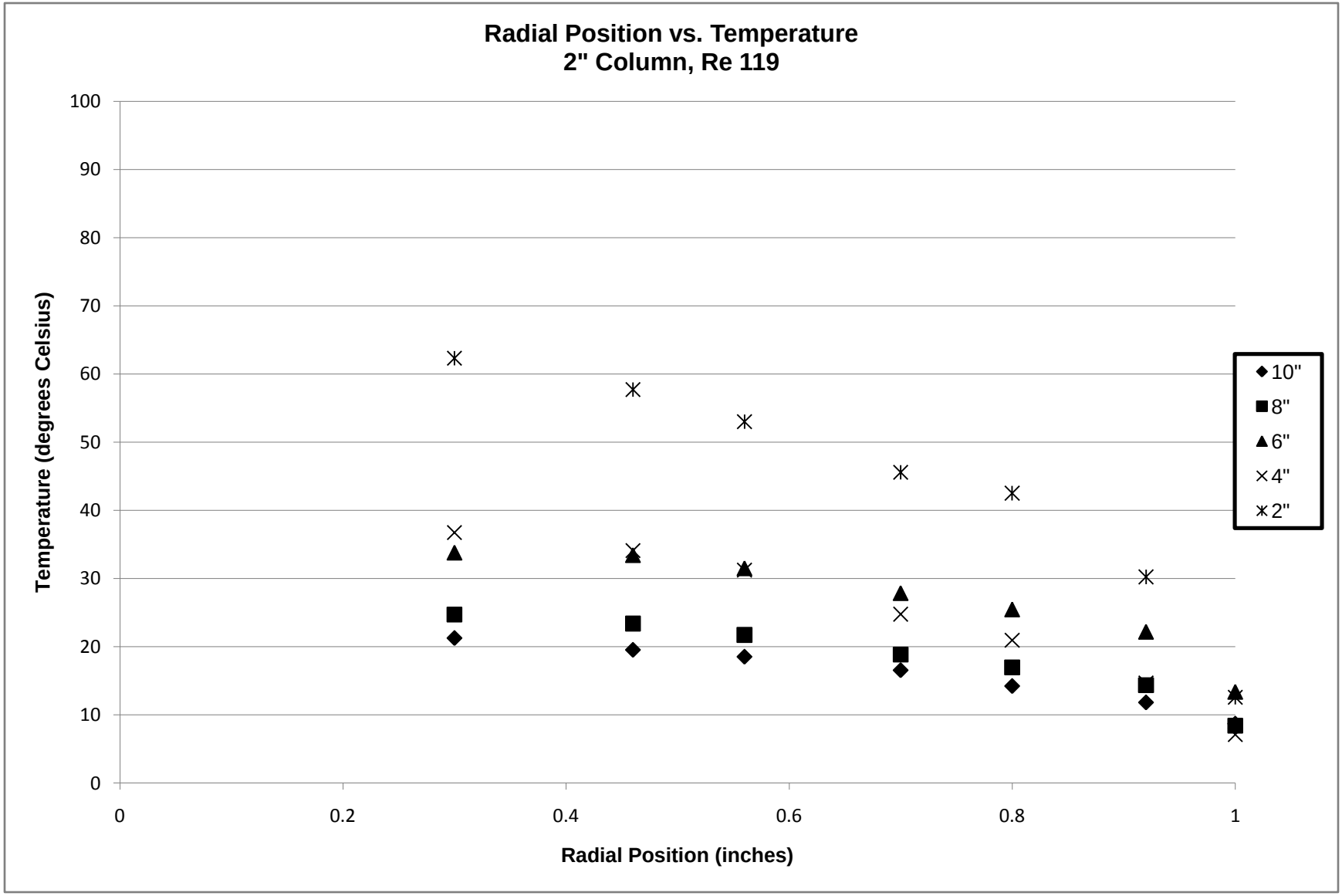
Radial Position vs. Temperature
2" Column, Re 119
Temperature (degrees Celsius)
100
90
80
70
60
50
40
30
20
10
0
0
0.2
0.4
0.6
0.8
1
Radial Position (inches)
10"
8"
6"
4"
2"

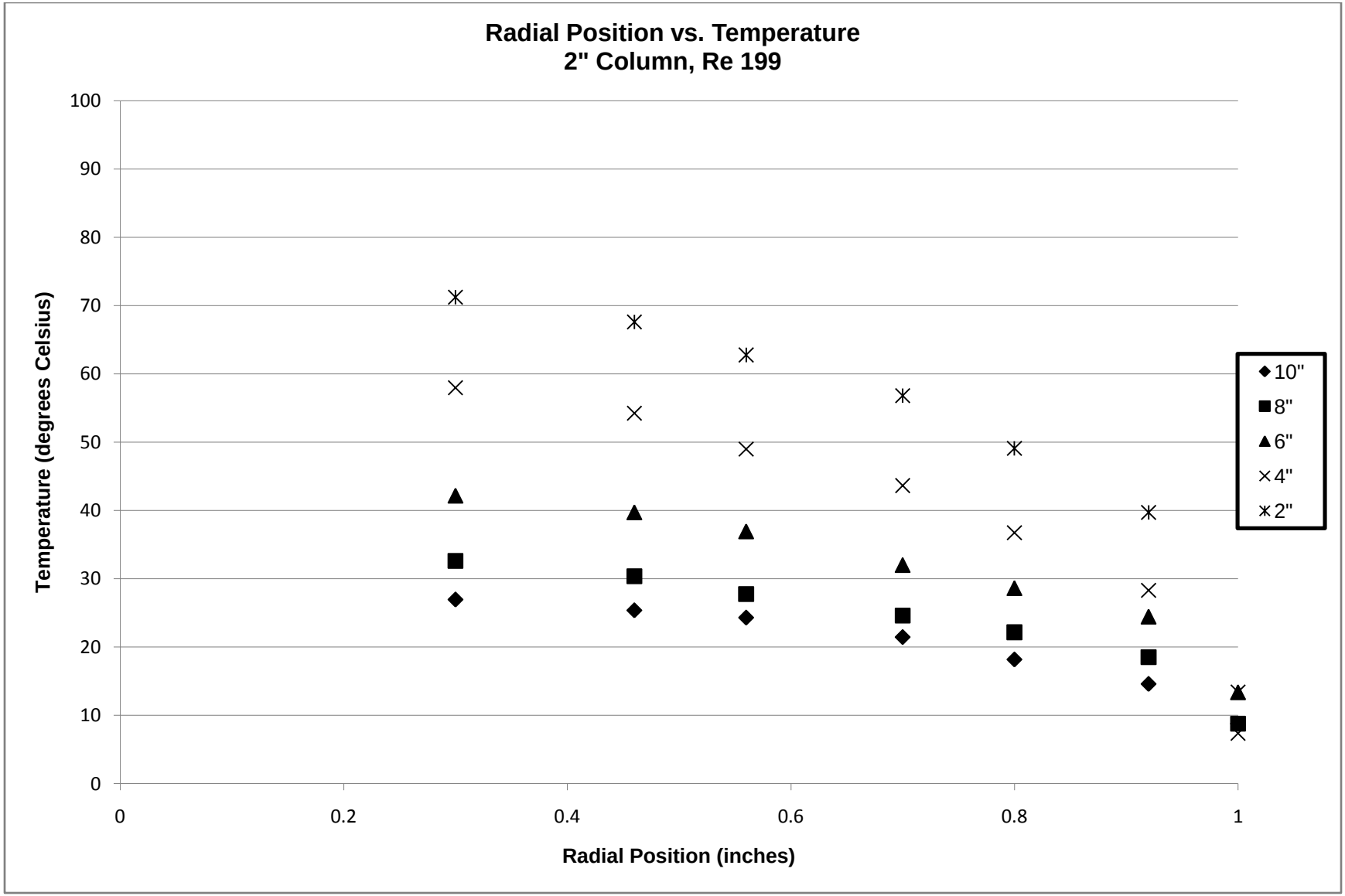
Radial Position vs. Temperature
2" Column, Re 199
Temperature (degrees Celsius)
100
90
80
70
60
50
40
30
20
10
0
0
0.2
0.4
0.6
0.8
1
Radial Position (inches)
10"
8"
6"
4"
2"

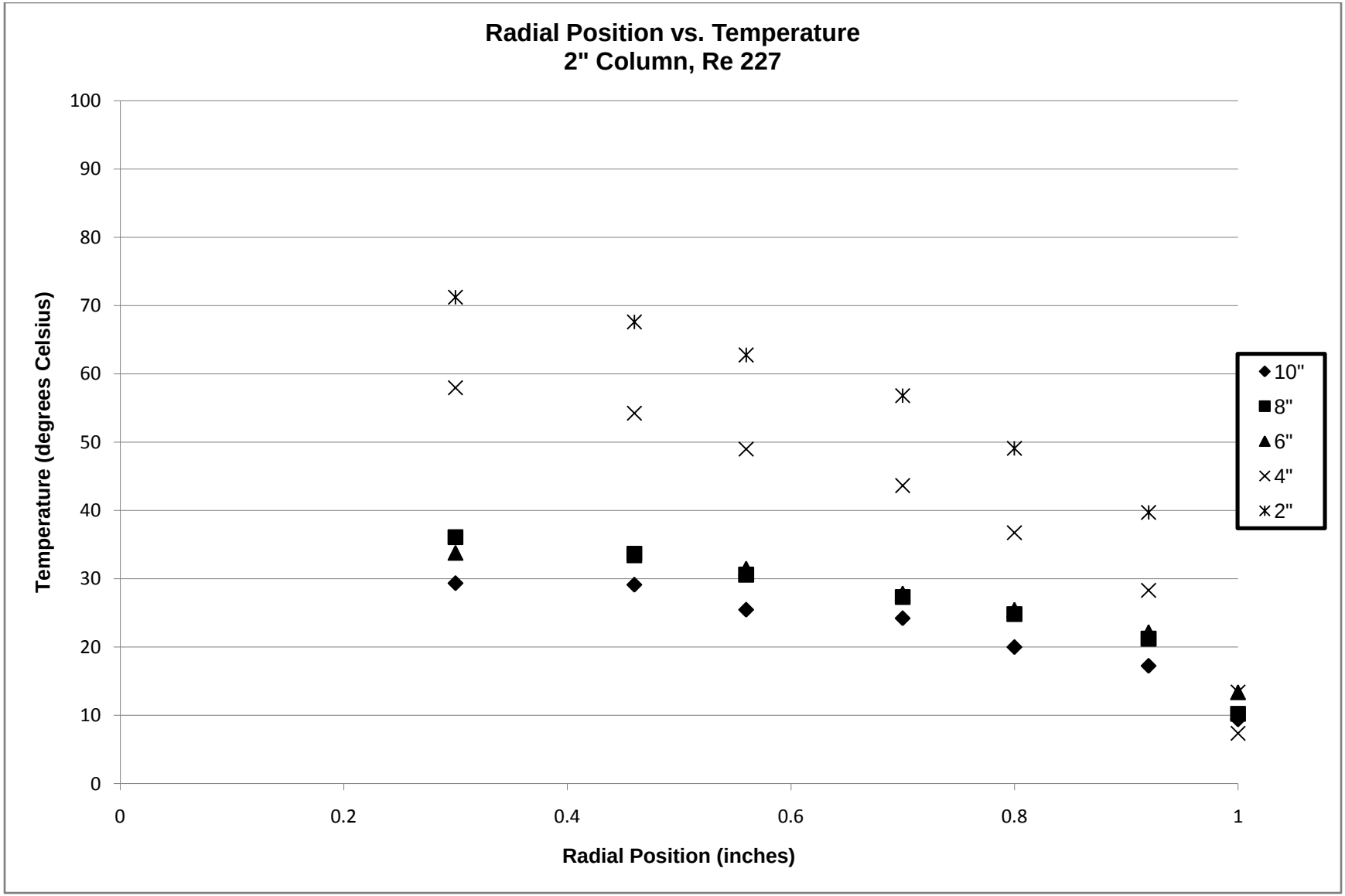
Radial Position vs. Temperature
2" Column, Re 227
Temperature (degrees Celsius)
100
90
80
70
60
50
40
30
20
10
0
0
0.2
0.4
0.6
0.8
1
Radial Position (inches)
10"
8"
6"
4"
2"

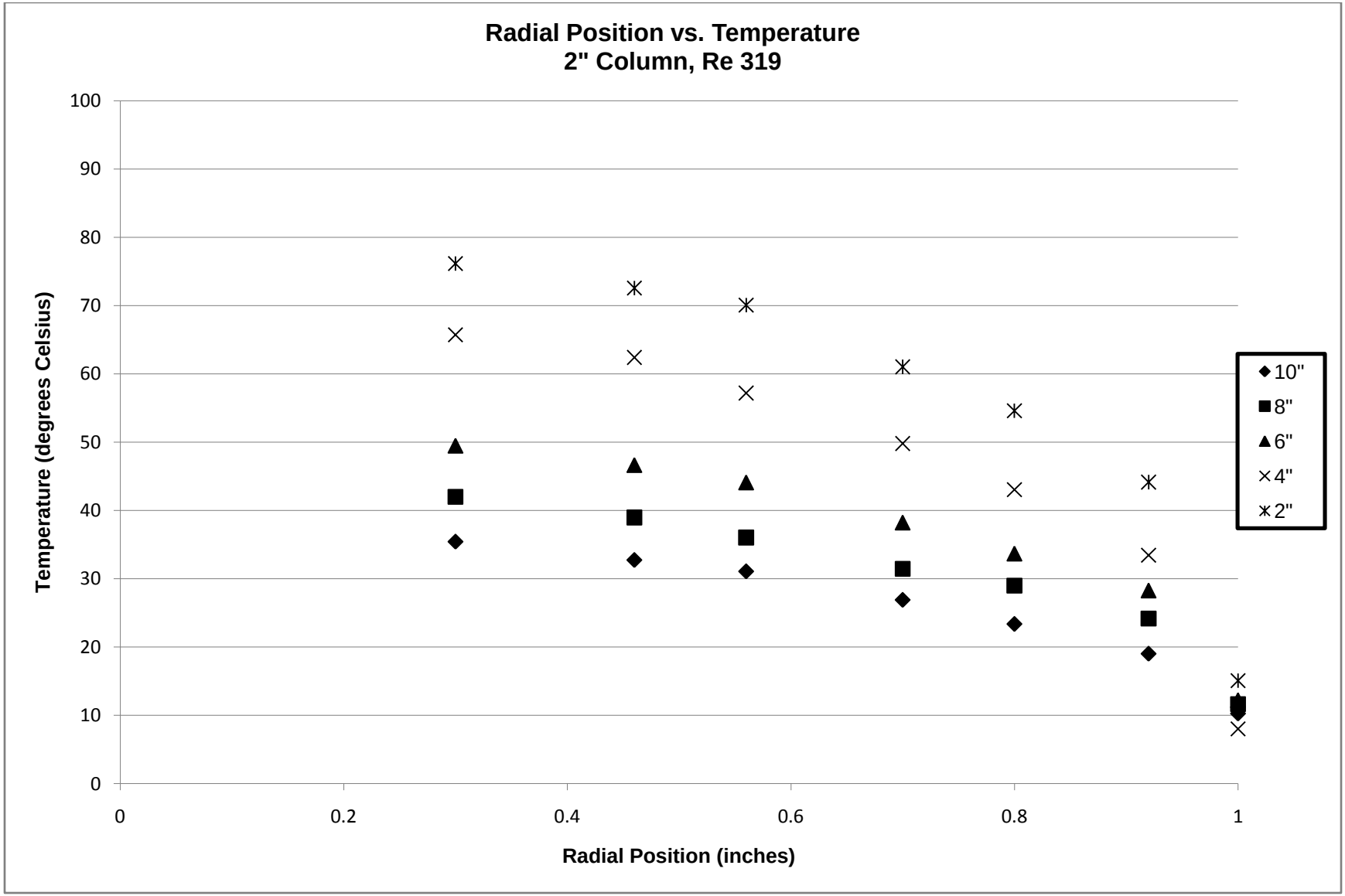
Radial Position vs. Temperature
2" Column, Re 319
Temperature (degrees Celsius)
100
90
80
70
60
50
40
30
20
10
0
0
0.2
0.4
0.6
0.8
1
Radial Position (inches)
10"
8"
6"
4"
2"

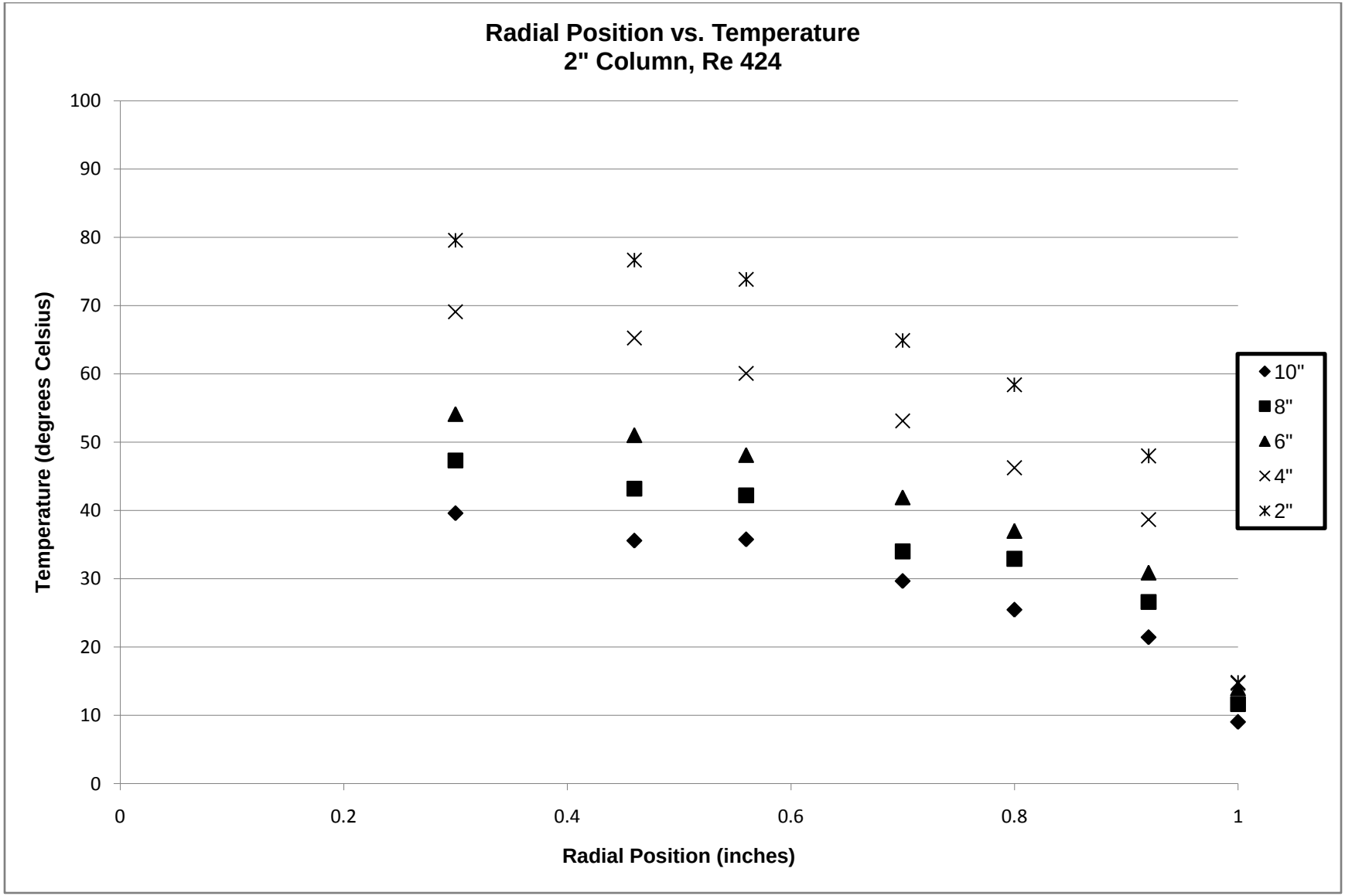
Radial Position vs. Temperature
2" Column, Re 424
Temperature (degrees Celsius)
100
90
80
70
60
50
40
30
20
10
0
0
0.2
0.4
0.6
0.8
1
Radial Position (inches)
10"
8"
6"
4"
2"

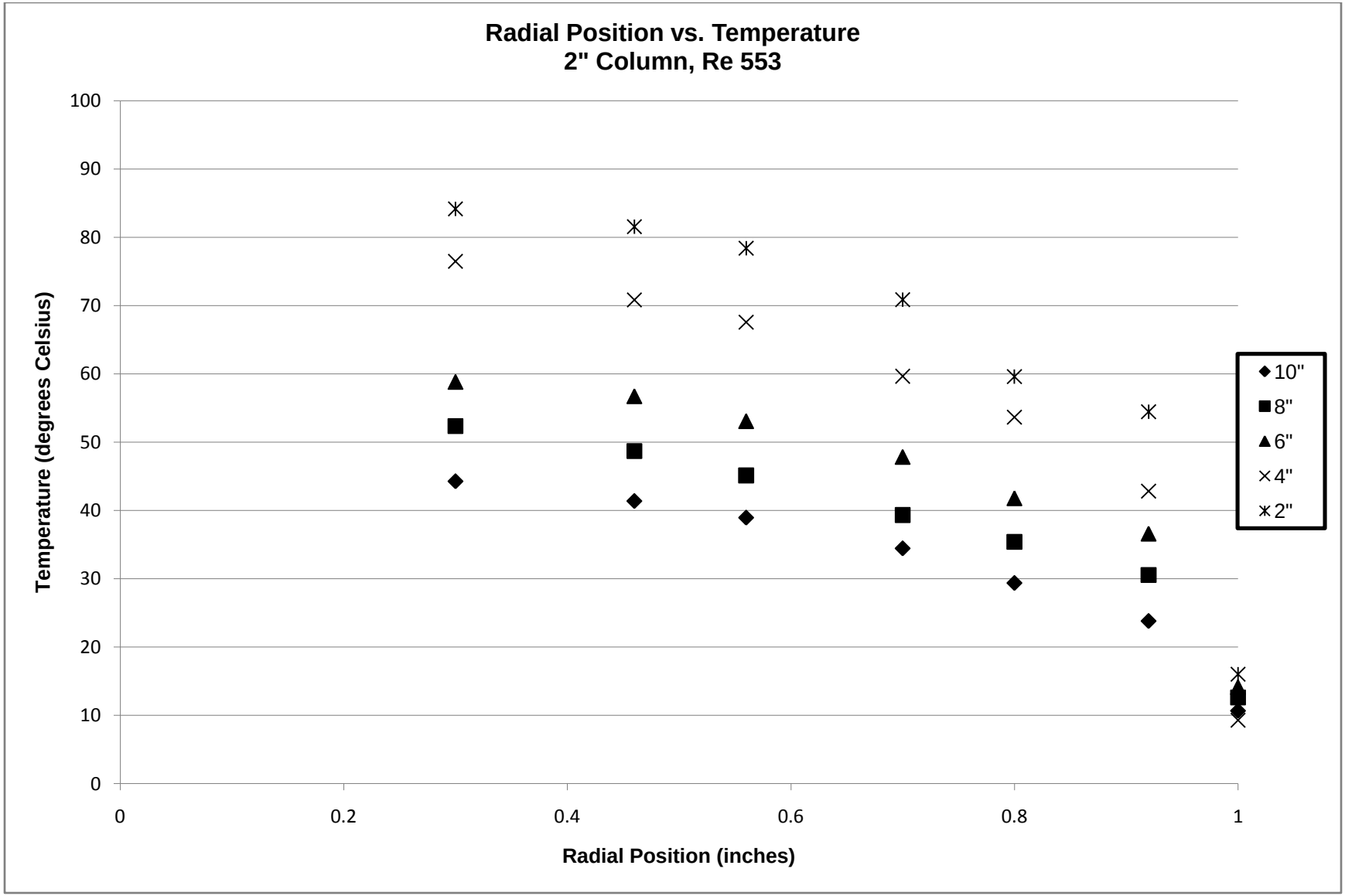
Radial Position vs. Temperature
2" Column, Re 553
Temperature (degrees Celsius)
100
90
80
70
60
50
40
30
20
10
0
0
0.2
0.4
0.6
0.8
1
Radial Position (inches)
10"
8"
6"
4"
2"

Appendix F: 4″ Column Temperature Profiles

F.1: Comparing Reynolds Numbers

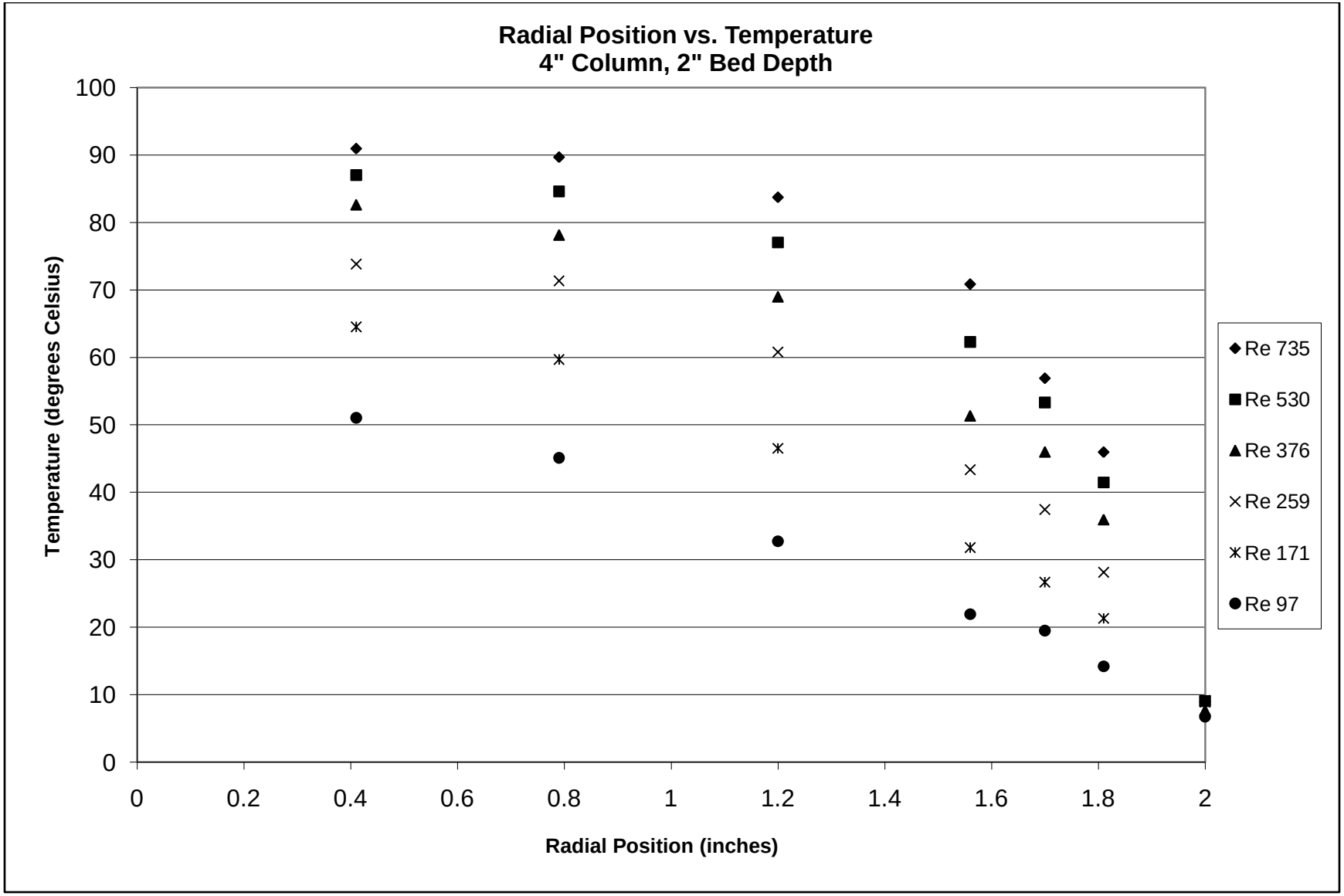
Radial Position vs. Temperature
4" Column, 2" Bed Depth
Temperature (degrees Celsius)
100
90
80
70
60
50
40
30
20
10
0
0
0.2
0.4
0.6
0.8
1
1.2
1.4
1.6
1.8
2
Radial Position (inches)
Re 735
Re 530
Re 376
Re 259
Re 171
Re 97

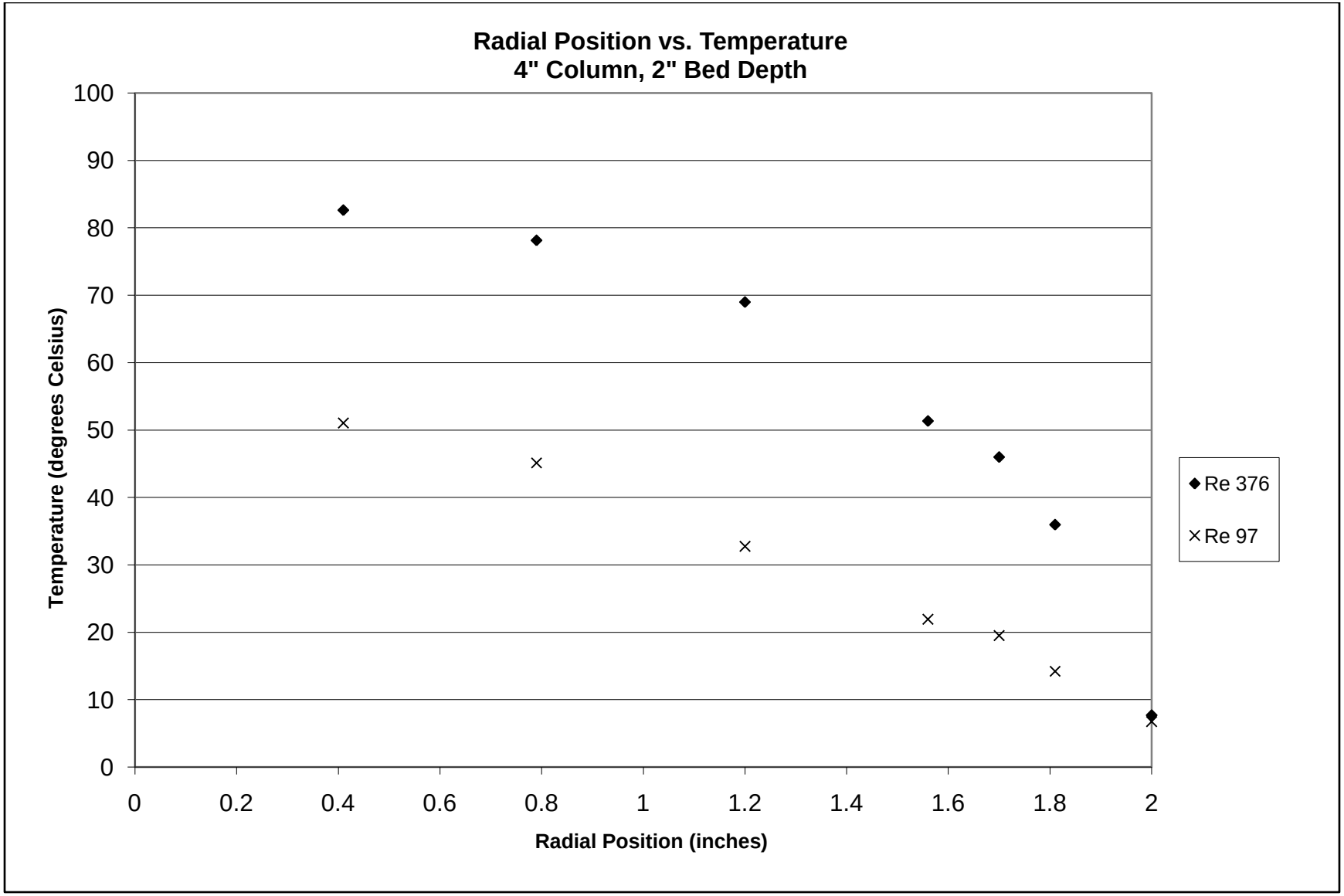
Radial Position vs. Temperature
4" Column, 2" Bed Depth
Temperature (degrees Celsius)
100
90
80
70
60
50
40
30
20
10
0
0
0.2
0.4
0.6
0.8
1
1.2
1.4
1.6
1.8
2
Radial Position (inches)
Re 376
Re 97

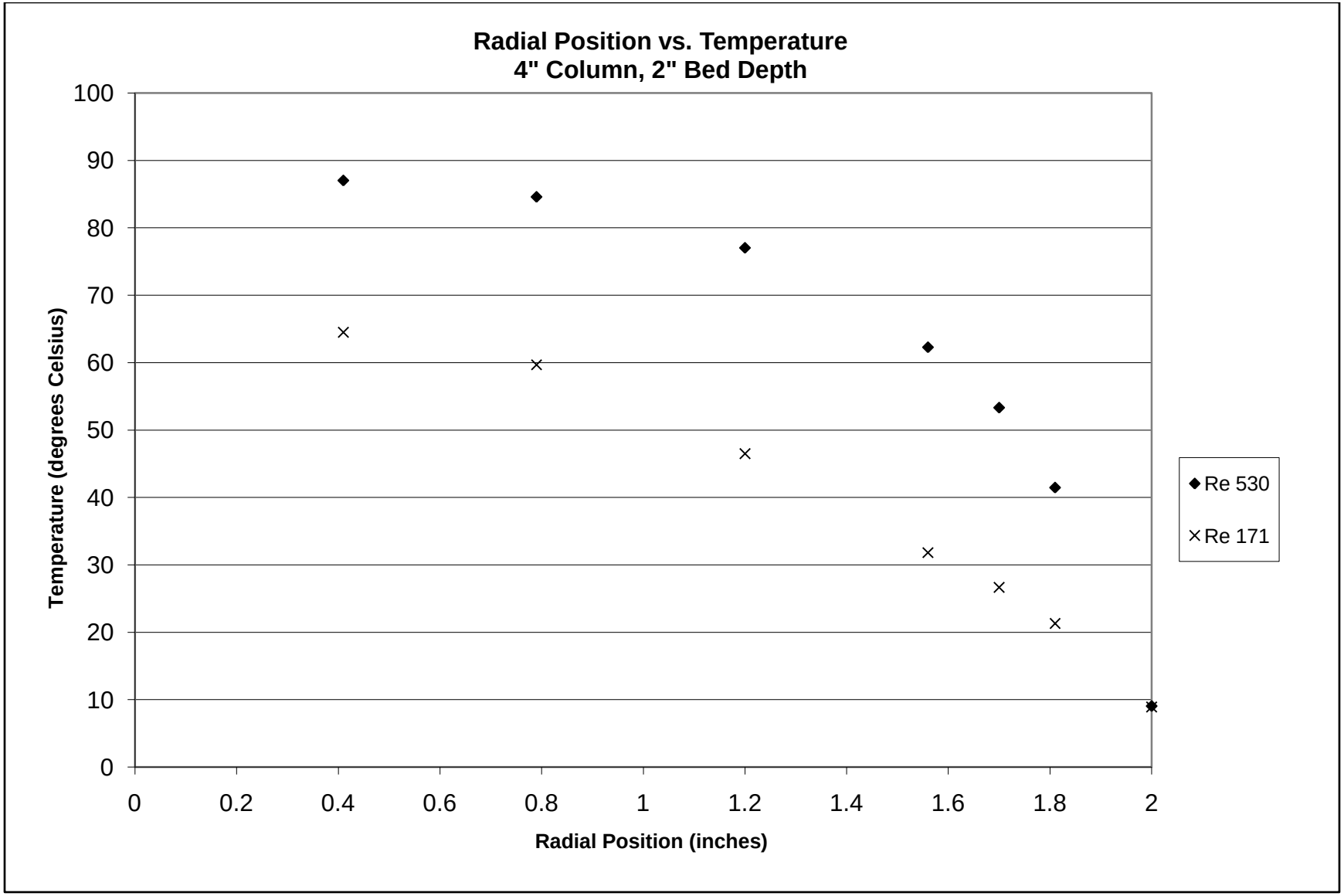
Radial Position vs. Temperature
4" Column, 2" Bed Depth
Temperature (degrees Celsius)
100
90
80
70
60
50
40
30
20
10
0
0
0.2
0.4
0.6
0.8
1
1.2
1.4
1.6
1.8
2
Radial Position (inches)
Re 530
Re 171

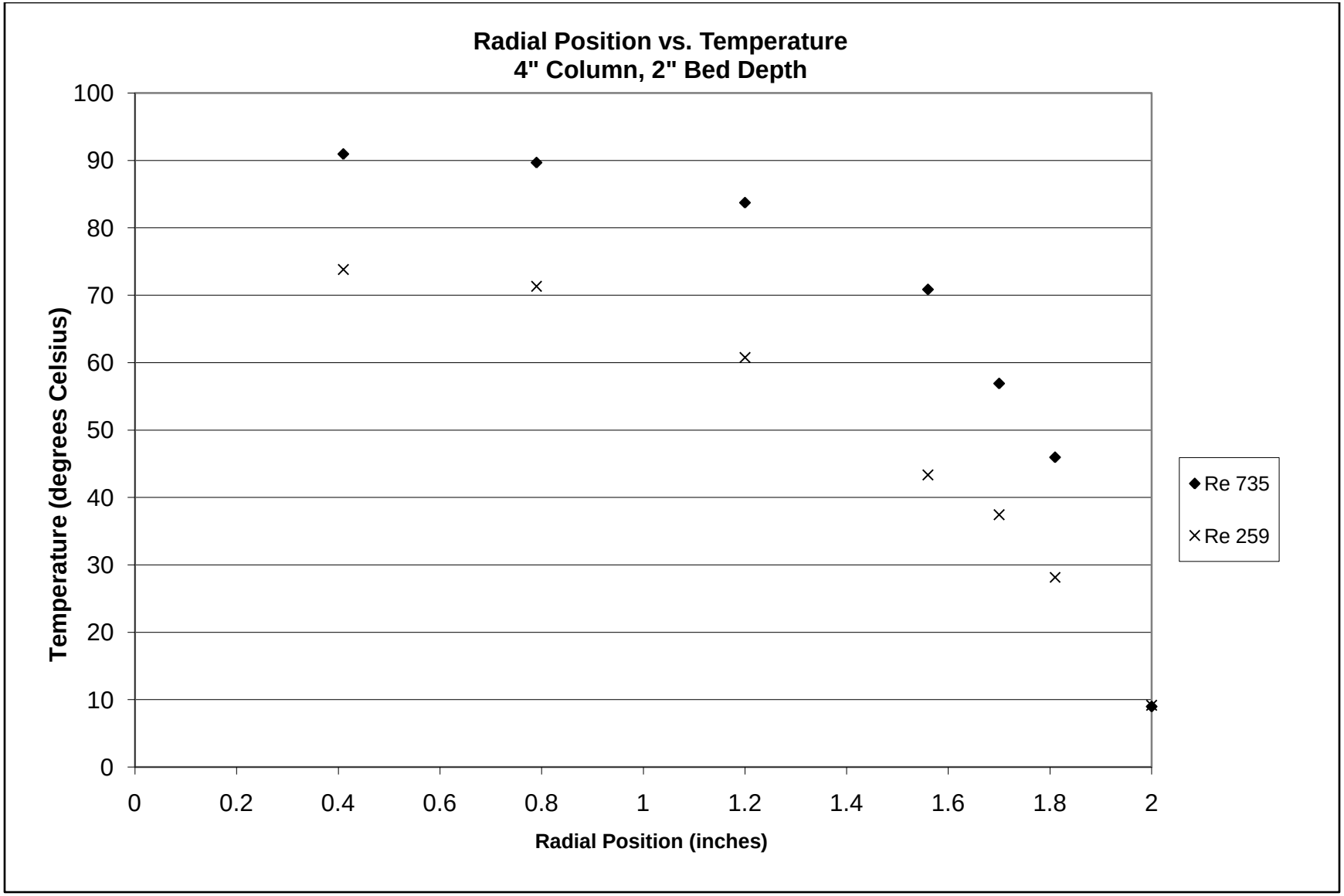
Radial Position vs. Temperature
4" Column, 2" Bed Depth
Temperature (degrees Celsius)
100
90
80
70
60
50
40
30
20
10
0
0
0.2
0.4
0.6
0.8
1
1.2
1.4
1.6
1.8
2
Radial Position (inches)
Re 735
Re 259

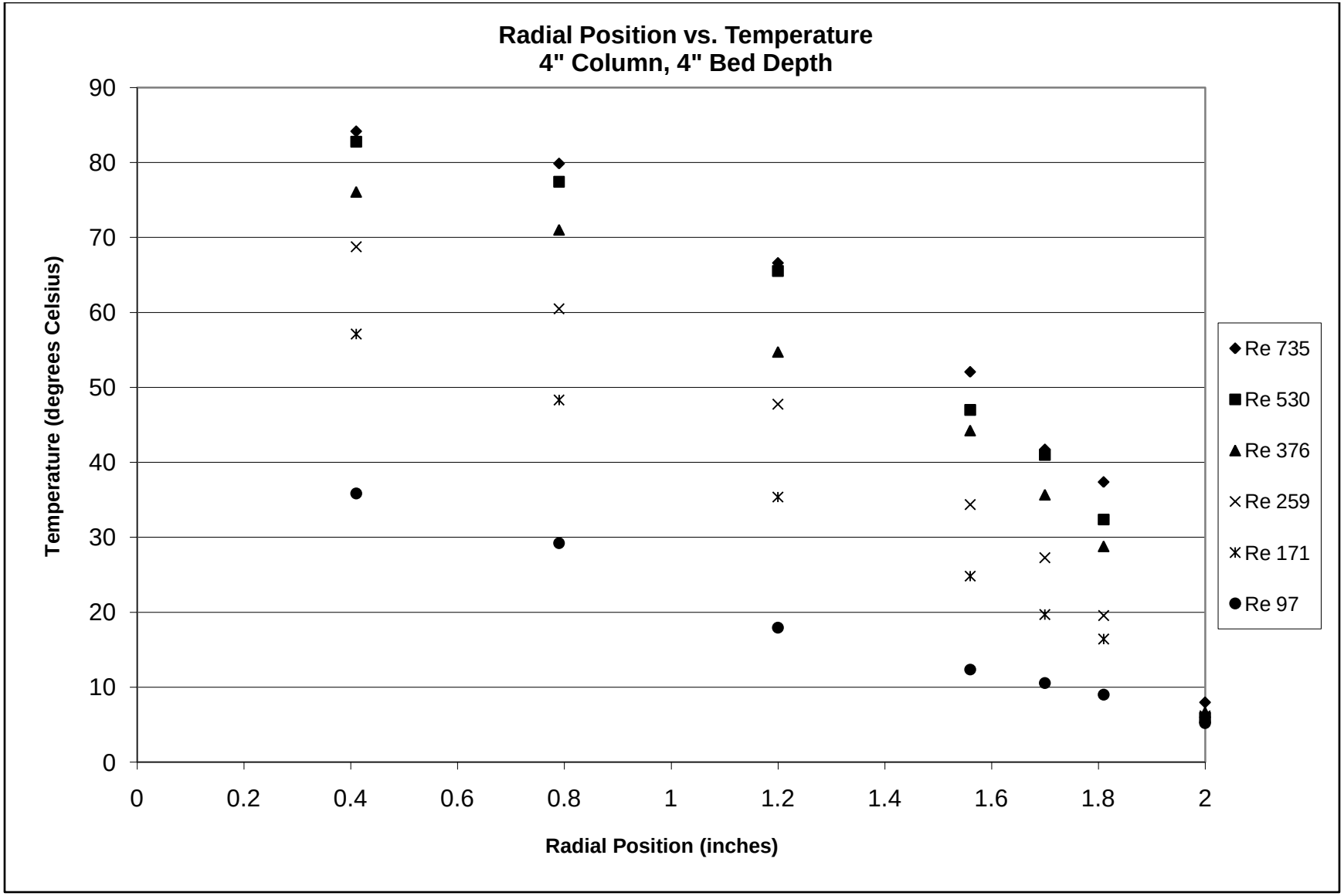
Radial Position vs. Temperature
4" Column, 4" Bed Depth
Temperature (degrees Celsius)
90
80
70
60
50
40
30
20
10
0
0
0.2
0.4
0.6
0.8
1
1.2
1.4
1.6
1.8
2
Radial Position (inches)
Re 735
Re 530
Re 376
Re 259
Re 171
Re 97

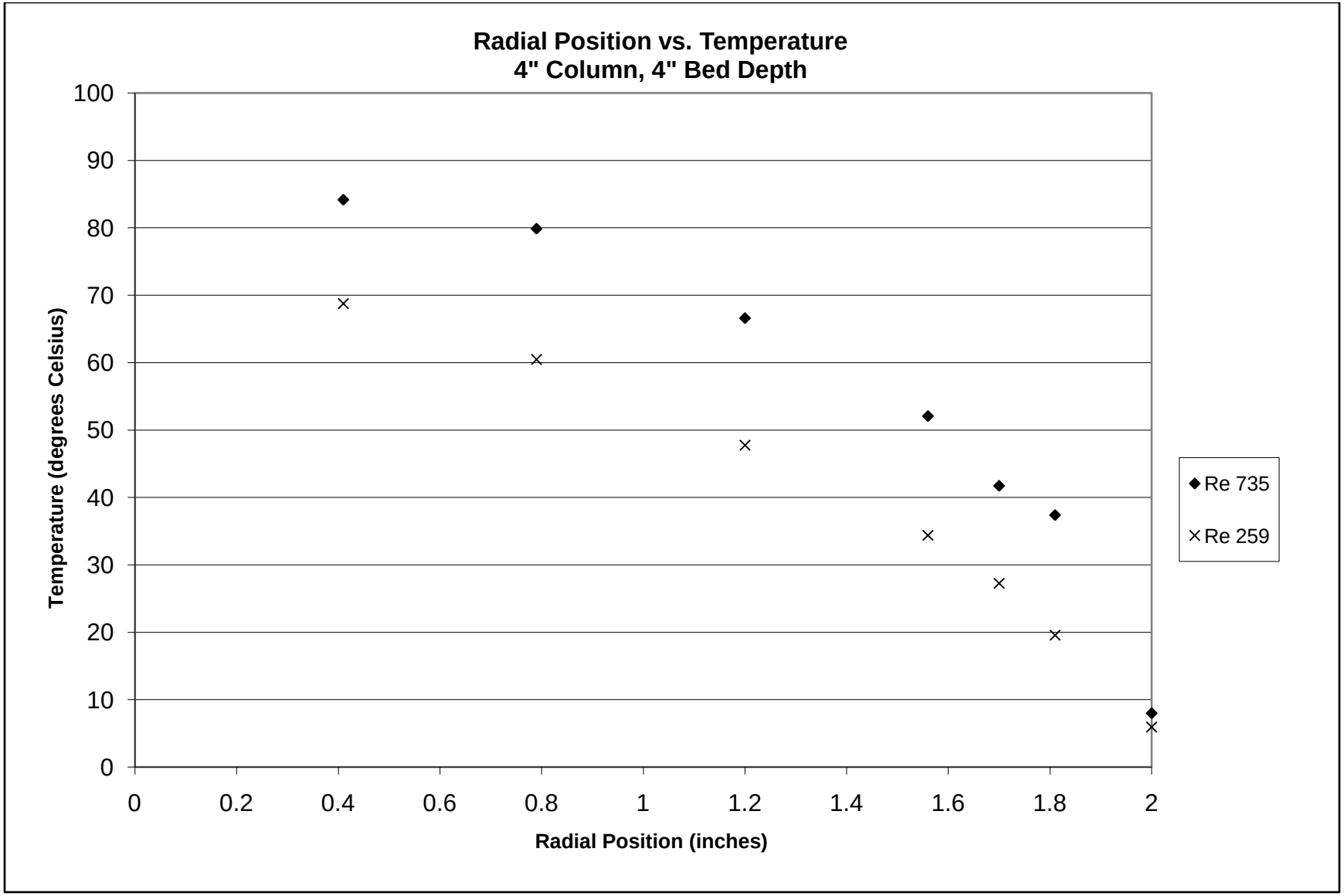
Radial Position vs. Temperature
4" Column, 4" Bed Depth
Temperature (degrees Celsius)
100
90
80
70
60
50
40
30
20
10
0
0
0.2
0.4
0.6
0.8
1
1.2
1.4
1.6
1.8
2
Radial Position (inches)
Re 735
Re 259

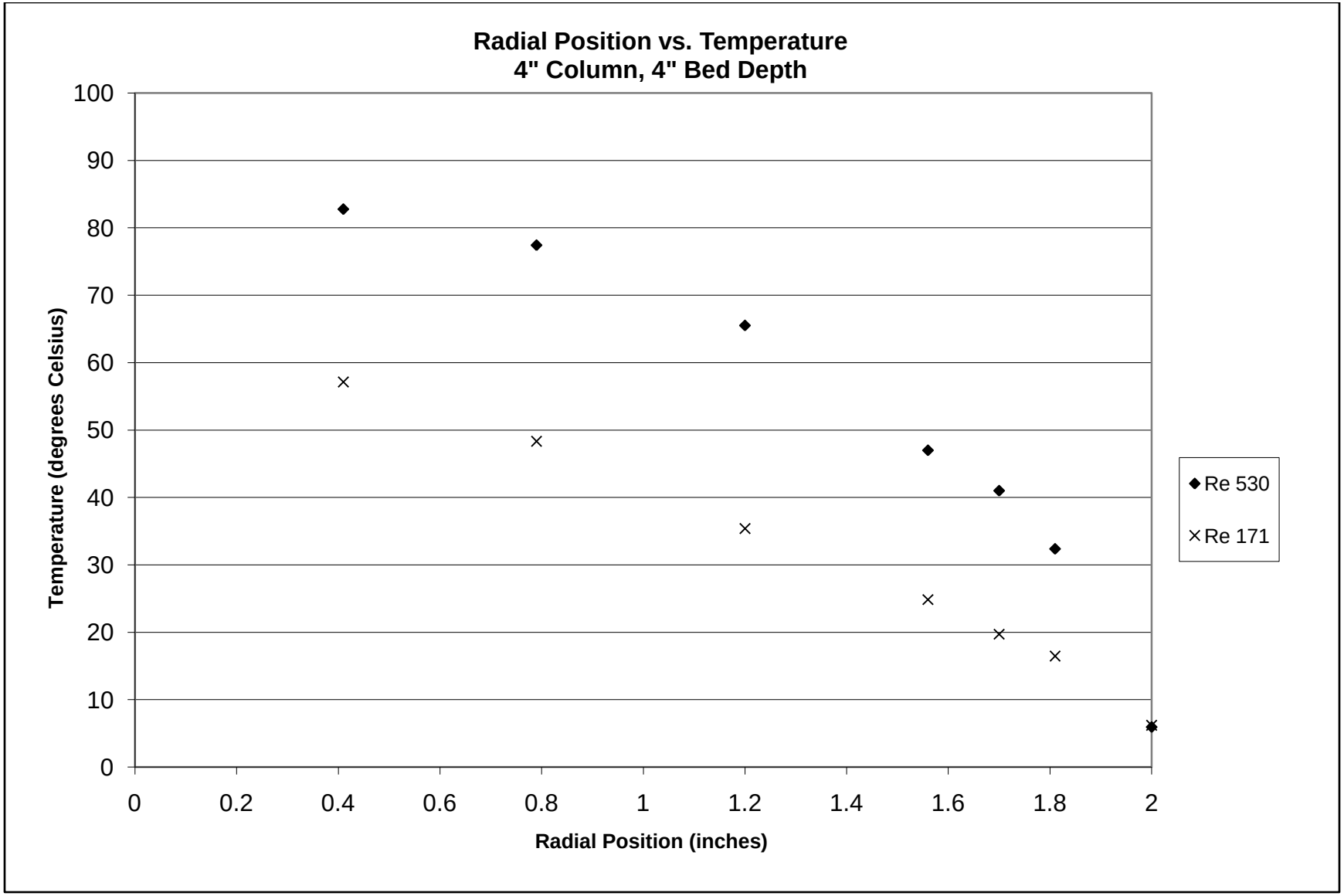
Radial Position vs. Temperature
4" Column, 4" Bed Depth
Temperature (degrees Celsius)
100
90
80
70
60
50
40
30
20
10
0
0
0.2
0.4
0.6
0.8
1
1.2
1.4
1.6
1.8
2
Radial Position (inches)
Re 530
Re 171

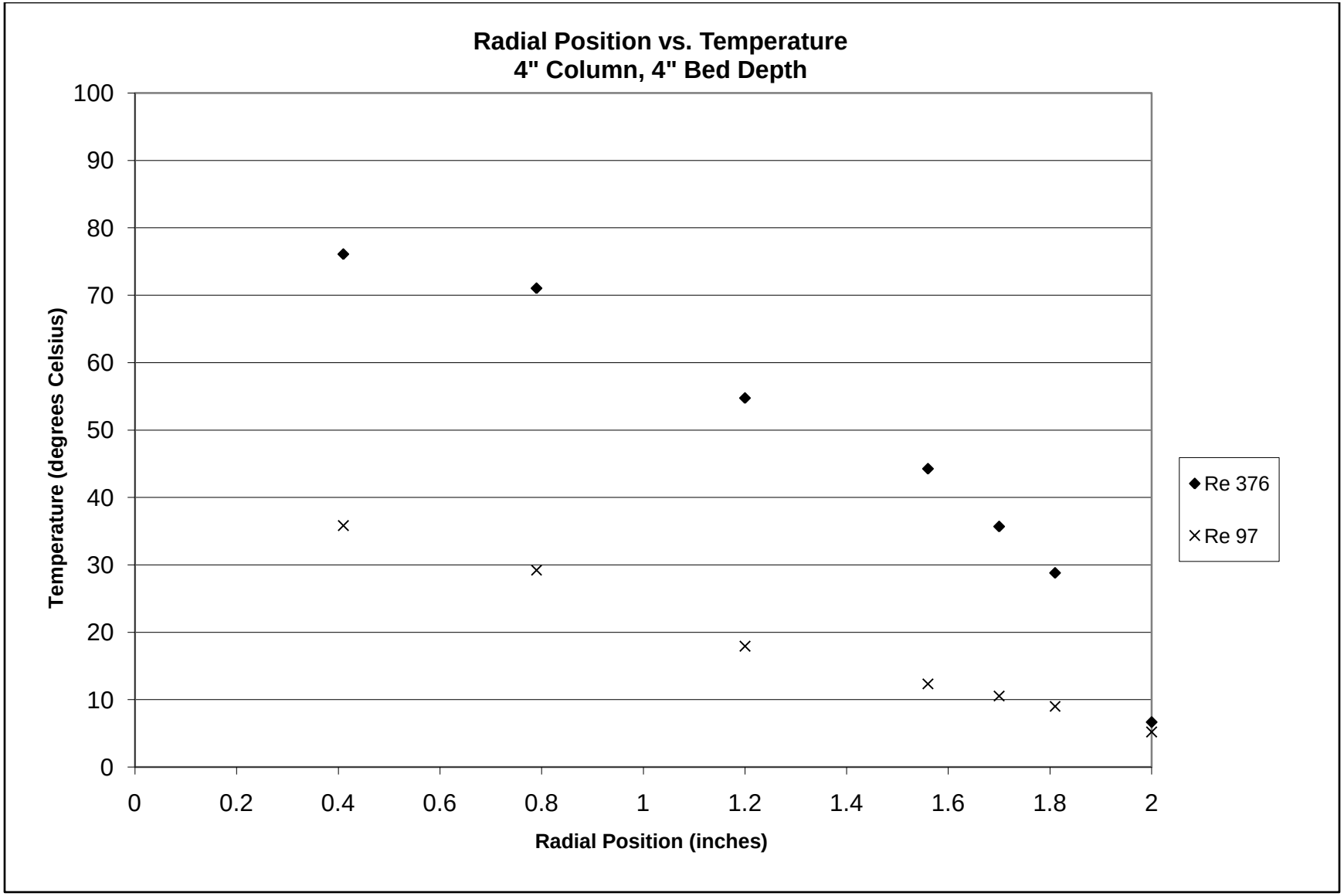
Radial Position vs. Temperature
4" Column, 4" Bed Depth
Temperature (degrees Celsius)
100
90
80
70
60
50
40
30
20
10
0
0
0.2
0.4
0.6
0.8
1
1.2
1.4
1.6
1.8
2
Radial Position (inches)
Re 376
Re 97

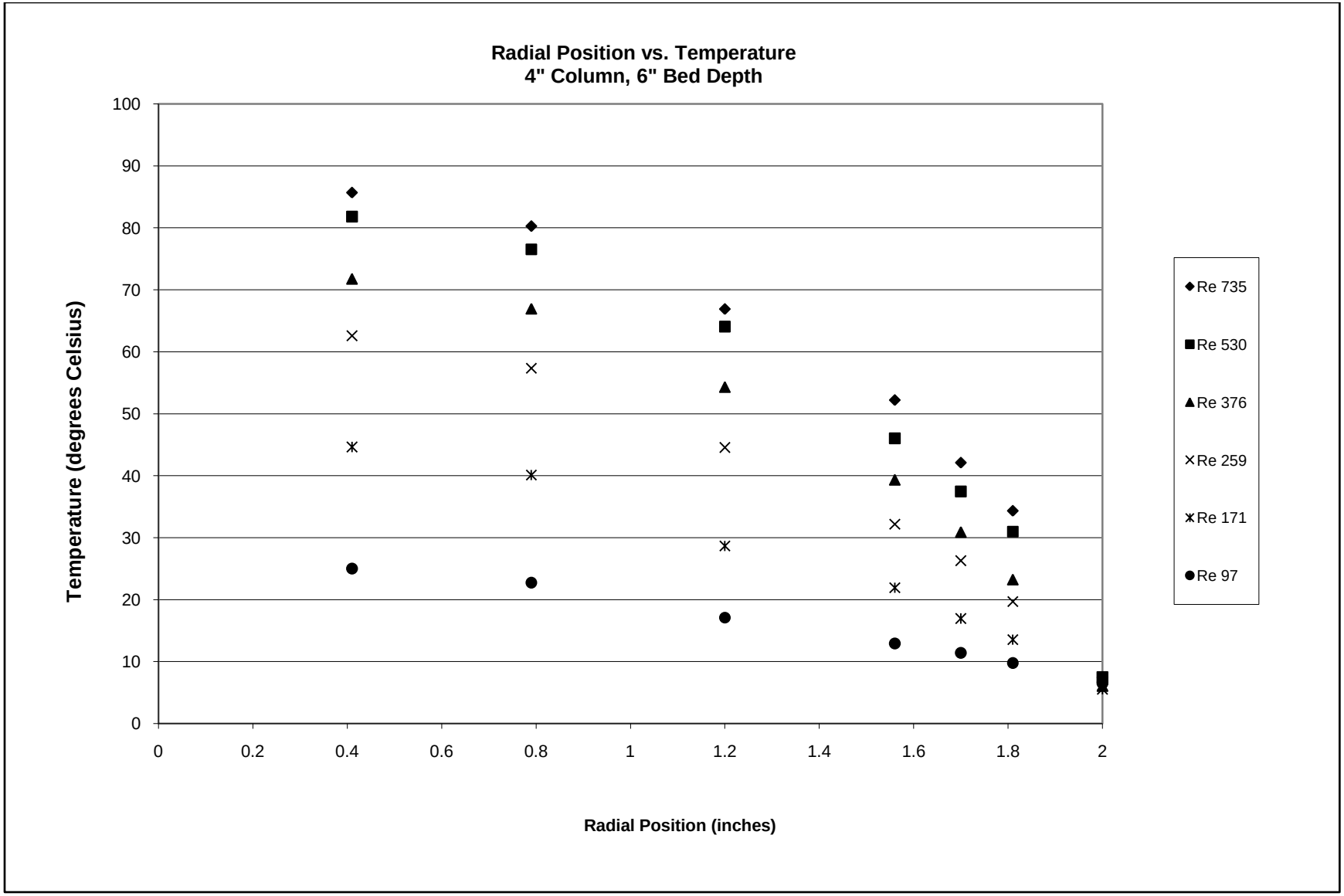
Radial Position vs. Temperature
4" Column, 6" Bed Depth
Temperature (degrees Celsius)
100
90
80
70
60
50
40
30
20
10
0
0
0.2
0.4
0.6
0.8
1
1.2
1.4
1.6
1.8
2
Radial Position (inches)
Re 735
Re 530
Re 376
Re 259
Re 171
Re 97

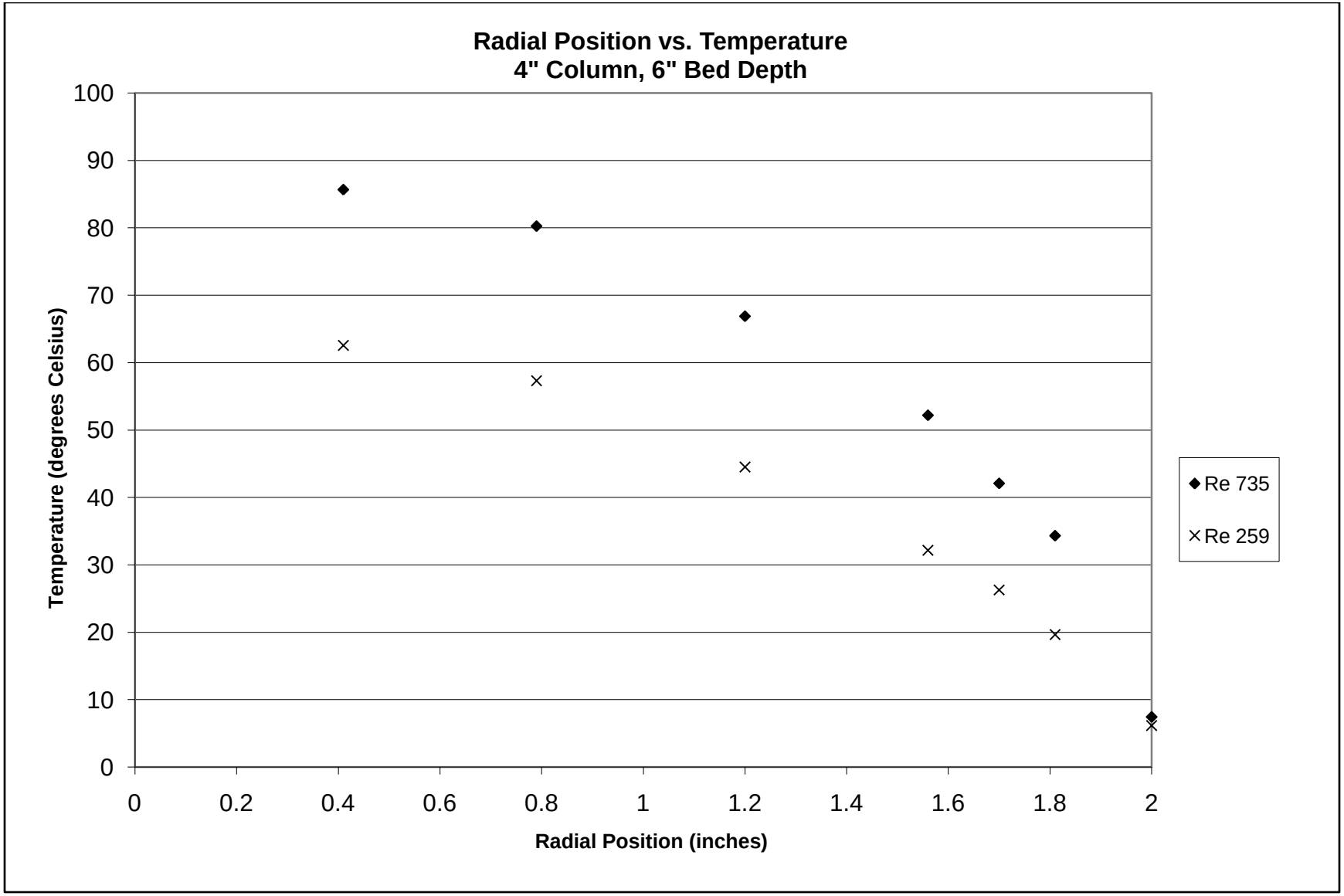
Radial Position vs. Temperature
4" Column, 6" Bed Depth
Temperature (degrees Celsius)
100
90
80
70
60
50
40
30
20
10
0
0
0.2
0.4
0.6
0.8
1
1.2
1.4
1.6
1.8
2
Radial Position (inches)
Re 735
Re 259

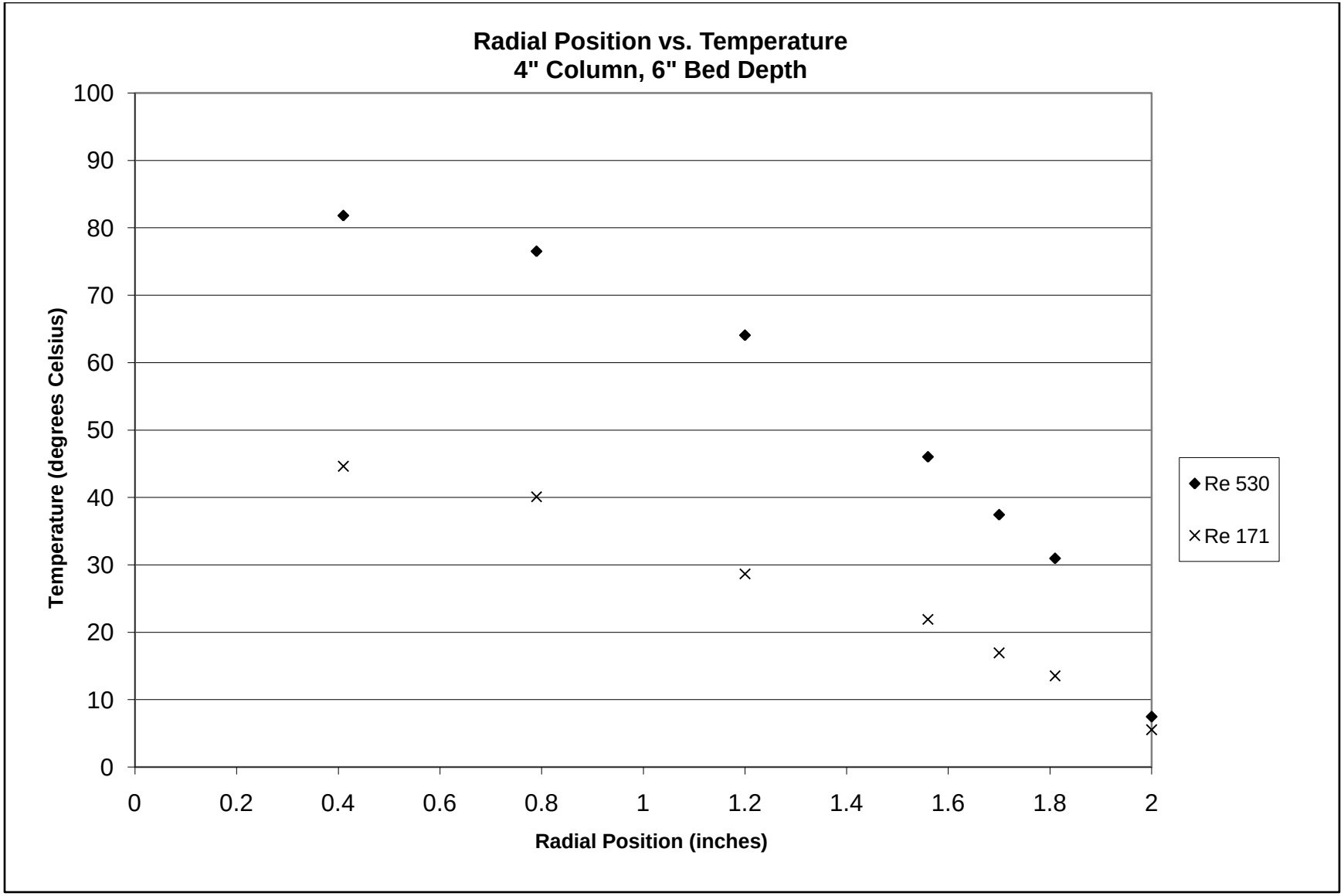
Radial Position vs. Temperature
4" Column, 6" Bed Depth
Temperature (degrees Celsius)
100
90
80
70
60
50
40
30
20
10
0
0
0.2
0.4
0.6
0.8
1
1.2
1.4
1.6
1.8
2
Radial Position (inches)
Re 530
Re 171

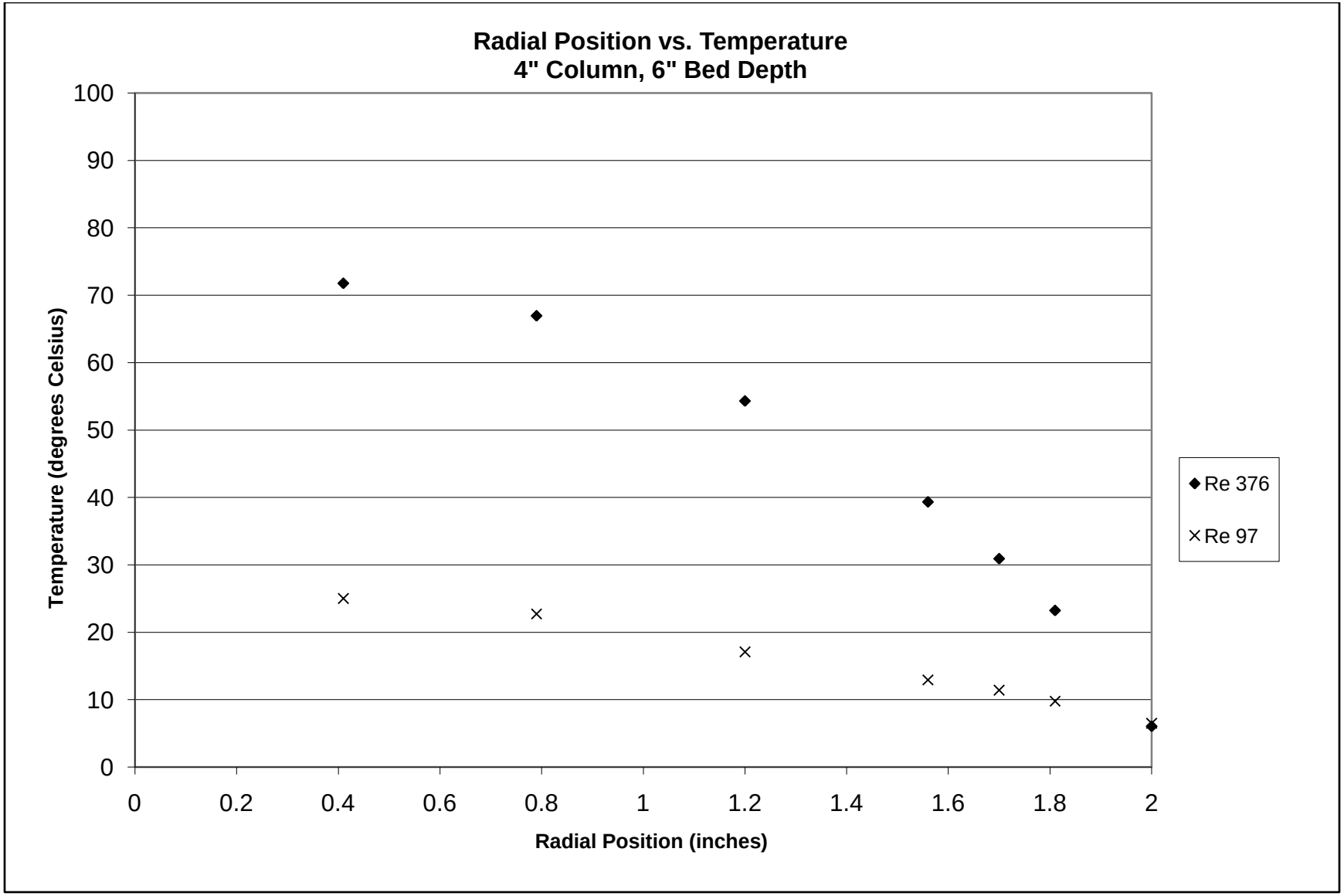
Radial Position vs. Temperature
4" Column, 6" Bed Depth
Temperature (degrees Celsius)
100
90
80
70
60
50
40
30
20
10
0
0
0.2
0.4
0.6
0.8
1
1.2
1.4
1.6
1.8
2
Radial Position (inches)
Re 376
Re 97

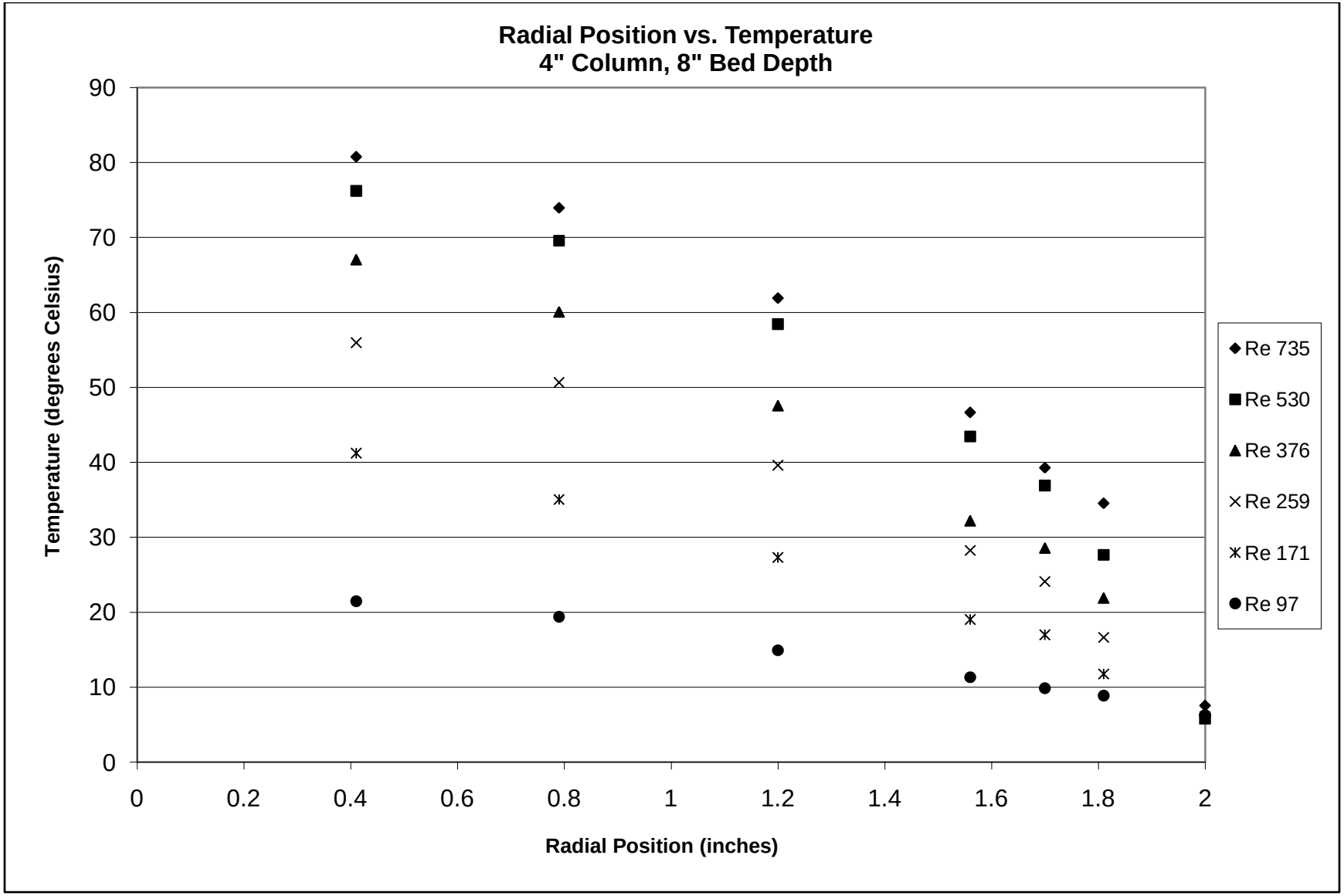
Radial Position vs. Temperature
4" Column, 8" Bed Depth
Temperature (degrees Celsius)
90
80
70
60
50
40
30
20
10
0
0
0.2
0.4
0.6
0.8
1
1.2
1.4
1.6
1.8
2
Radial Position (inches)
Re 735
Re 530
Re 376
Re 259
Re 171
Re 97

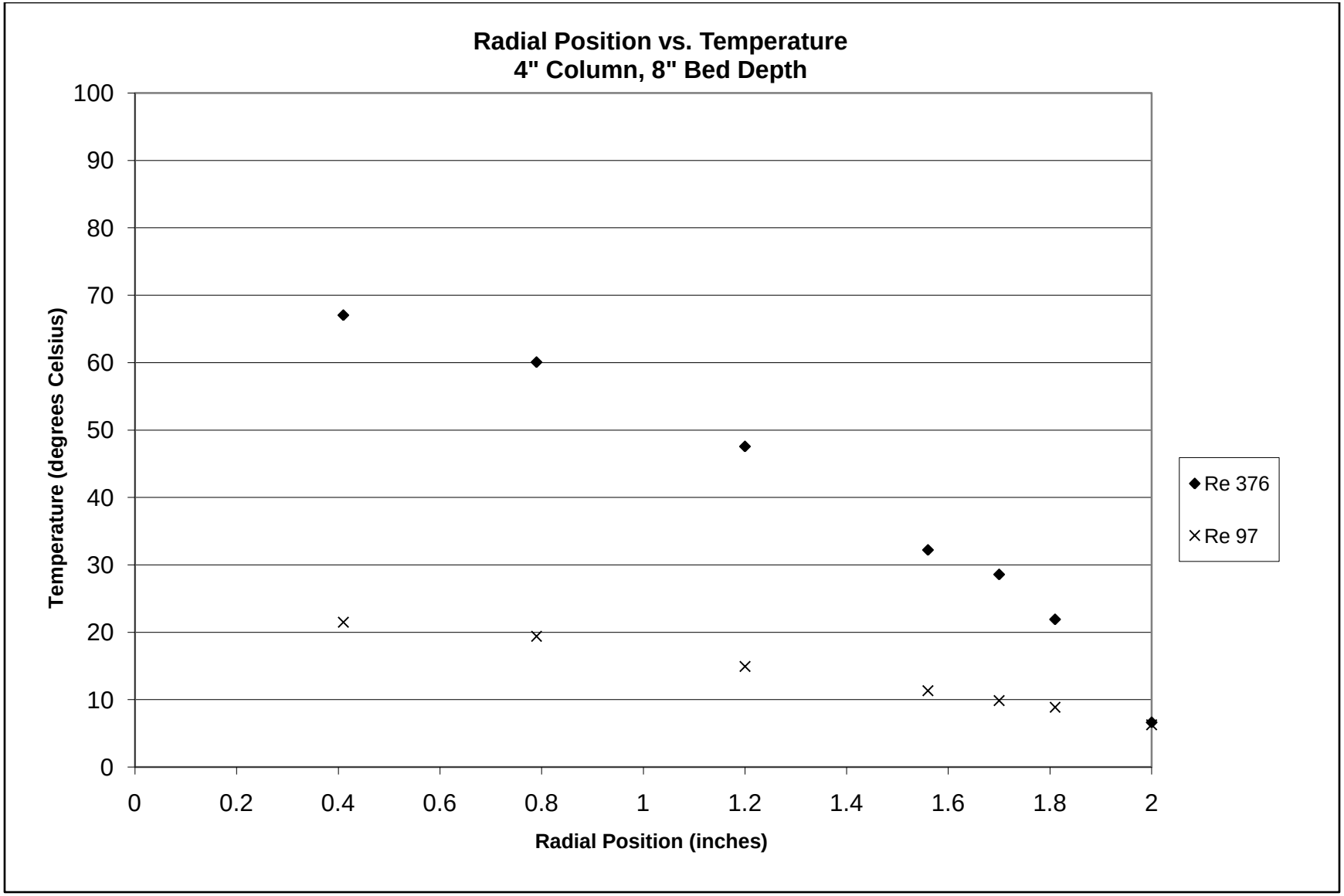
Radial Position vs. Temperature
4" Column, 8" Bed Depth
Temperature (degrees Celsius)
100
90
80
70
60
50
40
30
20
10
0
0
0.2
0.4
0.6
0.8
1
1.2
1.4
1.6
1.8
2
Radial Position (inches)
Re 376
Re 97

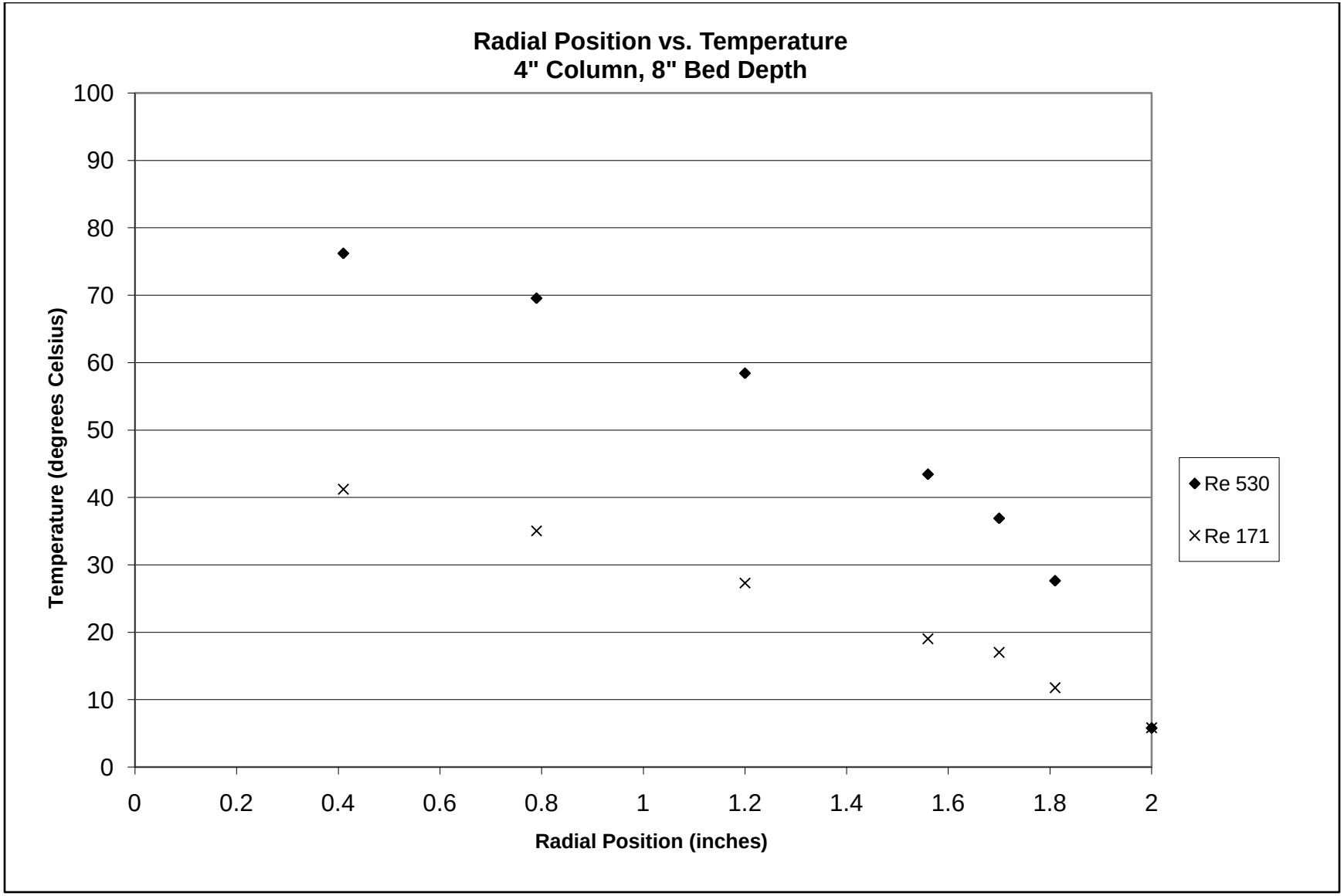
Radial Position vs. Temperature
4" Column, 8" Bed Depth
Temperature (degrees Celsius)
100
90
80
70
60
50
40
30
20
10
0
0
0.2
0.4
0.6
0.8
1
1.2
1.4
1.6
1.8
2
Radial Position (inches)
Re 530
Re 171

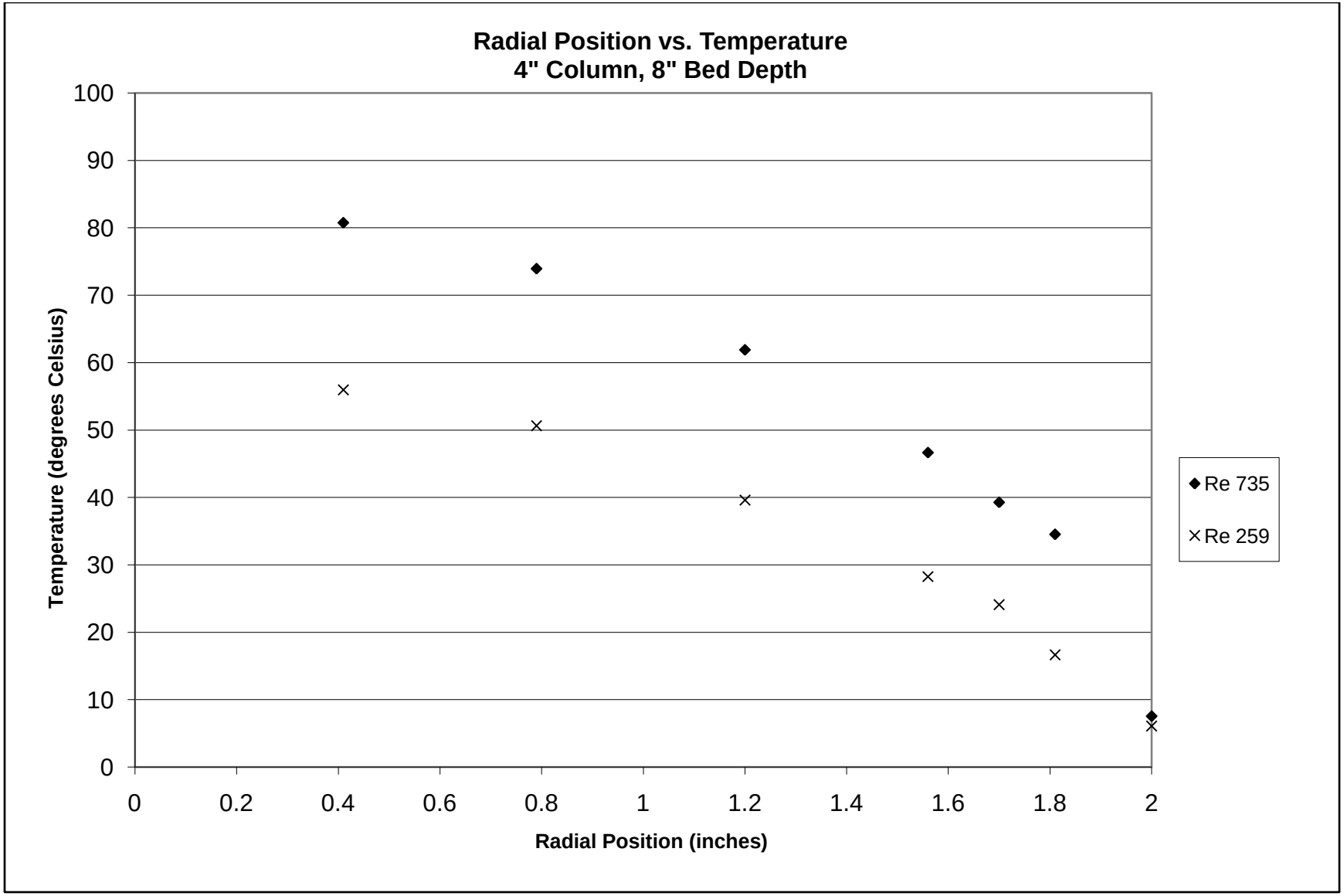
Radial Position vs. Temperature
4" Column, 8" Bed Depth
Temperature (degrees Celsius)
100
90
80
70
60
50
40
30
20
10
0
0
0.2
0.4
0.6
0.8
1
1.2
1.4
1.6
1.8
2
Radial Position (inches)
Re 735
Re 259

F.2: Comparing Bed Heights

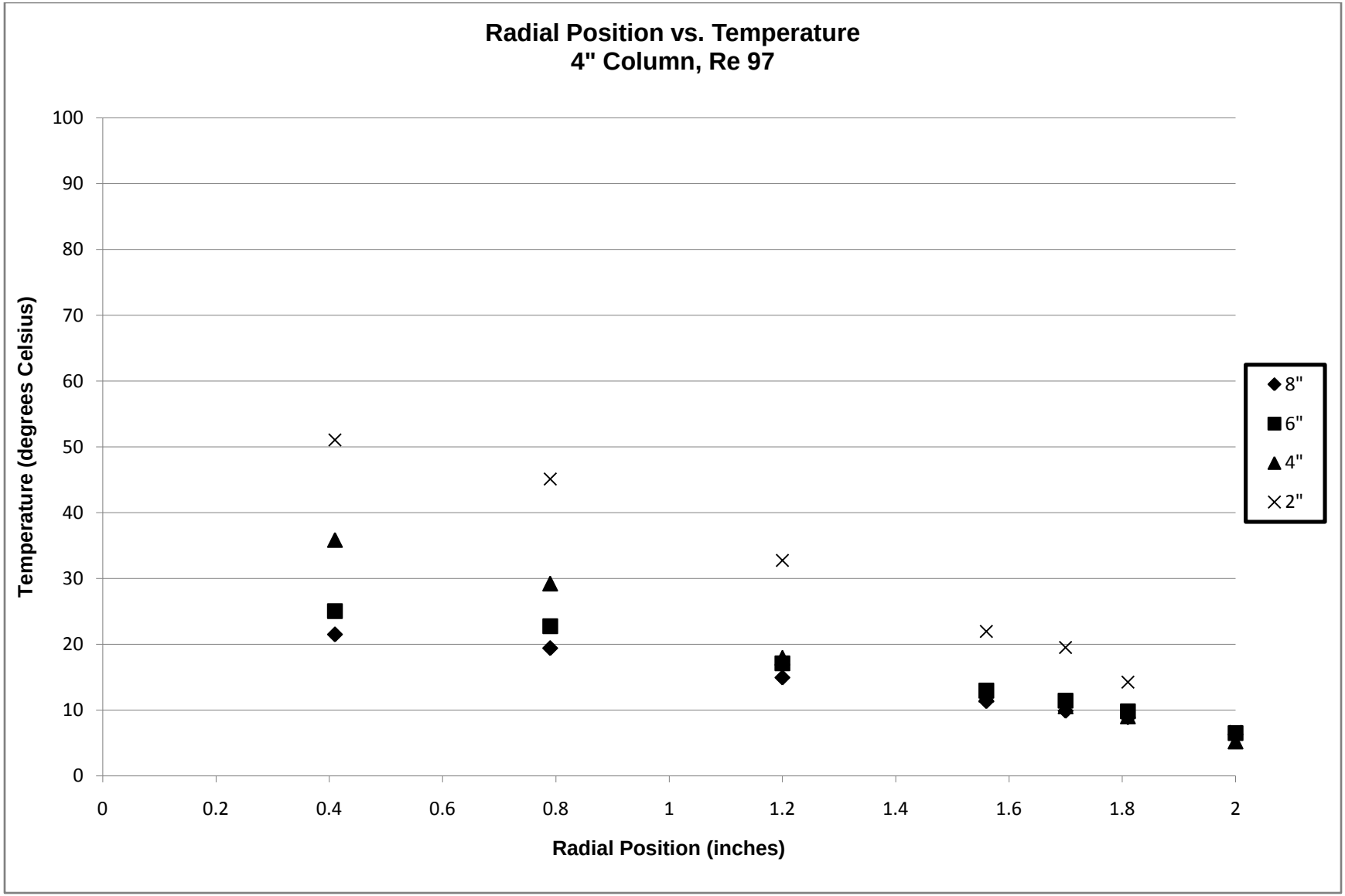
Radial Position vs. Temperature
4" Column, Re 97
Temperature (degrees Celsius)
100
90
80
70
60
50
40
30
20
10
0
0
0.2
0.4
0.6
0.8
1
1.2
1.4
1.6
1.8
2
Radial Position (inches)
8"
6"
4"
2"

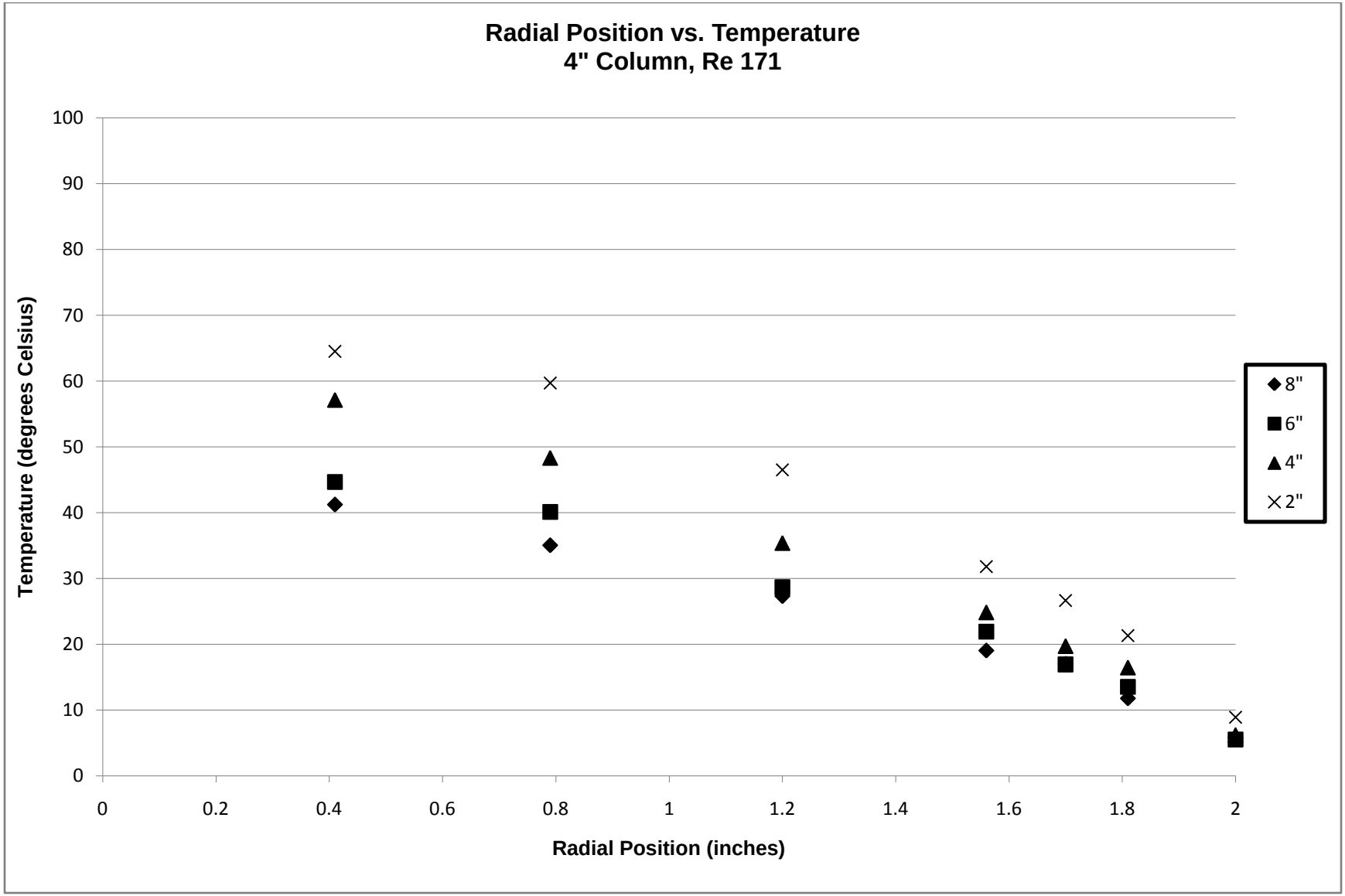
Radial Position vs. Temperature
4" Column, Re 171
Temperature (degrees Celsius)
100
90
80
70
60
50
40
30
20
10
0
0
0.2
0.4
0.6
0.8
1
1.2
1.4
1.6
1.8
2
Radial Position (inches)
8"
6"
4"
2"

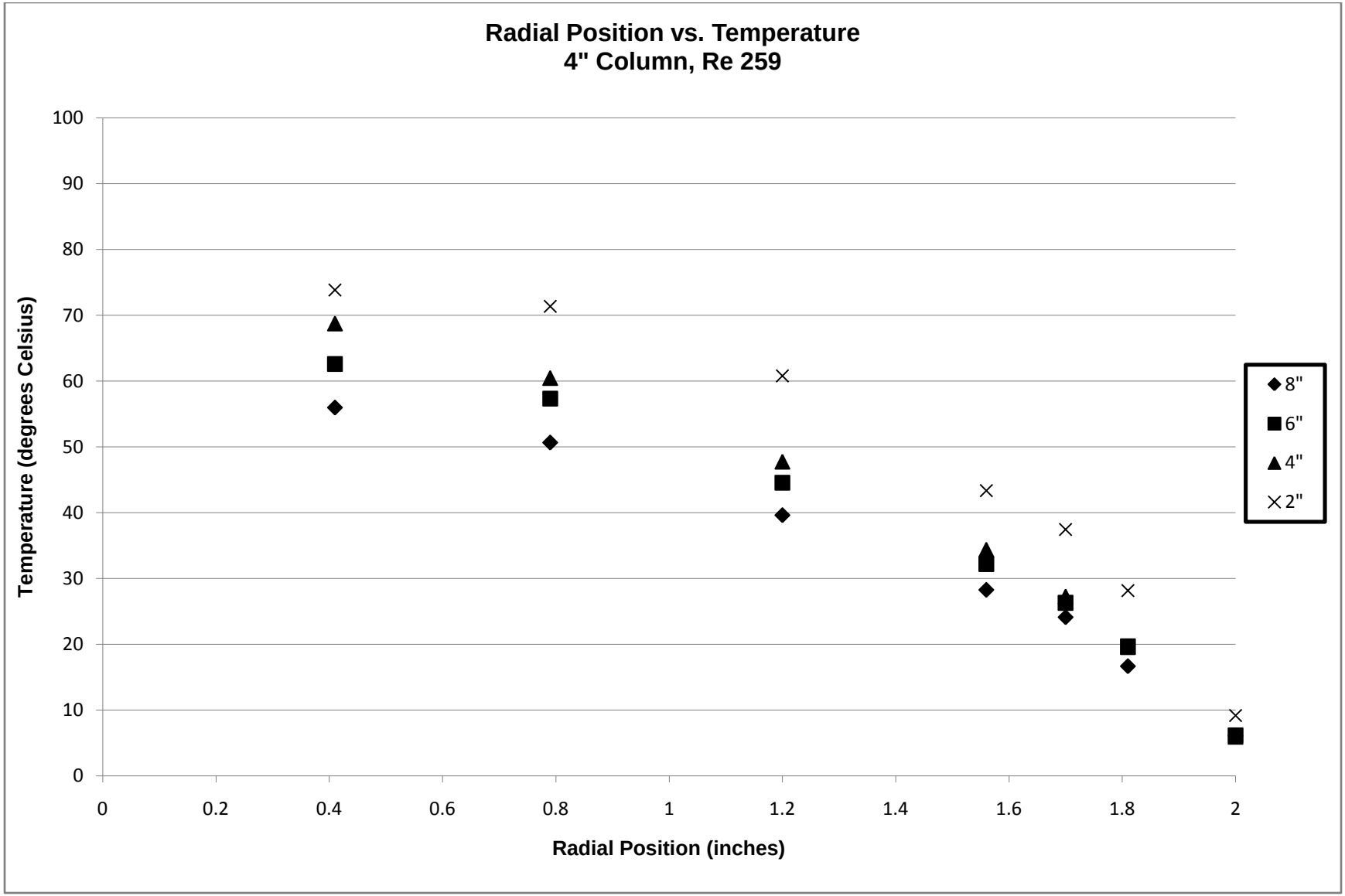
Radial Position vs. Temperature
4" Column, Re 259
Temperature (degrees Celsius)
100
90
80
70
60
50
40
30
20
10
0
0
0.2
0.4
0.6
0.8
1
1.2
1.4
1.6
1.8
2
Radial Position (inches)
8"
6"
4"
2"

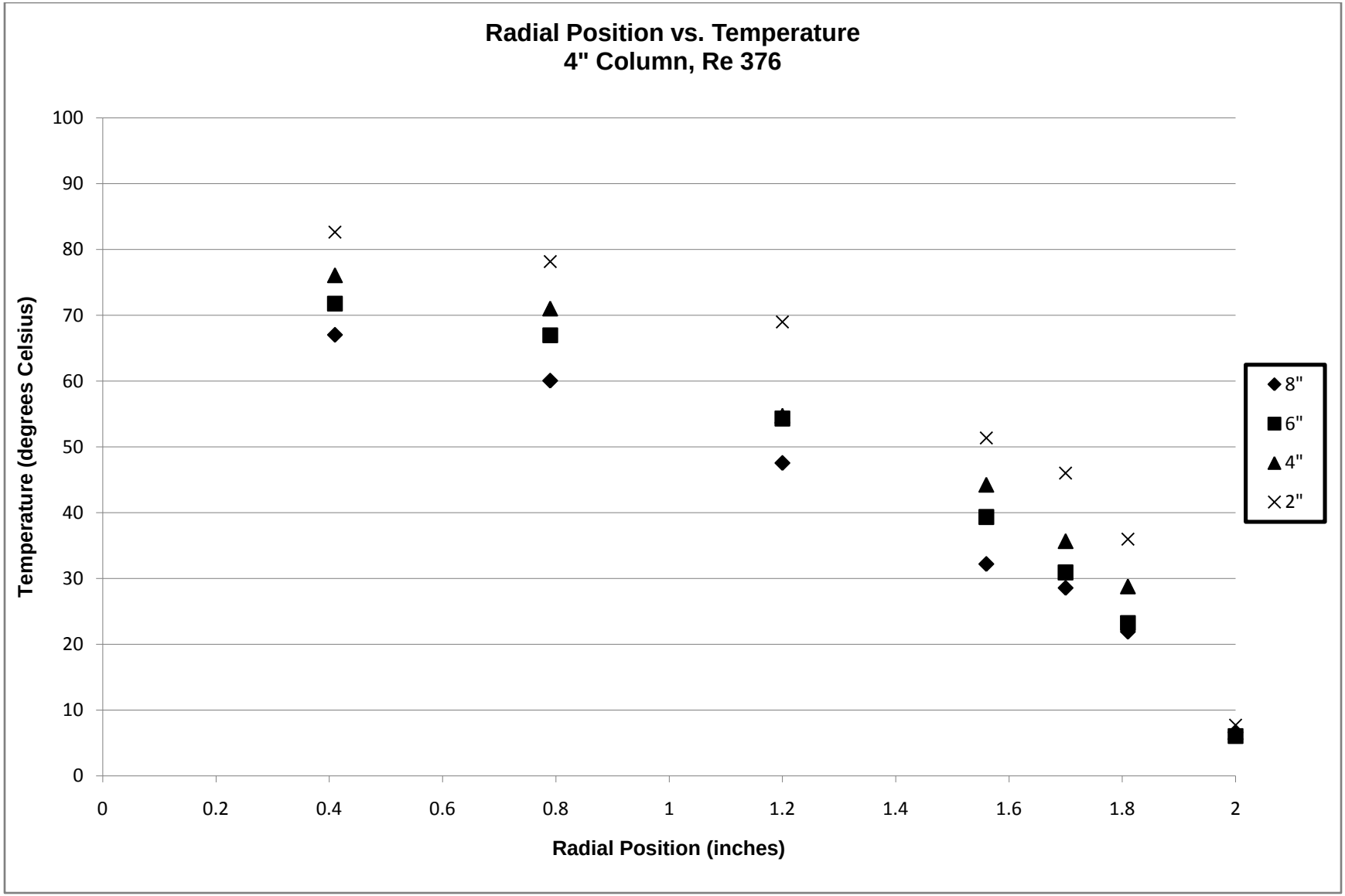
Radial Position vs. Temperature
4" Column, Re 376
Temperature (degrees Celsius)
100
90
80
70
60
50
40
30
20
10
0
0
0.2
0.4
0.6
0.8
1
1.2
1.4
1.6
1.8
2
Radial Position (inches)
8"
6"
4"
2"

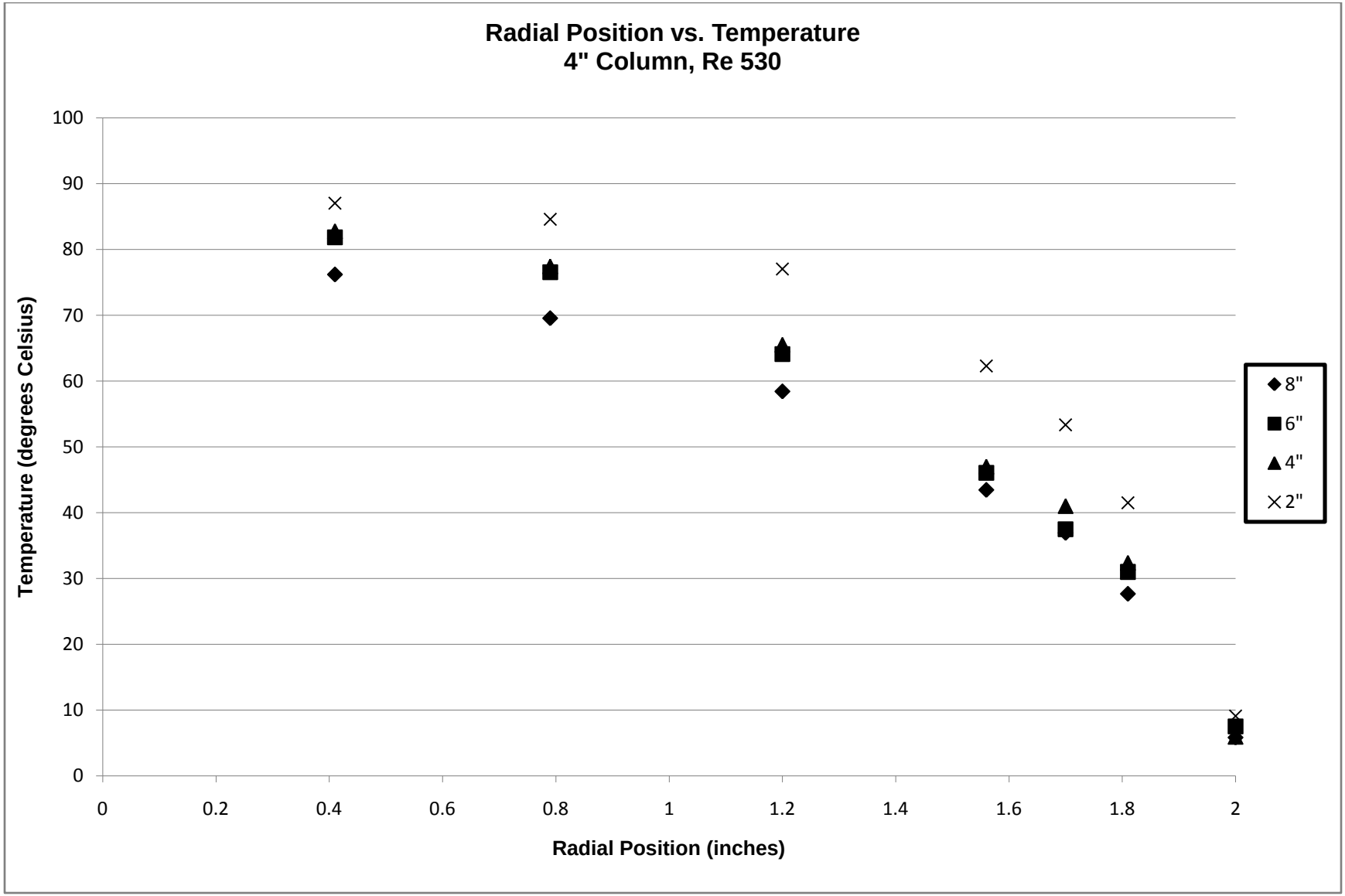
Radial Position vs. Temperature
4" Column, Re 530
Temperature (degrees Celsius)
100
90
80
70
60
50
40
30
20
10
0
0
0.2
0.4
0.6
0.8
1
1.2
1.4
1.6
1.8
2
Radial Position (inches)
8"
6"
4"
2"

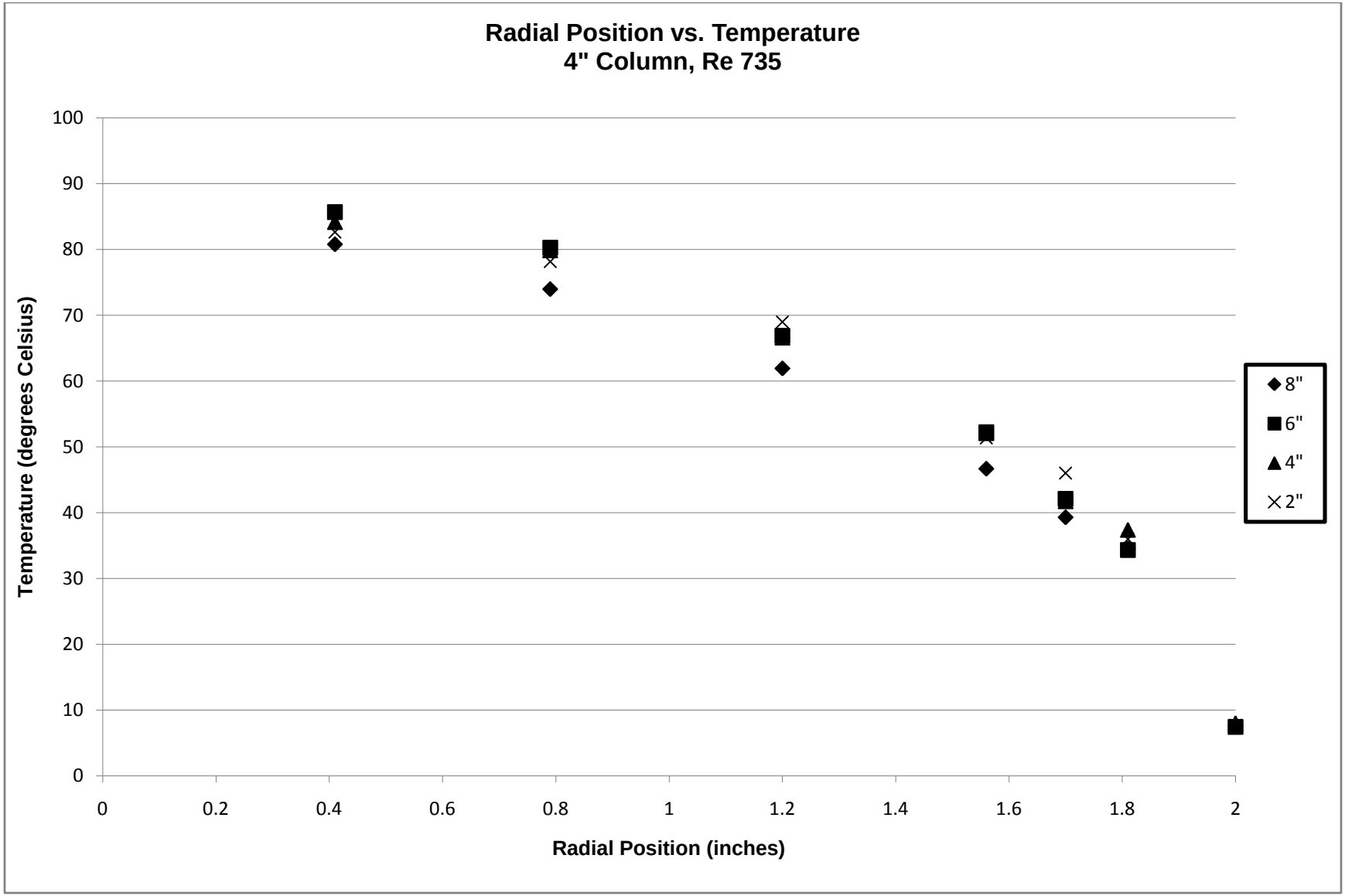
Radial Position vs. Temperature
4" Column, Re 735
Temperature (degrees Celsius)
100
90
80
70
60
50
40
30
20
10
0
0
0.2
0.4
0.6
0.8
1
1.2
1.4
1.6
1.8
2
Radial Position (inches)
8"
6"
4"
2"

Appendix G: Dimensionless Temperature Profile Comparisons

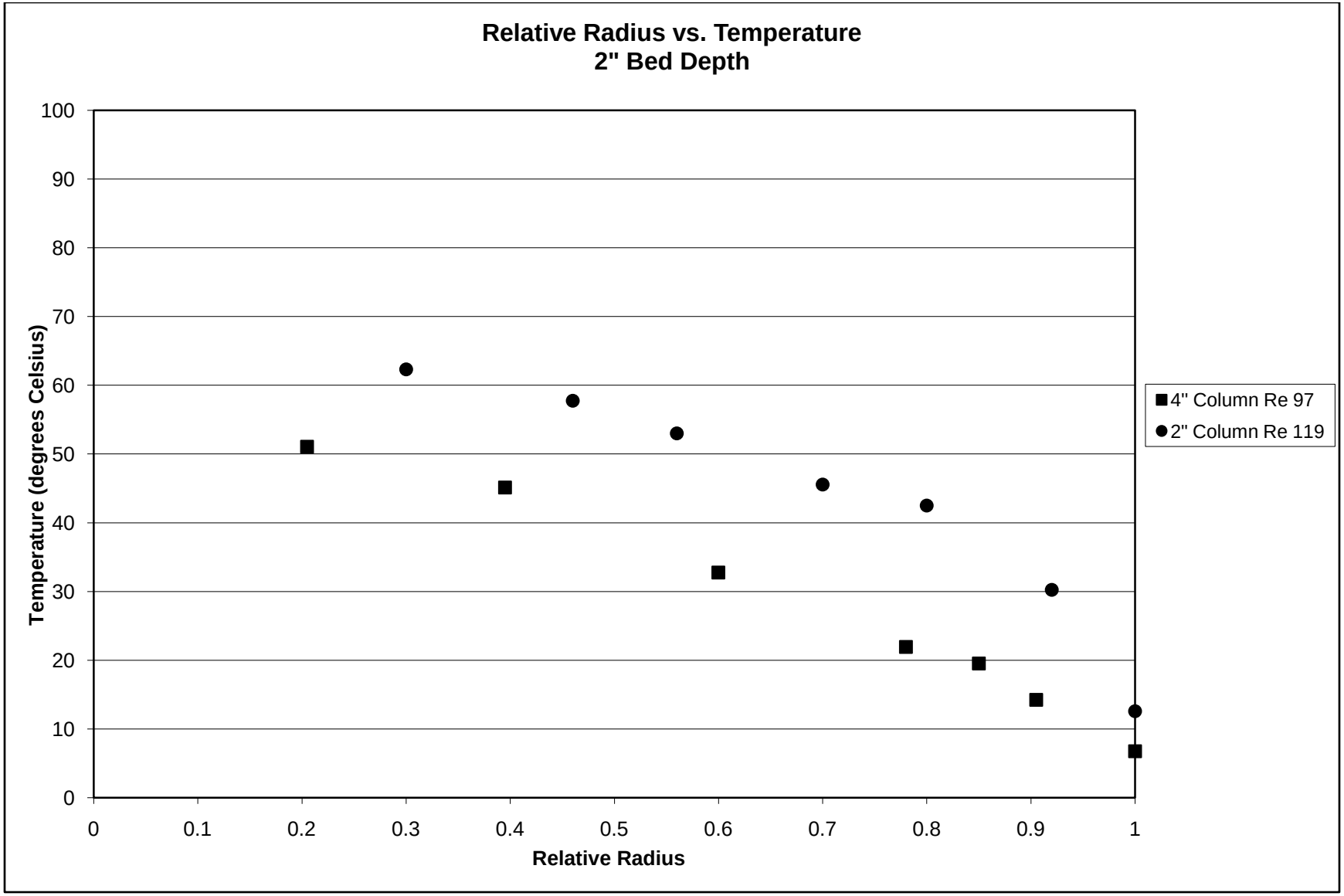
Relative Radius vs. Temperature
2" Bed Depth
Temperature (degrees Celsius)
100
90
80
70
60
50
40
30
20
10
0
0
0.1
0.2
0.3
0.4
0.5
0.6
0.7
0.8
0.9
1
Relative Radius
4" Column Re 97
2" Column Re 119

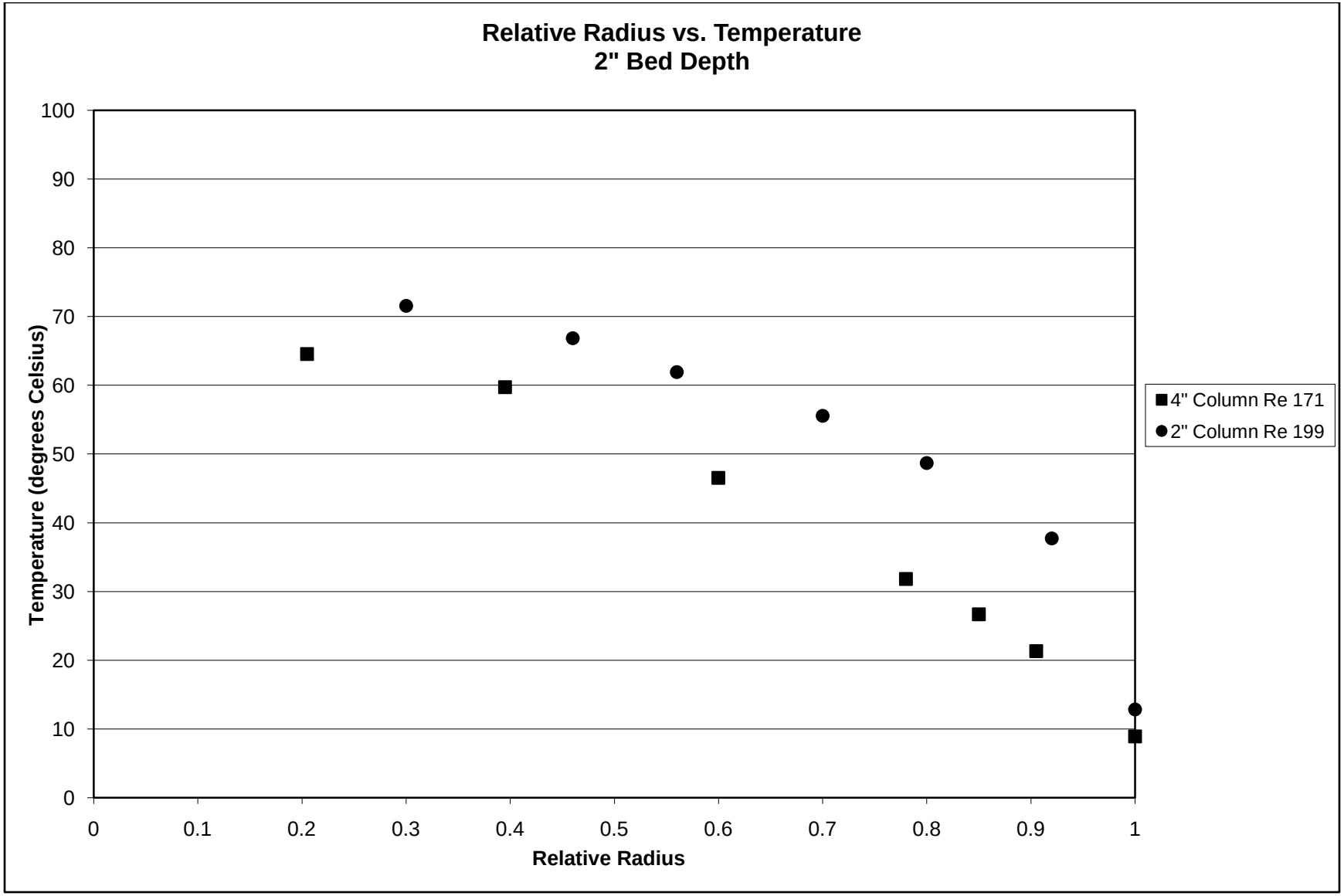
Relative Radius vs. Temperature
2" Bed Depth
Temperature (degrees Celsius)
100
90
80
70
60
50
40
30
20
10
0
0
0.1
0.2
0.3
0.4
0.5
0.6
0.7
0.8
0.9
1
Relative Radius
4" Column Re 171
2" Column Re 199

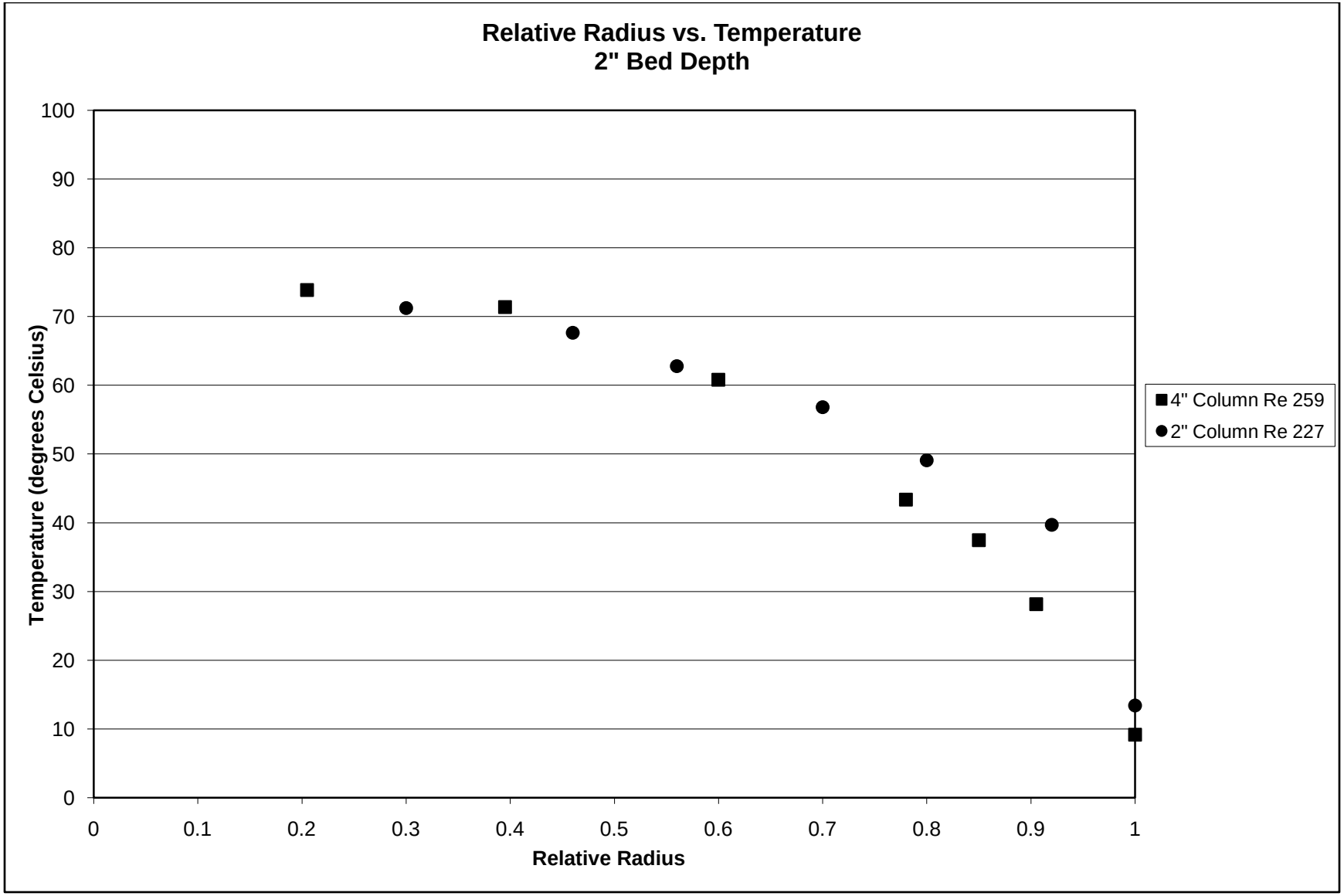
Relative Radius vs. Temperature
2" Bed Depth
Temperature (degrees Celsius)
100
90
80
70
60
50
40
30
20
10
0
0
0.1
0.2
0.3
0.4
0.5
0.6
0.7
0.8
0.9
1
Relative Radius
4" Column Re 259
2" Column Re 227

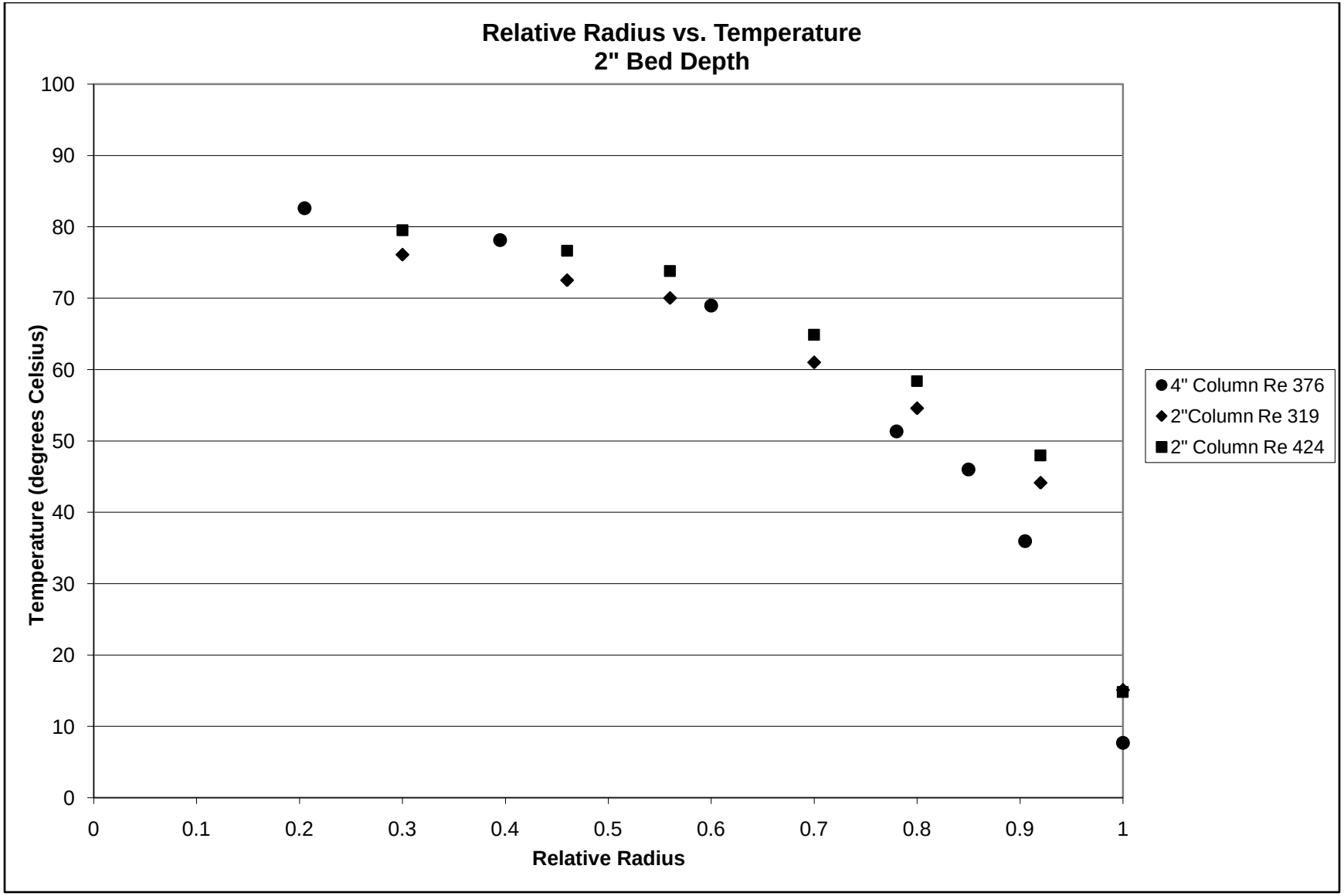
Relative Radius vs. Temperature
2" Bed Depth
Temperature (degrees Celsius)
100
90
80
70
60
50
40
30
20
10
0
0
0.1
0.2
0.3
0.4
0.5
0.6
0.7
0.8
0.9
1
Relative Radius
4" Column Re 376
2"Column Re 319
2" Column Re 424

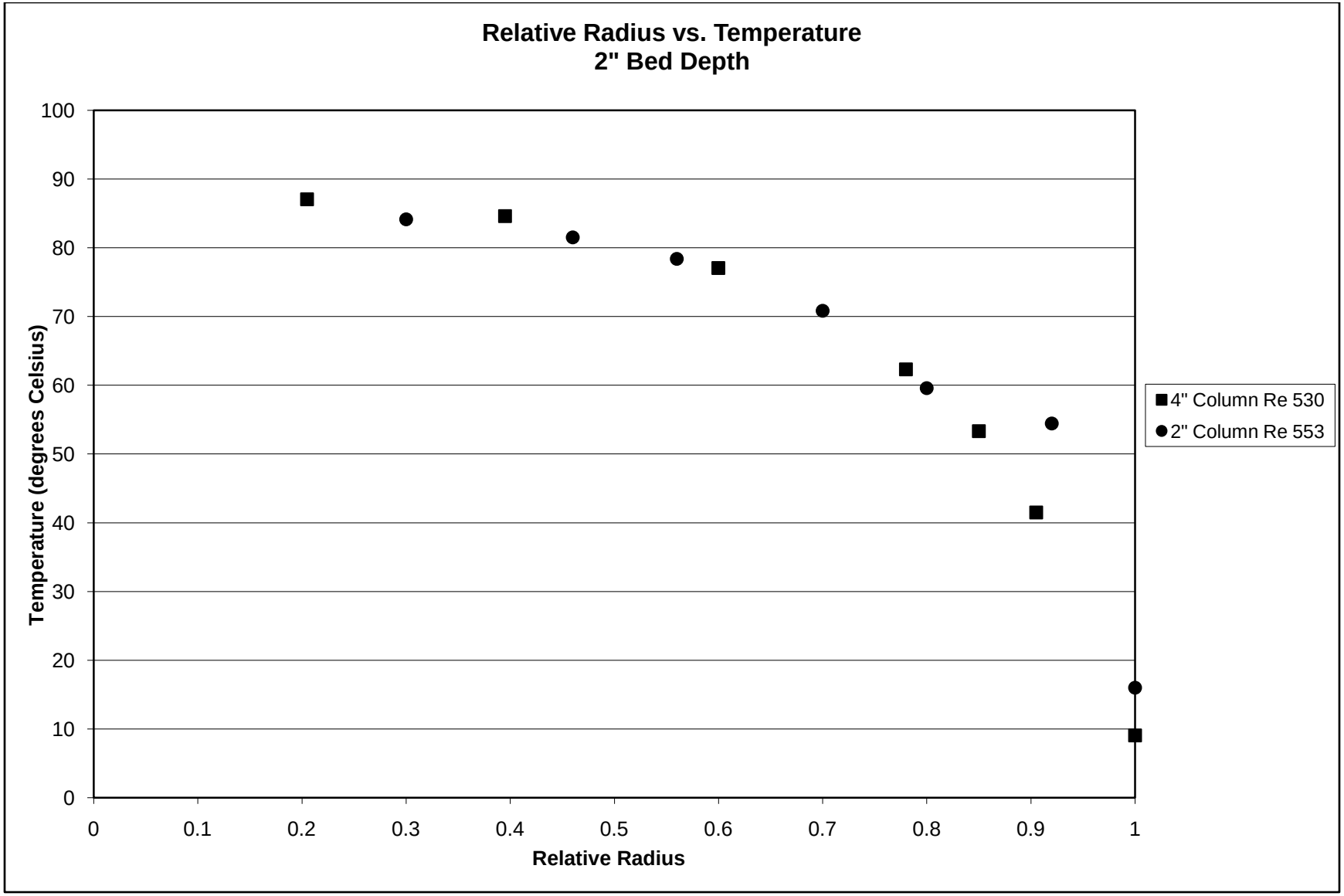
Relative Radius vs. Temperature
2" Bed Depth
Temperature (degrees Celsius)
100
90
80
70
60
50
40
30
20
10
0
0
0.1
0.2
0.3
0.4
0.5
0.6
0.7
0.8
0.9
1
Relative Radius
4" Column Re 530
2" Column Re 553

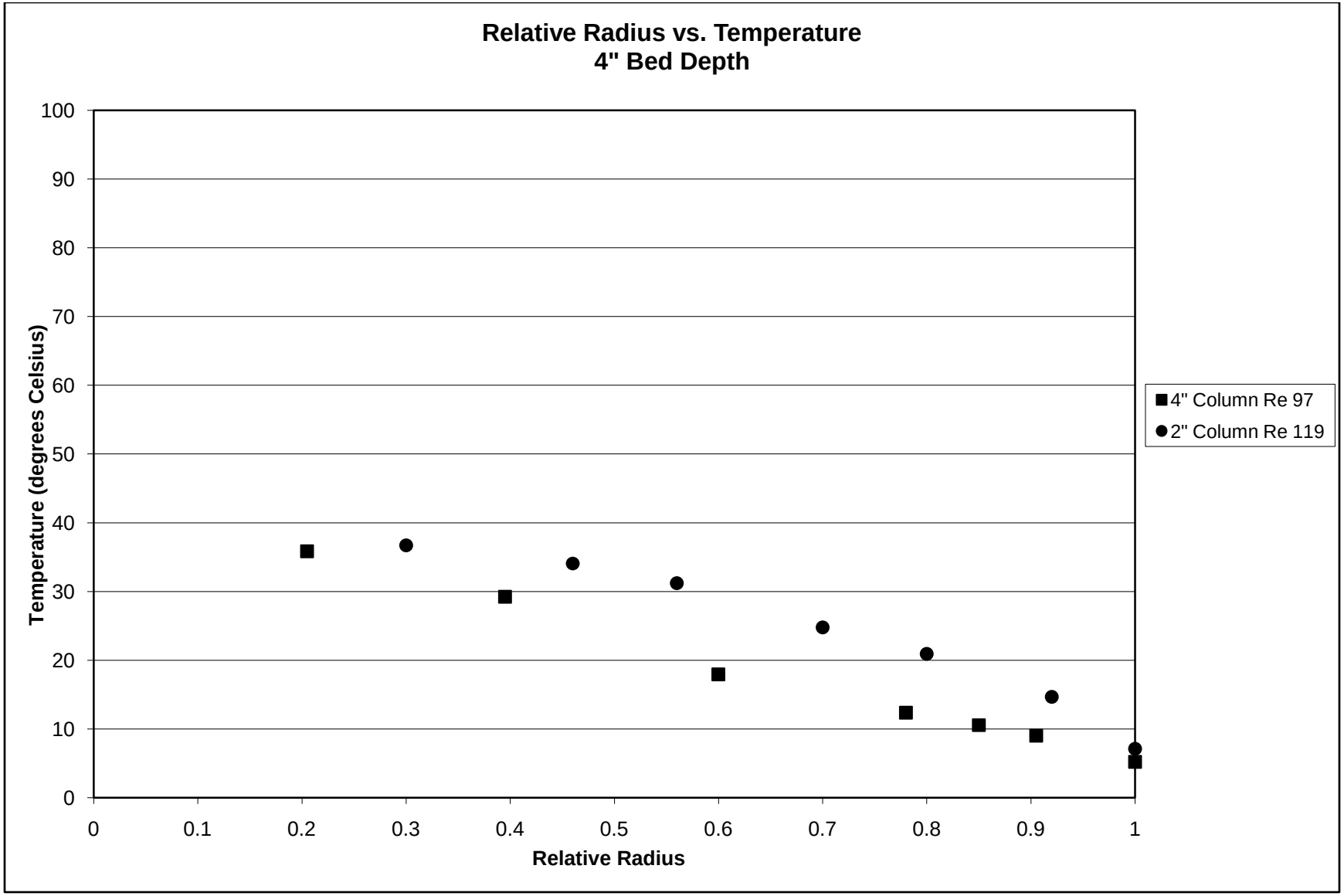
Relative Radius vs. Temperature
4" Bed Depth
Temperature (degrees Celsius)
100
90
80
70
60
50
40
30
20
10
0
0
0.1
0.2
0.3
0.4
0.5
0.6
0.7
0.8
0.9
1
Relative Radius
4" Column Re 97
2" Column Re 119

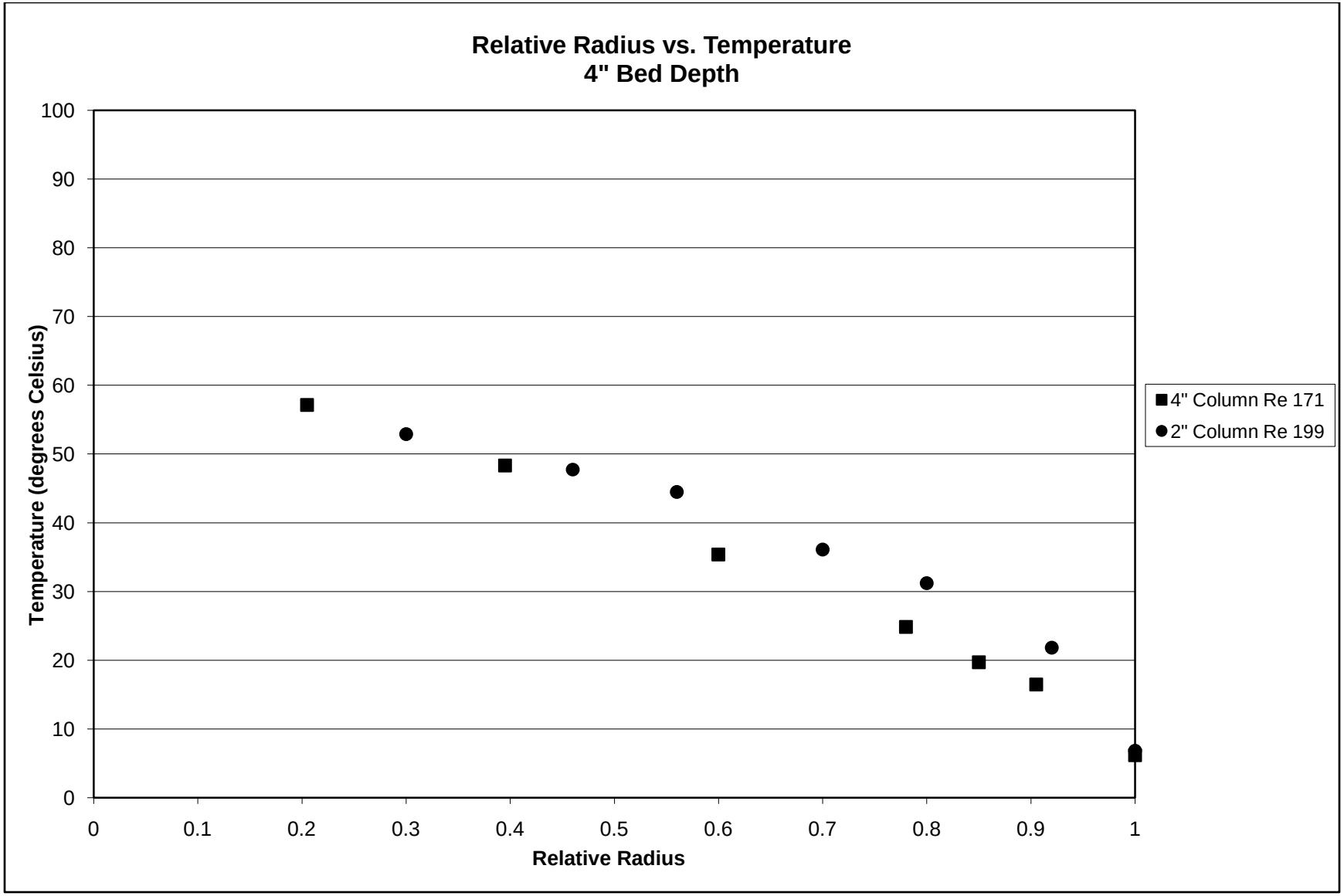
Relative Radius vs. Temperature
4" Bed Depth
Temperature (degrees Celsius)
100
90
80
70
60
50
40
30
20
10
0
0
0.1
0.2
0.3
0.4
0.5
0.6
0.7
0.8
0.9
1
Relative Radius
4" Column Re 171
2" Column Re 199

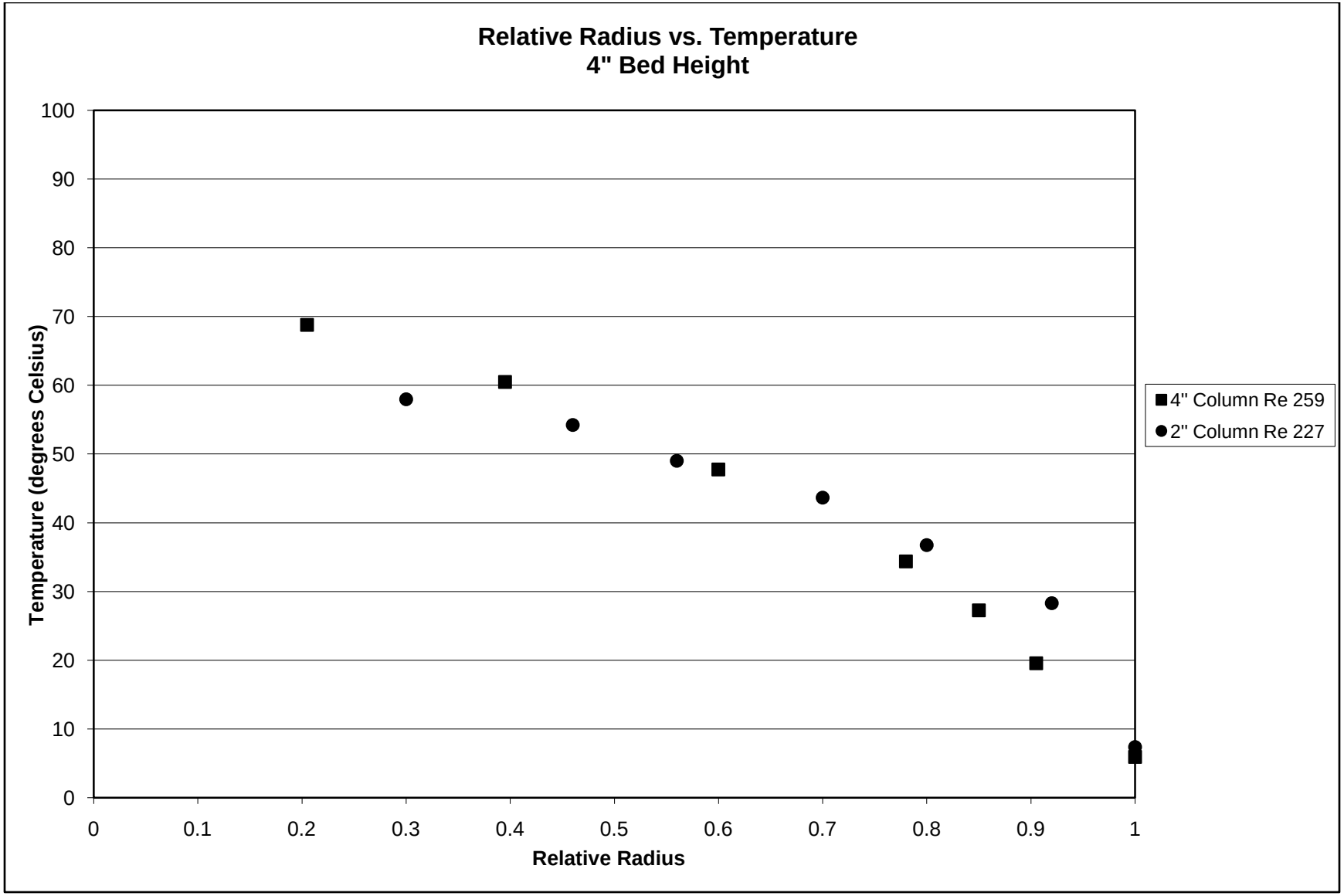
Relative Radius vs. Temperature
4" Bed Height
Temperature (degrees Celsius)
100
90
80
70
60
50
40
30
20
10
0
0
0.1
0.2
0.3
0.4
0.5
0.6
0.7
0.8
0.9
1
Relative Radius
4" Column Re 259
2" Column Re 227

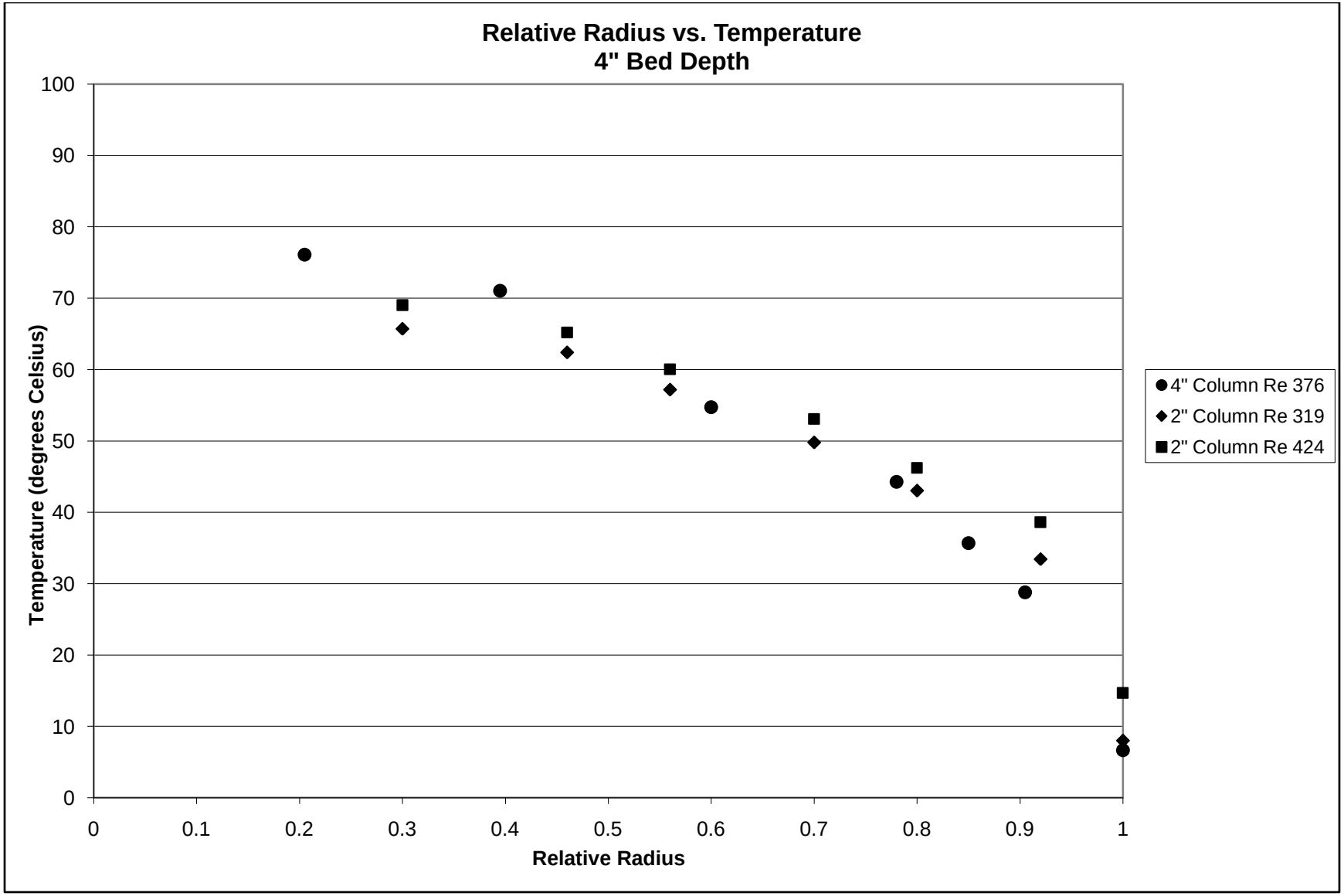
Relative Radius vs. Temperature
4" Bed Depth
Temperature (degrees Celsius)
100
90
80
70
60
50
40
30
20
10
0
0
0.1
0.2
0.3
0.4
0.5
0.6
0.7
0.8
0.9
1
Relative Radius
4" Column Re 376
2" Column Re 319
2" Column Re 424

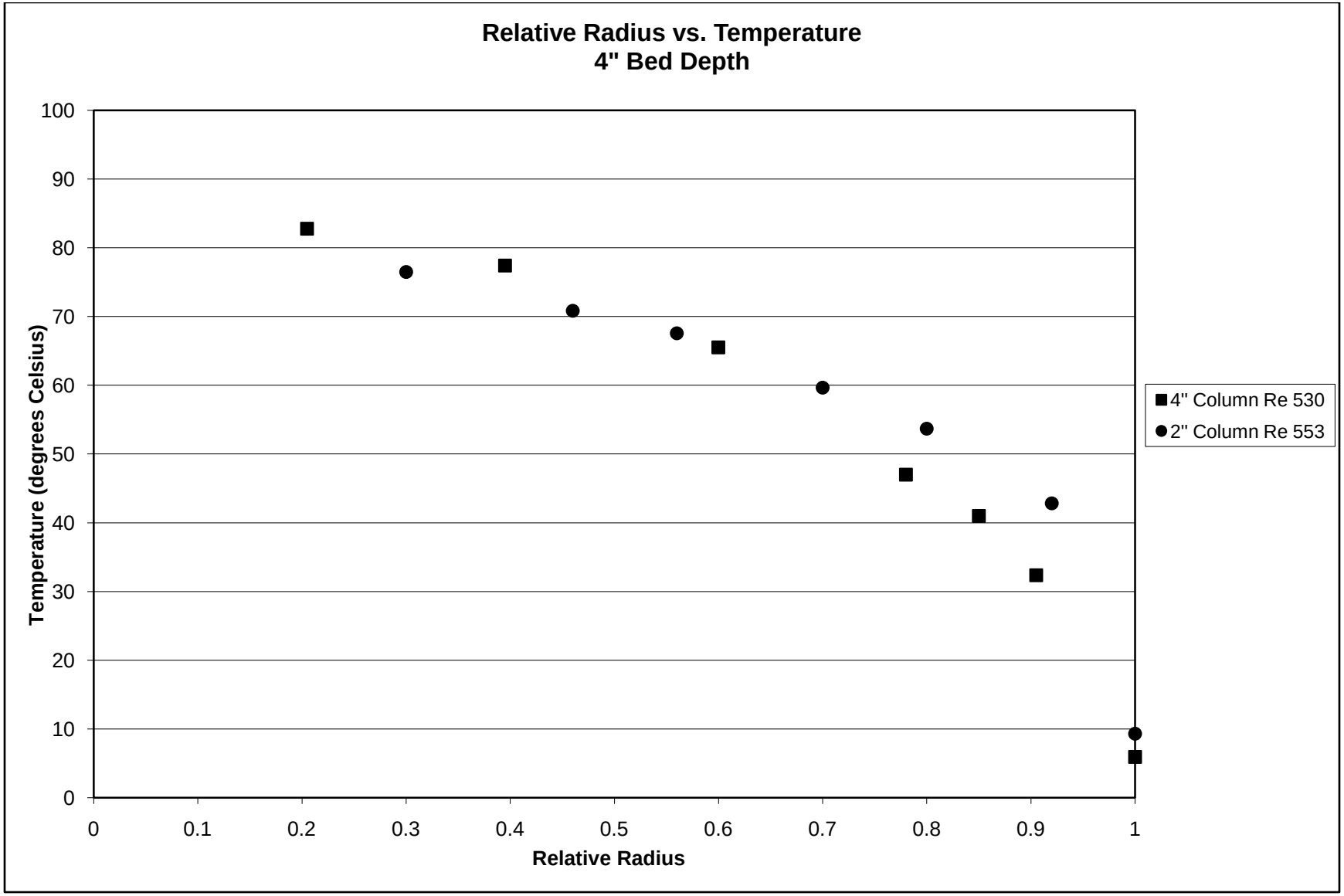
Relative Radius vs. Temperature
4" Bed Depth
Temperature (degrees Celsius)
100
90
80
70
60
50
40
30
20
10
0
0
0.1
0.2
0.3
0.4
0.5
0.6
0.7
0.8
0.9
1
Relative Radius
4" Column Re 530
2" Column Re 553

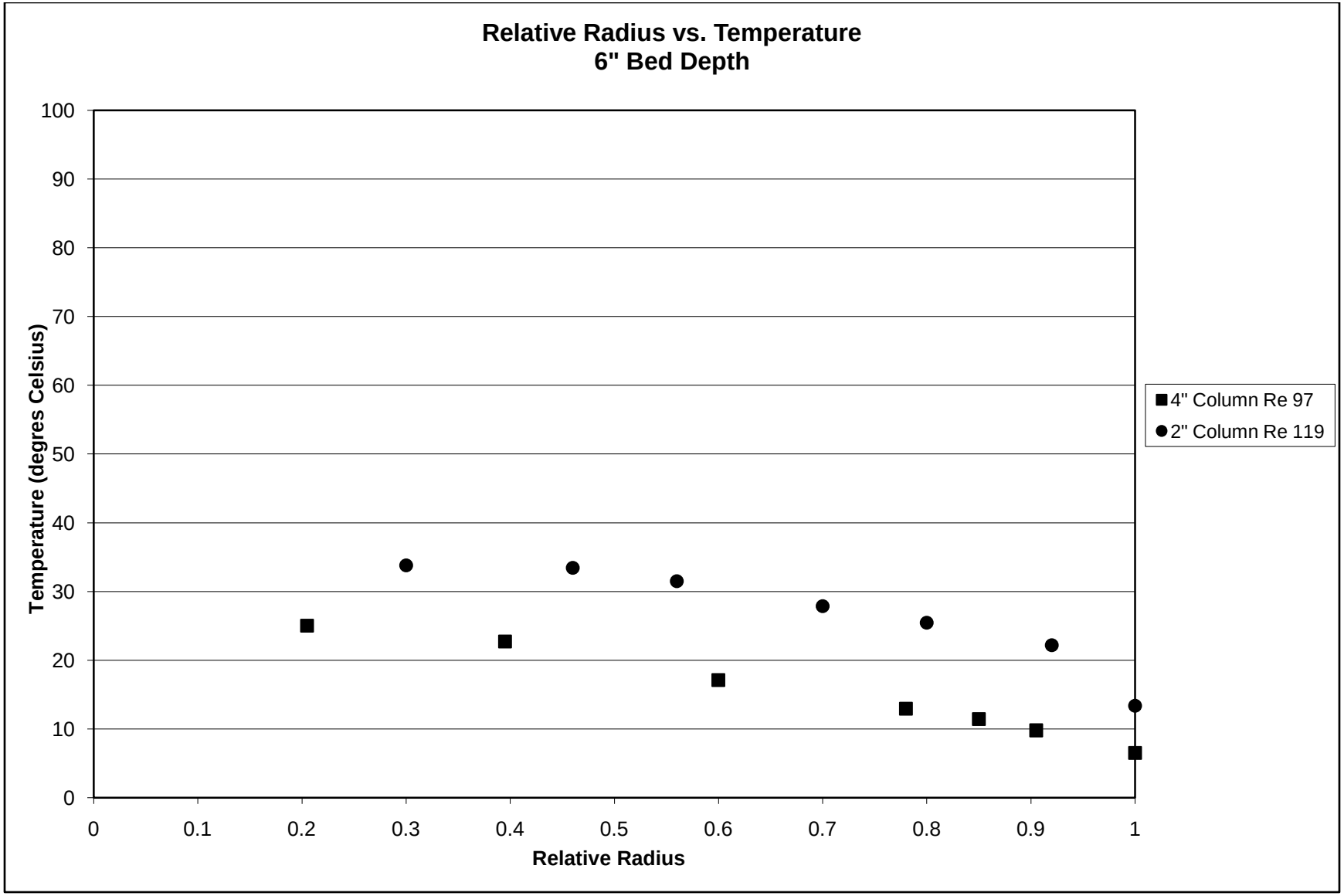
Relative Radius vs. Temperature
6" Bed Depth
Temperature (degres Celsius)
100
90
80
70
60
50
40
30
20
10
0
0
0.1
0.2
0.3
0.4
0.5
0.6
0.7
0.8
0.9
1
Relative Radius
4" Column Re 97
2" Column Re 119

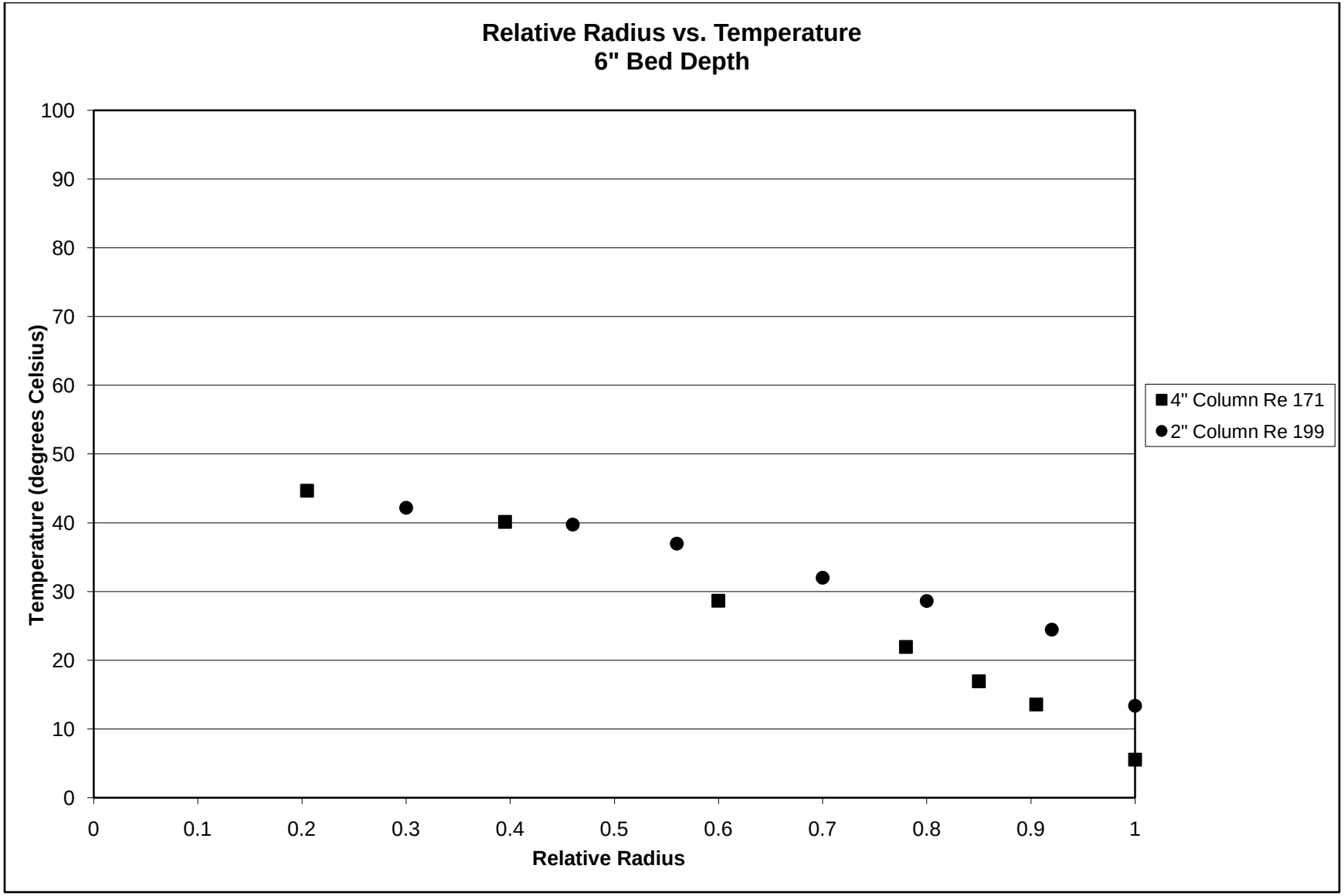
Relative Radius vs. Temperature
6" Bed Depth
Temperature (degrees Celsius)
100
90
80
70
60
50
40
30
20
10
0
0
0.1
0.2
0.3
0.4
0.5
0.6
0.7
0.8
0.9
1
Relative Radius
4" Column Re 171
2" Column Re 199

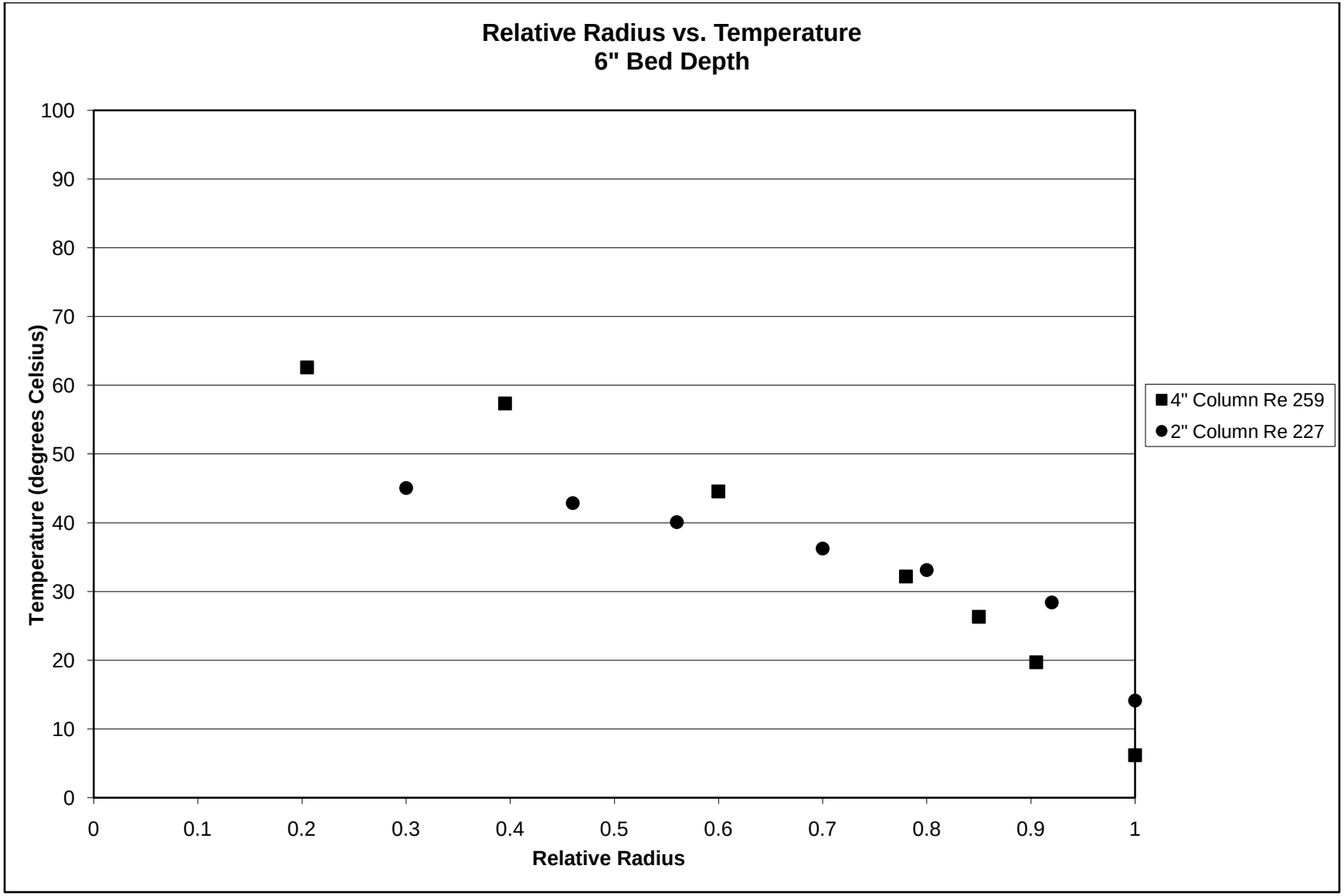
Relative Radius vs. Temperature
6" Bed Depth
Temperature (degrees Celsius)
100
90
80
70
60
50
40
30
20
10
0
0
0.1
0.2
0.3
0.4
0.5
0.6
0.7
0.8
0.9
1
Relative Radius
4" Column Re 259
2" Column Re 227

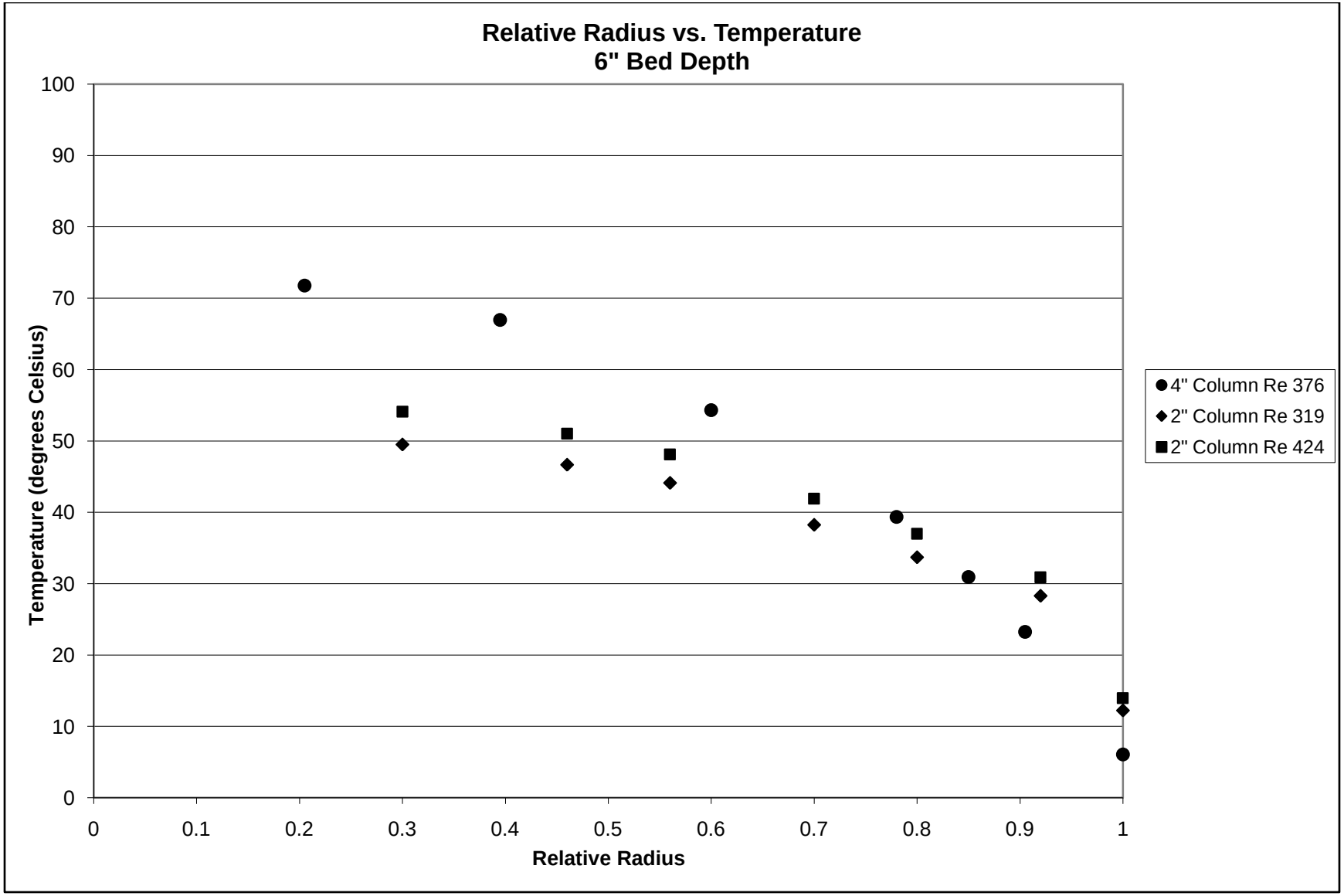
Relative Radius vs. Temperature
6" Bed Depth
Temperature (degrees Celsius)
100
90
80
70
60
50
40
30
20
10
0
0
0.1
0.2
0.3
0.4
0.5
0.6
0.7
0.8
0.9
1
Relative Radius
4" Column Re 376
2" Column Re 319
2" Column Re 424

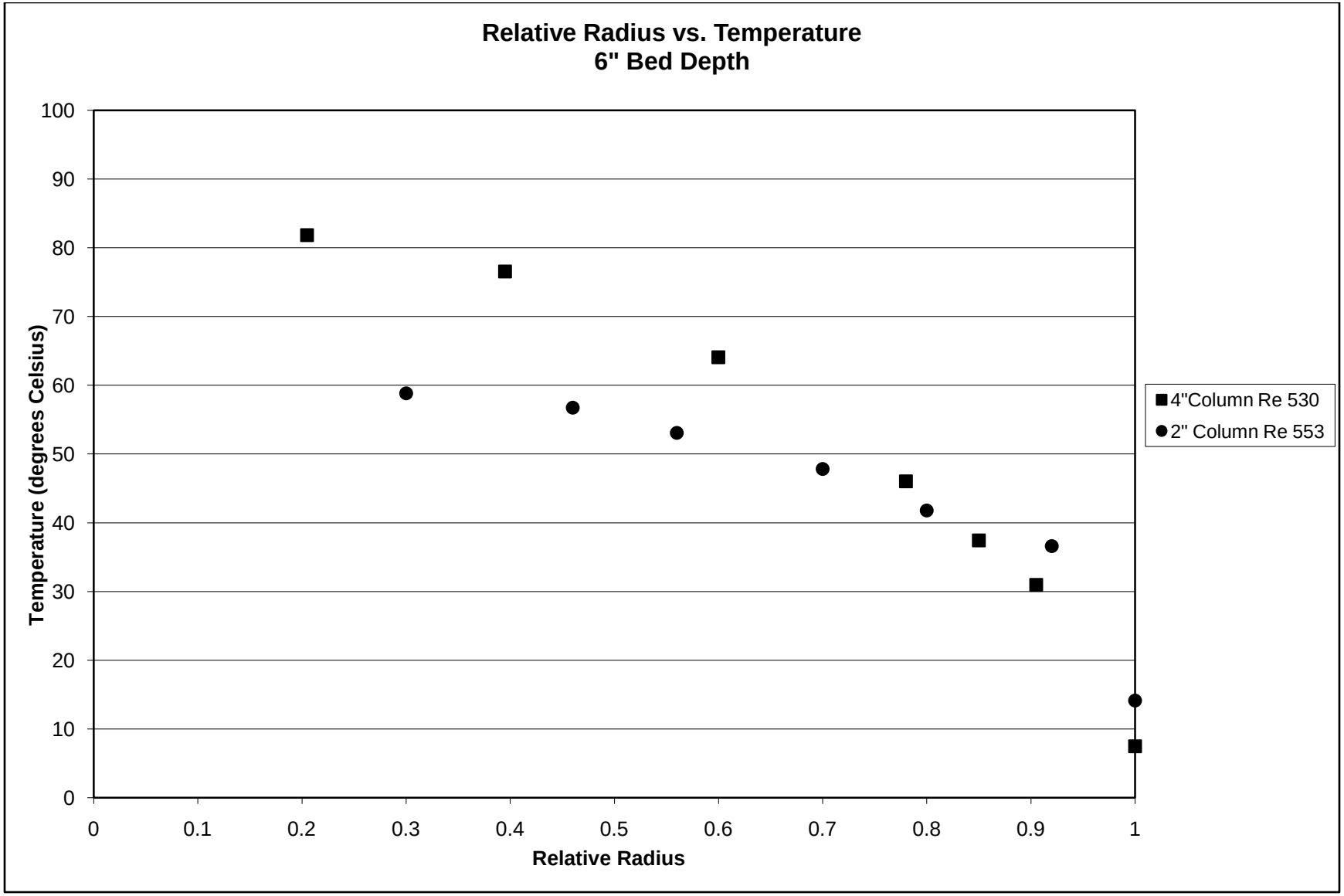
Relative Radius vs. Temperature
6" Bed Depth
Temperature (degrees Celsius)
100
90
80
70
60
50
40
30
20
10
0
0
0.1
0.2
0.3
0.4
0.5
0.6
0.7
0.8
0.9
1
Relative Radius
4"Column Re 530
2" Column Re 553

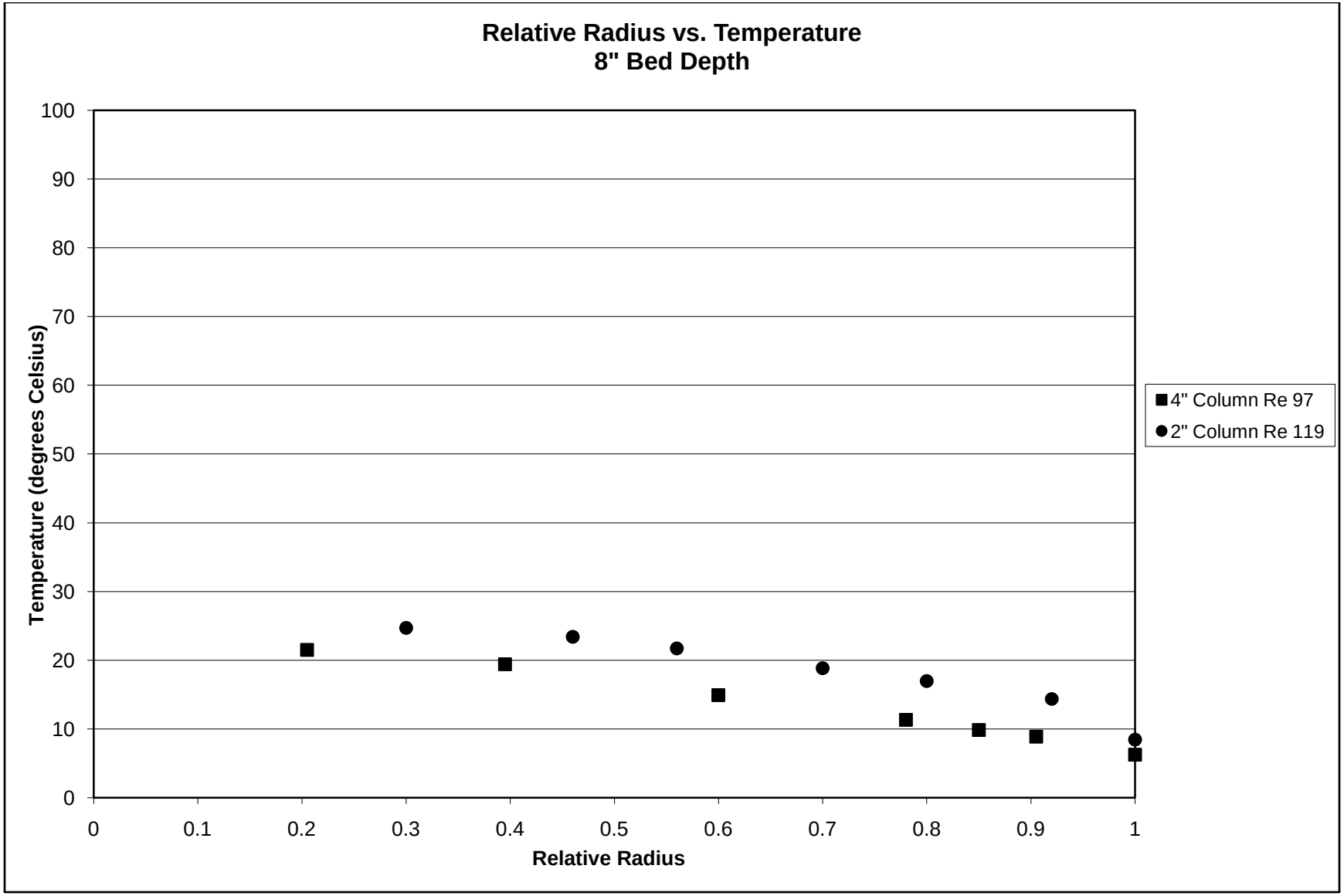
Relative Radius vs. Temperature
8" Bed Depth
Temperature (degrees Celsius)
100
90
80
70
60
50
40
30
20
10
0
0
0.1
0.2
0.3
0.4
0.5
0.6
0.7
0.8
0.9
1
Relative Radius
4" Column Re 97
2" Column Re 119

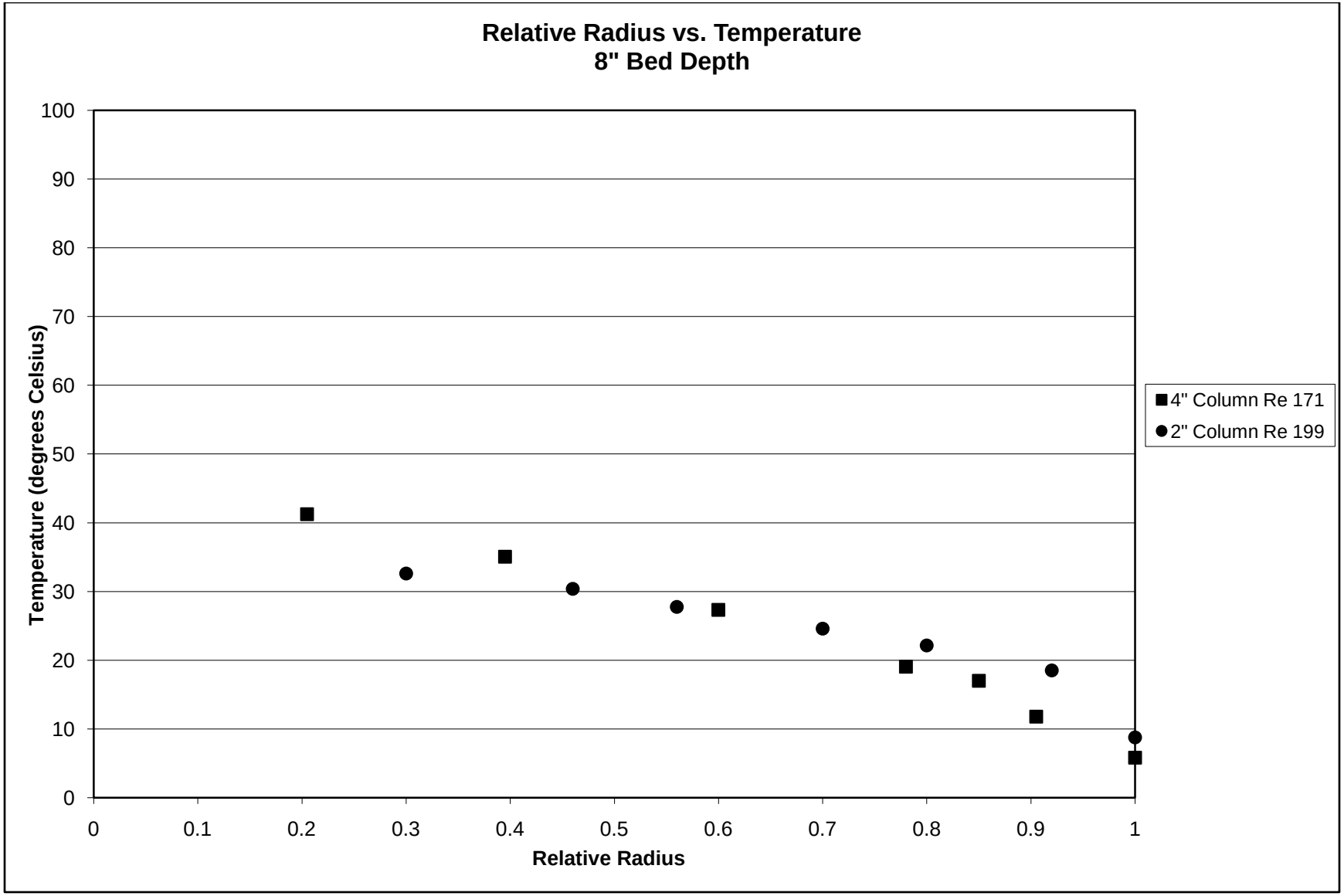
Relative Radius vs. Temperature
8" Bed Depth
Temperature (degrees Celsius)
100
90
80
70
60
50
40
30
20
10
0
0
0.1
0.2
0.3
0.4
0.5
0.6
0.7
0.8
0.9
1
Relative Radius
4" Column Re 171
2" Column Re 199

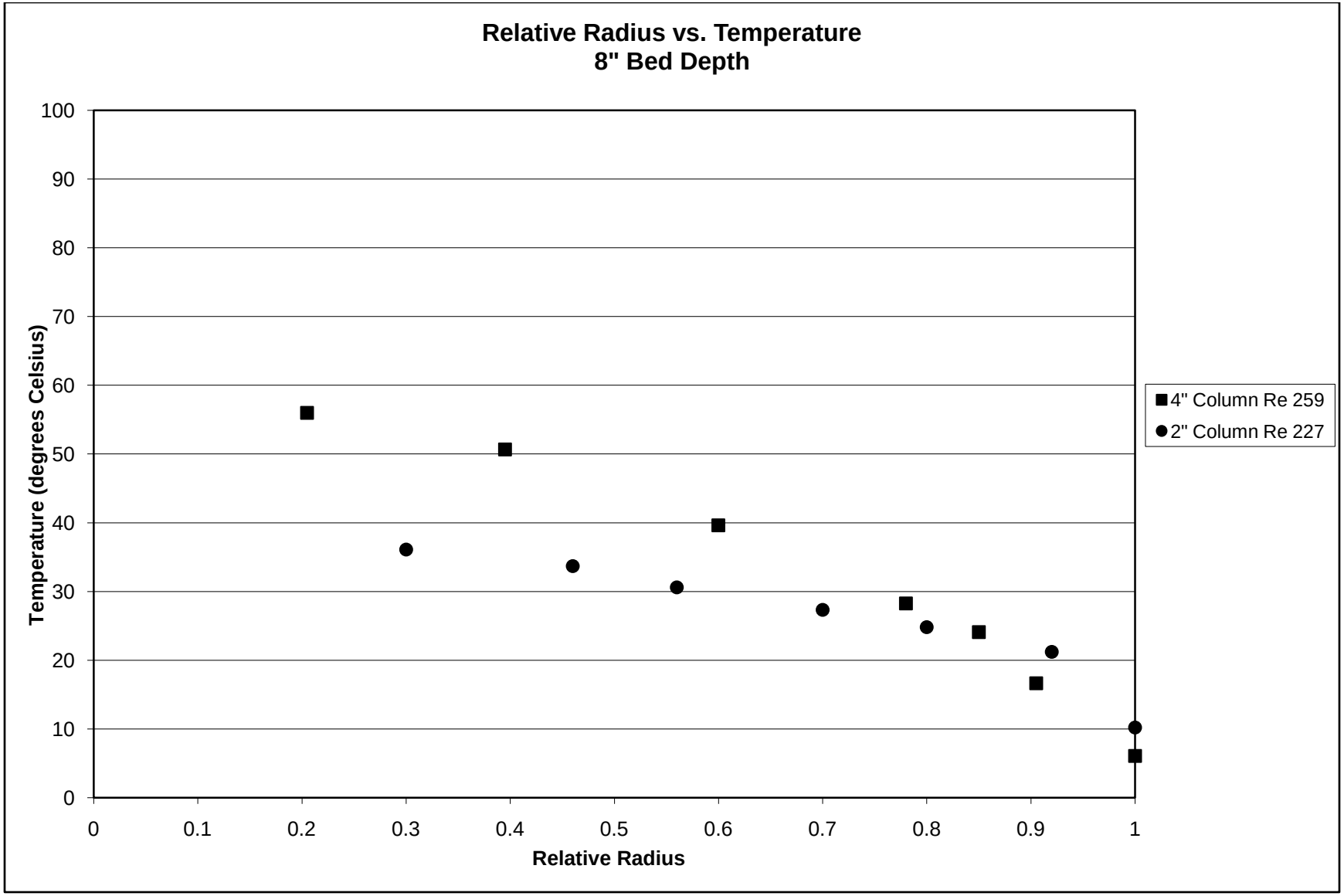
Relative Radius vs. Temperature
8" Bed Depth
Temperature (degrees Celsius)
100
90
80
70
60
50
40
30
20
10
0
0
0.1
0.2
0.3
0.4
0.5
0.6
0.7
0.8
0.9
1
Relative Radius
4" Column Re 259
2" Column Re 227

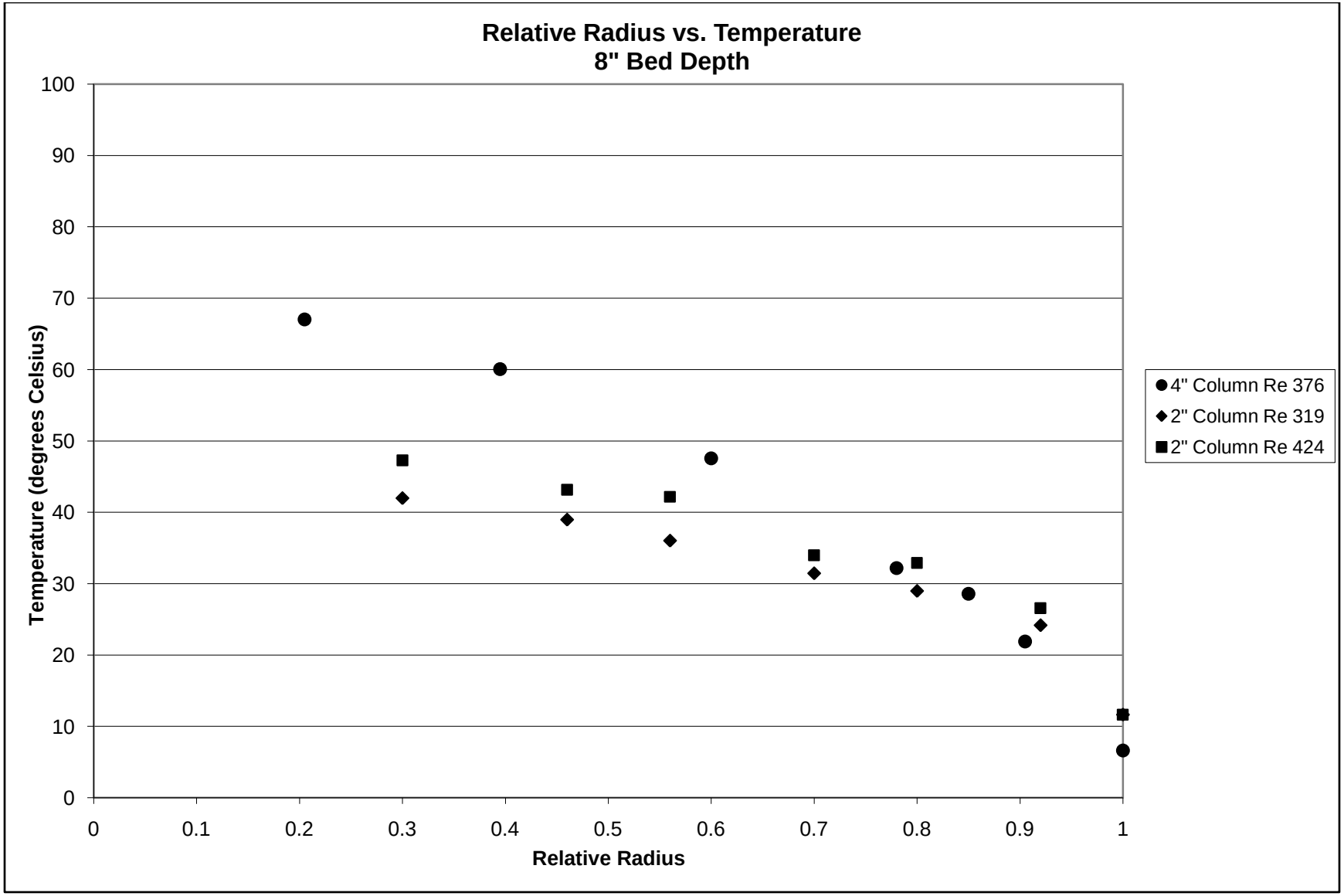
Relative Radius vs. Temperature
8" Bed Depth
Temperature (degrees Celsius)
100
90
80
70
60
50
40
30
20
10
0
0
0.1
0.2
0.3
0.4
0.5
0.6
0.7
0.8
0.9
1
Relative Radius
4" Column Re 376
2" Column Re 319
2" Column Re 424

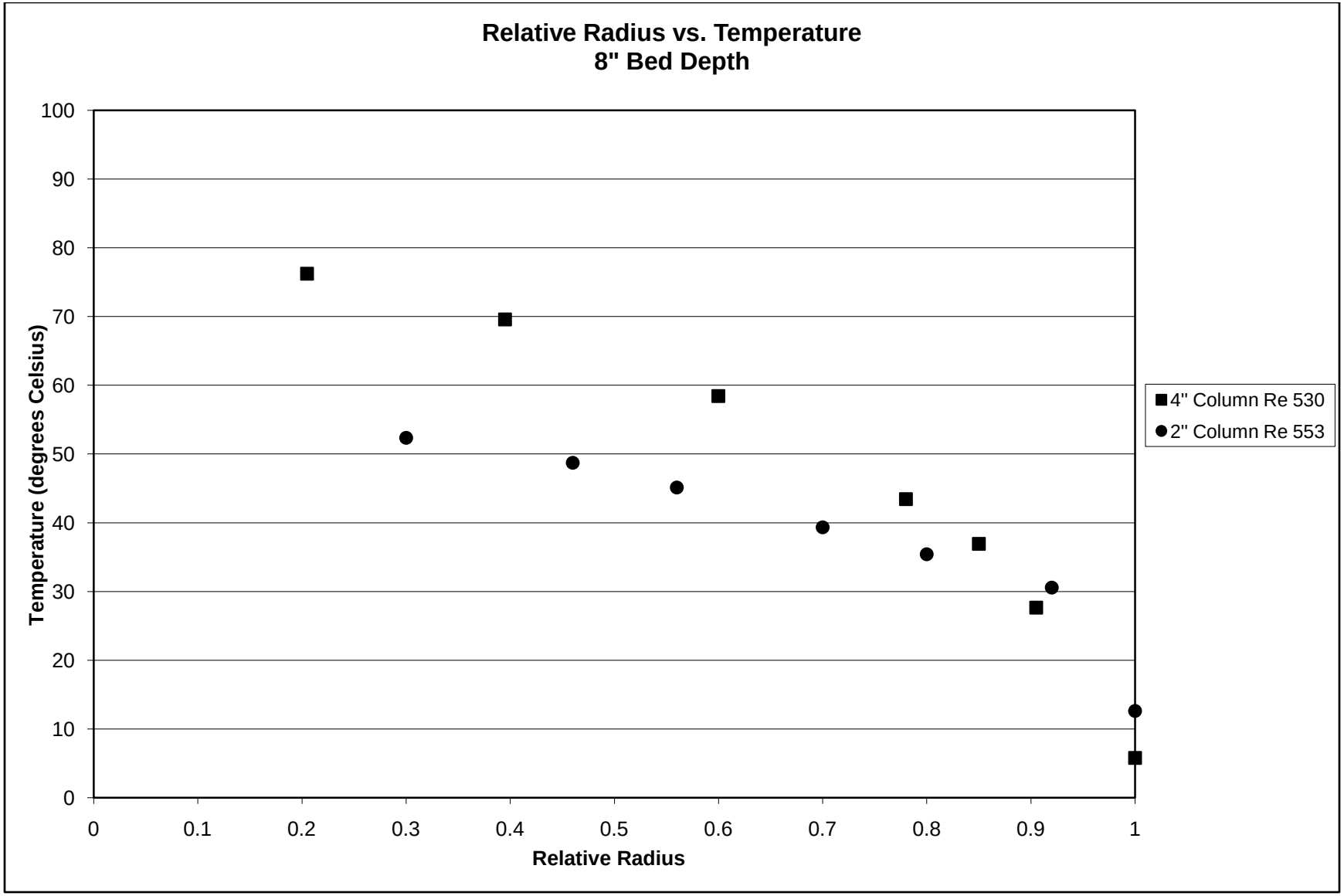
Relative Radius vs. Temperature
8" Bed Depth
Temperature (degrees Celsius)
100
90
80
70
60
50
40
30
20
10
0
0
0.1
0.2
0.3
0.4
0.5
0.6
0.7
0.8
0.9
1
Relative Radius
4" Column Re 530
2" Column Re 553

Appendix H: ExceLinx example input files

ExceLINX KEITHLEY A Greater Measure of Confidence

Task: Scan DMM Channels			
Task	Name	DMM Scan	
	Description		
	Created By	akgurnon	
	Company	Worcester Polytechnic Institute	
	Date Created	9/5/2008	
	Date Modified	12/8/2008	
	Status/Cmds	Stop	
Configuration	Worksheet	DMM Config	
Trigger	Model	Scan	
	Source	Timer	
	Delay	Auto	sec
	Reading Count		200
	Timer	180	sec
	Monitor	None	
	Monitor Limits	None	
Data Location	Worksheet	Run 4	
	Starting Col	B	
	Starting Row	2	
	Organize By	Rows	
	Autoincrement	Use one table	
	Auto Wrap	On	
	Log File		
	Format	Delimited text (comma)	
Data Display	Add Channel Tags	No	
	Add Channels	No	
	Add Units	No	
	Scroll Display	No	
	Limits	None	
	Timestamp	None	
	Update Interval	100	msec

Task Data

Appendix I: ExceLinx example output data file

Run 4	1	2	3	4	5	6	7	8	9	14	15
3	23.42068	22.89231	24.15695	24.55585	21.73233	21.71314	21.71959	21.75516	21.96574	21.81278	23.04303
6	45.46783	22.14618	20.79641	20.70528	22.29508	21.97647	22.02942	23.15322	26.64588	21.99551	21.84852
9	81.27805	19.50862	19.20297	19.23104	23.22986	23.92041	24.76518	29.87285	38.9371	23.85067	22.23216
12	112.2899	18.30693	18.08257	18.25646	27.67336	29.67327	32.27566	41.807	54.45057	32.65987	26.999
15	120.7242	18.12541	17.92116	18.2014	35.33142	38.59314	42.87508	53.77184	65.65064	24.75389	22.40983
18	116.9603	18.2819	18.20545	18.65032	43.54183	47.66985	52.67157	62.11267	70.86792	62.31419	44.09758
21	108.5563	18.24665	18.2356	18.67501	49.56139	54.31194	59.17772	66.16344	71.85067	73.79693	48.66024
24	99.68188	18.39477	18.33914	18.85131	52.66684	58.003	62.36086	67.11557	70.68762	78.43517	49.593
16	17	18	19	20	21	22	37	38	27	28	29
22.97531	23.3842	22.47248	22.66327	22.79073	22.50956	22.60727	22.17102	22.06856	22.10971	21.97283	22.25034
21.89478	21.73333	22.16018	22.00609	22.03364	22.15192	22.1	22.1969	22.20714	21.99326	21.99705	21.99238
22.16558	21.18283	22.79833	23.09288	22.39907	22.7608	23.01923	24.01003	24.20629	23.61322	24.21452	23.24875
26.8036	23.75037	28.72795	29.81625	27.5273	28.88945	29.25391	32.8391	33.35365	31.66516	33.97026	30.72334
24.71649	24.32467	31.80025	25.13455	24.22877	34.27325	25.18208	24.13188	28.49396	25.10085	24.73715	24.34565
45.08158	45.18689	35.01489	39.21066	42.39716	45.20304	41.72604	64.86517	62.63232	60.50227	62.07847	58.44077
49.2494	50.58122	38.26109	43.81696	47.52755	50.67738	46.39891	75.56685	73.0098	70.04592	71.62896	66.84672
53.8886	52.207	39.54292	45.46283	49.99112	52.95296	48.19687	79.70708	77.10088	74.43485	75.44035	69.21192
30	31	32	33	34	35	36	23	24	25	26	
21.97965	22.02357	22.15718	21.94589	22.00514	22.01565	21.9323	22.73674	22.71786	22.4656	22.26586	9.9E+37
22.07528	22.09348	22.02782	22.12819	22.08112	22.07286	22.06569	21.91866	22.01448	22.16994	22.15831	9.9E+37
23.74146	23.94634	23.76043	23.81844	23.89008	24.1765	24.45362	23.46047	22.91199	23.12764	23.49709	9.9E+37
32.21735	32.47439	32.02926	32.3935	32.53386	33.47192	34.55238	30.86107	28.99323	29.94559	30.94534	9.9E+37
33.18301	29.29628	26.19975	27.83124	25.52773	23.82443	25.69066	22.85061	24.91571	31.25646	28.40454	9.9E+37
60.02003	58.08753	65.01016	63.49944	64.28442	66.8538	65.85761	52.30237	62.69295	55.70084	51.7772	9.9E+37
69.10031	67.99407	75.84504	74.29359	73.83496	77.91532	76.43806	58.74007	73.21168	64.09735	58.17078	9.9E+37
72.85588	72.29625	80.15862	78.85751	77.02613	81.99568	80.69933	62.85204	77.34766	67.26083	60.33762	9.9E+37

Appendix J: Example Notepad File for 2-parameter model Input

4 rows of thermocouple data

7 accounts for the number of radial positions

8 accounts for the 8 thermocouples in the wall and calming sections of the bed

2 accounts for the two angles measured

The second row is the radial positions in inches.

The third row has the locations for the thermocouples in the wall.

The fourth row is the bed radius and the particle diameter.

The fifth row has the Reynolds number, bed height and angle.

The sixth row is the inlet temperature.

The seventh row has all of the temperature readings for the thermocouples in the wall.

The following rows have the temperature readings for the thermocouples on the cross

corresponding with the thermocouple locations in the second row.

4 7 8 2
0.0 0.30 0.46 0.56 0.70 0.80 0.92
-5.0 -3.0 -1.0 -0.625 -0.25 3.0 9.0 15.0
1.0 0.25
785 2.0 0
98.39
80.58 81.11 78.16 74.55 68.60 16.25 15.24 15.72
85.14 85.37 80.90 79.54 67.86 50.48 54.14
-1.00 83.06 85.29 76.33 79.10 60.46 53.31
-1.00 84.71 82.20 75.64 75.70 54.73 50.59
-1.00 81.31 81.46 74.81 65.67 54.73 45.99
785 2.0 45
98.64
80.68 81.29 78.37 74.76 68.80 16.44 15.53 16.96
84.70 83.36 82.01 76.86 69.00 62.13 64.41
-1.00 85.08 78.93 80.37 68.32 64.39 53.34
-1.00 85.68 83.58 82.72 70.82 66.50 57.86
-1.00 84.50 77.81 80.83 70.26 63.35 55.81
-1.00 0.00 0.00

Appendix K Comparing Calculated Predictions and Experimental Data

K.1 Radial Position vs. Temperature, 2" Column

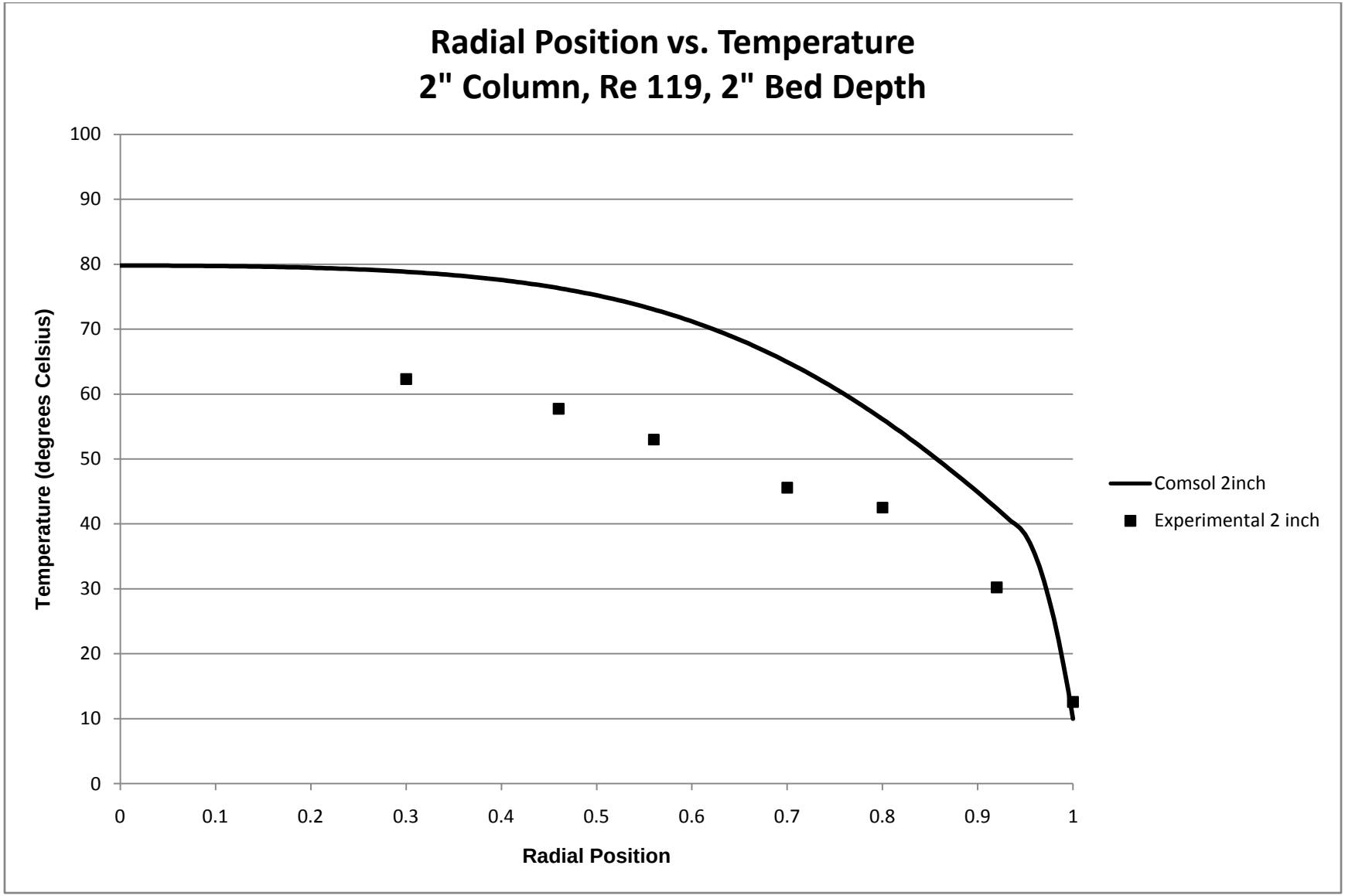
Radial Position vs. Temperature
2" Column, Re 119, 2" Bed Depth
Temperature (degrees Celsius)
100
90
80
70
60
50
40
30
20
10
0
0
0.1
0.2
0.3
0.4
0.5
0.6
0.7
0.8
0.9
1
Radial Position
Comsol 2inch
Experimental 2 inch

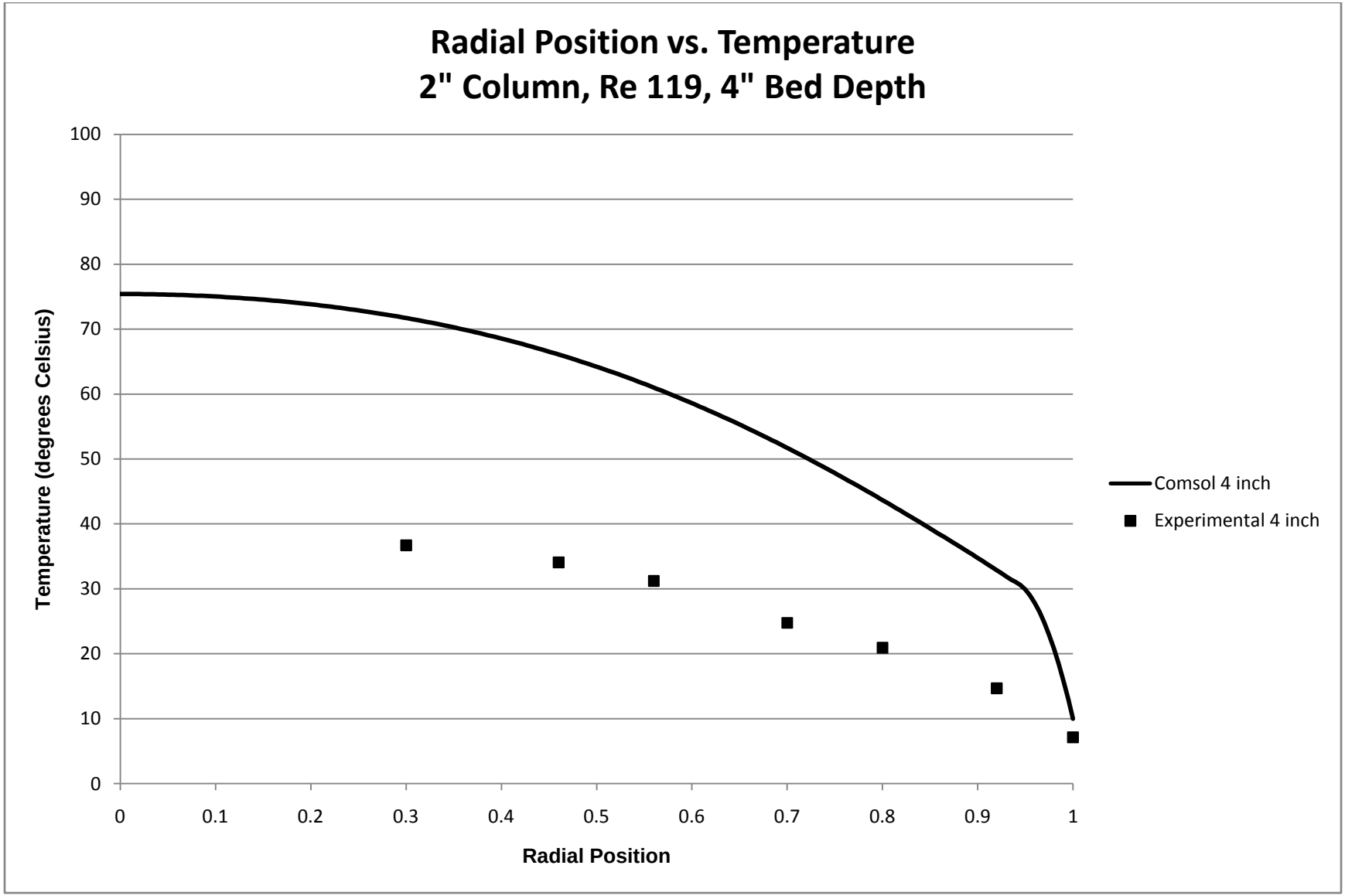
Radial Position vs. Temperature
2" Column, Re 119, 4" Bed Depth
Temperature (degrees Celsius)
100
90
80
70
60
50
40
30
20
10
0
0
0.1
0.2
0.3
0.4
0.5
0.6
0.7
0.8
0.9
1
Radial Position
Comsol 4 inch
Experimental 4 inch

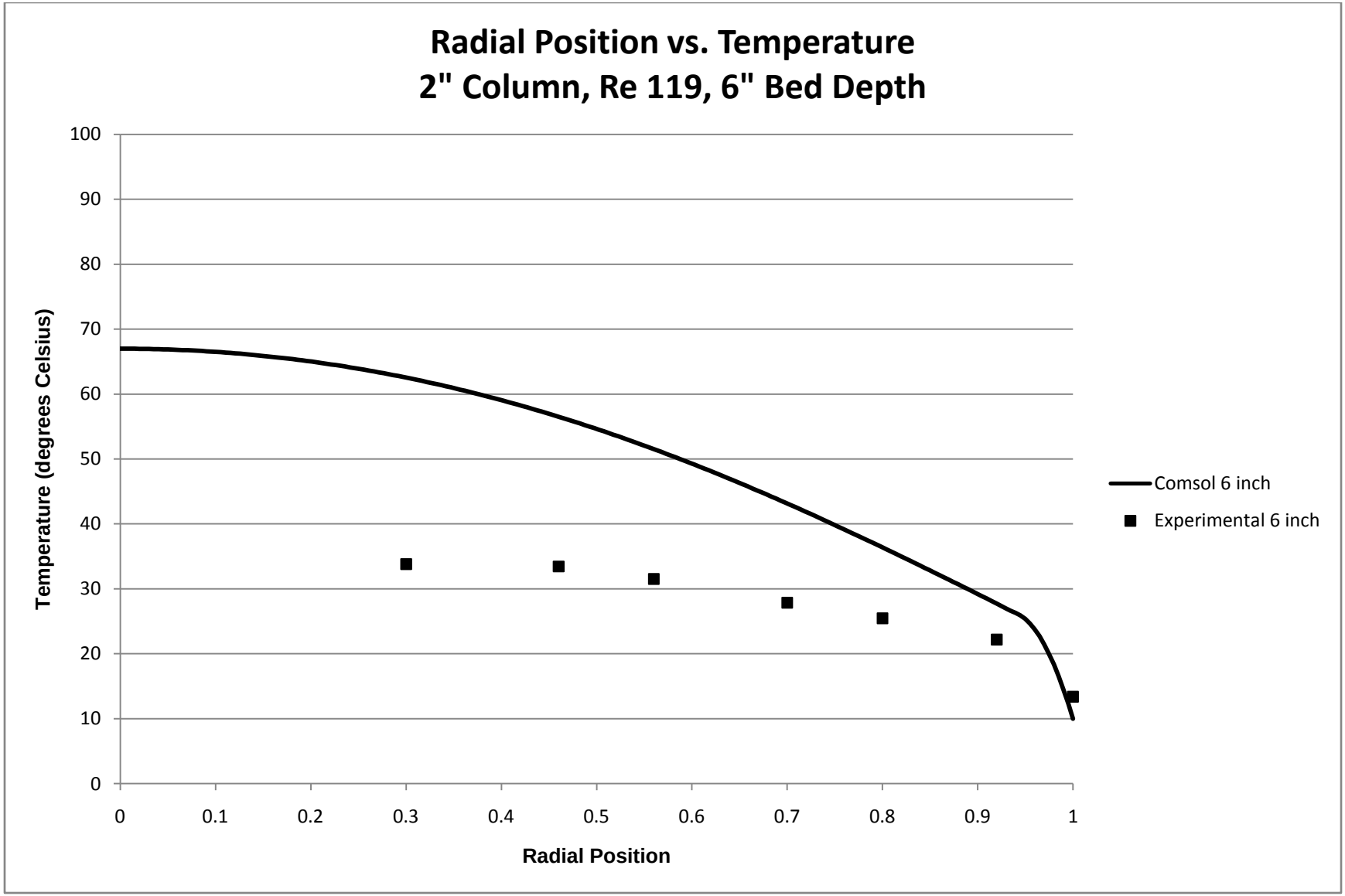
Radial Position vs. Temperature
2" Column, Re 119, 6" Bed Depth
Temperature (degrees Celsius)
100
90
80
70
60
50
40
30
20
10
0
0
0.1
0.2
0.3
0.4
0.5
0.6
0.7
0.8
0.9
1
Radial Position
Comsol 6 inch
Experimental 6 inch

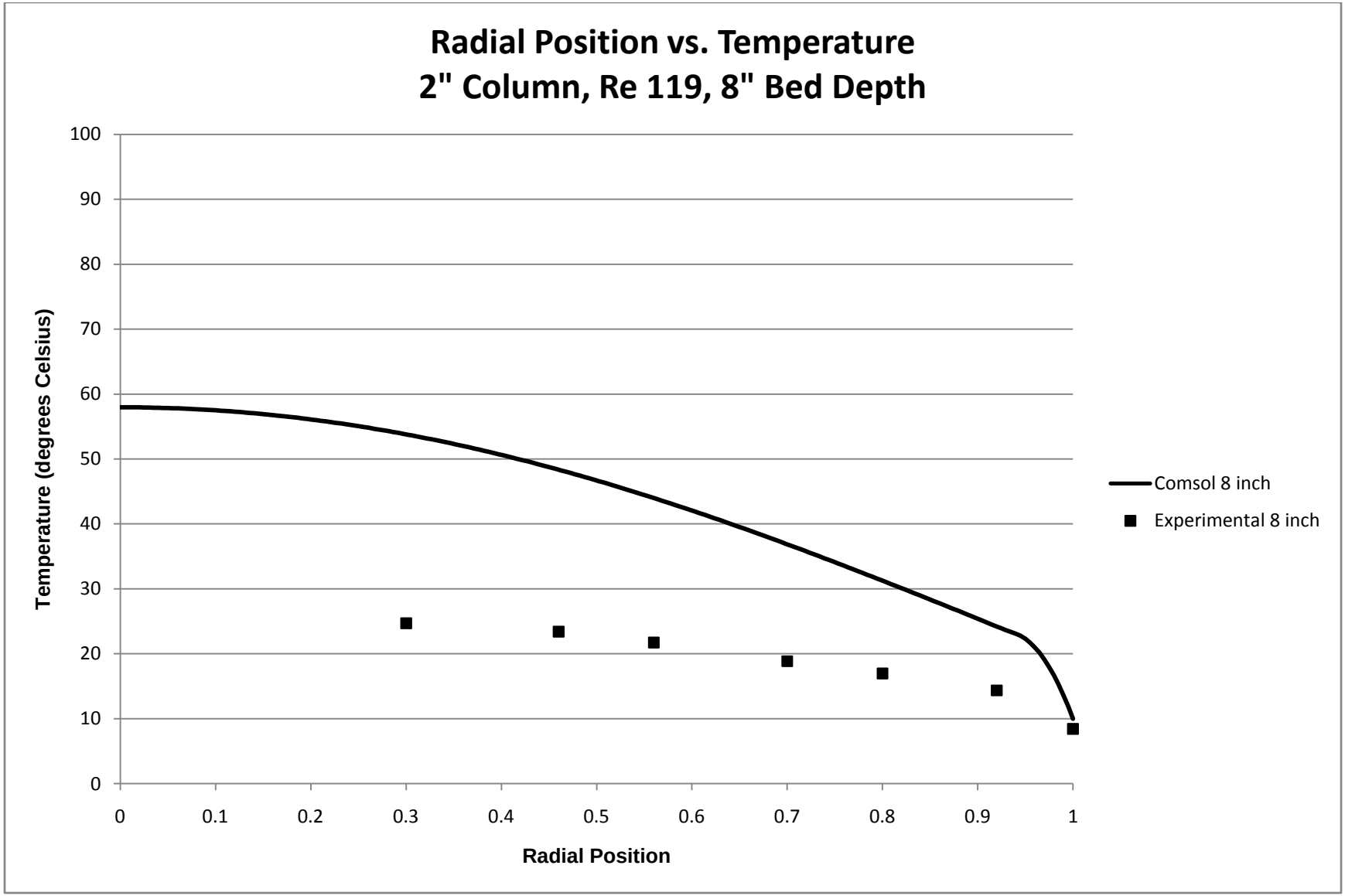
Radial Position vs. Temperature
2" Column, Re 119, 8" Bed Depth
Temperature (degrees Celsius)
100
90
80
70
60
50
40
30
20
10
0
0
0.1
0.2
0.3
0.4
0.5
0.6
0.7
0.8
0.9
1
Radial Position
Comsol 8 inch
Experimental 8 inch

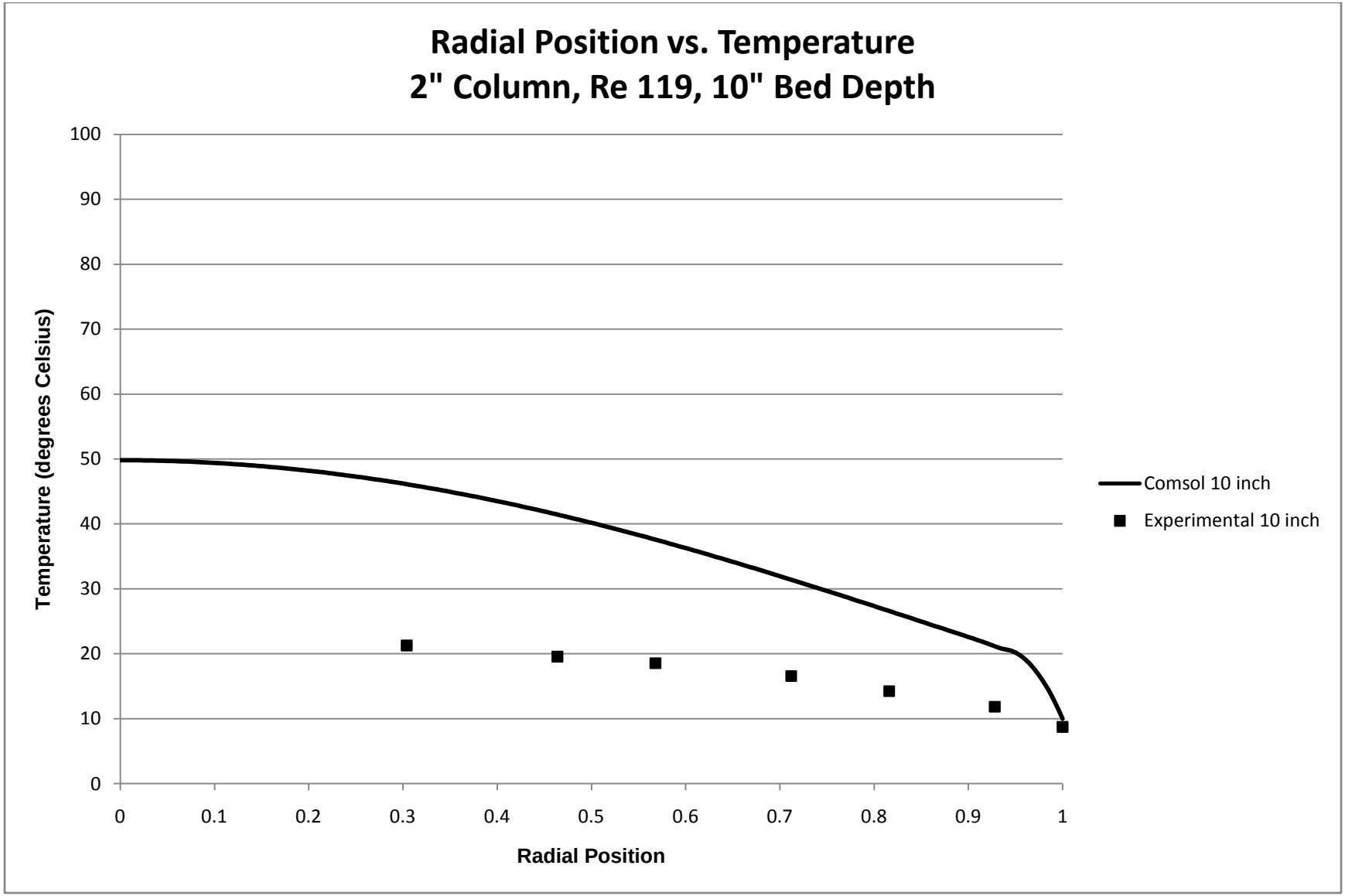
Radial Position vs. Temperature
2" Column, Re 119, 10" Bed Depth
Temperature (degrees Celsius)
100
90
80
70
60
50
40
30
20
10
0
0
0.1
0.2
0.3
0.4
0.5
0.6
0.7
0.8
0.9
1
Radial Position
Comsol 10 inch
Experimental 10 inch

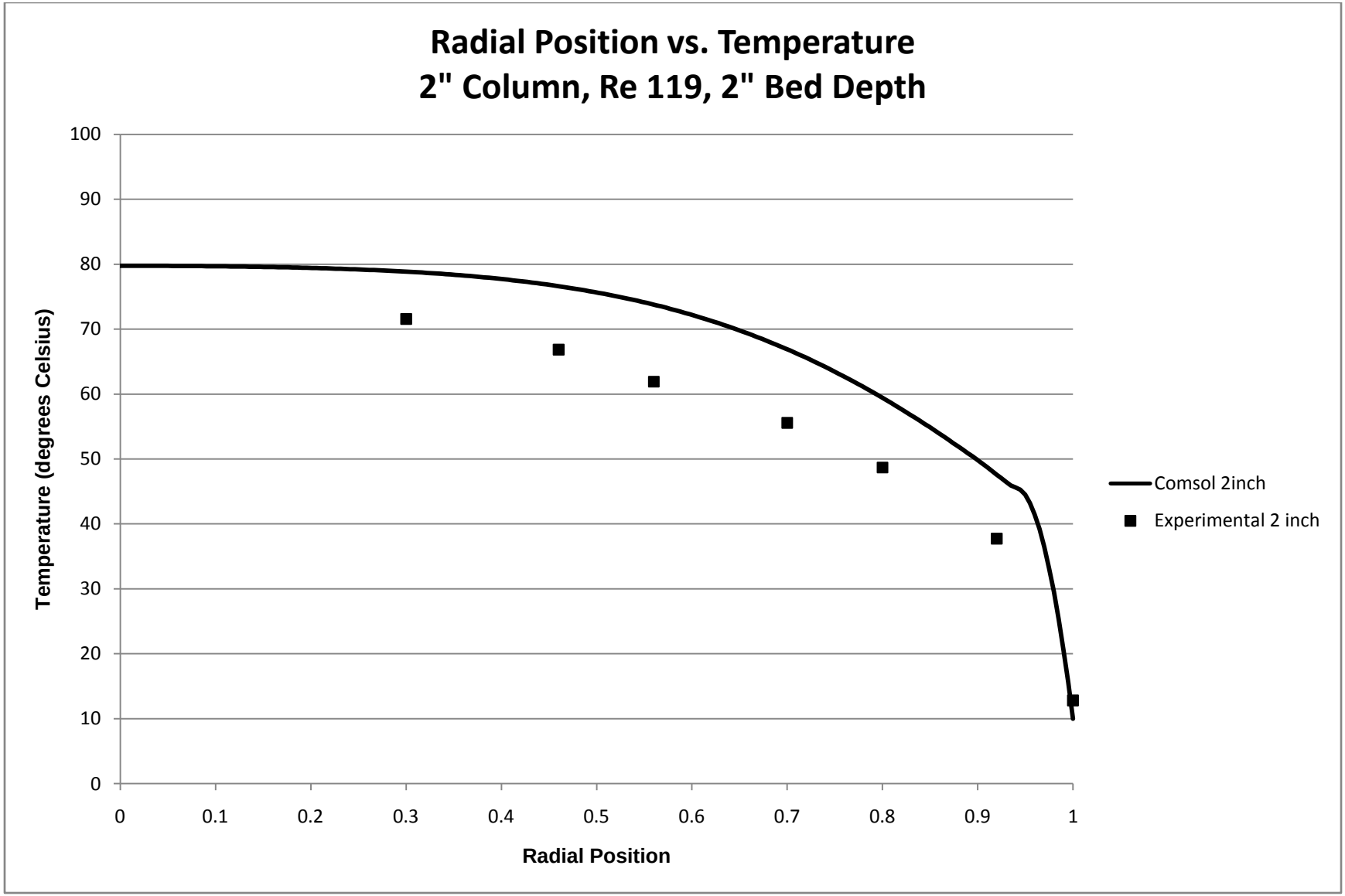
Radial Position vs. Temperature
2" Column, Re 119, 2" Bed Depth
Temperature (degrees Celsius)
100
90
80
70
60
50
40
30
20
10
0
0
0.1
0.2
0.3
0.4
0.5
0.6
0.7
0.8
0.9
1
Radial Position
Comsol 2inch
Experimental 2 inch

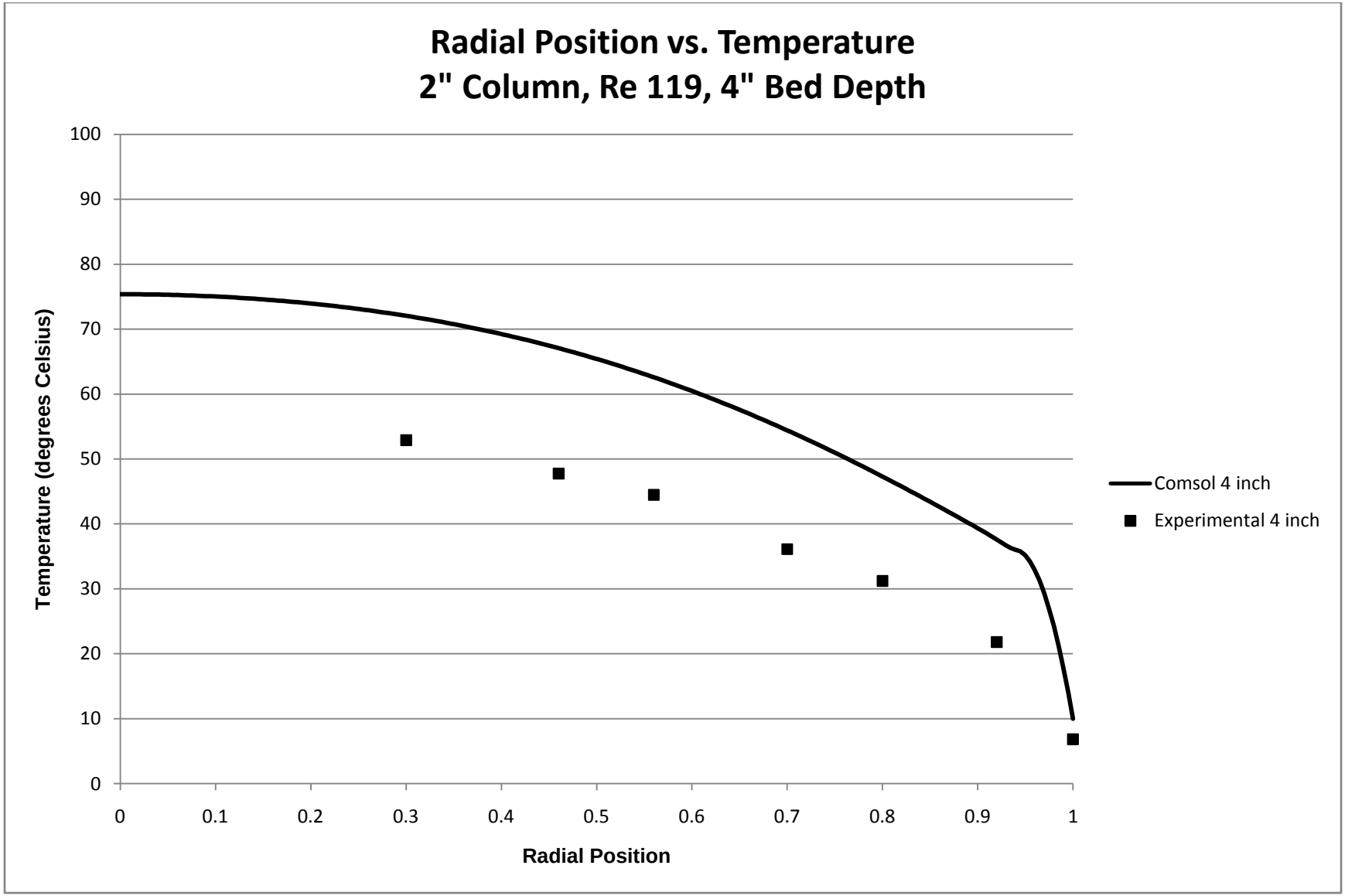
Radial Position vs. Temperature
2" Column, Re 119, 4" Bed Depth
Temperature (degrees Celsius)
100
90
80
70
60
50
40
30
20
10
0
0
0.1
0.2
0.3
0.4
0.5
0.6
0.7
0.8
0.9
1
Radial Position
Comsol 4 inch
Experimental 4 inch

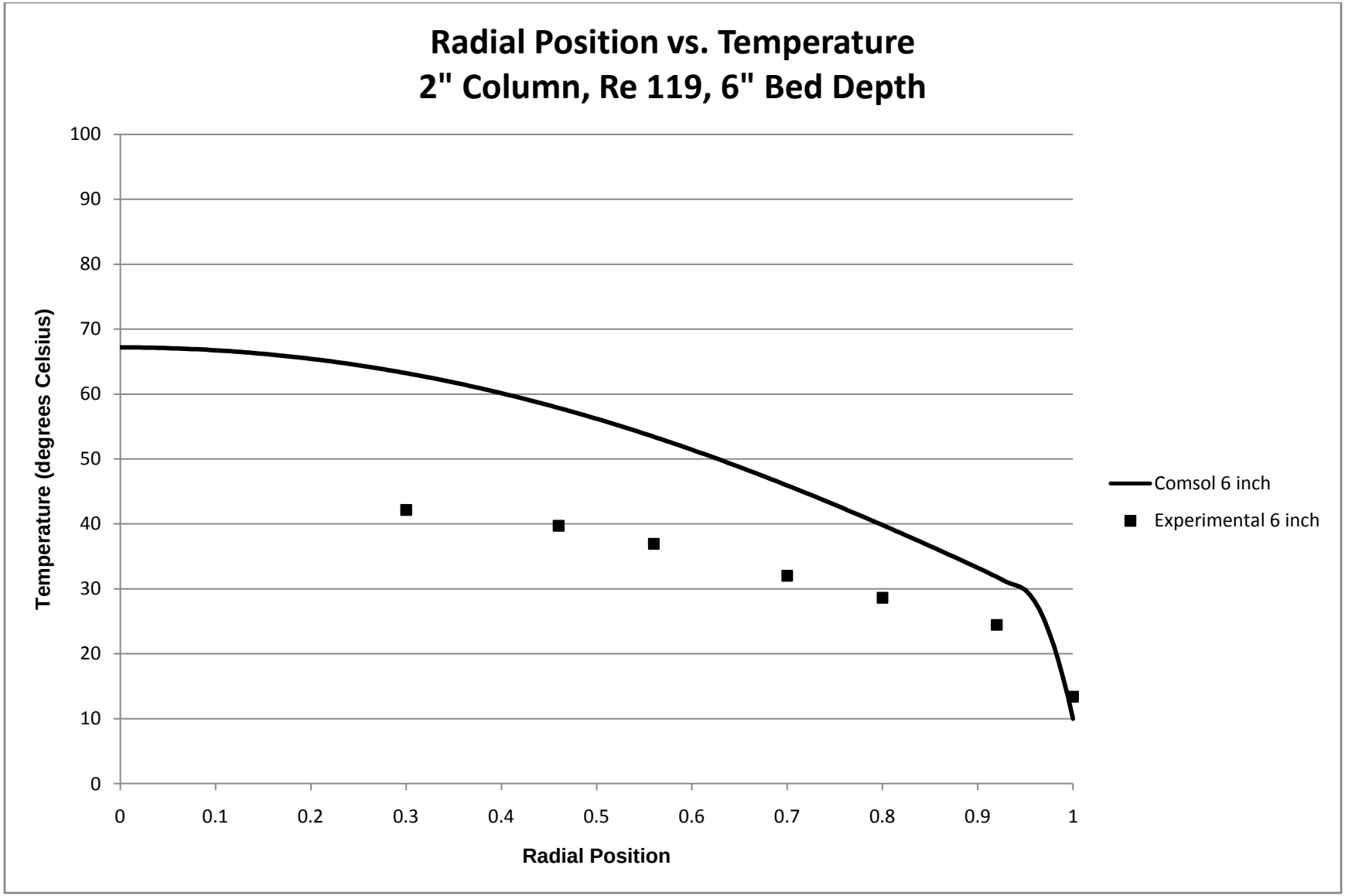
Radial Position vs. Temperature
2" Column, Re 119, 6" Bed Depth
Temperature (degrees Celsius)
100
90
80
70
60
50
40
30
20
10
0
0
0.1
0.2
0.3
0.4
0.5
0.6
0.7
0.8
0.9
1
Radial Position
Comsol 6 inch
Experimental 6 inch

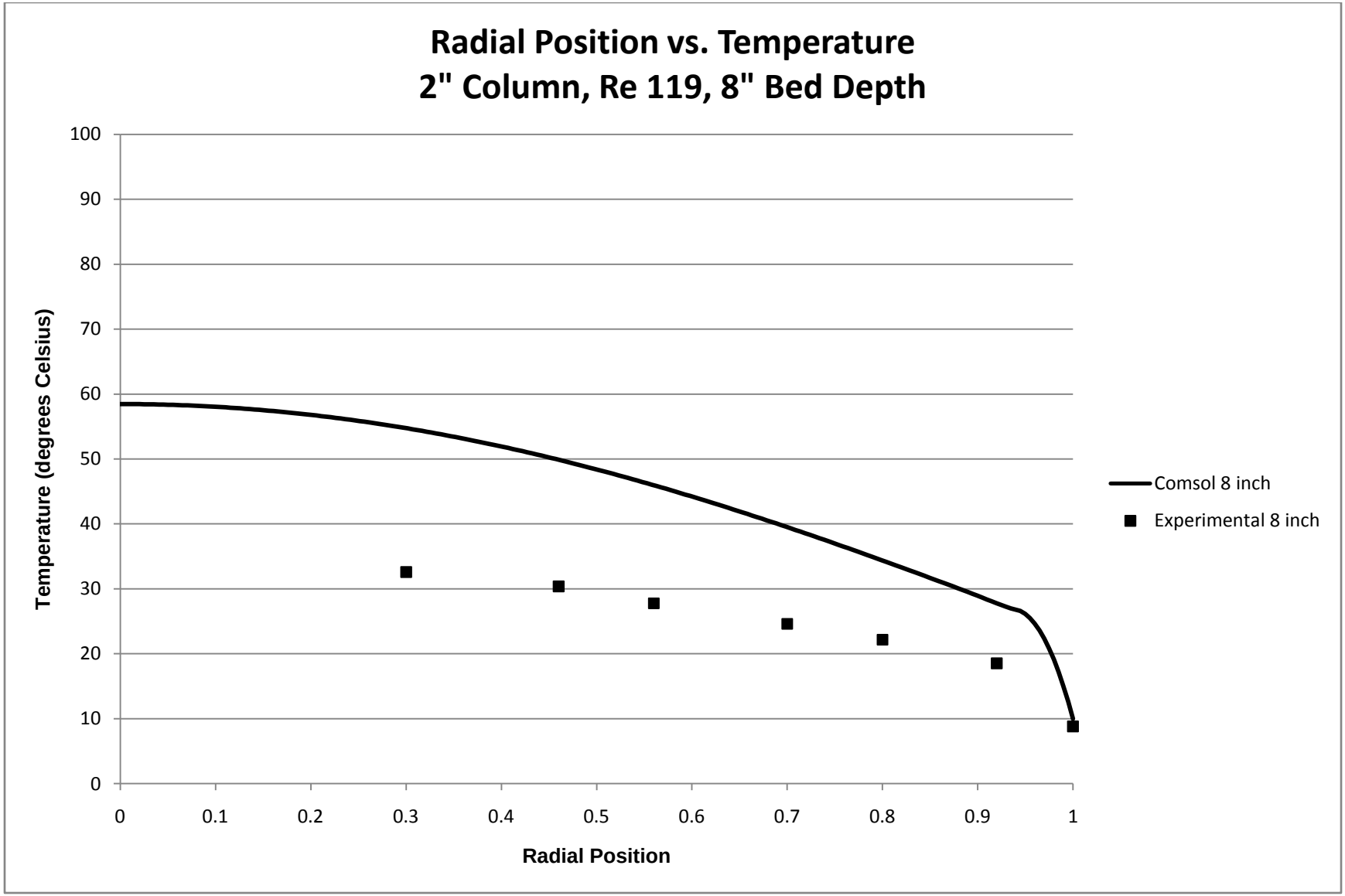
Radial Position vs. Temperature
2" Column, Re 119, 8" Bed Depth
Temperature (degrees Celsius)
100
90
80
70
60
50
40
30
20
10
0
0
0.1
0.2
0.3
0.4
0.5
0.6
0.7
0.8
0.9
1
Radial Position
Comsol 8 inch
Experimental 8 inch

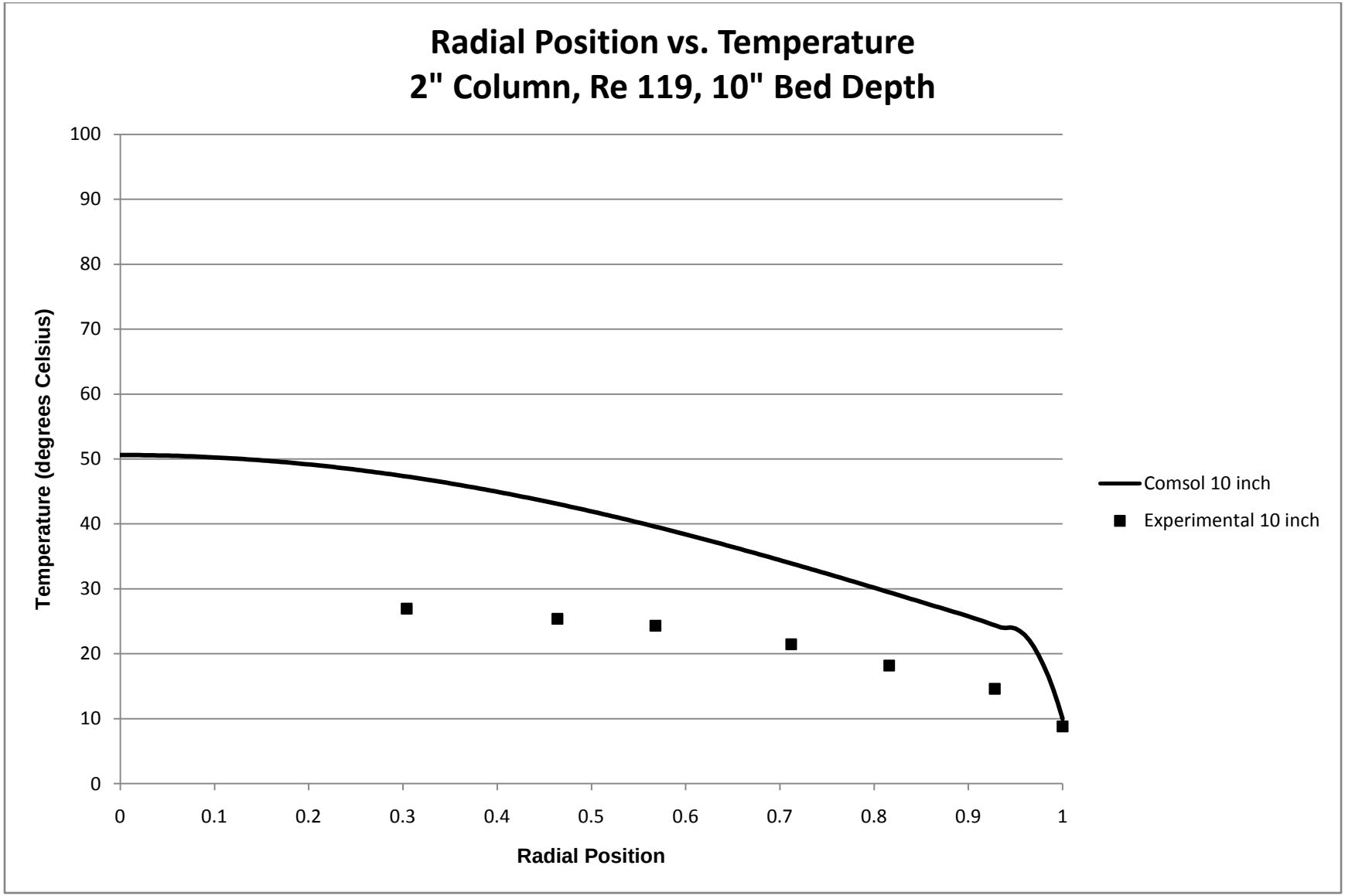
Radial Position vs. Temperature
2" Column, Re 119, 10" Bed Depth
Temperature (degrees Celsius)
100
90
80
70
60
50
40
30
20
10
0
0
0.1
0.2
0.3
0.4
0.5
0.6
0.7
0.8
0.9
1
Radial Position
Comsol 10 inch
Experimental 10 inch

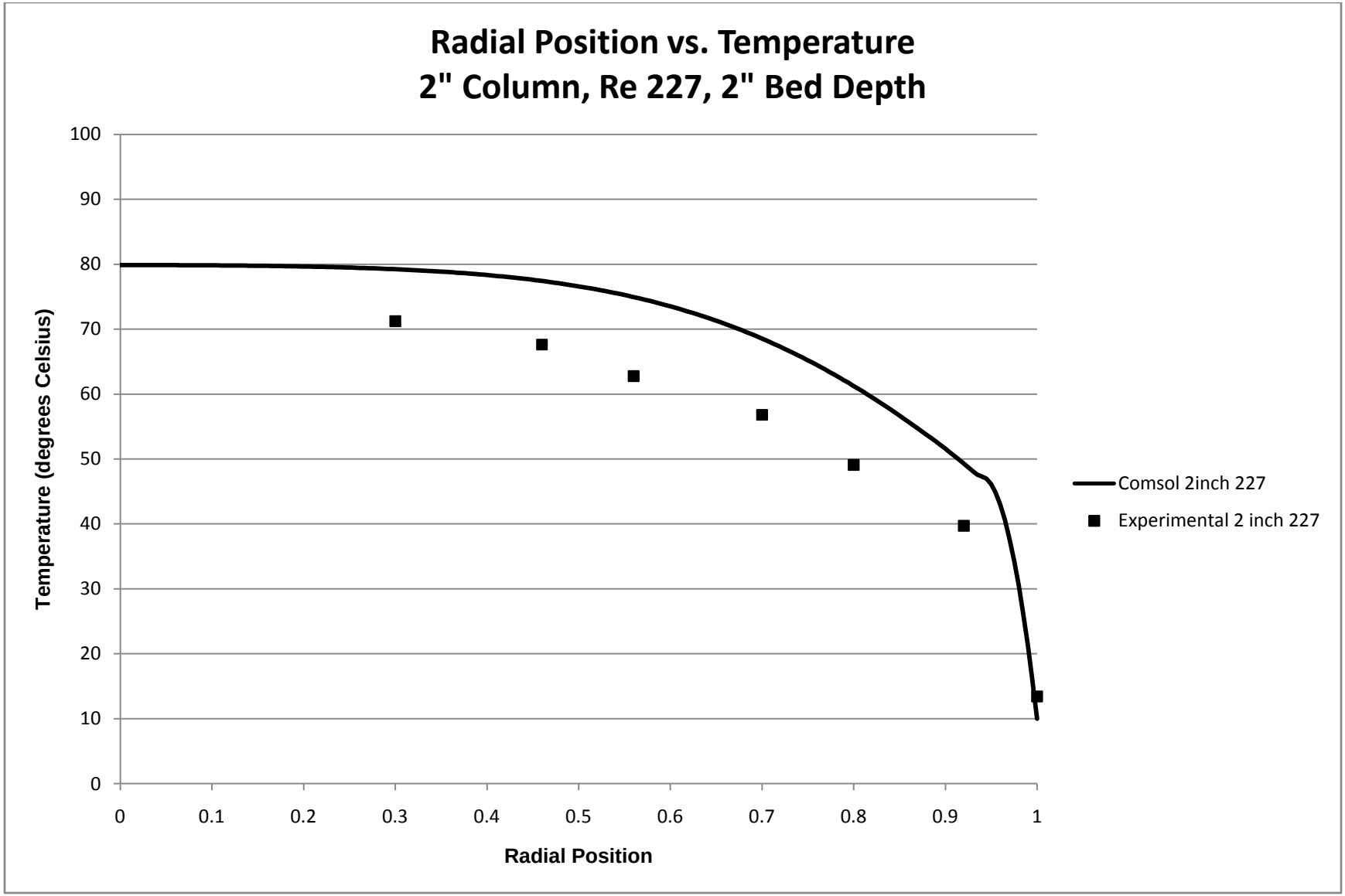
Radial Position vs. Temperature
2" Column, Re 227, 2" Bed Depth
Temperature (degrees Celsius)
100
90
80
70
60
50
40
30
20
10
0
0
0.1
0.2
0.3
0.4
0.5
0.6
0.7
0.8
0.9
1
Radial Position
Comsol 2inch 227
Experimental 2 inch 227

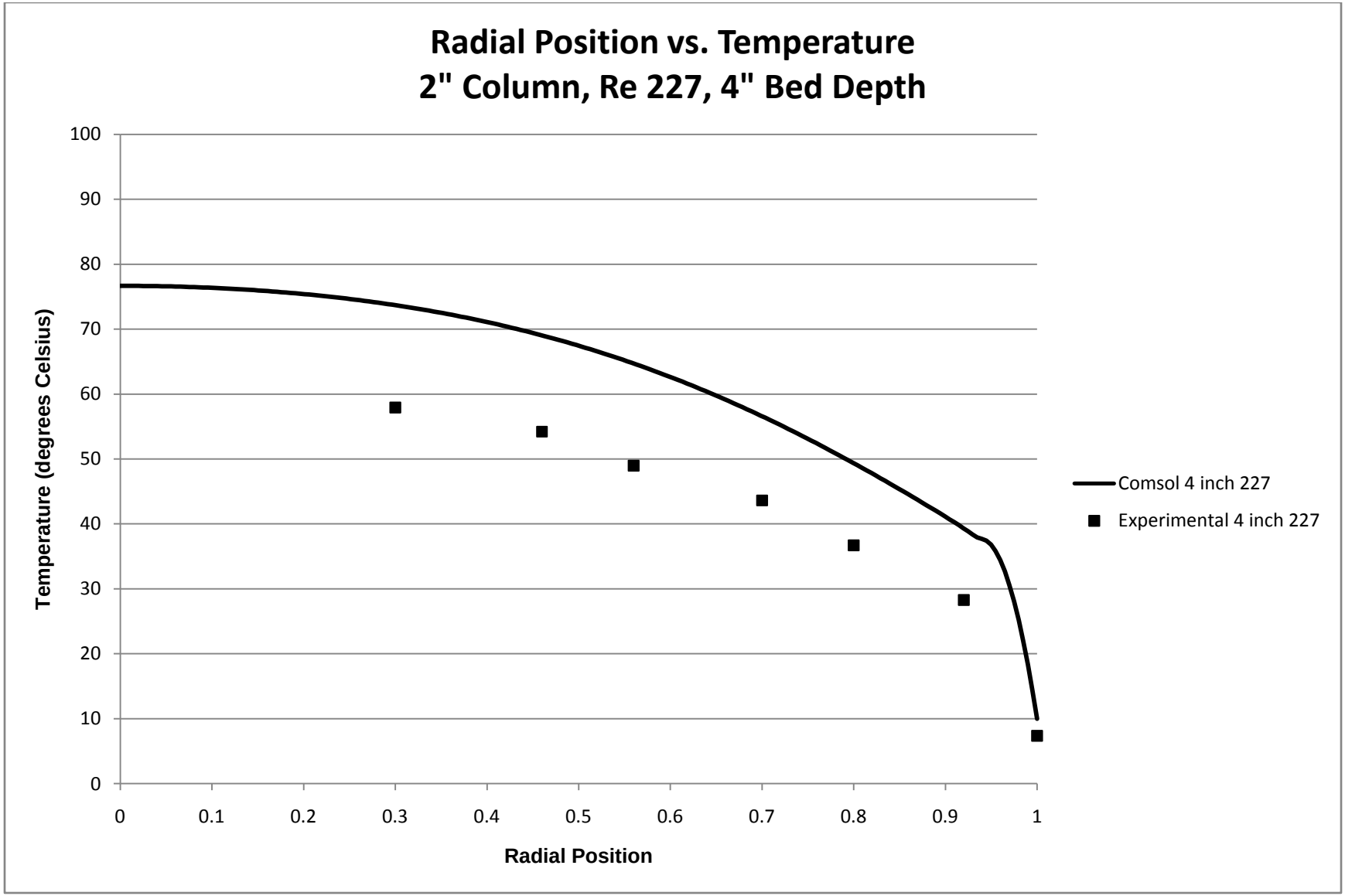
Radial Position vs. Temperature
2" Column, Re 227, 4" Bed Depth
Temperature (degrees Celsius)
100
90
80
70
60
50
40
30
20
10
0
0
0.1
0.2
0.3
0.4
0.5
0.6
0.7
0.8
0.9
1
Radial Position
Comsol 4 inch 227
Experimental 4 inch 227

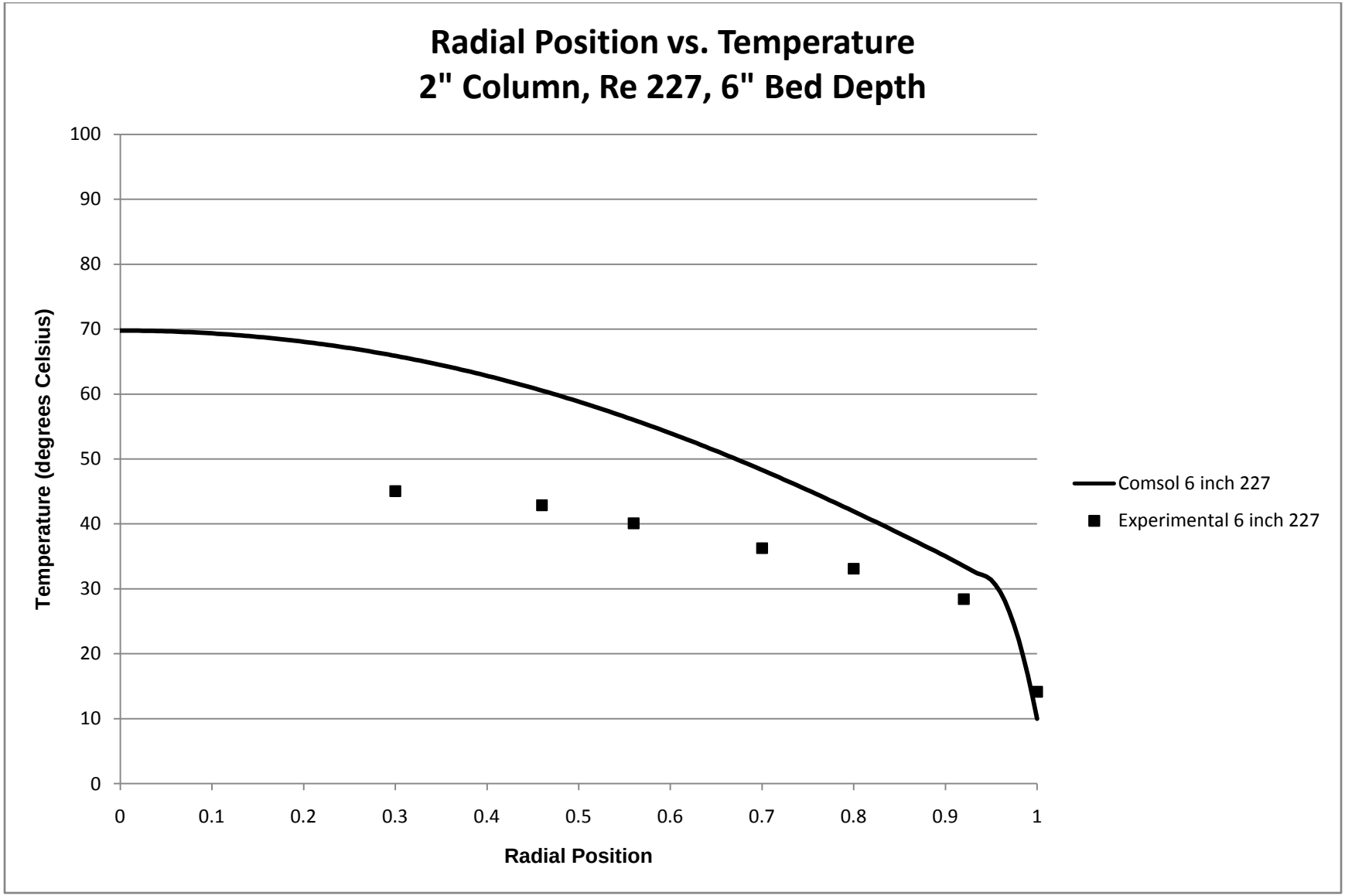
Radial Position vs. Temperature
2" Column, Re 227, 6" Bed Depth
Temperature (degrees Celsius)
100
90
80
70
60
50
40
30
20
10
0
0
0.1
0.2
0.3
0.4
0.5
0.6
0.7
0.8
0.9
1
Radial Position
Comsol 6 inch 227
Experimental 6 inch 227

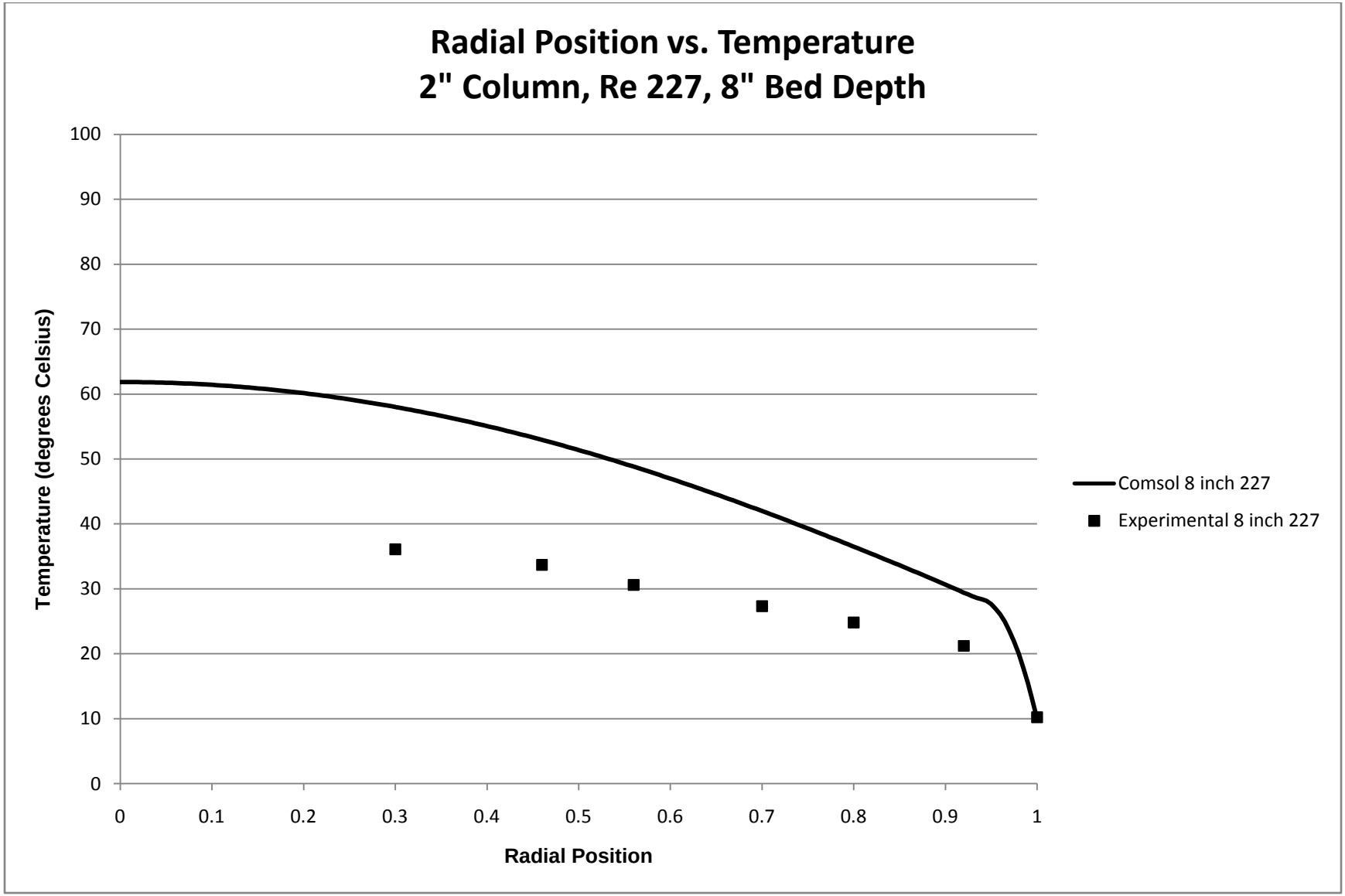
Radial Position vs. Temperature
2" Column, Re 227, 8" Bed Depth
Temperature (degrees Celsius)
100
90
80
70
60
50
40
30
20
10
0
0
0.1
0.2
0.3
0.4
0.5
0.6
0.7
0.8
0.9
1
Radial Position
Comsol 8 inch 227
Experimental 8 inch 227

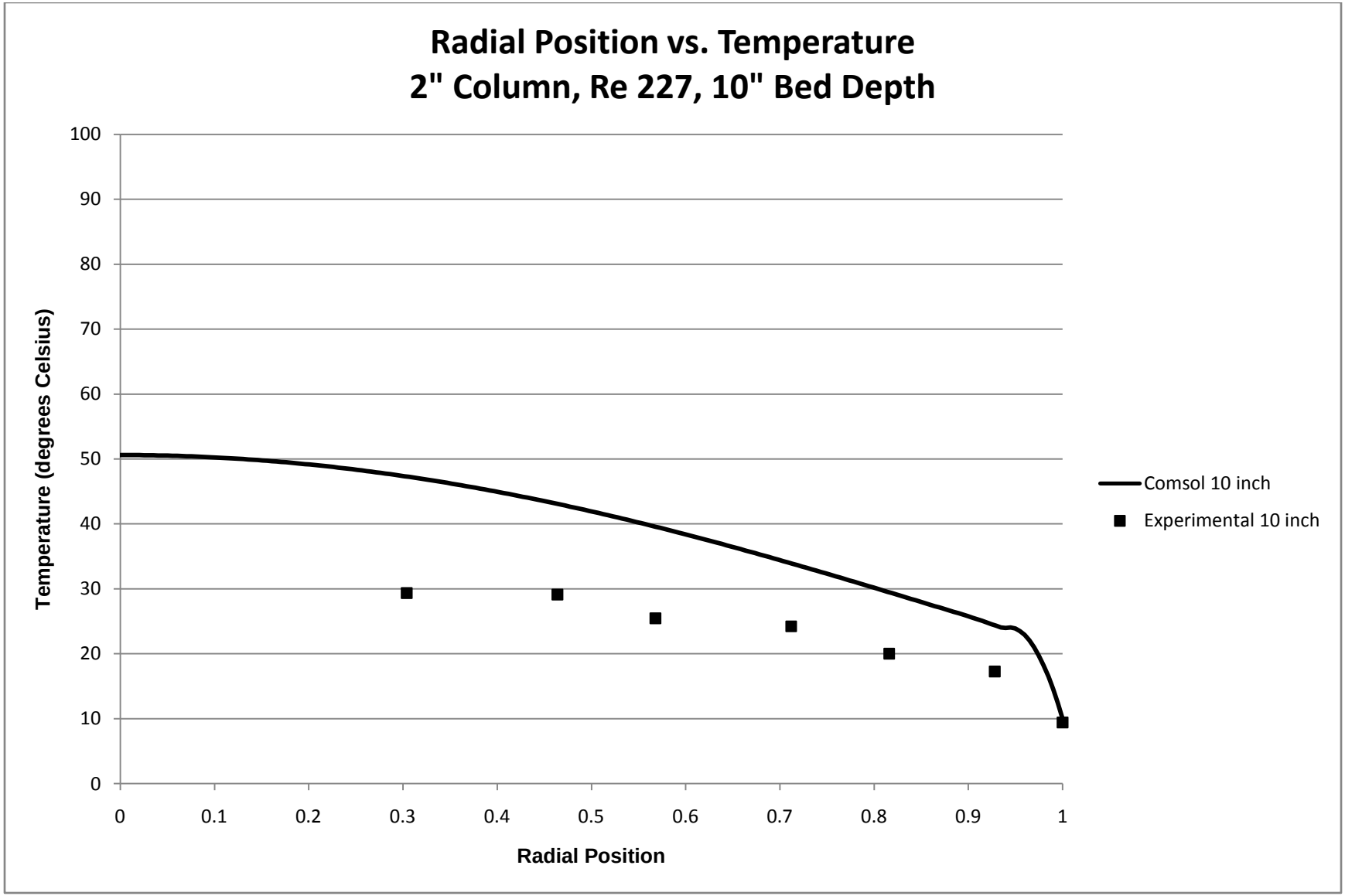
Radial Position vs. Temperature
2" Column, Re 227, 10" Bed Depth
Temperature (degrees Celsius)
100
90
80
70
60
50
40
30
20
10
0
0
0.1
0.2
0.3
0.4
0.5
0.6
0.7
0.8
0.9
1
Radial Position
Comsol 10 inch
Experimental 10 inch

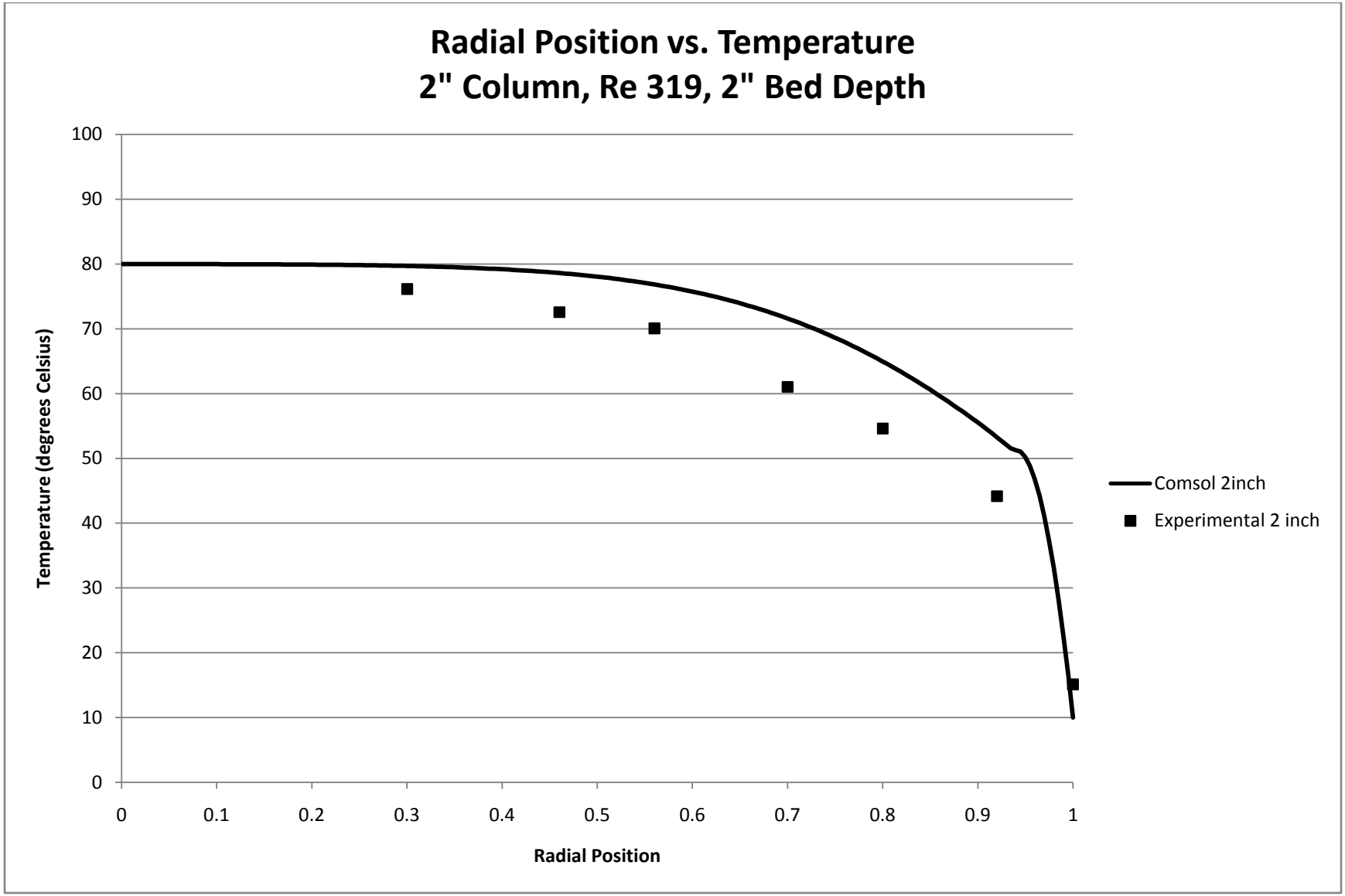
Radial Position vs. Temperature
2" Column, Re 319, 2" Bed Depth
Temperature (degrees Celsius)
100
90
80
70
60
50
40
30
20
10
0
0
0.1
0.2
0.3
0.4
0.5
0.6
0.7
0.8
0.9
1
Radial Position
Comsol 2inch
Experimental 2 inch

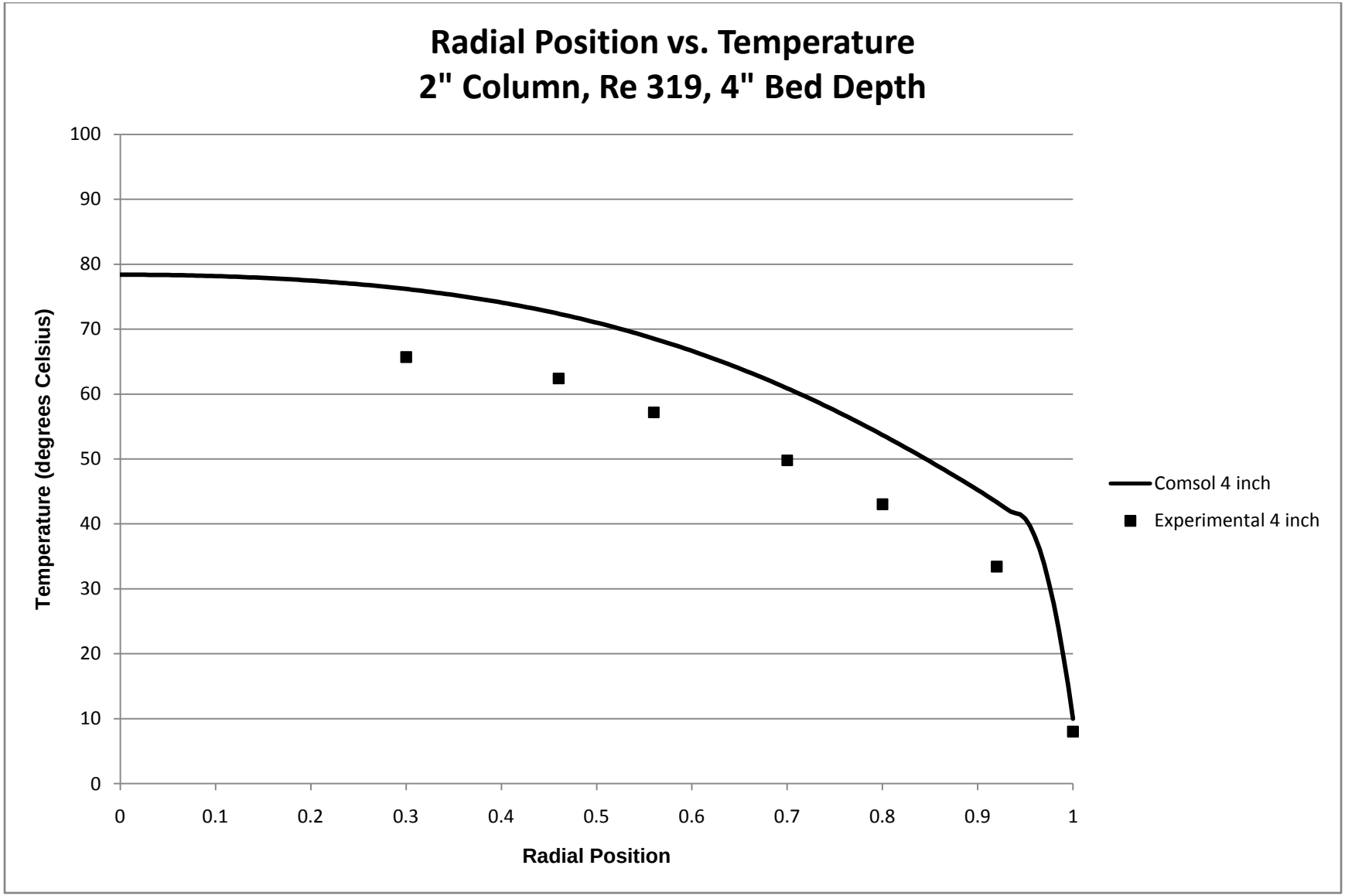
Radial Position vs. Temperature
2" Column, Re 319, 4" Bed Depth
Temperature (degrees Celsius)
100
90
80
70
60
50
40
30
20
10
0
0
0.1
0.2
0.3
0.4
0.5
0.6
0.7
0.8
0.9
1
Radial Position
Comsol 4 inch
Experimental 4 inch

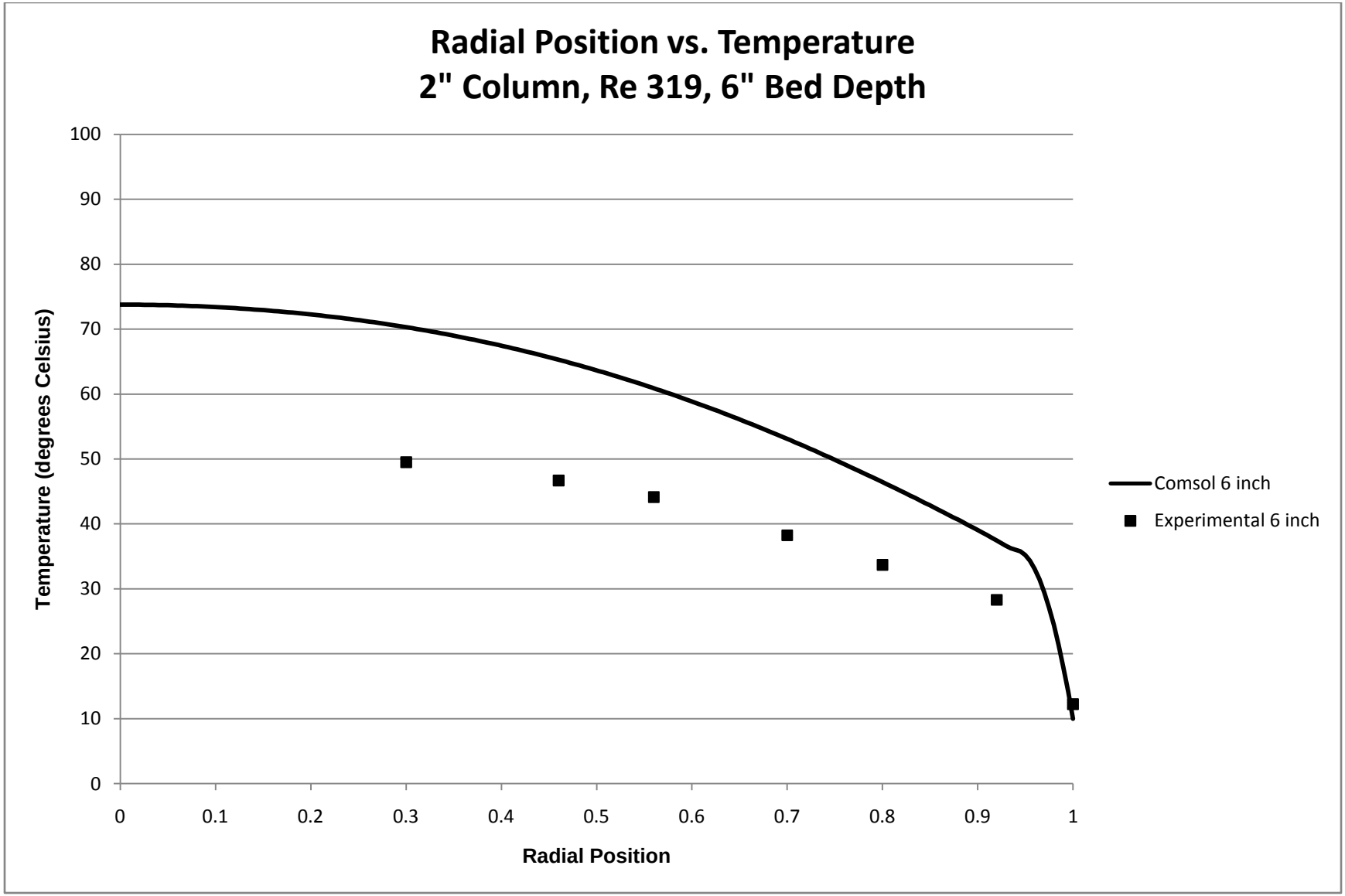
Radial Position vs. Temperature
2" Column, Re 319, 6" Bed Depth
Temperature (degrees Celsius)
100
90
80
70
60
50
40
30
20
10
0
0
0.1
0.2
0.3
0.4
0.5
0.6
0.7
0.8
0.9
1
Radial Position
Comsol 6 inch
Experimental 6 inch

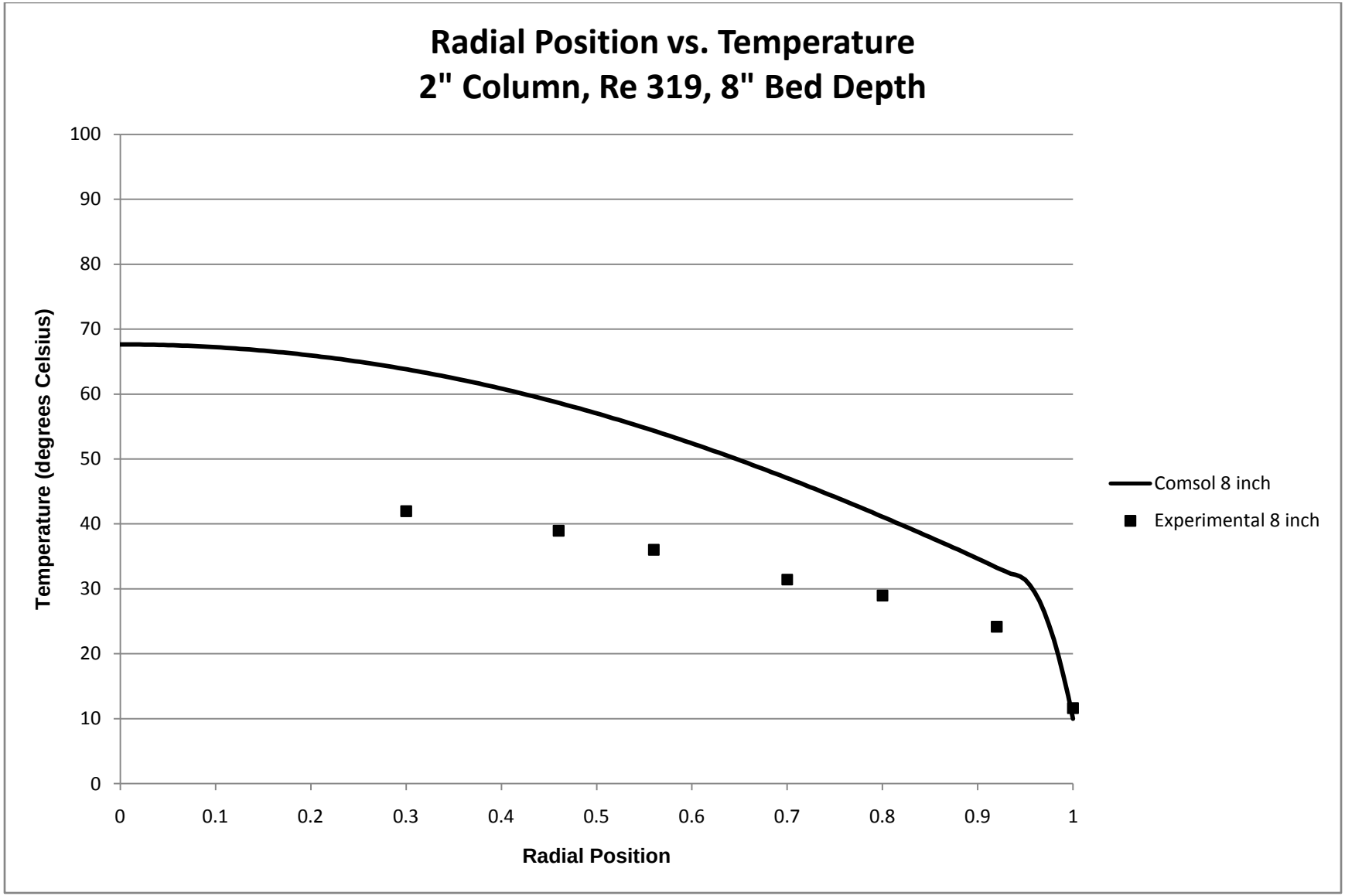
Radial Position vs. Temperature
2" Column, Re 319, 8" Bed Depth
Temperature (degrees Celsius)
100
90
80
70
60
50
40
30
20
10
0
0
0.1
0.2
0.3
0.4
0.5
0.6
0.7
0.8
0.9
1
Radial Position
Comsol 8 inch
Experimental 8 inch

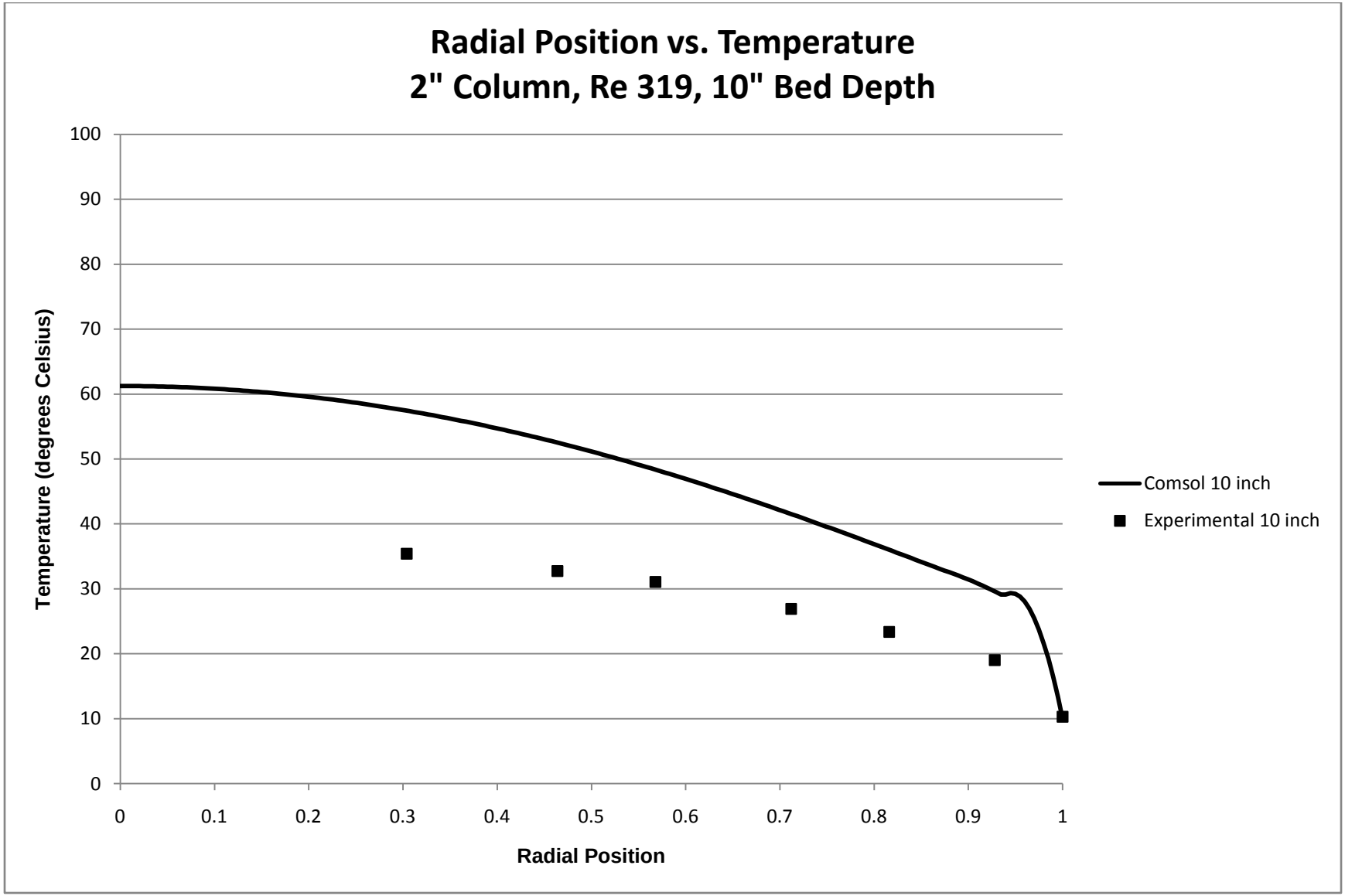
Radial Position vs. Temperature
2" Column, Re 319, 10" Bed Depth
Temperature (degrees Celsius)
100
90
80
70
60
50
40
30
20
10
0
0
0.1
0.2
0.3
0.4
0.5
0.6
0.7
0.8
0.9
1
Radial Position
Comsol 10 inch
Experimental 10 inch

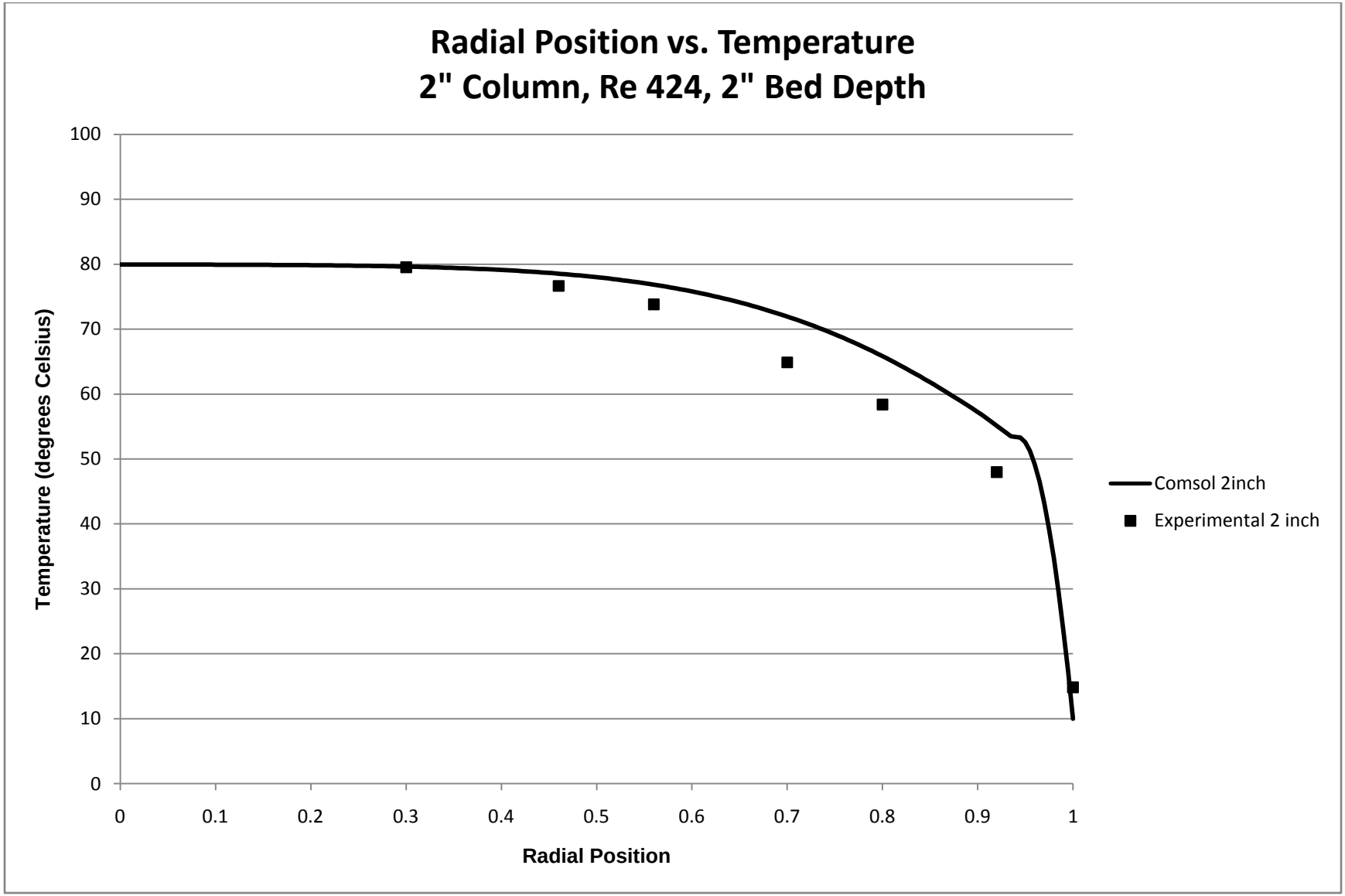
Radial Position vs. Temperature
2" Column, Re 424, 2" Bed Depth
Temperature (degrees Celsius)
100
90
80
70
60
50
40
30
20
10
0
0
0.1
0.2
0.3
0.4
0.5
0.6
0.7
0.8
0.9
1
Radial Position
Comsol 2inch
Experimental 2 inch

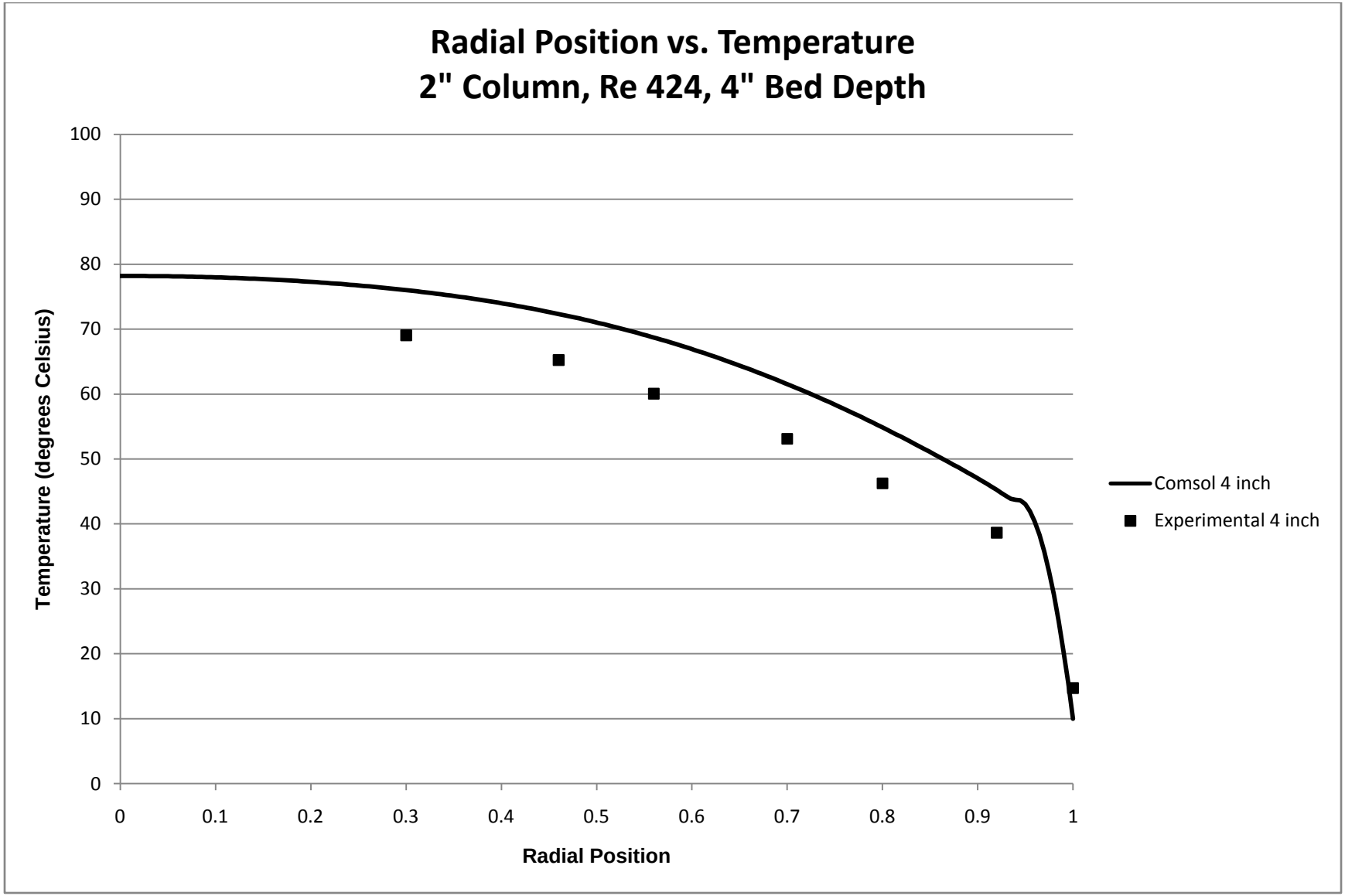
Radial Position vs. Temperature
2" Column, Re 424, 4" Bed Depth
Temperature (degrees Celsius)
100
90
80
70
60
50
40
30
20
10
0
0
0.1
0.2
0.3
0.4
0.5
0.6
0.7
0.8
0.9
1
Radial Position
Comsol 4 inch
Experimental 4 inch

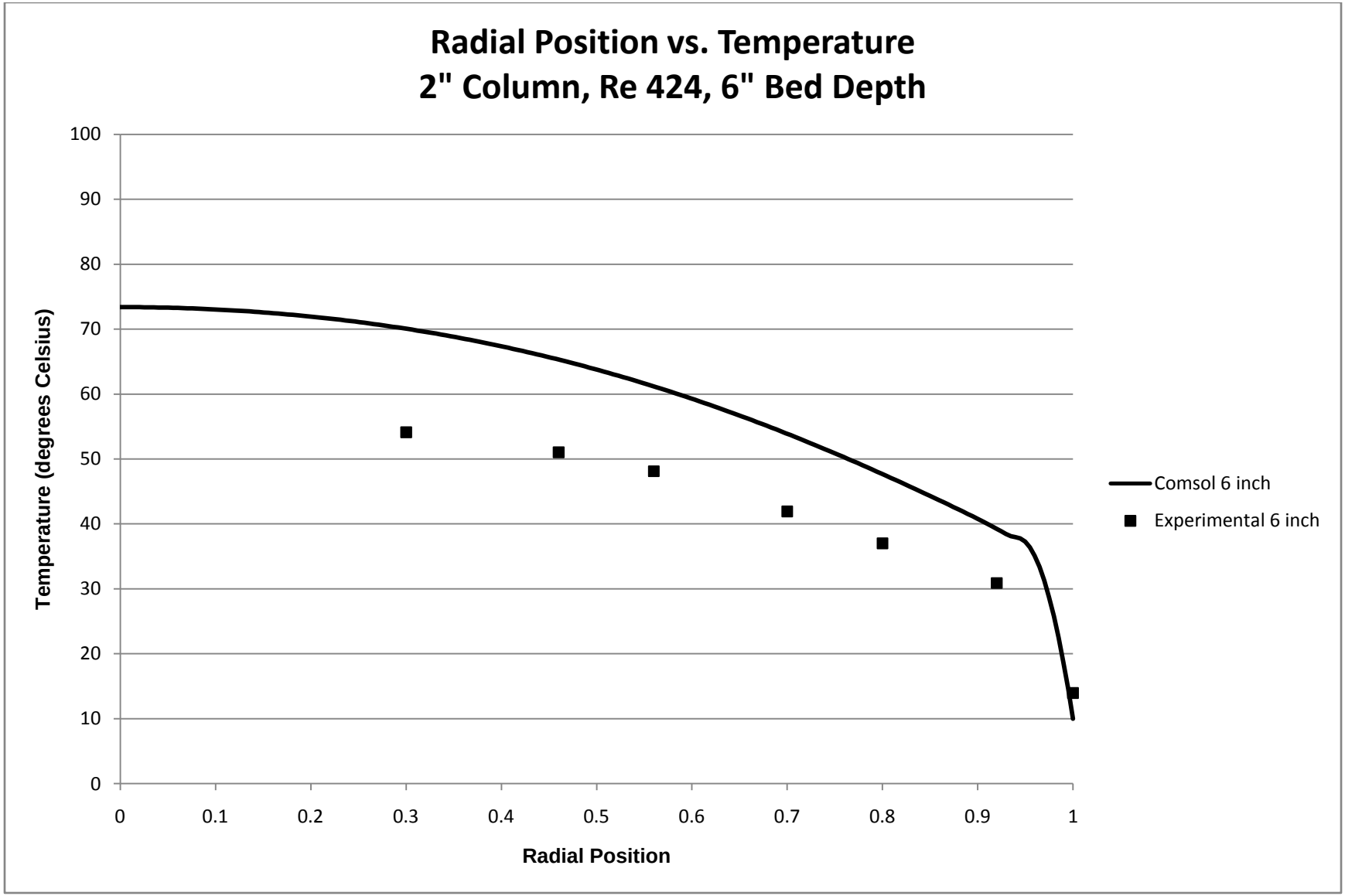
Radial Position vs. Temperature
2" Column, Re 424, 6" Bed Depth
Temperature (degrees Celsius)
100
90
80
70
60
50
40
30
20
10
0
0
0.1
0.2
0.3
0.4
0.5
0.6
0.7
0.8
0.9
1
Radial Position
Comsol 6 inch
Experimental 6 inch

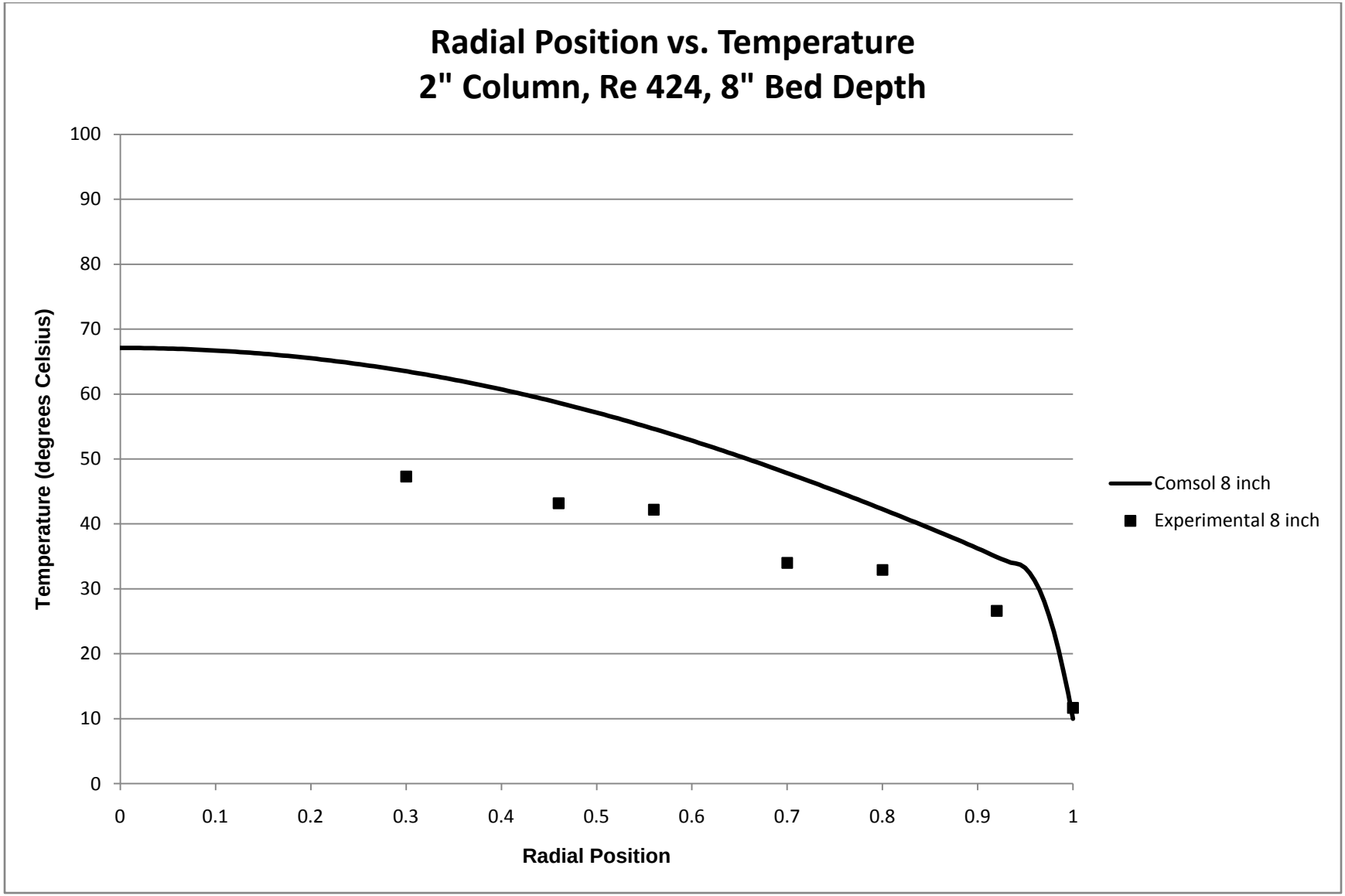
Radial Position vs. Temperature
2" Column, Re 424, 8" Bed Depth
Temperature (degrees Celsius)
100
90
80
70
60
50
40
30
20
10
0
0
0.1
0.2
0.3
0.4
0.5
0.6
0.7
0.8
0.9
1
Radial Position
Comsol 8 inch
Experimental 8 inch

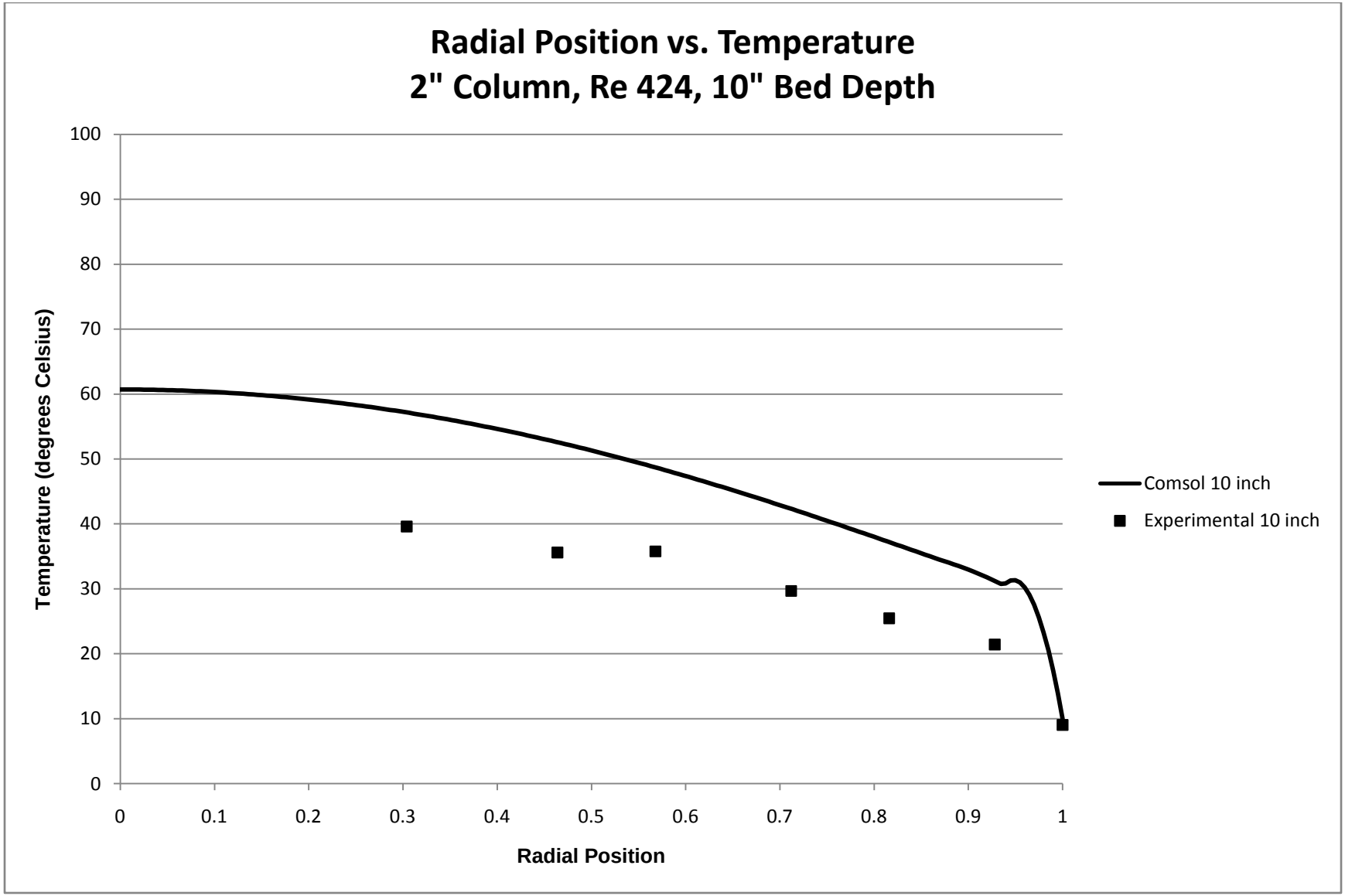
Radial Position vs. Temperature
2" Column, Re 424, 10" Bed Depth
Temperature (degrees Celsius)
100
90
80
70
60
50
40
30
20
10
0
0
0.1
0.2
0.3
0.4
0.5
0.6
0.7
0.8
0.9
1
Radial Position
Comsol 10 inch
Experimental 10 inch

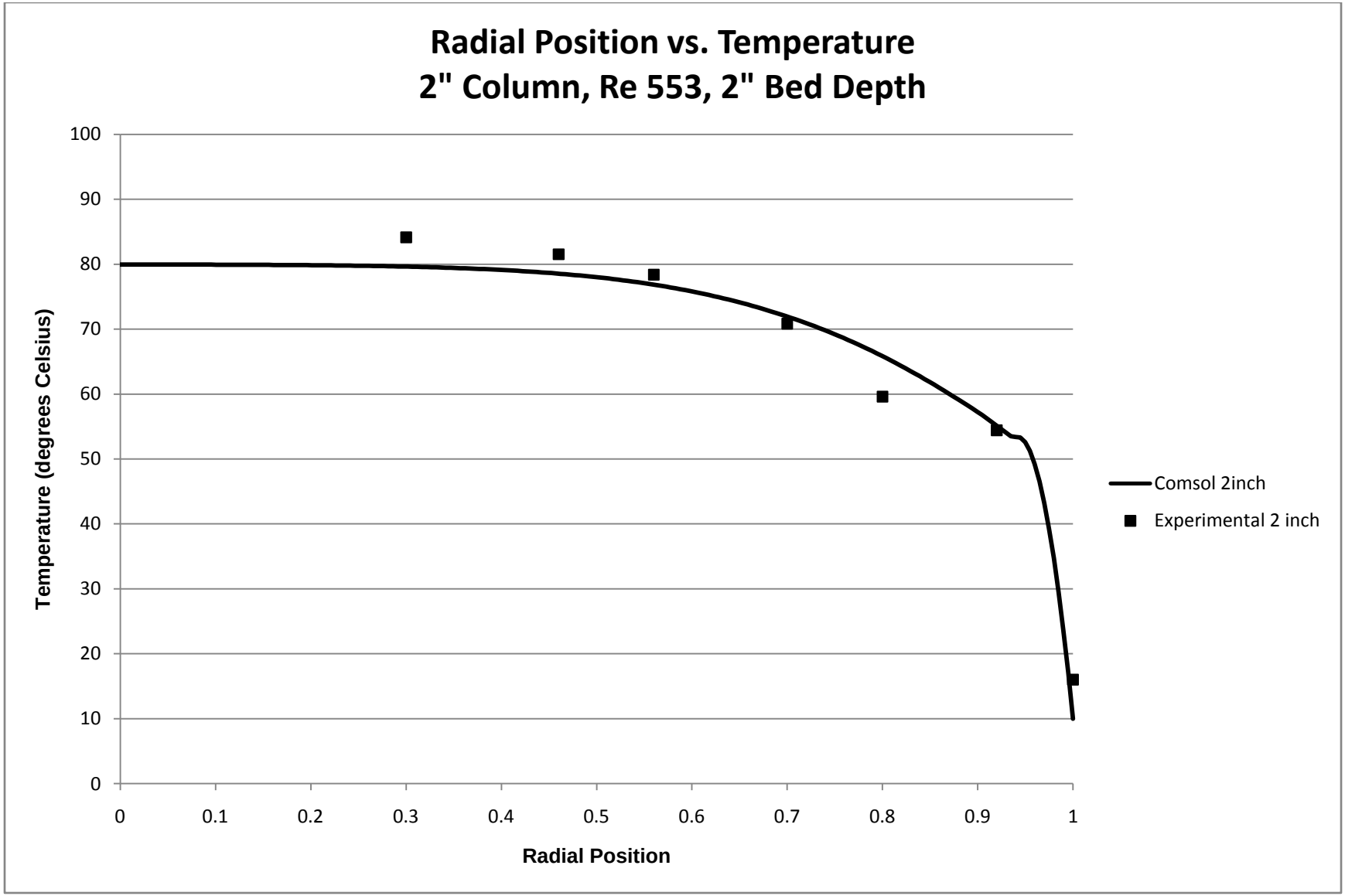
Radial Position vs. Temperature
2" Column, Re 553, 2" Bed Depth
Temperature (degrees Celsius)
100
90
80
70
60
50
40
30
20
10
0
0
0.1
0.2
0.3
0.4
0.5
0.6
0.7
0.8
0.9
1
Radial Position
Comsol 2inch
Experimental 2 inch

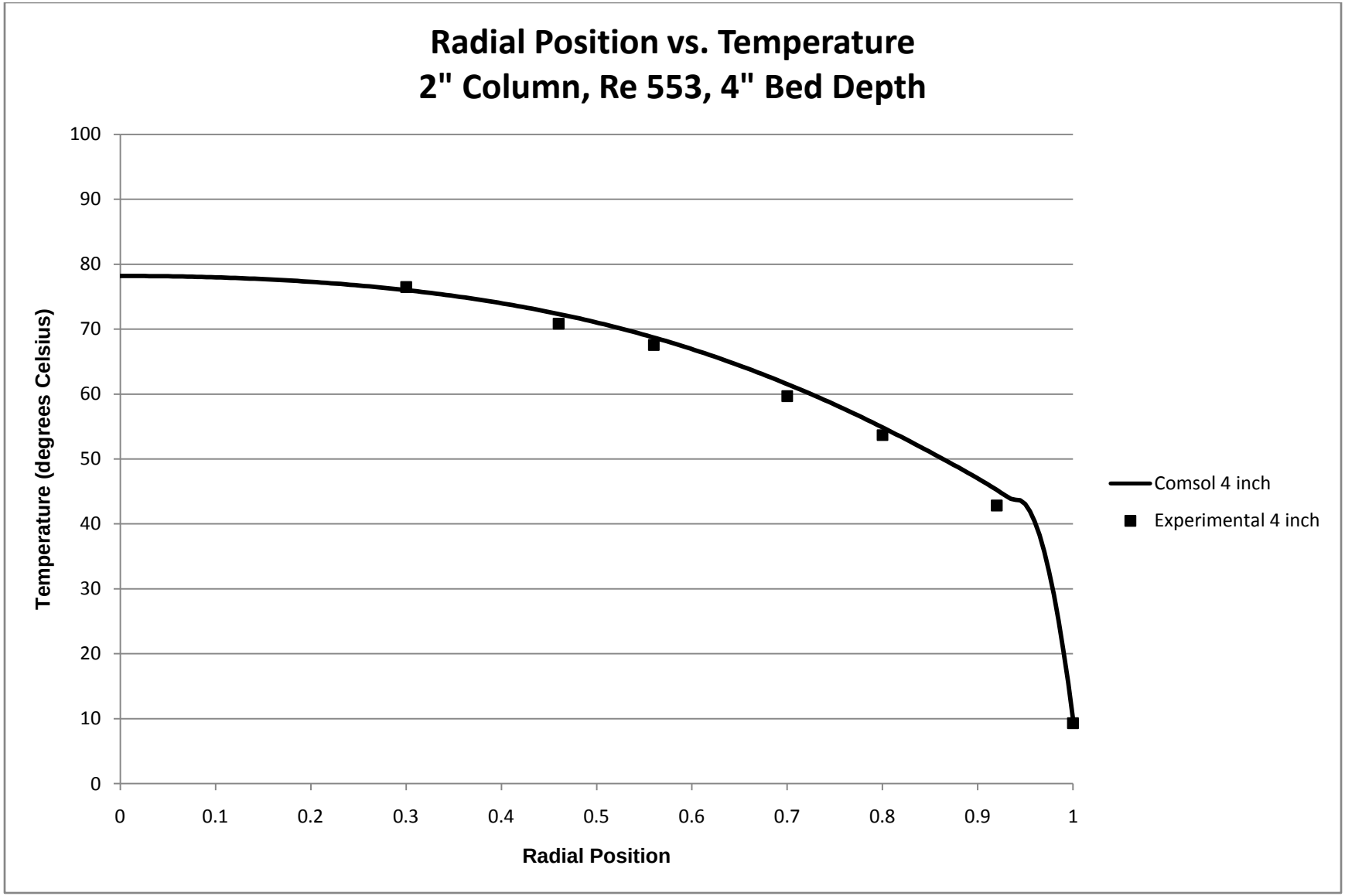
Radial Position vs. Temperature
2" Column, Re 553, 4" Bed Depth
Temperature (degrees Celsius)
100
90
80
70
60
50
40
30
20
10
0
0
0.1
0.2
0.3
0.4
0.5
0.6
0.7
0.8
0.9
1
Radial Position
Comsol 4 inch
Experimental 4 inch

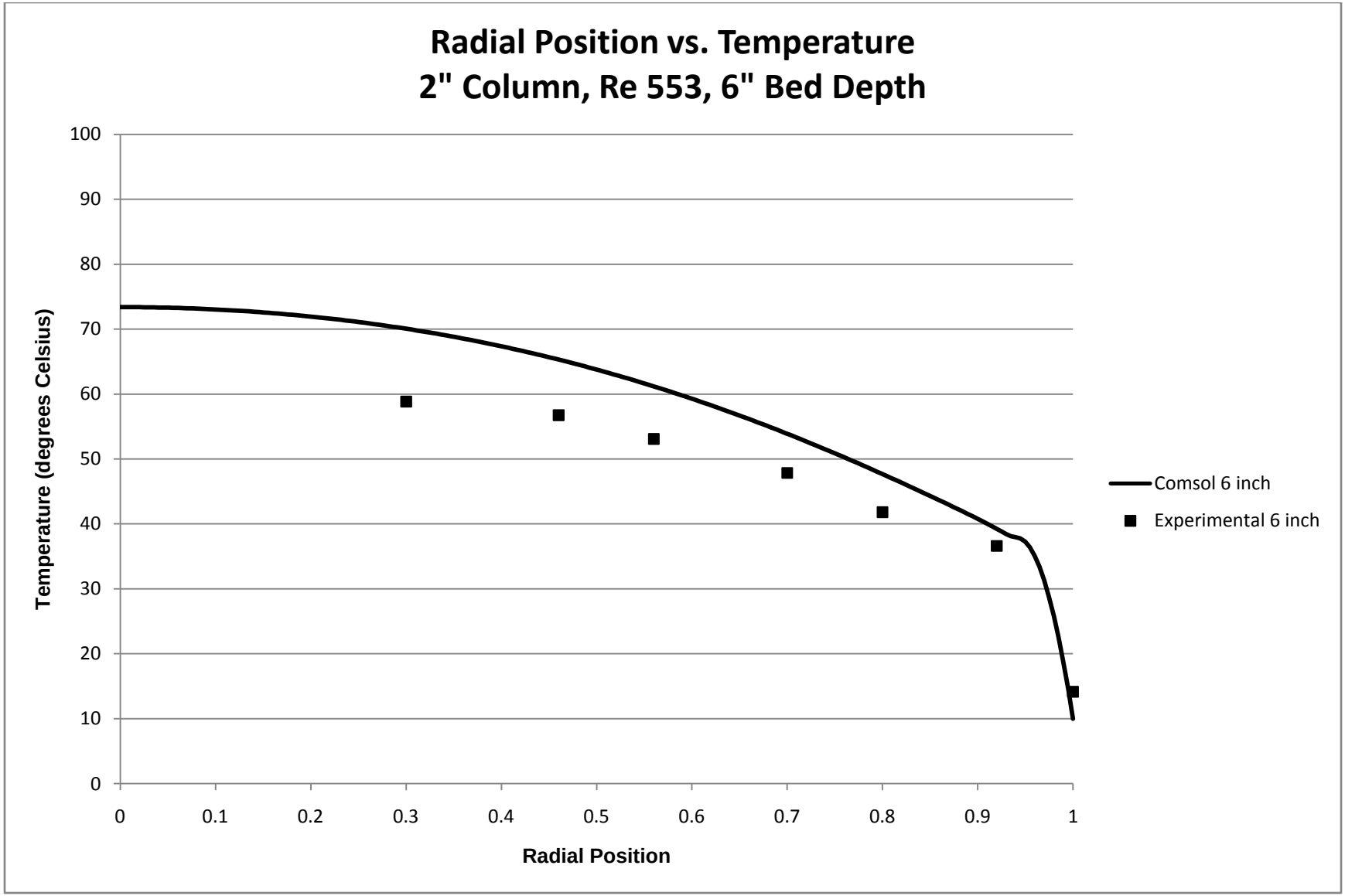
Radial Position vs. Temperature
2" Column, Re 553, 6" Bed Depth
Temperature (degrees Celsius)
100
90
80
70
60
50
40
30
20
10
0
0
0.1
0.2
0.3
0.4
0.5
0.6
0.7
0.8
0.9
1
Radial Position
Comsol 6 inch
Experimental 6 inch

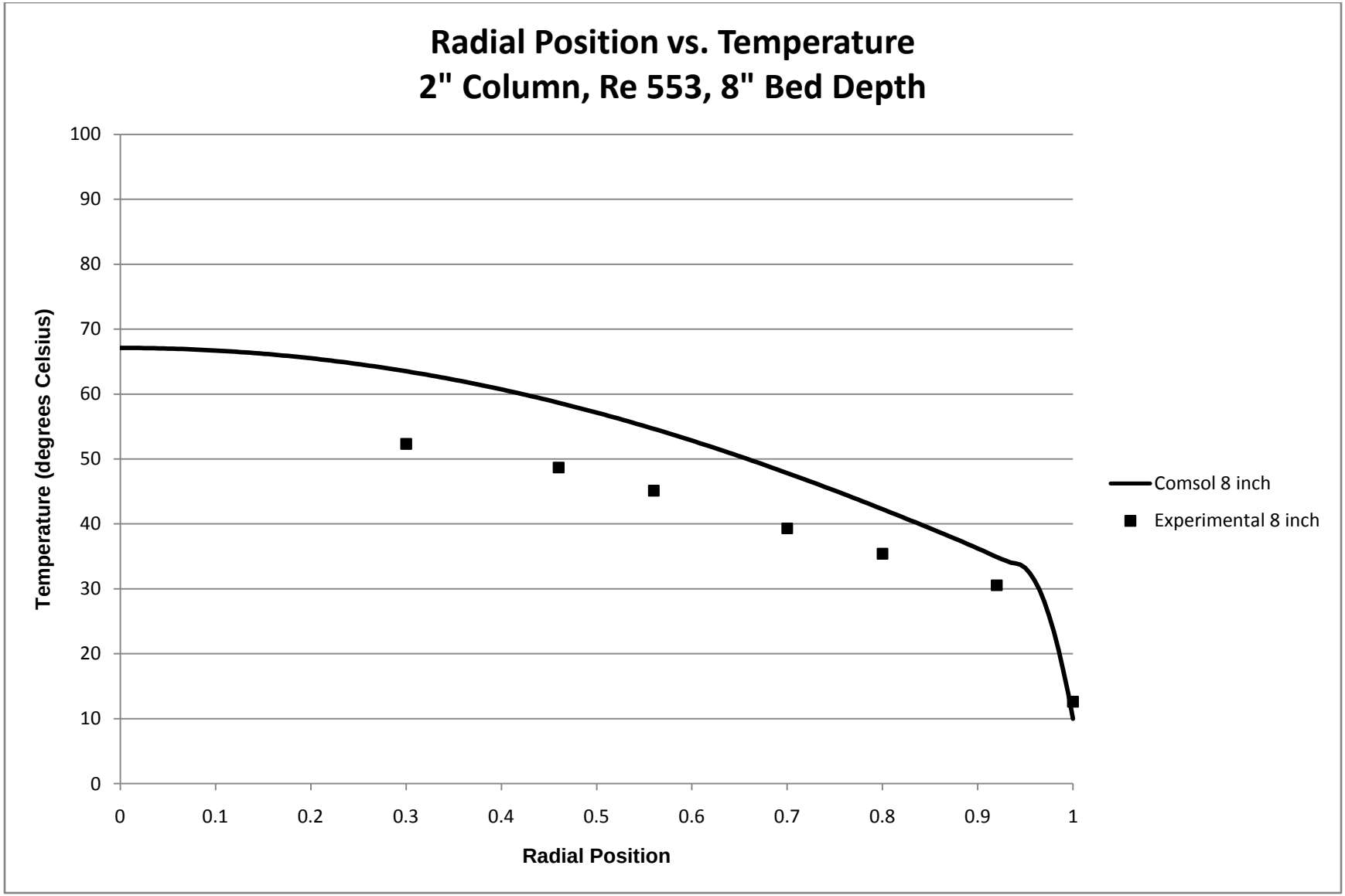
Radial Position vs. Temperature
2" Column, Re 553, 8" Bed Depth
Temperature (degrees Celsius)
100
90
80
70
60
50
40
30
20
10
0
0
0.1
0.2
0.3
0.4
0.5
0.6
0.7
0.8
0.9
1
Radial Position
Comsol 8 inch
Experimental 8 inch

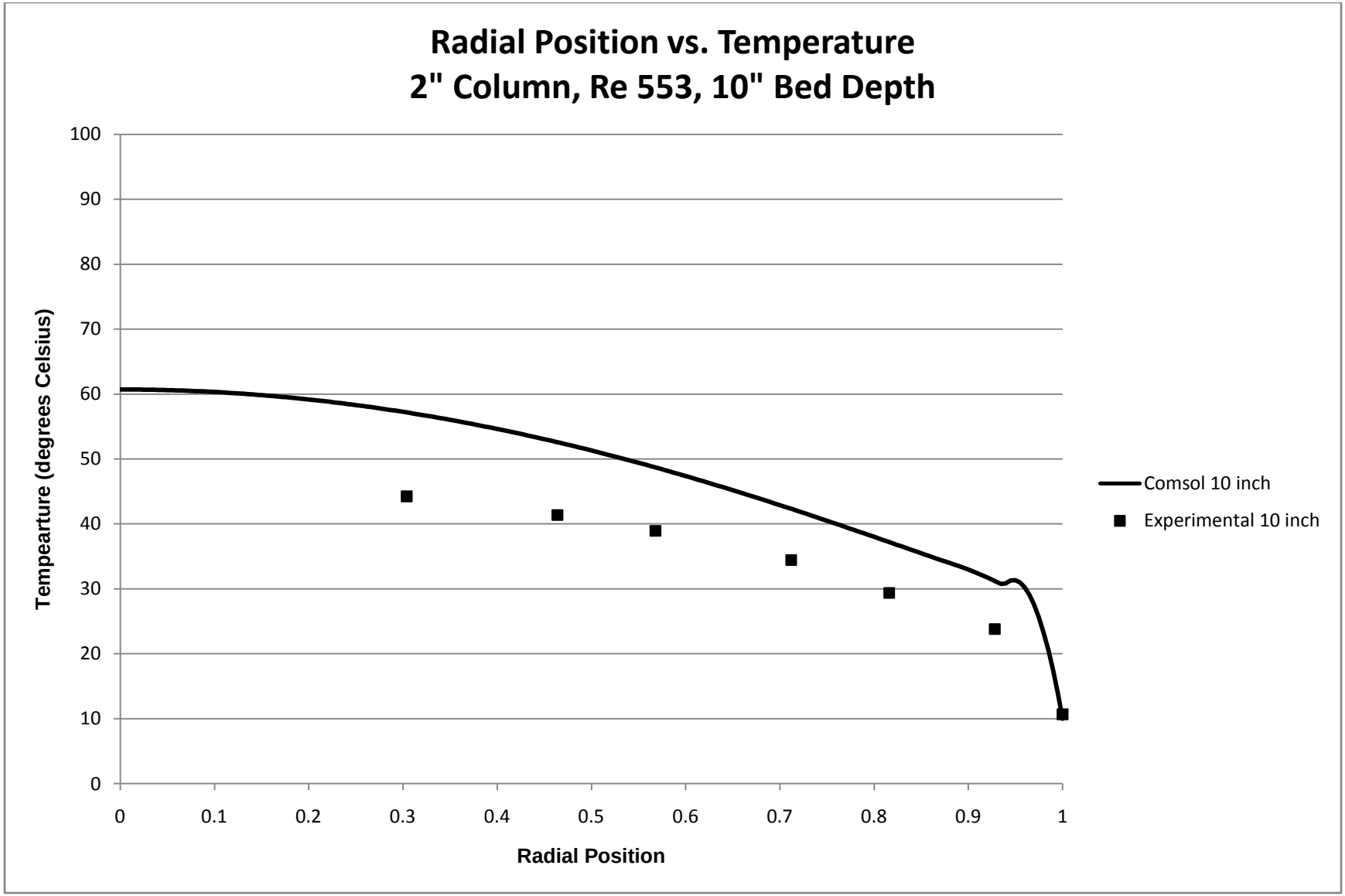
Radial Position vs. Temperature
2" Column, Re 553, 10" Bed Depth
Tempearture (degrees Celsius)
100
90
80
70
60
50
40
30
20
10
0
0
0.1
0.2
0.3
0.4
0.5
0.6
0.7
0.8
0.9
1
Radial Position
Comsol 10 inch
Experimental 10 inch

K.2 Radial Position vs. Temperature, 2" Column

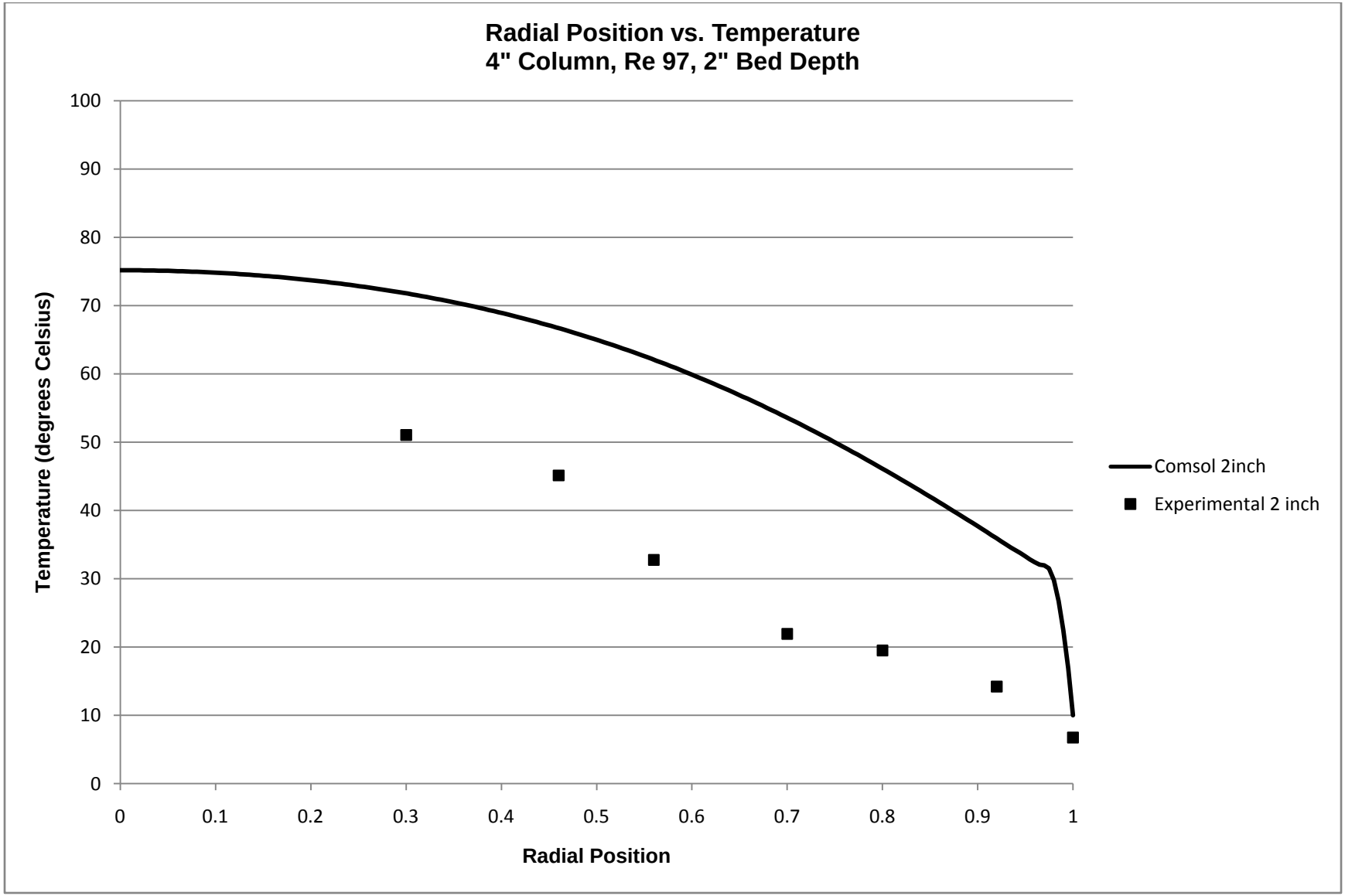
Radial Position vs. Temperature
4" Column, Re 97, 2" Bed Depth
Temperature (degrees Celsius)
100
90
80
70
60
50
40
30
20
10
0
0
0.1
0.2
0.3
0.4
0.5
0.6
0.7
0.8
0.9
1
Radial Position
Comsol 2inch
Experimental 2 inch

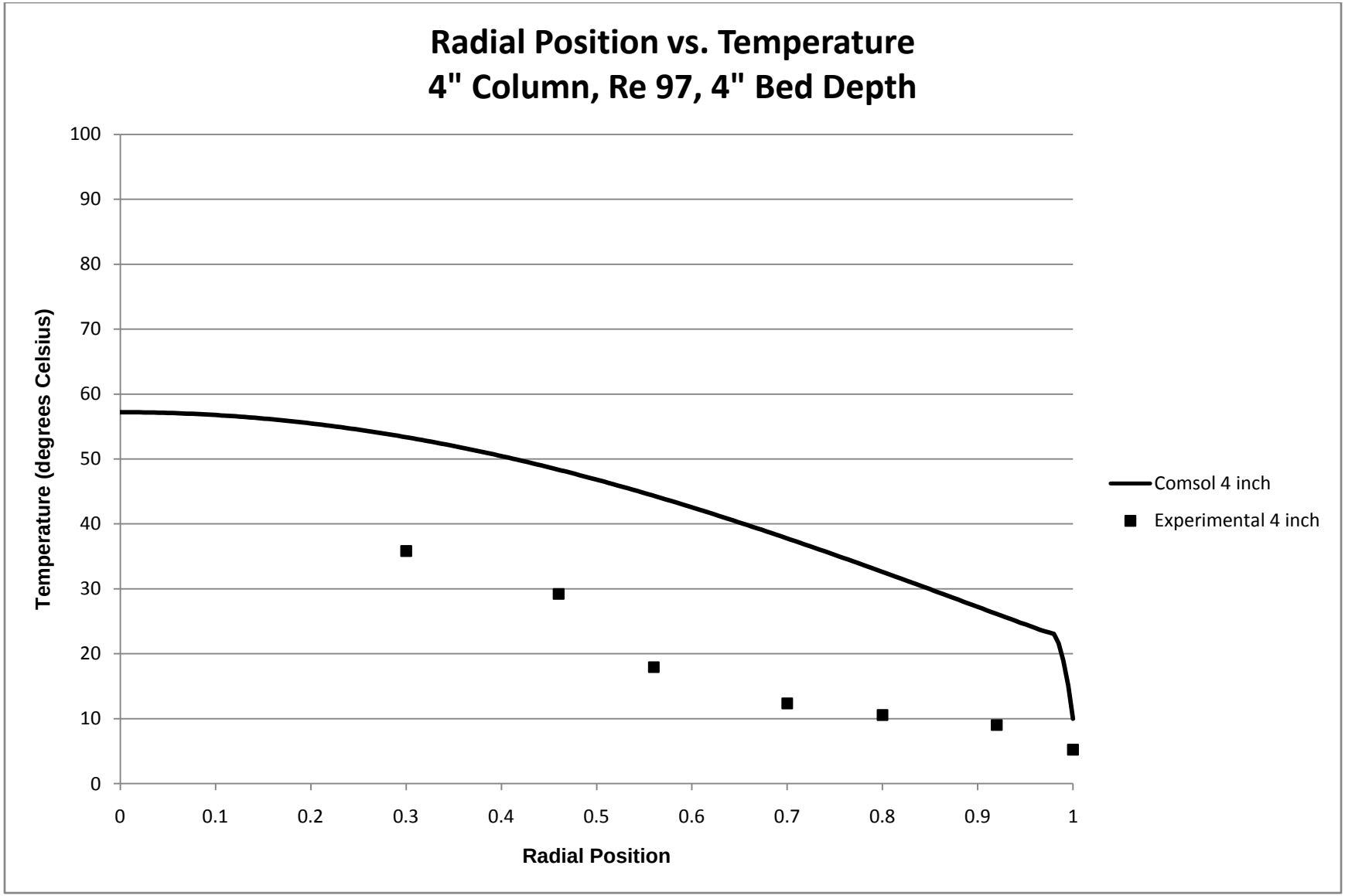
Radial Position vs. Temperature
4" Column, Re 97, 4" Bed Depth
Temperature (degrees Celsius)
100
90
80
70
60
50
40
30
20
10
0
0
0.1
0.2
0.3
0.4
0.5
0.6
0.7
0.8
0.9
1
Radial Position
Comsol 4 inch
Experimental 4 inch

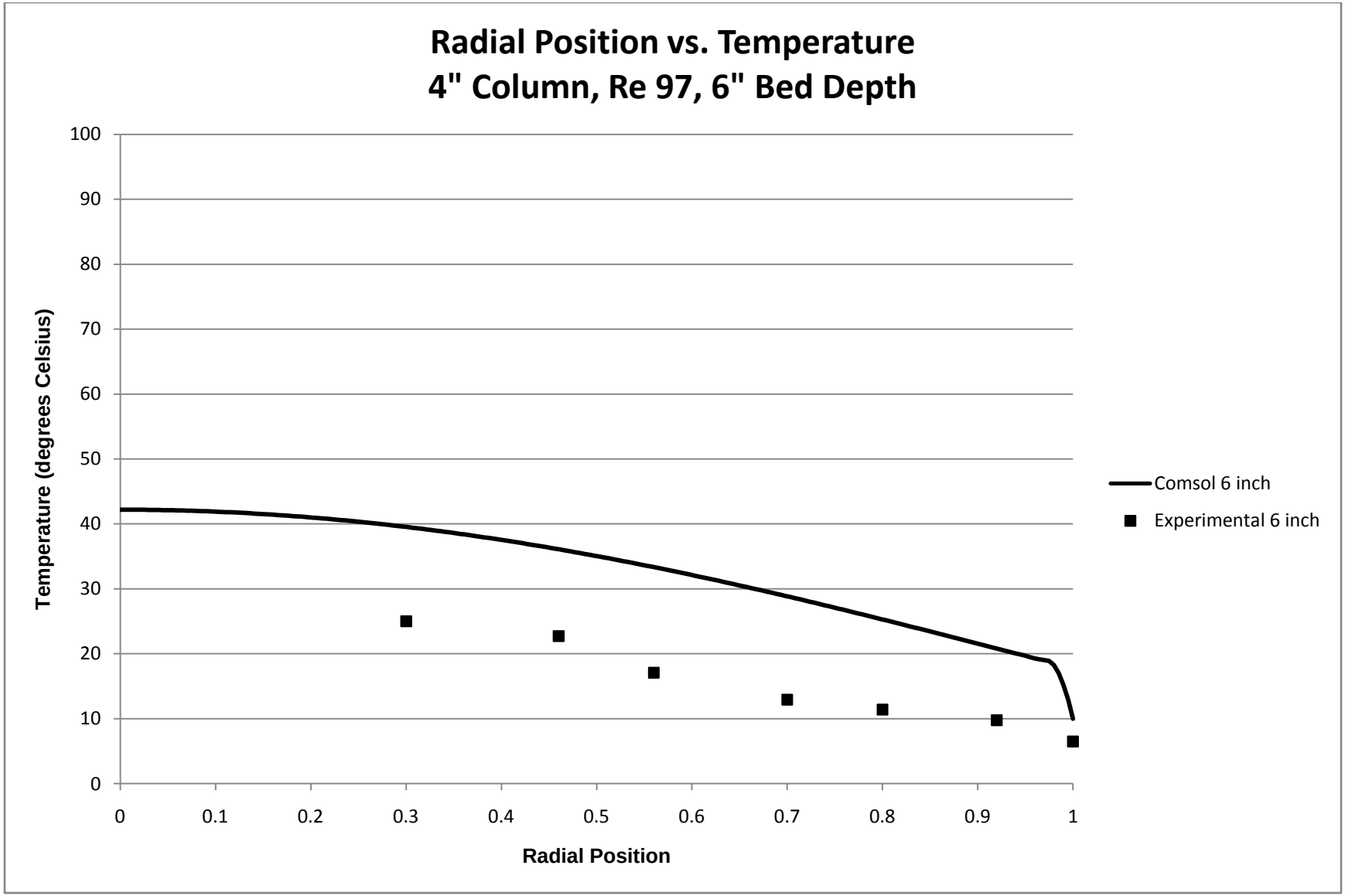
Radial Position vs. Temperature
4" Column, Re 97, 6" Bed Depth
Temperature (degrees Celsius)
100
90
80
70
60
50
40
30
20
10
0
0
0.1
0.2
0.3
0.4
0.5
0.6
0.7
0.8
0.9
1
Radial Position
Comsol 6 inch
Experimental 6 inch

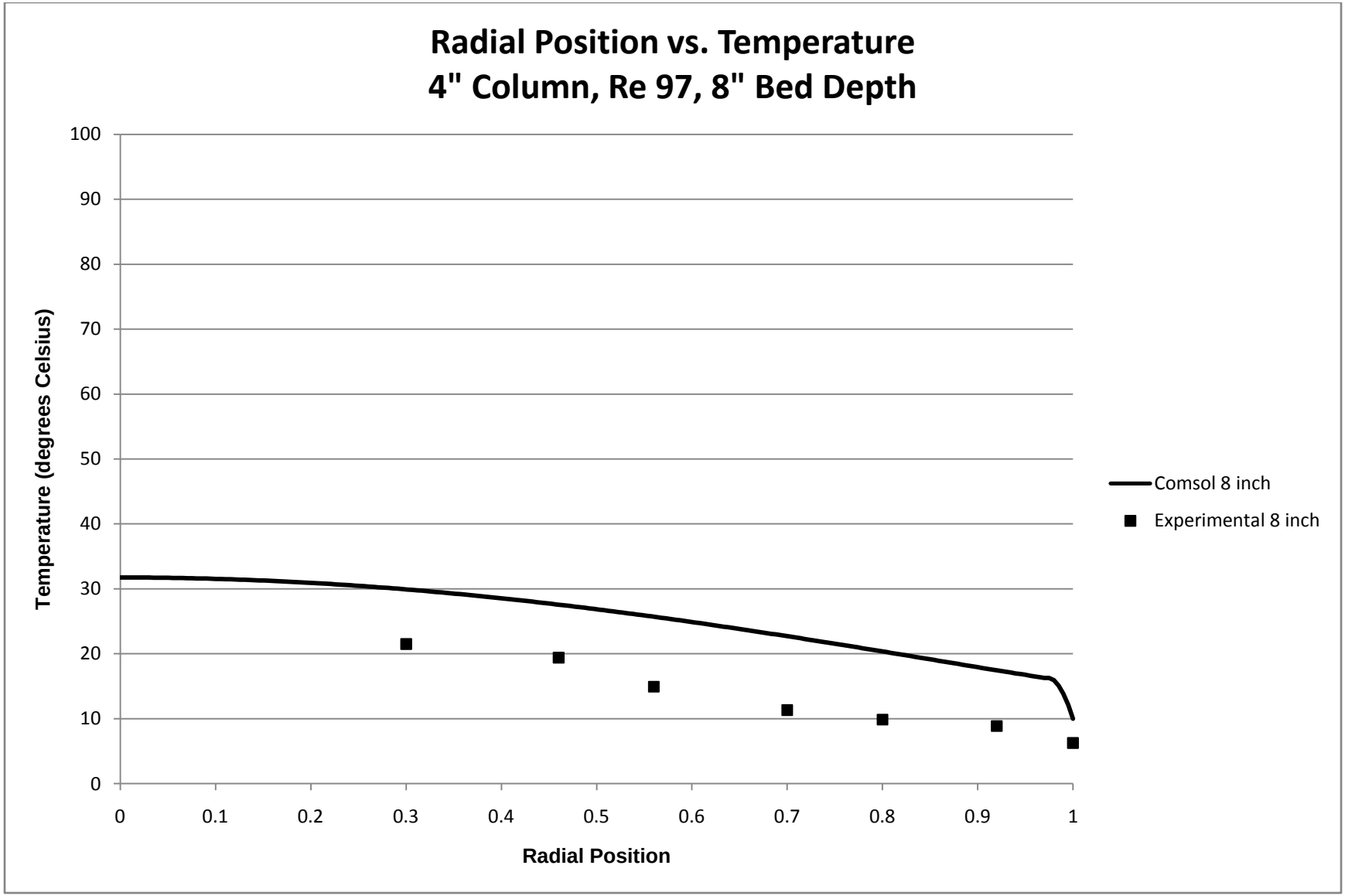
Radial Position vs. Temperature
4" Column, Re 97, 8" Bed Depth
Temperature (degrees Celsius)
100
90
80
70
60
50
40
30
20
10
0
0
0.1
0.2
0.3
0.4
0.5
0.6
0.7
0.8
0.9
1
Radial Position
Comsol 8 inch
Experimental 8 inch

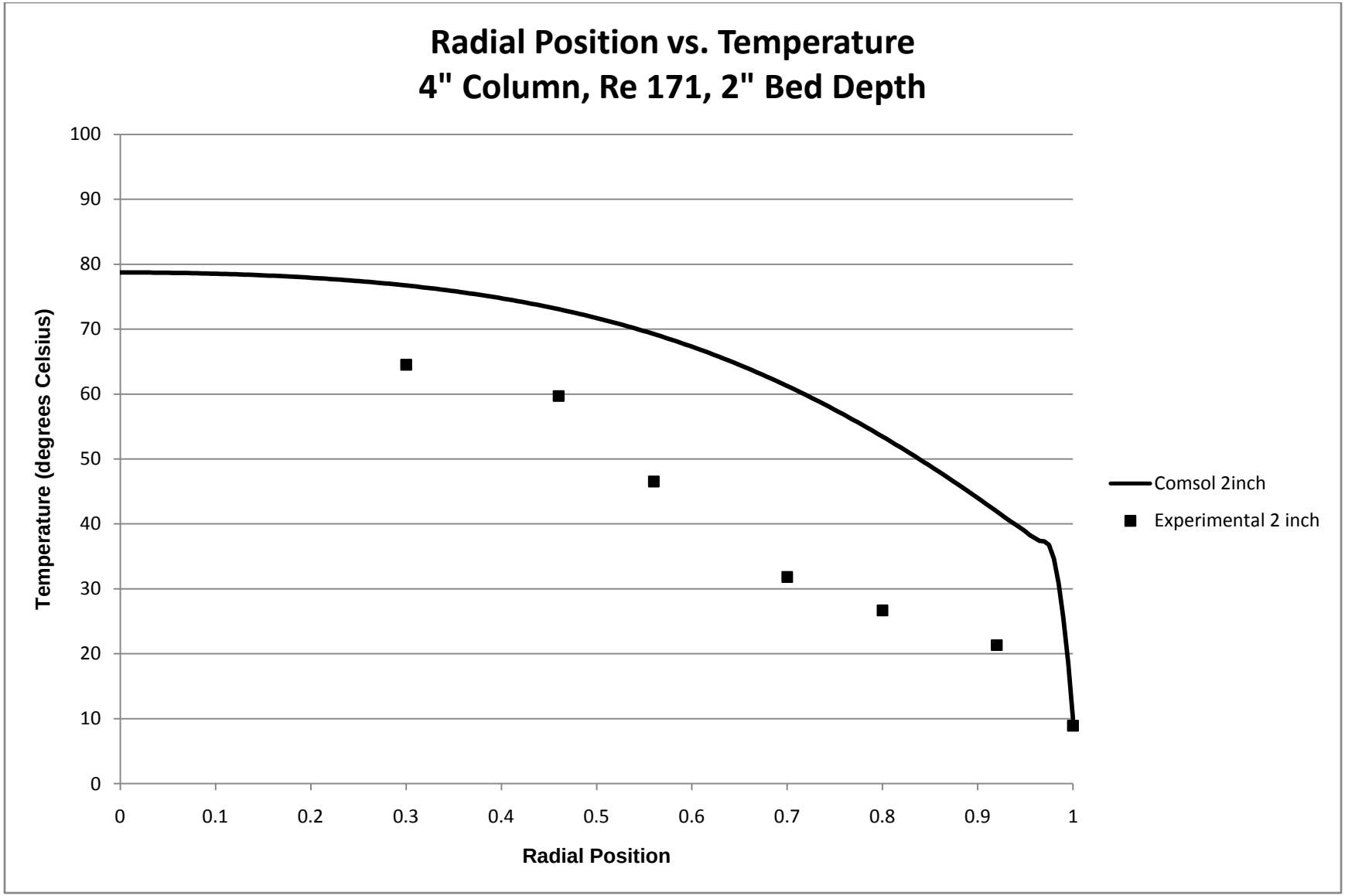
Radial Position vs. Temperature
4" Column, Re 171, 2" Bed Depth
Temperature (degrees Celsius)
100
90
80
70
60
50
40
30
20
10
0
0
0.1
0.2
0.3
0.4
0.5
0.6
0.7
0.8
0.9
1
Radial Position
Comsol 2inch
Experimental 2 inch

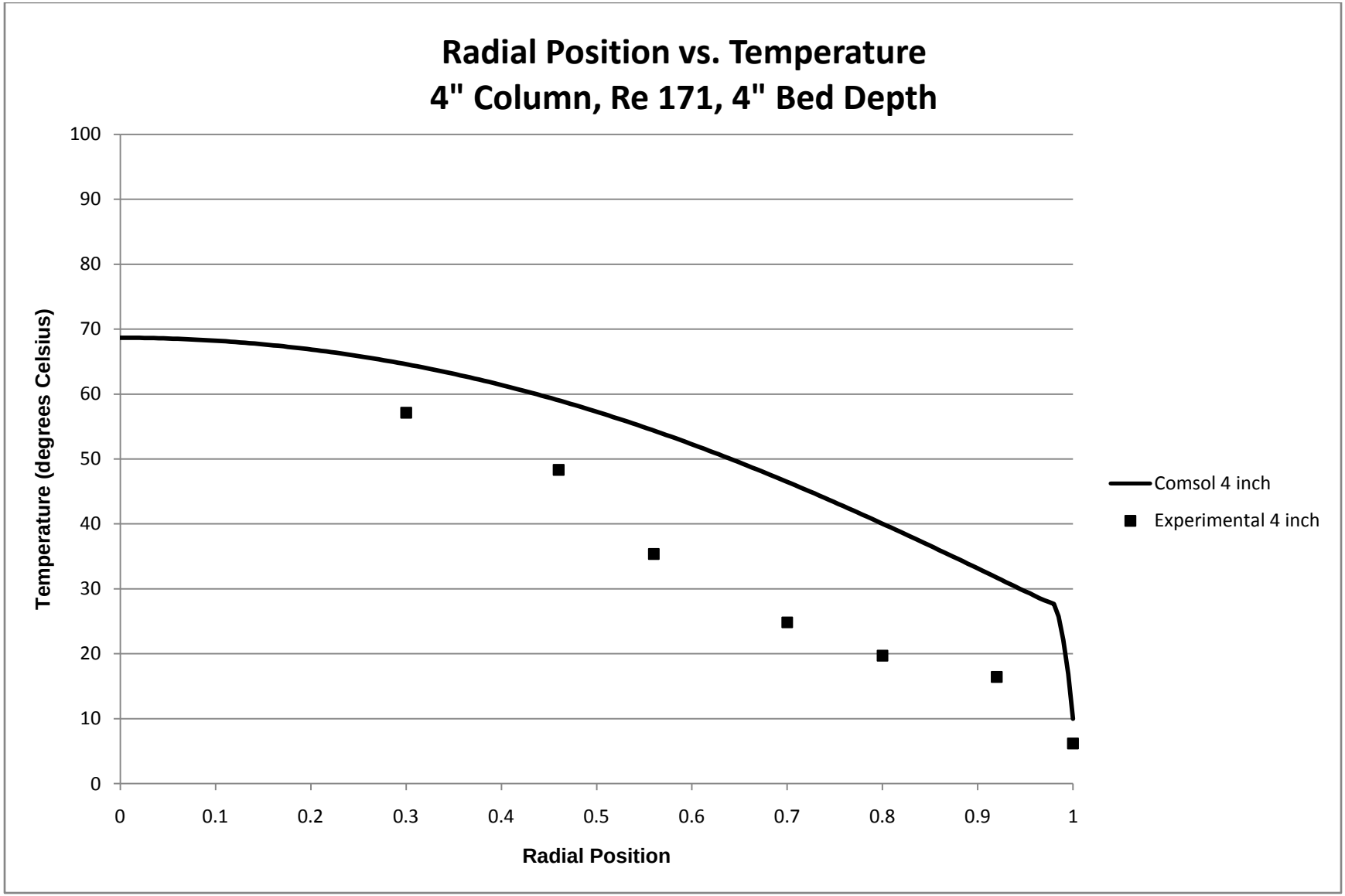
Radial Position vs. Temperature
4" Column, Re 171, 4" Bed Depth
Temperature (degrees Celsius)
100
90
80
70
60
50
40
30
20
10
0
0
0.1
0.2
0.3
0.4
0.5
0.6
0.7
0.8
0.9
1
Radial Position
Comsol 4 inch
Experimental 4 inch

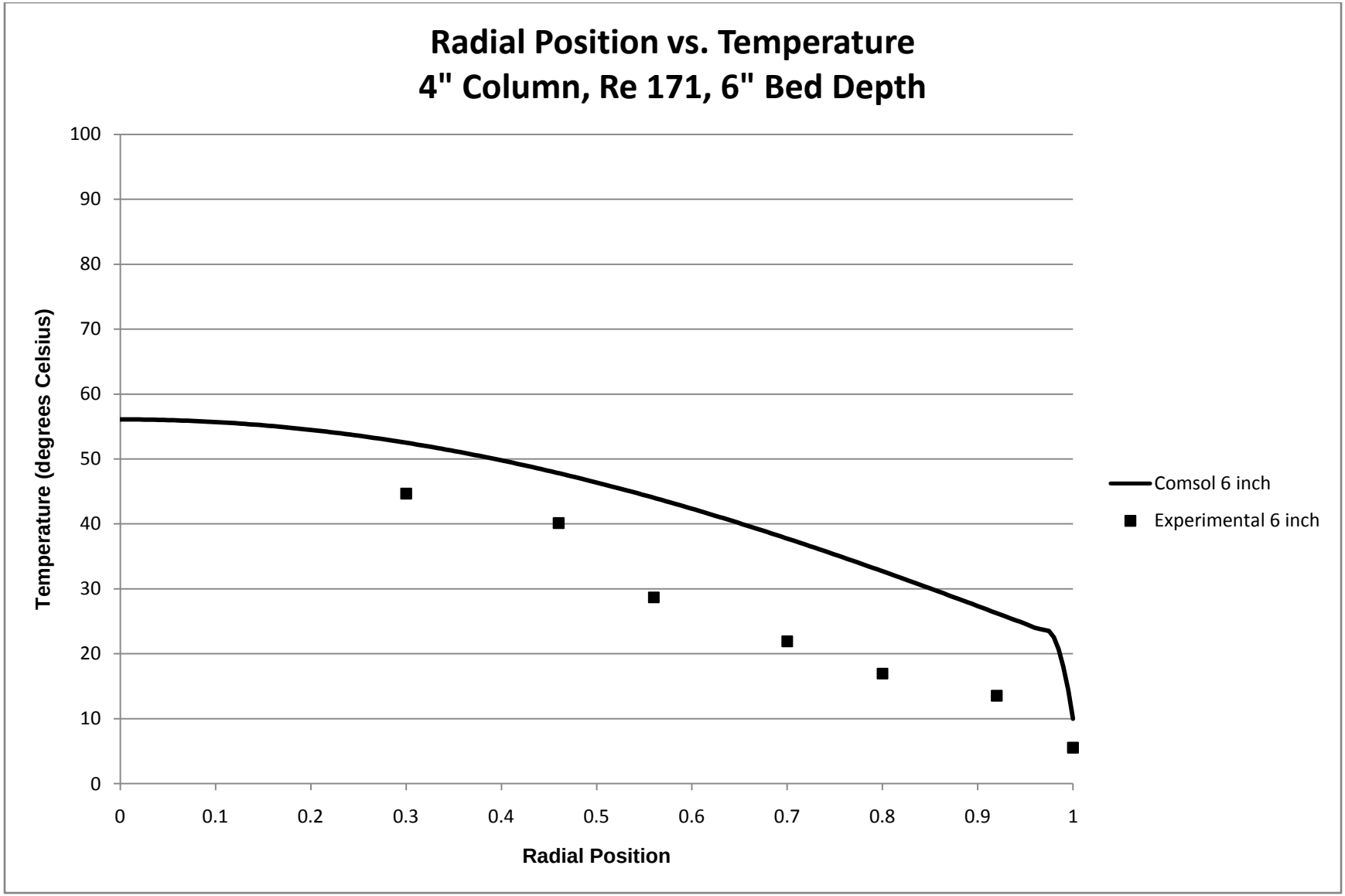
Radial Position vs. Temperature
4" Column, Re 171, 6" Bed Depth
Temperature (degrees Celsius)
100
90
80
70
60
50
40
30
20
10
0
0
0.1
0.2
0.3
0.4
0.5
0.6
0.7
0.8
0.9
1
Radial Position
Comsol 6 inch
Experimental 6 inch

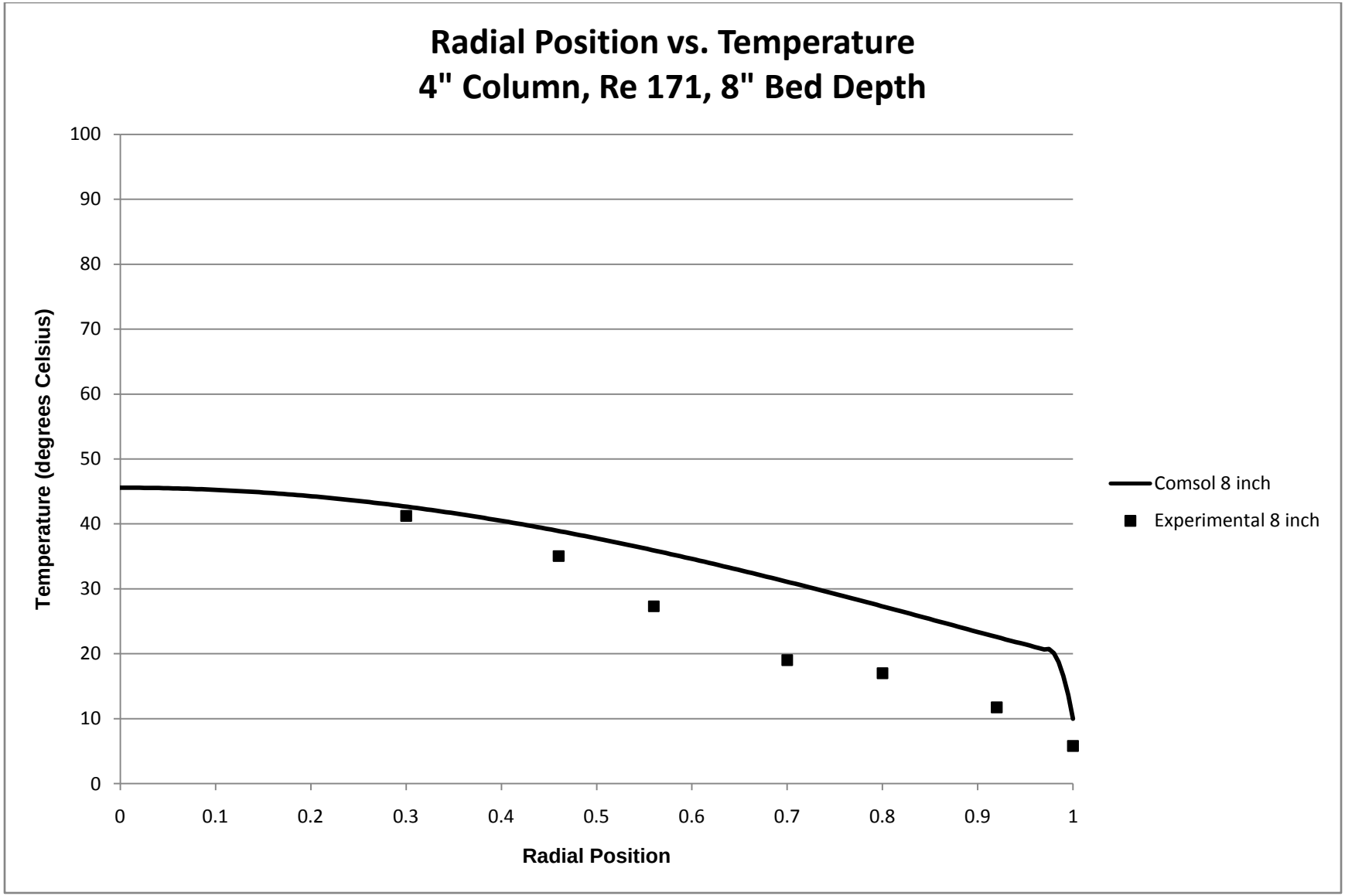
Radial Position vs. Temperature
4" Column, Re 171, 8" Bed Depth
Temperature (degrees Celsius)
100
90
80
70
60
50
40
30
20
10
0
0
0.1
0.2
0.3
0.4
0.5
0.6
0.7
0.8
0.9
1
Radial Position
Comsol 8 inch
Experimental 8 inch

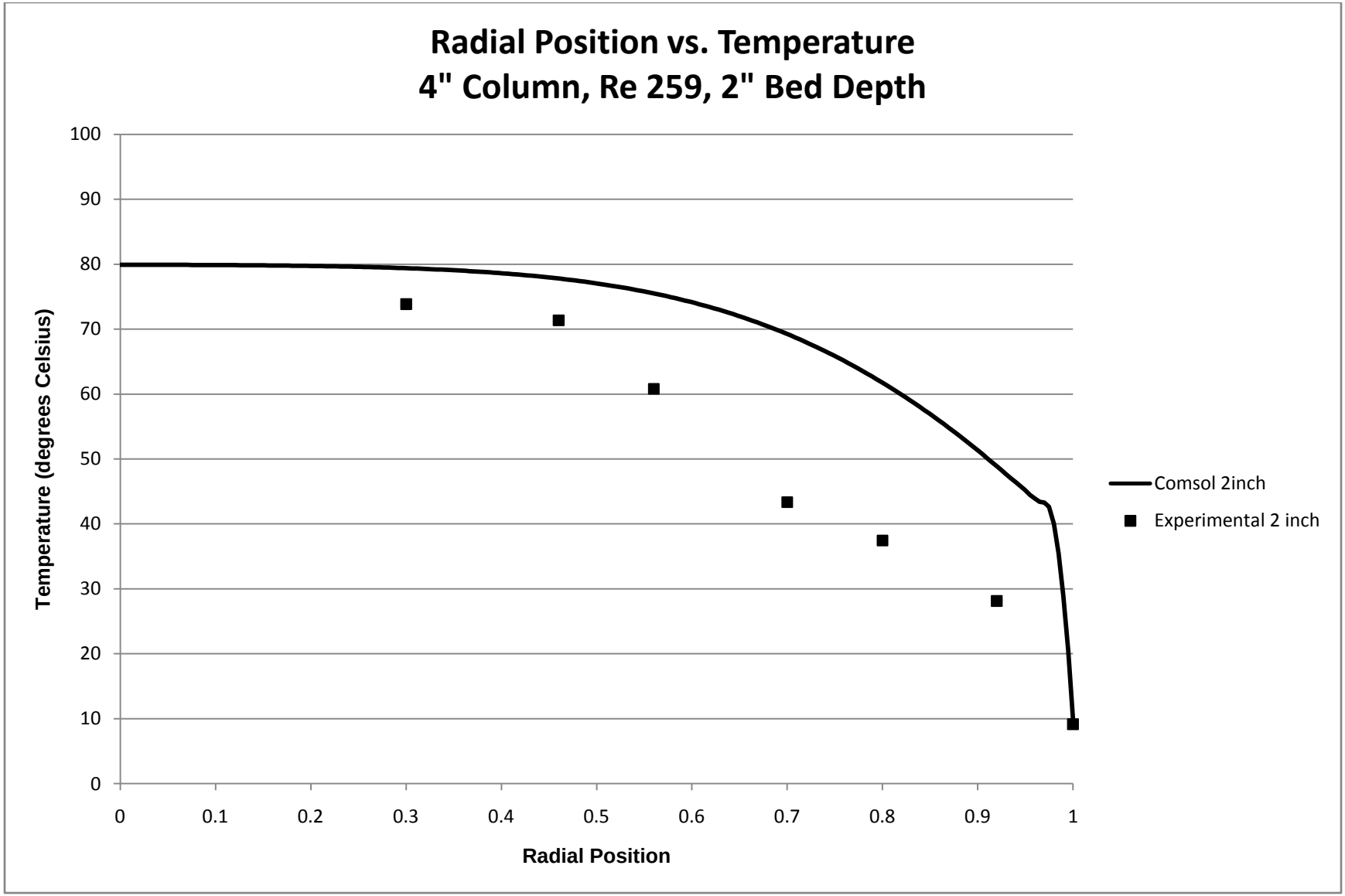
Radial Position vs. Temperature
4" Column, Re 259, 2" Bed Depth
Temperature (degrees Celsius)
100
90
80
70
60
50
40
30
20
10
0
0
0.1
0.2
0.3
0.4
0.5
0.6
0.7
0.8
0.9
1
Radial Position
Comsol 2inch
Experimental 2 inch

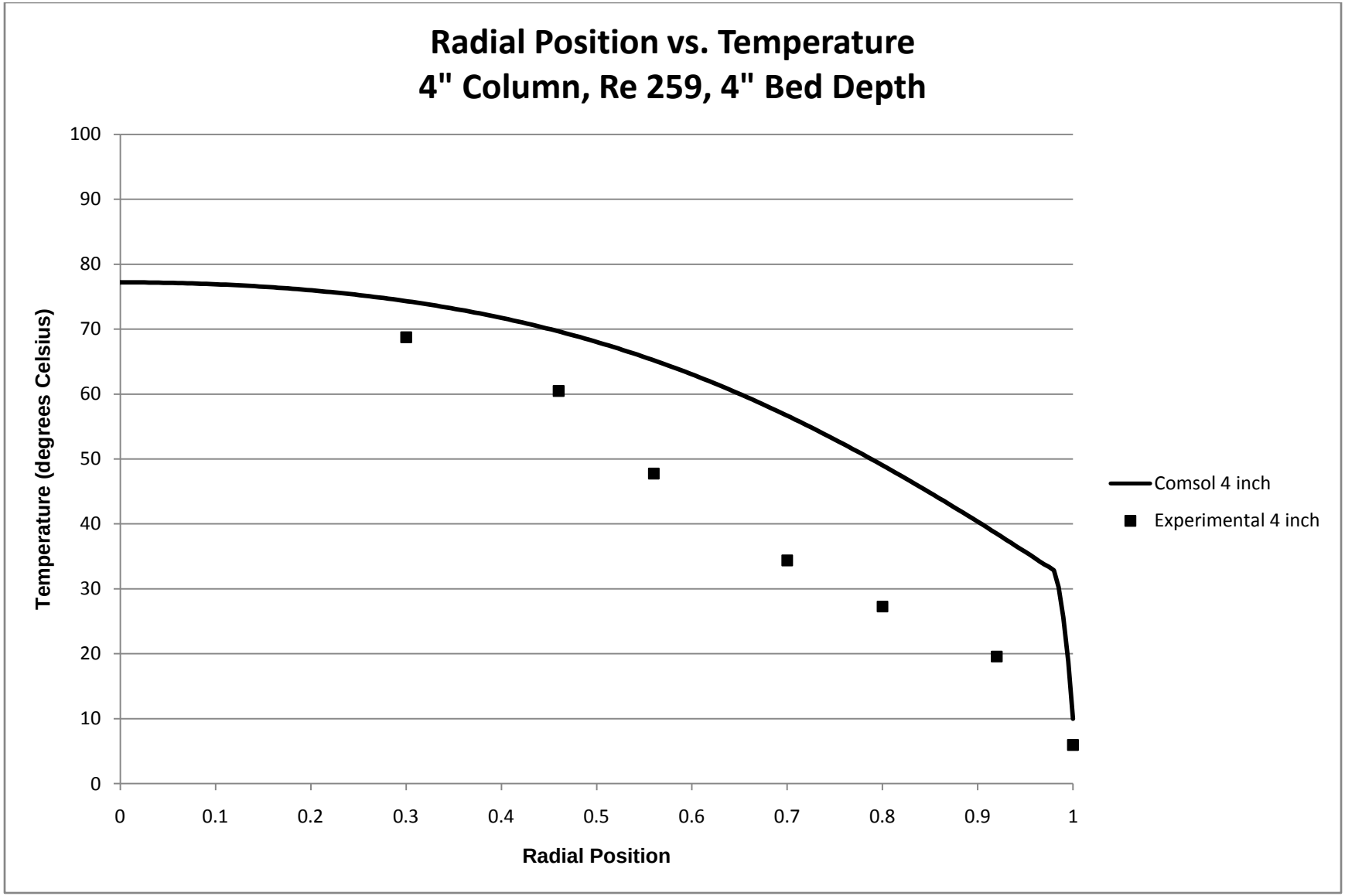
Radial Position vs. Temperature
4" Column, Re 259, 4" Bed Depth
Temperature (degrees Celsius)
100
90
80
70
60
50
40
30
20
10
0
0
0.1
0.2
0.3
0.4
0.5
0.6
0.7
0.8
0.9
1
Radial Position
Comsol 4 inch
Experimental 4 inch

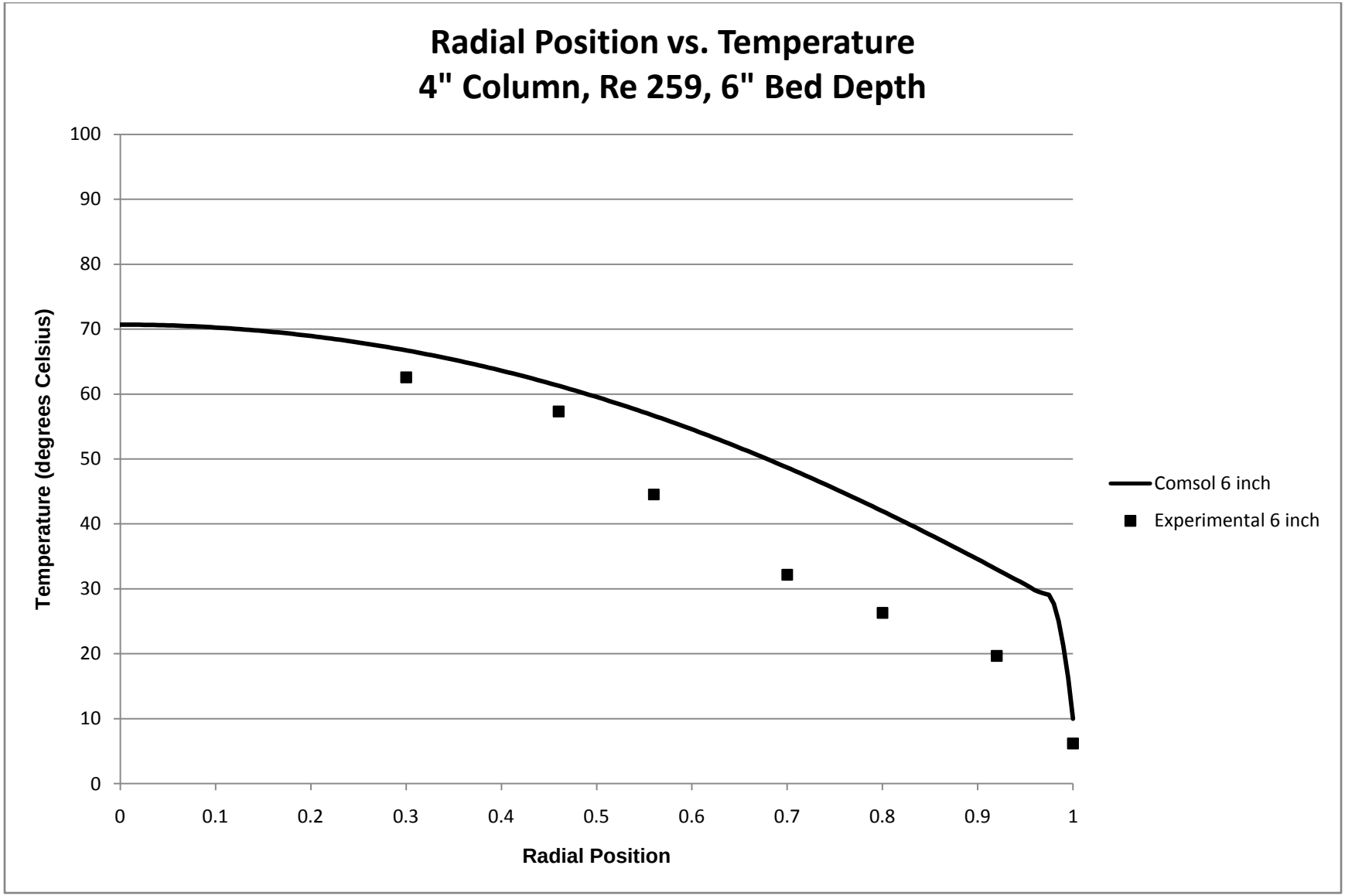
Radial Position vs. Temperature
4" Column, Re 259, 6" Bed Depth
Temperature (degrees Celsius)
100
90
80
70
60
50
40
30
20
10
0
0
0.1
0.2
0.3
0.4
0.5
0.6
0.7
0.8
0.9
1
Radial Position
Comsol 6 inch
Experimental 6 inch

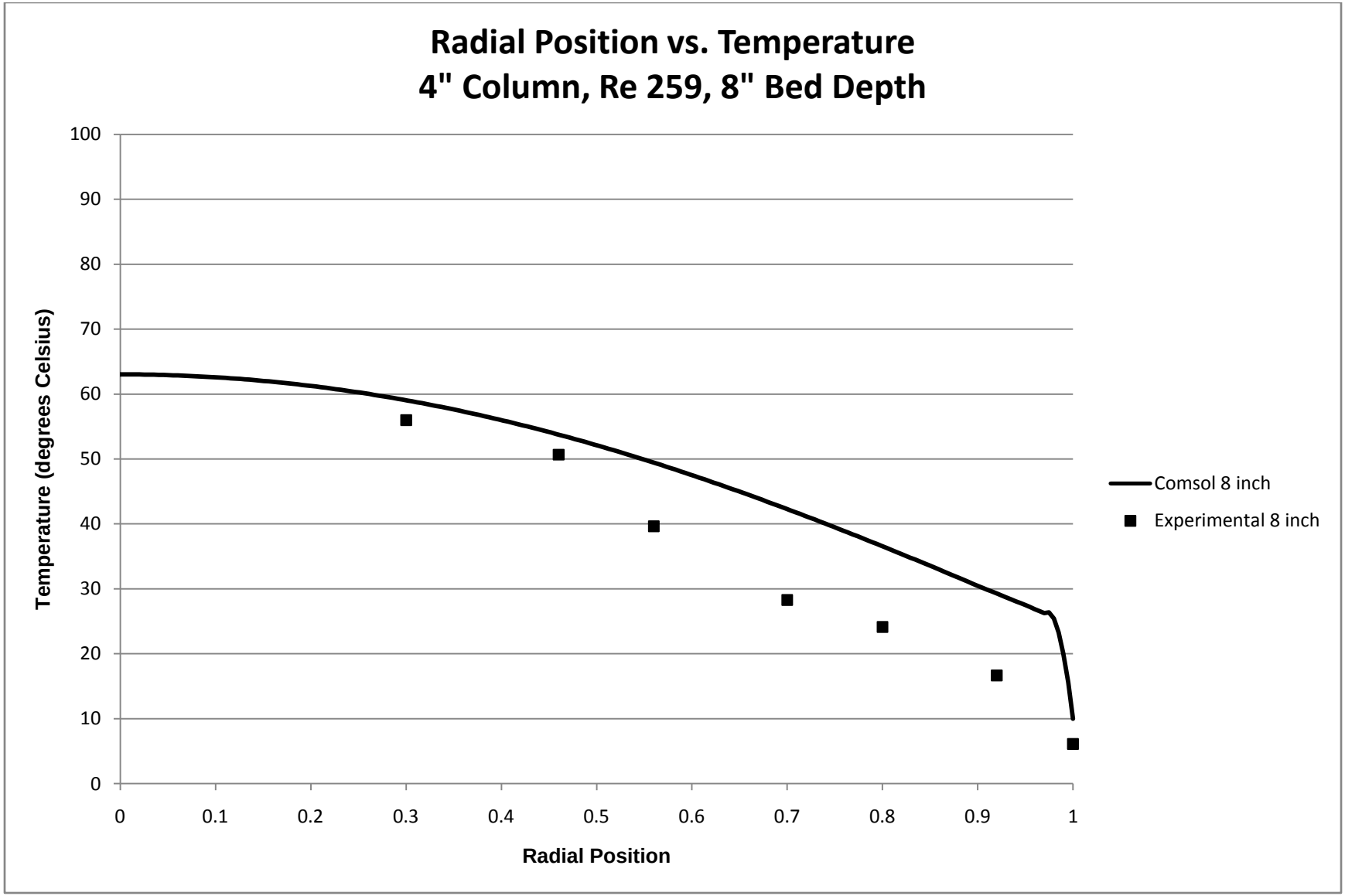
Radial Position vs. Temperature
4" Column, Re 259, 8" Bed Depth
Temperature (degrees Celsius)
100
90
80
70
60
50
40
30
20
10
0
0
0.1
0.2
0.3
0.4
0.5
0.6
0.7
0.8
0.9
1
Radial Position
Comsol 8 inch
Experimental 8 inch

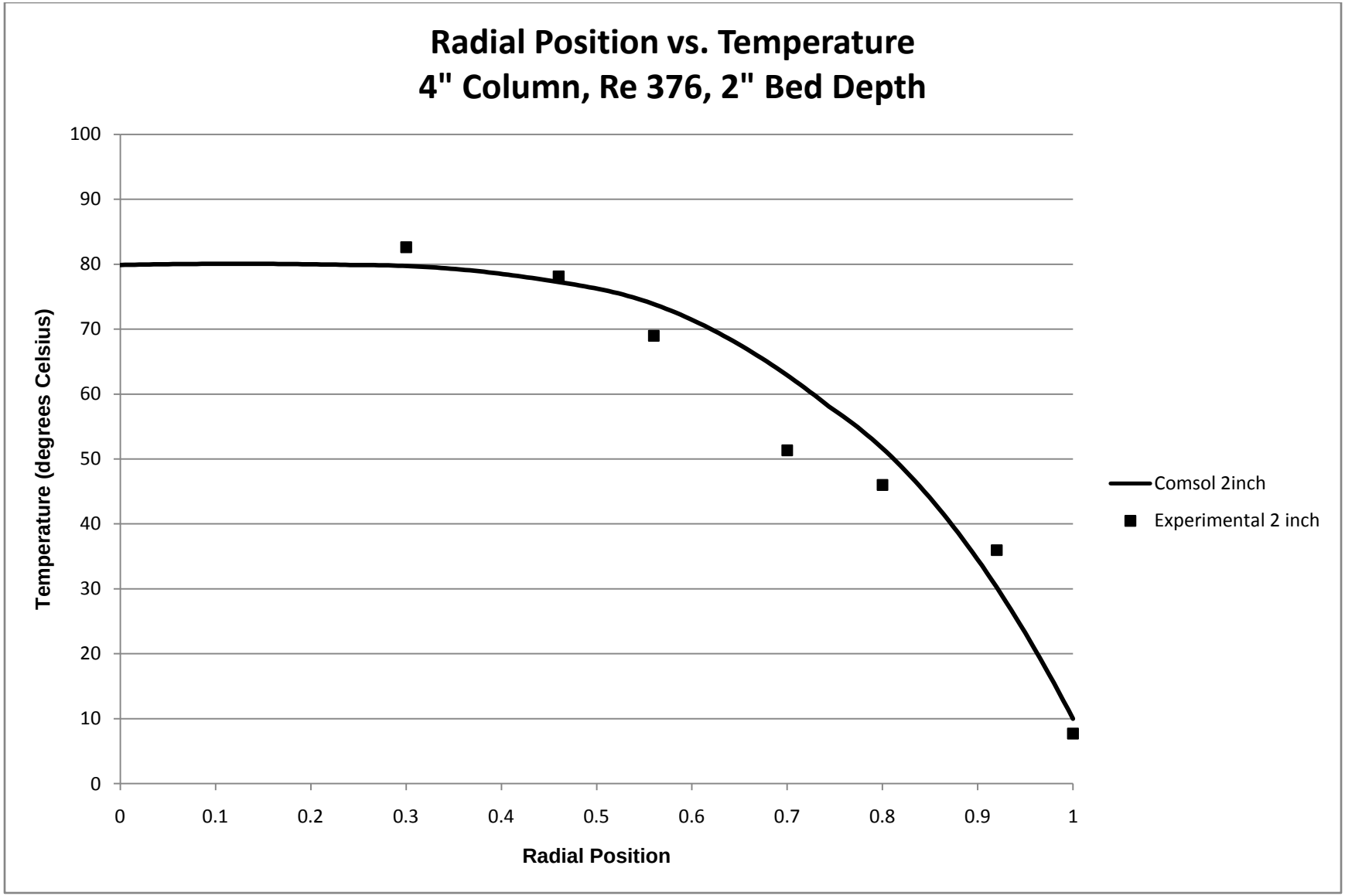
Radial Position vs. Temperature
4" Column, Re 376, 2" Bed Depth
Temperature (degrees Celsius)
100
90
80
70
60
50
40
30
20
10
0
0
0.1
0.2
0.3
0.4
0.5
0.6
0.7
0.8
0.9
1
Radial Position
Comsol 2inch
Experimental 2 inch

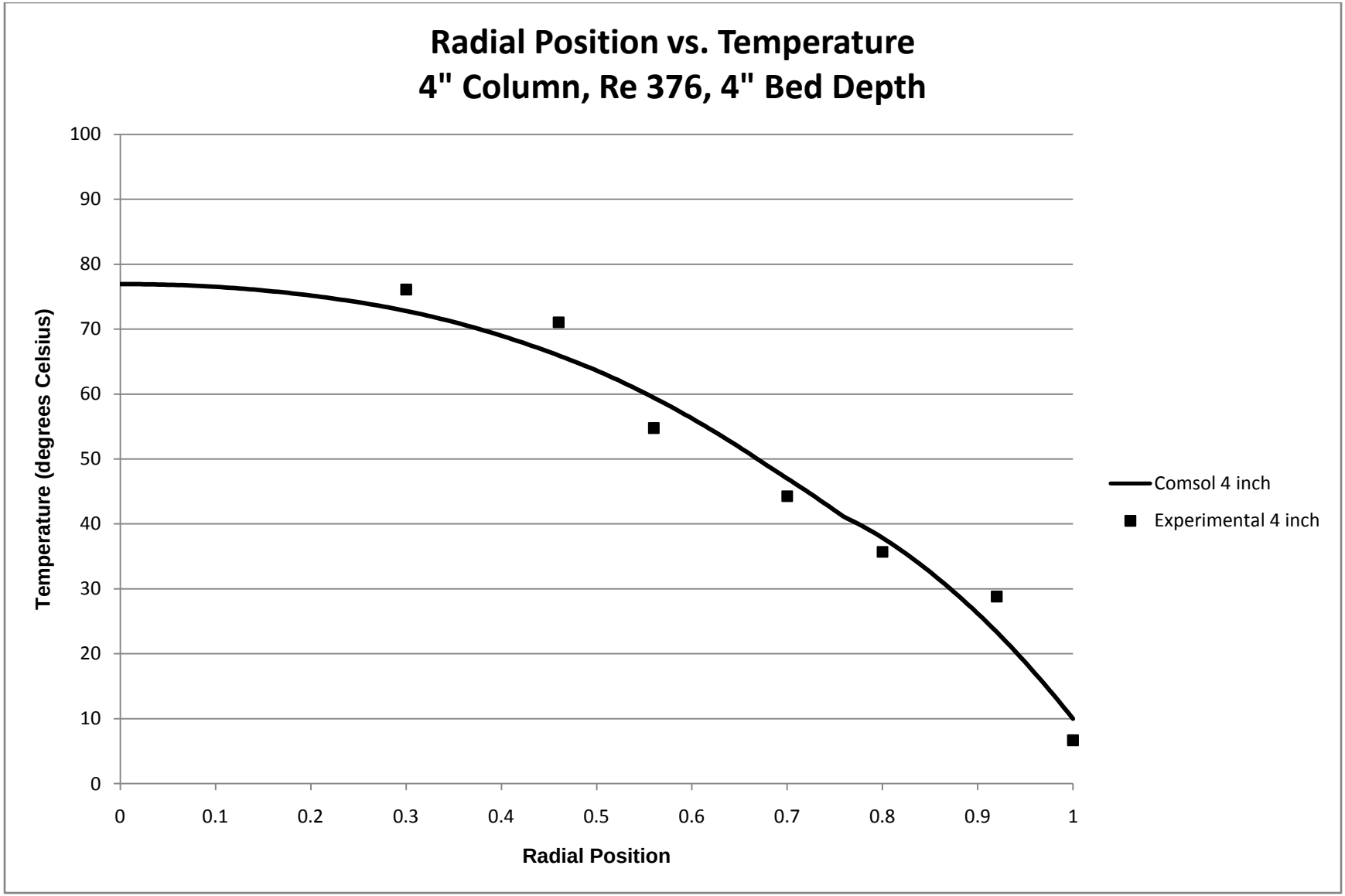
Radial Position vs. Temperature
4" Column, Re 376, 4" Bed Depth
Temperature (degrees Celsius)
100
90
80
70
60
50
40
30
20
10
0
0
0.1
0.2
0.3
0.4
0.5
0.6
0.7
0.8
0.9
1
Radial Position
Comsol 4 inch
Experimental 4 inch

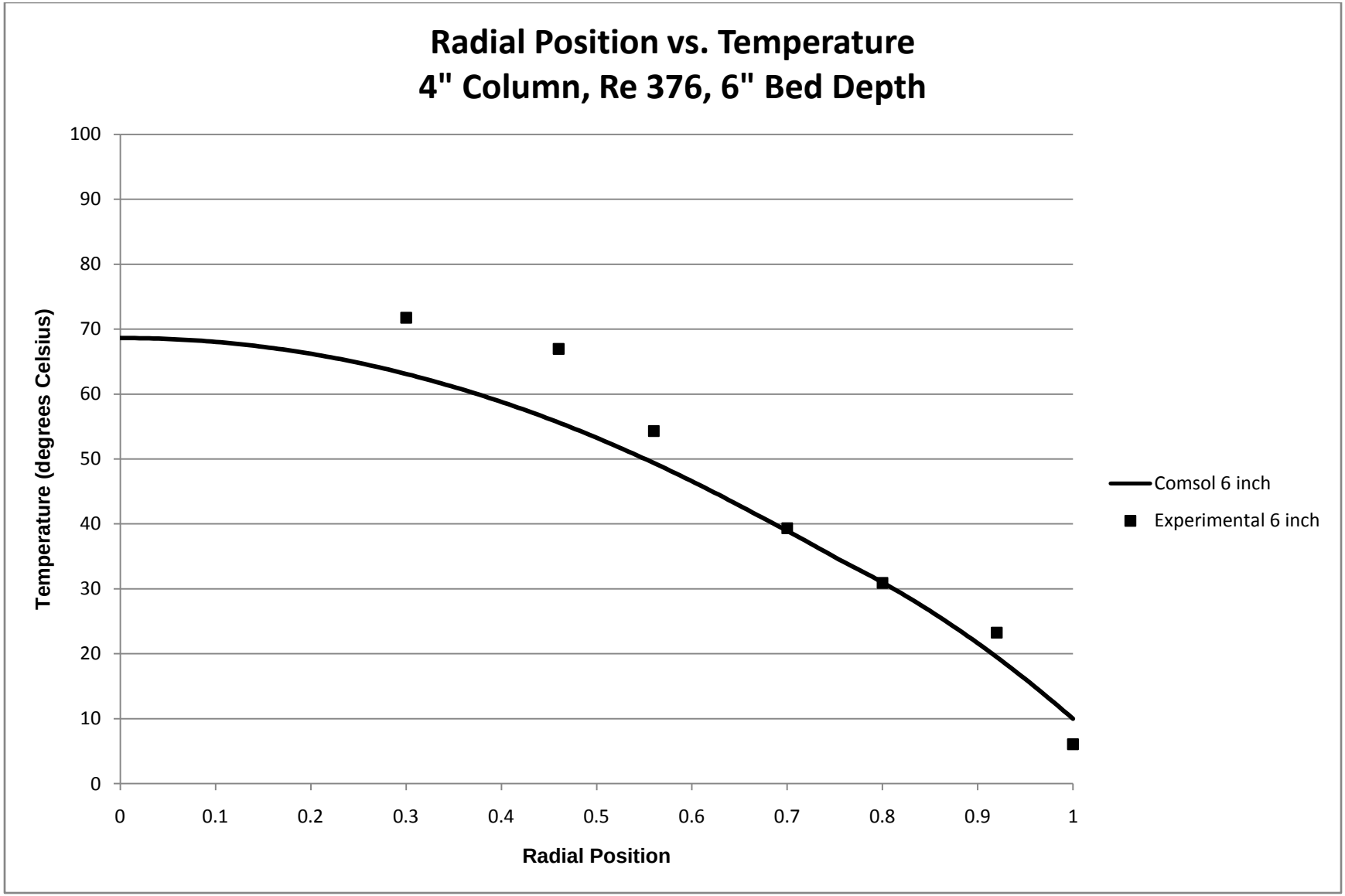
Radial Position vs. Temperature
4" Column, Re 376, 6" Bed Depth
Temperature (degrees Celsius)
100
90
80
70
60
50
40
30
20
10
0
0
0.1
0.2
0.3
0.4
0.5
0.6
0.7
0.8
0.9
1
Radial Position
Comsol 6 inch
Experimental 6 inch

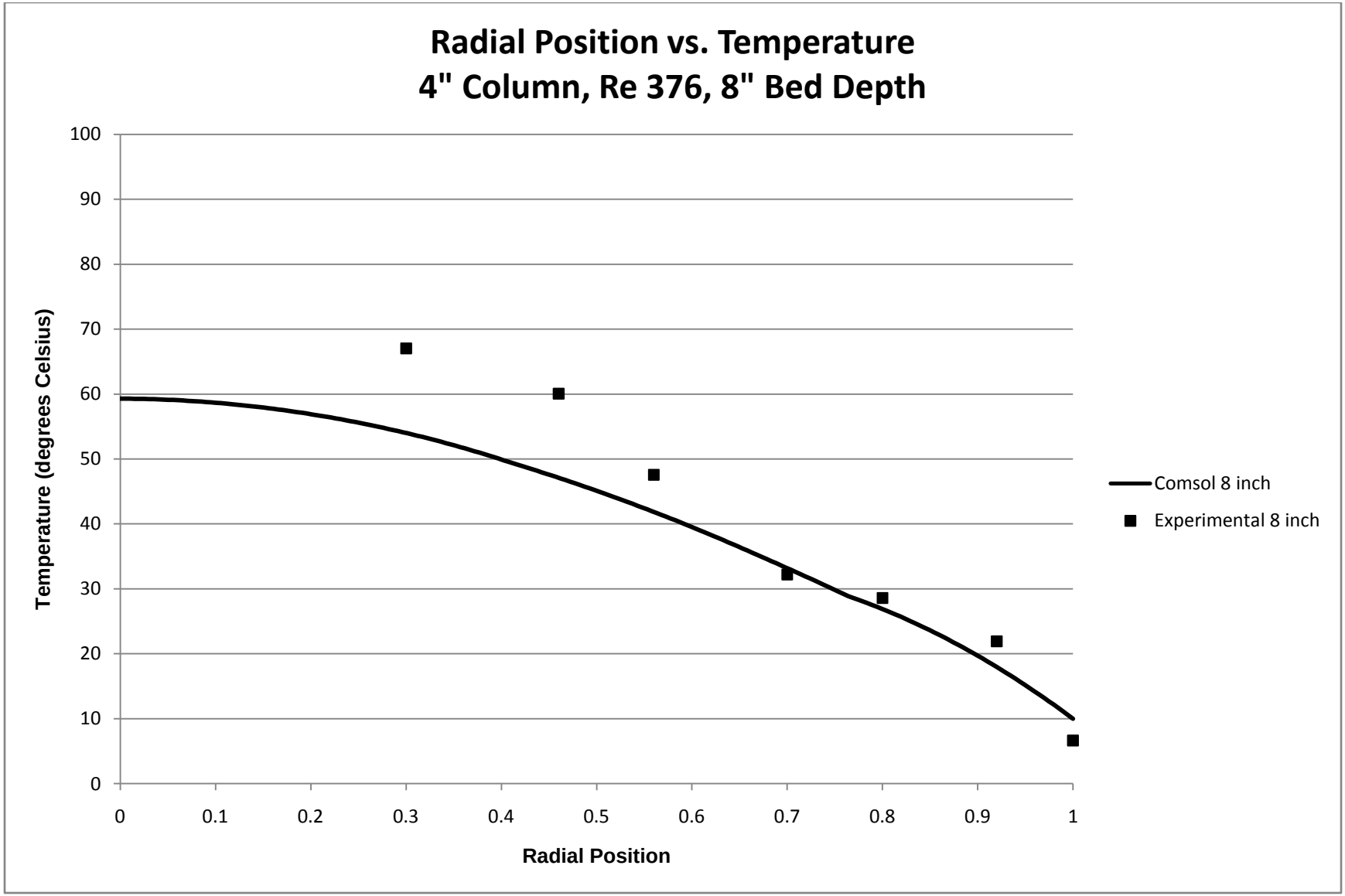
Radial Position vs. Temperature
4" Column, Re 376, 8" Bed Depth
Temperature (degrees Celsius)
100
90
80
70
60
50
40
30
20
10
0
0
0.1
0.2
0.3
0.4
0.5
0.6
0.7
0.8
0.9
1
Radial Position
Comsol 8 inch
Experimental 8 inch

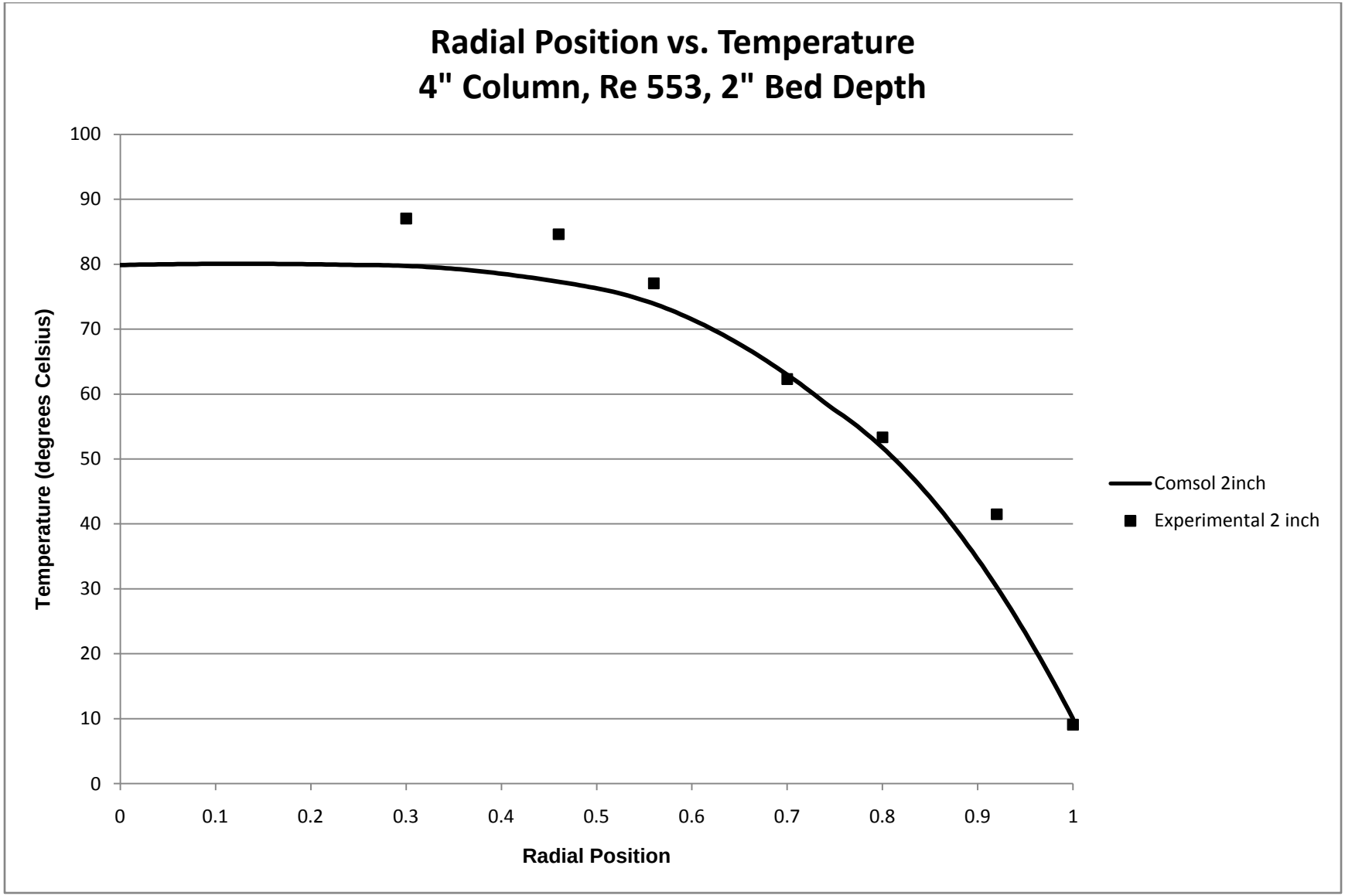
Radial Position vs. Temperature
4" Column, Re 553, 2" Bed Depth
Temperature (degrees Celsius)
100
90
80
70
60
50
40
30
20
10
0
0
0.1
0.2
0.3
0.4
0.5
0.6
0.7
0.8
0.9
1
Radial Position
Comsol 2inch
Experimental 2 inch

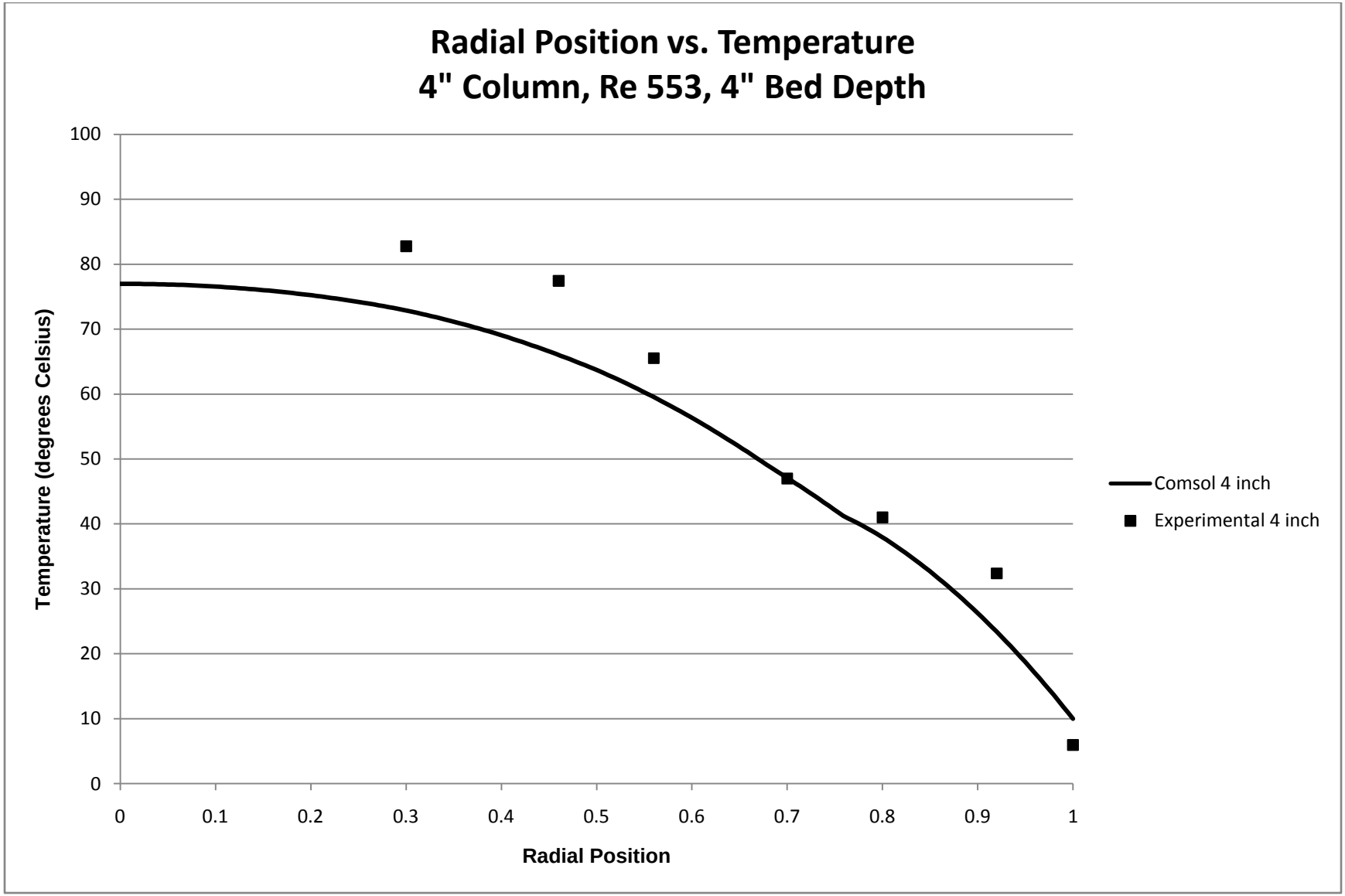
Radial Position vs. Temperature
4" Column, Re 553, 4" Bed Depth
Temperature (degrees Celsius)
100
90
80
70
60
50
40
30
20
10
0
0
0.1
0.2
0.3
0.4
0.5
0.6
0.7
0.8
0.9
1
Radial Position
Comsol 4 inch
Experimental 4 inch

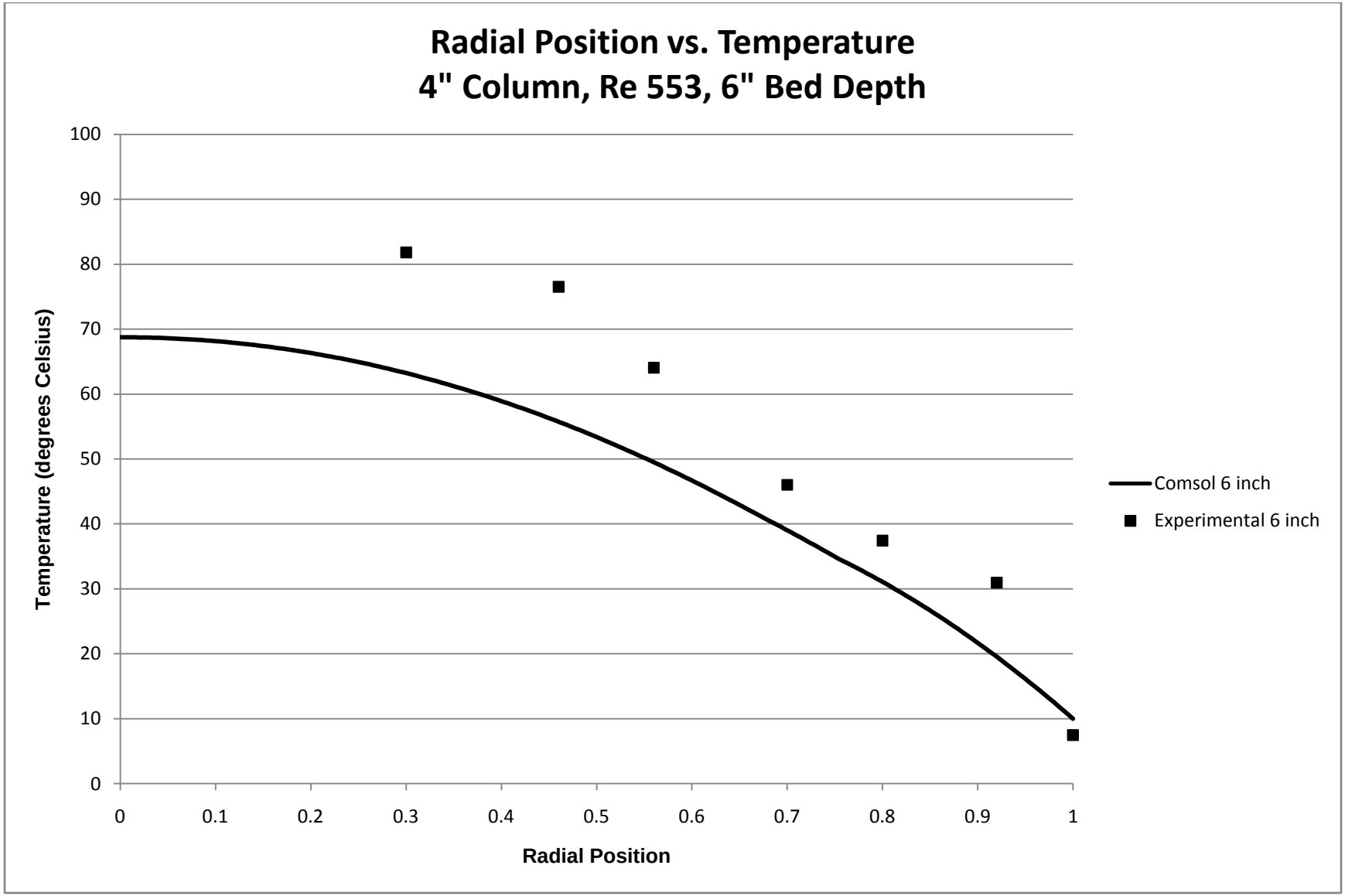
Radial Position vs. Temperature
4" Column, Re 553, 6" Bed Depth
Temperature (degrees Celsius)
100
90
80
70
60
50
40
30
20
10
0
0
0.1
0.2
0.3
0.4
0.5
0.6
0.7
0.8
0.9
1
Radial Position
Comsol 6 inch
Experimental 6 inch

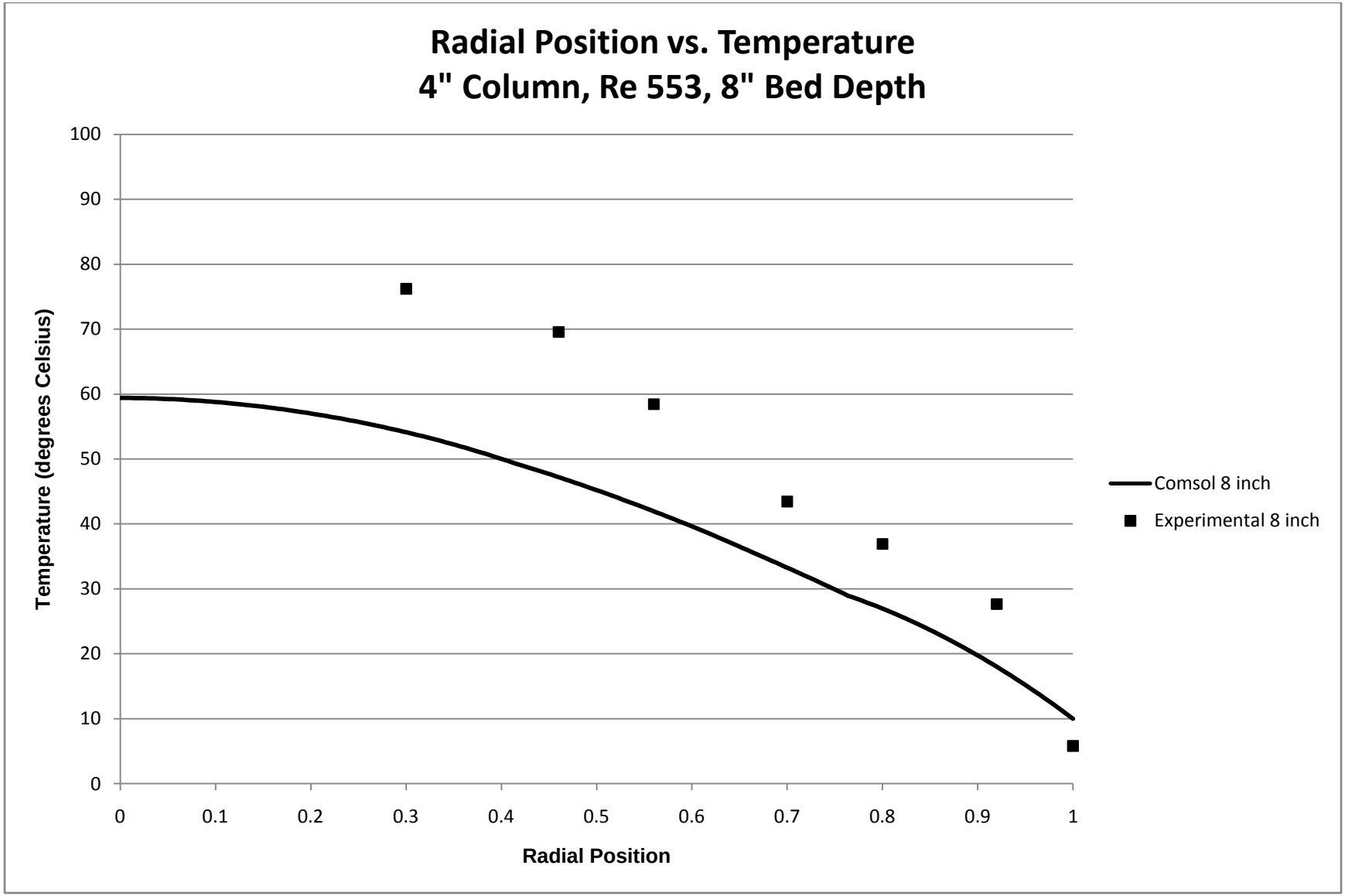
Radial Position vs. Temperature
4" Column, Re 553, 8" Bed Depth
Temperature (degrees Celsius)
100
90
80
70
60
50
40
30
20
10
0
0
0.1
0.2
0.3
0.4
0.5
0.6
0.7
0.8
0.9
1
Radial Position
Comsol 8 inch
Experimental 8 inch